SSC-N-354

RADIOLOGICAL SAFETY ASPECTS OF THE OPERATION OF PROTON ACCELERATORS

Ralph H. Thomas
Lawrence Berkeley Laboratory
and the School of Public Health
University of California
Berkeley, California
U.S.A

and

Graham R. Stevenson
European Laboratory for Particle Physics
European Organization for Nuclear Research
Geneva
Switzerland

July 1986

Note to Readers: This is a copy prepared for internal use only of a draft as submitted for publication in the Technical Report Series of the IAEA by the above authors. To reduce the bulk of this copy, double spaced text pages were reprinted as single spaced and the pages were renumbered with a numbering machine. Where these machine numbers appear they supercede previous page numbers. The order of contents in each chapter is 1) text, 2) references, 3) tables, 4) figure captions, 5) figures.

'Safety...there is no such thing as safety. There are so many seeking safety here now that they make a great danger. In seeking safety now you lose all!'

Pablo's Woman in
'For Whom the Bell Tolls'

Ernest Hemingway, 1940

FOREWORD

Particle accelerators are finding increased application in both the fundamental and applied sciences and in industry around the world. Recognizing this, the International Atomic Energy Agency began, in 1975, preparing a series of technical reports dealing with the radiological safety of accelerator operation. The first of these, IAEA Safety Series Report No. 42, entitled Radiological Safety Aspects of the Operation of Neutron Generators and written by R.F. Boggs, was issued in 1976. Radiological Safety Aspects of the Operation of Electron Linear Accelerators (IAEA Technical Report No. 188), written by W.P. Swanson, was issued in 1979. This present report covers positive-ion accelerators.

Since their first operation in the 1930s, positive-ion accelerators have been applied to a wide range of investigations in the fundamental sciences, including astronomy, biology, chemistry and physics. Indeed, the birth of the 'radiation sciences' — nuclear physics, fundamental particle physics, radiation biology and radiation chemistry— largely derives from the creation of positive-ion accelerators. While the use of positive-ion accelerators in the applied sciences and industry has perhaps been slower, and is less extensive, than has been the case for electron accelerators, it is now rapidly increasing. Positive-ion accelerators are being applied in a host of fields, including radiation damage studies, induced activation and dating measurements, radiography, radiotherapy and fusion research. Because positive-ion accelerators can be potent sources of neutrons, it is important that information concerning their safe operation be widely available.

This manual is conceived as a source book providing authoritative guidance in radiation protection from an important category of radiation sources. It thus supplements other manuals of the Agency related to the planning and implementation of radiation protection programmes. The authors, Ralph H. Thomas of the University of California and Graham R. Stevenson of the European Organization for Nuclear Research, were engaged as consultants by the Agency to compile and write the manual, and the Agency wishes to express its gratitude to them.

A draft was sent to a number of experts in various countries. The Agency gratefully acknowledges the helpful comments, which have been incorporated in the final text, from Dr. E. Benton, University of San Francisco, U.S.A; Dr. Liu Kuei-Lin, Institute of High Energy Physics — Academia Sinica, Beijing, People's Republic of China; Dr. Kazuaki Katoh, KEK, Japan; Dr. M. M. Komochkov, Joint Institute for Nuclear Research, Dubna, U.S.S.R; Prof. E. E. Kovalev, Institute of Biomedical Problems, Moscow, U.S.S.R; Dr. D. R. Perry, Rutherford-Appleton Laboratory, United Kingdom; Dr. S. Pszona, Institute of Nuclear Research, Swierk, Poland; Dr. A. Rindi, CEN, Frascati, Italy; Dr. K. Tesch, DESY, Federal Republic of Germany. The Agency's officer responsible for this project was F. N. Flakus of the Radiation Protection Section, Division of Nuclear Safety.

Comments from readers for possible inclusion in a later edition of the manual are welcome and should be addressed to:

The Director
Division of Nuclear Safety
International Atomic Energy Agency
Wagramerstrasse 5, P.O. Box 100
A-1400 Vienna
Austria

CONTENTS

INTRODUCTION

Purpose and Scope of the Manual

Terminology and Units

The Authors

Acknowledgements

1. CHARACTERISTICS OF POSITIVE-ION ACCELERATORS

1.1 Historical Review

1.2 Types of Positive-Ion Accelerators

1.3 Physical and Radiological Characteristics

1.4 Fields of Application

1.5 Examples of Accelerator Installations

References for Chapter 1

2. THE RADIATION ENVORONMENT OF POSITIVE-ION ACCELERATORS

2.1 Introduction

2.2 Prompt Radiation Fields

2.3 Induced Radioactivity

References for Chapter 2

3. RADIATION MEASUREMENTS AT ACCELERATORS

3.1 Dosimetry at Particle Accelerators

3.2 Historical Background

3.3 Mixed Radiation Field Dosimetry

3.4 Neutron Dosimetry at Accelerators

3.5 Radiation Surveys

3.6 Dose Equivalent Instruments versus Physical Measurements

3.7 The Determination of Neutron Spectra at Accelerators

3.8 Interpretation of Accelerator Radiation Measurements

References for Chapter 3

4. RADIATION SHIELDING
4.1 Introduction
4.2 Shielding Criteria, Materials and Other Considerations
Purpose and Scope of the Manual
Terminology and Units
The Authors
Acknowledgements

1. CHARACTERISTICS OF POSITIVE-ION ACCELERATORS
1.1 Historical Review
1.2 Types of Positive-Ion Accelerators
1.3 Physical and Radiological Characteristics
1.4 Fields of Application
1.5 Examples of Accelerator Installations
References for Chapter 1

2. THE RADIATION ENVORONMENT OF POSITIVE-ION ACCELERATORS
2.1 Introduction
2.2 Prompt Radiation Fields
2.3 Induced Radioactivity
References for Chapter 2

3. RADIATION MEASUREMENTS AT ACCELERATORS
3.1 Dosimetry at Particle Accelerators
3.2 Historical Background
3.3 Mixed Radiation Field Dosimetry
3.4 Neutron Dosimetry at Accelerators
3.5 Radiation Surveys
3.6 Dose Equivalent Instruments versus Physical Measurements
3.7 The Determination of Neutron Spectra at Accelerators
3.8 Interpretation of Accelerator Radiation Measurements
References for Chapter 3

INTRODUCTION

During the past 10 to 15 years, a great deal of operating experience with several high-energy proton accelerators has been gained, concurrently with some significant developments relating to accelerator radiation protection. These developments include the following:

(a) Radiation-protection practices are being standardized and national and international radiation-protection guidelines for medical accelerators have been developed.

(b) Operational flexibility, such as multibeam capability, has placed new demands on personnel protection systems.

(c) The development of sophisticated Monte-Carlo techniques has made it possible to undertake otherwise intractable calculational problems. Very useful calculations are now available on hadronic and electromagnetic cascade development, on neutron production and transport and on muon production and transport.

(d) The development of radiation protection practices at a wide variety of particle accelerators has provided a broad base of information. This worldwide experience was shared at conferences in 1965, 1969 and 1971.

(e) The growing sensitivity on the part of the general public to environmental concerns has required a greater degree of attention to radioactive releases. Although such releases have never been a serious problem at particle accelerators, an ability to make definite statements about the amounts produced and their disposal is still desirable.

Concurrently with these developments and with the increase in operating experience, several monographs have appeared that discuss accelerator radiation protection and associated topics in radiation physics. While these monographs have served to delineate accelerator radiation protection as a discipline in its own right, none has been truly comprehensive.

Because of the growing use of positive-ion accelerators in teaching institutions, their applications in industry and medicine and the interest in some industrially developing countries in designing and constructing proton accelerators, it was felt worthwhile to bring together in one place a general discussion of the radiological safety aspects of positive-ion accelerator operation. This manual is the result and is intended to both summarize the present state of our understanding and to serve as a source book for references to the literature.

PURPOSE AND SCOPE OF THE MANUAL

This manual is intended as a guide for the planning and implementation of radiation protection programs for all types of positive-ion accelerators. It is hoped that it will prove useful to accelerator users, managements of institutional and industrial accelerator installations, accelerator designers and manufacturers, government regulators and, most especially, to radiation safety officers and others

responsible for radiation safety at accelerators.

The manual is not designed to take into account various local, regional and national regulations for radiation protection that an accelerator installation may have to satisfy. Government authorities and qualified experts should be consulted to ensure that an installation meets all legal requirements.

There is a great diversity in the types of positive-ion accelerators in use, but many radiation protection problems are common to each. Although increasing energy results in a greater variety of particles present in the radiation fields close to primary beams, the problems of radiation protection outside shielding are dominated by photons, neutrons and (above about 10 GeV) muons.

The basic types of accelerator are briefly described, followed by a detailed description of several installations covering the energy range from 10 MeV to 500 GeV. Positive-ion accelerators are used primarily in fundamental research, so there is little standardization in design (as has developed in recent years, for example, for electron linacs used in radiotherapy); each facility is unique. Nevertheless, we feel that the discussion of these varied installations will demonstrate the typical radiation protection problems to be investigated for new installations.

Special discussions are devoted to the production of ionizing radiation and its transmission through shielding so that the fundamentals of shielding may be understood. Of particular importance has been the development during the past 10 years of computer techniques for shield design. Extensive references to the published literature will facilitate shielding design for particular facilities.

Measurements of radiation fields around accelerator installations may present special problems because of both the pulsed nature of the beam and the varying contribution of low-LET and high-LET radiations. Considerable discussion, again supported by reference to the literature, is given of radiation measurement and its interpretation.

Public interest in nuclear installations of all types has increased substantially during the past decade, and consequently the radiological impact of accelerators on the environment is discussed in some detail. The subjects of air and water activation are reviewed.

Space does not permit a complete treatment of radiation protection for the great variety of positive-ion accelerators in operation. Rather, our intention is to present a balanced treatment of the major radiation protection problems and to indicate general methods for their solution. A discussion of the sources of information on accelerator radiation protection together with an extensive bibliography will assist those responsible for accelerator radiation protection. One should have a selection of these references readily available.

The material presented here is derived from the work of many people working at a large number of installations, and no originality is claimed by the authors save in the manner of presentation.

TERMINOLOGY AND UNITS

The terminology and concepts used here correspond with the current recommendations of the International Commission on Radiological Protection and the International Commission on Radiation Units and Measurement (ICRP and ICRU), as expressed in ICRP Report 26 and ICRU Report 33. Wherever possible the International System of Units is used, but in some cases cgs units are used when quoting from the original documents. In many cases, numerical values are given in SI units with the special unit equivalent in parentheses.

THE AUTHORS

Ralph H. Thomas was educated at University College, London (B.Sc.[Physics] 1955, Ph.D. Nuclear Physics 1959), and the School of Public Health of the University of California at Berkeley (M.P.H. 1981). He is currently a member of the Director's Office of the Lawrence Berkeley Laboratory, responsible for Occupational Health. Dr. Thomas is also Adjunct Senior Lecturer at the School of Public Health at Berkeley. With more than 400 publications Dr. Thomas' research has largely centered on radiological protection from accelerator-produced ionizing radiation, and in 1979 he was awarded the degree of D.Sc. by the University of London for these studies. Before moving to Berkeley Dr. Thomas worked at the Atomic Energy Research Establishment (Harwell), the Research Laboratories of Associated Electrical Industries (Aldermaston), the Rutherford Laboratory (Chilton) and Stanford University (California). In 1977 Dr. Thomas was a Visiting Scholar to the National Laboratory of High Energy Physics in Japan (KEK); in 1984 he was a guest of the Academia Sinica to the Institute of High Energy Physics in Beijing, People's Republic of China. During the academic year 1985-86 he was a Visiting Scholar at the Radcliffe Science Library and Fellow at Keble College of the University of Oxford, United Kingdom.

Dr. Thomas has been a member of committees of the National Council on Radiation Protection and Measurements, the International Commission on Radiological Protection and the International Commission on Radiation Units and Measurements.

Graham R. Stevenson was educated at the University of Bristol, where he graduated in Physics in 1959. In 1963 he was awarded the degree of Ph.D. for his research on the composition and time variations of the galactic cosmic radiation.

He worked briefly as a research assistant in the Cosmic Ray Group at Bristol University before taking up an appointment at the Headquarters of the Radiological Protection Service of the United Kingdom, Sutton, Surrey in 1963. As a member of the Neutron Group Dr. Stevenson was involved in definitive studies of the use of NTA film in neutron personal dosimetry.

From 1966 Dr. Stevenson served as Senior Scientific Officer in the Radiological Protection Group of the Rutherford Laboratory. During the period 1966-1971 his work included research in the fields of neutron spectrometry, accelerator shielding, dose equivalent estimation and the production of induced activity by particle accelerators. From 1969

until 1971 he also had a concurrent appointment as lecturer in Radiological Physics at the University of Surrey.

Since 1971 Dr. Stevenson has worked at the European Centre for Nuclear Research (CERN) in Geneva, most recently as a Senior Physicist with the Radiation Protection Group. His current assignment is as Radiation Safety Officer of the CERN 400-GeV Super Proton Synchrotron, and his research interests include hadronic cascade development, skyshine, muon production and shielding, dosimetry and induced activity. His research is described in over two hundred publications in the scientific literature and in internal reports.

Dr. Stevenson is a member of the Society for Radiological Protection (UK) and has served on the Task Force on External Radiation of Committee 3 of the International Commission for Radiological Protection.

ACKNOWLEDGEMENTS

The authors gratefully acknowledge the encouragement and support of the International Atomic Energy Agency, the Lawrence Berkeley Laboratory of the University of California and the European Organization for Nuclear Research during the preparation of this report. We particularly wish to thank Dr. Franz N. Flakus of the IAEA, who was responsible for the preparation of the report; Dr. Andrew M. Sessler and Dr. David A. Shirley (Directors, Lawrence Berkeley Laboratory), Mr. Walter D. Hartsough (Associate Director—Facilities Management and Technical Services Division, Lawrence Berkeley Laboratory), Dr. Albert Herz (Head, Health and Safety Division, CERN), Dr. Fritz Ferger (Head, Technical Inspection and Safety Commission, CERN), and Dr. Klaus Goebel (Leader, Radiation Protection Group, CERN), for their forbearance in permitting us time to work on this report, although this diminished the time available for our usual duties.

In particular RHT wishes to express his thanks to Mr. Clayton Sealy, Dr. H. Henry Stauffer and Mr. Jensen Young of the Occupational Safety Section of the Lawrence Berkeley Laboratory for shouldering extra burdens, making it possible for him to take up an appointment in Oxford. He also is indebted to the Radcliffe Science Library of Oxford University for its hospitality during the Academic Year 1985-86 in making its facilities available during the final completion of this handbook during his tenure as a Visiting Scholar. Dr. D. Shaw, Keeper of the Scientific Books, is to be thanked for his generosity in making the invitation and his many kindnesses during the year. The Warden, C.J.E. Ball, and the Governing Body of Keble College, Oxford graciously made available a Visiting Fellowship during the academic year 1985-86. He also wishes to thank Pergamon Press (Oxford), especially Mr. R. Miranda of their New York office, and the Central Electricity Generating Board of the United Kingdom, particularly Dr. B.M. Wheatley of the Berkeley Nuclear Laboratories, for financial support at Oxford during this period.

We are deeply indebted to Dr. W.P. Swanson of the Lawrence Berkeley Laboratory, University of California, for valuable comments on

preliminary drafts and to our colleagues A. Fasso, K. Goebel, M. Hoefert and A. Sullivan of CERN, J.B. McCaslin and A.R. Smith of the Lawrence Berkeley Laboratory and H. Wade Patterson (formerly of the Lawrence Berkeley and Lawrence Livermore Laboratories, now retired) for valuable advice and helpful information. Our greatest appreciation is extended to the Technical Information Department of the Lawrence Berkeley Laboratory for their great efforts in typing the early drafts of this report, preparing many of the diagrams and providing editorial assistance.

Many individuals from several other organizations were extremely helpful in supplying data and information. These include:

M. R. Altman	Bureau of Radiological Health, U.S.A.
T. E. Burlin	The Polytechnic of Central London, U.K.
H. Book	Nuclear Regulatory Commission, U.S.A.
A.B. Chilton	University of Illinois, Champaign-Urbana, U.S.A.
J. Drouet	Saclay, France
E. Freytag	DESY, B.R.D.
S. Fukomoto	KEK, Japan
K. Goebel	CERN, Switzerland
J. T. Hyman	Rutherford-Appleton Laboratory, U.K.
K. Katoh	KEK, Japan
A.J. Miller	Los Alamos National Laboratory, U.S.A.
D. Myers	Lawrence Livermore National Laboratory, U.S.A.
M. O'Riordan	National Radiological Protection Board, U.K.
P. Pellerin	SCRPI, France
M. Pelliccioni	Laboratori Nazionali Di Frascati, Italy
D.R. Perry	Rutherford-Appleton Laboratory, U.K.
T.M. Putnam	Los Alamos National Laboratory, U.S.A.
G. Ryder	Daresbury Laboratory, U.K.
K. B. Shaw	NRPB, U.K.
G. B. Stapleton	Rutherford-Appleton Laboratory, U.K.
K. Tesch	DESY, B.R.D.
S. R. Wagner	Physikalisch-Technichse Bundesanstalt, B.R.D.
R. G. P. Voss	Daresbury Laboratory, U.K.

This work was supported in part by the European Centre for Nuclear Research (CERN) and by the U.S. Department of Energy under Contract No. DEAC03-76SF00098 with the University of California and by the Radcliffe Science Library of the University of Oxford.

CHAPTER 1

Characteristics of Positive-Ion Accelerators

'And now I see with eye serene,
The very pulse of the Machine,
A being breathing thoughtful breath,
A traveller betwixt life and death;
The reason firm, the temperate will,
Endurance, foresight, strength and skill;
A perfect woman nobly planned,
To warn, to comfort and command,
And yet a spirit still, and bright
With something of angelic light.'

from 'Simon Lee'
William Wordsworth (1770-1850)

CHAPTER 1 CONTENTS

1.1 Historical Review

1.2 Types of Positive-Ion Accelerators

1.3 Physical and Radiological Characteristics

1.4 Fields of Application

1.5 Examples of Accelerator Installations

30-MV Electrostatic Generator: Daresbury Laboratory

800-MeV Proton Linear Accelerator: The Clinton P. Anderson Meson Physics Facility Laboratory

800-MeV Proton Synchrotron: Spallation Neutron Source — Rutherford Appleton Laboratory

Multi-GeV Heavy-Ion Facility: The Bevalac of the Lawrence Berkeley Laboratory

12-GeV Strong Focussing Proton Synchrotron: KEK

The CERN Super Proton Synchrotron (SPS)

References for Chapter 1

Figure Captions for Chapter 1

CHAPTER 1

CHARACTERISTICS OF POSITIVE-ION ACCELERATORS

1.1. HISTORICAL REVIEW

The year 1932 was an extremely important one both for nuclear physics and for particle accelerators. Not only was it the year in which the neutron was discovered (Ch 32), but Cockcroft and Walton at Cambridge (Co 32a,b) and Lawrence and Livingston at Berkeley (La 32a,b) independently designed, constructed and operated particle accelerators as research instruments to investigate nuclear structure. Thus was born-in this annus mirabilis-the discipline of nuclear physics as we know it today (Ha 84).

With particle accelerators came the need to study the radiations produced by them, their interaction with biological tissue, and the birth of accelerator health physics.

The early accelerators were of such low energy and intensity that their radiations were of little biological consequence. However, it was not long before concerns for these unusual radiations were to be expressed. Apochryphal stories abound. One such story was about death of mice exposed to a neutron beam of the Crocker Cyclotron at the University of California at first ascribed to radiation but then found to be due to asphyxiation (Va 75).

In addition to the low intensity of the early cyclotrons many were constructed underground in order to avoid anticipated but unquantified radiation problems (see Chapter 6 in Pa 73). Thus the identification and solution of radiation problems during the first 25 years of the history of particle accelerators tends to have been centered at those groups with accelerators constructed above ground-largely because of a real need to go beyond a merely empirical solution of radiation problems (Li 61a, McC 81, Mo 58, Pa 73, Ri 73).

In the early fifties a sense of urgency was given to accelerator radiation studies by reports in the literature of the observation of cataracts in several French and U.S. cyclotron workers (Ha 53, Up 68).

As more particle accelerators were constructed of increased energy and intensity, and as the variety of accelerator types proliferated, radiation phenomena became an increasingly important aspect of both operation and design. The second 25 years of accelerator history has included detailed investigation of accelerator radiation protection phenomena, and the foundation of these studies was laid in the mid to late fifties at Berkeley and Brookhaven (Li 57, Mo 57, Pa 57, So 57). Any understanding of accelerator radiation protection first requires a knowledge of the types of particle accelerator and their various characteristics, and such a discussion is given in this chapter. The chapter begins with a historical review of accelerator development and a description of the various types of positive-ion accelerator and their characteristics and application, and it concludes by describing several typical accelerator installations.

The brief historical review given here cannot attempt to do justice to such an extensive subject, and only the highlights can be indicated.

Interested readers are referred to some of the standard texts on the subject (Bu 68, Li 61b, Li 62, McM 59, Wi 68a,b and the Bibliography in Chapter 7).

Livingston has compiled 28 of the classic papers of accelerator physics to which he has added an extremely valuable linking commentary. These papers demonstrate the development of particle accelerators from the early theoretical suggestions of the 1920s to the design and construction and operation of the first alternating gradient synchrotrons in the late fifties and early sixties (Li 66). In this review the authors have drawn heavily upon the material compiled by Livingston.

A glimpse into the future of high-energy research has been given by Panofsky in an article entitled 'Needs Versus Means in High-Energy Physics' (Pa 80).

At the time of writing (mid-1985) planning or construction is underway on several large high-energy accelerators. At CERN a large electron-positron storage ring (LEP) is under construction, and it will begin its experimental program in 1989 (Fa 84a). The addition of superconducting RF cavities will make feasible an increase in centre-of-mass (c.m.) energy to 200 GeV by about 1992. A preliminary design of a large hadron collider facility (LHC) to be constructed in the LEP tunnel has been carried out (Br 84, Fa 84b,c). With magnetic fields of 10 tesla, the LHC could reach an energy of 17 TeV (c.m.).

In the Federal Republic of Germany at the DESY laboratory in Hamburg the first electron-proton collider (HERA) is under construction to operate about 1990.

Plans in the Soviet Union envisage a 3-TeV superconducting proton synchrotron (UNK). UNK will first operate in fixed-target mode (80 GeV c.m.) and then in a collider mode against a 400-GeV conventional protron ring (2.2 TeV c.m.).

Finally, in the United States a 20-TeV colliding proton facility is being planned (DOE 84, McC 83). These vast accelerator complexes will eventually bring with them new and interesting radiological problems.

THE PHASES OF ACCELERATOR DEVELOPMENT

Livingston (Li 66) has recognized four distinct phases in the development of particle accelerators:

- Direct-Voltage Acceleration
- Resonance Acceleration
- Synchronous Acceleration
- Alternating Gradient Focussing

to which should be added a fifth phase:

- Colliding Beam Technology

Direct-Voltage Acceleration is perhaps the most obvious method of charged-particle acceleration, and in fact the first accelerator to

demonstrate the disintegration of atomic nuclei by artifically accelerated particles was of this type (Co 30, Co 32a,b, Co 34).

The principal difficulty in direct voltage acceleration is to maintain a DC potential that is stable (i.e., free from AC ripple or voltage surges such as occur, for example, from insulator breakdown). Successful solutions to these problems have included the voltage multiplier (as used by Cockcroft and Walton [Co 32a]), its modern successor the Dynamitron (Bu 68, Cl 65) and the insulated electrostatic generator.

Versions of accelerators using the voltage multiplication principle are now widely used in industry and research. Low-energy accelerators in the voltage range from 100 kV are used as inexpensive neutron generators by accelerating deuterons and taking advantage of the exoenergetic (D,D, 2.3-MeV) and (D,T, 14.7-MeV) reactions. Such accelerators are also used as injectors or pre-injectors to higher-energy facilities that consist of an assembly of several accelerators in tandem (see Section 1.5, Examples of Accelerator Installations).

The basic principle of the electrostatic generator had been discovered in the nineteenth century and applied to machines used to demonstrate electrostatic phenomena in the lecture-theatre (Je 08).

The belt-charged electrostatic generator derives from the work of R.J. Van de Graaff, who in 1931 reported attaining a steady potential of approximately 1.5 MV (Va 31). By 1936 Van de Graaff and his colleagues at MIT had successfully designed and constructed generators for experimental use that were operated for many years at a terminal potential of 2.75 MV (Va 33, Va 36).

Van de Graaff's work was extended by colleagues at other institutions. Tuve et al. have described a high-voltage generator that was constructed at the Carnegie Institution. Beam currents of 20 μA were obtained (Tu 35).

The principal difficulty in the operation of these high voltage generators lay in their unstable terminal voltage due to corona discharges or sparking. This problem was solved by placing the generator in a pressurized housing. The first report in the literature of a pressure-insulated generator and was made in 1932 by Van Atta and his colleagues (Ba 32). This development made possible the use of Van de Graaff generators as a practical nuclear physics research instrument. One such instrument, operating reliably at 400 kV in the mid-thirties, has been described by Herb et al. (He 35).

A useful review of these developments up to 1948 has been given by Van de Graaff, Trump and Buechner (Va 48). At this time the terminal voltage was limited for several technical reasons to about 10 MV. Developments since the Second World War have now made terminal voltages of 20 MV to 30 MV possible. Section 1.5 describes one such accelerator designed and constructed at the Daresbury Nuclear Physics Laboratory in England and recently put into operation.

Resonance Acceleration. Suggestions for particle accelerators based upon a resonance principle date from the mid-1920s. Wideröe, in 1928 (Wi 28), was the first to demonstrate radio-frequency resonance, but the first application of the principle to a practical accelerator

was at Berkeley, following the invention of the cyclotron by Lawrence and his colleagues (La 30, Li 31).

The first practical cyclotron used a magnet with a 10-inch-diameter pole face with which protons of an energy of 1.2 MeV were obtained (La 32a,b). Concurrently with the application of the 1-MeV cyclotron to nuclear disintegration studies a larger (27-inch) cyclotron was immediately designed. This accelerator operated in 1934, producing 3-MeV protons and 5-MeV deuterons (La 34).

Lawrence has described the early development of the cyclotron in his Nobel Lecture (La 51). A progression of cyclotrons followed the 27-inch one at Berkeley. This latter cyclotron was modified so as to have a magnet pole-face diameter of 37 inches and produce 8-MeV deuterons (La 36).

The first applications of the cyclotron to medical problems started, also in Berkeley, with the operation of the Crocker 60-Inch Cyclotron (La 39). This cyclotron was capable of accelerating deuterons to an energy of 20 MeV and served as a model for similar cyclotrons at other laboratories (Li 66).

Resonance acceleration is also the basic principle by which proton and heavy-ion linear accelerators operate (Is 24). Sloan and Lawrence operated the first such accelerator and demonstrated the acceleration of singly charged Hg ions to an energy of 1.26 MeV, at a beam current of 0.1 μA. Although the authors concluded from their experiments that the acceleration of ions to energies as high as 10 MeV seemed possible, their linear accelerator was not practical for nuclear physics experiments (Sl 31).

The development of high-power radio-frequency supplies during the Second World War made feasible the construction of proton linear accelerators for use in nuclear physics. The first such instrument was designed and built by Alvarez and his colleagues and accelerated protons to 32 MeV (Al 46). This linac has been the basis for more advanced designs, and proton linear accelerators up to an energy of 200 MeV are often used as injectors to high-energy synchrotrons (see Section 1.5). The highest-energy proton linac in operation at the present time is at the Los Alamos National Laboratory with an energy of 800 MeV (see Section 1.5).

Synchronous Acceleration. The energy of particles accelerated by fixed-frequency cyclotrons is limited to about 25 MeV because of the relativistic increase in mass of the accelerated ions.

In 1945 Veksler and McMillan independently suggested a method of synchronous acceleration that permitted acceleration to higher energies (McM 45, Ve 45). The first demonstration in the laboratory of such synchronous acceleration was achieved by Goward and Barnes in England in 1946, who modified a betatron to operate as a 70-MeV electron synchrotron (Go 46).

The principle of phase stability discovered by McMillan and Veksler was also rapidly applied to the synchronous acceleration of protons. Modulation of the frequency of the accelerating field applied across the cyclotron dees would lead to stable oscillations of the accelerated

particles about the equilibrium phase. The principle was first demonstrated on a 37-inch-diameter cyclotron magnet (Ri 46), and the theory of the synchrocyclotron, as it became known, was developed by Bohm and Foldy (Bo 47). With this demonstrated success, plans to construct a 184-inch fixed-frequency cyclotron at Berkeley were drastically modified, and 184-Inch Synchrocyclotron was designed and brought into operation in 1946, producing deuterons of energy 130 MeV and helium ions of energy 380 MeV (Br 47). Still in operation, this accelerator is now totally dedicated to medical research. After several modifications it now accelerates protons to an energy of 720 MeV and helium ions to an energy of 920 MeV. Throughout its long career the '184-Inch' has made an enormous contribution to nuclear physics and medical research (Ca 77). Following the success of the 184-Inch, six other synchrocyclotrons were constructed around the world in the energy range 400–700 MeV.

The principle of phase stability had been anticipated during the Second World War by Oliphant, who, in 1943, proposed construction of a proton accelerator of the type now called a synchrotron (Co 81). In 1947, after the publication of Veksler's and McMillan's work, Oliphant and his colleagues at Birmingham proposed and designed a 1-GeV proton synchrotron (Go 47, Ol 47). For a variety of reasons including inadequate financial resources, the operation of the accelerator was delayed until 1953.

Meanwhile, in the United States, planning for two synchrotrons began, at Brookhaven National Laboratory and the University of California Radiation Laboratory.

At Brookhaven a 3-GeV accelerator–the Cosmotron–first operated in 1952 (Co 53, Li 50). At Berkeley, after first building a quarter size scale model, a 6-GeV proton synchrotron (the Bevatron) was constructed (Br 48, Se 50). It is still operating, although now used to accelerate heavy ions (see Section 1.5).

It is worth noting that much of our present understanding of the radiological phenomena around high-energy accelerators is based upon studies made at the 184-Inch Synchrocyclotron, the Cosmotron, and the Bevatron [see for example So 57].

Alternating-Gradient Focussing. The technical advance in accelerator design known as alternating-gradient focussing or strong-focussing was first invented by Christofilos (Ch 56) but independently discovered by Courant et al. and reported by them in 1952 (Co 52).

Alterating-gradient (AG) focussing is not a new principle of particle acceleration but a technical improvement in magnet design applied to synchrotron accelerators:

> 'Charged particles traversing a gradient field (one which is strong on one side and weak on the other) are deviated through different angles, depending on incident locations and directions. In a 'positive' gradient the particle trajectories will converge, while in a 'negative' gradient they will diverge (or vice versa, depending on definition of terms). Also, a gradient which is converging in one transverse plane is diverging in the perpendicular transverse plane. The alternating gradient prin-

ciple uses a sequence of magnet sectors in which the sense of the gradient alternates. Analysis shows that in such a sequence of alternately focusing and defocusing sectors, the net effect is focusing in both transverse coordinates. This net focussing about the equilibrium orbit is much stronger than that obtained in uniform-gradient fields such as are used in the betatron or the synchrotron. Amplitudes of particle oscillations about the equilibrium orbit are much smaller, and therefore magnets and vacuum chambers can be smaller. It becomes economically practical to design circular, magnetic accelerators of much larger orbit radius and thus for much higher energies.' (Li 66)

The principle of strong-focussing was rapidly applied to accelerator design both in Brookhaven (Bl 56) and Geneva (Ad 53, Re 59). The design and construction of 30-GeV proton synchrotrons began in both centres leading to operation by 1960.

Since then strong-focussing proton synchrotrons have been brought into operation at Serpukhov (70 GeV) in 1967; Batavia (200 GeV)* in 1972; and CERN (400 GeV) in 1976. The SPS at CERN is briefly described in Section 1.5.

Colliding-Beam Technology. In high-energy physics experiments the centre-of-mass energy (which is available for the production of new particles) is a parameter of great importance. When an accelerator beam impinges on a stationary target the center-of-mass energy is $\sqrt{2ME}$, where E is the energy of the particles in the beam and M is the mass of the target particles. However, if beams of energy E are made to collide head on, the centre-of-mass energy is 2E.

Colliding-beam technology began in 1955 at the Midwest Universities Research Association (MURA) at Madison, Wisconsin, which was interested in building a colliding-proton-beam facility. At that time adequate technology had not been developed to permit the construction of a proton facility, but several groups rapidly developed the idea and applied it to electron facilities.

In 1957 a collaboration between Princeton and Stanford Universities led to the construction of two 500-MeV electron storage rings. This facility was used with great success to experimentally investigate the predictions of quantum electrodynamics during the early to mid-sixties.

Other storage ring facilities followed-this time electron-positron rings-in Italy ADA (started 1961) and ADONE (started 1962) and in the USSR VEPP-2 (also started in 1962). The design of SPEAR (Stanford Positron Electron Accelerator Ring) began in 1961; funding was provided in 1970 and beam obtained in April 1972.

The successful exploitation of the early storage-ring facilities led to the construction of several other electron-positron rings, at the DESY laboratory in Hamburg, at Novosibirsk in the USSR and at Cornell in the U.S.A.

---

*At the time of writing (mid-1985) the Fermilab accelerator is operating at 800 GeV.

The first hadron collider was the CERN Intersecting Storage Rings (ISR) facility. Construction of this machine started in 1966, and it came into operation in 1971. Two separate rings containing 31.4-GeV protons were made to collide at eight intersection points. This gave an equivalent energy for a normal fixed-target accelerator of 2 TeV. Toward the end of its period of exploitation the current in each of the two rings exceeded 30 amperes, and the beams were stored for periods of more than 70 hours without any significant degradation in beam quality. This unique facility was dismantled for economic reasons in 1984.

The first proton-antiproton collider was brought into operation at CERN in 1981 (see section 1.5). Because of the success of this facility, several others are now envisaged (see Historical Review). In particular it is planned that a proton-antiproton colliding beam facility providing centre-of-mass energies up to 2 TeV will come into operation at Fermilab in 1986.

1.2. TYPES OF POSITIVE-ION ACCELERATORS

A basic understanding of the principles of accelerator operation is essential for those concerned with radiation protection at these installations. Space does not permit a discussion here, but several references are given in the bibliography (Chapter 7).

Positive-ion accelerators may be classified in a variety of ways, but the parameters of most importance for radiation protection are the particles accelerated, their energy and intensity and the time-structure of the accelerated particle beams. These parameters are to a large degree determined by the type of accelerator. Table 1.1 summarizes the various types of accelerator and indicates whether they accelerate electrons or heavy ions.

1.3. PHYSICAL AND RADIOLOGICAL CHARACTERISTICS OF POSITIVE-ION ACCELERATORS

PARTICLE ENERGY

In their text on particle accelerators Livingston and Blewett (1962) first showed a plot of the energies achieved by several types of accelerators as a function of time. Such a plot has become known as a Livingston plot and has been constantly revised. Figure 1.1 shows a current version due to Panofsky (Pa 80, Pa 81).

Now almost 25 years after the first Livingston plot their general conclusions remain unchanged:

'Energies achieved with accelerators have increased at an almost exponential rate during the past 30 years. The field has been characterized by a sequence of new concepts or inventions, each leading to a new type of machine capable of still higher energies, and each stimulating the development and construction of a new generation of accelerators. At times, the new developments have come so fast that it as been difficult to determine which laboratory or machine held the current energy record. The record has been held in turn by voltage multipliers,

cyclotrons, betatrons, synchrotrons, synchrocyclotrons, proton synchrotrons and alternating-gradient synchrotrons. In the figure energies achieved with several accelerator types are plotted on a logarithmic scale against the dates of publication of the results. Separate curves show the rise in energy with time for the different machines and identifies the useful energy range for each type. An envelope enclosing all the curves shows a ten-fold increase in energy every six years' (Li 62).

Livingston and Blewett made their analysis when only strong-focussing proton accelerators were in operation (the AGS at Brookhaven and the CPS). Some 20 years later Panofsky was unable to change the conclusions of Livingston and Blewett very much: 'The whole progress of this field (high-energy physics) has been nurtured by a succession of new inventions. As any one invention ran out of steam, a new one has followed, and the result of all these inventions has led high-energy physics to [a] succession of spectacular discoveries' (Pa 81). The Livingston plot still indicates a growth in equivalent energy by about a factor of 10 every 6 or 7 years (Ri 84).

At the present time (mid-1985) the highest-energy accelerator in the world is the CERN proton-antiproton colliding-beam facility (see Section 1.5) with a normal centre-of-mass energy of 540 GeV. Recently in a new mode of pulsed collider operation, maximum centre-of-mass energies of 900 GeV have been achieved. [Protons and antiprotons are composite particles made from quarks, and thus the centre-of-mass energy is considerably higher than the effective centre-of-mass energy.] (Qu 85, Ri 85)

At Fermilab the Tevatron (a superconducting positron synchrotron of 1 TeV) is currently operating in the fixed-target mode at about 800 GeV, giving centre-of-mass energies up to 45 GeV. The SPS operates in fixed-target mode at 450 GeV, and the Serpukhov synchrotron operates at 70 GeV.

BEAM INTENSITY

Available beam intensities of the highest-energy accelerators tend to be significantly lower than those from lower-energy accelerators, as may be seen by inspecting Fig. 1.2. In this figure, prepared in 1971, the two parameters, maximum beam energy and maximum average current, are plotted for various accelerators. For the highest-energy proton accelerators, average currents of a few microamperes were feasible (CERN II, NAL), whereas at the Stanford Linear Accelerator Center (which accelerates electrons) the beam current was an order of magnitude higher.

At these energies the available beam power was almost 1 MW (670 kW at SLAC), and dissipation of the heat generated by the interaction of such beams presents a difficult engineering problem. Experiments at SLAC, with the electron beam focussed to a spot of approximately 1 mm in diameter, have demonstrated that 30-cm-thick metal beam stops are melted through in times ranging from 1 to 10 seconds, depending upon the thermal properties of the metal (Bu 69a). The thermal energy density produced in targets, collimators and backstops by such accelerator beams exceeds that in the cores of fast reactors used for generating

electricity. At proton accelerators, too, the energy in the beam provides similar engineering problems. 'Lost' beams have easily ruptured vacuum chambers in the ISR and SPS machines. Beam dumps, targets and collimators at the SPS and Fermilab accelerators have to be designed to resist the thermal shock provided by a 20-microsecond pulse of several-hundred-GeV protons.

Figure 1.3, prepared in 1982, shows the effective luminosity, L, versus centre-of-mass energy for several operating accelerators and for accelerators then planned for construction. The luminosity of an accelerator, L, is related to intensity by the equation

$$L = \frac{fN_1N_2}{4\pi\sigma^2} \qquad (1.1)$$

where f = collision frequency, N_1,N_2 = particles per bunch, and σ = beam radius. Figures 1.2 and 1.3 both indicate the same general principle: the higher the accelerator energy the lower its intensity.

NUMBER OF ACCELERATORS

The technological achievements of increasing energy and intensity have made possible the development of a large variety of commercially available particle accelerators that can accelerate a wide range of particles to high energies at high beam intensities. This has made possible the industrial application of accelerators to a host of diverse tasks (Av 73, Bo 71, Ev 73, Fo 61, Ma 79, Pa 79, Ro 71, Se 75, To 71).

Burrill (Bu 69b) documented the increasing uses of accelerators in industry and medicine during the period ending December 1968 and showed the number of accelerators in use to be increasing at the rate of roughly 10% a year (Fig. 1.4). Morgan (Mo 73) showed that the annual rate of increase during the period 1968–1972 had more than doubled over the estimate of Burrill.

1.4. FIELDS OF APPLICATION

Although positive-ion accelerators are still used primarily for fundamental research, they have found increasing application in many other areas. Of particular significance for radiation protection is the increasing use of small accelerators* in teaching and research because personnel at smaller institutions may not be familiar with their potential radiation hazards.

Small accelerators have also been applied to problems in atomic physics, astrophysics, archeology, mineralogy, environmental science, nuclear structure, surface physics, solid state physics, radiological

*The term small accelerator was first used to mean Cockcroft-Walton or Van de Graff accelerators with terminal voltage below 500 kV. It now includes linear accelerators and small cyclotrons that accelerate ions up to 50 MeV. The radiological safety aspects of small neutron generators has been discussed by Boggs (Bo 76).

physics and fusion research.

Applications in industry include oil-well logging, ion implantation, trace-element studies in environmental samples, aerosol composition studies and radiation sterilization.

In medicine, small accelerators have been used for radiotherapy, trace-element studies, body-calcium assays, in-vivo neutron activation and radiography.

The widening use of small accelerators has been conveniently documented in the proceedings of a series of conferences held at Oak Ridge National Laboratory and North Texas State University (Du 68, Du 70, Du 74, Du 76).

Table 1.2, taken from NCRP Report 51, summarizes these applications of particle accelerators in the energy range 0.1 MeV to 100 MeV (NCRP 77).

Apart from fundamental research, positive-ion accelerators at energies above 100 MeV have also been widely used in medicine. As early as 1946, Wilson (Wi 46) suggested that the energy-loss mechanisms of protons could be used to provide distributions of absorbed dose in human tissue far superior to those obtained from ^{60}Co photons. Tobias and his colleagues confirmed Wilson's thesis in 1952, using 190-MeV deuterons from the 184-Inch Synchrocyclotron at Berkeley for radiobiological studies (To 56).

Somewhat later, the Berkeley group reported the first therapeutic use of high-energy ion beams in attempts to destroy the endocrine function of the pituitary gland in cancer patients (To 52). Subsequently, protons and other ions have been used for radiotherapy or radiosurgery at many centers around the world, including Uppsala, Harvard, Moscow, Dubna, and Leningrad. Larsson has recently reviewed this work (La 80).

A recent review of the use of particle accelerators to generate protons, ion beams, neutrons or pions for use in therapy and diagnosis may be found in the proceedings of the third course of the International School of Radiation Damage and Protection held at the Ettore Majorana Centre for Scientific Culture (Th 80).

1.5. TYPICAL INSTALLATIONS

Examples of actual positive-ion accelerators used in research or medicine are presented in this section together with a number of general points that should be considered in planning new facilities in research settings such as universities and national laboratories. There is usually a small staff knowledgeable in radiation protection. This staff should be consulted as early as possible in the planning stages. In small institutions, where the management and staff may not be familiar with the detailed requirements for radiation safety, expert advice should be obtained at the architectural planning stage to ensure that adequate provision is made for radiation shielding and other features such as radiation and other safety interlocks and requirements for utilities. Whatever the setting, planning for the radiation safety

programme must consider the physical layout (see Chapter 5).

Radiation shielding is generally of large dimensions at accelerators, which are therefore often constructed at or below ground level to avoid the necessity of constructing massive shield supports. Except where space is at a premium ordinary concrete or earth is usually the cheapest means of providing shielding. Steel or heavy-aggregate concretes are used to minimize shield thickness, but at some cost premium (see Chapter 4).

The external radiation field of positive-ion accelerators is usually dominated by neutrons, with a smaller contribution from photons (see Chapter 2). Shield thicknesses are therefore often determined by neutron dose-equivalent rates. Other important considerations are adequate roof design to reduce neutron skyshine to acceptable levels (Chapter 6) and the design of labyrinths and other penetrations through the shield to minimize radiation streaming (Chapter 4).

The installations described cover the energy span from 20 MeV to 400 GeV and are generally used for fundamental research. Although the accelerators described are diverse, it will subsequently be shown that they exhibit great similarity in radiation protection features.

30-MV Electrostatic Generator-Daresbury Laboratory
[Based on information supplied by R. Ryder]

An excellent review of the first 15 years (1931–1946) of development, which essentially brought the single-stage electrostatic generator to maturity, has been given by Van de Graaff et al. (Va 48). The terminal voltage of such accelerators was limited by a variety of technical reasons to about 10 MV.

Since World War II, technical innovations have made feasible the development and construction of tandem accelerators. In such accelerators a negative heavy ion, for example, is extracted from the ion source and accelerated towards a positive terminal; on the way, it passes through a charge stripper (either a gas or a thin metal foil), becomes a positive ion, and is then repelled towards the negative (ground) terminal. This technique can immediately double the energy of the particles accelerated, and improvements in column design, vacuum and operating technique have made it possible to operate at voltages above 30 MV.

In 1974, the Daresbury Laboratory of the United Kingdom began constructing a tandem Van De Graaff electrostatic accelerator that would operate at 20 MV on the terminal but be capable of development to 30 MV and that could be used as an injector to a heavy-ion synchrotron or superconducting linac. The accelerator produced its first beam in 1982, and since then a wide range of beams have been accelerated including deuterons, tritons and carbon-14. It is capable of accelerating polarised light ions and of producing beams of bunched ions (Vo 78). The accelerator is to be used mainly for two areas of research in nuclear physics: coulomb excitation of heavier nuclei and the study of neutron-deficient nuclei.

Figure 1.5 shows the overall appearance of this facility. The main tower houses the accelerator and is surmounted by the injector room. The smaller tower at the side contains a passenger lift, service hoist,

stairway and utilities. In a cutaway view, Fig. 1.6 clearly shows the ion source and inflector magnet that directs this beam down the accelerating column towards the centre terminal; from the centre terminal, the beam goes down the lower column to an analysing magnet, which selects beams for the experimental areas. Figure 1.7 gives additional details of the column design, and Fig. 1.8 shows a plan of the experimental area.

The pressure vessel enclosing the accelerator is 45 m high and 8.2 m in diameter and has been pressure-tested to 8 atmospheres. The vessel normally operates with an internal filling of sulphur hexafluoride at pressures of up to 8 atmospheres. A considerable R&D programme was devoted to the design of the accelerating column so that it would control and prevent electrostatic breakdown.

Ion pumps maintain the pressure inside the beam tube to a value of 10^{-7} atmospheres, and a cryopump is used in the terminal when a gas stripper is used. In the accelerator, the control system operates at potentials up to 30 MV and is achieved by means of an infrared link modulated at 10 MHz (Vo 78).

Table 1.3 gives expected beam intensities and charge states for various ions and for two terminal voltages at the accelerator.

Isotropic neutron fluence rates at 1 metre from the target of 1.6×10^{6}, 3.1×10^{6} and 4.8×10^{6} n $cm^{-2}/\mu C$ are expected. These will result from 60-MeV protons interacting with optimum targets of aluminum, copper and tantalum. In the forward direction fluence rates at 1 m of 4.3×10^{7}, 3.5×10^{7} and 2.2×10^{7} n $cm^{-2}/\mu C$ will be produced by 60-MeV deuterons incident upon similar targets. The ratio of the forward deuteron yield at angles of 10, 30, 60° and thereafter is 0.50, 0.02 and 0.07 (Ry 82).

Helium and heavier particles produce fewer neutrons. Carbon-13 ions accelerated to 168 MeV produce 6.0×10^{5} n $cm^{-2}/\mu C$ at 1 m when interacting with an optimum tantalum target (Hu 60). For both protons and deuterons the number of neutrons of energy greater than 10 MeV falls considerably at angles greater than 60°, allowing shorter attenuation lengths to be used at large angles (Ry 82).

The tandem Van de Graaff is housed in a tower whose walls are constructed of 1 m of concrete, density 2.3×10^{3} kg m^{-3}, and the experimental areas have concrete side walls and roofs, 1 m thick. The end walls, in the forward direction, are 1.6-m-thick concrete. Since beam losses are generally less than 5% this permits 1-μA beams of 60-MeV protons and deuterons to be utilised. Regions of intense beam loss, e.g., faraday cups, beam stops, aperture defining slits, etc., have been identified and local shielding constructed to reduce radiation to permitted levels (see Fig. 1.8).

During light-ion operation, personnel are excluded from the experimental areas. However, access will be allowed to beam lines using heavy ions, subject to radiation survey.

Triton beams are generated from a Middleton sputter-ion source, which uses approximately 200 Ci of tritium for 500 hours of beam time at 5 μA. Most of the gaseous tritium released is trapped within the first

two turbo-pumps, and only 300 mCi will be passed by the gas restriction and 30 mCi by the inflector magnet (Ry 80). The contaminated ion source, turbo-pumps, and associated beam-line components before the gas restriction are decontaminated in a glove box equipped with facilities for the collection and disposal of cleaning water.

Induced activity at these energies is not a great problem. With short light-ion runs (2 to 5 days) followed by long heavy-ion beams (5 to 16 days) dose rates at 10 cm from faraday cups, etc., of 20 to 100 mrem h^{-1} are experienced. However maximum dose rates at 10 cm from tantalum beam stops of 0.47 and 0.76 gray h^{-1} (47 and 76 rad h^{-1}) are expected immediately after running periods of 30 days with 1-μA beams of 60-MeV protons and deuterons. These will decay to 39 and 66 mGy h^{-1} after 1 day and 12 and 18 mGy h^{-1} after 7 days (Ho 80).

800-MeV Linear Accelerator-The Clinton P. Anderson Meson Physics Facility

[Based on information supplied by T.M. Putnam and A.J. Miller]

Introduction

The Clinton P. Anderson Meson Physics Facility, otherwise known as LAMPF,* is operated by the Los Alamos National Laboratory of the University of California for the U.S. Department of Energy. (Figure 1.9 is an overhead view of the facility). The heart of the installation is a high-intensity linear accelerator (linac) producing proton (H^+) beams of energy 800 MeV at an average current of up to 1 mA, variable energy (300 to 800 MeV) H^- beams at up to 10-μA average current, or variable energy polarized H^- beams up to 10-nA average current. The accelerator is pulsed at a repetition rate of 120 Hz with a duty factor of from 6% to 9%.

Although primarily a tool for atomic, nuclear and elementary particle physics and nuclear chemistry research, LAMPF is used for extensive research in solid-state physics. It also has important applications in medical radioisotope production and materials science.

The LAMPF Facility

LAMPF consists of a three-stage high-intensity proton linear accelerator approximately 800 metres long with research facilities capable of supporting the simultaneous performance of as many as 12 experiments.

The first stage of the accelerator comprises three Cockcroft-Walton-type accelerator systems (injectors) that produce high-intensity H^+ and lower-intensity H^- or polarized H^- beams. Two beams are accelerated on alternate half cycles of the radio-frequency field in the subsequent second and third stages of the accelerator.

The second stage is a drift-tube type linac that accelerates the beams to 100 MeV. This stage is about 62 metres long.

---

*An acronym for Los Alamos Meson Physics Facility.

The third stage is a side-coupled wave-guide-type accelerator. It is about 685 metres long and accelerates the protons to a maximum energy of 800 MeV.

Variable energy is achieved by using only some of the accelerating stages on a given pulse and letting the beam drift through to the end of the accelerator. In this manner energies between 300 MeV and 800 MeV may be obtained.

When the particles leave the accelerator they enter a switchyard, where the two beams are separated and directed by magnets along three beam lines to the various experimental areas shown in Fig. 1.10. The high-intensity H^+ beam passes straight ahead through two production targets in the meson experimental hall, through up to six isotope production targets, and finally, to the main beam stop. H^- or polarized H^- beams are directed to the High Resolution Proton Spectrometer and the research areas in the Nucleon Physics Laboratory. Pulses of H^- beam are also directed to the Proton Storage Ring and/or the Weapons Neutron Research Facility.

General Radiological Safety

Physical Controls. Radiation shielding for the accelerator, beam switchyard, targets, beam stops and experimental caves consists of poured concrete, compacted earth and/or steel and concrete slabs and blocks. The injectors require no shielding, but rope barriers and signs warn personnel of the presence of x-ray fields in front of the H^- injector. The drift-tube linac channel is shielded by concrete walls and a roof varying in thickness from 0.6 metres at the low-energy end to 1.5 metres at the 100-MeV end. The side-coupled wave-guide section and the beam switchyard are in a tunnel about 9 metres underground. Access to the beam channel is controlled by locked and interlocked doors and gates.

The beam line and target cells in the meson experimental hall are shielded by massive stacks (~60,000 tons) of steel slabs and concrete blocks. There are 2.5 metres of magnetite and regular concrete beneath the line to limit ground shine. The experimental caves are shielded by 1-metre-thick concrete blocks 2.5 metres high; there is no roof shielding over the experiments. Both the Nucleon Physics and the High Resolution Proton Spectrometer areas are closed to access when beam is directed to these areas.

Activation of accelerator components from beam spill is controlled by 100 accelerator-protect/beam-spill monitors consisting of small scintillation detectors and fast-shut-down circuitry capable of turning the beam off during a pulse. This system prevents excessive induced activity in accelerator components and minimizes external radiation fields in occupied areas.

Administrative Controls. The control of personnel radiation exposures and the monitoring and control of radioactive materials, including waste disposal and radioactive contamination control, are the two major radiological safety concerns at a high-intensity accelerator. A health physics staff provides 24-hour control and surveillance for all activities in radiation areas that involve radioactive materials. They make

frequent radiation surveys of occupied areas using instruments that allow for the pulsed nature of the proton beam and provide guidance and assistance in the handling and disposal of radioactive materials (see below).

Everyone working in the accelerator buildings and experimental areas is required to wear a TLD personal dosimetry badge. Personnel entering high-radiation areas or working near radioactive components are issued pocket ionization chambers. TLD finger rings are worn for close work on radioactive materials. With these efforts personnel exposures are maintained well below the established legal regulations for radiation workers.

Special Radiological Problems

The intense proton beams at LAMPF have created numerous special problems and magnified many others.

Induced Radioactivity. The intense primary proton beams, secondary pion and neutron beams and scattered particles induce radioactivity in accelerator and target components, shielding and nearby equipment. Surface contamination is not as serious a problem as the induced activity. The major part of the activity is within solid materials, requiring careful surveillance and control during maintenance activities. However, cooling water systems and the air surrounding the targets and beam stops also suffer considerable induced activity. The activity in the cooling water systems is controlled by passing part of the circulating water through deionization columns. This removes most radionuclides except tritium, which can be removed from the system by evaporation techniques. In case of leaks, a drain system has been provided that connects to two 2500-gallon underground storage tanks. The liquid in the tanks is pumped out and disposed of in a manner depending on an analysis of its activity. The activities in the radioactive air consist primarily of ^{11}C, ^{13}N, ^{15}O and a little ^{41}A, all with relatively short half lives. This activity is exhausted to the atmosphere through a ventilation stack. The gaseous and particulate effluents are continuously monitored.

Control of Radioactive Materials. The control of radioactive materials involves experiment safety reviews, health physics surveillance and doorway radiation monitors. To detect the unauthorized movement of such materials from the LAMPF site, a sensitive gateway monitoring system has been developed. This detection system consists of a 12-cm-diameter NaI crystal detector placed beneath the roadway at the exit to the site with sensitive electronics that continuously update the background level. This system provides an alarm if the activity level increases to approximately twice background level. An inductive loop, buried in the road around the detector, provides a coincident signal with the radiation detector, indicating that a vehicle is present when the alarm sounds. The system will alarm if a source of radiation passing through the detector's cone of sensitivity [at speeds of up to 25 km h^{-1} (15 mph) increases the radiation level at the detector to about twice the background, or 400 nGy h^{-1} (0.04 mrad h^{-1}).

The disposal of massive highly radioactive items, such as a steel shielding block from a target cell or beam stop, has proven to be a difficult problem. Rigging such a block, painting it with fast drying paint to prevent the spread of contamination, loading it into a cask for transportation, and ultimately unloading and depositing it in a hole for burial, all involve special equipment and handling techniques to keep the spread of contamination and exposures to personnel within allowable range. At LAMPF, remote handling techniques are used as much as possible.

Remote Maintenance of Target Cells. The intense proton beams create such high levels of radioactivity in the target cells and main beam stop that all maintenance work must be done using remote handling techniques. Two sophisticated remote manipulator systems have been developed for LAMPF using commercial components (see Fig. 1.11).

These systems enable technicians to use wrenches, cut water lines, solder fittings, and connect or disconnect hooks from radio-controlled cranes. The remote handling staff can perform almost any operation that one can do by hand; it just takes 8 to 10 times longer. The manipulator systems are force-reflective so that the operator can 'feel' the amount of pressure he is exerting. Six television cameras are used to give an adequate view of the operation, and a microphone is mounted on the manipulator so that any special noises associated with the work can be heard. Without such a system, repair of water leaks and electrical connections or the replacement of faulty components would be almost impossible.

800-MeV Proton Synchrotron: Spallation Neutron Source at Rutherford Appleton Laboratory

[Based on material supplied by J.T. Hyman and G.B. Stapleton]

Interest in applying pulsed proton accelerators to produce pulsed neutron sources has been growing. Compared with conventional nuclear reactors, such pulsed sources are less expensive and have the technical advantages of a greatly increased effective flux of neutrons within the higher neutron temperature range, with reduced problems of source cooling and radiation damage (Ho 77).

Manning has given a detailed review of the broad scope scientific research that may be undertaken with such facilities in biology, chemistry, engineering and medical physics (Ma 78). Manning also discussed the relative merits of various accelerator systems for neutron production.

The Rutherford Appleton Laboratory has completed the construction of a spallation neutron source (SNS), the main feature of which is a high-intensity 800-MeV rapid-cycling proton synchrotron that will deliver high-energy protons onto a depleted-uranium target. The main parameters of this neutron source are given in Table 1.4 (Bo 85). A description of the accelerator and target station, as finally built, is given in Ref. Bo 85. The most recent status of the project is included in Refs. Gr 85 and Le 85, which describe some of the early commissioning and preliminary results with the first neutron beams.

Figure 1.12 is a general view of the facility, consisting of three accelerators, beam transport systems and a target station. Important parameters for each accelerator are also shown in Table 1.4. Figure 1.13 shows the 665-keV pre-injector.

Several important radiation protection issues are involved with the design and operation of such a powerful neutron source as SNS. These include shielding the accelerator, shielding the target station, personnel protection, radioactivity induced in the accelerator, beam transport components and target and environmental impact. These issues have been discussed in the design report (Pe 77).

Shielding the 800-MeV synchrotron was largely achieved by using an existing building designed to house a 7-GeV weak-focussing proton synchrotron (Nimrod). Additional local shielding was added near beam scrapers, which are regions of controlled localized beam loss.

Shielding the neutron target itself presents a formidable problem. Figure 1.14 shows a schematic view of the target and Fig. 1.15 the proposed shield configuration.

Approximate steel-equivalent shield thicknesses vary from 2.2 m along the 800-MeV proton beam transport line to about 5.5 m in the forward direction. Because space is at a premium, very dense material, such as steel, is preferred for bulk shielding. However, a composite shield must be constructed to remove intermediate-energy neutrons transmitted by iron (see Chapter 4).

Calculations show that dose-equivalent rates due to induced radioactivity of 0.01 to 0.1 Sv h^{-1} (1–10 rem h^{-1}) are to be expected at regions of localized beam loss around the accelerator. Remote handling systems for accelerator maintenance are required at these levels.

After six months irradiation by the 200-μA proton beam the ^{238}U target has a total inventory of activity one day after shutdown of the order of 7×10^{15} Bq (200 kilocuries); at saturation, the targets will contain 1×10^{14} Bq (3 kilocuries) of ^{131}I (At 80). Remote handling equipment will be used to work with irradiated targets, surrounding hardware and shielding.

Approximately 5×10^{9} Bq (0.12 curies) and 7×10^{10} Bq (0.2 curies) of tritium and ^{7}Be will be produced in the target cooling (heavy) water per day (At 81). Calculations show the environmental radiological impact of SNS is negligible (see Chapter 6).

Multi-GeV Heavy-Ion Facility:
The Bevalac of the Lawrence Berkeley Laboratory
[Based on material supplied by R.E. Lemmon (Le 81)]

The Bevalac is an accelerator complex consisting of the SuperHILAC used as an injector to the Bevatron.

The SuperHILAC (Fig. 1.16) is a heavy-ion linear accelerator that can operate in a time-shared mode with a pulse-to-pulse energy variability [in the range from 2.4 MeV/amu to 3.5 MeV/amu]. Ions of all elements up to uranium may be accelerated. Three injectors give the SuperHILAC a unique ability to accelerate multiple high-mass ($A \geq 100$) high-intensity ion beams.

During normal time-shared operation, 32 pulses per second are used by the principal research group, 2 pulses per second (usually of ions of a different species) are used to inject into the Bevatron and 2 pulses per second of either ion species (at a different energy if desired) are used for a secondary experiment at the SuperHILAC II experimental area. Major experimental facilities include an actinide-target bombardment area, a gas-filled magnetic spectrometer, and a new on-line isotope separator with high mass resolution and overall efficiency as high as 20% for nuclides throughout the periodic table.

The research program at the SuperHILAC includes the production of new heavy elements (e.g., ^{102}No and ^{103}Lr), elucidating many of the global features of the fusion, deeply inelastic (damped) and fission reactions that empitomize collective nuclear phenomena. Because of its very-high-charge and -mass beams, the SuperHILAC also plays an essential role in studies of nuclear structure, including such aspects as pairing correlations, nuclear collective structures and the effects of high nuclear temperature. Atomic physics work at the SuperHILAC concentrates on atomic spectroscopy (especially of very-high-charge-state, low-velocity recoil ions) and inner-shell ionization processes during high-Z ion-atom collisions. (Many of these projects are relevant to the study of the interstellar medium, to the design of fusion devices and to the design of an x-ray laser device.) Finally, work in the area of exotic nuclei involves the study of elements near the limits of particle and fission stability, the synthesis of new elements and isotopes, the study of reaction mechanisms for their production and the investigation of their radioactive and chemical properties.

The Bevatron (Fig. 1.17) is a synchrotron that can accelerate heavy ions from either the SuperHILAC (the Bevalac mode) or its local injector to any energy between 50 MeV/amu (where it overlaps with lower energy machines) and 2100 MeV/amu (where it is the only facility in the world with such high-energy heavy ions).

Several large detector facilities are used in the research program at the Bevalac:

- HISS–a very-large-volume heavy-ion superconducting spectrometer with large-area detection systems.
- Plastic Ball and Wall–a multiplicity detector with over 1000 detector elements, jointly funded by the German Federal Republic and the U.S.A.
- TASS–a two-armed magnetic-spectrometer system.
- TOPAZ TPC–a pion detector system jointly funded by Japan and the U.S.A.
- LEBL–a low-energy beam line designed to host a variety of experiments at energies from 50-250 MeV.

The Bevalac has a unique capability to study collisions between nuclei at energies sufficient to convert nuclear matter into hadronic matter in which neutrons and protons, their excited states such as delta resonances and free pions all coexist. It supports programs in peripheral fragmentation reactions, pion production with heavy ions, central

collisions that create nuclear matter complexes under extreme conditions of compression and stress and reactions in which the nucleonic character of nuclei is isolated from effects of coherent nuclear matter. One-third of the Bevalac operating time is used in support of biomedical research, including a trial programme of heavy-ion cancer therapy.

The heavy Charged-Particle Treatment Facility is used to benefit certain cancer patients who have been referred by physicians. The medical staff at LBL reviews each case with the patient's physician to determine whether or not this type of radiotherapy could be of help to the patient. If the treatment seems to be appropriate, the therapy is planned and carried out by the specialized medical staff. Both the 184-Inch Synchrocyclotron and the Bevalac are used in these treatments.

12-GeV Strong-Focussing Proton Synchrotron (KEK)
[Based on material supplied by S. Fukomoto and K. Katoh (Ka 85, Ke 84)]

The National Laboratory for High Energy Physics (Ko-Enerugi-Ken, or KEK) of Japan is situated at Tsukuba some 90 kilometres north of Tokyo.

The first accelerator constructed at the Laboratory was a 12-GeV strong-focussing proton synchrotron, which operated in 1976.* A 2.5-GeV synchrotron radiation facility, photon factory, was completed in 1982. Construction of a 30-GeV electron-positron colliding beam accelerator (TRISTAN) began in 1981. Only the proton synchrotron is described here.

12-GeV Proton Synchrotron

Figure 1.18 schematically shows the four stages of the KEK proton synchrotron:

- 750-kV Cockcroft-Walton pre-injector
- 20-MeV linac
- 500-MeV fast cycling booster
- 12-GeV main synchrotron

The principal parameters of the synchrotron are given in Table 1.5.

Pre-injector. There are two 750-kV Cockcroft-Walton pre-injectors. One had accelerated ion beams of about 600–700 mA and injected 300-mA protons into the linac with a pulse duration of 5 μs since 1974. This has been modified to accelerate H^- ions. The duoplasmatron was replaced by a multicusp H^- ion source, and 20-mA H^- beams are injected into the linac in routine operation. Its pulse duration is adjustable up to 120 μs. The other was constructed in 1982 to accelerate polarised H^- beams. An optically pumped polarised ion source is installed in its high-voltage terminal.

Linac. The linac was designed to provide a 100-mA proton beam at an

*A 2.5-GeV synchrotron radiation facility (photon factory) was completed in 1982.

energy of 20 MeV. It is an Alvarez-type linac with a single tank 15.5 m in length, operated at a frequency of 201.06 MHz with a peak power of 3 MW. The maximum capture efficiency is 55% with a prebuncher. For protons, the typical linac beam was 140 mA, but a maximum current of 200 mA was achieved. For H^- ions, however, the beam intensity is 10 mA, so that no extensive beam-loading compensation is needed. Another Alvarez linac 13 m long will be made to upgrade the beam energy from 20 MeV to 40 MeV in the fall of 1985. It is not only effective for increasing the booster beam but also favorable for improving injection efficiency.

Booster Synchrotron. The booster synchrotron is a 500-MeV alternating gradient synchrotron that operates at a repetition rate of 20 Hz. Its entire magnet is constructed of eight combined-function submagnets. The mean orbit radius is 6 m (one ninth of the main-ring radius). In one cycle, nine pulses from the booster synchrotron are injected into the main ring.

The 3×10^{12} protons (100 mA, pulse duration 5 μs) were injected into the booster by multiturn injection. During the injection, about half of the injected protons was lost. Immediately after injection, 1.2×10^{12} circulating protons were observed. Due to the beam loss during acceleration, the maximum intensity achieved at 500 MeV was 6.6×10^{11} protons/pulse. The booster started with an RF accelerating cavity, and an additional one was installed in 1977 to improve the stability and efficiency of operation. The extraction of the beam from the booster is performed by four fast-kicker magnets and one septum magnet.

H^- charge-exchange injection increased the maximum booster beam to 9.1×10^{11} protons/pulse. During typical operation more than 85% of the injected protons are accumulated in the booster.

Pulses from the booster synchrotron not needed for injection into the main ring are switched to a beam line that directs them to a separate booster synchrotron utilization facility.

Main Ring. The magnet configuration of the main ring is a separated-function-type magnet with a FODO structure. The number of superperiods is four, each period consisting of five normal cells and two cells from which one of the two bending magnets is omitted; one normal cell involves two bending magnets and two quadrupole magnets. Four straight sections are provided for beam injection, fast extraction to the bubble chamber, slow extraction to the counter experimental hall and the RF accelerating station. Nine pulses from the booster are injected into the main ring during the injection period of 0.7 s. The acceleration is performed for the following 0.5–0.8 s depending on the maximum energy and a 0.5-s flat top is used for high-energy physics experiments. The magnetic field is 0.15 T at the injection energy and 1.75 T at 12 GeV. The high magnetic field with good characteristics was achieved, even in this C-type magnet, by virtue of the oriented low-carbon steel.

The designed frequency of betatron oscillations was $\nu_H = \nu_V = 7.25$. But in practice, it was determined after an extensive survey on tune diagram that the best operating point is $\nu_H = 7.12$ and $\nu_V = 6.28$ with correction of the octupole magnets. The maximum beam intensity achieved

is 4.5×10^{12} protons per pulse, and in recent runs the average beam intensity is 4.2×10^{12}.

Operation. Figure 1.22 summarizes the growth of beam intensity achieved since operation of the various component accelerators of the KEK PS.

The entire accelerator has worked with great reliability (less than 5% breakdown time) and has exceeded its design specification for intensity by more than a factor of 2.

Table 1.6 summarizes design parameters and performance achieved as of July 1985 (Ka 85).

The CERN Super Proton Synchrotron (SPS)

Only three proton synchrotrons in the world operate above 50 GeV: a 70-GeV synchrotron first operated in 1967 at the Institute of High Energy Physics in Serpukhov, USSR; the 500-GeV synchrotron at the Fermi National Accelerator Laboratory in the United States (first operated at 200-GeV in March 1972); and, most recently, the synchrotron of the European Organization for Nuclear Research (CERN), which began operating in Geneva at 400-GeV in June 1976.

These proton synchrotrons are in fact complexes of accelerators. The Geneva synchrotron uses four distinct accelerators: a 50-MeV linear accelerator; an 800-MeV booster proton synchrotron; and finally a 28-GeV proton synchrotron (PS) that injects particles into the main ring for acceleration to 450-GeV.

Such large accelerators are major feats of civil, electrical and mechanical engineering. Some idea of the scale of the undertaking may be seen from Fig. 1.23, which is an aerial view of the site. The diameter of the main ring is 2.2 km and crosses the Franco-Swiss frontier. A schematic drawing (Fig. 1.24) shows the arrangement of the component accelerators.

To provide adequate structural stability, the main ring was built 18 to 64 m below ground. This incidentally provided enough shielding by the surrounding rock against ring-produced radiation to allow public access to the outer shield surface. Fig. 1.25 shows the synchrotron in its underground tunnel.

The SPS is currently operated in two distinct modes, first as a standard proton accelerator in which the beam is accelerated up to 400–450 GeV, extracted from the machine and directed toward production targets to provide secondary beams for the experimental program (fixed target mode) and in a second mode in which separate beams of protons and antiprotons are injected in opposite directions into the ring structure, accelerated to 270 GeV, and held stable at this energy for as long as possible, usually up to 24 hours at a time, before instabilities render the beam useless for observing the proton-antiproton collisions. This mode of operation is termed the collider mode. The main parameters of the SPS are given in Table 1.7.

The beam intensities of these two modes are very different. In the fixed-target mode, two or three pulses each of about 1.5×10^{13} protons are extracted from the PS at an energy of 10 GeV to provide SPS pulses, accelerated to energy 400 or 450 GeV depending on requirements and

extracted towards the three major target areas, one serving the west experimental area, another the north experimental areas and a third the neutrino beam lines. On its way towards the north areas the beam is split into three parts, each serving a separate target. One of these is usually very thin, and the protons that do not interact in it may be recovered for use in a further target station (the NAHIF area). Table 1.8 gives a summary of the principal beam lines of the SPS as of Summer 1983. Some 10–15 experiments may be taking beam simultaneously.

In the collider mode, the accelerator contains 2×10^{11} protons and the same number of antiprotons. The only exception to this is during accelerator tests, when as many as 2×10^{12} protons per pulse may be accelerated. These particles are accelerated once per day instead of having a pulse repetition rate of one every 10 seconds in the fixed-target mode. Thus the radiation protection problems of the SPS are limited mainly to those from the fixed-target mode. Even the shielding between the collider experimental areas (ECX) and their associated assembly areas (ECA) is designed for continuous occupation of the ECA areas during fixed-target operation, rather than for collider considerations. Thus the radiological problems of collider mode operation are minimal and will not be discussed further except to mention that periods of collider operation provide a valuable cooling-down time to allow dose rates in the highly radioactive target stations to decay before maintenance and replacement operations.

The main problems of radiation protection at the SPS are in fact maintenance operations in areas where the beam is lost, either intentionally at the internal or external dumps and target stations or accidentally during extraction at the electrostatic and magnetic septa or at regular points around the ring. It is interesting to note the correspondence between the measurements of dose rate from induced activity around the ring with the variation of the momentum compaction function, see Fig. 1.26. Wherever this function is large, the protons are preferentially lost. Dose rates from remanant activity near the extraction systems reach several hundreds of mrem/h and near the dumps and target stations several rem/h. However there are remarkably few points other than the dump or extraction regions where the dose rate exceeds 10 mrem/h, and if a person were to travel at a uniform speed around the SPS ring during a typical shut-down, the average dose rate would only be 1 to 2 mrem/h.

In the occupied experimental areas the dose rates during operation are generally very low (0.1–1 mrem/h), and a monitor/alarm system allows any beam mis-steering to be quickly identified and corrected. However, the problem of muons downstream of the dumps of the secondary beam lines is a particular problem of high-energy accelerators, and special precautions must be taken. This will be discussed in a later chapter. Problems arising from radioactive air and water are dealt with by the provision of closed circuits wherever this is necessary, for example in the target stations.

REFERENCES FOR CHAPTER 1

Ad 53 Adams, J.B., Hine, M.G.N. and Lawson, J.D., Nature 171, 926 (1953).

Al 46 Alvarez, L.W., 'The Design of a Proton Linear Accelerator', Phys. Rev. 70, 799 (1946)

At 80 Atchinson, F. Rutherford Appleton Laboratory Internal Note SNS/TCAM/P5/80, unpublished (1980).

At 81 Atchinson, F. 'A Theoretical Study of a Target Reflector and Moderator Assembly for SNS'. Rutherford Appleton Laboratory Internal Report RL-81-006 (April 1981).

Av 73 Avery, R.T. and Keefe, D., 'Shattering Rock with Intense Bursts of Energetic Electrons', IEEE Trans. Nucl. Sci. NS-20, 3, 1010 (1973).

Ba 32 Barton, H.A., Mueller, D.W. and Van Atta, L.C. 'A Compact High Potential Electrostatic Generator', Phys. Rev. 42, 901 (1932).

Bl 56 Blewett, J.P., 'The Proton Synchrotron', Rep. Prog. Physics 19, 37 (1956).

Bo 47 Bohm, D. and Foldy, L., 'The Theory of the Synchro-Cyclotron', Phys. Rev. 72, 649 (1947).

Bo 76 Boggs, R.F., 'Radiological Safety Aspects of the Operation of Neutron Generators', Safety Series Report No. 42, IAEA, Vienna (1976).

Bo 71 Boone, M.L. and Wiley, A.L., 'Fast Neutrons and π^- Mesons in Cancer Therapy', IEEE Trans. Nucl. Sci. NS-18, 3, 36 (1971).

Bo 85 Boardman, B. (Ed.), Rutherford Appleton Laboratory, Chilton, Didcot, Oxon OX110QX, U.K., Report RL-82-006 (1985).

Br 47 Brobeck, W.M., Lawrence, E.O., MacKenzie, K.R., McMillan, E.M., Serber, R., Sewell, D.C., Simpson, K.M. and Thornton, R.L., 'Initial Performance of the 184-Inch Cyclotron of the University of California', Phys. Rev. 71, 449 (1947).

Br 48 Brobeck, W.M., 'Design Study for a Ten-BeV Magnetic Accelerator', Rev. Sci. Instr. 19, 545 (1948).

Br 84 Brianti, G., and Hübner, K., 'Large Hadron Collider in the LEP Tunnel— A Feasibility Study of Possible Options', CERN Report DIR-TECH/84-01 (1984).

Bu 68 Burrill, E.A., 'Van de Graaff Accelerators for Radiation Research and Applications' in Radiation Sources, (Ed. A. Charlesby), Pergamon Press, London, (1968).

Bu 69a Busick, D. et al., 'Beam Safety Considerations of the Stanford Linear Accelerator', Proc. Second Int. Conf. on Accelerator Dosimetry, Stanford, CA, November 5-7, 1969, USAEC Report CONF-691101, p. 782 (1969).

Bu 69b Burrill, E.A., 'The Expanding Use of Particle Accelerators in Research Medicine and Industry: A Statistical Review', in Proc. Second Int. Conf. on Accelerator Dosimetry, Stanford, CA, November 5-7, 1969, USAEC Report CONF-6911101, p. 9 (1969).

Ca 77 Castro, J.R., Quivey, J.M., Lyman, J.T., Chen. G.T.Y., Tobias, C.A., Kanstein, L.L. and Walton, R.E., 'Heavy-Ion Therapy in Biological and Medical Research with Accelerated Heavy Ions at the Bevalac', Lawrence Berkeley Laboratory Report LBL-5610 (1977).

Ch 32 Chadwick, J., 'Possible Existence of a Neutron', Nature 129, 312 (1932). See also 'Tne Existance of of a Neutron', Proc. Roy. Soc. A 36, 692 (1932).

Ch 56 Christofilos, H., 'Focussing System for Ions and Electrons', U.S. Patent 2736799 issued 28 February 1956.

Cl 65 Cleland, M., 'Dynamitrons of the Future', IEEE Trans. Nucl. Sci. 12(3), 227 (June 1965).

Co 30 Cockcroft, J.D. and Walton E.T.S., 'Experiments with High-Velocity Positive Ions', Proc. Roy. Soc. A129, 477 (1930).

Co 32a Cockcroft, J.D. and Walton E.T.S., 'Experiments with High Velocity Positive Ions. I. Further Developments in the Method of Obtaining High Velocity Positive Ions', Proc. Roy. Soc. A136, 619 (1932).

Co 32b Cockcroft, J.D. and Walton, E.T.S., 'Experiments with High-Velocity Positive Ions: II. The Disintegration of Elements by High-Velocity Protons', Proc. Roy. Soc. A137, 229 (1932).

Co 34 Cockcroft, J.D. and Walton, E.T.S., 'Experiments with High-Velocity Ions: III. The Disintegration of Lithium, Boron and Carbon by Heavy Hydrogen Ions', Proc. Roy. Soc. A144, 706 (1934).

Co 52 Courant, E.D., Livingston, M.S. and Snyder, H.S., 'The Strong-Focusing Synchrotron. A New High Energy Accelerator', Phys. Rev. 88, 1190 (1952).

Co 53 Cosmotron Staff, 'The Cosmotron', Rev. Sci. Instr. 24, 723 (1953).

Co 81 Cockburn, S. and Ellyard, D., 'Oliphant', Axiom Books, Adelaide (1981).

DOE 84 U.S. Dept. of Energy, 'Superconducting Super Collider: Reference Design Study for the U.S. Dept. of Energy, 8 May 1984', (1984).

Du 68 Duggan, J.L. (Ed)., Proc. Conf. on the Use of Small Accelerators for Teaching and Research, Oak Ridge National Laboratory, USAEC Rep. CONF-688411 (1968).

Du 70 Duggan, J.L. (Ed.), Proc. Second Oak Ridge Conf. on the Use of Small Accelerators for Teaching and Research, Oak Ridge National Laboratory, USAEC Rep. CONF-700322 (1970).

Du 74 Duggan, J.L., and Morgan, I.L. (Eds.), Proc. Third Conf. on Application of Small Accelerators, North Texas State University, Denton, Texas. LU-1970 (2 vols.) USERDA CONF-741040 (1974).

Du 76 Duggan, J.L. and Morgan, I.L., (Eds.), Proc. Fourth Conf. on the Scientific and Industrial Applications of Small Accelerators, North Texas State University, IEEE Publication 76CH 1175-9 NPS (1976).

Ev 73 Evans, A.E., 'The Expanding Role of the Small Van de Graaff in Nuclear Nondestructive Analysis', IEEE Trans. Nucl. Sci. NS-20, 3, 989 (1973).

Fa 84a Fasso, A., Goebel, K., Hoefert, M., Rau, G., Schoenbacher, H., Stevenson, G.R., Sullivan, A.H., Swanson, W.P. and Tuyn, J.W.N., 'Radiation Problems in the Design of the Large Electron-Positron Collider (LEP)', European Organization for Nuclear Research (CERN), CERN 84-02 (March 1984).

Fa 84b Fasso, A., Goebel, K., Hoefert, M., Shoenbacher, H. and Stevenson, G.R., 'Environmental Considerations for a Large Hadron Collider', CERN Technical Memorandum TIS-RP/TM/84-16, 9 March 1984.

Fa 84c Fasso, A., Goebel, K., Hoefert, M., Schoenbacher, H. and Stevenson, G.R., 'Radiation Protection for a Large Hadron Collider', CERN Internal Report TIS-RP/IR/84-20 (March 1984).

Fo 61 Fowler, P.H. and Perkins, D.H., 'The Possibility of Therapeutic Applications of Beams of Negative Mesons', Nature 189, 524 (1961).

Go 46 Goward, F.K., and Barnes D.E., 'Experimental 8 MeV Synchrotron for Electron Acceleration', Nature 158, 413 (1946).

Go 47 Gooden, J.S., Jensen, H.H. and Symonds, J.L., Proc. Phys. Soc. (London) 59, 677 (1947).

Gr 85 Gray, D.A., 'The Spallation Neutron Source at the Rutherford Appleton Laboratory', Proceedings of a Conference on Neutron Scattering in the 'Ninties, Jülich, 14-18 January 1985 IAEA, Vienna (1985).

Ha 53 Ham, W.T., 'Radiation Cataract', Arch. Ophthal. 50, 618 (1953).

Ha 84 Hartcup, G. and Allibone, T.E., 'Crockcroft and the Atom'. Adam Hilger (Bristol) (1984).

He 35 Herb, R.G., Parkinson, D.B. and Kerst D.W., 'A Van de Graaff Electrostatic Generator Operating Under High Pressure', Rev. Sci. Inst. 6, 261 (1935).

Ho 77 Hobbis, L.C.W., Rees, G.H. and Stirling, G.C. (Eds.), 'A Pulsed Neutron Facility for Condensed Matter Research', Rutherford Appleton Laboratory Internal Report RL-77-064/C, unpublished (June 1977).

Ho 80 Holbourn, M.P., 'An Assessment of the Induced Activity within the NSF', Daresbury Laboratory, Daresbury Laboratory Report HP

80/135, (1980).

Hu 60 Hubbard, E.L., et al., 'Neutron Production by Heavy Ion Bombardment', Phys. Rev. 118, 507 (1960).

Is 24 Ising, G., 'Prinzip einer Methode zur Herstellung von Kanalstrahlen hoher Voltzahl', Arkiv. för Matematik, Astronomi och Fysik 18, 1 (1924) (Translated by F.W. Brasse as: The Principle of a Method for the Production of Canal Rays of High Voltage' in (Li 66), p. 88).

Je 08 Jeans, J.H., 'The Mathematical Theory of Electricity and Magnetism', Cambridge University Press (1908).

Ka 85 Katoh, K, National Laboratory for High-Energy Physics, Tsukuba, Japan. Private communication (April 1985).

Ke 84 Ko-Enerugi-Ken (National Laboratory for High Energy Physics), Tsukuba, Japan, Outline of KEK (May 1984).

La 30 Lawrence, E.O. and Edlefsen, N.E., 'On the Production of High Speed Protons', Science 72, 376 (1930).

La 32a Lawrence, E.O. and Livingston, M.S., 'The Production of High Speed Light Ions Without the Use of High Voltages', Phys. Rev. 40, 19 (1932).

La 32b Lawrence, E.O., Livingston, M.S. and White, M.G., 'Disintegration of Lithuim by Swiftly Moving Protons', Phys. Rev. 42 150 (1932).

La 34 Lawrence, E.O. and Livingston, M.S, 'The Multiple Acceleration of Ions to Very High Speeds', Phys. Rev. 45, 608 (1934).

La 36 Lawrence, E.O. and Cooksey, D., 'On the Apparatus for the Multiple Acceleration of Light Ions to High Speeds', Phys. Rev. 50, 1131 (1936).

La 39 Lawrence, E.O. Alvarez, L.W., Brobeck, W.M., Cooksey, D., Corson, D.R., McMillan, E.M., Salisbury, W.W. and Thornton, R.L., 'Initial Performance of the 60-Inch Cyclotron of the William W. Crocker Radiation Laboratory, University of California', Phys. Rev. 56, 124 (1939).

La 51 Lawrence, E.O., 'Nobel Lecture: The Evolution of the Cyclotron', from Les Prix Nobel en 1951, Imprimerie Royale, P.A. Norstedt and Söner, Stockholm (1952) p. 127.

La 80 Larsson, B., 'Dosimetry and Radiobiology of Protons as Applied to Cancer Therapy and Neurosurgery', Advances in Radiation Protection and Dosimetry in Medicine, (Thomas, R.H. and Perez-Mendez, V., Eds.) Plenum Press, New York, p. 367 (1980).

Le 81 Lemmon, R.M. (Ed.), 'User Facilities at the Lawrence Berkeley Laboratory', Pub-426, November 1981 (Rev. July 1982).

Le 85 Leadbetter, A.J. et al., 'First Neutron Results from SNS', Rutherford Appleton Laboratory, Chilton, Didcot, Oxon OX110QX, U.K., Report RAL-85-030 (1985).

Li 31 Livingston, M.S., The Production of High Velocity Hydrogen Ions Without the Use of High Voltages', Ph.D. Thesis. Dept. of Physics, University of California at Berkeley, April 16, 1931.

Li 50 Livingston, M.S., Blewett, J.P., Green, G.K. and Haworth, L.J., 'Design Study for a Three-Bev Proton Accelerator', Rev. Sci. Inst. 21, 7 (1950).

Li 57 Lindenbaum, S.J., 'The Brookhaven National Laboratory Proton Synchrotron' in (So 57), p. 28 (1957).

Li 61a Lindenbaum, S.J., 'Shielding of High-Energy Accelerators', Ann. Rev. Nucl. Sci. 11, 213 (1961).

Li 61b Livingood, J.J., 'Principles of Cyclic Particle Accelerators', de Van Nostrand (1961).

Li 62 Livingston, M.S. and Blewett, J.P., 'Particle Accelerators', McGraw Hill, New York, (1962).

Li 66 Livingston, M.S., 'The Development of High-Energy Accelerators', Dover Publications, New York (1966).

Ma 78 Manning, G., 'Spallation Neutron Sources for Neutron Beam Research', Contemp. Phys. 19, No. 6, 505-529 (1978).

Ma 79 Mason, J.F., 'Particle-Beam Weapons: A Controversy', IEEE Spectrum 16 (6), 30 (1979).

McC 81 McCaslin, J.B. and Thomas, R.H., 'Practical Neutron Dosimetry at High Energies', Proceedings of the European Seminar on Radiation Protection Quantities for External Exposure, Braunschweig, Fed. Rep. of Germany, 13-15 October 1980, Edited by G. Burger, H.G. Ebert, D. Harder, R. Kramer and S. Wagner, Harwood Academic Publishers for CEC, London, EUR-7101 EN, p. 137 (1981).

McC 83. McCasin, J.B. and Thomas, R.H., 'General Shielding for the 20 TeV Hadron Collider Facility: Hadron Considerations', in Report of the 20 TeV Hadron Collider Technical Workshop, Cornell University, April 1983.

McM 45 McMillan, E.M., 'The Synchrotron—A Proposed High Energy Particle Accelerator', Phys. Rev. 68, 143 (1945).

McM 59 McMillan, E.M., 'Particle Accelerators', Part XII in Experimental Nuclear Physics Vol. III (Ed. E. Segrè), John Wiley and Sons Inc., New York (1959).

Mo 57 Moyer, B.J., 'Buildup Factors', in (So 57), p. 26 (1957).

Mo 58 Moyer, B.J., 'Practical Control of Radiation Hazards in Physics Research', Ann. Rev. Nucl. Sci. 8, 327 (1958).

Mo 73 Morgan, I.L., 'Impact of Accelerators on Technology', IEEE Trans. Nucl. Sci. NS-20, 3, (1973).

NCRP 77 National Council on Radiation Protection and Measurements, 'Radiation Protection Design Guidelines for 0.1-100 MeV Particle Accelerator Facilities', NCRP Report 51, Washington D.C. (1977).

Ol 47 Oliphant, M.E., Gooden, J.S. and Hyde, G.S., Proc. Phys. Soc. (London) 59, 666 (1947).

Pa 57 Patterson, H.W., 'The University of California Synchrocyclotron', in (So 57), p. 99 (1957).

Pa 73 Patterson, H.W. and Thomas, R.H., 'Accelerator Health Physics', Academic Press, New York (1973).

Pa 79 Parmentola, J. and Tsipsis, K., 'Particle-Beam Weapons'. Scientific American 240 (4), 54 (1979)

Pa 80 Panofsky, W.K.H., 'Needs versus Means in High-Energy Physics', Physics Today 33(6), 24 (1980).

Pa 81 Panofsky, W.K.H., 'The State of SLAC. SLAC Beam Line Nos. 1, 2 and 3', SLAC, Stanford, CA (1981).

Pe 77 Perry, D. and Stapleton, G., Chapter 3, 'Shielding, Radioactivity and Radiation Damage', in Appendix II, Project Description: 'A Pulsed Neutron Facility for Condensed Matter Research', Rutherford Appleton Laboratory Report RL-77-064/C, (Eds.) L.C.W. Hobbs, G.H. Rees, and G.C. Stirling (June 1977).

Qu 85 Quigg, C., 'Elementary Particles and Forces', Scientific American 252, 4 (1985), p. 84.

Re 59 Regenstreif, E., 'The CERN Proton Synchrotron', Excerpts from the CERN Proton Synchrotron Part I, CERN Internal Report, August 21, 1959. Translated by P.C.P. Mollet [from Li 66] (1969).

Ri 46 Richardson, J.R., MacKenzie, K.R., Lofgren, E.J. and Wright, B.T., 'Frequency Modulated Cyclotron', Phys. Rev. 69, 669 (1946).

Ri 73 Rindi, A. and Thomas, R.H., 'The Radiation Environment of High-Energy Accelerators', Ann. Rev. Nucl. Sci. 23, 315 (1973).

Ri 84 Richter, B. 'An Informal History of SLAC - Part III: Collider Beams at Stanford', SLAC Beam Line, Special Issue No. 7, Nov. 1984.

Ri 85 Richter, B. 'Future Needs of High-Energy Physics. Remarks to Energy Research Advisory Board', U.S. Department of Energy, February 1985.

Ro 71 Rosen, L., 'Relevance of Particle Accelerators to National Goals', IEEE Trans. Nucl. Sci. NS-18 3, 29 (1971).

Ry 80 R. Ryder, 'Use of a Tritium Source in the NSF', Daresbury Laboratory. Daresbury Laboratory Internal Report HP 80/131 (1980).

Ry 82 R. Ryder, 'Neutron Production from Protons and Deuterons', Daresbury Laboratory Internal Report DL/NUC/TM 60A (1982).

Se 50 Sewell, D.C., Brobeck, W.M. and Lawrence, E.O., 'Design of the Bevatron Quarter Scale Operating Model', Phys. Rev. 78, 85 (1950).

Se 75 Servian, J.G., 'Production of Radionuclides and Labelled Compounds from Accelerators', Int. J. Applied Radiation and Isotopes 26, 763 (1975).

Sl 31 Sloan, D.H. and Lawrence, E.O., 'The Production of Heavy High Speed Ions Without the Use of High Voltage', Phys. Rev. 38, 2021 (1931).

So 57 Solon, L.E., Ed., Proceedings of the Conference on Shielding High-Energy Accelerators, New York April 11-13, 1937. USAEC Report TID-7545 (1957).

Th 80 Thomas, R.H. and Perez-Mendez, V., Eds., 'Advances in Radiation Protection and Dosimetry in Medicine', Proc. Third Symp. International School of Radiation Damage and Protection, Ettore Majorana Centre for Scientific Culture, Erice, Italy, Sept. 1979, Plenum Press, New York (1980).

To 52 Tobias, C.A., Anger, H.O. and Lawrence, J.H., 'Radiological Use of High Energy Deuterons and Alpha Particles', Am. J. Roentgenol. 67, 1 (1952).

To 56 Tobias, C.A., Roberts, J.C., Lawrence, J.H., Low-Beer, B.V.A., Anger, H.O., Born, J.L., McCombs, R. and Huggins, C. Irradiation Hypophysectomy and Related Studies Using 340-MeV Protons and 190-MeV Deuterons', Proc. Int. Conf. on Peaceful Uses of Atomic Energy, Geneva, Vol. 10, United Nations (1956).

To 71 Tobias, C.A., Lyman, J.T. and Lawrence, J.H., 'Some Considerations of Physical and Biological Factors in Radiotherapy with High-LET Radiations Including Heavy Particles, pi-Mesons and Fast Neutrons', Chapt. 6 in Progress in Atomic Medicine, 3, 167 (1971), Grune and Stratton, Inc.

Tu 35 Tuve, M.A., Hafstad, L.R. and Dahl, O., 'High Voltage Technique for Nuclear Physics', Phys. Rev. 48, 315 (1935).

Up 68 Upton, A.C., 'Effects of Radiation on Man', Ann. Rev. Nucl. Sci. 18, 495 (1968).

Va 31 Van de Graaff, R.J., 'A 1,500,000 Volt Electrostatic Generator', Phys. Rev. 38, 1919 (1931).

Va 33 Van de Graaff R.J., Compton, K.T. and Van Atta, L.C., 'The Electrostatic Production of High Voltage for Nuclear Investigations', Phys. Rev. 43, 149 (1933).

Va 36 Van Atta, L.C. Northrup, D.L., Van Atta, C.M. and Van de Graaff, R.J., 'The Design, Operations and Performance of the Round Hill Electrostatic Generator', Phys. Rev. 49, 761 (1936).

Va 48 Van de Graaff, R.J., Trump, J.G. and Buechner, W.W., 'Electrostatic Generators for the Acceleration of Charged Particles', Rep. Prog. Phys. 11, 1 (1948).

Va 75 Vale, J., Lawrence Berkeley Laboratory, private communication (1975).

Ve 45 Veksler, V., 'A New Method of Acceleration of Relativistic Particles', J. Phys. USSR 9 153 (1945), Translated by L. Bell in

(Li 66), p. 202.

Vo 78 Voss, R.G.P., 'The Nuclear Structure Facility at Daresbury Laboratory', in Proc. Int. Conf. Nuclear Structure, Tokyo, 1977. J. Phys. Soc. Japan 44, Suppl. p. 577-588, T. Murumori, Ed. (1978).

Wi 28 Wideröe, R., 'Über ein neues Prinzip zur Herstellung hoher Spannungen'. Archiv für Electrotechnick 21, 387 (1928). Translated by G.E. Fischer, F.W. Brasse, H. Kumpfert and H. Hartmann as 'A New Principle for the Generation of High Voltages', in (Li 66), p. 92.

Wi 46 Wilson, R.R., 'Radiological Use of Fast Protons', Radiology 47, 487 (1946).

Wi 68a Wideröe, R., 'Betatrons and Synchrotrons', Sect. 2.2.1.3. in Engineering Compendium on Radiation Shielding Vol. 1, Springer Verlag, Berlin (1968).

Wi 68b Wideröe, R., 'Linear Electron Accelerators', Sect. 2.2.1.4. in Engineering Compendium on Radiation Shielding Vol. 1, Springer Verlag, Berlin (1968).

Table 1.1
Types of particle accelerators.

Direct (Potential-Drop)
(Single-stage for acceleration of either ions or electrons;
Two-stage [tandem] for acceleration of ions)

1. Electrostatic high-voltage generators:
   a. belt-charging system (e.g., Van de Graaff, Pelletron)
   b. rotating-cylinder charging system
2. High-voltage transformers:
   a. transformer-rectifier set
   b. voltage-multiplying system (e.g., Cockcroft-Walton, Dynamitron)
   c. cascaded-transformer system (e.g., Insulating-Core Transformer)

Indirect (Cyclic)

1. Linear Beam Trajectory:
   a. ion linear accelerator
   b. electron linear accelerator
2. Circular or Spiral Beam Trajectory:
   a. cyclotron (ions only)
   b. synchrotron (ions or electrons)
   c. betatron (electrons only)
   d. microtron (electrons only)

Source: NCRP Report 51. (NCRP 77)

Table 1.2
Applications of particle accelerators.

	Electron	X-Ray	Ion	Neutron
Diagnostic radiology		*		
Radiotherapy	*	*	*	*
Industrial radiography		*		
Analysis of materials, e.g.,				
activation analysis,			*	*
microscopy, electron or ion	*		*	
X-ray fluorescence analysis	*	*	*	
Ion implantation, polishing			*	*
Radioisotope production			*	
Research and training, e.g., nuclear-structure physics neutron physics atomic and solid-state physics biology, chemistry radiation effects on materials	*	*	*	*

Source: NCRP Report 51.

Table 1.3
Expected beam intensities, transmission efficiencies and charged states of ions at the Daresbury 30 MV accelerator.[a]

		20 MV						30 MV					
		1st Stripper	2nd Stripper		Final			1st Stripper	2nd Stripper		Final		
Ion type	Initial beam (μA-ev)	% Trans.	Charge state	%	Charge state	%	Final energy (MeV)	beam (pnA)	% Trans.	Charge state	%	Charge state	%	Final energy (MeV)	beam (pnA)
Cl	10	14	8	35	13	39	246	1400	15	9	35	14	44	400	1500
Fe	0.5	8	8	29	17	27	300	40	8	9	29	19	29	500	40
Br	10	6	8	25	20	23	340	600	6	9	25	23	23	580	600
I	10	4	7	20	21	20	346	400	5.6	9	20	27	28	660	560
Ta	1.3	3.1	7	17	23	18	373	40	3.9	9	17	29	23	700	50
Au	10	3.1	7	17	23	18	373	300	3.7	9	17	30	22	720	360
Pb	0.5	3.1	7	17	23	18	373	15	3.6	9	17	30	21	720	18
Bi	0.3	3.1	7	17	23	18	373	9	3.6	9	17	30	21	720	10
U	2	2.9	7	16	23	18	373	58	3.2	9	16	30	20	720	64

[a]The percentage transmissions quoted are in terms of the number of particles in the incident negative ion beam. The charge states quoted for each stripper are the most probable states and the percentages quoted at each stripper are for the number of particles transmitted for further acceleration, taking into account the fraction in the charge state, the initial emittance of the incident particle beam and the multiple scattering introduced by the stripper. The estimated final beams are, as is usual, quoted in particle nanoamps. The maximum input beam has been limited to 10 μA for convenience.

Table 1.4.
Main design parameters of SNS.

Final Proton Energy	800 MeV
Proton Pulse Repetition Rate	50 Hz
Injection Energy	70.44 MeV (H^- ions)
Proton Intensity per Pulse	2.3×10^{13}
Extracted Proton Pulse Duration	0.4 μs
Average Neutron Production Rate	3×10^{16} s^{-1}

Table 1.5
Parameters of KEK 12-GeV Proton Synchrotron.

Main Ring:	
Construction started	April 1971
First beam obtained	March 1976 (8 GeV) December 1976 (12 GeV)
Maximum energy	12 GeV
Injection Energy	500 MeV
Maximum beam intensity	4.5×10^{12} protons/pulse
Repetition rate	0.4 Hz
Ring diameter	108 m
Injector	20-MeV linac + 500-MeV booster
Focussing type	AG, separated function
Focussing order	FODO
Betatron frequency	$\nu_H = 7.1$, $\nu_V = 6.2$
Bending field	0.15 T (injection), 1.75 T (extraction)
Number of RF cavities	4
Harmonic number	9
RF range	6.02-7.96 MHz
Booster (also used for Booster Synchrotron Utilisation Facility):	
Construction started	April 1971
First beam obtained	December 1974
Maximum energy	500 MeV
Maximum beam intensity	6.6×10^{11} protons/pulse[a] 9.1×10^{11} protons/pulse[b]
Repetition rate	20 Hz
Ring diameter	12 m
Focussing type	AG, combined
Focussing order	FDFO
Betatron frequency	$\nu_H = 2.2$, $\nu_V = 2.3$
Bending field	0.197 T (injection), 1.1 T (extraction)
Linac:	
Construction started	April 1971
First beam obtained	August 1974
Maximum energy	20 MeV[c]
Injection energy	750 keV
Maximum beam current	200 mA[a] 12 mA[b]
Ion source	Duoplasmatron[a] Multicusp[b] Optically pumped polarised H source
Injector	Open-type Cockcroft-Walton
Total length	15.5 m
Number of tanks	1
Repetition rate	20 Hz
RF frequency	201 MHz

[a] Proton, multiturn injection.

[b] H^- ion, charge-exchange injection.

[c] The linac will be upgraded to 40 MeV in the fall of 1985.

Table 1.6

	Design (shielding)	Approval	Present	Expected (1985)
Proton Linac:				
Energy (MeV)	20	21	20	40
Intensity (μA)	30	30	20	30
Booster Synchrotron:				
Energy (MeV)	500	500	500	500
Intensity (p s^{-1})	2×10^{13}	2×10^{13}	1.8×10^{13}	6×10^{13}
= (μA)	3.2	3.2	3.0	~10
Power (kW)	1.6	1.6	1.5	5.0
Booster Synchrotron Utilisation Facility:				
Energy (MeV)	500	500	500	500
Intensity (p s^{-1})	2×10^{13}	2×10^{13}		6×10^{13}
= (μA)	3.2	3.2	~1.8	~10
Power (kW)	1.6	1.6	0.9	5.0
Medical Facility:				
Energy (MeV)	500	500	500	500
Intensity (p s^{-1})	1.25×10^{13}	1.25×10^{13}		1.25×10^{13}
= (μA)	2	2	~1.8	2
Main Ring:				
Energy (GeV)	12	12	12	12
Intensity (p s^{-1})	1×10^{13}	5×10^{12}	2×10^{12}	4×10^{12}
= (μA)	1.6	0.8	0.32	0.64
Power (kW)	19.2	9.6	3.6	7.2

Table 1.7
Principal parameters of the CERN SPS.

	Accelerator		Collider
Peak Energy (GeV)	450		270×270
Accelerated Particles	$p,(e^+,e^-)$		$p,\bar{p}$
Construction Started	1971		1978
First Beam	1976		1981
Injector	PS at 10 GeV/c		PS at 26 GeV/c
Ring Diameter		2200 m	
Number of Super-periods		6	
Number of Dipoles		744	
Number of Quadrupoles		216	
Dipole-magnet length (m)		6.26	
Quadrupole-magnet length (m)		3.05	
Maximum dipole field (T)	2.025		1.215
Peak power— dipoles (MW)		180	
Average power— dipoles (MW)		40	
Number of RF cavities	4		2×2
RF power— peak (kW)	3000		2×1500
RF voltage (kV)	9800		2×4900
RF average mains power consumption (MW)		8	
Vacuum chamber aperture (mm)		150×150	
Average pressure (torr)		2×10^{-9}	
Number of ion pumps		1500	
Peak intensity particles/pulse or beam	2.7×10^{13}		1.4×10^{11} p 2×10^{9} $\bar{p}$
particles/s	2.3×10^{12}		
Design value	10^{13} p/p		10^{30} $cm^{-2}s^{-1}$
Number of experimental areas	4		2

Table 1.8
Principal secondary beam lines of the SPS.

Experimental Area	Target	Beam Line	Experiments
West	T1	H1/E1	Hadron or electron beam of up to 5×10^7 particles/pulse serving one experiment.
		H3	Hadron beam of up to 5×10^7 particles per pulse serving two experiments alternately.
		X5	Hadron test beam of 10^5 particles per pulse serving up to three test areas.
		X7	Same as X5.
North	T2	H2	Hadron beam of up to 10^7 particles per pulse serving up to two experiments.
		H4/E4	Hadron or electron beam of up to 10^7 particles/pulse serving two experiments alternately.
	T4	H6	Hadron beam of 3×10^6 particles per pulse serving one experiment.
		H8	Same as H2.
	T6	M2	Muon beam of up to 10^7 muons per pulse serving two experiments simultaneously.
NAHIF	T8	H10	Hadron beam of 10^{10} particles per pulse dedicated to one experiment.
	T10	E12	Electron/photon beam of 10^8 particles/pulse dedicated to one experiment. This beam runs alternately with H10.
Neutrino	T9	N1	Wide-band neutrino beam serving three in-line experiments.
	T11	N3	Narrow-band neutrino beam serving the same experiments as N1 and running alternately with this beam.

FIGURE CAPTIONS FOR CHAPTER 1

Figure 1.1. A 'Livingston Plot' showing the increase in particle energy produced by accelerators with time. An increase in energy by a factor of ten every seven years is evident. A new technology has thus far always appeared when previous technologies have saturated. [After Panofsky (Pa 80), (Pa 81)].

Figure 1.2. Worldwide inventory of particle accelerators (1971). Each accelerator is plotted on coordinate system of beam energy versus intensity measured in μA. [After Rosen [Ro 71]).

Figure 1.3. Effective luminosity versus center-of-mass energy for the largest accelerators now operating or planned. For fixed-target accelerators the target is assumed to be liquid hydrogen 1 metre thick (except in the case of SPS muons, where a 50-metre-thick liquid-hydrogen target is assumed). [After Panofsky (Pa 81)].

Figure 1.4. The annual increase in the number of particle accelerators throughout the world during the period 1930-1968. The dashed line indicates rate of increase of 10% per annum. [After Burrill (Bu 69b).]

Figure 1.5. The 30-MV Van De Graaff Accelerator at Daresbury Nuclear Physics Laboratory, Great Britain. (Courtesy Daresbury Laboratory.)

Figure 1.6. Cutaway view of the 30-MV Van de Graaff Accelerator at Daresbury. (Courtesy Daresbury Laboratory.)

Figure 1.7. Details of column design of the 30-MV Van de Graaff Accelerator at Daresbury. (Courtesy Daresbury Laboratory.)

Figure 1.8. Provisional layout of experimental areas of the 30-MeV Van de Graaff Accelerator at Darsebury. (Courtesy Daresbury Laboratory.)

Figure 1.9. An overhead view of the Clinton P. Anderson Meson Physics

Facility. (Courtesty Los Alamos National Laboratory.)

Figure 1.10. Plan of the experimental areas of the Clinton P. Anderson Meson Physics Facility. (Courtesy Los Alamos National Laboratory.)

Figure 1.11. Remote manipulator systems developed for LAMPF using commercial components. (Courtesy Los Alamos National Laboratory.)

Figure 1.12. General view of the synchrotron facility at the Rutherford Appleton Laboratory; major parameters of the three accelerators are also shown. (Courtesy Rutherford-Appleton Laboratory.)

Figure 1.13. View of the 665-keV pre-injector of the SNS. (Courtesy Rutherford-Appleton Laboratory.)

Figure 1.14. Target station block shield schematics. (SNS) (Courtesy Rutherford-Appleton Laboratory.)

Figure 1.15. Target assembly with four wing moderators. (Courtesy Rutherford-Appleton Laboratory.)

Figure 1.16. View of the Superhilac, shown here during modification without its usual shield. (Courtesy Lawrence Berkeley Laboratory.)

Figure 1.17. The Bevalac of the Lawrence Berkeley Laboratory. This is the only accelerator facility in the world that provides ions as heavy as uranium at relativistic energies. The arrow shows the path of the heavy ions, which are produced and accelerated at the SuperHILAC (rear) then steered through a transfer line into the Bevatron (the circular building in the foreground), where they are further accelerated and routed to the various research areas. (Courtesy Lawrence Berkeley Laboratory.)

Figure 1.18. Schematic diagram of KEK 12-GeV Synchrotron. (Courtesy National Laboratory for High-Energy Physics, Tsukuba.)

Figure 1.19. KEK 20-MeV Alvarez-Type Linac. (Courtesy National Laboratory for High-Energy Physics, Tsukuba.)

Figure 1.20. KEK 500-MeV Booster Synchrotron. (Courtesy National Laboratory for High-Energy Physics, Tsukuba.)

Figure 1.21. View of Main Ring of KEK 12-GeV Synchrotron. (Courtesy National Laboratory for High-Energy Physics, Tsukuba.)

Figure 1.22. The growth of beam intensity at the KEK 12-GeV Protron Synchrotron. (Courtesy National Laboratory for High-Energy Physics, Tsukuba.)

Figure 1.23. Aerial view of the CERN site with location of the 400-GeV proton synchrotron picked out by dashed white lines. The links with previously existing CERN installations and the beam-line direction out to the North Experimental Area (to the left) are also indicated. The Franco-Swiss frontier, which crosses the site, is drawn as a dotted white line. The city of Geneva and the Alps are in the background. (Courtesy Swissair.)

Figure 1.24. Schematic drawing of the CERN 400-GeV proton synchrotron showing the link (via transfer tunnel TT10) with the PS, which serves as injector. Six auxiliary buildings (1-6) and access shafts, located on the long straight sections of the machine, are indicated, together with a seventh (7) located over the beam line to the West Experimental Area and the Puits Génié Civil (PGC), used during the machine tunnel construction. The transfer tunnels TT60 and TT20 send accelerated beam to the West Experimental Area and North Experimental Area, respectively. The experimental halls and the location of some detection systems are also shown. (Courtesy CERN.)

Figure 1.25. SPS magnet in tunnel. (Courtesy CERN.)

Figure 1.26. Parts of a chart record of dose rates from induced radioactivity in the SPS tunnel. Also shown is the momentum compaction function as a function of distance on the same horizontal scale for a typical sextant. Note that the horizontal scale corresponds to a real distance in the accelerator tunnel of approximately 1 km. (Courtesy CERN.)

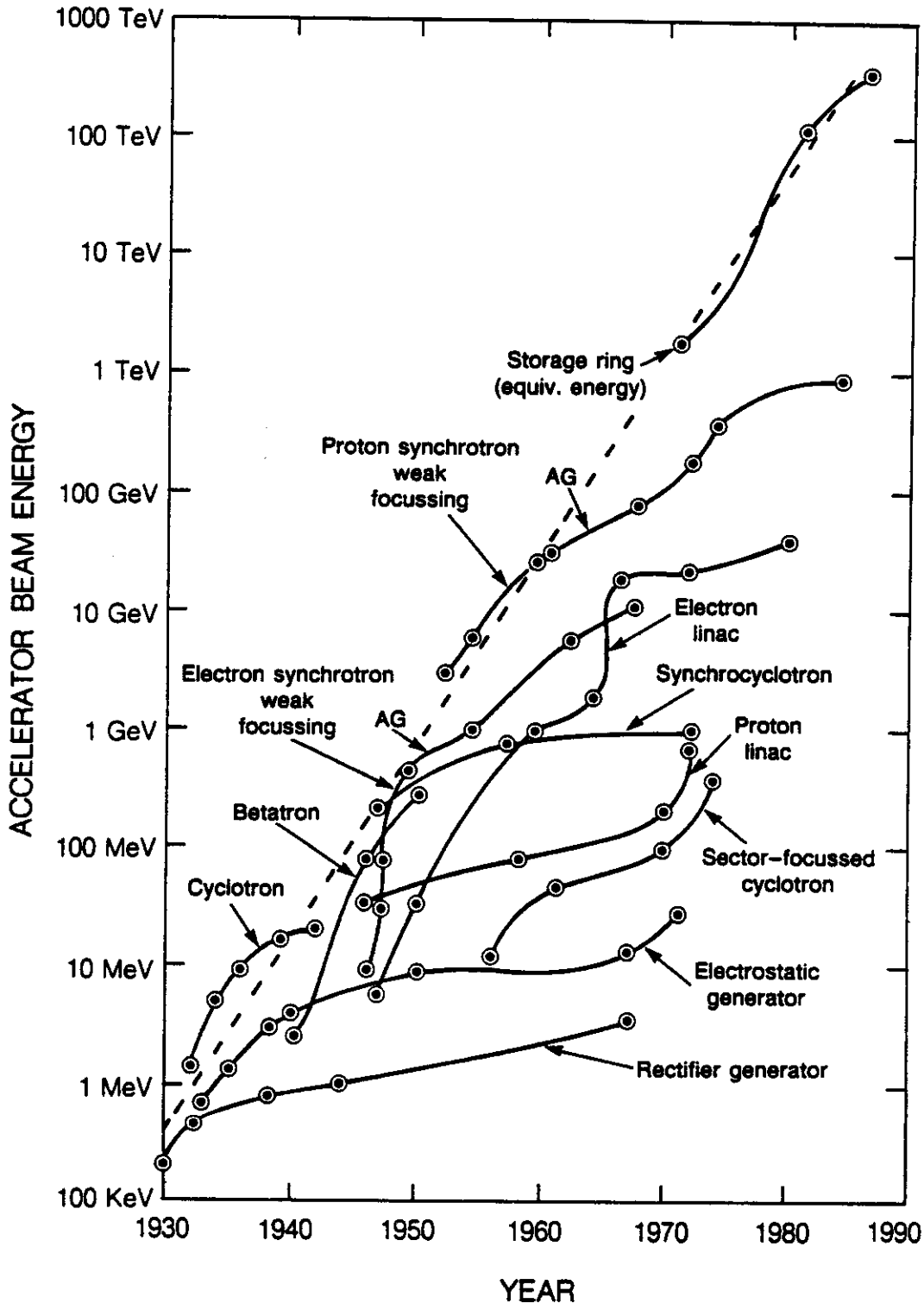
1000 TeV
100 TeV
10 TeV
1 TeV
100 GeV
10 GeV
1 GeV
100 MeV
10 MeV
1 MeV
100 KeV
ACCELERATOR BEAM ENERGY
1930
1940
1950
1960
1970
1980
1990
YEAR
Storage ring
(equiv. energy)
Proton synchrotron
weak
focussing
AG
Electron
linac
Electron synchrotron
weak
focussing
AG
Synchrocyclotron
Proton
linac
Betatron
Sector-focussed
cyclotron
Cyclotron
Electrostatic
generator
Rectifier generator
XBL 853-10145

Fig. 1.1

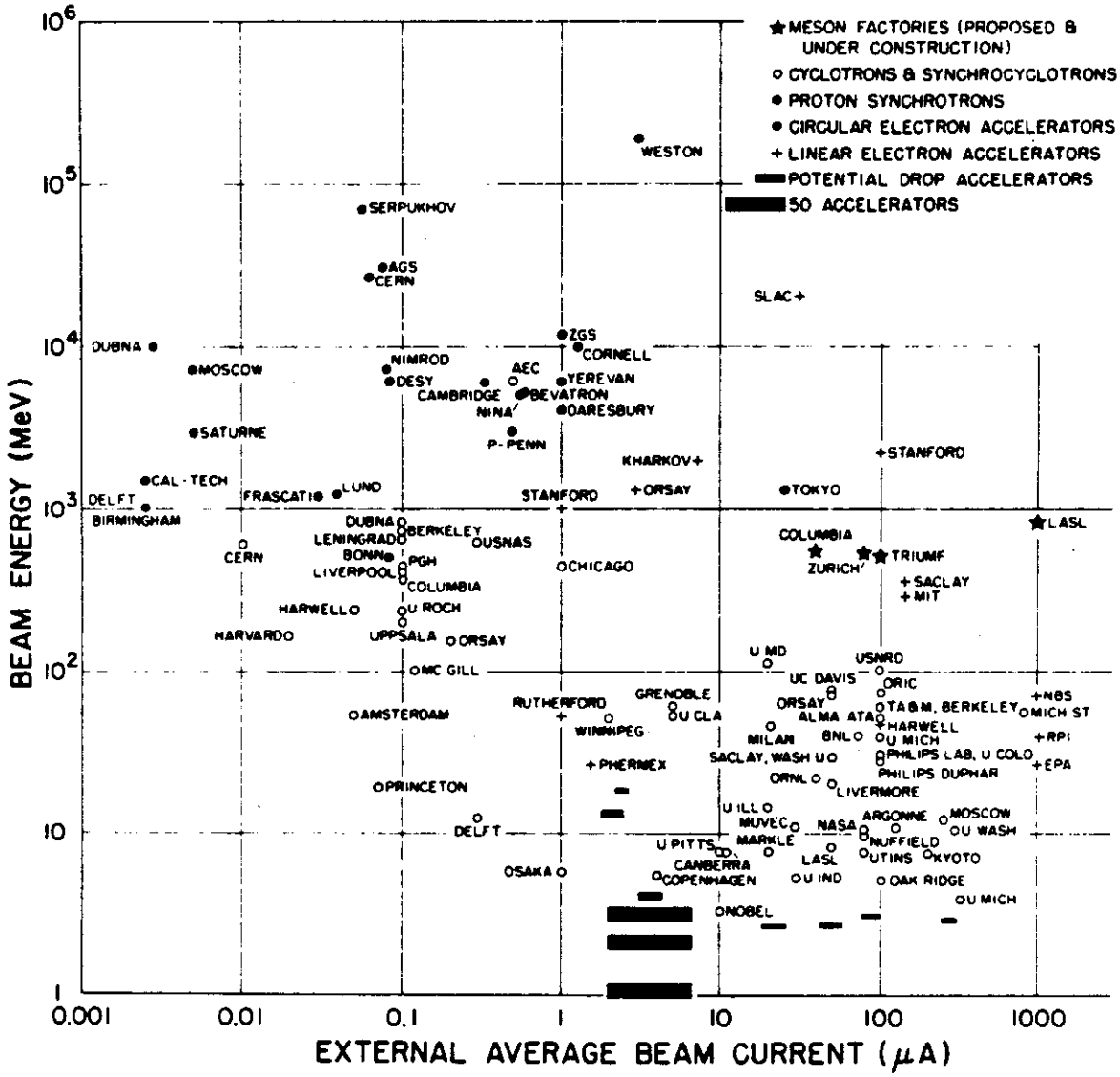

XBL 855-2644

Fig. 1.2

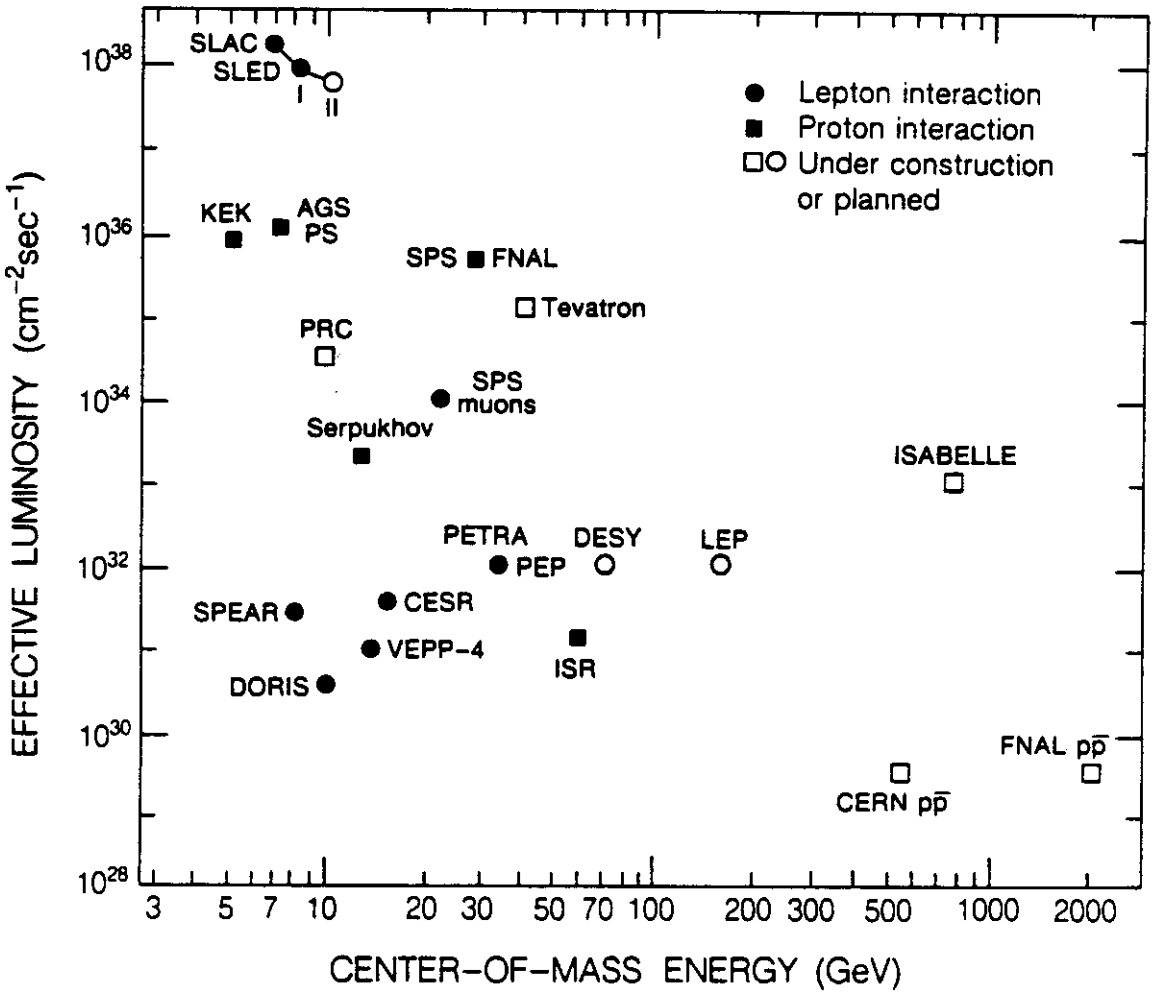

XBL 853-10144

Fig. 1.3

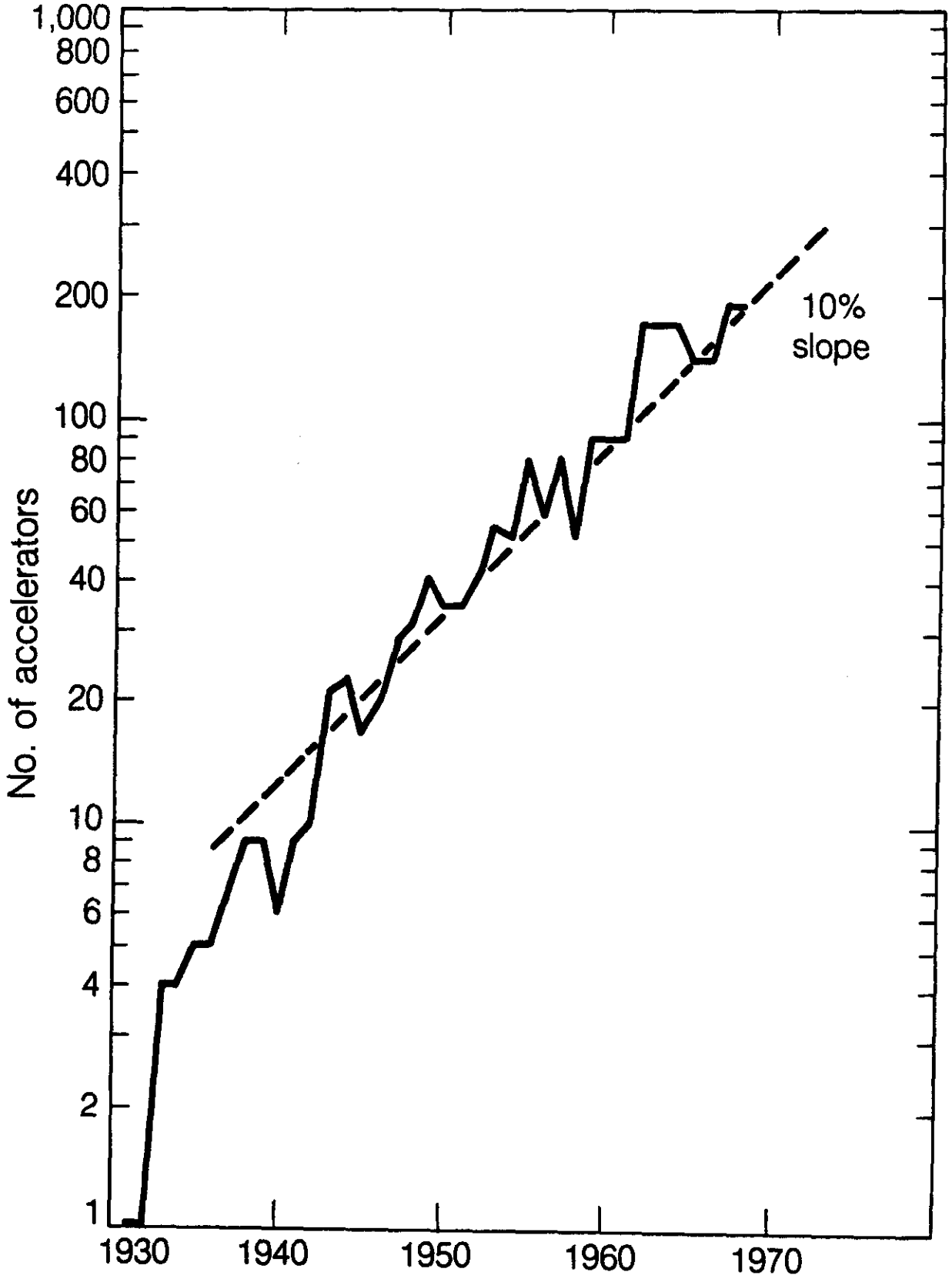

XBL 855-9979

Fig. 1.4

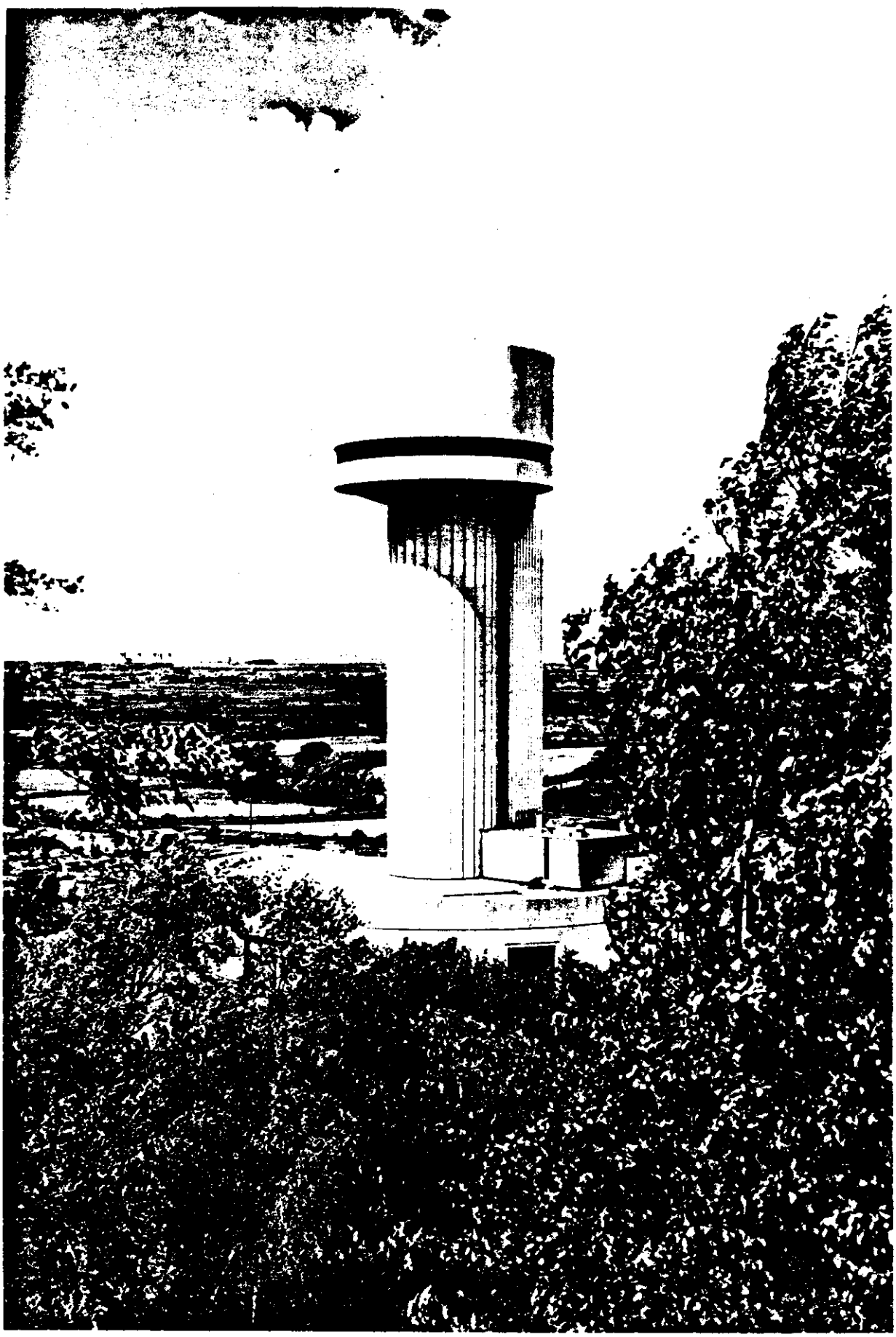

Fig. 1.5

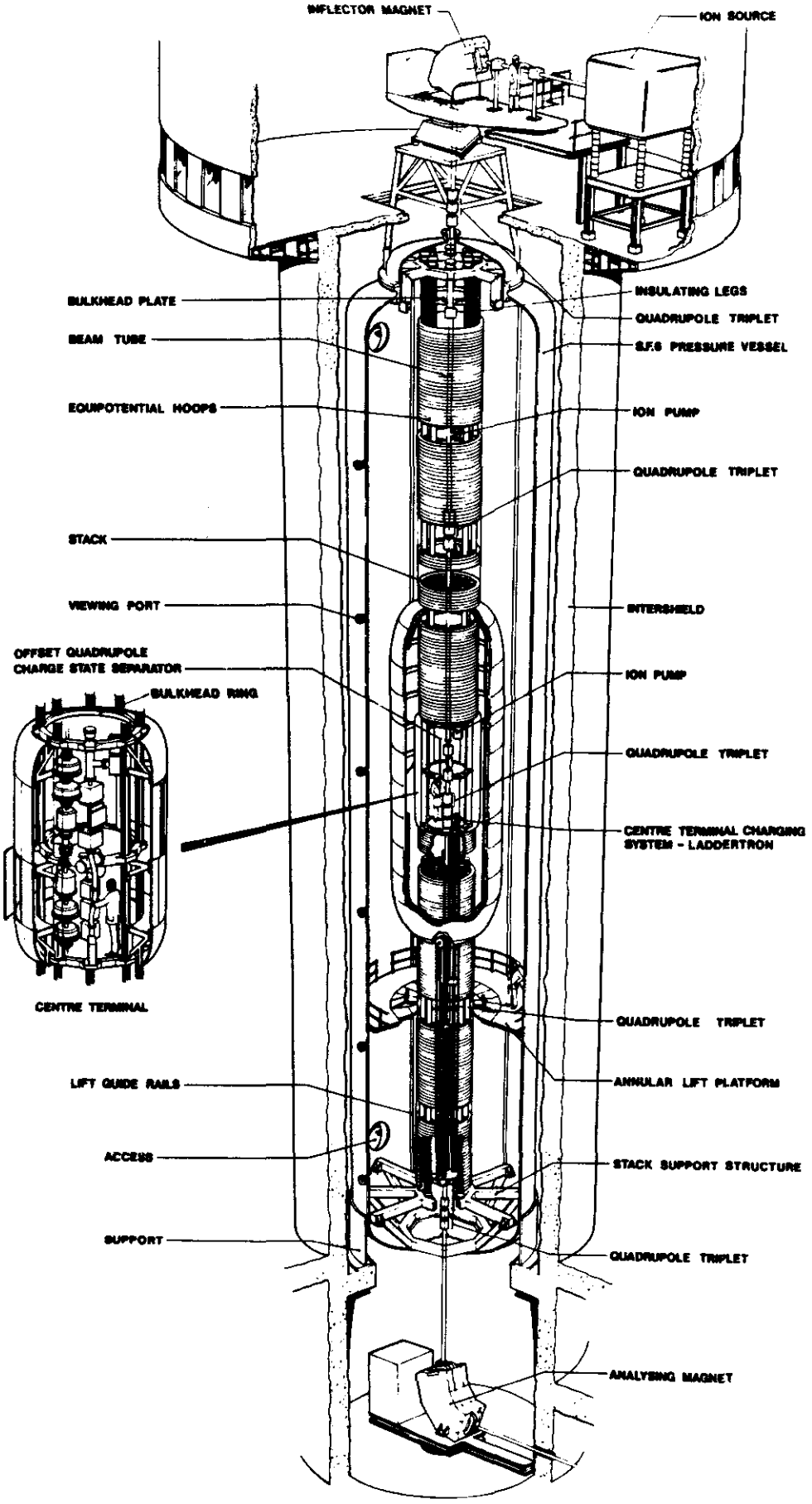
DEFLECTOR MAGNET
ION SOURCE
BULKHEAD PLATE
BEAM TUBE
EQUIPOTENTIAL HOOPS
STACK
VIEWING PORT
OFFSET QUADRUPOLE
CHARGE STATE SEPARATOR
BULKHEAD RING
CENTRE TERMINAL
LIFT GUIDE RAILS
ACCESS
SUPPORT
INSULATING LEGS
QUADRUPOLE TRIPLET
S.F.6 PRESSURE VESSEL
ION PUMP
QUADRUPOLE TRIPLET
INTERSHIELD
ION PUMP
QUADRUPOLE TRIPLET
CENTRE TERMINAL CHARGING
SYSTEM - LADDERTRON
QUADRUPOLE TRIPLET
ANNULAR LIFT PLATFORM
STACK SUPPORT STRUCTURE
QUADRUPOLE TRIPLET
ANALYSING MAGNET

Fig. 1.6

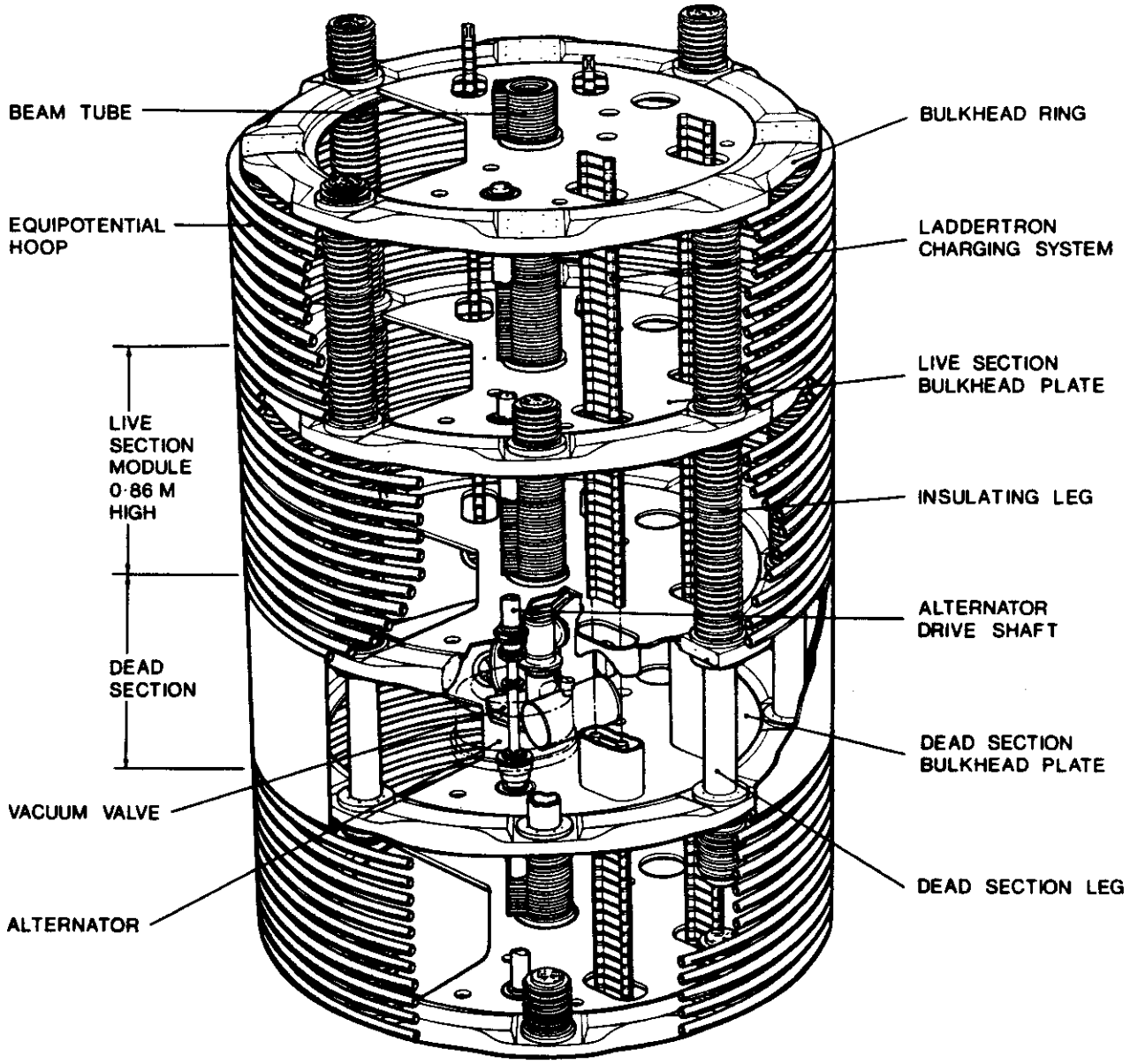

TYPICAL STACK SECTION INDICATING MAIN STRUCTURAL & ELECTROSTATIC ELEMENTS

Fig. 1.7

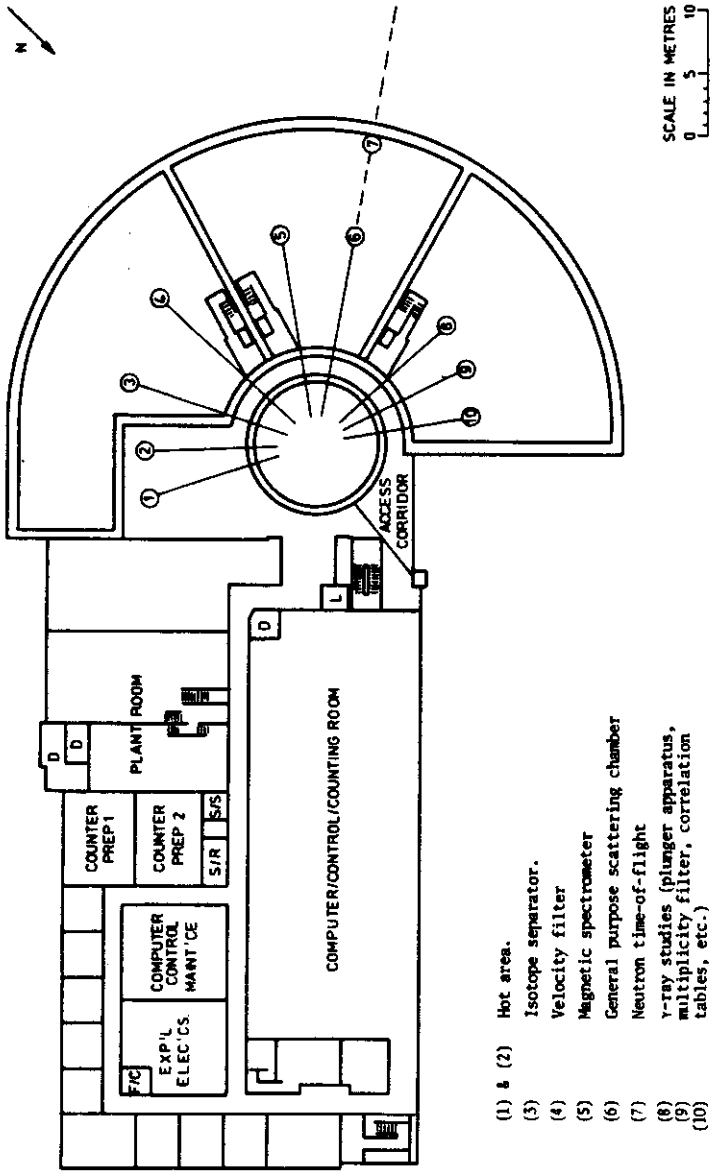
N
SCALE IN METRES
0 5 10
ACCESS CORRIDOR
PLANT ROOM
COUNTER PREP 1
COUNTER PREP 2
S/R
S/S
COMPUTER CONTROL MAINT'CE
EXP'L ELEC'CS.
F/C
COMPUTER/CONTROL/COUNTING ROOM
D
L
(1) & (2) Hot area.
(3) Isotope separator.
(4) Velocity filter
(5) Magnetic spectrometer
(6) General purpose scattering chamber
(7) Neutron time-of-flight
(8) γ-ray studies (plunger apparatus,
(9) multiplicity filter, correlation
(10) tables, etc.)

Fig. 1.8

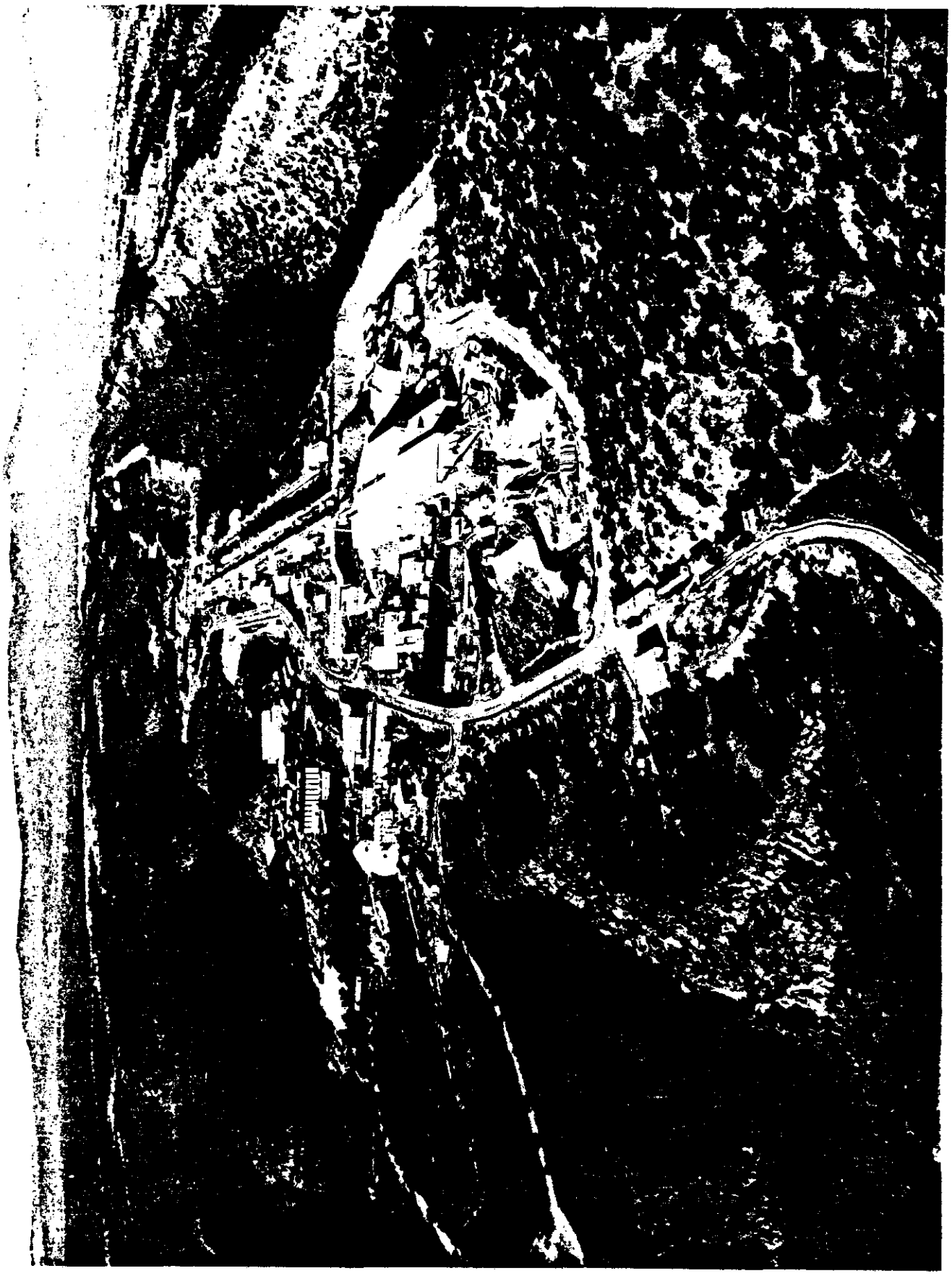

Fig. 1.9

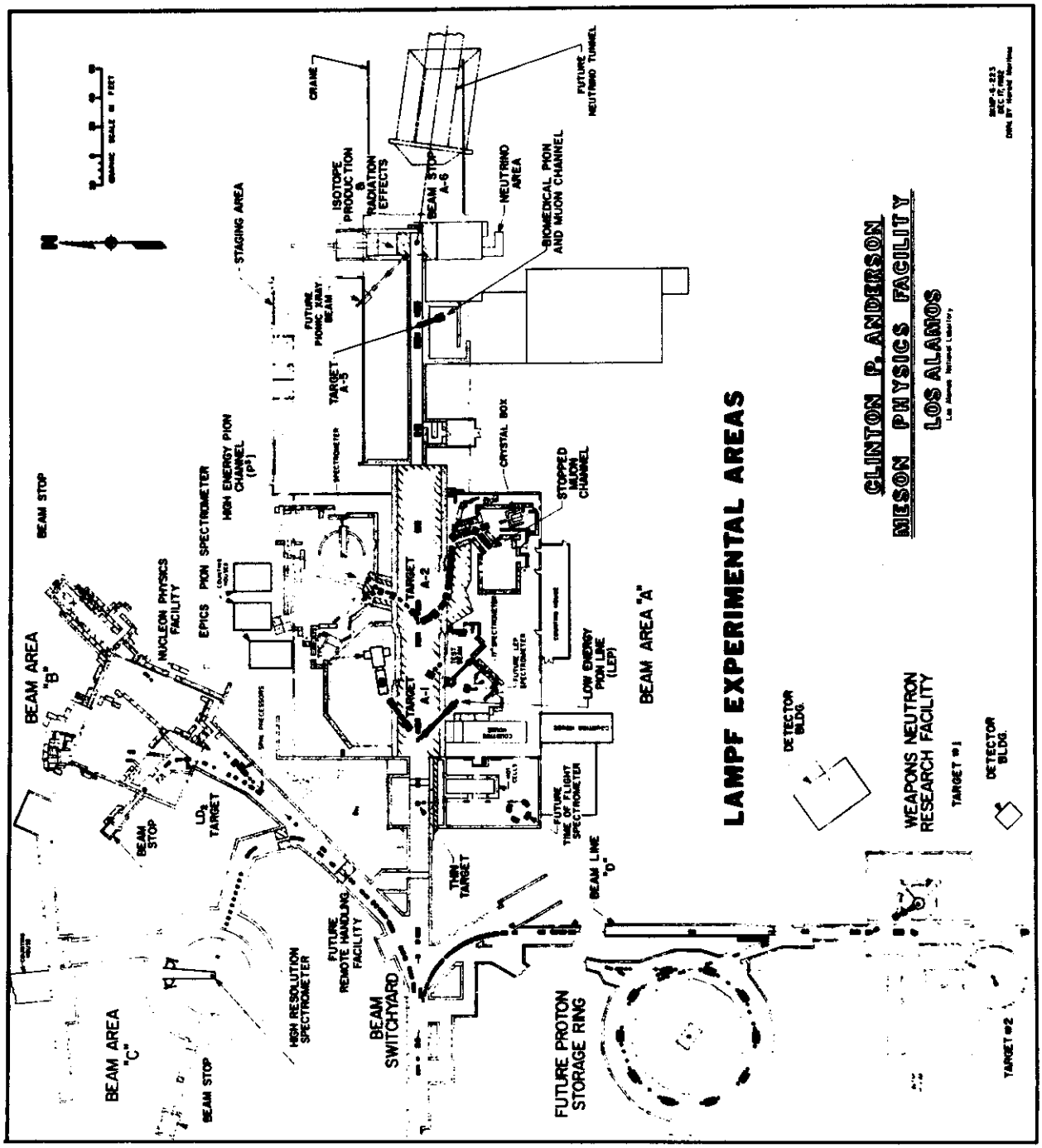
CLINTON P. ANDERSON
MESON PHYSICS FACILITY
LOS ALAMOS
LAMPF EXPERIMENTAL AREAS
BEAM AREA "B"
BEAM AREA "C"
BEAM AREA "A"
BEAM STOP
NUCLEON PHYSICS FACILITY
EPICS
PION SPECTROMETER
HIGH ENERGY PION CHANNEL (P3)
STAGING AREA
CRANE
ISOTOPE PRODUCTION & RADIATION EFFECTS
BEAM STOP A-6
NEUTRINO AREA
FUTURE NEUTRINO TUNNEL
BIOMEDICAL PION AND MUON CHANNEL
TARGET A-5
CRYSTAL BOX
STOPPED MUON CHANNEL
TARGET A-2
TARGET A-1
LOW ENERGY PION LINE (LEP)
FUTURE TIME OF FLIGHT SPECTROMETER
LD_2 TARGET
BEAM STOP
THIN TARGET
BEAM LINE "D"
FUTURE REMOTE HANDLING FACILITY
HIGH RESOLUTION SPECTROMETER
BEAM SWITCHYARD
FUTURE PROTON STORAGE RING
DETECTOR BLDG.
WEAPONS NEUTRON RESEARCH FACILITY
TARGET #1
TARGET #2

Fig. 1.10

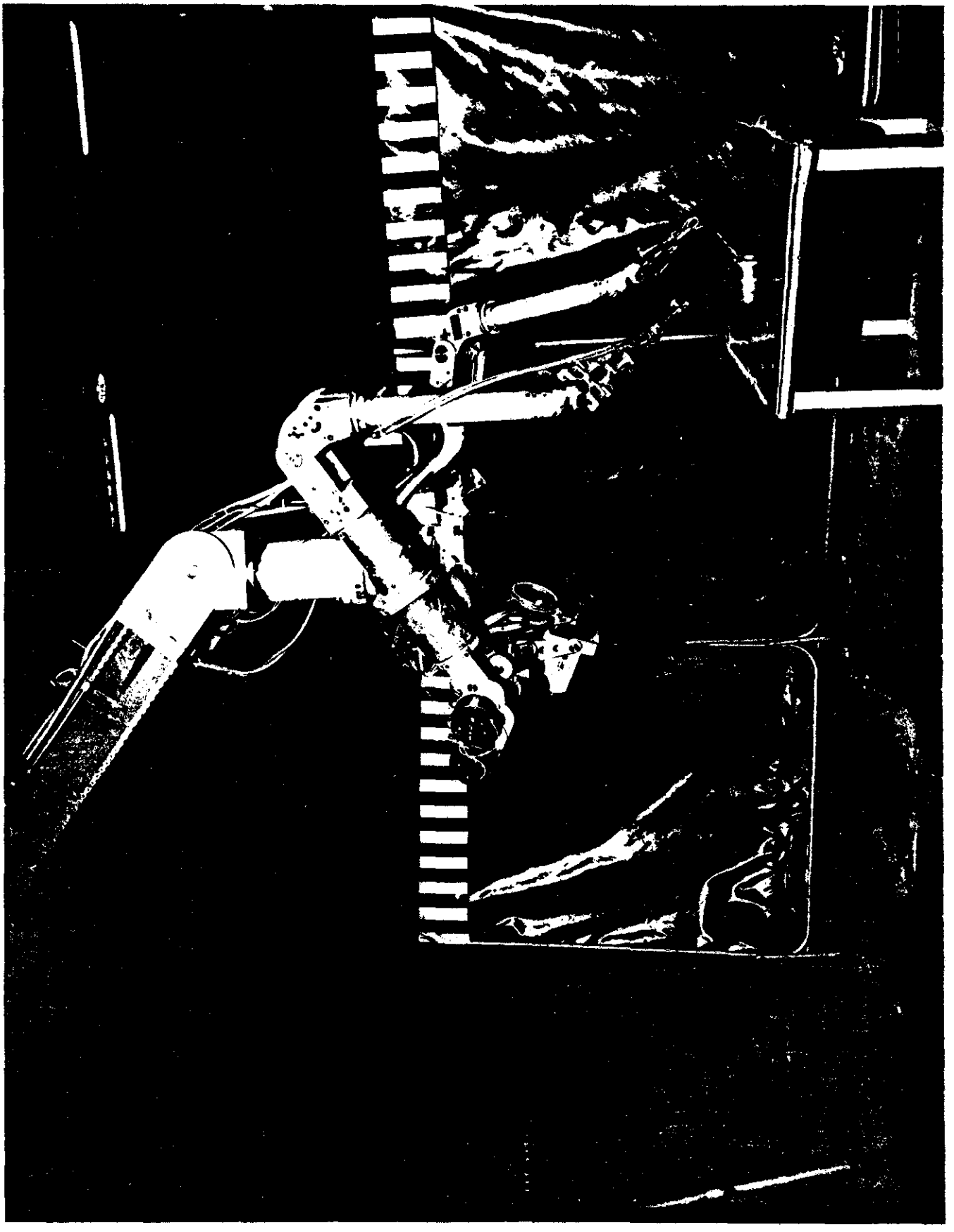

Fig. 1.11

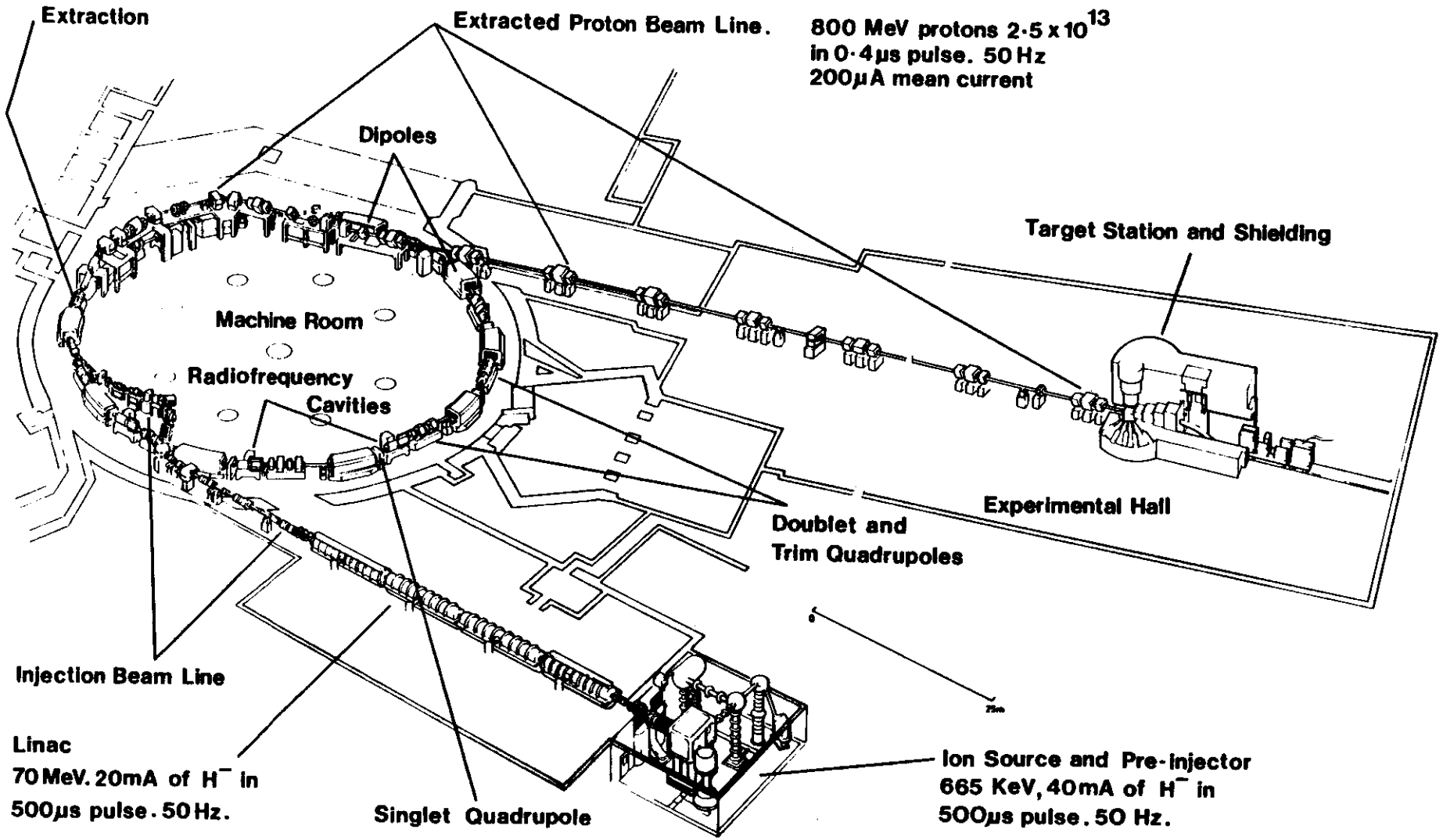

SPALLATION NEUTRON SOURCE

Fig. 1.12

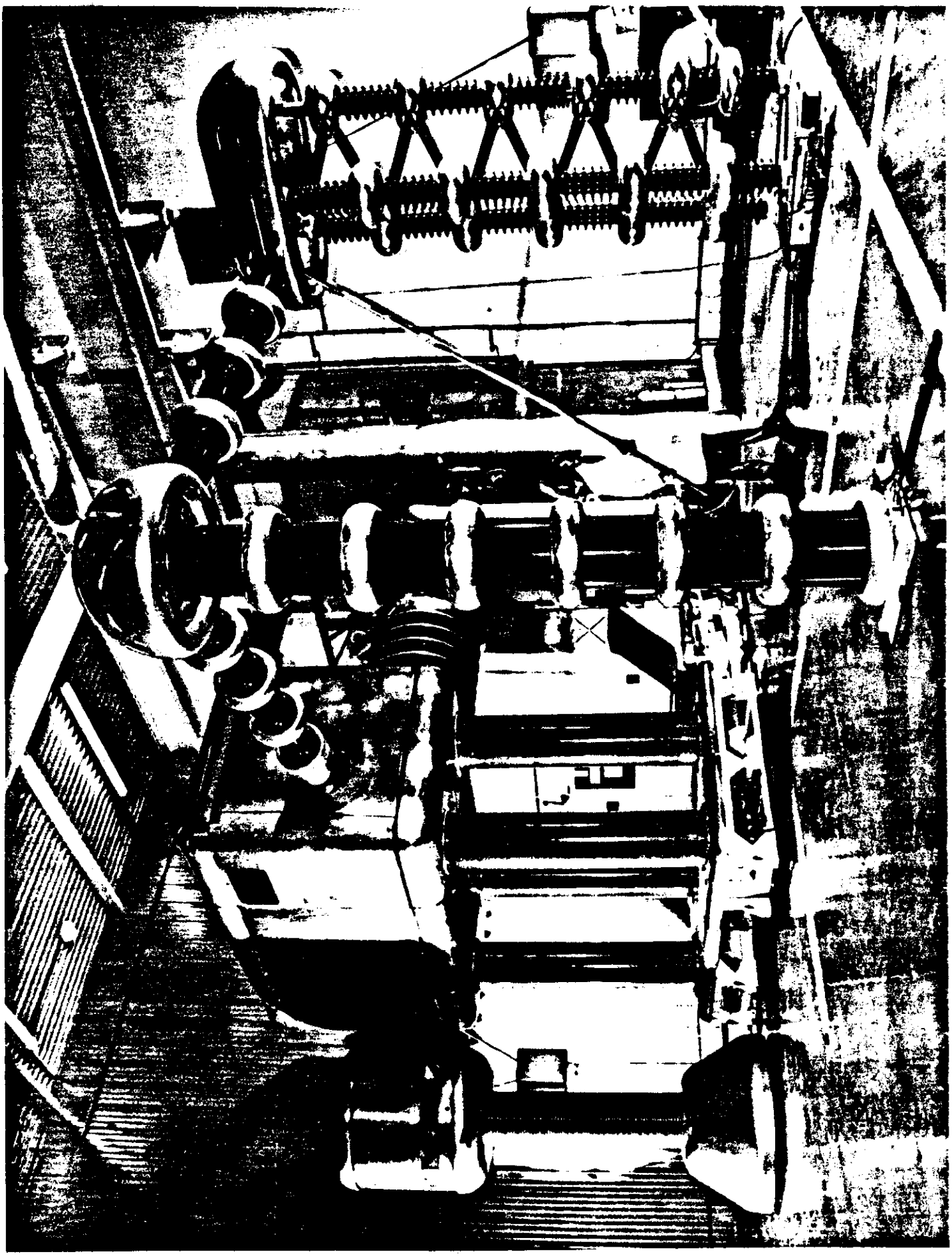

Fig. 1.13

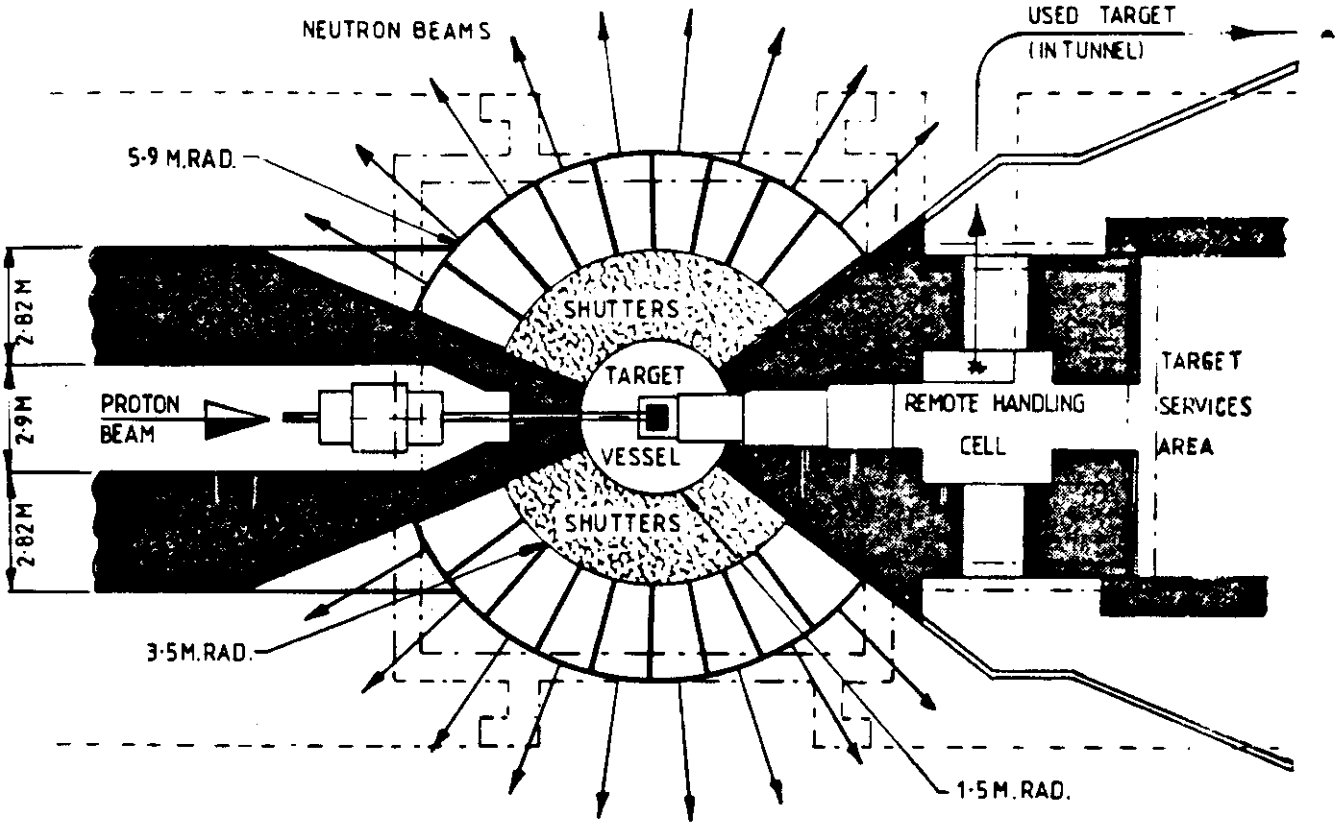

a) PLAN VIEW

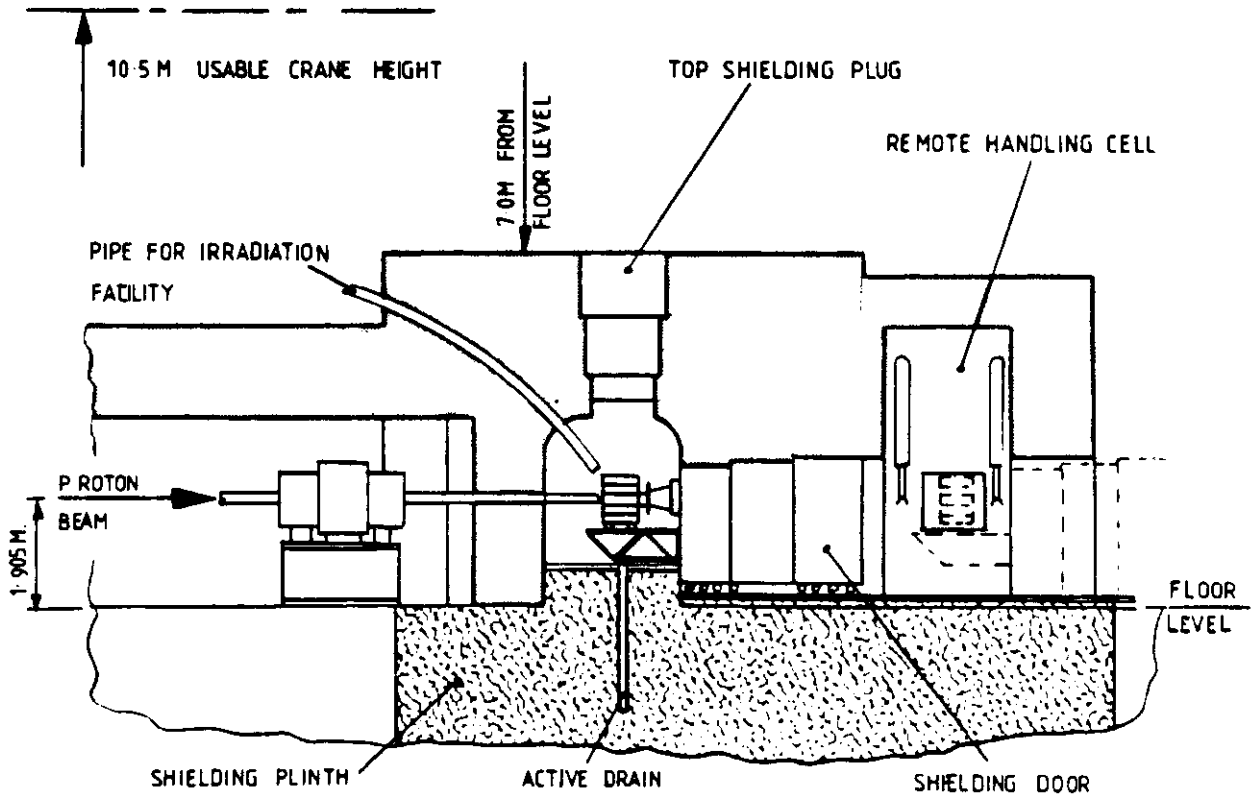

b) VERTICAL SECTION

Fig. 1.14

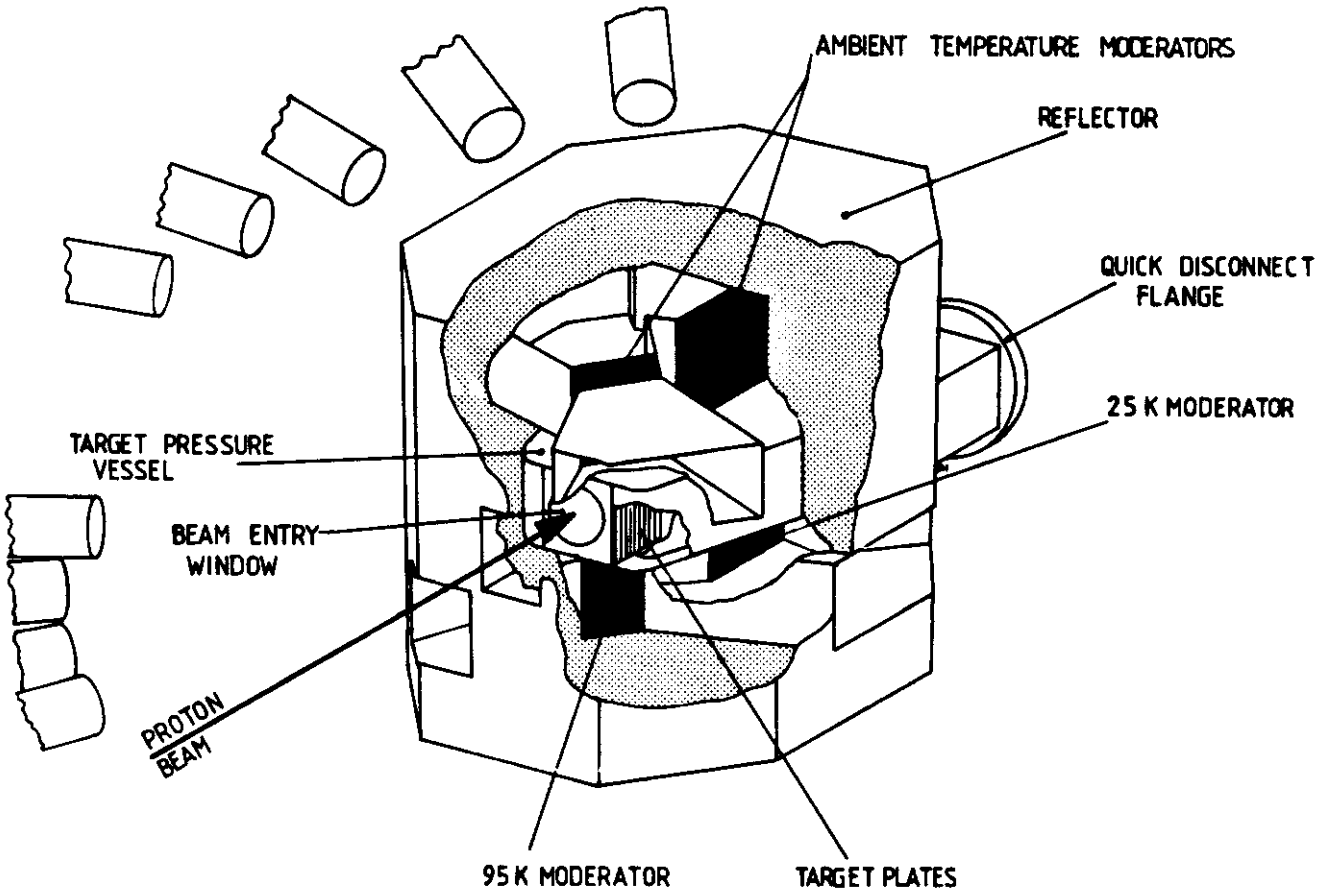
AMBIENT TEMPERATURE MODERATORS
REFLECTOR
QUICK DISCONNECT FLANGE
25 K MODERATOR
TARGET PRESSURE VESSEL
BEAM ENTRY WINDOW
PROTON BEAM
95 K MODERATOR
TARGET PLATES

Fig. 1.15

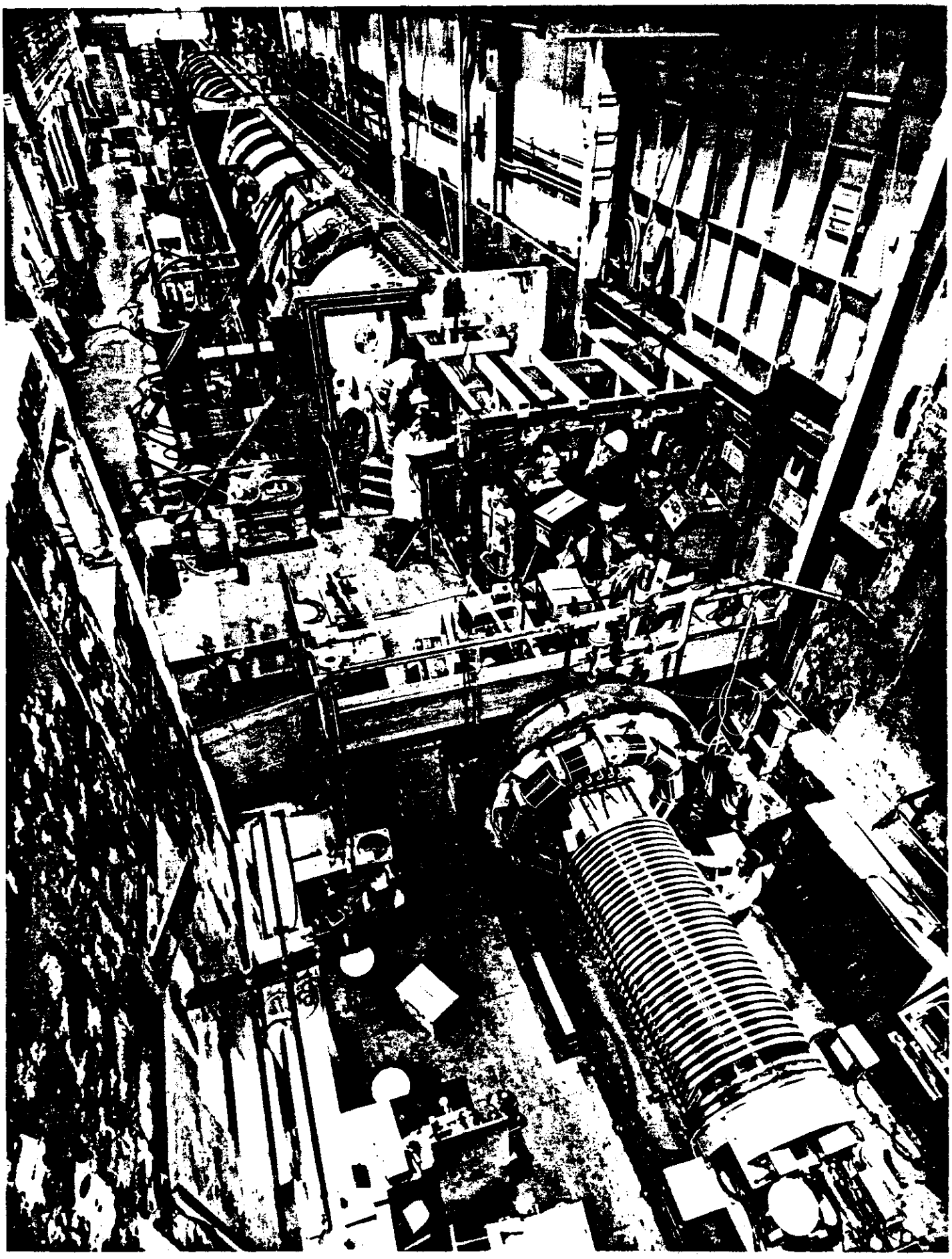

Fig. 1.16

Fig. 1.17

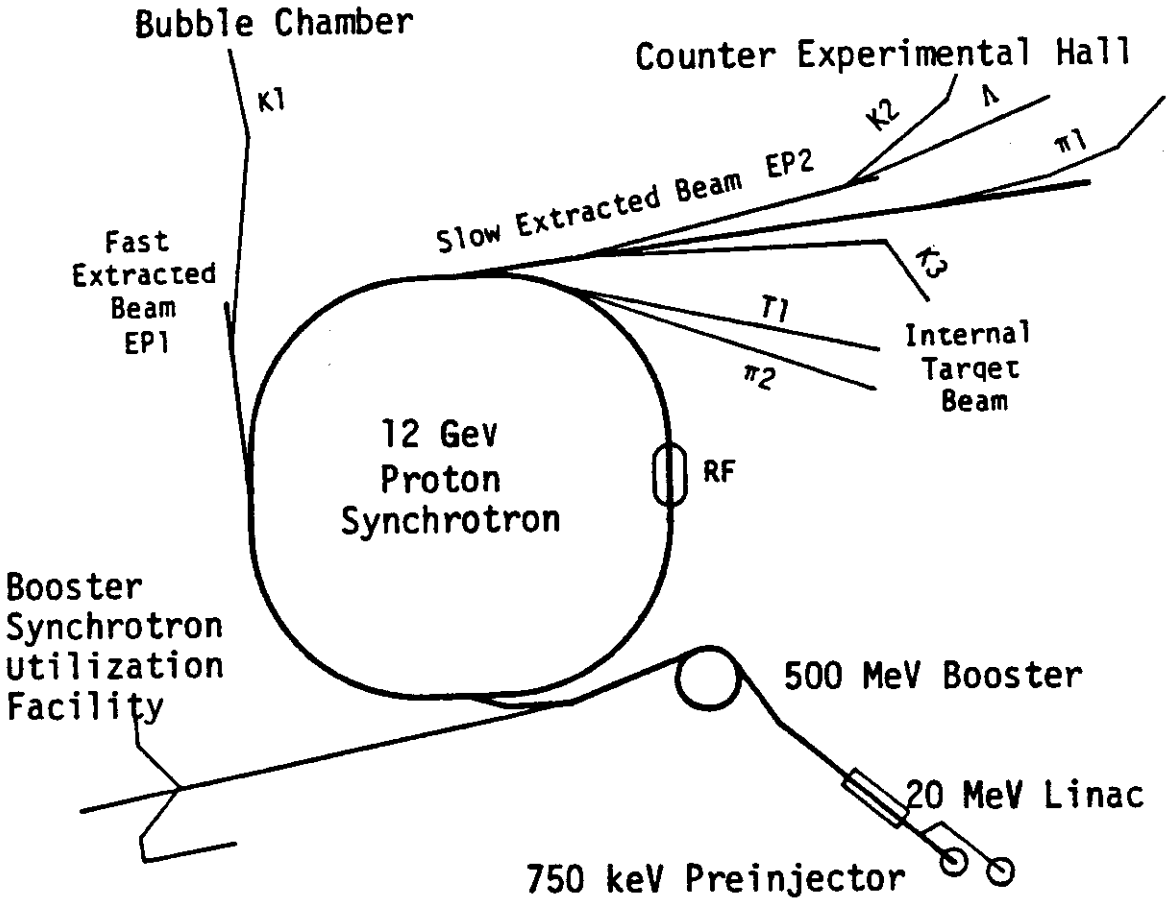
Bubble Chamber
K1
Counter Experimental Hall
K2
Λ
π1
Slow Extracted Beam EP2
Fast
Extracted
Beam
EP1
K3
T1
Internal
Target
Beam
π2
12 GeV
Proton
Synchrotron
RF
Booster
Synchrotron
Utilization
Facility
500 MeV Booster
20 MeV Linac
750 keV Preinjector

Fig. 1.18

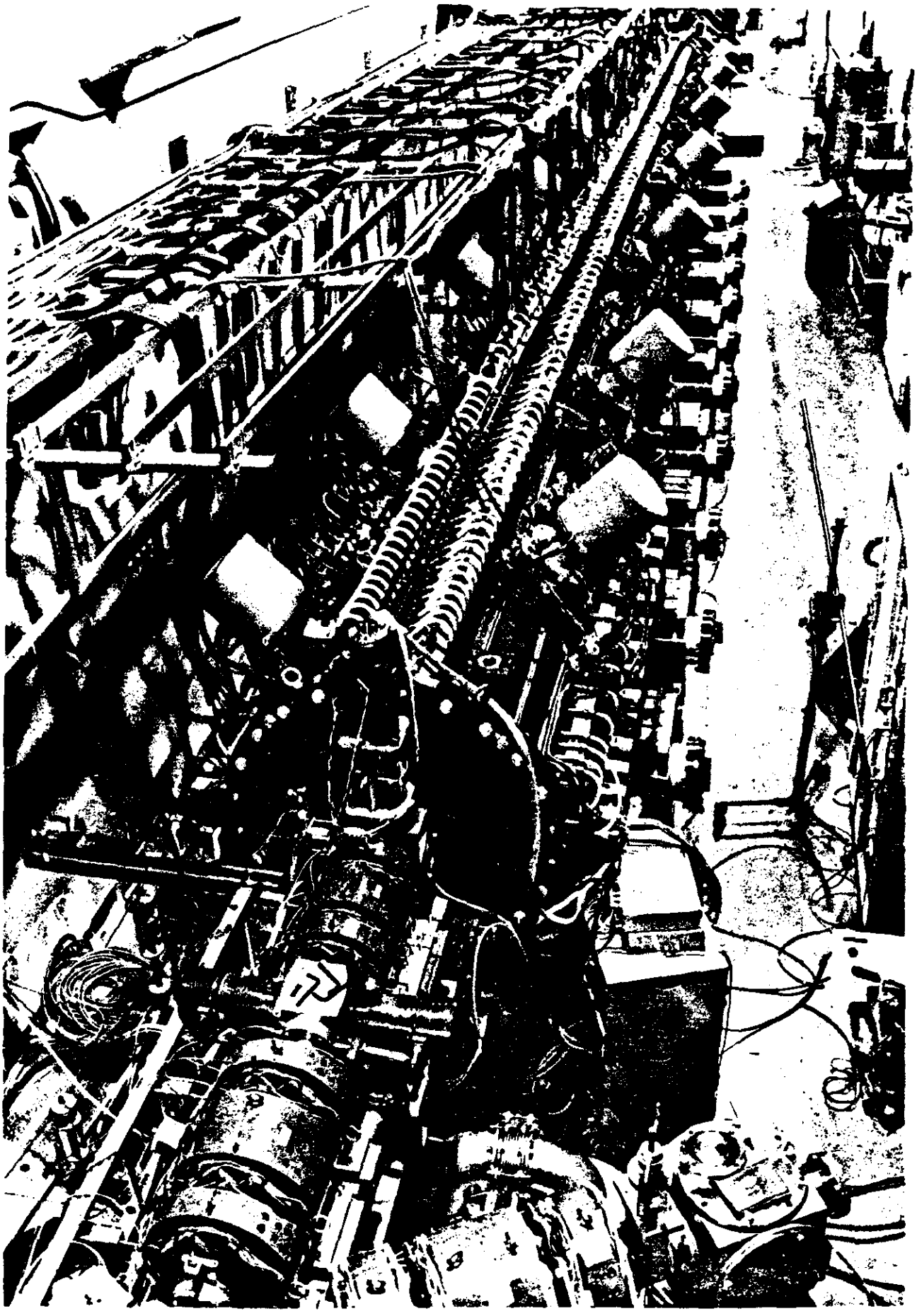

Fig. 1.19

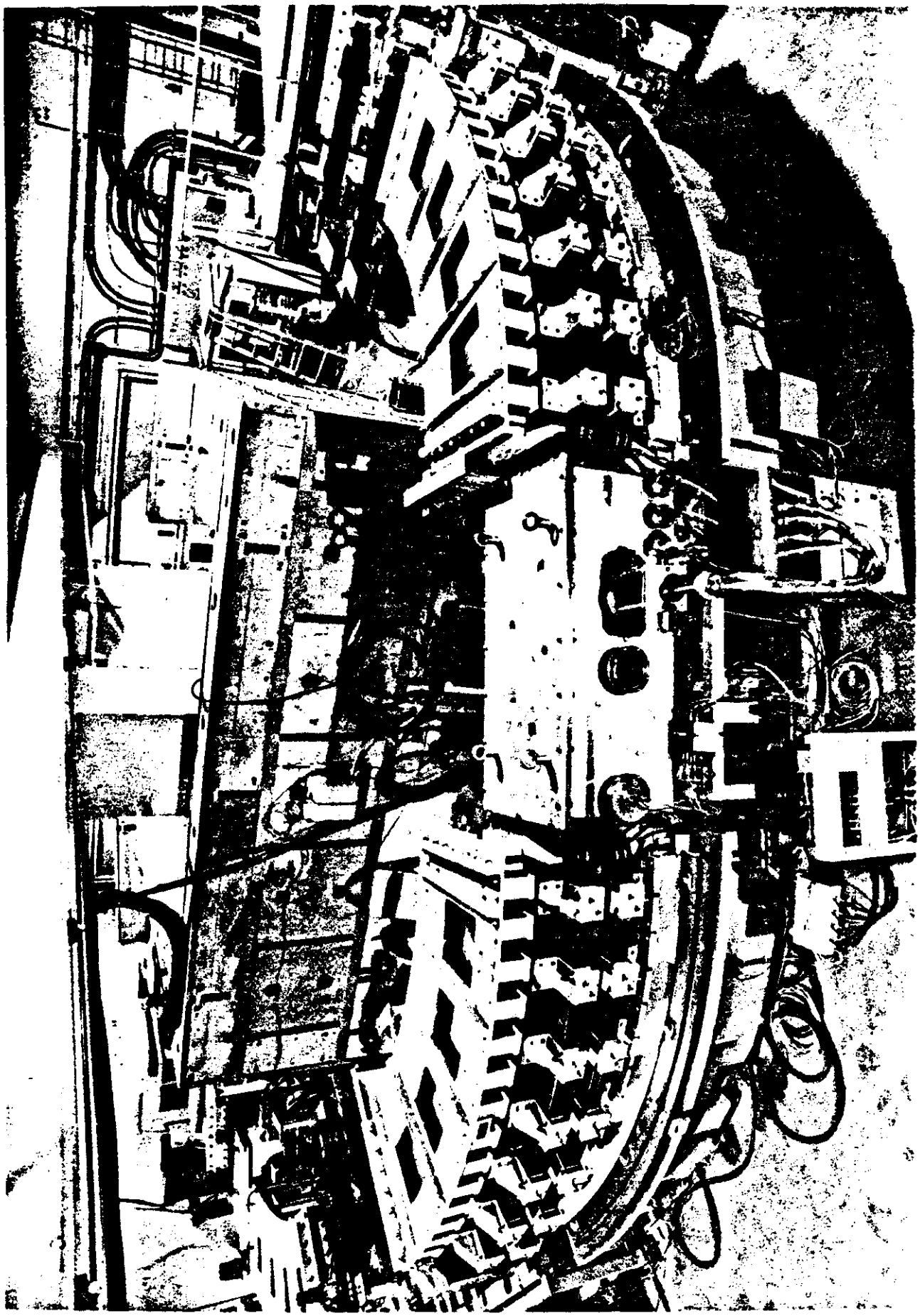

Fig. 1.20

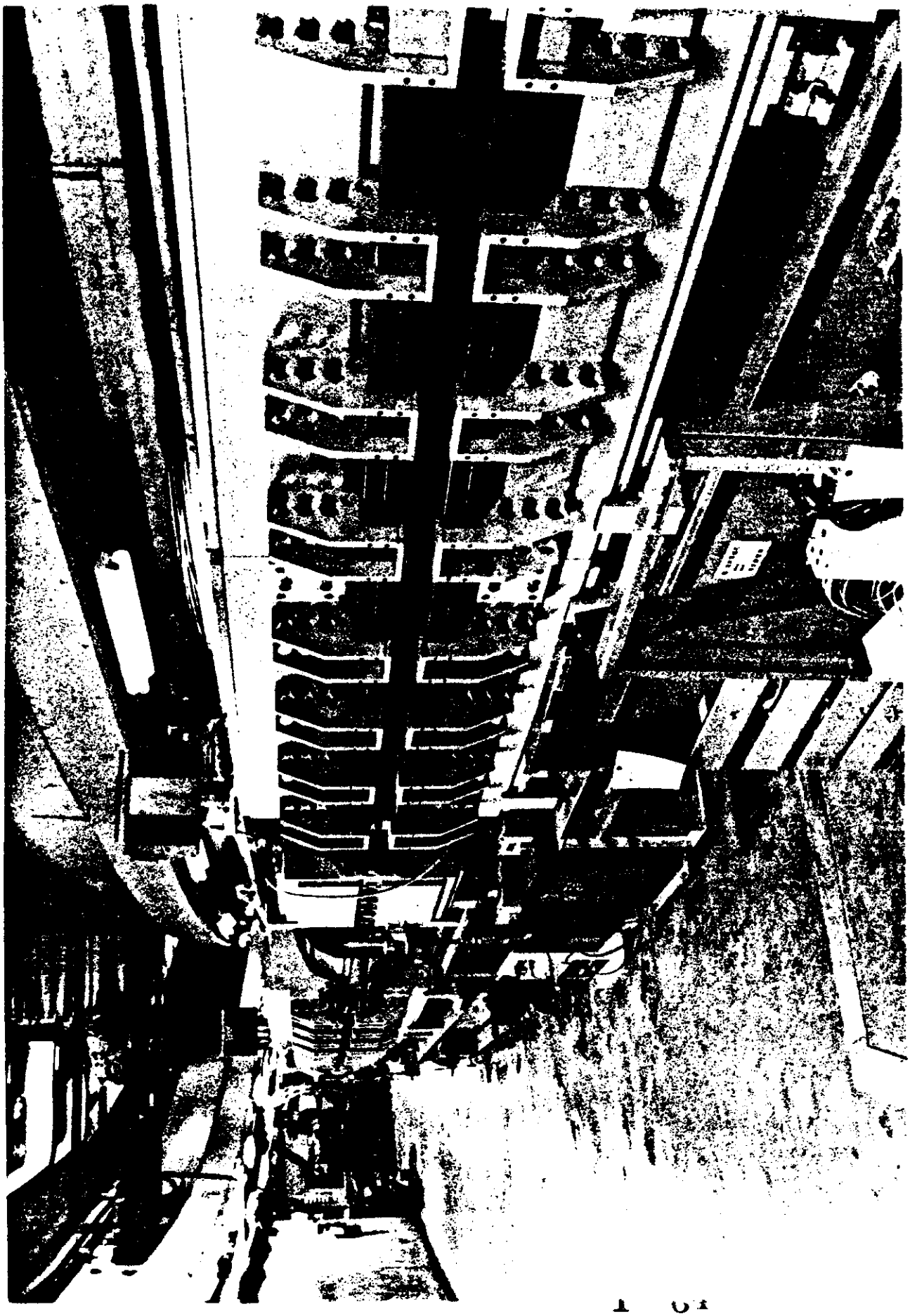

Fig. 1.21

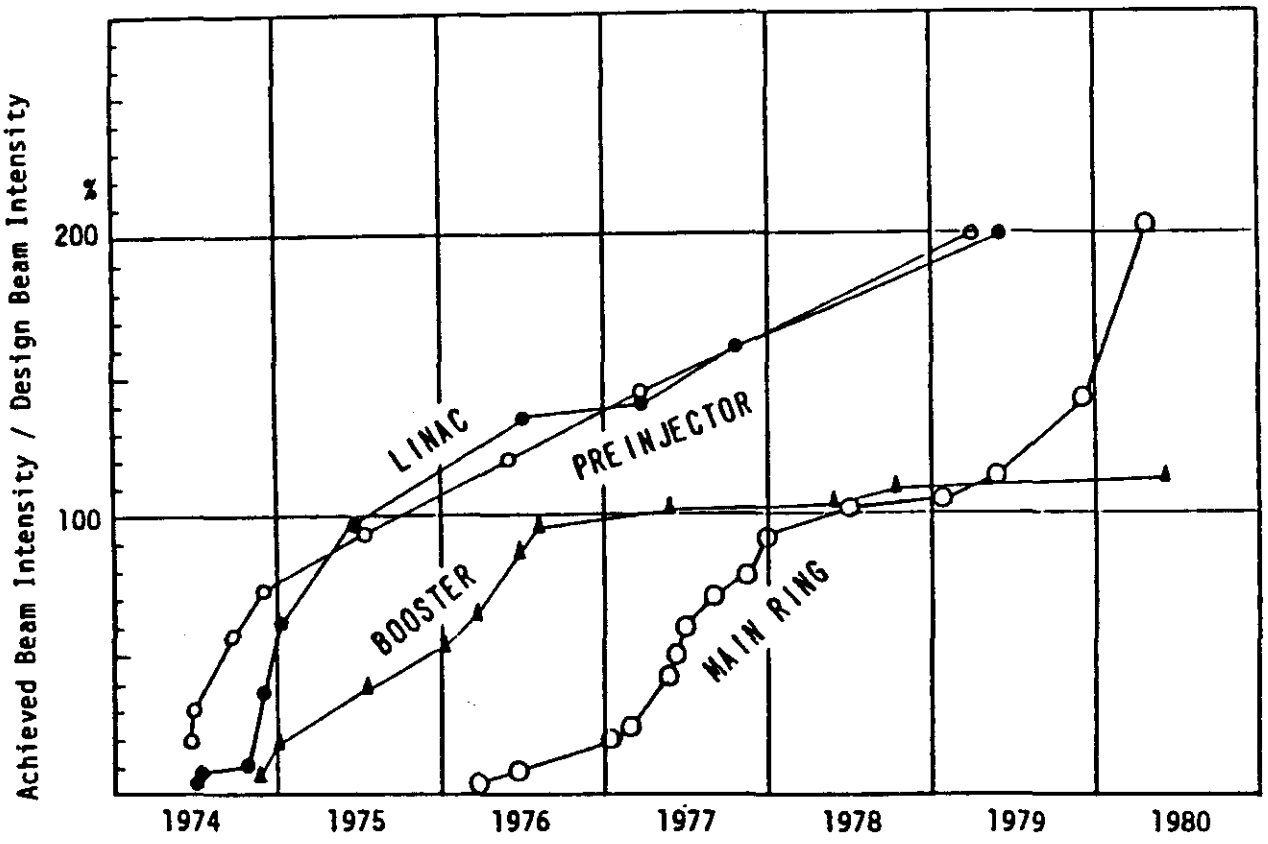
Achieved Beam Intensity / Design Beam Intensity
%
200
100
LINAC
PREINJECTOR
BOOSTER
MAIN RING
1974
1975
1976
1977
1978
1979
1980
Design Beam Intensity
Preinjector 200 mA
Linac 100 mA
Booster 6x10^11 ppp
Main Ring 2x10^12 ppp

Fig. 1.22

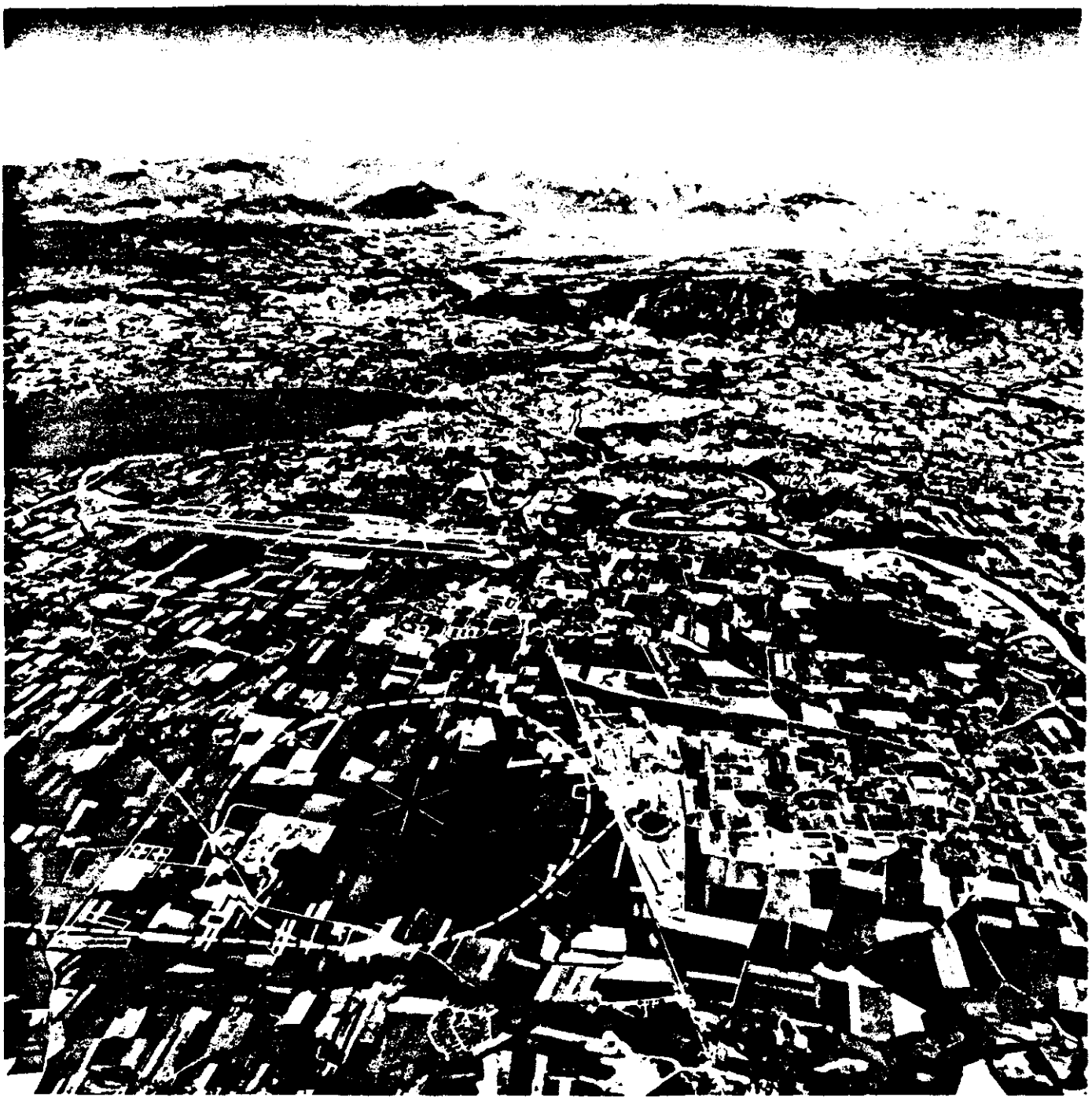

Fig. 1.23

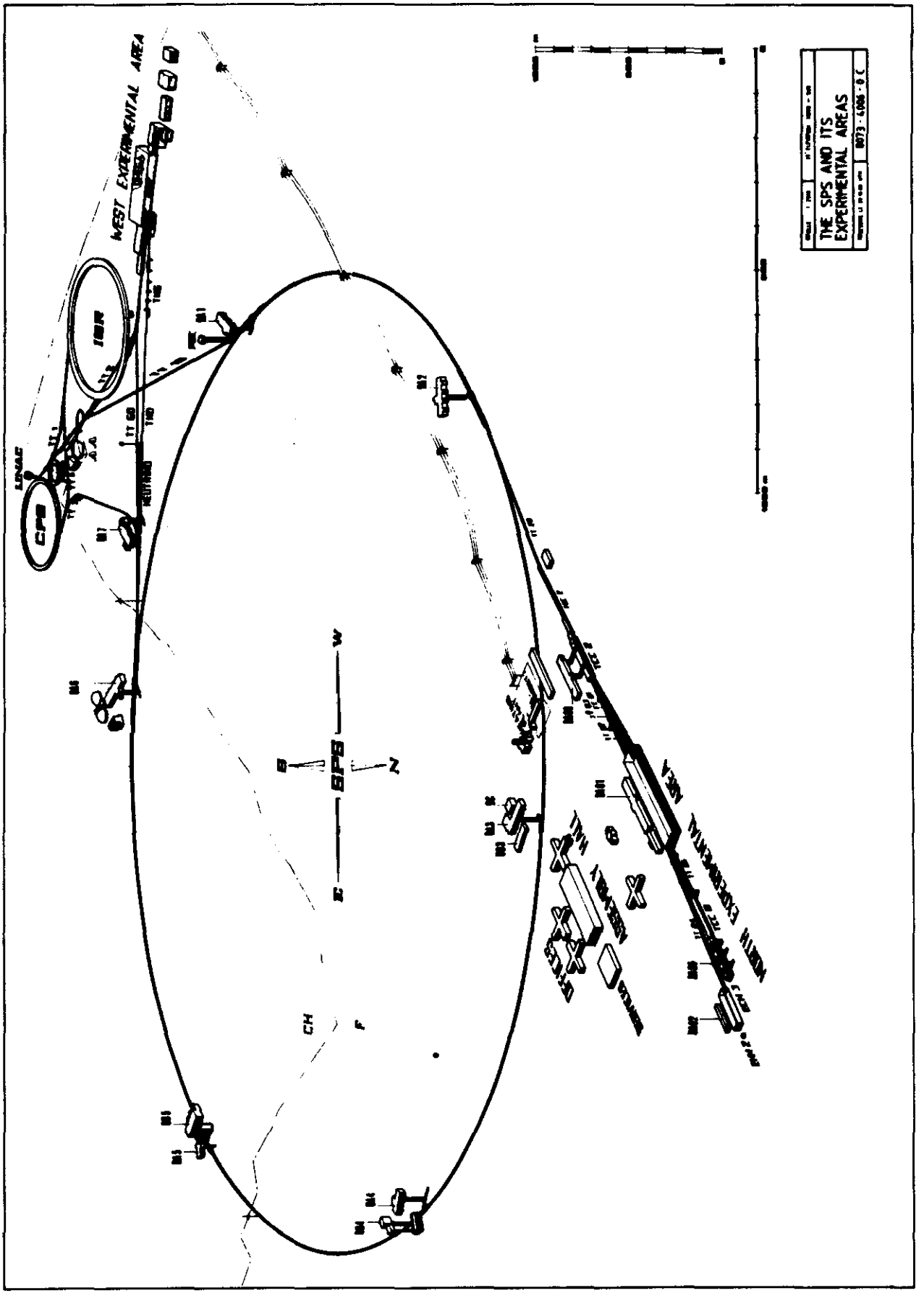
THE SPS AND ITS
EXPERIMENTAL AREAS
WEST EXPERIMENTAL AREA
NORTH EXPERIMENTAL AREA
CPS
IBR
LINAC
SPS
W
N
E
CH
F

Fig. 1.24

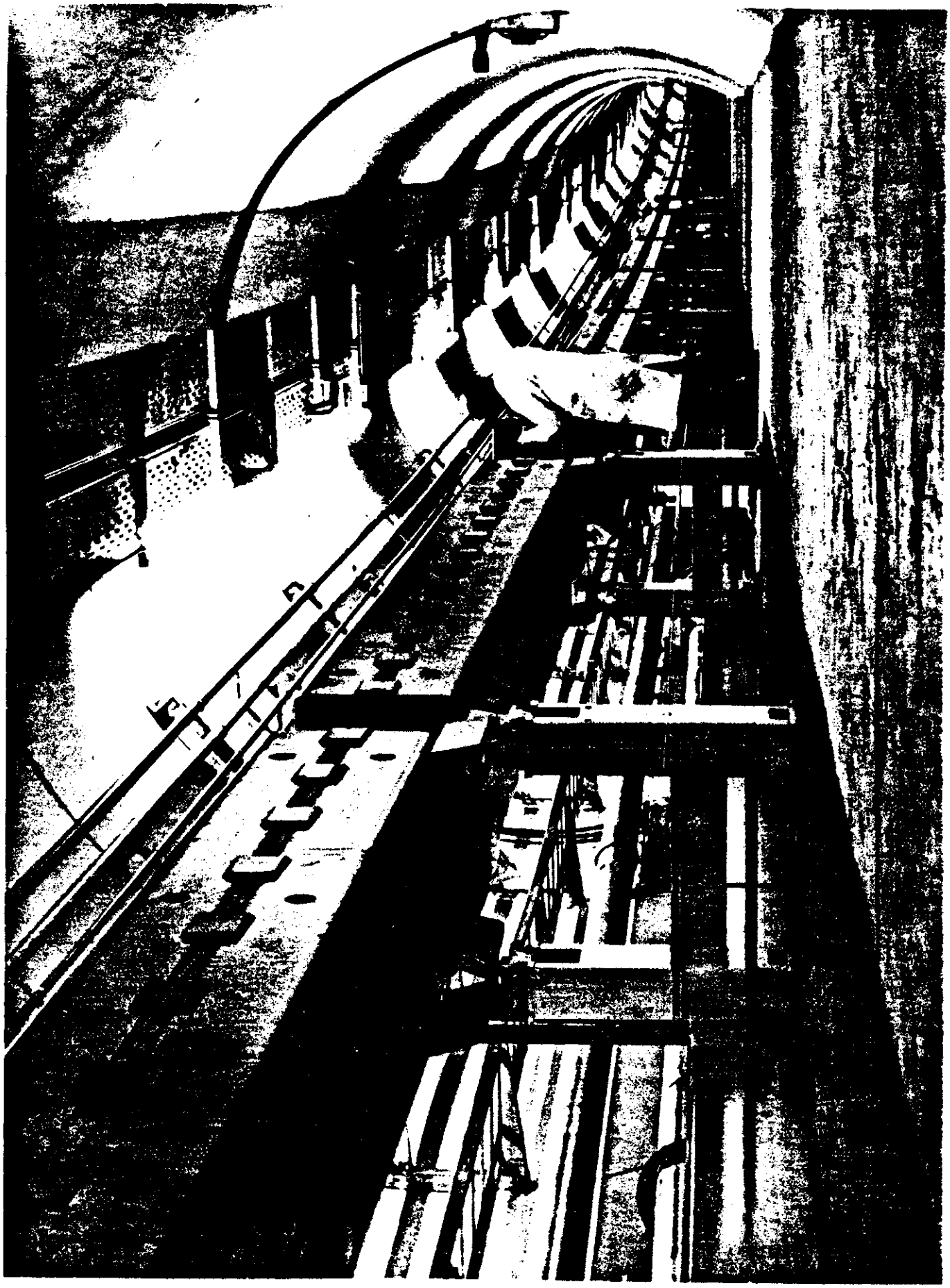

Fig. 1.25

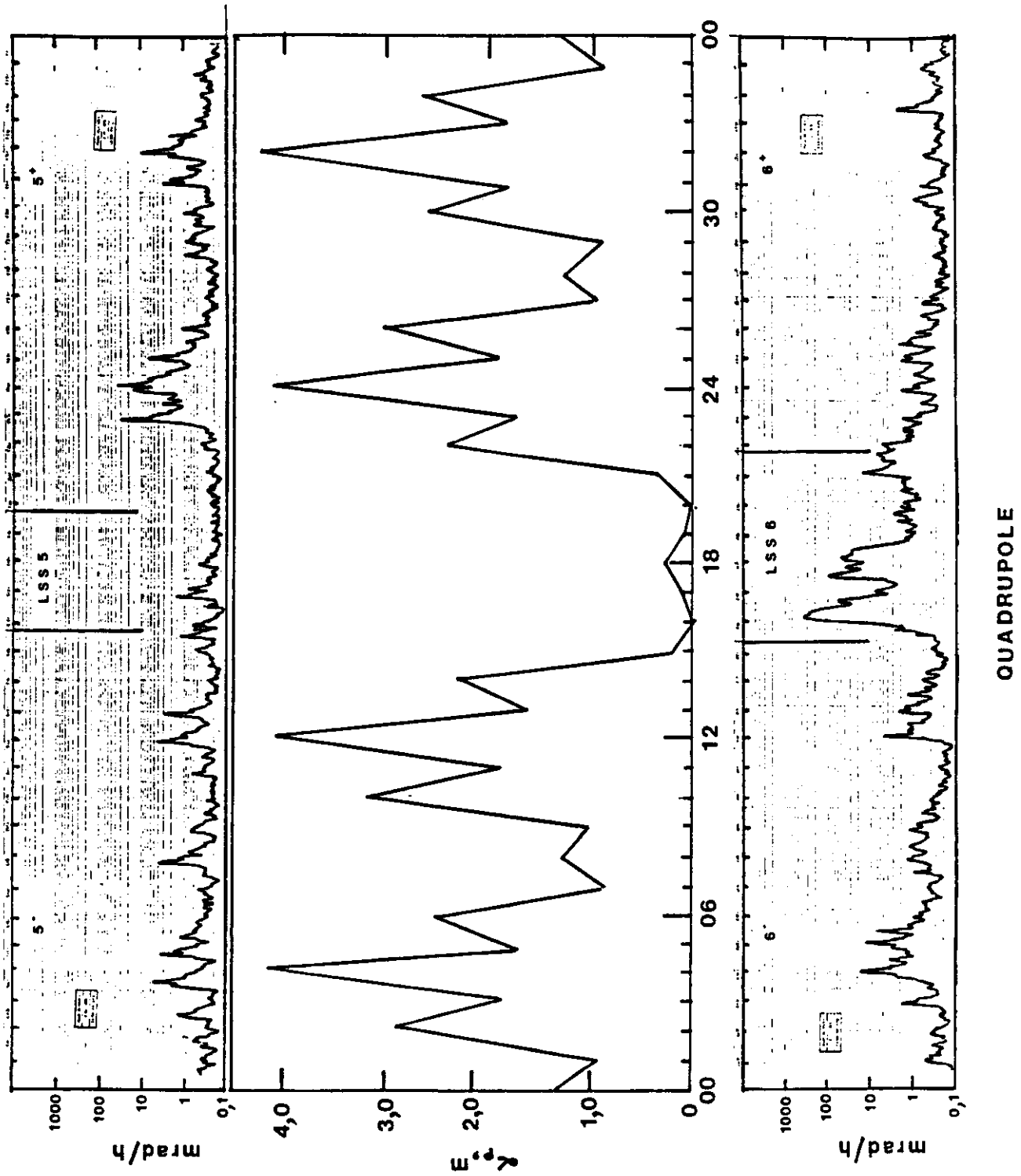

QUADRUPOLE
mrad/h
1000
100
10
1
0,1
LSS 5
5⁻
5⁺
4,0
3,0
2,0
1,0
0
00
06
12
18
24
30
00
LSS 6
6⁻
6⁺

Fig. 1.26

CHAPTER 2

The Radiation Environment of Positive-Ion Accelerators

'Strange to the world, he wore a bashful look,
The Fields his study, Nature was his book'

from 'The Farmer's Boy-Spring'
Robert Bloomfield (1766-1823)

CHAPTER 2 CONTENTS

2.1 Introduction

2.2 Prompt Radiation Fields

- Historical Background
- Operational Experience at High-Energy Accelerators
- Typical Neutron Spectra at Proton Accelerators
- Charged Particle Environments outside High-Energy Proton Accelerator Shields
  - Muons
  - Protons
- Heavy-Ion Accelerators
- Interpretation of Accelerator Radiation Measurements
  - The Evaluation of Dose Equivalent Produced by Neutrons
  - Operational Dose-Equivalent Quantities for Neutrons
  - Recent Developments

2.3. Induced Radioactivity

- Introduction--The Remanent Radiation Field
- Characteristics of the Remanent Radiation Field
  - Particle Energy
  - Radionuclides Produced
  - Reaction Cross Sections
  - The Decay of Residual Radioactivity
- Magnitude of the Problem of Induced Radioactivity
- Induced Radioactivity
  - Dose Rate from Electrons and Positrons
  - Ferrous Materials
  - Non-Ferrous Materials
- Maintenance and Handling of Radioactive Accelerator Components
- Disposal of Radioactive Accelerator Components

References for Chapter 2

Figure Captions for Chapter 2

CHAPTER 2

THE RADIATION ENVIRONMENT OF POSITIVE-ION ACCELERATORS

2.1 INTRODUCTION

The 'prompt' radiation of particle accelerators exists only while they are in operation. It results as a natural consequence of the acceleration process and the utilisation of the accelerated beam.

As we saw in Chapter 1, particle acceleration is achieved by the interaction of charged particles (ions) with stable or varying electrical and magnetic fields. Under such conditions there are many potential sources of radiation. The acceleration process is not totally efficient: particles are lost before achieving the maximum energy and interact with the accelerator structure. Such losses may occur, for example, close to focussing or bending elements. In many positive-ion accelerators it is possible for electrons to back-stream along the potential gradients in a direction opposite to that travelled by the positive ions. The interaction of such accelerated electrons with accelerator components may result in the copious production of x-rays. Beam which is fully accelerated and utilised interacts with target elements, which are then sources of radiation.

In general the higher the energy of the particles accelerated the more complex the character of the 'prompt' radiation field may be. Thus at accelerators such as the 70-GeV Synchrotron at Serpukhov or the 800-GeV proton synchrotron at Batavia it is possible to find a wide range of radiation environments, depending upon the thickness of the shielding, in which, for example, thermal neutrons dominate, intermediate energy neutrons dominate, fast neutrons dominate or muons dominate the radiation field (An 78, McC 77, McC 81).

The most complex radiation environments around particle accelerators will generally arise at locations where the shielding between the radiation source and the point of measurement is 'thin'. Before interacting the accelerated beam is, of course, essentially monoenergetic, consisting of only one particle type. Passage through the accelerator structure, experimental equipment, or thin shielding will lead to the partial development of electromagnetic and hadronic cascades and the production of many types of particle distributed over a wide range of energies. Accident dosimetry at particle accelerators may be particularly difficult because of this complexity of the radiation field in regions of high intensity where the cascades may only be partially developed (Pa 73). The production of secondary radiations may also be of concern, for example, in the application of charged particles to therapy where the absorbed dose to tissues adjacent to the irradiated tumour must be assessed (McC 84b, Sm 81, Sw 80). Neither of the previous two examples can be considered routine radiological protection, but thin or intermediate shields may cause even routine problems. Two examples will suffice: firstly at very high energies; secondly for a heavy-ion accelerator.

During the past ten years the radiation environments around high-energy accelerator facilities have undergone a subtle change. The external radiation fields from the earliest proton synchrotrons

(Cosmotron, Bevatron) mainly came from the bulk shielding of the accelerators themselves. As the shielding of the accelerator proper was improved the dominant radiation sources came from the extracted primary beam lines (AGS, CPS, Nimrod). Secondary beams from these second generation proton synchrotrons were of little importance as radiation sources. However, at the highest energy facilities (Fermilab and the CERN SPS) it is possible for secondary beams to have intensities equal to or greater than the intensity of the early synchrotrons. These secondary beams are typically transported through lightly shielded areas, often without roof shielding, because beam losses are small. It is expected that the quality of the radiation fields around these unshielded, or lightly shielded high energy (>100 GeV) beams will be very different from those found around the well shielded second generation proton synchrotrons. Theoretical cascade calculations predict the presence of protons and charged pions under certain circumstances. The existence of this charged component in the field is of great importance; the techniques currently used to measure dose equivalent may not be entirely adequate. The conventional dosimeters (e.g., film) may be incorrect. Charged particle fluence to dose equivalent conversion coefficients (particularly for negatively charged pions) need to be determined' (Th 85a). [See also later in this chapter.]

In the second example McCaslin and his colleagues have found regions outside the shielding of the Biomedical Facility of the Bevalac where a small charged particle field exists (McC 83, McC 84a). It is suggested that tritons produced at the target have sufficient energy to penetrate the shield wall. These energetic charged particles can perturb the response of many radiation detectors.

Outside thick shields, however, the situation becomes simpler. Despite the large variety of high-energy particle accelerators, both with respect to beam characteristics and utilization, their external radiation environments outside thick shields are often quite similar, and are usually dominated by photons and neutrons or possibly by muons at the highest energies (de S 62a,b).

In many branches of radiation protection it has been customary to quantify radiation fields solely in terms of gross properties such as exposure, absorbed dose or dose equivalent. This procedure is inadequate at accelerators. In order to perform properly the tasks required of a health physicist at an accelerator (such as personal dosimetry, the design and construction of radiation-measuring instruments, general radiation and particle beam dosimetry, shielding design or determination of induced activity), it is vital that the detailed composition of the radiation environment be understood in terms of the constituent particles. The study of these environments in terms of the energy spectra of their separate components is still being developed, and more extensive measurements are required. The published information only describes neutron spectra and is limited but, when supplemented by information from cosmic-ray experiments and neutron transport theory, enables some general conclusions to be made concerning radiation fields produced by proton accelerators.

Shielding studies have shown that the radiation field reaches an equilibrium condition within a few mean-free paths inside an accelerator

shield (see Chapter 4). The shape of the neutron spectrum observed at a shield-air interface is very close to that which exists within the shield, but may be perturbed at the low-energy end, due to the scattering and leakage through holes in the shielding.

2.2 PROMPT RADIATION FIELDS

HISTORICAL BACKGROUND

In the early fifties, following the successful operation of several accelerators in the GeV energy region, interest in accelerator radiation problems had become widespread. A conference held in New York in 1957 indicated the concern of several laboratories in the United States (So 57) and by 1962 an international meeting was organized in Paris (Bo 62).

Experience at the 184-Inch Synchrocyclotron at Berkeley and the early proton synchrotrons-the Cosmotron and Bevatron-rapidly established the qualitative nature of their radiation environments outside thick shielding (Pa 65, Sm 58, Sm 62). A general rule emerged showing that neutrons between 0.1 and 10 MeV contributed more than 50% to the dose-equivalent contribution of the radiation field; γ-rays and low energy neutrons contributed about 10–20%, with the balance made up by neutrons greater than 10 MeV in energy.

In order to quantify the high-energy neutron contribution to dose-equivalent more precisely, Patterson et al. (Pa 59) suggested that the equilibrium neutron spectrum low down in the atmosphere produced by the interaction of the primary galactic cosmic radiation (mainly protons) must be very similar to that generated in the shield of a high-energy proton accelerator. The cosmic ray neutron spectrum had previously been measured at several altitudes by Hess et al. (He 59) and was shown to reach equilibrium rapidly (at depths greater than 200 g/cm^2). Using the Hess spectrum and fluence to dose-equivalent conversions given in NBS Handbook 63 (NCRP 57), Patterson et al. concluded that 'by far the largest contribution to total neutron dose equivalent comes from neutrons in the energy interval from 0.10 to 30 MeV' (Pa 59). Somewhat later Tardy-Joubert (Ta 65) pointed out that, at energies above 50 MeV, the Hess spectrum was consistent with that deduced from an analysis of the prong-number distribution of stars produced in nuclear emulsion exposed at various altitudes above the earth's surface (Ro 54).

These similarities to the cosmic ray spectrum also explain the relative unimportance of protons in contributing to the dose-equivalent (Pe 66). At energies greater than a few hundred MeV, protons are present in numbers comparable with neutrons. At lower energies, however, protons are depleted by ionization losses. Puppi and Dallaporta (Pu 65) have suggested that the neutron to proton ratio (N/P) in an equilibrium spectrum is of the form:

$$\frac{N}{P} = \frac{W^2}{W^2 - (m_0c^2)^2} \qquad (2.1)$$

where

W is the nucleon total energy,

m_0c^2 is the nucleon rest mass.

Given Eq. (2.1) it is trivial to show that protons contribute little to the dose-equivalent in an equilibrium cascade spectrum.

By early 1965 there was sufficient experience at high-energy accelerators at Berkeley (Sm 58, Sm 62, Pa 65), CERN (Ba 65a, b), the Rutherford Laboratory (Pe 65, Pe 66), Saclay (Ta 65) and elsewhere (Ko 70, USAEC 65) to confirm that the cosmic-ray- and accelerator-produced neutron spectra were indeed quite similar. Thus, for example, at the 1966 Vienna meeting Perry (Pe 66) summarized experience at the British 7-GeV proton synchrotron as follows:

> '...the energy spectrum varies from place to place but always falls off rapidly with increasing energy. Most of the neutron flux and dose equivalent is due to neutrons with energies between 0.1 and 10 MeV. The dose contributions from thermal and very high energy neutrons are both very small'.

Table 2.1 shows a summary of data given by Perry showing the composition of the radiation field outside the shielding of a 7-GeV proton beam.

This experience with accelerators in the GeV energy region gave increased confidence in the earlier arguments of Patterson et al. (Pa 59) concerning the probable shape of the neutron equilibrium spectrum and led to the use of the Hess spectrum as the design neutron spectrum for the specification of the shields of several high-energy accelerators in the early sixties (CERN 64, Co 65, de S 62a,b, LBL 65, Th 67). For this assumption to be valid it was necessary that the equilibrium spectrum be determined by the character of the interaction mechanisms of the nuclear cascade and be essentially independent of the energy of the incident proton. Some theoretical cascade calculations by Riddell (Ri 65) lent support to this assumption but the extrapolation from experience in the GeV energy region to hundreds of GeV could not be made without reservation. Patterson (Pa 65) indicated the need for more detailed information of the neutron spectrum between 1 and 10 MeV where 'there may or may not be a flattening due to the production and scattering of evaporation neutrons'. Nevertheless by early 1965 there was both a good qualitative and fair quantitative understanding of the radiation environments outside high-energy proton accelerator shielding.

OPERATIONAL EXPERIENCE AT HIGH-ENERGY ACCELERATORS

As we have just seen, in the latter part of the fifties, experience at the 184-Inch Synchrocyclotron and Bevatron (Lawrence Berkeley Laboratory) and the Cosmotron (Brookhaven) allowed estimation of the qualitative nature of their radiation environments outside thick shielding. Although detailed spectra were not obtained, a general rule emerged for proton accelerators showing that neutrons between 0.1 and 10 MeV contributed more than 50% to the total dose equivalent in the radiation field. This fact was explained by analogy with the cosmic-ray-produced neutron spectrum. By 1965 there was sufficient experience at many high-energy proton accelerators around the world to confirm that the neutron spectra outside accelerator shields and the cosmic-ray spectrum were, in general, quite similar.

There were, however, some data that pointed to exceptions to this simple general rule. Table 2.2 (Ba 64, Ba 65a,b, Ca 65) gives a typical example where the relative composition of dose equivalent measured through thick shielding above accelerator targets is given at the same accelerator, the CERN proton synchrotron (CPS). Data are given for a concrete shield and for an earth shield. The measurements above the concrete shield are very similar to those reported at other accelerators, such as the British 7-GeV proton synchrotron Nimrod (Pe 65, Pe 66) and suggest a neutron spectrum similar to that produced by cosmic rays (Pa 59), while the data measured above an earth shield indicate a relatively large contribution to the dose equivalent by high-energy neutrons.

Relative data, of the type given in Table 2.2, are not adequate to determine whether the high fraction of dose equivalent contributed by high-energy particles was due to a deficit of low-energy neutrons or to a surfeit of high-energy neutrons. For this, a more detailed understanding of the neutron spectrum is necessary. In the past 20 years more specific information on the neutron spectra found around accelerators has been obtained by the use of nuclear emulsions and activation detectors (Th 73, Th 85a).

TYPICAL NEUTRON SPECTRA AT PROTON ACCELERATORS

A few examples of neutron spectrum measurements selected from the available literature are shown in Figs. 2.1 through 2.5.

Throughout Chapters 2 and 3 we will refer to several neutron spectra, measured at particle accelerators or calculated, by convenient abbreviations. It is appropriate at this juncture to define these symbols.

1/E the familiar 1/E differential energy spectrum.

RT a neutron spectrum determined at the CERN 28-GeV proton synchrotron (CPS) above the earth shielding with a target intercepting the beam as a primary radiation source.

PSB measured at the CPS above a concrete shield, again with a target acting as the primary source.

BEV measured at the University of California Radiation Laboratory (now Lawrence Berkeley Laboratory) 6.3-GeV proton synchrotron.

X2 measured at the 7-GeV proton synchrotron of the Rutherford Laboratory, outside concrete shielding.

P1 measured as for X2 but outside steel shielding.

PLA the ambient neutron spectrum around the 50-MeV proton linac of the Rutherford Laboratory.

CR the Hess cosmic-ray neutron spectrum.

PPA measured at the Princeton-Pennsylvania Proton Acclerator using Bonner spheres.

Figure 2.1 shows spectra measured by the Lawrence Berkeley Laboratory Group during the middle 1960s (Gi 68, He 59, Pa 59). A four-detector combination was used: a boron trifluoride counter in a

cylindrical moderator, the $^{27}Al-^{24}Na$ and $^{12}C-^{11}C$ passive activation detectors, and a bismuth ionization chamber (see Chapter 3). These spectra are reasonably well constrained in the 100-keV to 100-MeV region. Outside this energy range the spectra are not well determined by the measurements but general physical principles are invoked to give reasonable spectral shapes. From these early measurements several features emerge. The 'ring-top' spectrum (RT) was measured above the earth shielding of the CERN 28-GeV proton synchrotron. This earth contained more moisture than the concrete shield of the PS bridge at the same accelerator where the PSB spectrum was measured. The Bevatron spectrum (BEV) shows a broad peak in the 1–100 MeV region; the negative slope of the cosmic-ray spectrum (CR) in this energy region coupled with the response of the moderated BF_3 counter implies a peak in the spectrum below 1 MeV.

Spectra were obtained at the 7-GeV proton synchrotron accelerator of the Rutherford Laboratory, 'Nimrod', using the multisphere technique with a ^{6}LiI scintillator as the thermal neutron detector (St 67). Some of these are shown in Fig. 2.2. All the spectra shown are relatively flat: the X2 spectrum, taken directly outside the shield around an extracted beam target, is significantly harder than the P1 spectrum, which was measured in an environment where the outer surface of the direct shield was of iron and there was a significant contribution to the field from neutrons scattered by local concrete blocks.

Spectra obtained by the Princeton-Pennsylvania Health Physics Group, also using Bonner spheres (see Fig. 2.3), show a much more oscillatory character (Aw 66), probably reflecting the different spectrum unfolding routine used from that used at the Rutherford Laboratory.

Figure 2.4 shows the results of a theoretical calculation by O'Brien (OB 68, OB 71) where the observed features of a 1/E type spectrum coupled with a peak in the 1–10 MeV energy range are confirmed. In addition the calculation by O'Brien reveals a second peak in the 100 MeV energy region, where none of the measurements described above would be expected to give good resolution. This high-energy peak was confirmed experimentally by Madey et al. (Ma 76) and also in calculations reported by Stevenson of the high-energy cascade in iron [see Fig. 2.5 (St 84)].

CHARGED PARTICLE ENVIRONMENT OUTSIDE HIGH ENERGY PROTON ACCELERATOR SHIELDS

Muons

Muons arise from the decay of pions and kaons, either in particle beams or in the cascade induced by high-energy hadrons. They can also be produced directly in high-energy hadron-nucleus interactions. Since muons are weakly interacting particles, they can only be stopped by 'ranging them out'. The mean muon range as a function of energy for different materials is given in Fig. 2.6, taken from the data of Richard-Serre (Ri 71). The physics of muon production and scattering is discussed by Stevenson (St 76). Muons from pion decay have a momentum spectrum that extends from 57% of the momentum of the parent pion to the pion momentum itself. Secondary pion beams generally have endstops of longitudinal depths of about 1-2 m of iron, calculated from hadron attenuation considerations alone. Thus Fig. 2.6 indicates that decay

muons will penetrate the endstops for pion beams whose momentum is greater than some 2 to 3 GeV. The decay length for a pion is approximately 55 m per GeV/c of pion momentum. Thus in a decay path of about 20 m, the decay probability of a 10-GeV/c pion is almost 4% or, in other words, there will be a beam of muons whose intensity is some 4% of the incident pion beam which penetrates an endstop designed purely for hadron attenuation. Special care must be taken to avoid radiological hazards of this nature by making sure that sufficient shielding is provided to range out the muons or that diffusion by multiple scattering reduces the flux density to sufficiently low levels.

Hadron endstops for proton beams are typically 4 to 5 m in depth (Fr 71). Because the spectrum of muons resulting from meson decay in the hadron cascade is rather soft, the depth required to reduce muon flux densities to acceptable levels corresponds to the range of a muon having a momentum of about 75% of that of the incident proton (Ke 64, Ke 68). Thus muons can be expected to dominate longitudinal shielding considerations for proton beam dumps at proton energies of above 20 GeV. Cowan (Co 62) reported that substantial muon intensities were observed downstream from targets when the BNL 33-GeV AGS first came into operation. Muons have been observed behind low-energy pion beams at the Nimrod accelerator. They are a regular feature of the radiation field at all the multi-GeV CERN accelerators (Be 71, Ni 74) and at Fermilab (Co 83, Ka 72, Th 71). Cones of muon beams are relatively easy to find by measurement, but an exact diagnosis of the origin of the muons is often difficult (see for example the work of Moore and Velen [Mo 74]).

Except for their higher mass, muons are similar in every respect to electrons. In principle the dose from muons can be measured by normal ionization chamber techniques, but Hoefert (Ho 84) has noted discrepancies of up to 30% between the readings of different detector types in pure muon fields. The problem of muon dosimetry in general and of fluence to dose-equivalent conversion in particular is discussed by Stevenson (St 83).

Cossairt has described muon measurements made at the Fermi National Accelerator Laboratory using a portable muon telescope (Co 83).

Protons

We have already seen that early investigations suggested that the presence of protons in the equlibrium radiation field outside the shielding of the high-energy accelerators would not significantly contribute to the dose equivalent that was largely due to neutrons. We have also mentioned the reservations to this generally correct observation for accelerators in the 100-GeV energy region (Th 85a).

It may indeed be quite convenient to investigate radiation fields outside accelerator shielding by studying the protons in equilibrium with the neutrons. Unfortunately very few laboratories have used this technique for the purposes of radiation protection. Penfold and Stevenson (Pe 68) have reported the use of a proton telescope to detect intense sources of radiation inside thick shields along an external proton beam. The most important work has been done at Dubna where Aleinikov et al. have reported proton spectrum measurements using counter telescope techniques (Al 75). Using a proton telescope and a (dE/dx)

spectrometer these authors have reported studies of both the energy and angular distributions of protons greater than 40 MeV outside the 2 metre thick concrete shield of the 660-MeV Dubna synchrocylotron (Al 75, Al 79). In appropriate geometrical configurations the proton spectra observed are qualitatively of the form predicted by Eq. (2.1), having a broad maximum at a proton energy of about 100 MeV. Figures 2.7 (a and b) show proton spectra measured by the Dubna group for the locations shown in Fig. 2.8. The spectrometer was positioned so as to point along a beam channel through the iron shielding wall [approximately 3000 g cm^{-2} thick] (position A) or orthogonally to the shield wall (position B). The proton spectra are seen to have distinct differences in character for these two settings of the spectrometer.

The application of spark chambers to this problem should prove extremely helpful; Hajnal et al. (Ha 69) have reported the use of an optical spark chamber to study the secondary-neutron energy spectra emerging from a 40-cm-thick iron shield bombarded by 2.9-GeV protons. Rindi (Ri 69) and his co-workers (Li 73, Ma 74, Ri 74) have described the construction of an instrument that utilizes multiwire spark chambers with magnetostrictive readout and that may be used for measuring neutron and proton spectra up to energies of about 300 MeV in low-intensity fields.

It is now possible to investigate the charged-particle spectra outside shielding using radiation transport code calculations. As an example of what is possible Stevenson has reported some work using the analogue Monte Carlo hadron cascade FLUKA82 (Aa 83, Aa 84, St 84), which was used to generate proton, neutron and charged-pion spectra above a kinetic energy limit of 50 MeV. Protons of 30 GeV were allowed to interact along the axis of an iron cylinder of density 7.8 g cm^{-3}. Particles were scored as they crossed plane surfaces at depths of 0.5, 1.0, 1.5 and 2.0 m into the cylinder and at cylindrical surfaces of 0.2, 0.4, 0.6 and 0.8 m radius. The geometry of the calculation is illustrated in Fig. 2.9 and the energy spectra obtained are shown in Figs. 2.10 and 2.11. The 'forward' spectra are related to the flux densities integrated laterally over planes perpendicular to the incident protons; the 'lateral' spectra are related to the flux densities integrated longitudinally over cylindrical surfaces centered on the beam direction. The energy binning used for this analysis is again based on a lethargy scale. Each decade of energy is divided into five equal logarithmic intervals. This representation has the advantage of showing departures from a 1/E spectrum since, if x is put equal to log E, $\phi(x)$ equals $E\phi(E)$, and if $\phi(E)$ is proportional to 1/E, $\phi(x)$ is constant.

Of the secondary particles produced in the cascade about 9% were charged pions, equally of either sign.

The ratios of the numbers of particles crossing successive scoring boundaries for each particle type are given in Table 2.3. In the 'forward' case the ratios are essentially constant beyond a depth of 1 m. There is no evidence for an energy dependence in any of these ratios. In the 'lateral' case, a similar conclusion may not be drawn because of the poor statistical accuracy of the calculations (no protons were observed beyond the 0.2-m boundary and no pions beyond the 0.4-m boundary).

The ratios of the number of protons to the number of neutrons and of number of pions to number of neutrons are plotted as a function of energy at the various depths in Figs. 2.12 and 2.13. As expected, the proton-neutron and pion-neutron ratios are significantly less than unity at lower energies where slowing down removes many charged particles from the cascade. At energies greater than 1 GeV the proton-neutron ratio is constant and slightly greater than unity, whereas the pion-neutron ratio decreases after peaking at about 1 GeV. In the 'forward' case there is some evidence that the ratios initially decrease with increasing depth in the iron block but that they remain constant after a depth of about 1 m. It is not possible to draw a similar conclusion in the 'lateral' case because of the statistical limitations of the calculation. However, both the proton-neutron and the pion-neutron ratios are significantly lower than for the 'forward' case.

Thus, within the statistical accuracy of the calculation, one can talk of equilibrium spectra of particles at longitudinal depths of greater than 1 m and, at least for the neutron component, at radial distances of greater than 0.4 m. These calculations are important in that they demonstrate the essential validity of the conclusions of the workers in the fifties and sixties whose work has been described.

HEAVY-ION ACCELERATORS

Very little information currently exists on the radiation environments of heavy-ion accelerators. Little new information has been obtained since that described in the review provided more than 10 years ago by Patterson and Thomas (Hu 60, Pa 73, St 69).

Aleinikov et al. have reported the angular distribution of dose equivalent and the neutron spectrum around a thick target bombarded by 6.6 MeV/amu ^{58}Ni ions (Al 85). An analytical expression for the dose equivalent angular distribution is obtained that fits the experimental data well between 0° and 135°. The total neutron yield was estimated to be 1.6×10^{-4} neutrons per incident ion. In this paper references are given to other work at Darmstadt and Oak Ridge where the dose equivalent was determined at a fixed angle for a series of ions (Fe 80, Oh 80) or at different angles for $^{12}C^{+6}$ and $^{232}U^{+4}$ ions (Fe 80). Ryder has reported neutron fluence rates for deuteron and other ions incident on optimum-thickness targets of Al, Cu and Ta (Ry 82, see also Chapter 1).

Smith and his colleagues have reported measurements of the neutron production by a 920-MeV alpha particle beam incident on various targets (McC 84b, Sm 81) and McCaslin et al. have begun to make measurements in the areas around the Bevalac (see Section 1.5 and Refs. McC 83, McC 84a, b, McC 85). Many of these measurements are preliminary, but the radiation environment outside their shielding may indicate some interesting departures from the usual radiation fields found at proton accelerators. Detailed investigation of these fields as a function of ion energy, ion species and target as well as attenuation measurements in shielding are needed (McC 85).

INTERPRETATION OF ACCELERATOR RADIATION MEASUREMENTS
(See also Section 3.8)

Perhaps the most difficult aspect of radiation protection dosimetry at particle accelerators is the interpretation of measurements in terms of the particular dose-equivalent quantities required by regulation and statute.

The quantity dose equivalent was first formally defined as recently as 1968 (ICRU 68), although its origins go back a further twenty years to the application of RBE-dose to radiological protection (Pa 48). Thomas has reviewed the long-standing discussion concerning the definition of both the quantity and its units (Th 85b). For sources of radiation exposure external to the body the dose equivalent, H, is defined by the equation:

$$H = \int_0^\infty Q(L_\infty) \frac{dD(L_\infty)}{dL_\infty} dL_\infty \qquad (2.2)$$

where L_∞ = the linear collision stopping power in water, $\frac{dD(L_\infty)}{dL_\infty}$ = the absorbed dose in the stopping power increment from L_∞ to $L_\infty + dL_\infty$, $Q(L_\infty)$ is the quality factor as a function of stopping power as defined by ICRU and ICRP (ICRP 73, ICRU 68), and the integral of Eq. (2.2) is evaluated over the entire L_∞ spectrum.

In the determination of the dose equivalent in the radiation fields of particle accelerators Eq. 2.2 is not normally used directly, for example by the determination of the absorbed dose distribution as a function of L_∞. Alternative means are usually taken. Since in most cases we are concerned with measurements of neutrons, the interpretation of neutron measurements in terms of dose equivalent will be discussed in more detail.

The Evaluation of Dose Equivalent Produced by Neutrons

The evaluation of dose equivalent from neutrons, particularly at high energies, poses severe technical difficulties which are compounded by 'inadequate or incomplete definition of the quantity to be measured' (Wa 84, Wa 85). McCaslin and Thomas have reviewed neutron dosimetry intercomparisons made by several high-energy laboratories and while they found reasonable agreement in the determination of the physical parameters of the radiation field, the conversion of these data to dose-equivalent produced disagreement by almost as much as a factor of two (McC 81). They concluded that these discrepancies were often due to the use of different dose-equivalent quantities.

Operational Dose-Equivalent Quantities for Neutrons

The primary limits for radiation exposure recommended by ICRP are expressed in terms of the dose equivalent to various tissues, H_T, the whole body dose equivalent, H_{wb}, and the effective dose equivalent, H_E. For external radiation exposure secondary limits are expressed in terms of the shallow and deep dose equivalent indexes $H_{I,s}$ and $H_{I,d}$ (ICRP 77). Since, in general, neither the primary nor the secondary limits may be measured directly operational quantities must be developed (Ha 81, ICRP 82, ICRU 85, Wa 85).

The most widely used operational dose equivalent quantity for neutrons is the dose equivalent, H_c, determined from a measured neutron fluence, ϕ_m, and a fluence-to-dose-equivalent conversion coefficient, h or g,* according to the equations:†

$$H_c = h\phi_m \tag{2.3a}$$

$$\dot{H}_c = \phi_m/g \tag{2.3b}$$

Equations (2.3a and b) assume monoenergetic neutrons but, of course, both ϕ and h are functions of neutron energy. Thus, more exactly:

$$H_c(E) = h(E)\phi_m(E) \tag{2.4a}$$

$$\dot{H}_c(E) = \frac{\phi_m(E)}{g(E)} \tag{2.4b}$$

Tabulations of the conversion coefficients h(E) or g(E) for various neutron energies have been given for example in NCRP Report 38 (NCRP 71) or ICRP Publication 21 (ICRP 70, ICRP 73). (For a discussion of the derivation of these conversion coefficients see the references given in the review article by Thomas [Th 85b].) The ICRP has recently revised the conversion coefficients published in 1973 and these should now be used (ICRP 86).

The conversion coefficients of NCRP Report 38 and ICRP Publication 21 were determined for an incident broad parallel beam of incident neutrons on a tissue-equivalent phantom (e.g., 30-cm-thick tissue-equivalent slab, 30-cm-diameter by 60-cm-high tissue-equivalent cylinder) (Al 70, Ar 73, Au 68, Ir 67, Ne 66, Sn 50, Sn 57, Sn 71, Wr 69, Ze 65) or the ICRU sphere (Ch 78, Ch 79, Ch 81a,b, Sh 83).

The conversion coefficients determined in this way define a set of conversion coefficients $h_m(E)$ for monoenergetic neutrons as a function of energy E. These conversion coefficients may be used to determine a quantity originally called the maximum dose equivalent (MADE), H_m, (ICRU 71) defined by the equation

---

*Two conversion coefficients have been in common use. The first h(E) is expressed in units of dose equivalent per unit fluence (e.g., rem cm^2, or Sv cm^2), while the second g(E) (now obsolete) was expressed in units of fluence rate required to produce a dose-equivalent rate of 2.5 millirem h^{-1} or 1 millirem h^{-1}.

† Throughout this text the subscripts m, p and s indicate parameters, e.g., dose equivalent, H, or conversion coefficients, g(E), corresponding to dose equivalents determined at the maximum, m, or surface, s, in the human body or according to the method of Shaw et al. (Sh 69).

$$H_m = \int_{E_{min}}^{E_{max}} h_m(E)\phi(E)\, dE \qquad (2.5)$$

where $\phi(E)\, dE$ is the differential energy neutron spectrum.

This procedure is not entirely logically consistent since the argument of the integral contains two elements–the first a hypothetical neutron fluence, which would exist if the phantom or body were not present; the second a fluence-to-dose-equivalent conversion coefficient for a particular neutron energy. These conversion coefficients are, however, determined by locating the maximum dose equivalent that occurs in the phantom. The location of this maximum varies with neutron energy. The procedure of integration (summation) of maximum dose equivalents that occur at different positions in the phantom will thus overestimate the actual dose equivalent in typical accelerator spectra. However, this procedure was used at several British and U.S. high-energy accelerators in the 1960s and was endorsed in the recommendations of ICRP Publication 21. This concept was further formalised by Harvey to define the dose-equivalent ceiling (Ha 75). It has now been realised that ceiling quantities are a special subgroup of the so-called 'aligned quantities' (ICRU 85, Wa 85). (See Recent Developments.)

In order to avoid the overestimation resulting from the use of ceiling quantities, a somewhat different method of determining dose equivalent in practical situations at accelerators was adopted at CERN (St 73a, St 73b). Here it was argued that in many cases the radiation penetrating a thick concrete shield essentially had achieved an equilibrium particle spectrum that would not be significantly altered by the presence of the human body. In such circumstances the human body merely acts as additional attentuating material, and the maximum of the depth-dose-equivalent distribution will lie close to the body surface. Furthermore, it is a feature of the radiation survey instruments that are commonly used in operational health physics (e.g., tissue-equivalent ionization chambers), that the wall thickness is selected so that the measurement determines the dose near the body surface. With this philosophy one can take the values of the dose equivalent at or near the surface of the phantom in the calculations mentioned above to define a new conversion function, $h_s(E)$, which when integrated with the spectrum as before, defines a surface dose equivalent, H_s, in a way which is rigorously correct for particle-spectra because a definite position in the phantom is now chosen.

$$H_s = \int_{E_{min}}^{E_{max}} h_s(E)\phi(E)dE \qquad (2.6)$$

Yet another approach was suggested by Shaw et al. (Sh 68a,b, Sh 69) who calculated the distribution of dose equivalent relative to depth in a 30-cm parallel-sided phantom irradiated bilaterally with broad neutron spectra typical of those to be found outside the shielding of high-energy proton accelerators. The maximum of the depth-dose-equivalent curves was taken to define another dose equivalent quantity, the

practical dose equivalent, H_p. The relationship between the three quantities, normalised to H_p, for the spectra used by Shaw et al. is given in Table 2.4. Inspection of Table 2.3 shows that H_m is systematically greater than and sometimes nearly twice as large as H_p, whereas for these spectra H_s never underestimates H_p by more than 15%, but may overestimate it by as much as 70%.

In the past decade the ICRU and ICRP have introduced concepts with the intention of clarifying the quantities to be determined for radiation protection purposes.

In 1973 the ICRU first introduced the concept of the 'dose-equivalent index' (ICRU 73) and three years later extended the concept to include shallow and deep indices (ICRU 76). There is, however, no practical means of locating the maximum dose equivalent in a 30-cm tissue-equivalent sphere, and there are many undesirable properties of the index quantities including nonadditivity (spatial and secular) and non-point specificity. At high energies there is very little difference to be expected between fluence to dose-equivalent conversion coefficients derived either from a 30-cm diameter sphere or a 30-cm-thick parallel-sided slab. These considerations led Stevenson et al. (St 73a,b) to suggest that the concept dose-equivalent index was in fact redundant for dosimetry at accelerator laboratories and that H_s, determined for the appropriate condition of unilateral or bilateral irradiation, was an adequate quantity to 'attempt to relate the absorbed dose to the risk of the resulting biological effects' (ICRP 66).

Recent Developments

During the past decade there have been significant developments that will have a considerable influence in the future on the matter of the interpretation of radiation field quantities in terms of biological risk.

Interestingly enough there have been two different, and perhaps ultimately conflicting, approaches. The first approach has been to improve the basic definition of the quantity dose-equivalent and to derive operational dose equivalent quantities that are suitable for measurement. The second approach has been to suggest changes that require either a partial or a total change in the dose-equivalent system.

In 1977 the ICRP introduced the effective dose equivalent as the primary quantity to be evaluated in radiation protection (ICRP 77). ICRP 26 went on to suggest that for 'external exposures to ionizing radiation, on those occasions when information is lacking concerning the actual distribution of dose equivalents in the bodies, it is possible to assess the maximum value of dose equivalent that would occur in a 30-cm sphere (the deep dose equivalent, $H_{I,d}$,)'. Almost immediately, following the publication of ICRP 26 there were debates published in the literature suggesting that the dose-equivalent indexes might not necessarily provide precise estimates of the effective dose equivalent (Kr 79, Kr 80, OB 78, OB 80).

It has been necessary to assemble a considerable quantity of data, showing the relationship of many dosimetric quantities to the geometry

of the irradiation and physical parameters of the radiation field, in order to be able to determine the accuracy with which the index quantities approximate the effective dose equivalent. Over the past nine years this has been accumulated for photons of energy up to 10 MeV and neutrons of energy up to 14 MeV (Bu 78, Bu 83, Ch 79, Ch 81a,b, Ch 81c, Di 79, Dr 78, Kr 82, Sh 83). Committees of both international commissions have been reviewing these data-the ICRP with a view to revising fluence-to-dose-equivalent conversion coefficients and the ICRU with a view to improving the definitions of operational dose-equivalant quantities (So 83, Wy 83).

Dose-equivalent quantities have one important property for radiation protection-they provide a system that is unified for all radiation. [At the present time different operational quantities are used for photons (exposure), for β-particles and electrons (absorbed dose in air or tissue), and for neutrons (fluence, dose-equivalent ceiling).] There is then some argument for retaining the use of some form of dose-equivalent quantity(ies) in the future. The dose-equivalent indexes have, however, not been widely used in radiation monitoring because of both practical and theoretical difficulties in their application. In searching for improved quantities it is possible to list the desirable properties of dose-equivalent operational quantities used in monitoring. They should be:

- Measurable under operating conditions
- Compatible with existing instruments
- Physically realizable in standards laboratories
- Calculable
- Related to primary limits
- Durable
- Additive, single-valued, point specific
- Relatable to a specific phantom.

The choice of a specific phantom is not easy. The ICRU sphere has the advantage of being uncomplicated and accepted by international authorities; the specification of its composition (tissue) is unlikely to be changed; it has an isotropic response to radiation. Furthermore, it is a reasonable phantom for calibration purposes (e.g., for personal dosimeters worn on the human abdomen). Such properties make it suitable as the basis of a calibration standard to be set up in a national standards laboratory.

The ICRU sphere, however, can clearly never be used to determine organ dose equivalents or the effective dose equivalent. For this purpose an anthropoid phantom is needed. Several simple alternatives to the sphere have been used for calculation (the 30-cm-thick tissue slab, cylinder, etc.) but all have the principal defect of the sphere. Several complex anthropoid phantoms have been constructed to facilitate organ dose measurements (e.g., Alderson Rando phantom, Plastinaut, Mr. Adam). Extensive calculations of effective dose equivalent have been made in the modified MIRD-5 phantoms ADAM and EVA. Such phantoms are

most important for accurate calculation but doubtless will be subject to continuing improvement. Furthermore, individual anatomical variation in monitored individuals is quite significant, and the accurate determination of organ dose and effective dose equivalent must always demand individual attention. Such arguments tend to suggest that measurements based upon calibrations with the ICRU sphere may be linked, with sufficient accuracy for routine monitoring, both to radiation field quantities and to calculations of dose equivalent in anthropoid phantoms.

The development of suitable operational dose-equivalent quantities requires one further set of simplifications. It is only practicable, for routine monitoring, to specify maximal conditions. (Consideration of the host of alternative radiation conditions is just too complicated.) Such conditions are, in general, obtained when the human body is irradiated by a broad unidirectional parallel beam of radiation incident on the anterior face of the body and leaving from the posterior face.

In discussing radiation fields it is then convenient to define two concepts: expansion and alignment of a radiation field as was done in ICRU Report 39 (ICRU 85). An expanded radiation field is a hypothetical field that everywhere in space has the same particle flux density, energy and angular distribution as the unperturbed field at the point of reference. An aligned and expanded radiation field is a hypothetical field that everywhere in space has the same particle fluence density and energy distribution as the unperturbed actual field at the point of reference but with all radiation incident in one direction. With these conditions of the radiation field specified it is then possible to define quantities including these conditions-making it possible to calibrate physically small instruments, which have an isotropic response, in terms of these quantities which are then referred to as 'aligned dose-equivalent quantities'.

As we have seen, as early as 1973 workers at high-energy accelerator laboratories have found it helpful to define what is, in effect, the aligned dose equivalent at a depth of 10 mm in a tissue-equivalent phantom (St73a,b). Other depths at which these aligned dose equivalents might be specified are 0.07 mm and 3 mm, because of the specification of the thickness of the skin and the depth of the lens by the ICRP (ICRP 77).

Another concept that is of great value in clarifying dose equivalent quantities is that of 'energy summation'. Here the separate maximum dose equivalents from each energy increment of the incident aligned and expanded radiation field, irrespective of where these maximum dose equivalents occur, are summed. The value of the 'energy-summed' quantity is equal to this sum. Aligned and energy-summed quantities were first identified as ceiling quantities by Harvey in 1975 (Ha 75) and are of great practical importance because the so-called neutron 'rem-meters' are designed to measure this quantity.

In 1985 the ICRU published Report 39 entitled 'Determination of Dose Equivalents for External Radiation Sources' in which the conclusions of considerations similar to those given above are summarised. The Commission has selected four operational quantities for the determination of dose equivalents resulting from exteral ionizing radiation

sources. These are:

	Symbol
Ambient Dose Equivalent	$H^*(d)$
Directional Dose Equivalent	$H'(d)$
Individual Dose Equivalent, Penetrating	$H_p(d)$
Individual Dose Equivalent, Superficial	$H_s^p(d)$

These quantities provide a sound metrological basis for the implementation of the current recommendations of the ICRP, are within the International System of Units and achieve a uniform basis for the dosimetry of all types of ionizing radiation. In addition, the quantities are compatible with current practice in radiation monitoring and will not require replacement of existing instruments (ICRU 85).

The ICRU is preparing a second report giving the supporting data and reasons for its recommendations contained in Report 39 (ICRU nd). A third report is planned to discuss the design and construction of instruments to measure the new operational quantities (Wy 83).

The ICRP is currently revising and extending data on fluence-to-dose-equivalent conversion coefficients contained in Publication 21 (ICRP 73). The new data will include conversion coefficients to the maximum dose equivalence (MADE), the index quantities and the ambient dose-equivalent quantities (So 83, ICRP 86). Some of the conversion coefficients are discussed in Chapter 3.

These improvements in the definitions of the dose-equivalent quantities and the improved precision of the conversion coefficients will lead to better agreement between measurements.

Nonspecific comparisons of 'dose equivalent' derived from fluence measurements may be expected to show large differences. Proper comparisons will only follow when the dose-equivalent quantities to be examined are rigorously specified. Many of the apparent discrepancies reported in the literature arise from ambiguity in the definition of the dose equivalent actually determined.

Concurrently with these improvements in clarity of the definitions of dose-equivalent quantities and the ability to remove these quantities there have been some developments that suggest fundamental or partial changes in the present dose-equivalent-based system.

The principal suggestions for piecemeal changes lie in the modification quality factor for neutrons. This has most recently been expressed by the ICRP in the recent statement (ICRP 85):

'The Value of the Quality Factor in the Case of Neutrons

The information now available on the relative biological effectiveness (RBE) of neutrons for a variety of cellular effects in vitro, and for life shortening in the mouse, is being reviewed by the Commission. The implications of this information will be considered as part of a larger review of recommendations to be undertaken by the Commission over the next four years or so. Meanwhile, in the

case of neutrons the Commission recommends an increase in Q by a factor of 2. The permitted approximation for $\bar{Q}$ for fast neutrons thus changes from 10 to 20. These changes relate only to neutrons, and no other changes in Q are recommended at this time.'

Such a view has previously been expressed by the NCRP and by Rossi and his colleagues (NCRP 80, Ro 77, Ro 78). It is not universally supported, however, and is even contested [see for example (St 85a)].

Even more fundamental challenges to the present dose-equivalent system have been suggested on a radiobiological basis by Mole (Mo 79) and on a physical basis by Rossi (Ro 77) [see Section 3.6]. Another challenge is mounted on the grounds that a risk-based system of radiation protection is to be preferred (NCRP 82).

Casarett has succinctly evaluated the disadvantages of our present dose-equivalent-based system of radiation (Ca 82):

> 'It is proper to distinguish the dose equivalent from biological risk. The utilization of rem for dose is inappropriate in the context of risk because the rem is frozen within the LET-dependent quality factor system. Because of the rigidity of this interlocking physically defined system, a change in MPD for one radiation, e.g., on the basis of a new risk estimate, requires, for consistency, changes in the MPDs for the other radiation. If an exception were made and, in effect, the Q for that one radiation were changed instead, that would be tantamount to injecting a bit of the risk system into the current system. For consistency, either the other Q values would need to be changed according to the LET-dependence in the current system or changed on the basis of risk. With the current system, Q is an especially knotty problem in regard to the internal emitter field'.

It is difficult to predict the detailed changes that will occur in our dosimetry systems over the next 10 years. It is perhaps time for a cautious review that can incorporate our present understanding without producing a major disruption in operational radiological protection.

2.3 INDUCED RADIOACTIVITY

INTRODUCTION: THE REMANENT RADIATION FIELD

In addition to the prompt radiation field just described there may exist a radiation field that, by contrast, remains or lingers on after shut-down. This remanent radiation field results from the decay of radioactivity induced in the accelerator structure and its ancillary components by the interaction of the constituent particles of the prompt radiation field: its precise characteristics will depend upon many factors such as the type and energy of the particles accelerated, the beam intensity and materials irradiated by the primary beam and secondary radiations.

The specification of the properties of this remanent radiation field merits some effort because it may have consequences for:

- The exposure of personnel working in accelerator environments when the accelerator is not operating.
- The maintenance of accelerator components--in particular the control of the spread of contamination during operations such as the turning, drilling or milling of radioactive components.
- The administrative control of movement of items from accelerator areas that might be radioactive.
- The environment of particle accelerators into which radioactive contaminants--particularly in gaseous or liquid form--may be generated.
- The disposal of unwanted accelerator components.

This chapter discusses the general characteristics of the remanent radiation field and its consequences for accelerator operation. Chapter 5 discusses the administrative controls necessary and suitable at a particle accelerator laboratory while Chapter 6 discusses the magnitude and consequences of induced radioactivity in the environment.

CHARACTERISTICS OF THE REMANENT RADIATION FIELD

Particle Energy

All particle accelerators whose energy exceeds 10 MeV will produce some induced radioactivity. This radioactivity results from the interaction of the particles (including photons) of the prompt radiation field with the accelerator and its surroundings. The precise energy at which radioactivity is produced depends upon the particles accelerated and the target being irradiated: certain nuclear reactions with light target nuclei (such as Be or Li) will produce neutrons, and hence radioactivity, at energies well below 10 MeV. Neutron generators always have a potential for the induction of radioactivity. NBS Handbook 107 gives rules of thumb for determining whether particle accelerators whose energy is below 10 MeV may present a problem with induced radioactivity (ANSI 70). Only a small fraction of accelerators give cause for concern in this respect. Thus Opelka et al. found that less than 5% of some 1200 accelerators in the USA might have significant induced activity problems (Op 82).

Radionuclides Produced

Barbier has given an excellent summary of the mechanisms for the production of radioactivity by particle accelerators (Ba 69). In the interaction of a hadron of sufficient energy with a nucleus an intranuclear cascade is generated. The emission of particles produced during this cascade from the nucleus (spallation) is followed by the evaporation of nucleons from the excited residual nucleus. The number of radionuclides that might be produced is in principle very large, but in practice only a relatively small number are of consequence in radiological protection. Although, in principle, all the nuclides that have a mass number and atomic number equal to the sum of these numbers for the projectile and target nuclei may be generated, in practice it is found that the number of radionuclides of concern in radiological protection is limited by a combination of production cross section and radioactive half life.

The daughter nuclei are not necessarily radioactive and in addition not all the radioactive nuclei contribute significantly to the dose-equivalent rates several hours after irradiation. Those isotopes that have very short half lives have already decayed, while those with very long half lives are both produced and decay very slowly so as to make only a small contribution to the dose-equivalent rate. The remanent dose rate does not therefore have a simple dependence upon the mass and atomic numbers of the target nuclei and one may therefore most conveniently resort to experience. Several authors have reported experimental studies of the radionuclides commonly identified in materials used at particle accelerators (for a review see Patterson and Thomas, Chapter 7, Induced Radioactivity [Pa 73]). Of the principal radionuclides produced with a half life longer than 1 hour, Charalambus and Rindi showed that 70% were gamma emitters (Ch 67). However, radionuclides of even shorter half life than 1 hour may be of concern in radiological protection if produced in large quantities. Table 2.5, adapted from Patterson and Thomas, summarises experience at particle accelerators and lists radionuclides commonly identified in solid materials; half lives shorter than 10 minutes are excluded.

Reaction Cross Sections

Most of the radionuclides listed in Table 2.5 are produced by simple nuclear reactions [e.g., (n,xn), (p,xn), (p,xnyp), etc.], but some result from spallation, fragmentation or capture reactions. Compilation of measured cross sections have been prepared by Bruninx (Br 61, Br 62, Br 64). An empirical formula that permits interpolation between measured data has been developed by Rudstam (Ru 66) while Bertini has written a computer code that predicts reaction cross sections from calculations of the intranuclear cascade (Be 69).

The Decay of Residual Radioactivity

The decay of the radioactivity in accelerator structures is a complex function of time both because of the large number of radionuclides produced and because the operation of the accelerator may be quite variable. The earliest information on the decay of dose rate of accelerator structures was empirical (see Ri 73, Pa 73). Sullivan and Overton (Su 65) have derived an approximate analytical expression that gives the dose rate at time t after the irradiation ceases, $\dot{D}(t)$:

$$\dot{D}(t) = B\phi \ln [(T + t)/t] \qquad (2.7)$$

where T is the irradiation time, ϕ is the fluence rate of irradiating particles, and B is a parameter that depends upon the target, geometrical and irradiation conditions. Equation (2.7) is in good qualitative agreement with observation and Sullivan has reported values of the parameter B for medium-to-heavy materials that give reasonable absolute agreement with measurements (Su 72a,b) [see the section on induced radioactivity for a more detailed discussion].

The computer programmes that model the development of the hadron and electromagnetic cascades in matter (see Chapter 4) make it possible to combine the reaction cross-section data to predict the spatial distribution of radionuclides in external components such as magnets, other

beam transport components or shielding. Such distributions may then be combined with photon transport calculations to predict the dose rate due to photons outside irradiated materials. Examples of such calculations are given for both ferrous and nonferrous materials in later subsections.

MAGNITUDE OF THE PROBLEM OF INDUCED RADIOACTIVITY

There a several means by which the scope of the problem of induced radioactivity at particle accelerators may be measured:

- The fraction of accelerators with induced radioactivity problems.
- The total quantities and specific activities of the radioactivity produced.
- The radiation exposure to operating and maintenance personnel at particle accelerators.

The majority of particle accelerators used in medicine and research are below the beam energy and intensity at which induced radiation presents a problem. Thus, for example, Opelka et al. report that of 1200 particle accelerators operating in the USA during 1982 at least 50 could 'produce neutron fluxes that cause significant induced activation, are capable of producing significant fluences of particles, and several hundred more are capable of producing neutron fluxes that could result in non-negligible activation of the accelerator facility' (Op 82).

The total quantities of radioactivity produced by particle accelerators are quite small. Compare for example the radioactive inventory of an 1100 MW_e PWR at shutdown of 6.3×10^{20} Bq or 1.7×10^{10} Ci [5.6×10^{18} Bq or 1.5×10^{8} Ci after 1 year] with that of a 500 GeV proton accelerator operating at 10^{13} protons per second, which amounts to about 9×10^{15} Bq or 0.24 MCi [see Chapter 6] (APS 75). Proton or heavy-ion accelerators are considerably more efficient in producing radioactivity than are electron accelerators. Comparisons of the total activity generated by high-energy electron and proton accelerators show that differences of about a factor of 100 in the radioactivity produced for the same beam power (Pa 73, Sw 79).

Not only is the total amount of radioactivity produced by accelerators rather small, but

> "It should be remembered...that in general the specific activity induced in accelerator structures is much lower than that found in reactor irradiated materials. With the notable exception of targets, collimators, etc., placed directly in the beam, or in beam dumps, the specific activity is not high. The extent of the radioactivity is widespread, however, it is not 'concentrated and confined', but rather 'diluted and dispersed'. In consequence the total volume may be large. Control of this low-specific-activity material at accelerator laboratories may represent a major administrative problem" ((Pa 73).

Some indication of the consequences of induced radioactivity have already been discussed in Chapter 1. The principal problems will be associated with accelerator components directly irradiated by the primary beam. As is shown in Chapter 6, the largest fraction of the

induced radioactivity will be produced in the accelerator structure and beam transport components. It is estimated, for example, in the case of strong focussing accelerators such as the 30 GeV proton synchrotrons at Brookhaven and CERN that about 90% of the total radioactivity is induced in the magnet, accelerator components and concrete accelerator room. Something less than 10% of the total activity produced is produced outside the accelerator room at such accelerators. [See for example Climent (Cl 64), Golvachick et al. (Go 69) and the references given in Chapter 6.]

Typical dose rates found at particle accelerators vary widely and some typical dose rates from accelerator components at a variety of particle accelerators has been given in Chapter 1. Opelka et al. have prepared an extremely useful compilation of reported measurements of exposure rates observed under varied conditions at many particle accelerators (see Table 2.6). Such a compilation is valuable in showing the magnitude of the induced activity problem and the need, under some conditions, for special care in controlling exposures to personnel during routine maintenance.

Although the fraction of accelerators capable of producing significant quantities of radioactivity is small, induced radioactivity may nevertheless be the major source of personnel exposure at some particle accelerators. This is particularly so at research installations where frequent changes in experimental arrangements are often required.

Although detailed studies have not been made there is a strong suggestion that there is a correlation between personnel exposures and accelerated beam intensity. This has been observed at several accelerator laboratories such as CERN, Brookhaven National Laboratory and the Lawrence Berkeley Laboratory (Pa 73, St 76, Th 75). The largest source of personnel exposure at accelerator laboratories is from routine maintenance exposures on radioactive accelerator components. In the remainder of this section the estimation of induced activity in the accelerator structure and it surroundings will be discussed.

INDUCED RADIOACTIVITY

The basic information needed for the calculation of dose rates from materials irradiated in accelerator radiation environments are the specific reaction cross sections for the production of a given radionuclide from a target material bombarded by specified radiations. These cross sections may be obtained by experimental means (Br 61) or empirical interpolations of measured data (Ru 66) [see also (Pa 73), Chapter 7].

The estimation of the radioactivity induced in materials in accelerator radiation environments is simplest when the radiation field is simple. Such irradiation conditions occur, for example, when small accelerator components such as targets or magnet-septa are directly struck by a proton beam and there has been little or no development of the hadron cascade (see Chapters 2 and 3). Such calculations have been discussed in detail by Barbier (Ba 69) [see section on Ferrous Materials].

In complex radiation environments (e.g., when the electromagnetic and hadronic cascades are well developed) it is necessary to first determine the irradiating field. This is most conveniently done using computer programmes. For example, HETC (High Energy Transport Code) is a Monte Carlo hadron cascade programme that is capable of predicting the production of radionuclides from its own models of the intranuclear cascade and nuclear evaporation phases of hadron-nucleus interactions (see Chapter 4). Specific examples using HETC to predict induced radioactivity in iron are given later (Ar 69a,b,c).

The variation of dose rate with time, D(t), due to a single radionuclide is given by the equation

$$\dot{D}(t) = G\phi(1 - e^{-\lambda T})\, e^{-\lambda t} \qquad (2.8)$$

where λ is the decay constant of the radionuclide,
T is the irradiation time,
t is the decay time,
ϕ is the fluence rate (assumed constant), and
G is a constant that depends upon many parameters such as the macroscopic production cross section for the nuclide considered, the particle spectrum in which the sample is irradiated, geometrical and self-shielding factors, and the accelerator parameters.

The result of irradiation of material in an accelerator radiation environment is not, however, to produce one radionuclide, but many. The number of radionuclides is, in fact, so large that Sullivan and Overton have described an analytical method for predicting the variation of radioactive buildup and decay by assuming a continuum of radioactive decay constants, λ (Su 65). This assumption is reasonable for target nuclei of medium mass number, A, (for example, iron) where Sullivan and Overton observed that the number of radionuclides, n, with decay constants greater than λ, can be represented by the empirical expression

$$n = a \ln \lambda \qquad (2.9)$$

where a is an arbitrary constant

Equation (2.9) is accurate to within ± 10% for medium A nuclei for values of λ corresponding to half lives between about 15 minutes and 100 years.

The contribution to the dose rate from the dn radionuclides with decay constants between λ and $\lambda + d\lambda$, $d\dot{D}(t)$ may be written

$$d\dot{D}(t) = G\phi\,(1 - e^{-\lambda T})\, e^{-\lambda t}\, dn \qquad (2.10)$$

dn may be obtained by differentiating Eq. (2.9). Substituting the result into Eq. (2.10) we obtain

$$d\dot{D}(t) = Ga\phi(1-e^{-\lambda T})\, e^{-\lambda t} d\lambda/\lambda \qquad (2.11)$$

Assuming that any variation of G with λ is negligible, the dose rate from radionuclides with decay constants between λ_1 and λ_2 is then

$$D(t) = Ga\phi \int_{\lambda_1}^{\lambda_2} (1 - e^{-\lambda T}) \, e^{-\lambda t} d\lambda/\lambda \qquad (2.12)$$

With the approximations $\lambda_2 \to \infty$; $\lambda_1 \to 0$ Eq. (2.12) has the solution (Su 65, Chapter 7 of Pa 73):

$$\dot{D}(t) = B\phi \ln [(T + t)/t)] \qquad (2.7)$$

where B is a constant.

Many studies have been published in the literature that have shown that Eq. (2.7) is a good approximation to measured data (Fr 68, Go 71, Su 65, Su 72a).

It is interesting to explore the asymptotic values of Eq. (2.7) with respect to T and t (Su 83). When the decay time is long compared with the irradiation time, Eq. (2.7) reduces to

$$\dot{D}(t) = B\phi \, T/t \quad (t \gg T) \qquad (2.13)$$

i.e., the dose rate is inversely proportional to the decay time.

When the irradiation is very long with respect to the decay time, Eq. (2.7) reduces to

$$\dot{D}(t) = B\phi \, (\ln T - \ln t) \quad (T \gg t) \qquad (2.14)$$

i.e., a logarithmic decrease in dose rate with decay time.

It has been a convenient rule of thumb at accelerators to use an effective half life, T_H, that is approximately equal to the decay time, t. Freytag has given a firm basis for this rule of thumb (Fr 68). By differentiating Eq. (2.7) with respect to decay time t we obtain

$$\frac{d[\dot{D}(t)]}{dt} = - \frac{T}{t^2(1 + T/t)} \times \frac{\dot{D}(t)}{\ln (1 + T/t)} \qquad (2.15)$$

Equation (2.15) may be written in terms of an effective half life, T_H,

$$T_H = \frac{t^2}{T} (1 + T/t) \ln (1 + T/t) \ln 2 \qquad (2.16)$$

and by substituting $x = T/t$

$$T_H = [((1 + x)/x) \ln (1 + x)] \ln 2 \qquad (2.17)$$

For values of $x \to 0$, 1 and 10 the corresponding values of effective half life, T_H, obtained from Eq. (2.17) are then 0.69t, 1.0t, and 1.7t respectively. This result shows the rule of thumb obtained empirically to be quite accurate and can be understood on fundamental principles.

Dose Rate from Electrons and Positrons

It is most important to determine the dose rate produced by electrons in addition to those produced by photons. This is particularly true when close contact to irradiated materials cannot be avoided, as, for example, during accelerator component maintenance, or the machining of irradiated materials. There is one important difference between proton accelerator irradiated and reactor irradiated materials in that in the former case positron emitters are much more likely to be produced than in the latter. Doses produced by both positive and negative electrons should therefore be considered.

Sullivan has given a simple discussion to show the magnitude of the dose rate due to electrons (Su 83). Consider a thin foil irradiated by protons. The dose rate in contact with the foil due to β^- particles, $\dot{D}_\beta$, is given by

$$\dot{D}_\beta = 1.6\times10^{-10}\ N_\beta (dE/dx)_\beta \quad \text{Sv s}^{-1} \tag{2.18}$$

where N_β is the number of β^- particles emitted per cm^2 per second.

$(dE/dx)_\beta$ is the average stopping power in MeV g^{-1} cm^2.

The corresponding photon dose rate, $\dot{D}_\gamma$ is

$$\dot{D}_\gamma = 1.6\times10^{-10}\ \mu\ N_\gamma\ E_\gamma \quad \text{Sv s}^{-1} \tag{2.19}$$

where N_γ is the number of photons emitted per cm^2 per second.

E_γ is the average photon energy

μ is the mass energy attenuation coefficient in cm^2 g^{-1}

The ratio of the dose rates in then given by

$$\dot{D}_\beta/\dot{D}_\gamma = \frac{N_\beta\ (dE/dx)_\beta}{\mu\ N_\gamma\ E_\gamma} \tag{2.20}$$

For the case

$N_\beta/N_\gamma = 1$; $(dE/dx)_\beta = 2$ MeV g^{-1} cm^2; $E_\gamma = 1$ MeV and $\mu = 0.3$ cm^2 g^{-1},

Eq. (2.20) gives

$$\dot{D}_\beta/\dot{D}_\gamma \approx 70$$

In practice the electron dose rate is not so high as this treatment suggests for several reasons. The self absorption of even very thin

foils considerably reduces the dose due to electrons below that estimated by this simple method. The electron dose is even further reduced in those radionuclides where electron capture is a competing mode of decay. When the electrons emitted have a positive charge, the positrons stopping in the foil emit two annihilation photons of 0.511 MeV.

Sullivan has measured the ratios of doses due to electrons and photons at the surface of metallic foils 0.1 mm thick and reported values for $\dot{D}_\beta/\dot{D}_\gamma$ of 12, 7 and 9 for aluminium, steel and copper respectively (Su 82), considerably lower than the value of ~ 70 predicted by simple analysis. The actual value of $\dot{D}_\beta/\dot{D}_\gamma$ will be a function of thickness of the irradiated foil. Beyond 0.1 mm it might be expected that the electron dose will increase only slowly with foil thickness but that the photon dose rate will increase almost linearly with thickness. Sullivan predicts that for copper or steel foils the electron and photon surface dose rates will be equal at a foil thickness of about 1 mm (Su 83).

The ratio $\dot{D}_\beta/\dot{D}_\gamma$ also clearly depends upon the radionuclide produced in the foils and thus on the irradiation time, T, and the decay time, t. As an example, for aluminium foils, the positron emitter ^{18}F (T_H = 110 m) is the major contributor to surface dose rates for decay times of less than a few hours. As another example, organic materials (e.g., mylar) when irradiated may produce only positron emitters (e.g., ^{11}C) and in thin foils annihilation may not occur to any great degree. Sullivan has demonstrated that the dose rates indicated by standard survey instruments in contact with irradiated materials may underestimate surface dose rates by a factor of as much as 200 (Su 82). Dose rate measured at distances of 30 cm from the surface of thin foils were lower by a factor of 10^4 than the surface dose rates. Such facts emphasize the caution given at the beginning of this section that great care must be taken in assessing the hazards of handling accelerator irradiated materials particularly thin foils, such as used, for example, in beam monitoring equipment or vacuum windows.

Ferrous Materials

Because ferrous materials comprise a large fraction of the total mass of materials used in accelerator structures (e.g., magnet yokes, stainless steel vacuum pipes, magnet supports) and because the relatively high density of iron makes it extremely useful for shielding, it is important to study the production of radioactivity in ferrous materials in some detail.

Table 2.7, due to Barbier, gives values of dose rate due to photons at a distance of 1 metre from a 1 kg mass or iron irradiated by monoenergetic protons for an infinite time. Values of the dose rate (in Sv h^{-1}) are given for decay times up to 360 days and for bombarding proton energies from 50 MeV to 2.9 GeV. The dose rate are normalized to a proton beam fluence rate of 10^{12} protons m^{-2} s^{-1} (Ba 69). Gollon (Go 76) has shown how the data of Table 2.7 may be used to determine the dose rates, $\dot{D}$, for different irradiation times, T, and decay times, t, using the relation

$$\dot{D}(T,t) = \dot{D}(\infty,T) - \dot{D}(\infty,T+t) \qquad (2.21)$$

Armstrong has used the computer code HETC to calculate production of radionuclides in a large iron block bombarded by 1 and 3 GeV protons (Ar 69a). The results of the calculation are shown in Fig. 4.11 together with a comparison with experimental measurements. Armstrong and Alsmiller have combined hadron cascade calculations, using Monte Carlo methods, to determine the distribution of radionuclides in materials with photon transport calculations in order to predict the dose rate due to photons at the surface of irradiated materials (Ar 69b). In particular Fig. 2.14 (Go 71) shows the results of their calculations for a model magnet, carried out for the Fermi National Accelerator Laboratory. Also shown in this figure are measured values of the relative dose rates from a CPS magnet, and values of relative dose rate computed using the empirical formula due to Sullivan and Overton.

Armstrong and Barish (Ar 69c) have reported calculations of the relative photon dose rate outside a steel cylinder irradiated by a pencil beam of protons. Two proton energies--200 MeV and 3 GeV--were used. Figure 2.15 shows the results of the calculations for the relative dose rate at the surface of the cylinder for an infinitely long irradiation. The dominant radionuclides that contribute to the dose rate are ^{54}Mn (280 d), ^{52}Mn (5.6 d), ^{48}V (16 d), ^{51}Cr (27.8 d), ^{56}Mn (2.6 h), ^{52m}Mn (21 m), ^{56}Co (77.3 d), ^{51}Mn (46.5 m), ^{44}Sc (4 h) and ^{49}Cr (42 m).

The prediction of surface dose rates is a complex matter because evidently the energy spectrum of the photons emitted from the iron will depend upon the chemical composition of the irradiated steel, the time of irradiation and the decay time. Hirayama et al. have recently reviewed this problem in detail (Hi 82).

Knowledge of the photon spectrum emitted from irradiated ferrous materials is of practical importance for radiological protection in those cases where local shielding is to be designed around "hot spots" at the accelerator, so that the dose to individuals engaged in maintenance operations may be kept as low as possible. The transmission of photons through lead is of particular interest in this regard. Figure 2.16 shows measurements made of the transmission through lead of the photons emitted by irradiated steel accelerator components of the CPS made by Goebel (Go 67). Examination of Fig. 2.16 shows that the transmission curves lie between those for ^{137}Cs and ^{226}Ra and would roughly correspond to that for photons with an energy of 800 keV.

Using this information of the average photon energy, and by making some reasonable assumptions, it is possible to estimate photon dose rates due to induced radioactivity from Monte Carlo calculations. In Chapter 6 the use of these computer methods to calculate the "star" (inelastic reaction) production rate is described. We now make, with Sullivan (Su 71, Su 72a), the following reasonable assumptions:

- Half the radionuclides produced in irradiated materials have decay constants in the range $10\ m^{-1} \geq \lambda \geq 10^{-6}\ m^{-1}$.
- 25% of the radionuclides produced have radioactive daughter products.

- The average number of photons emitted per radioactive disintegration is 1.5.
- A hadron 'star' is identical to an interaction that produces a radionuclide.

With these assumptions and taking the density of iron to be 7.8 g cm^{-3} the specific activity corresponding to unit star density (1 star cm^{-3} s^{-1}) is

$$\frac{0.5 \times 1.25 \times 1.5}{7.8} = 0.12 \text{ Bq } g^{-1}$$

The dose rate due to photons from photon-emitters distributed in a semi-infinite plane is given by:

$$\dot{D}_\gamma = 1.07 \text{ C E} \quad \text{rem } h^{-1} \tag{2.20}$$

where C is the specific activity measured in μCi g^{-1}
E is the photon energy in MeV.

In SI units with C measured in Bq g^{-1} and $\dot{D}_\gamma$ in Sv h^{-1}, Eq. (2.22) becomes

$$\dot{D}_\gamma = 2.9\times10^{-7} \text{ C E} \quad \text{Sv } h^{-1} \tag{2.22a}$$

By combining the fact that unit star density corresponds to a specific activity of 0.12 Bq g^{-1} with Eq. (2.22a) and the average photon energy is 0.8 MeV, we see that the surface dose rate from an infinite slab of irradiated iron in which unit star density has been produced will be

$$\dot{D}_\gamma = 2.9\times10^{-7} \times 0.12 \times 0.8 = 2.8\times10^{-8} \quad \text{Sv } h^{-1}$$

To predict dose rates from steel irradiated for a finite time and after some decay, we may define a parameter--referred to in the literature as the 'ω factor'--as the dose rate due to photons at the surface of iron or steel in which unit star density has been produced for irradiation time, T, after decay time, t. The ω factor is written $\omega(T,t)$.

Inspection of Fig. 2.17 shows that in steel for an irradiation time of 30 days and a decay time of 1 day the surface dose rate is reduced by a factor of about 2.8 over the dose rate after an infinite irradiation and with no decay. Thus:

$$\omega(30,1) = 10^{-8} \text{ Sv } h^{-1}/\text{star cm}^{-3}\ s^{-1}.$$

This value for $\omega(30,1)$ is in fair agreement with other estimates. Values for $\omega(30,1)$ derived from the ORNL calculations are in the range $1.2\text{–}1.5 \times 10^{-8}$ Sv h^{-1}/star cm^{-3} s^{-1} (Go 71, St 73c), whereas Hoefert et al. have suggested that measurements give a somewhat smaller value of 5×10^{-9} Sv h^{-1}/star cm^{-3} s^{-1} (Ho 75a). A value of 1.0×10^{-8} Sv h^{-1}/star cm^{-3} s^{-1} seems to be a reasonable value to use in practice. When

combined with the time variation formula of Sullivan and Overton reasonably accurate predictions of photon dose rates due to remanent radioactivity in steel are possible.

Non-Ferrous Materials

Barbier has comprehensively discussed the induction of radioactivity in non-ferrous materials (Ba 69). Figure 2.17 gives examples of the remanent dose rate due to photons from irradiated elements as a function of atomic number of the element. The specific example given is for an irradiation by 2.9 GeV protons lasting 5000 days; two decay times are given (Go 71). Inspection of Fig. 2.17 shows that the pattern is not widely different for the two decay times shown and that the specific dose rate (dose rate per unit mass of material) varies in a somewhat irregular way with atomic number. For elements with atomic number in the range from about 22 to 42 (titanium to molybdenum) there is a tendency for the dose rate per unit mass of material to increase with atomic number. Thereafter there is a slow but generally steady decline with increasing number, but Barbier has mentioned that the Rudstam formula used in his calculations is of limited validity in the high-Z region (Ba 69, Ru 66). Of particular note is a region of low specific dose rate for the elements with Z of 18, 19 and 20 (Ar, K, Ca). This trough in the general tendency is due to the absence of radioactive photon emitters of sufficiently long half life in this region of the table of radionuclides. For elements with lower atomic number there is a general increase and photons emitted from the radionuclides of sodium often predominate. For example, in the case of irradiated aluminium, after a few hours of decay almost the entire dose rate is due to ^{24}Na; at even longer decay times it may be due to ^{22}Na.

The trough in the specific dose rate in the calcium region can be turned to practical advantage. Both Barbier and Hoefert have recommended facing the outer surface of steel shielding (such as, for example, in a beam-stop) with marble ($CaCO_3$) to reduce the dose rates due to remanent radioactivity (Ba 69, Ho 75b). Such a step would reduce personnel exposures when performing maintenance in the vicinity of the beam stop. As another example of the use of low atomic number elements to reduce remanent-activity dose rates we may cite the use of graphite liners on the inner surfaces of cyclotron or weak-focussing synchrotron vacuum chambers. Such liners will preferentially absorb beam lost during acceleration or beam scattered from targets or septa resulting in the production of ^{7}Be (53 d) as the only significant long-lived radionuclide.

Of the heavier elements the dose rate from the radionuclides produced in lead is of interest because lead is often used as a shield for photons. Local lead shielding may be added after accelerator shut down, but this is often inconvenient and time consuming. Of greater interest is installation of the lead before accelerator operation. Sullivan has shown that the dose rate from accelerator irradiated lead decays as $t^{-1.4}$ for decay times long compared with the irradiation time (Su 72b). This is somewhat faster than the decay for medium atomic number materials, like iron, that decay as $t^{-1.0}$ (see previous sections). Furthermore it was observed that the average dose rate from lead was only one-fifth of that from steel, both materials having been irradiated for one

year and observed during a shut-down period of one month at CERN (Su 72b). This empirical result is in contradiction to the predictions of Fig. 2.17 and adds weight to the caveat given by Barbier (Ba 69). However Sullivan's observations have been confirmed by calculations by Gabriel and Santoro who used the HETC, the Monte Carlo hadron cascade code, coupled with MORSE, the neutron and photon transport code, to study the effect of lead collars around iron beam stops irradiated by 200 GeV photons (Ga 72). Figure 2.18 shows the results. Infinitely long cylinders are irradiated by a pencil beam of 200 GeV protons, and the dimensions of the iron cylinder and lead collars are given in the figure. Irradiation times between one day and infinity are assumed and the dose rates for decay times from 0.1 h to 100 h are indicated. For all the irradiation times and decay times considered the lead collars are seen to have substantially reduced the dose rate compared with that calculated for the bare iron cylinder. Furthermore, as predicted by Sullivan, the decay of dose rate from the lead shielded cylinders is faster than for the bare iron.

Plastics and oils comprise a most important group of non-ferrous materials in wide use at accelerators. In such materials the most important radionuclides of concern will be ^{7}Be, ^{11}C, ^{13}N, ^{15}O and the radioactive isotopes of chlorine (Pa 73). Care must be taken to avoid tritium contamination of neutron generators, where tritium targets are used, in vacuum pump oil and at accelerators where cryogenic magnets are used (Pa 73, Po 81, Wa 69).

In addition to concerns of the radioactivity induced in solid materials care must be taken to avoid contamination from radioactive dust, chips and filings. In general the radiological hazard in accelerator areas from these sources is negligible when compared with that from the external radiological hazard from close-by radioactive accelerator components. Patterson and Thomas have summarized experience with dust activation (Chapter 7 of Pa 73). Baarli et al. indicate that, as expected, the radioactivity in dust closely correlates with the dose rates from the remanent activity in near-by accelerator components (Ba 66). The radionuclides most commonly found are ^{7}Be, ^{48}V, ^{51}Cr, ^{56}Mn and ^{59}Fe, with ^{54}Mn alone accounting for more than 40% of the total activity (Ba 66, Ch 67). When heavy element targets or shields are used, heavier radionuclides are also observed. Thus, for example, Patterson et al. have reported finding ^{181}W and ^{237}Np in accelerator areas (Pa 69) and Kitao and Ohata have measured ^{138}Re, ^{184}Re, ^{185}Os and ^{182}Ta in dust in cylotron areas (Ki 71).

Concrete

Most if not all accelerators are housed in concrete rooms or are surrounded by concrete shielding blocks. Constituent particles of the electromagnetic and hadronic cascades generated in the accelerator structure may cross the air gap and enter the concrete, inducing radioactivity in the shielding. The fraction of water (a few percent) present in all concrete provides sufficient hydrogen to slow down evaporation neutrons to thermal energies. These thermal neutrons may leak back into the accelerator room, resulting in significant thermal neutron fluence rates. Experience shows that in the accelerator vault the thermal neutron fluence rates are comparable to the fluence rates of

neutrons of about 1 MeV in energy (Pa 58, Pa 73). Radioactivity may be induced in the concrete walls by both the thermal and fast neutrons, but as we shall show, the thermal neutron capture usually dominates the production of radionuclides that are important in the short term.

Unlike many of the materials used in the accelerator structure such as aluminium, copper and iron, concrete is a heterogenous substance whose chemical composition may vary widely (see for example IAEA 75). Nevertheless many experimental studies show that one radionuclide, ^{24}Na, usually dominates the radiation field at the surface of concrete irradiated in accelerator environments (de S 62b, Gi 64a, Gi 64b, Gi 64c, Gi 65, Mi 65, Na 66). These empirical conclusions have been confirmed by calculation (Ar 69d, Ar 70). For example Armstrong and Barish (Ar 70) show that 10 minutes after accelerator shut-down the dose rate due to ^{24}Na is about 20 times that from all other radionuclides (^{7}Be, ^{11}C, ^{13}N, ^{22}Na, ^{34}Cl and ^{38}K). One hour from shut-down this ratio has increased to about 100. Calculations by Armstrong and Barish suggest that after about 100 hours after accelerator shut-down the dose rates produced by induced radioactivity are almost entirely due the radionuclides induced in the accelerator structure.

The ^{24}Na in concrete is principally formed by thermal neutron capture in the elemental sodium present in the cement and aggregate. Although ^{24}Na may also be formed in spallation reactions in constituents of the concrete, experience shows that the (n,γ) reaction is the most important contributor. Thus for an aggregate containing 1% sodium by weight Armstrong and Barish calculate that 25 times as much ^{24}Na activity is produced by thermal neutron capture in ^{23}Na as from all spallation reactions (Ar 70). Gilbert et al. estimated that from 50% to 90% of the ^{24}Na was produced by the (n,γ) reaction in several aggregates studied (Gi 69).

It is important to have some understanding of the magnitude of the dose rates produced by the decay of induced radioactivity in accelerator rooms. It may be readily shown that the dose rate due to remanent radioactivity inside a cylindrical void whose walls have been uniformly irradiated will be independent of position within the void and equal to the dose rate at the inner wall of the shield. Superimposed on the uniform field will be the radiation level produced by the decay of radioactivity induced in the accelerator structure (Ar 70, Pa 73). Gilbert and Thomas have reported measurements made in the accelerator tunnel of the Brookhaven National Laboratory AGS and determined that the some 6 hours after accelerator shut-down the uniform dose rate inside the tunnel due to concrete was about 10 $\mu Sv\ h^{-1}$ (1 millirem per hour) (Gi 65). Armstrong and Barish made calculations for a simulated 3 GeV proton accelerator magnet situated in a concrete-walled tunnel of 2-metre radius. The accelerator magnet was represented by a solid iron cylinder of about 20-cm radius (160 g cm^{-2}). The dose equivalent rate due to induced activation from a uniform beam in the concrete some 6 minutes after shut-off was 1.5×10^{-13} Sv h^{-1} per primary proton interaction per metre per second. This value may be scaled linearly with primary proton energy and the dose rate will decay with the 15-hour half life of ^{24}Na. Thus for a 30 GeV proton synchrotron operating at 10^{13} protons per second of radius 100 metres in which 1% of the beam is distributed

uniformly the radiation level due to ^{24}Na induced in the concrete would be

$$1.5 \times 10^{-13} \times \frac{30}{3} \times \frac{10^{-2} \times 10^{13}}{2\pi \times 100} = 2.5 \times 10^{-4} \text{ Sv h}^{-1}$$

The dominance of ^{24}Na in contributing to the short-term radiation levels from concrete and the mechanisms by which it is produced offer some possibility for amelioration. It will not, in general, be cost effective to take steps to reduce the ^{24}Na levels if entry into the accelerator room will take place some considerable time after shut down. Thus, as we have seen, after 100 hours, the residual radiation levels will be dominated by the accelerator structure and even after 24 hours the dose rate from the concrete activity will equal or be smaller than the dose rate from the magnet iron (Ar 70, St 76). The problems posed by induced activity in the concrete for long-term access to accelerators are therefore usually trivial.

However if access is required shortly after accelerator shut down there may be some virtue in attempting to reduce the quantities of ^{24}Na induced so as to reduce personnel exposures. The simplest way in which this may be done is by the choice of low-sodium aggregates and cement. The natural sodium content of these substances may vary by about an order of magnitude, so that aggregates containing only about 0.1% sodium by weight may be found. Such a course of action is only economically feasible if the aggregate is locally available. High transportation costs can easily make this course of action impracticable. A second method of amelioration is to add a neutron poison either to the concrete mix or on the inner surface of the accelerator room.

Table 2.8 shows the reduction in ^{24}Na production that may be achieved by such courses of action.

Barbier has proposed lining the inner shield walls with marble ($CaCO_3$), which has a chemical composition that produces rather low levels of induced radioactivity in accelerator environments (Ba 69).

HANDLING AND MAINTENANCE OF RADIOACTIVE ACCELERATOR COMPONENTS

As we have already suggested, the control of the enormous number of items irradiated in the environment of particle accelerators may present a formidable administrative problem. The problem is exacerbated in some countries where there are no clear guidelines for the disposal of accelerator-induced radioactivity (Op 82).

All accelerator laboratories should determine what policies should be implemented with regard to controlling the movement of objects (such as for example tools, accelerator components or targets) that have been irradiated in the accelerator room. A general discussion of such problems is given by Goebel et al. (Go 71). Details of the practical control of radioactive materials during the decommissioning of a facility at a large high-energy research laboratory are given by Schönbacher and Tavlet (Sc 85) while Chapter 5 of this report describes an administrative control program suitable for a large multidisciplinary research laboratory using particle accelerators. Stewart discusses the general aspects of controlling contamination from the use of radioactive

materials in national laboratories (St 81).

A convenient rule of thumb for assessing the dose rate to be expected from γ-emitting irradiated materials is to remember that the dose rate, $\dot{D}$, in a cavity surrounded by a uniform distribution of radioactivity is given by

$$\dot{D} = 2.14\ C\ E \quad \text{rad h}^{-1} \tag{2.23}$$

where C is the specific activity measured in μCi g^{-1} and E is the γ-ray energy in MeV. Thus for photon energies of a little less than 1 MeV the dose rate in contact with a large slab of material [half that given by Eq. (2.23)] will be about C rad h^{-1}. Caution must be exercised in the use of this simple rule of thumb for two reasons: firstly, it is often necessary to handle small radioactive objects when surface dose rates may be more than a factor of 10 higher than that from a large object of the same specific activity, and secondly, the presence of soft x rays or β particles may increase the radiation field intensity by sometimes as much as a factor of 100 (Sc 70).

It is not uncommon for the surface dose rate of objects placed in or near high intensity accelerator beams to exceed tens or even hundreds of rads per hour. It is advisable to minimize the need for maintenance in such regions by adequate design and to provide adequate means of remote handling to perform any necessary maintenance. Early studies at the Argonne and Brookhaven national laboratories (Fl 65, Go 65) have led to sophisticated equipment at high intensity, high-energy laboratories such as CERN and LAMPF (Bu 77, El 71, Ho 75c, Ho 75d, Ho 78). Ellefsplass, Horne and Madsen have given an excellent summary of the use of remote handling equipment in accelerators, to which the reader is referred for further information (El 71).

DISPOSAL OF RADIOACTIVE ACCELERATOR COMPONENTS

Perhaps the most extensive study of the scope of the problems involved in the disposal of unwanted particle accelerators has been made at the Argonne National Laboratory by Opelka and his colleagues (Op 82). This study was occasioned by the closing of the Zero Gradient Synchrotron (ZGS) but its scope was expanded to include an assessment of the problem of accelerator disposal within the United States. Although the report deals with the particular problems of one country much of its discussion is of general relevance.

The Argonne study begins with a brief review of accelerator technology similar in scope to that given in Chapter 1 of this report. This is followed by a history of particle accelerator decommissioning in the U.S.A., a discussion of the appropriate U.S. regulations and details of how to plan for and estimate the cost of particle accelerator decommissioning. Nine appendices include a census of U.S. particle accelerators and details of various aspects of decommissioning.

The report classifies accelerator components into three categories based on expected levels of conducted activity:

- 'Those components or materials that were either directly struck by the accelerated-particle beam or in proximity to those points of

beam interaction will contain the highest levels of induced activity. Examples of these types of components are targets, target holders and positioning mechanism, beam stops, collimators and beam-defining slits, extraction magnets and channels, beam pipes or inner chambers, and local shields around targets and slits.

- Components that are part of the accelerator itself, and nearby auxiliary items that are subjected to irradiation by the scattered beam or secondary particles (neutrons, protons, etc.), will in general have lower concentrations of induced activity but may be suspected of having radiation levels similar to those of materials in the proximity category. Examples of these items are electrostatic shields, cyclotron vacuum chambers, magnet-pole tips (cyclotrons),magnet winding, bending and focussing magnets, synchrotron magnets and coils, and linac drift tubes.
- A third general category includes materials used in the building structure housing the accelerator facility and any other similar materials having been subjected to low-level neutron irradiation. The residual induced activity in these types of materials would generally be of extremely low concentration, if any exists at all. Examples of these types of material are floors and walls of accelerator vaults (concrete), support structures (steel, concrete), cyclotron magnet yokes (steel), shielding blocks (iron, concrete, lead), earth surrounding underground vaults, and any materials or components located within the vault' (Op 82).

This classification enables decisions to be made as to the deployment of appropriate levels of health physics surveillance in the absence of precise knowledge of either the specific activity or surface dose rate for the materials to be handled. Detailed information from radiation surveys on operating accelerators, such as that given in Table 2.6, is extremely useful in this regard, as is experience obtained from past decommissionings.

Opelka et al. have reported that 81 particle accelerators of energy above 1 MV had been taken out of operation in the U.S.A. by mid 1978 and these are listed in Table 2.9.

Of the 81 particle accelerators listed in Table 2.9 Opelka et al. selected five decommissionings for detailed study: the two synchrocyclotrons of the Carnegie Mellon University and the University of Rochester, the HILAC of Yale University and the 5 GeV Cambridge Electron Accelerator. Details are given in the report by Opelka et al., but features common to all decommissionings were apparent: useful equipment and components, even if some radioactivity was exhibited, were salvaged and put to other use.

Opelka et al. suggest four alternatives for accelerator decommissioning:

- Mothballing
- Entombment
- Dismantling with storage of components

- Dismantling with disposal of components

'Mothballing would involve a general cleanup around the accelerator, with loose contamination packaged for disposal. Following cleanup, access to the accelerator would be prohibited by blocking all entrances. Entombment would be similar to mothballing with the additional step of sealing all accesses to the accelerator with concrete. Because there is a relatively small amount of induced activity with short half-lives, a marked difference between decommissioning of an accelerator and that of other radioactive facilities (such as nuclear reactors) is the potential recycle of the accelerator-component materials. This reuse potential is directly addressed in the option of dismantling the accelerator and placing components in retrievable storage of a period of time to allow for radioactive decay. On dismantlement, the only components that would require storage are the potentially valuable ones not immediately claimed by other accelerator facilities for reuse. The option of dismantlement with disposal of all radioactive material, as addressed in this report, assumes no recycle of accelerator components and, therefore, gives an upper bound on the magnitude of the problem both in terms of cost and quantities of radioactive waste.

'In most cases, the induced radioactivity is confined to relatively few parts of the machine, and disposition of these parts (assuming no recycle potential) is through normal radioactive-waste channels without complication. The radioactivity is generally low-level (less than 100 R/h at the surface) and has a short half-life (5.26 years for ^{60}Co). The waste-disposal problem is complicated because most research accelerators leave a legacy of low-level induced radioactivity in massive components (10 to 1000 Mg). Examples of such items are large magnets, shield blocks, beam stops of concrete, earth, or iron, and even the walls and floors of the building itself. These massive components need to be dealt with in a manner so as to pose no potential health hazards to persons in the vicinity or the public at large' (Op 82).

Typical quantities of radioactive waste that would have to be disposed of from some 30 particle accelerators are summarized in Table 2.10.

Given such information it is possible to prepare cost estimates for the various options for decommissioning, and this Opelka et al. have done for four accelerators at the Argonne National Laboratory. For the case where is is assumed that the accelerator will be dismantled and all components immediately disposed of their results are shown in Table 2.11.

Of the remaining three options for accelerator decommissioning proposed by Opelka et al. entombment does not appear warranted from the quantities of radioactivity generated and the maximum surface dose rates encountered. The other three options have been utilized both in the United States and elsewhere (St 85b).

Opelka et al., recommend the development of national guidelines for the recycling of valuable materials such as those used in accelerator components containing induced radioactivity. To date this has not been done.

REFERENCES FOR CHAPTER 2

Aa 83 Aarnio P.A., Ranft J. and Stevenson G.R., 'A Long Write-up of the FLUKA82 Program', CERN Divisional Report, CERN, Geneva, Switzerland, TIS-RP/106 (1983).

Aa 84 Aarnio P.A., Ranft J. and Stevenson G.R., 'First Up-date of FLUKA82 Including Particle Production with a Multi-Chain Fragmentation Model (EVENTQ)', CERN Divisional Report, CERN, Geneva, Switzerland, TIS-RP/129 (1984).

Al 70 Alsmiller, R.G., Jr., Armstrong, T.W. and Coleman, W.A., 'The Absorbed Dose and Dose Equivalent from Neutrons in the Energy Range 60 to 3,000 MeV and Protons in the Energy Range 400 to 3,000 MeV', Nucl. Sci. Eng. 42, 367 (1970).

Al 75 Aleinikov, V.E., Gerdt, V.P. and Timoshenko, G.N., 'Measurement of Spectra of High-Energy Protons Generated in the Shielding of a 680 MeV Synchrocyclotron', Joint Institute of Nuclear Research, Dubna, Report JNIR-P16-9400 (1975).

Al 79 Aleinikov, V.E., Komochov, M.M., Krilov, A.R., Timoshenko, G.N. and Hahn, G., 'The Energy Angle Distributions of the Proton Component of the Radiation Field behind the 660-MeV Synchrocylotron Shielding', Joint Institute for Nuclear Research, Dubna, U.S.S.R, Preprint 16-12732 (1979).

Al 85 Aleinikov, V.E., Cherevatenko, A.P., Clapier, F.B. and Tsofbun, V.I., 'Neutron Radiation Field Due to 6.6 MeV/amu ^{58}Ni Beams Bombarding a Thick Cu Target', Rad. Prot. Dosem. 11, 245 (1985).

ANSI 70 American National Standards Institute, Radiological Safety in Design and Operation of Particle Accelerators', American National Standard N43-1, National Bureau of Standards Handbook 107 (1970).

APS 75 American Physical Society, 'Report of the Study Group on Light Water Reactor Safety', Rev. Mod. Phys. 47, Suppl. 1 (1975).

An 78 Antipov, A.V., Bajshev, I.S., Golovachik, V.T., Krupnyji, G.I., Kustarev, V.M., Lebedev, V.N. and Hoefert, M., 'Comparison of Dose Equivalent Measurements behind the IHEP Accelerator Shielding Using Different Methods', Institute of High Energy Physics, Serpukhov, Report IFVEORI 78-15 (in Russian), 1978. [Available in English Translation by B.C. Hodge as CERN Internal Report CERN TRANS 78-01].

Ar 69a Armstrong, T.W. 'Monte Carlo Calculations of Residual Nuclei Production in Thick Iron Targets Bombarded by 1 and 3 GeV Protons and Comparison with Experiement', J. Geophys. Res. 74, 1361 (1969).

Ar 69b Armstrong, T.W. and Alsmiller, R.G., 'Calculation of the Residual Photon Dose Rate around High-Energy Proton Accelerators', Nucl. Sci. Eng. 38, 53 (1969).

Ar 69c Armstrong. T.W. and Barish, J., 'Calculation of the Residual Photon Dose Rate Induced in Iron by 200 MeV Protons', Nucl. Sci. Eng. 38, 271 (1969).

Ar 69d Armstrong, T.W. and Barish, J., 'Calculation of the Residual Photon Dose Rate Due to the Activation of Concrete by Neutrons from a 3-GeV Proton Beam in Iron', Nucl. Sci. Eng. 38, 265 (1969).

Ar 70 Armstrong, T.W. and Barish, J., 'Reduction of the Residual Photon Dose Rate around High-Energy Proton Accelerators', Nucl. Sci. Eng. 40, 128 (1970).

Ar 73 Armstrong, T.W. and Chandler, K.C., 'Calculation of the Absorbed Dose and Dose Equivalent from Neutrons and Protons in the Energy Range from 3.5 GeV to 1.0 TeV', Health Physics 24, 227 (1983).

Au 68 Auxier, J.A., Snyder, W.S. and Jones, T.D., 'Neutron Interactions and Penetration in Tissue', In: Attix, F.H. and Roesch, W.D., Eds., Radiation Dosimetry, 2nd ed., Vol. 1, p. 275, Academic Press, New York (1968).

Aw 66 Awschalom, M., 'The Use of Multisphere Neutron Detector for Dosimetry of Mixed Radiation Fields', Princeton-Pennsylvania Accelerator Laboratory Report PPAD 596E (1966).

Ba 64 Baarli, J. 1964. Private communication to Middlekoop, W.C., reported in CERN Intern. Rep. AR/INT/SG 64-6.

Ba 65a Baarli, J. and Sullivan, A.H., 'Radiation Dosimetry for Protection Purposes Near High-Energy Particle Accelerators', Health Physics 11, 353 (1965).

Ba 65b Baarli, J. and Sullivan, A.H., 'Health Physics Survey Methods around the CERN High-Energy Accelerators', in Proceedings of the First Symposium on Accelerator Radiation Dosimetry and Experience, USAEC Report CONF 651109, p. 103 (1965).

Ba 66 Baarli, J., Charalambus, S., Dutrannois, J., Goebel, K. Hubell, H.H., Overton, T.R., Rindi, A. and Sullivan, A.H., 'Hazards from Induced Radioactivity near High-Energy Accelerators', CERN Internal Report DI/HP/84 (1966).

Ba 69 Barbier, M., Induced Radioactivity, North Holland, Amsterdam (1969).

Be 69 Bertini, H.W., 'Intranuclear Cascade Calculation of the Secondary Nuclear Spectra from Nucleon-Nucleus Interactions in the Energy Range from 340 to 2900 GeV, and Comparison with Experiment', Phys. Rev. 188, 1711 (1969).

Be 71 Bertel, E., Freytag, E., de Séréville, B. and Wachsmuth, E., in Shielding against Muons, Chapter 6 in 'Radiation Problems Encountered in the Design of Multi-GeV Facilities' (Ed. K. Goebel) CERN Internal Report 71-21, p. 79 (1971).

Bo 62 Bonet-Maury, P., Duhamel, M. and Perrin, F., Proc. 'Premier Colloque International sur la Protection auprès des Grands

Accelératéurs', Paris, France, January 18-20, 1961, Presses Universitaire de France, 108 Bd. Saint-Germain, Paris (1962).

Br 61 Bruninx, E., High-Energy Nuclear Reaction Cross Sections Vol. 1, CERN Report CERN 61-1 (1961).

Br 62 Bruninx, E., High-Energy Nuclear Reaction Cross Sections Vol. 2, CERN Report CERN 62-9 (1962).

Br 64 Bruninx, E., High-Energy Nuclear Reaction Cross Sections Vol. 3, CERN Report CERN 64-17 (1964).

Bu 77 Burgerjon, J.J., et al., 'A Solution for Remote Handling in Accelerator Installations', IEEE Trans. Nucl. Sci. NS-24, 1580 (1977).

Bu 78 Burger, G., Morhart, A. and Schraube, H., 'Recent Results in Neutron Depth Dose Calculations', in Proceedings of the Third Symposium on Neutron Dosimetry in Biology and Medicine, EUR 5848, CEC, Brussels, p. 125 (1978).

Bu 83 Burger, G. and Williams, G., 'Organ Doses and Risks from Neutron Exposure', in Proceedings of the Seminar on Neutron Cancer Risk, Delft, 1982, to be published as an EUR document, CEC, Luxembourg (1983).

Ca 65 Capone, T. et al., 'A Radiation Survey Inside and Outside the CPS Tunnel', CERN Internal Report DI/HP/71 (1965).

Ca 82 Casarett, G.W., Scientific Committee on Basic Radiation Protection Criteria, Reports on Selected Activites in Critical Issues in Setting Radiation Dose Limits, Proceedings of the Seventh Annual Meeting of the NCRP, 8-9 April 1981, p.272 National Council on Radiation Protection and Measurements, Washington D.C. (1982).

CERN 64 CERN, 'Report on the Design Study of a 300 GeV Proton Synchrotron by the CERN Study Group on New Accelerators' (2 vols.), CERN Internal Report, CERN 563 (1964).

Ch 67 Charalambus, S. and Rindi, A., 'Aerosol and Dust Radioactivity in the Halls of High-Energy Accelerators', Nucl. Instr. and Methods 56, 125 (1967).

Ch 78 Chen, S.Y., 'Calculation of Neutron-Fluence-to-Dose-Index Conversion Factors for the Standard ICRU Tissue Phantom by the Monte Carlo Method', Ph.D. Thesis, Nuclear Engineering Dept., Univ. of Illinois at Urbana-Champaign (1978).

Ch 79 Chen, S.Y. and Chilton, A.B., 'Calculation of Fast Neutron Depth-Dose in the ICRU Standard-Tissue Phantom and the Derivation of Neutron Fluence-to-Dose Index Conversion Factors', Radiat. Res. 78, 335 (1979).

Ch 81a Chilton, A.B. and Shiue, Y.L., 'Progress Report on Studies Concerning Doses in the ICRU Sphere Resulting from Neutron Beams', in Proceedings of the Fourth Symposium on Neutron Dosimetry, Vol. I, Radiation Protection Aspects, Edited by G. Burger and H.G. Ebert, Report EUR 7448-EN, CDC, Luxembourg, p. 63 (1981).

Ch 81b Chilton, A.B., 'Calculated Index Quantities for Neutrons', in Proceedings of the European Seminar on Radiation Protection Quantities for External Exposure, Braunschweig, Fed. Rep. of Germany, October 13-15, 1980. EUR 7101-EN, p. 89, Harwood Academic Publishers, Chur, Switzerland (1981).

Cl 64 Climent, V.H., 'Analysis of the Residual Radioactivity of a Large Accelerator', Radiation Research 22, 32 (1964).

Co 62 Cowan, F.P., 'A Preliminary Report on Health Physics Problems at the Brookhaven Alternating Gradient Synchrotron', in op. cit. Bo 62, p. 143 (1962).

Co 65 Cochran, D.R.F. and Israel, H.I., 'The Radiation and Shielding Design Factors for the Los Alamos Meson Physics Facility', Proc. First Symposium on Accelerator Radiation Dosimetry and Experience USAEC Report CONF 651109, p. 459 (1968).

Co 83 Cossairt, J.D., 'Recent Muon Fluence Measurements at Fermilab', Health Phys. 45, 651 (1983).

deS 62a de Staebler, H.,'Transverse Shielding for the Stanford Two-Mile Accelerator,' Stanford Linear Accelerator Center Report SLAC-9, Nov. 1962. See also 'Similarity of Shielding Problems at Electron and Proton Accelerators', Proc. First Symposium on Accelerator Dosimetry and Experience, USAEC Report CONF 651109, p. 429 (1965).

deS 62b de Staebler, H., 'Average Radiation Levels inside the Accelerator Housing When the Machine is Off', Stanford Linear Accelerator Center Internal Report SLAC-TN 6270 (October 1972).

Di 79 Dimbylow, P.J. and Francis, T.M., 'A Calculation of the Photon Depth-Dose Distributions in the ICRU Sphere for a Broad Parallel Beam, a Point Source, and an Isotropic Field', National Radiological Protection Board Report NRPB-R92 (1979).

Dr 78 Drexler, G. and Kramer, R., 'Die Grosse Aquivalentdosindex (ADI) und ihre praktische Bedeutung im Strahlenschutz', 12th Jahrestagung, Norderney, 2-6 October 1978 (Fachverband für Strahlenschutz ev) (1978).

El 71 Ellefsplass, M. Horne, R.A. and Madsen, J.B., 'Remote Handling Equipment and Its Use in Accelerators', Chapter X in Radiation Problems Encountered in the Design of Multi-GeV Research Facilities (K. Goebel, Ed.), CERN Report CERN 71-21 (1971).

Fe 80 Festag, J.C., 'Dose Rates During Experiments with Heavy Ions', in Proc. Vth Congress of International radiation Protection Association, Jerusalem, p. 743 (March 1980).

Fl 65 Flateau, C.R., 'Proposed Remote Handling Method for a Modified AGS', IEEE Trans. Nucl. Sci. NS-12, 656 (1965).

Fl 68 Freytag, E., 'Halbwertzeiten der Aktiverung bei Beschleunigern', Health Physics 14, 267 (1968).

Fr 71 Freytag, E., and Ranft, J., 'Hadronic and Electromagnetic Cascades', Chapter III in Radiation Problems Encountered in the

Design of Multi-GeV Research Facilities, ed. K. Goebel, CERN Report CERN 71-21 (1971).

Ga 72 Gabriel, T.A. and Santoro, R.J., 'Photon Dose Rates from the Interactions of 200 GeV Protons in Iron and Iron-Lead Beam Stops', Oak Ridge National Laoratory Report ORNL TM-3945 (1972).

Gi 64a Gilbert, W.S., 'Induced Activity and Radiation Damage', Lawrence Berkeley Laboratory Report UCID-10014 (1964).

Gi 64b Gilbert, W.S., 'Self-Shielding of γ's from Induced Activity in Accelerator Tunnel Walls', Lawrence Berkeley Laboratory Internal Report UCID-10013 (1964).

Gi 64c Gilbert, W.S., 'Decay of Shut-Down Field in BNL AGS Tunnel', Lawrence Berkeley Laboratory Internal Report UCID-10119 (1864).

Gi 65 Gilbert, W.S. and Thomas R.H., 'Problems of Induced Activity around the 200-BeV Alternating Gradient Synchrotron', Trans. Nucl. Sci. 12, 665 (1965).

Gi 68 Gilbert, W.S. et al., 1966 CERN-LBL-RHEL Shielding Experiment at the CERN Proton Synchrotron, Lawrence Berkeley Laboratory Report UCRL-17941 (1968).

Gi 69 Gilbert, W.S., Goebel, K., Patterson, H.W. and Smith, A.R., 'Concrete Activation Experiment at the Bevatron', Lawrence Berkeley Laboratory Report UCRL-19368 (1969).

Go 65 Gorka, A.J., 'Induced Radioactivity and Remote Handling Methods for Accelerators', IEEE Trans. Nucl. Sci. NS-12, 656 (1965).

Go 67 Goebel, K. 'Personnel Exposure from β− γ radiation of Induced Activity at High Intensity Exploitation of the Proton Synchrotron', CERN Internal Report HP-47-1967 (1967).

Go 69 Golovachik, V.T., Britvich, G.I. and Lebedev, V.N., 'Induced Radioactivity at the IHEP Proton Synchrotron', Institute of High-Energy Physics, Serpukhov Internal Report IHEP 69-76 (1969) (in Russian). English translation available as CERN Trans 72-11 (1972).

Go 71 Goebel, K., Ranft, J. and Stevenson, G.R., 'Remanent Radioactivity in the Accelerator Structure', Chapter VIIIA in Radiation Problems Encountered in the Design of Multi-GeV Research Facilities (K. Goebel, Ed.), CERN Report CERN 71-21 (1971).

Go 76 Gollon, P., 'Production of Radioactivity in Particle Accelerators', IEEE Trans. Nucl. Sci. NS-23, 1395 (1976).

Ha 69 Hajnal, F., et al., 'A Study of the Neutron Cascade in Iron', Nucl. Instrum. Methods 69, 245 (1969).

Ha 75 Harvey, J.R., 'An Approach to the Surveying of Radiation Environments for Radiation Protection Purposes', Phys. Med. Biol. 20, 1003 (1975).

Ha 81 Harder, D., 'Recently Proposed Concepts and Quantities in Radiation Protection', in Proceedings of the European Seminar on

Radiation Protection Quantities for External Exposure, Braunschweig, Fed. Rep. of Germany, October 13-15, 1980. EUR 7101-EN, p. 15, Harwood Academic Publishers, Chur, Switzerland (1981).

He 59 Hess, W.N., Patterson, H.W., Wallace, R.W. and Chupp, E.L., 'Cosmic Ray Neutron Energy Spectrum', Phys. Rev. 116, 445 (1959).

Hi 82 Hirayama, H. Miura, S., Hozumi, K. and Ban, S., 'Measurements of Radionuclides Induced in the Accelerator Structure of KEK', Health Physics 43, 481 (1982).

Ho 75a Hoefert, M. et al., 'The Prediction of Radiation Levels from Induced Radioactivity; Discussion of an Internal Dump Target Facility in the PS', CERN Internal Report DI/HP/185 (1975).

Ho 75b Hoefert, M. and Bonifas, A., 'Measurement of Radiation Parameters for the Prediction of Dose Rates from Induced Radioactivity', CERN Internal Report HP-75-148 (1975).

Ho 75c Horne, R.A. and Ellefsplass, M., 'Long Range, High-Speed Remote Handling at the CERN 26 GeV Proton Synchrotron', in Proc. 23rd Conference on Remote Systems Technology, p. 247 (1975).

Ho 75d Horne, R.A. and Ekberg, E.L., 'Monitor--A Versatile Remote Handling System', Proc. 23rd Conference on Remote Systems Technology, p. 242 (1975).

Ho 78 Horne, R.A., 'Mantis--A Compact Mobile Remote-Handling System for Accelerator Halls and Tunnels', in Proc. 26th Conference on Remote Systems Technology, p. 55 (1978).

Ho 84 Hoefert, M., 'Muons and Exposure Dose', CERN Internal Report TIS-RP/IR/84-23 (1984).

Hu 60 Hubbard, E.L., Main, R.M. and Pyle, R.V., 'Neutron Production by Heavy-Ion Bombardments', Phys. Rev. 118, 507 (1960).

IAEA 75 International Atomic Energy Agency. Engineering Compendium on Radiation Shielding, Jaeger, R.G., Blizard, E.P., Chilton, A.B., Grotenhuis, M., Honig, A., Jaeger, T.A. and Eisenlohr, M.H., Eds., Vol. 2, 'Shielding Materials', Springer Verlag, Berlin [under auspices of the IAEA] (1975).

ICRP 66 International Commission on Radiological Protection, 'Recommendations of the International Commission on Radiological Protection', ICRP Publication 9 (Adopted Sept. 17, 1965), Paragraph 13, Pergamon Press, Oxford (1966).

ICRP 70 International Commission on Radiological Protection, 'Protection against Ionizing Radiation from External Sources', (Adopted by the Commission in Nov. 1969), ICRP Publication 15, Pergamon Press, Oxford (1970).

ICRP 73 International Commission on Radiological Protection, 'Data for Protection against Ionizing Radiation from External Sources: Supplement to ICRP Publication 15', (Adopted by the Commission in April 1971), ICRP Publication 21, Pergamon Press, Oxford

(1973).

ICRP 77 International Commission on Radiological Protection, 'Recommendations of the ICRP', ICRP Publication 26, Pergamon Press, Oxford (1977).

ICRP 82 International Commission on Radiological Protection, 'General Principles of Monitoring for Radiation Protection of Workers', ICRP Publication 35, para. 5, Pergamon Press, Oxford (1982).

ICRP 85 Internation Commission of Radiological Protection, 'The Value of the Quality Factor in the Case of Neutrons', Statement from the 1985 Paris Meeting of the ICRP, ICRP/85/G-03 (26 April 1985).

ICRP 86 International Commission on Radiological Protection, 'Data for Use in Protection against External Radiation', ICRP Publication 44, Pergamon Press, Oxford (1986).

ICRU 68 International Commission on Radiation Units and Measurements, 'Radiation Quantities and Units', ICRU Report 11, Washington, D.C. (1968).

ICRU 71 International Commission on Radiological Units and Measurements, 'Radiation Protection and Instrumentation and its Application', ICRU Report 20, Washington, D.C. (1971).

ICRU 73 International Commission on Radiation Units and Measurements, 'Dose Equivalent—Supplement to ICRU Report 19', ICRU Report 19S, Washington, D.C. (1973). See also: International Commission on Radiation Units and Measurements, 'Radiation Quantities and Units', ICRU Report 19, Washington, D.C. (1971); replaced by ICRU Report 33 (1980).

ICRU 76 International Commission on Radiation Units and Measurements, Conceptual Basis for the Determination of Dose Equivalent', ICRU Report 25, Washington, D.C. (1976).

ICRU 85 International Commission on Radiation Units and Measurements, 'Determination of Dose Equivalents Resulting from External Radiation Sources', ICRU Report 39, Washington, D.C. (1985).

ICRU nd International Commission on Radiation Units and Measurements, Report in preparation, Washington, D.C. (no date).

Ir 67 Irving, D.C., Alsmiller, R.G., Jr. and Moran, H.S., 'Tissue Current-to-Dose Conversion Factors for Neutrons with Energies from 0.5 to 60 MeV', Oak Ridge National Laboratory Report ORNL-4032 (1967).

Ka 72 Kang, Y., et al., 'Design of a Magnetized Iron Muon Shield for a High Energy Neutrino Laboratory', Particle Accel. 4, 31 (1972).

Ke 64 Keefe, D., 'Mu-Meson Shielding Problems at 200 GeV: Approximate Calculations', LBL Internal Report UCID-10018 (1964).

Ke 68 Keefe, D. and Noble, C.M., 'Radiation Shielding for High Energy Muons: The Case of a Cylindrically Symmetrical Shield and No Magnetic Fields', Nucl. Instrum. Methods 64, 173 (1968).

Ki 71 Kitao, K. and Ohata, T., 'Gamma-Ray Analysis on Radioactive Aerosols and Dust in the Machine Hall of a Cyclotron', Health Physics 21, 475 (1971).

Ko 70 Komochkov, M.M., 'The Dubna Synchro-Phasotron', Engineering Compendium on Radiation Shielding Vol. 3, p. 171, Springer-Verlag, New York (1970).

Kr 79 Kramer, R. and Drexler, G., 'Practical Implications of the Concept of Dose Equivalent Index', in Application of the Dose Limitation System for Radiation Protection: Practical Limitations', STI/PUB/521 IAEA, Vienna, p. 451 (1979).

Kr 80 Kramer, R. and Drexler, G., Letter to the Editor: 'The Dose Equivalent Index (DEI) as a Function of Angular Distribution of Photons', Health Phys. 38, 426 (1980).

Kr 82 Kramer, R. and Drexler, G., 'On the Calculation of the Effective Dose Equivalent', Rad. Prot. Dosim. 3(1/2), 13 (1982).

LBL 65 Lawrence Radiation Laboratory, '200 BeV-Design Study' (2 Vols.), Lawrence Radiation Laboratory Report UCRL-16000 (1965).

Li 73 Lim, C.B., 'The Development of a Neutron Spectrometer Using Multi-Wire Spark Chambers', Ph.D. Thesis, University of California, Lawrence Berkeley Laboratory Report LBL-1719 (1973).

Ma 74 Mamont-Čiesla, K. and Rindi, A., 'Spark Chamber Neutron and Proton Spectrometer: First Report on Performance', Lawrence Berkeley Laboratory Report LBL-3343 (1974).

Ma 76 Madey, R., Baldwin, A.R. and Waterman, F.M., 'Neutron Spectrum from 20 to About 600 MeV above the Brookhaven National Laboratory AGS Shielding', Trans. Am. Nucl. Soc. 23, 612 (1976).

McC 77 McCaslin, J.B., Smith, A.R., Stephens, L.D., Thomas, R.H., Jenkins, T.M., Warren, G.J. and Baum, J.W., 'An Intercomparison of Dosimetry Methods in Radiation Fields at Two High-Energy Accelerators', Health Phys. 33, 611 (1977).

McC 81 McCaslin, J.B. and Thomas, R.H., 'Practical Neutron Dosimetry at High Energies', in Proceedings of the European Seminar on Radiation Protection Quantities for External Exposure, Braunschweig, Fed. Rep. of Germany, October 13-15, 1980. EUR 7101-EN, p. 137, Harwood Academic Publishers, Chur, Switzerland (1981).

McC 83 McCaslin, J.B., LaPlant, P.R., Smith, A.R. and Thomas, R.H., Lawrence Berkeley Laboratory Internal Report: 'Bevalac Biomed Radiation Measurements Note H1' (September 1983).

McC 84a McCaslin, J.B., La Plant, P.R., Smith, A.R. and Thomas, R.H., Lawrence Berkeley Laboratory Internal Report: 'Bevalac Biomed Radiation Measurements Note H2' (February 1984).

McC 84b McCaslin, J.B., Smith, A.R., Chen, G.T. and Zink, S., 'Absorbed Dose Estimates of Neutrons from the Primary Beam Particle Interactions in a Water Phantom at the 184-Inch Synchrocyclotron Medical Facility', Lawrence Berkeley Laboratory Internal

Report HPN 142 (August 1984).

McC 85 McCaslin, J.B., La Plant, P., Smith A.R., Swanson, W.P. and Thomas, R.H., 'Neutron Production by Ne and Si Ions on a Thick Cu Target at 670 MeV.A with Application to Radiation Protection', Paper read by title at the 1985 Particle Accelerator Conference, Vancouver, British Columbia, May 13-16, 1985, IEEE Trans Nucl. Sci. NS-32, 3104 (1985).

Mi 65 Middlekoop, W.C. and de Raad, B., ' Induced ^{24}Na in the Concrete of the CPS Tunnel', CERN Internal Report AR/Int. SG/65-13 (1965).

Mo 74 Moore, C. and Velen, S., 'Muon Beam Halo Studies', Fermilab Internal Report TM-497 (1974).

Mo 79 Mole, R.H., "RBE for Carcinogenesis by Fission Neutrons," Health Physics 36, 463 (1979).

Na 66 Nachtigall, D. and Charalambus, S., 'Induced ^{24}Na Activity in the Concrete Sheilding of High-Energy Accelerators', CERN Report CERN 66-28 (1966).

NCRP 57 National Council on Radiation Protection and Measurements, 'Protection Against Neutron Radiation Up to 30 MeV', National Bureau of Standards (NBS Handbook No. 63), Washington, D.C. (1957).

NCRP 71 National Council on Radiation Protection and Measurements, 'Protection against Neutron Radiation', NCRP Report 38, Washington, D.C. (1971).

NRCP 80 National Council on Radiation Protection and Measurements, 'Statement on the Dose Limit for Neutrons', Washington, D.C. (Feb. 21, 1980).

NCRP 82 National Council on Radiation Protection and Measurements, Proceedings of the Seventh Annual Meeting, April 1981, Washington, D.C. (1982).

Ne 66 Neufeld, J., Snyder, W.S., Turner, J.E. and Wright, H.A., 'Calculation of Radiation Dose from Protones and Neutrons', Health Physics 12, 227 (1966).

Ni 74 Nielsen, B., 'Muon Measurements for Radiation Protection', CERN Internal Report HP-74-135 (1971).

OB 68 O'Brien, K. and McLaughlin, J.E., 'The Propagation of the Neutron Component of the Nucleonic Cascade at Energies Less than 500 MeV: Theory and a Solution to the Accelerator Transverse Shielding Problem', Nucl. Instrum. Methods 60, 129 (1968).

OB 71 O'Brien, K., 'Neutron Spectra in the Side-Shielding of a Large Particle Accelerator', USAEC Health and Safety Laboratory Report HASL-240 (1971).

OB 78 O'Brien, K., 'The Application of the Dose-Equivalent Index to the Natural Radiation Background', Health Phys. 35, 506 (1978).

OB 80 O'Brien, K., Letter to the Editor: 'Reply to "The Dose-Equivalent Index (DEI) as a Function of Angular Distribution of Photons"', Health Phys. 38, 428 (1980).

Oh 80 Ohnesorge, W.F., et al., 'Heavy Ion Target Area Fast Neutron Dose Equivalent Rates', 39, 633 (1980).

Op 82 Opelka, J.H., Mundis, R.L., Marmer, G.J., Peterson, J.M., Siskind, B. and Kikta, M.J., 'Particle Accelerator Decommissioning', Argonne National Laboratory Report ANL/ES-82 (1982).

Pa 48 Parker, H.M., 'Health Physics, Instrumentation, and Radiation Protection', Adv. Biol. Med. Phys. 1, 223 (1948).

Pa 58 Patterson, H.W. and Wallace, R., 'A Method of Calibrating Slow Neutron Detectors', Lawrence Berkeley Laboratory Report UCRL-8359 (1958).

Pa 59 Patterson, H.W., Hess, W.N., Moyer, B.J. and Wallace, R.W., 'The Flux and Spectrum of Cosmic Ray Produced Neutrons as a Function of Altitude', Health Phys. 2, 69 (1959).

Pa 65 Patterson, H.W., 'Accelerator Radiation Monitoring and Shielding at the Lawrence Radiation Laboratory, Berkeley', in Proceedings First Symposium on Accelerator Radiation Dosimetry and Experience, Brookhaven National Laboratory, November 1965, USAEC Report CONF-651109, p. 3 (1965).

Pa 69 Patterson, H.W., Low-Beer, A.G. and Sargent, T.N., 'Whole-Body Counting and Bioassay Determination of Accelerator Workers', Health Physics 17, 621 (1969).

Pa 73 Patterson, H.W. and Thomas, R.H., 'Accelerator Health Physics', Academic Press, New York (1973).

Pe 65 Perry, D.R. and Shaw, K.B., 'Radiation Levels in and around Nimrod', Proceedings First Symposium on Accelerator Radiation Dosimetry and Experience, USAEC Report CONF 651109, p. 20 (1965).

Pe 66 Perry, D.R., 'Neutron Dosimetry Methods and Experience on the 7-GeV Proton Synchrotron, Nimrod', Proc. Symp. on Neutron Monitoring for Radiological Protection, IAEA, Vienna, p. 355, STI/PUB/136 (1966).

Pe 68 Penfold, J. and Stevenson, G.R.,'Preliminary Measurements of the Angular Distribution of the Stray Radiation Field, Rutherford Laboratory Internal Report, RP/PN/29 (1968).

Po 81 Pollock, R.W., 'Tritium Contamination in Accelerator Cryogenic Facilities', Health Physics 40, 565 (1981).

Pu 65 Puppi, G. and Dallaporta, N., 'The Equilibrium of the Cosmic Ray Beam in the Atmosphere,' in Progress in Cosmic Ray Physics, Vol. 1, p. 317 (Wilson, J.G., ed.) (1965).

Ri 65 Riddell, R.J., 'High Energy Nuclear Cascades in Matter', Lawrence Berkeley Laboratory Internal Report UCRL-11989 (April 1965).

Ri 69 Rindi, A., 'Present and Projected Uses of Multiwire Spark Chambers in Health Physics', Proc. Second Symposium on Accelerator Dosimetry and Experience, Stanford, California, November 1969, USAEC Report CONF-691101, p. 660 (1969).

Ri 71 Richard-Serre, C., 'Evaluation de la perte d'énergie unitaire et du parcours pour des muons de 2 à 600 GeV dans un absorbant quelconque', CERN Report CERN 71-18 (1971).

Ri 73 Rindi, A. and Thomas, R.H., 'The Radiation Environment of High-Energy Accelerators', Ann. Rev. Nucl. Sci. 23, 315 (1973).

Ri 74 Rindi, A., 'A Spectrometer for Measuring Charged Particles and Neutrons', Nucl. Instr. Methods 116, 471 (1974).

Ro 54 Rossi, B., 'High-Energy Particles', Prentice-Hall, New York (1954), p. 488.

Ro 77 Rossi, H.H., 'A Proposal for the Revision of Quality Factors', J. Envir. Biophys. 14, 275 (1977).

Ro 78 Rossi, H.H. and Mays, C.W., 'Leukemia Risk from Neutrons', Health Phys. 34, 353 (1978).

Ru 66 Rudstam, G., 'Systematics of Spallation Yields', Z. Naturforsch. 21a, 1027 (1966).

Ry 82 Ryder, R., 'Neutron Production from Protons and Deuterons', Daresbury Laboratory Internal Report DL/NUC/TM60A (1982).

Sc 70 Schönbacher, H., Sullivan, A.H. and Baarli, A.H., 'The Surface Dose Hazard from Radioactivity Induced in High-Energy Particle Accelerators', CERN Internal Report DI/HP/126 (1970).

Sc 85 Schönbacher, H. and Tavlet, M. 'Demontage des ISR. Activites du Service Radioprotection', CERN Internal Report TIS-RP/IR/85-03 (1985).

Sh 68a Shaw, K.B., Stevenson, G.R. and Thomas, R.H., 'Evaluation of Dose Equivalent from Neutron Energy Spectra', Rutherford Laboratory Report RPP/R5 (1968).

Sh 68b Shaw K.B., Stevenson, G.R. and Thomas, R.H., 'Depth Dose and Dose Equivalent Data as Functions of Neutron Energy', Rutherford Laboratory Report RHEL/M149 (1968).

Sh 69 Shaw, K.B., Stevenson, G.R. and Thomas, R.H., 'Evaluation of Dose Equivalent from Neutron Energy Spectra', Health Phys. 17, 459 (1969).

Sh 83 Shiue, Y.L. and Chilton, A.B., 'Calculation of Low-Energy Dose Indices and Depth Doses in the ICRU Sphere', Radiat. Res. 93, 421 (1983).

Sm 58 Smith, A.R., 'The Stray Radiation Field of the Bevatron', Lawrence Berkeley Laboratory Internal Report UCRL-8377, July 1958.

Sm 62 Smith, A.R., 'Measurements of Radiation Field Around High Energy Accelerators', op. cit., Ref. Bo 62, p. 137 (1962).

Sm 81 Smith, A.R., Schimmerling, W., Kanstein, L.L., McCaslin, J.B. and Thomas, R.H., 'Neutron Flux Density and Secondary-Particle Energy Spectra at the 184-Inch Synchrocyclotron Medical Facility', Medical Physics 8(5), 668 (1981).

Sn 50 Snyder, W.S., 'Calculations for Maximum Permissible Exposure to Thermal Neutrons', Nucleonics 6(2), 46 (1950).

Sn 57 Snyder, W.S., 'Depth Dose, in Protection Against Neutron Radiation up to 30 Million Electron Volts', op. cit. NRCP 57, p. 39.

Sn 71 Snyder, W.S., 'Dose Distribution in a Cylindrical Phantom for Neutron Energies up to 14 MeV', op. cit., Ref NCRP 71, p. 46.

So 57 Solon, L.R. (Ed.), Proc. Conf. on Shielding of High-Energy Accelerators, New York, New York, April 11-13, 1957, USAEC Report TID-7545 (1957).

So 83 Sowby, F.D., International Commission on Radiological Protection, private communication (1983).

St 67 Stevenson, G.R., 'Neutron Spectrometry from 0.025 eV to 25 GeV', Rutherford Laboratory Report RHEL/R 154 (1967).

St 69 Stephens, L.D. and Miller, A.J., 'Radiation Studies at a Medium Energy Accelerator', in Proceedings of the Second International Conference on Accelerator Dosimetry and Experience, Stanford, California, 5-7 November 1969, USAEC Report CONF 691101, p. 459 (1969).

St 73a Stevenson, G.R., Hoefert, M., Neufeld, J., Rindi, A., Routti, J.T., and Pretre, S., 'Standardizing the Fluence-to-Dose Equivalent Conversion Factors for Whole-Body Neutron Exposures', in Proceedings of the Symposium on Neutron Monitoring for Radiation Protection Purposes, Vol. 1, p. 177, IAEA, Vienna, STI/PUB/318 (1973).

St 73b Stevenson, G.R., et al., Discussion in op. cit., Ref. St 73a, p. 185.

St 73c Stevenson, G.R., 'The Determination of Remanent Dose Rates from Hadron-Cascade Star Densities--A Reappraisal of the Oak Ridge Comparisons', CERN Internal Report LABII-RA/Note/73-17 (1973).

St 76 Stevenson, G.R., 'The Radiation Environment of Proton Accelerators and Storage Rings, CERN Report CERN 76-04 (1976).

St 81 Stewart, D.C., Handling of Radioactivity, John Wiley, New York (1981).

St 83 Stevenson, G.R., 'Dose and Dose Equivalent from Muons', CERN Divisional Report TIS-RP/099 (1983).

St 84 Stevenson, G.R., 'The Estimation of Dose Equivalent from the Activation of Plastic Scintillators', Health Physics 47, 837 (1984).

St 85a Straume, T., 'A Radiobiological Basis for the Establishment of Exposure Limits to Neutrons', Health Physics 49, 883 (1985).

St 85b Stapleton, G.B., Rutherford-Appleton, private communication, September 1985.

Su 65 Sullivan, A.H. and Overton, T.R., 'Time Variation of the Dose Rate from Radioactivity Induced in High-Energy Particle Accelerators', Health Phys. 11, 1101 (1965).

Su 71 Sullivan, A.M., 'An Approximate Relation for the Estimation of the close Rate from Radioactivity Induced in High Energy Particle Accelerators', CERN Internal Report MP-71-196 (1971).

Su 72a Sullivan, A.H., 'An Approximate Relation for the Prediction of the Dose Rate from Radioactivity Induced in High-Energy Particle Accelerators', Health Phys. 23, 253 (1972).

Su 72b Sullivan, A.H., 'Induced Radioactivity Dose Rates from Steel and Lead', CERN Internal Report HP-72-106 (1972).

Su 82 Sullivan, A.H., 'Dose Rates from Radioactivity Induced in Thin Foils', CERN Internal Report HS-RP/IR/82-46 (1982).

Su 83 Sullivan, A.H., 'Some Ideas on Radioactivity Induced in High-Energy Particle Accelerators', CERN Internal Report TIS-RP/TM/83-27 (1983).

Sw 79 Swanson, W.P., 'Radiological Safety Aspects of the Operation of Electron Linear Accelerators', Technical Report 188, IAEA, Vienna (1979).

Sw 80 Swanson, W.P., 'Estimate of the Risk in Radiation Therapy Due to Unwanted Neutrons', Medical Physics 7(2), 141 (1980).

Ta 65 Tardy-Joubert, P., 'Methods and Experience Acquired in Dosimetry at the Synchrotron Saturne', Proc. First Symposium on Accelerator Radiation Dosimetry and Experience USAEC Report CONF-651109, p. 117 (1965).

Th 67 Thomas, R.H., 'Radiation Field Observed around High Energy Accelerators', in Progress in Radiology, Vol. 2, Excerpta Medica Foundation, Amsterdam, p. 1829 (1967).

Th 71 Theriot, D., Awschalom, M., Lee, K., 'Muon Shielding Calculations: Heterogeneous Passive and Active Shields, Applications to Experimental Beams and Areas', in Proc. Int. Cong. Radiat. Prot. Accel. and Space Radiat., Geneva, CERN 71-16, p. 641 (1971).

Th 73 Thomas, R.H., 'Neutron Dosimetry at High-Energy Particle Accelerators', in Neutron Monitoring for Radiation Protection Purposes, Vol. 1, p. 327, IAEA, Vienna, STI/PUB/318 (1973).

Th 75 Thomas, R.H., 'Implementing the Requirements to Reduce Radiation Exposure to...as Low as Practicable at the Lawrence Berkeley Laboratory', Lawrence Berkeley Laboratory Report LBL-3604 (1975).

Th 85a Thomas, R.H. and Stevenson, G.R., 'Radiation Protection around High-Energy Accelerators', Rad. Prot. Dosim. 10 (1-4), 283 (1985).

Th 85b Thomas, R.H., 'Dosimetric Aspects', in Some Important Issues in Developing Radiation Protection Issues, Proceedings of the 1984 Annual Meeting of the National Council on Radiation Protection and Measurements, Washington, D.C., NCRP, Washington, D.C., p. 182 (1985).

USAEC 65 Proc. First Symp. on Accelerator Radiation Dosimetry and Experience, Brookhaven National Laboratory, November 3-5, 1965, USAEC Report CONF-651109 (1965).

Wa 69 Watson, E.E., Cloutier, R.J. and Berger, J.D., 'Tritium Concentrations in Neutron Generator Pump Oil', Health Phys. 17, 739 (1969).

Wa 84 Wagner, S.R., 'Definition and Realization of the Operational Quantities Used or Proposed for Radiation Protection Measurements', paper presented at the EURADOS-Workshop 'Practical Implementation of Microdosimetric Counts in Radiation Protection', Homburg/Saar, May 15-17, 1984, Rad. Prot. Dosim. 9, 153 (1984).

Wa 85 Wagner, S.R., 'Quantities and Units for Neutron Dosimetry in Radiation Protection', Radiation Protection Dosimetry 10 (1-4), 23 (1985).

Wr 69 Wright, H.A., Anderson, V.E., Turner, J.E., Neufeld, J. and Snyder, W.S., 'Calculation of Radiation Dose due to Protons and Neutrons with Energies from 0.4 to 2.4 GeV', Health Physics 16, 13 (1969).

Wy 83 Wyckoff, H., International Commission on Radiation Units and Measurements, private communication (1983).

Ze 65 Zerby, C.D. and Kinney, W.E., 'Calculated Tissue Current-to-Dose Conversion Factors for Nucleons below 400 MeV', Nucl. Instrum. Meth. 36, 125 (1965).

Table 2.1
Radiation spectrum above Nimrod extracted proton beam shielding (Pe 66).

Type of radiation	Energy range	Estimated % of neutron flux density	Estimated % of total dose-equvialent
Neutrons	<1 eV	<7	<1
Neutrons	1 eV-0.7 MeV	70	20
Neutrons	0.7-3 MeV	15	35
Neutrons	3-7 MeV	7	25
Neutrons	7-20 MeV	1.5	5
Neutrons + protons	20-100 MeV	1	5
Neutrons + charged particles	>100 MeV	0.5	4
Other particles + gammas	—	—	<2

Table 2.2
Composition of radiation fields above thick shields at the CPS

Radiation component	Percentage of dose equivalent	
	Above concrete shield bridge[a]	Above target through earth shield[b]
Thermal neutrons	11-12	<1-3
Fast neutrons (0.1 MeV < E < 20 MeV)	50-70	10-37
High-energy particles (E > 20 MeV)	2-25	52-89
γ rays and ionization from charged particles	2-19	1-13

[a](Ba 64)
[b](Ba 65a,b), (Ca65)

Table 2.3
Calculated ratios of particles at different depths in the cascade.[a]
[after Stevenson (St 84)].

Forward Direction:	Particle	$R(z_1/z_2)$:	z_1 = 1.0 m, z_2 = 0.5 m	z_1 = 1.5 m, z_2 = 1.0 m	z_1 = 2.0 m, z_2 = 1.0 m
	p		0.27 ± 0.02	0.19 ± 0.03	0.03 ± 0.01
	n		0.35 ± 0.03	0.27 ± 0.02	0.04 ± 0.01
	π		0.23 ± 0.02	0.24 ± 0.03	0.04 ± 0.01
Lateral Direction:	**Particle**	$R(r_1/r_2)$:	r_1 = 0.4 m, r_2 = 0.2 m	r_1 = 0.6 m, r_2 = 0.4 m	r_1 = 0.8 m, r_2 = 0.4 m
	p		[b]	[b]	[b]
	n		0.25 ± 0.01	0.28 ± 0.2	0.07 ± 0.1
	π		0.01 ± 0.01	[c]	[c]

[a] The ratio $R_x = N_x(z_1/N_x(z_2)$ or $R_x = N_x(r_1)/N_x(r_2)$ is calculated where x is the particle type (p, n, π) and $N_x(z)$ or $N_x(r)$ is the number of particles of type x at depth z or radius r.

[b] No protons detected beyond r = 0.2 m.

[c] No pions detected beyond r = 0.4 m.

Table 2.4
Comparison of calculated values of various dose-equivalent quantities in several typical accelerator neutron spectra.

Spectrum	H_m	H_s	H_p
RT	1.21	0.86	1.00
RSB	1.33	0.99	1.00
BEV	1.58	1.26	1.00
X2	1.23	0.96	1.00
P1	1.73	1.49	1.00
PLA	1.94	1.68	1.00
CR	1.73	1.53	1.00

Table 2.5
Radionuclides commonly identified in solid materials irradiated around accelerators (adapted form Paterson and Thomas).

Irradiated material	Radionuclides
Plastics, oils	^{7}Be, ^{11}C
Concrete, aluminium	As above, plus ^{22}Na, ^{24}Na, ^{32}P, ^{42}K, ^{45}Ca
Iron, steel	As above, plus ^{44}Sc, ^{44m}Sc, ^{46}Sc, ^{47}Sc, ^{48}Sc, ^{48}V, ^{51}Cr, ^{52}Mn, ^{52m}Mn, ^{54}Mn, ^{56}Mn, ^{57}Co, ^{58}Co, ^{60}Co, ^{57}Ni, ^{55}Fe, ^{59}Fe
Copper	As above, plus ^{65}Ni, ^{61}Cu, ^{64}Cu, ^{63}Zn, ^{65}Zn

Table 2.6
Summary of reported radiation measurements at U.S. accelerators [adapted *from Opelka et al. (Op 62)*].

Size	Energy	Location	Time from shutoff	Measured radiation exposure from: Accelerator components	Accelerator surface	External Beam-line components	Room or general area
Cyclotrons:							
31 in. diam.	15 MeV	Duke	Immed.			<2.5 mR/h to >1 R/h @ 3 ft @ contact	--
38 in. diam.	22 MeV	Medi-Phys.	4 h	0.5-5.5 R/h @ 3 ft		0.3-1.5 R/h @ 3 ft	30 mR/h
38 in. diam.	22 MeV	NE Nucl.	Immed.	--	1.25 R/h @ 25 ft	--	--
38 in. diam.	22 MeV	UCLA	2-3 wk	--	125 R/h @ 1 ft		
52 in. diam.	28 MeV	U. of Colo.	0.25 h	--	50-400 mR/h @ 3 ft		
60 in. diam.	40 MeV	ANL	--	--	25 mR/h @ 1 ft 300 mR/h @ 2 ft	up to 50 mR/h	5-15 mR/h
60 in. diam.	40 MeV	U. of Wash.	16 h	--	100-245 mR/h @ 3 ft	1-60 mR/h @ 3 ft	3.6-13 mR/h
76 in. diam.	50 MeV	NRL	0.33 h	--	1-13 mR/h @ 3 ft	1-6 mR/h @ 3 ft	0.75-2 mR/h
83 in. diam.	55 MeV	NASA Lewis	0.5 h	--	0.16-2.0 R/h @ 3 ft	3.5-180 mR/h @ 3 ft	--
88 in. diam.	60 MeV	LBL	0.2 h		<1 R/h @ 3 ft	>2.5 to <1 R/h @ 3 ft	--
88 in. diam.	60 MeV	Texas A&M	--	--	0-100 mR/h @ contact	--	0.2-2 mR/h
Synchro-cyclotrons:							
95 in. diam.	160	Harvard	--	--	0.5-3.0 R/h @ contact	1-800 mR/h @ contact	--
184 in. diam.	730 MeV	LBL	--	>1 R/h @ 3 ft	--	<1 R/h @ 3 ft	--
197 in. diam.	680 MeV	NASA/SREL	--				
Synchrotrons:							
60 ft diam.	3 GeV	PPA	8 d	5-7 R/h @ contact	250 mR/h @ contact	1-80 mR/h 1-4 mR/h @ 3 ft	
100 ft diam.	6.2 GeV	LBL Bev.	32 h	--	2-800 mR/h @ contact 1.5-450 mR/h @ 12 in.	--	--
180 ft diam.	12.5 GeV	ANL-ZGS	10 d		10-200 mR/h @ contact	--	7-60 mR/h
860 ft diam.	33 GeV	BNL-AGS	--	>1 R/h @ 3 ft	--	<1 R/h @ 3 ft	--
5000 ft diam.	500 GeV	FNAL	"Short"	>1 R/h @ 3 ft	--	>1 R/h @ 3 ft	--
Electron linacs:							
30 ft long	35 MeV	IRT	--	<1 mR/h @ 3 ft	--		
600 ft long	400 MeV	MIT/Bates	"Short"	--	2-60 mR/h @ contact	up to 110 R/h	
10000 ft long	22 GeV	SLAC	--	<2.5 mR/h @ 3 ft	--		@ contact --
Proton linac:							
2600 ft long	800 MeV	LAMPF	--	--	>1 R/h @ contact	>> 10^3 R/h @ contact	

-- no data.

Table 2.7
Photon dose rates from proton irradiation [from Barbier et al. (Ba 69)].

Proton energy	γ dose rates in μSv/h per kg at 1 m ($\phi = 10^2$ protons cm^{-2} s^{-1})							
(MeV)	0	1 h	6 h	1 d	7 d	30 d	180 d	360 d
50	0.350	0.287	0.271	0.265	0.237	0.204	0.144	0.097
100	0.462	0.352	0.329	0.318	0.267	0.220	0.142	0.045
600	0.347	0.271	0.249	0.225	0.161	0.100	0.048	0.029
2900	0.305	0.244	0.215	0.187	0.123	0.075	0.033	0.021

Table 2.8
Methods of reducing dose rates from activity induced in concrete.

Method	Reduction factor	Ref.
0.8% B addition by weight	10	Gi 69
0.3% B addition by weight	3	Na 66
0.1% B addition by weight	9	Ar 70
0.166 g/cm^2 B coating	3	Ar 70
1/32-inch Cd coating	2.7	Ar 70

Table 2.9
Particle accelerators with energy above 1 MeV that had been taken out of operation in the USA by mid-1978 (from Opelka et al.).

Institution	Identification	Disposition	Year
Brookhaven Nat. Lab.	Cosmotron (3-GeV proton synchrotron	Dismantled	1966
Brookhaven Nat. Lab.	18-in. FF cyclotron	Dismantled	1963
UCLA	41-in. synchrocylotron	Dismantled	1961
UCLA	50-in. AVF cyclotron	Dismantled	1973
Cal. Tech	1.1-GeV electron synchrotron	Dismantled	1968
Carnegie Inst.	60-in. FF cyclotron	Stored	1955
Carnegie Mellon	141-in. synchrotron	Dismantled	1973
Univ. of Chicago	170-in synchrotron	Partially dismantled	
Univ. of Chicago	100-MeV betatron	Dismantled	1955
Univ. of Chicago	32-in. FF cyclotron	Dismantled	1944
Univ. of Chicago	170-in. FF cyclotron	Dismantled	1971
Chicago Nuclear	3-MV Van de Graaff	Shut down	1972
Columbia Univ.	37-in. FF cyclotron	Dismantled	1965
Columbia Univ.	5.5-MV Van de Graaff	Shut down	1970
Cornell Univ.	Electron synchrotron (CES)	Dismantled	
Univ. of Florida	1-MV Van de Graaff	Dismantled	1965
General Electric	100-MeV betatron	Dismantled	1973
Harvard Univ.	Electron accelerator (CEA)	Dismantled	1973
Univ. of Illinois	50-in. FF cyclotron	Dismantled	1968
Univ. of Illinois	300-MeV betatron	Dismantled	1968
Univ. of Illinois	25-MeV betatron	Dismantled	1972
Indiana Univ.	45-in. FF cyclotron	Dismantled	1968
Iowa State Univ.	70-MeV electron synchrotron	Mothballed	1972
Iowa State Univ.	4-MV Van de Graaff	Dismantled	1964
Johns Hopkins Univ.	1-MV Van de Graaff	Dismantled	1962
Johns Hipkings Univ.	3-MV Van de Graaff	Dismantled	1974
Knolls Atomic Power Lab.	100-MeV betatron	Scrapped	1970
Univ. of Texas	2-MV Van de Graaff	Dismantled	1962
LBL	340-MeV electron synchrotron	To Smithsonian	1960
LBL	32-in. FF cyclotron	To Lawrence Hall	1940
LBL	27-in. FF cyclotron, 6 MeV	To Museum	
LBL	30-MeV proton linac	Decommissioned	1960
LLNL	90-in. FF cyclotron	Dismantled	1971
LLNL	35-MeV electron linac	Dismantled	1970
LASL	2.5-MV Van de Graaff	Dismantled	1963
LASL	2.5-MV Van de Graaff	Dismantled	1965
LASL	FF cyclotron	Dismantled	1974
LASL	Electron prototype accelerator (EPA)	Shut down(?)	~1970
LASL	15-MeV betatron	Scrapped	~1970
LASL	10-MeV "portable" betatron (10 units)	Scrapped	1955
Louisana State Univ.	10-MeV "portable" betatron, modified	To Univ. of N.M.	1960
MIT	1-MV Van de Graaff	Dismantled	1966
MIT	42-in. FF cyclotron	Mothballed	1973
MIT	300-MeV electron synchrotron	Dismantled	1960
MIT	2-MV Van de Graaff	To Boston Museum	1950
MIT	17-MeV electron linac	Dismantled	1968

Continued ↓

Continuation of Table 2.9

MIT	8-MV Van de Graaff	Dismantled	1960
Univ. of Michigan	100-MeV electron synchrotron	Dismantled	1960
Univ. of Michigan	83-in. 35-MeV AVF cyclotron	Dismantled	1978
Univ. of Michigan	50-in. proton linac	Dismantled	1968
Univ. of Minnesota	4-MV Van de Graaff	Dismantled	1966
Nat. Bureau of Stds.	50-MeV betatron	--	1965
Naval Research Lab.	2-MV Van de Graaff	Dismantled	1966
Northwestern Univ.	4.5 Van de Graaff	Stored	1968
Oak Ridge Nat. Lab.	63-in. FF cyclotron	To museum	1962
Ohio State Univ.	2-MV Van de Graaff	Dismantled	1962
Ohio State Univ.	45-in. FF cyclotron	Shut down	1972
Oregon State Univ.	37-in. AVF cyclotron	Dismantled	1973
Univ. of Pennsylvania	12-MV tandem Van de Graaff	Dismantled	1974
Penn. State Univ.	6-MV Van de Graaff	Shut down	1973
Univ. of Pittsburgh	45-in. FF cyclotron	Dismantled	1967
Princeton Univ.	3-GeV proton synchrotron (PPA)	Sent to ANL	
Princeton Univ.	35-in. synchrotron	Mothballed	1967
Purdue Univ.	37-in. FF synchrotron	Dismantled	1968
Purdue Univ.	300-MeV electron synchrotron	Dismantled	1961
Rensselaer Poly. Inst.	20-MeV betatron	Dismantled	1968
Univ. of Rochester	130-in. synchrotron	Dismantled	1968
Univ. of Rochester	240-MeV electron synchrotron	Stored	1968
Univ. of California	31-MeV proton linac	Dismantled	1967
Space Rad. Eff. Lab.	Synchrocyclotron	Mothballed	1979
Stanford Univ.	Mark I electron linac	Extended to Mark II	1947
Stanford Univ.	Mark II 1200-MeV electron linac	Sent to Brazil	1948
Stanford Univ.	Mark III electron linac	Dismantled, parts replaced	1963
Univ. of Texas	17.5-MV tandem Van de Graaff (CN + EN)	Mothballed	1977
Tulane Univ.	3-MV Van de Graaff	Sold	1973
Univ. of Virginia	70-MeV electron synchrotron	Stored	1968
Washington State. Univ.	2-MV Van de Graaff	Shut down	1973
Yale Univ.	Hilac	Dismantled	1974

Sources: 'Nuclear Science: A Survey of Funding, Facilities and Manpower', Vol. II, Part A, NAS, 1969; plus contributions from reviewers who helped update the list to mid-1978.

Table 2.10
Mass of radioactive waste from selected accelerators [from Opelka et al. (Op 82)].

Location	Energy and size	Estimated mass of material (> 1 R/h at 1 m) (kg)	Reported mass of material (> 2.5 mR/h at 1 m) (kg)	Reported mass of accelerator (kg)	Total mass of active material (kg)	Estimated amount of radioactivity (Ci)	Time-averaged beam (μA)	Use(s)	Remarks
Positive-ion cyclotrons and synchrotrons:									
Duke Univ.	15 MeV, 31 in.	--	--	--	--	7.6 E+1	30	R	
Medi-Phy, Emeryville, CA	22 MeV, 38 in.	--	--	2.0 E+4	2.2 E+4	1.5 E+4	400	I	
Medi-Phy, S. Plnfld., NJ	22 MeV, 38 in.	--	--	2.0 E+4	2.2 E+4	1.5 E+3	400	I	
New England Nuclear	22 MeV, 38 in.	--	--	2.0 E+4	2.2 E+4	4.1 E+2	100	I,D	
UCLA	22 MeV, 38 in.	--	2.3 E+3	2.3 E+4	2.5 E+4	1.1 E+2	30	I	
Univ. of Colo.	28 MeV, 52 in.	--	2.8 E+3	9.0 E+4	9.9 E+4	7.6 E+2	160		
ANL	20 MeV, 60 in.	4.8 E+1	8.7 E+3	2.9 E+5	3.2 E+5	--	--	R,I	
Univ. of Wash.	40 MeV, 60 in.	1.1 E+2	2.7 E+4	1.1 E+5	1.2 E+5	--	--	R	
Mich. State Univ.	50 MeV, 67 in.	2.5 E+0	3.9 E+2	2.0 E+5	2.2 E+5	1.7 E+2	20	R	
NASA Lewis	55 MeV, 83 in.	5.4 E+1	2.3 E+5	2.3 E+5	2.3 E+5	2.3 E+2	25	R	
LBL	60 MeV, 88 in.	1.4 E+1	6.7 E+2	3.0 E+5	3.3 E+5	1.9 E+3	190	R	
Texas A&M	60 MeV, 88 in.	0	6.4 E+4	2.6 E+5	3.0 E+5	2.9 E+3	285	R	
Harvard Univ.	160 MeV, 95 in.	4.2 E+2	8.0 E+3	7.1 E+5	7.8 E+5	5.4 E+1	0.5	M	
LBL	730 MeV, 184 in.	--	--	4.3 E+6	4.7 E+6	6.2 E+1	0.5	M	
NASA/SEEL	600 MeV, 197 in.	2.0 E+4	1.2 E+5	2.6 E+6	2.9 E+6	2.0 E+5	2.0	R	Shut down 1978
Indiana Univ.	225 MeV, 272 in.	--	--	2.0 E+6	2.2 E+6	--	--	R	
Proton Synchrotrons:									
Princeton Penn	3 GeV, 60 ft	--	--	1.4 E+6	1.5 E+7[b]	5.1 E+1	0.1	R	Shut down 1972
LBL Bevatron	6.2 GeV, 100 ft	--	--	9.8 E+6	1.1 E+7	9.5 E+2	0.9	R	w/ 50-MeV linac
ANL-ZGS	12.7 GeV, 180 ft	2.3 E+4	9.5 E+6	1.4 E+7	1.5 E+7[b]	2.2 E+2	0.1	R	w/ 50-MeV linac
BNL-AGS	33 GeV, 860 ft	6.0 E+6	3.7 E+7	1.8 E+8	2.0 E+8[c]	2.2 E+3	0.4	R	w/ 200-MeV linac
FNAL	400 GeV, 5000 ft	4.6 E+5	2.0 E+6	1.0 E+7	1.1 E+7[c]	6.8 E+3	0.1	R	w/ 8-GeV booster synchrotron and 200-MeV linac
Electron synchrotron:									
Cornell Univ.	12 GeV, 820 ft	--	--	1.3 E+5	--	--	0.8	R	
Electron linacs:									
IRT San Diego	35 MeV, 30 ft	0	3.1 E+2	1.0 E+4 to 1.0 E+5	--	--	500		
ANL	35 MeV, 30 ft	0	4.0 E+1	4.0 E+4[d]	--	--	--	R	Includes power supplies, etc.
MIT Bates Lab.	400 MeV, 600 ft	--	5.5 E+4[d]	--	--	--	--	R	
SLAC	20 GeV, 2 mi.	--	3.4 E+5	--	--	--	30	R	
Proton linacs:									
LAMPF	800 MeV, 2600 ft	--	5.5 E+7	--	--	9.5 E+4	700[e]	R	
Electrostatic									

Continued ↓

Continuation of Table 2.10

accelerators:							
ANL-Tandem	30 MeV	0	--	5.0 E+4	3.0 E+0	--	--
Univ. of Wash. Tandem	--	0	--	5.0 E+4	3.0 E+0	--	--

[a] R = research; I = isotope separation; D = machine developement; M = medical. [b] Total includes some shielding.
[c] No shield material. [d] Accelerator tank and beam stops only. [e] Design goal = 120 h/wk at 1000 mA.

Table 2.11
Estimated costs of dismantlement and immediate disposal of four prototypic accelerators (1978 thousand US$). (From Opelka et al.)

Facility	Dismantling	Packaging	Transportation	Disposal	Total[a]
ZGS	3700	410	1000	290	6300
60-in. cyclotron	800	40	200	600	1300
22-MeV electron linac	60	0.5	2	0.7	80
Tandem Van de Graaff	100	0.5	2	0.7	140

[a] Sum of dismantling, packaging, transportation, disposal and a 25% contingency factor for all activities.

FIGURE CAPTIONS FOR CHAPTER 2

Figure 2.1. Neutron spectra measured by the Health Physics Group of the Lawrence Berkeley Laboratory in the mid-1960s (see text for the explanation of the designations PSB, RT, BEV and CR).

Figure 2.2. Neutron spectra measured at the 7-GeV proton synchrotron (Nimrod) of the Rutherford Laboratory using Bonner spheres (see text for the explanation of the designations PLA, P1, X2).

Figure 2.3. Neutron spectra measured at the Princeton-Pennsylvania 3-GeV proton synchrotron using Bonner spheres.

Figure 2.4. O'Brien neutron spectrum (OB 68, OB 71).

Figure 2.5. Comparison of the three neutron spectra: the open circles indicate the lateral iron spectrum of Fig. 2-11; the solid line is the concrete spectrum of Fig. 2-4; and the crosses are the experimental data from Madey et al. (Ma 76).

Figure 2.6. Range-energy curves for muons in various materials [After Richard-Serre (Ri 71)].

Figure 2.7. The energy spectrum of protons from the iron shield wall (approximately 3000 g cm^{-2} thick) of the Dubna Synchrocyclotron which separates the cyclotron room from the experimental area.

a. Energy spectrum from a 'thin' shield with the spectrometer aligned as shown in inset A.

b. Energy spectrum from a 'thick' shield with the spectrometer aligned as shown inset B. [After Aleinikov et al. (Al 75)].

Figure 2.8. Plan view of the cyclotron and experimental area for the measurements of Fig. 2.7. The two locations of the proton spectrometer are shown.
1 - the vacuum chamber of the cyclotron.
2 - beam transport equipment
3 - the shield wall (3000 g cm^{-2} Fe)
S_1, S_2 and S_3 are the scintillation counters of the spectrometer.
[After Aleinikov et al (Al 75)].

Figure 2.9. Illustration of the geometrical configuration used in the Monte Carlo hadron cascade calculation. [After Stevenson (St 84)].

Figure 2.10. Forward particle spectra in Fe. The symbols •, ×, O and + correspond to depths of 0.5, 1.0, 1.5 and 2.0 m, respectively (St 84).

Figure 2.11. Lateral particle spectra in Fe. The symbols •, ×, O and + correspond to radii of 0.2, 0.4, 0.6 and 0.8 m, respectively (St 84).

Figure 2.12. Ratios of protons to neutrons and pions to neutrons as a function of energy for the forward spectra. The symbols •, × and O

correspond to depths of 0.5, 1.0 and 1.5 m, respectively (St 84).

Figure 2.13. Ratios of protons to neutrons and pions to neutrons as a function of energy at a radius of 0.2 m for the lateral spectra (St 84).

Figure 2.14. Relative photon dose rate from an irradiated iron block as a function of time after shut-down and irradiation time, from Goebel et al. (Go 71). Solid lines are the calculations of Armstrong and Alsmiller (Al 69b) for a cylinder of 40 cm diameter irradiated by 3-GeV protons. × = experimental data and Δ = points calculated from the Sullivan-Overton formula (Su 65) normalized to the curves at an irradiation time t_1 of 1 month and a cooling time of 1 day.

Figure 2.15. Relative photon dose rate from different isotopes at the surface of an iron cylinder as a function of time after shut-down for an infinite irradiation time. Proton energies are 3 GeV and 200 MeV. From Armstrong and Barish (Ar 69c).

Figure 2.16. Absorption curves for photons in lead. Curves for irradiated iron objects from Goebel (Go 67). Isotopic data from ICRP Publication 21 (ICRP 73).

Figure 2.17. Variation of remanent gamma dose rate with atomic number of the irradiated element, from Goebel et al. (Go 71) based on data from Barbier (Ba 69).

Figure 2.18. Comparison of the average total photon dose rates from an irradiated iron cylinder and for a cylinder surrounded by two thicknesses of lead for several irradiation times, from Gabriel and Santoro (Ga 72).

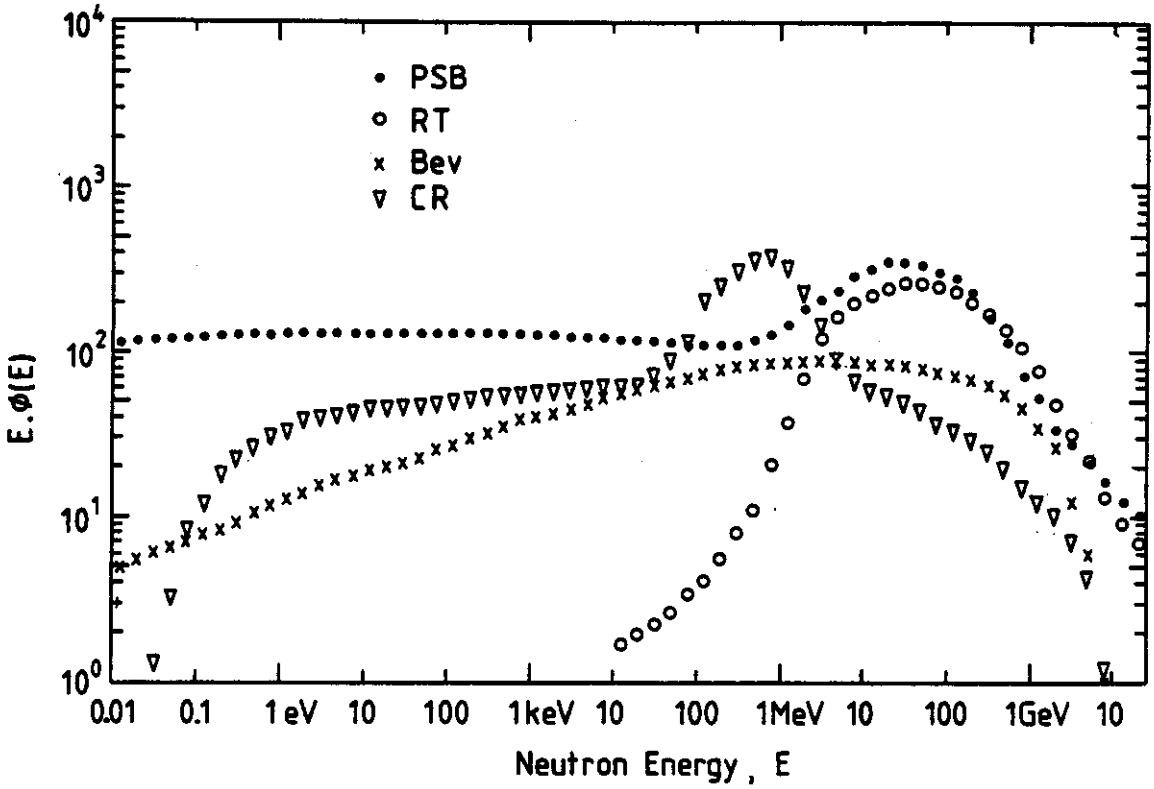

Fig. 1

XBL 8412-5057

2.1

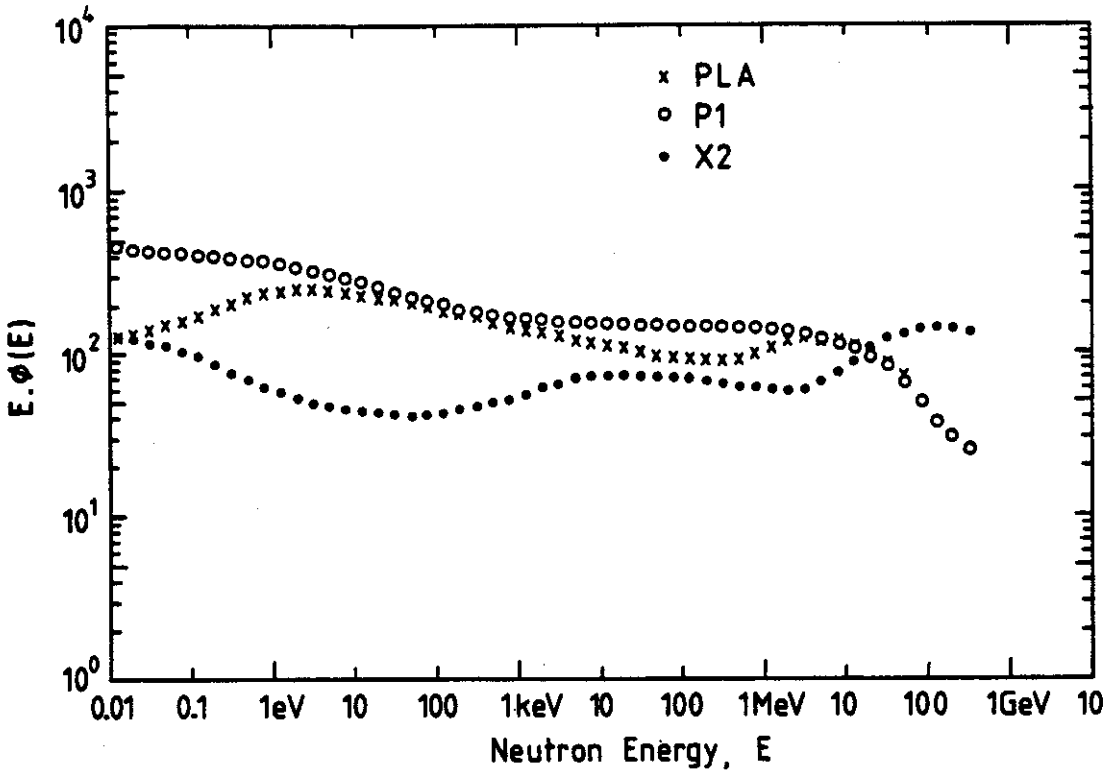

Fig. 2

XBL 8412-5058

67

2.2

2.2

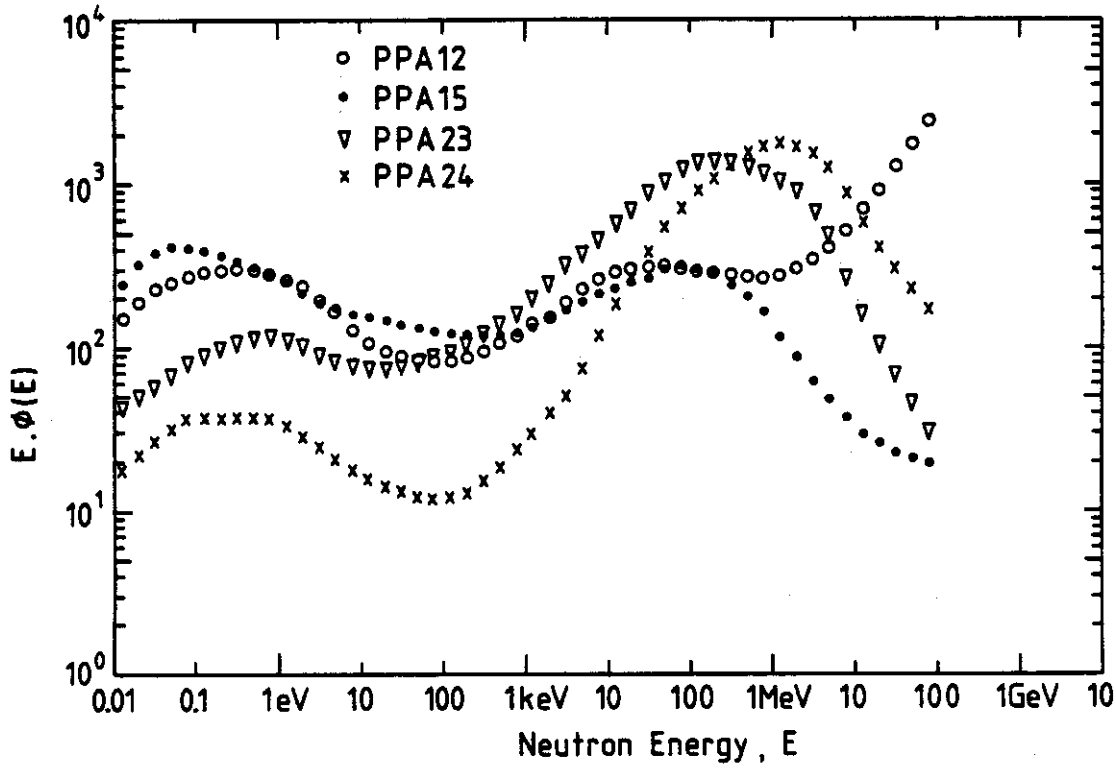

Fig. 3

XBL 8412-5059

2.3

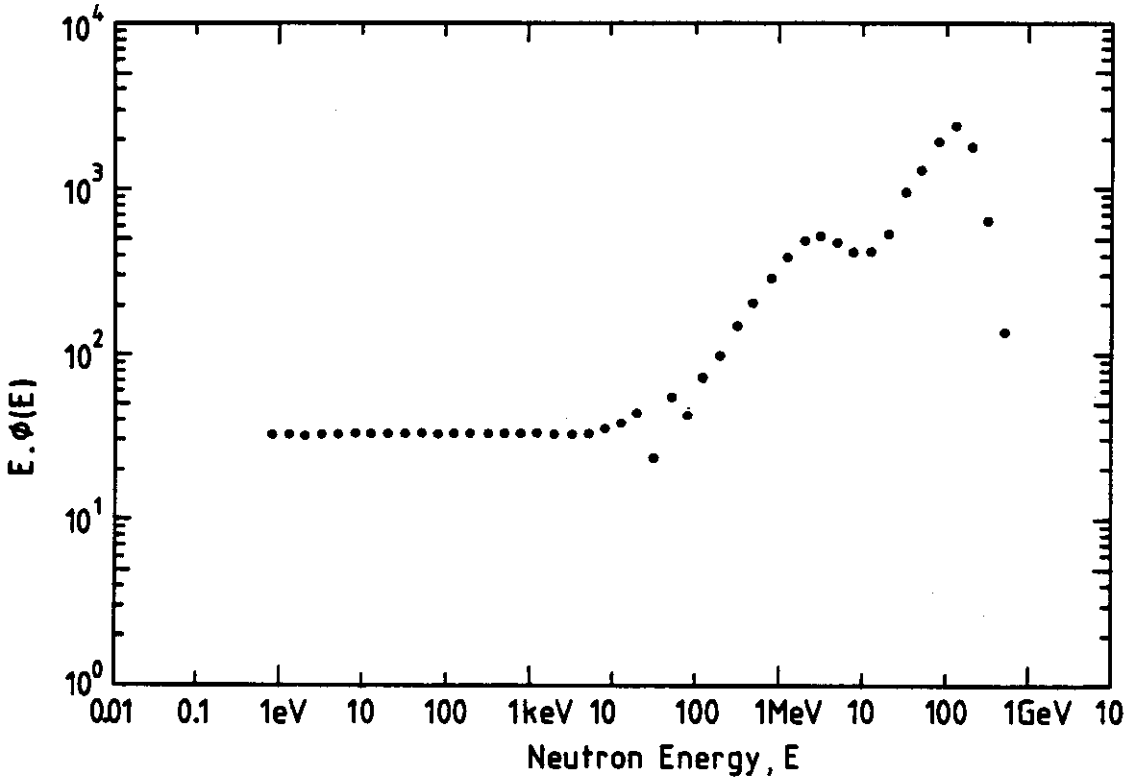

Fig. 4

XBL 8412-5060

2.4

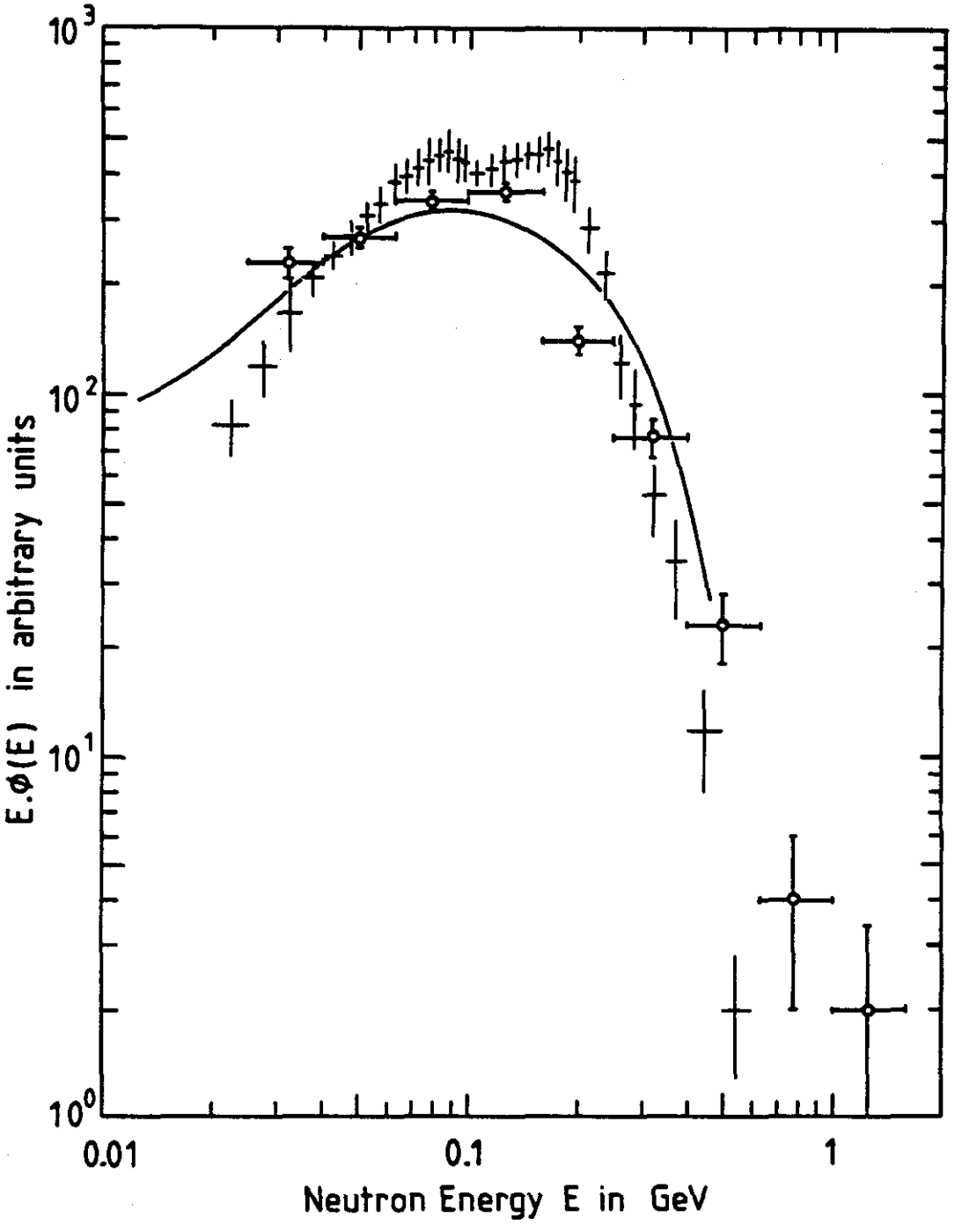

Fig. 5

XBL 8412-5061

2.5

2.5

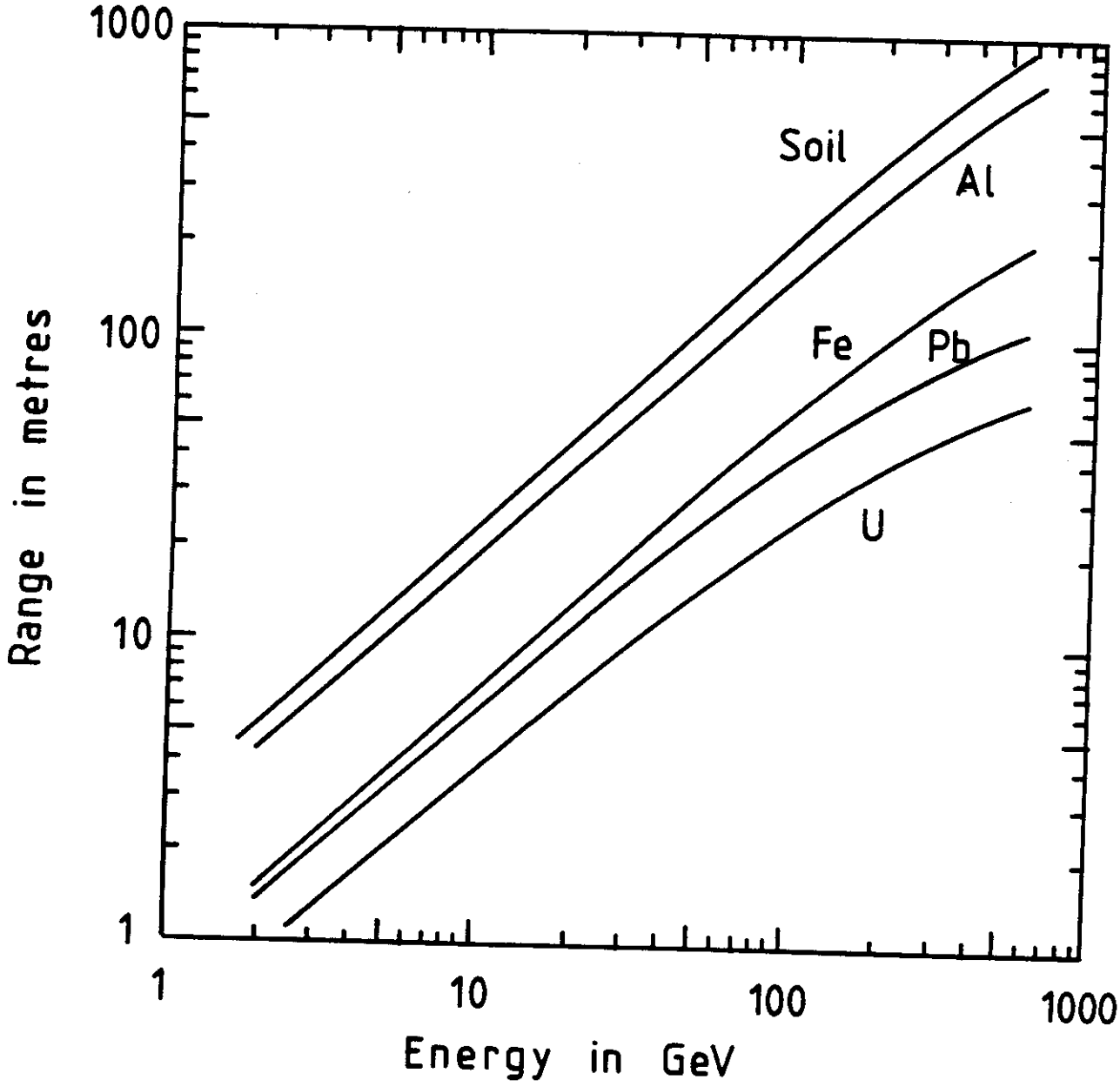
1000
100
10
1
Range in metres
Soil
Al
Fe
Pb
U
1
10
100
1000
Energy in GeV

2.6

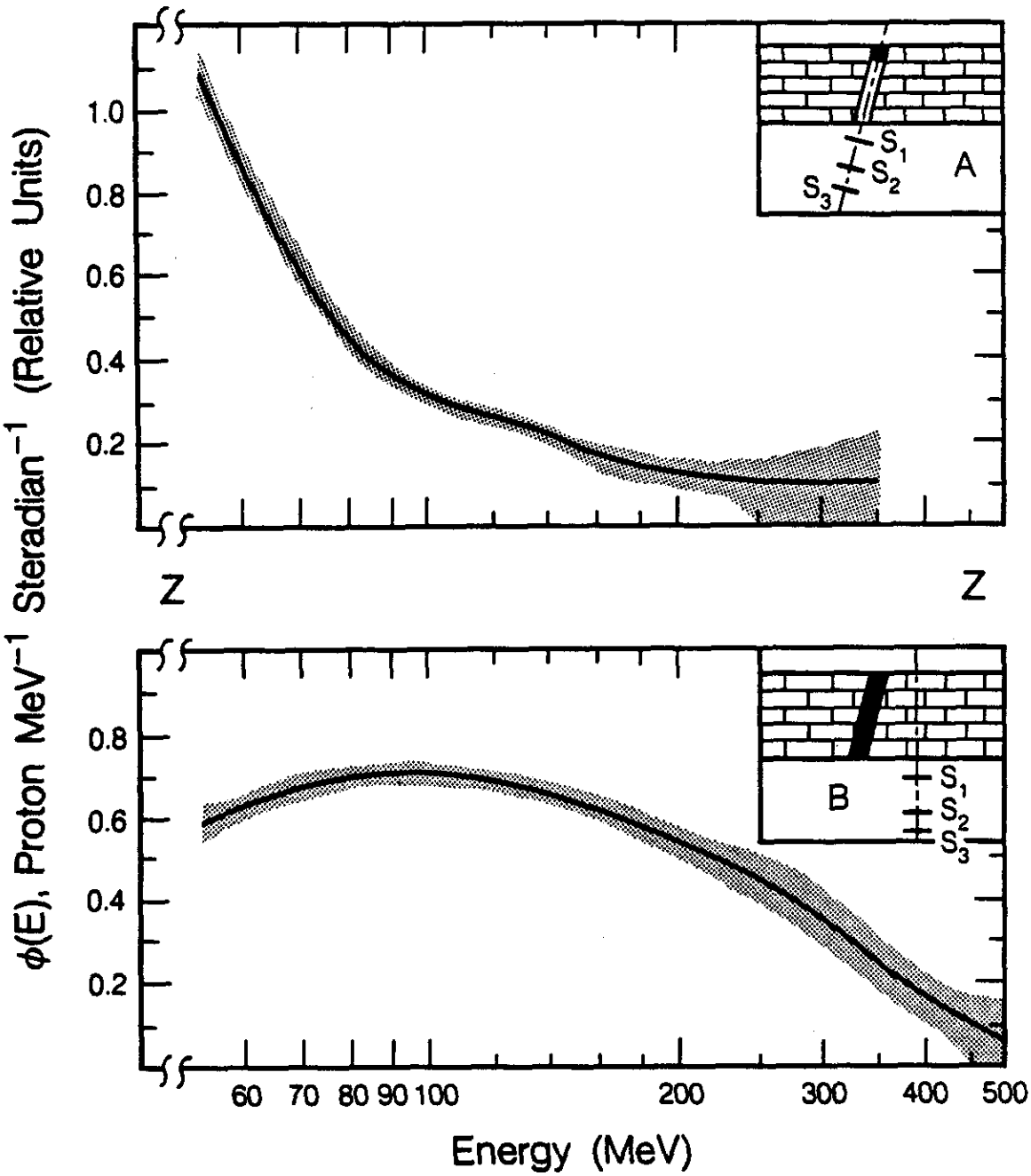

XBL 859-3856

2.7

2.7

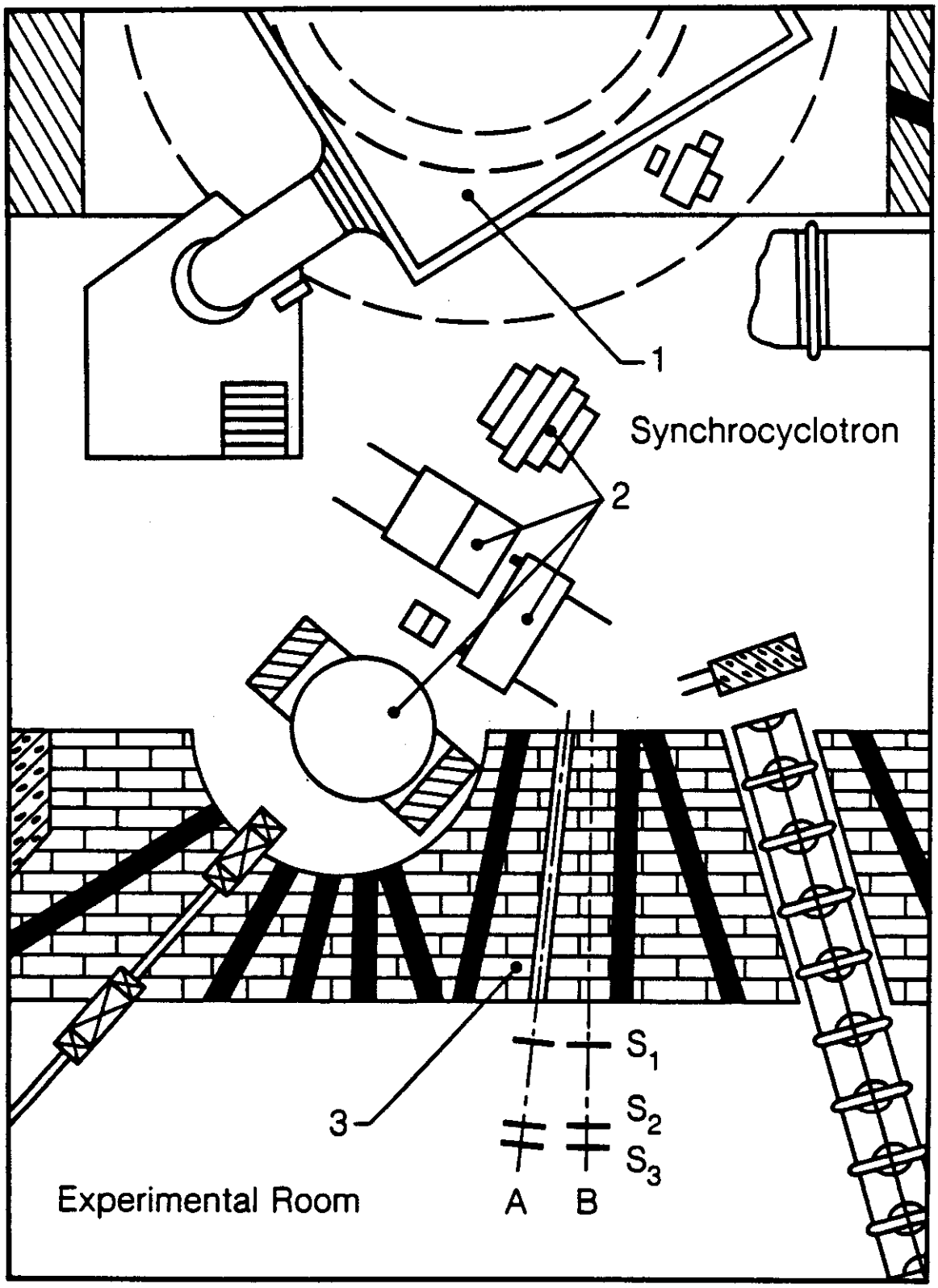

XBL 859-3857

2.8

2 73

2.8

a) Forward Calculation

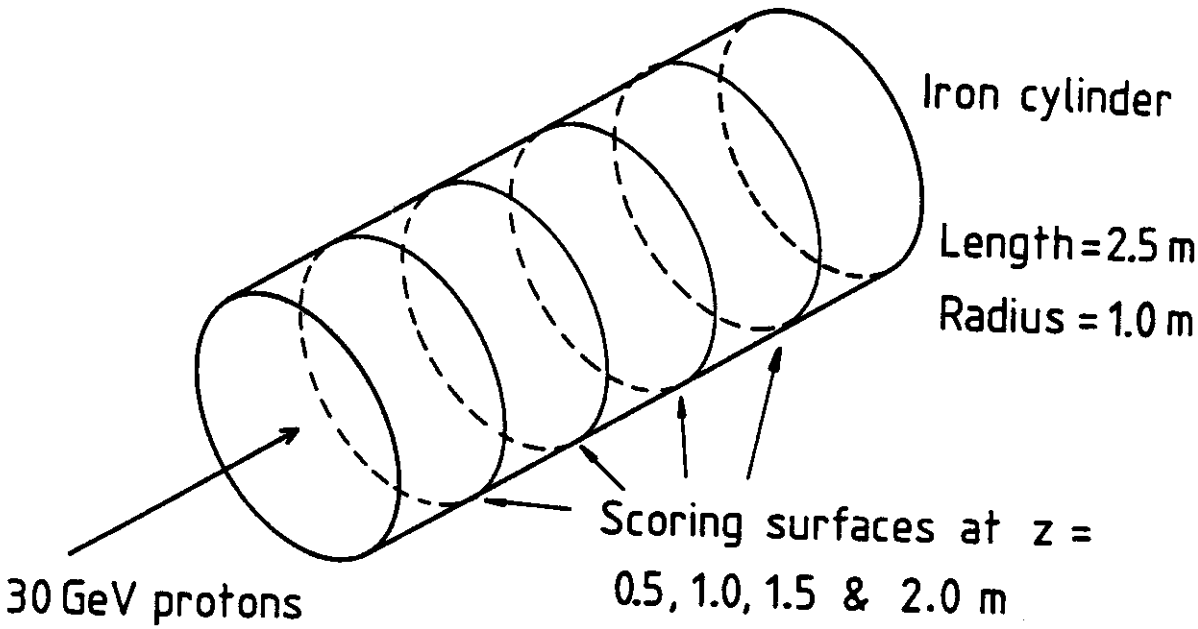

b) Lateral Calculation

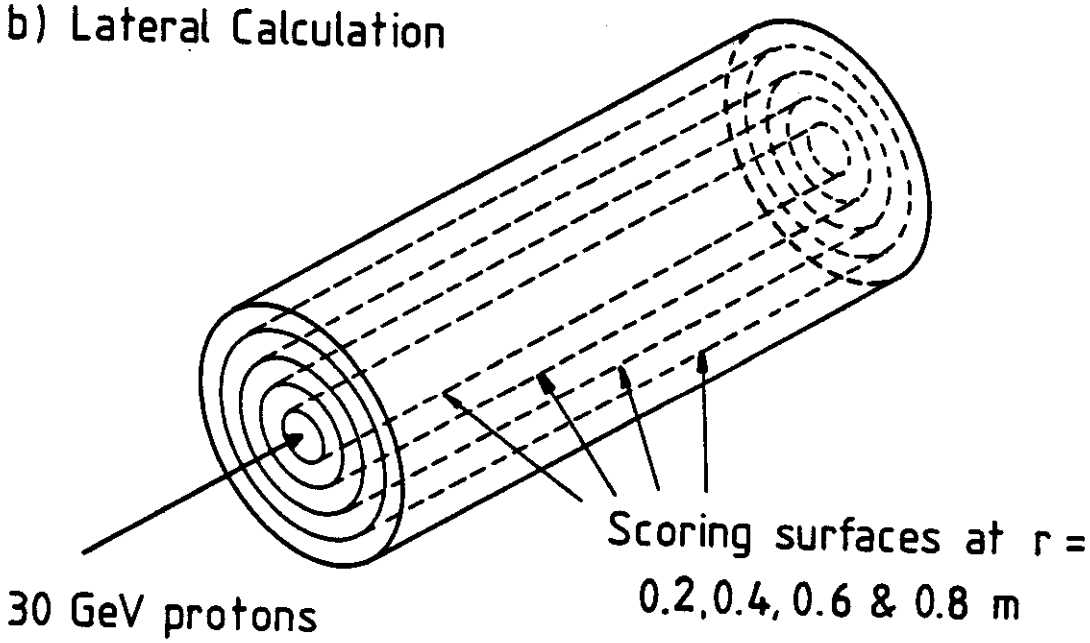

protons
neutrons
charged pions
Particles per Bin
1000
100
10
1
0.01
0.1
1
10
0.01
0.1
1
10
100
Kinetic Energy in GeV

2.10

54 2

protons
neutrons
charged pions
Particles per Bin
1000
100
10
1
0.01
0.1
1
10
0.01
0.1
1
10
100
Kinetic Energy in GeV

2.11

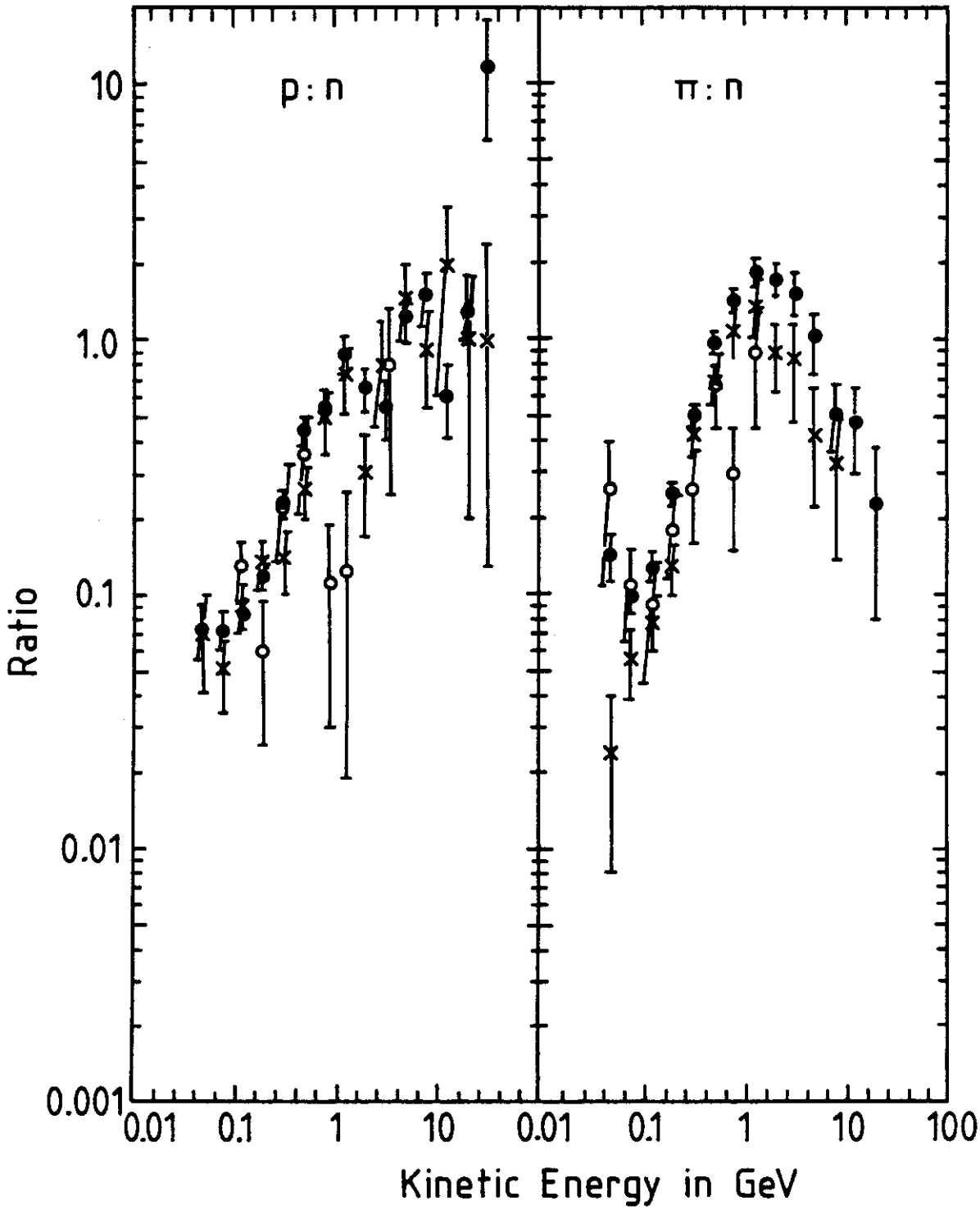
p : n
π : n
10
1.0
0.1
0.01
0.001
Ratio
0.01
0.1
1
10
0.01
0.1
1
10
100
Kinetic Energy in GeV

2.12

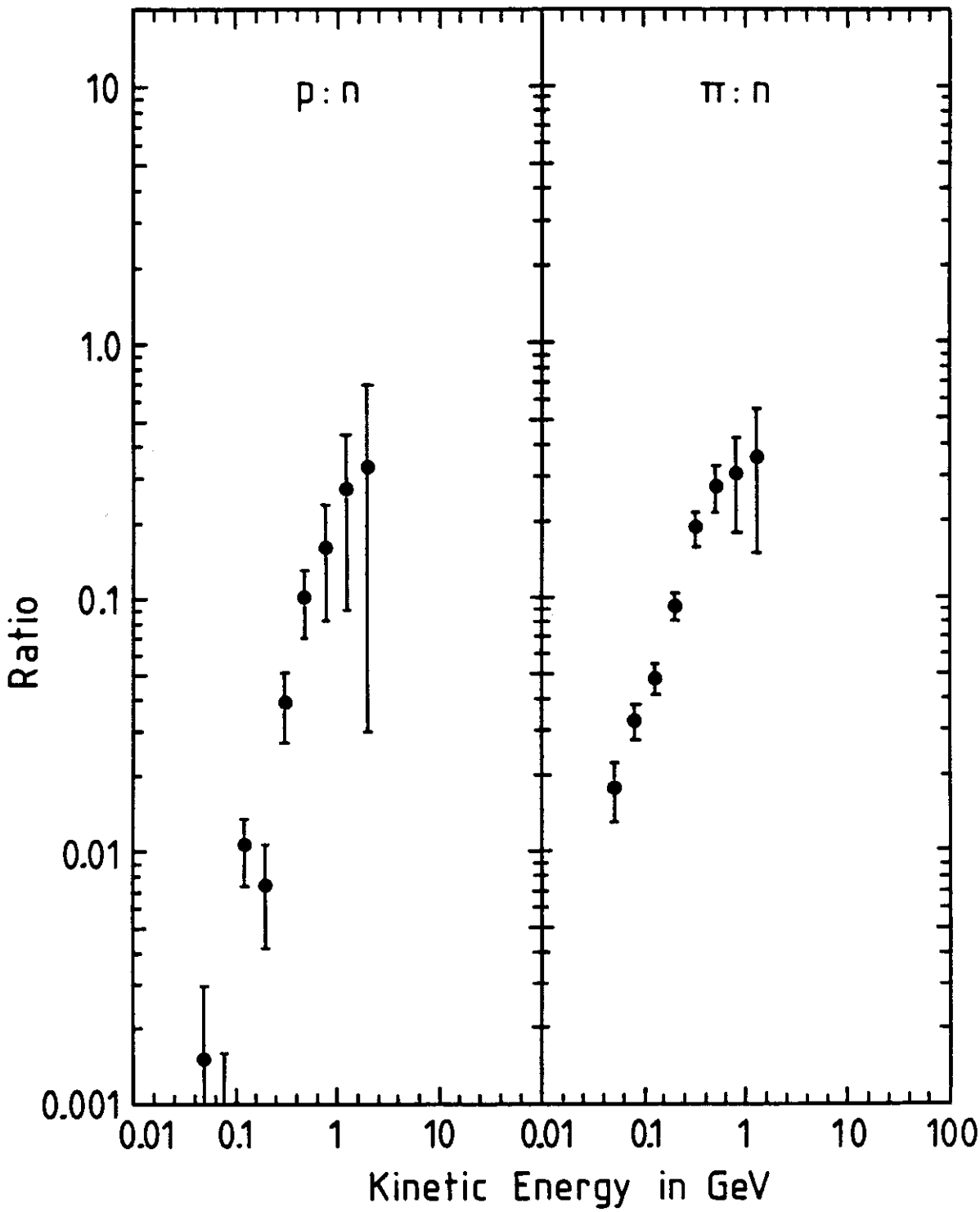
p : n
π : n
10
1.0
0.1
0.01
0.001
Ratio
0.01
0.1
1
10
0.01
0.1
1
10
100
Kinetic Energy in GeV

2.13

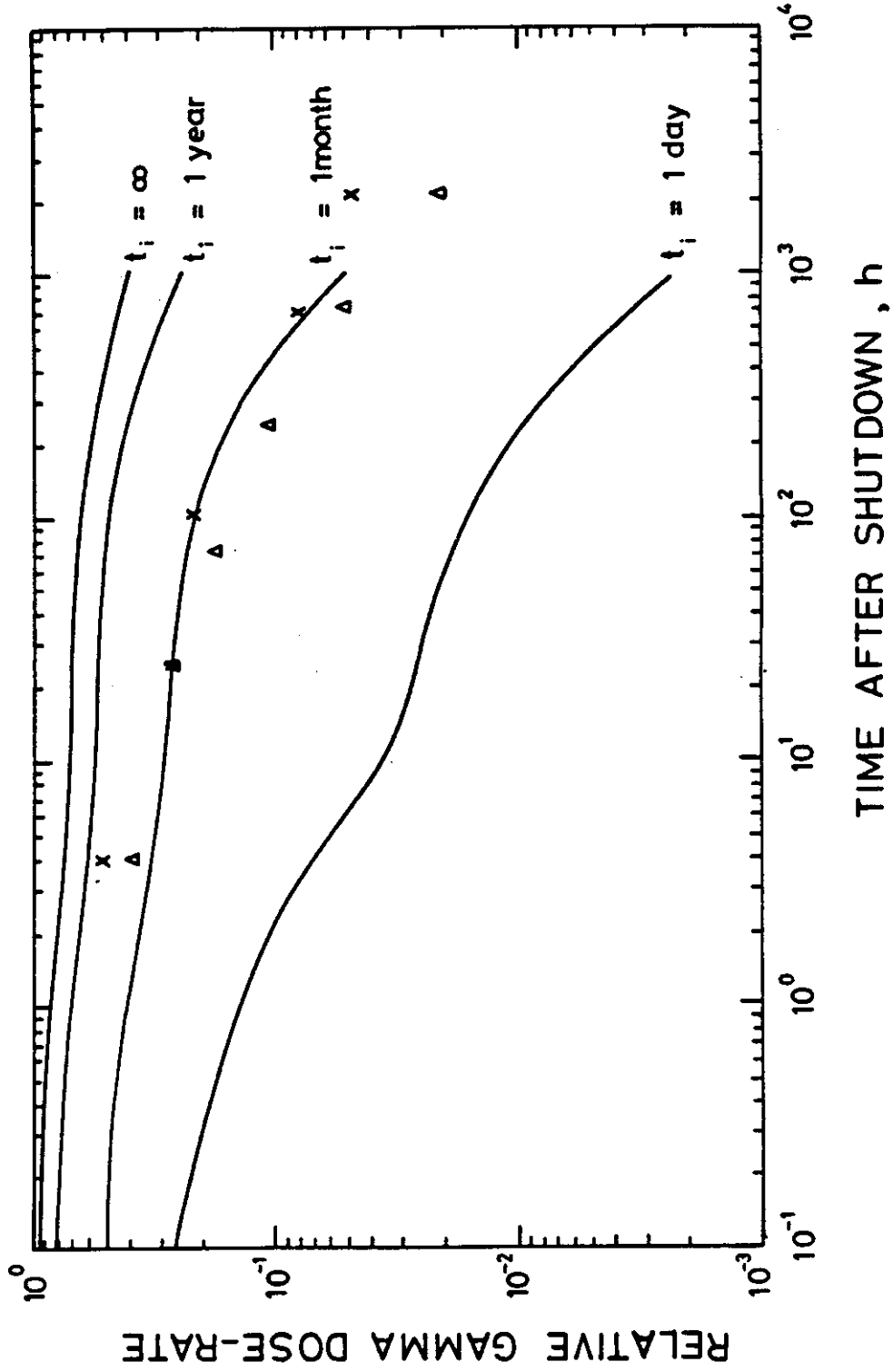
RELATIVE GAMMA DOSE-RATE
TIME AFTER SHUTDOWN , h
t_i = 8
t_i = 1 year
t_i = 1month
t_i = 1 day
10^0
10^{-1}
10^{-2}
10^{-3}
10^{-1}
10^0
10^1
10^2
10^3
10^4

2.14

2.14

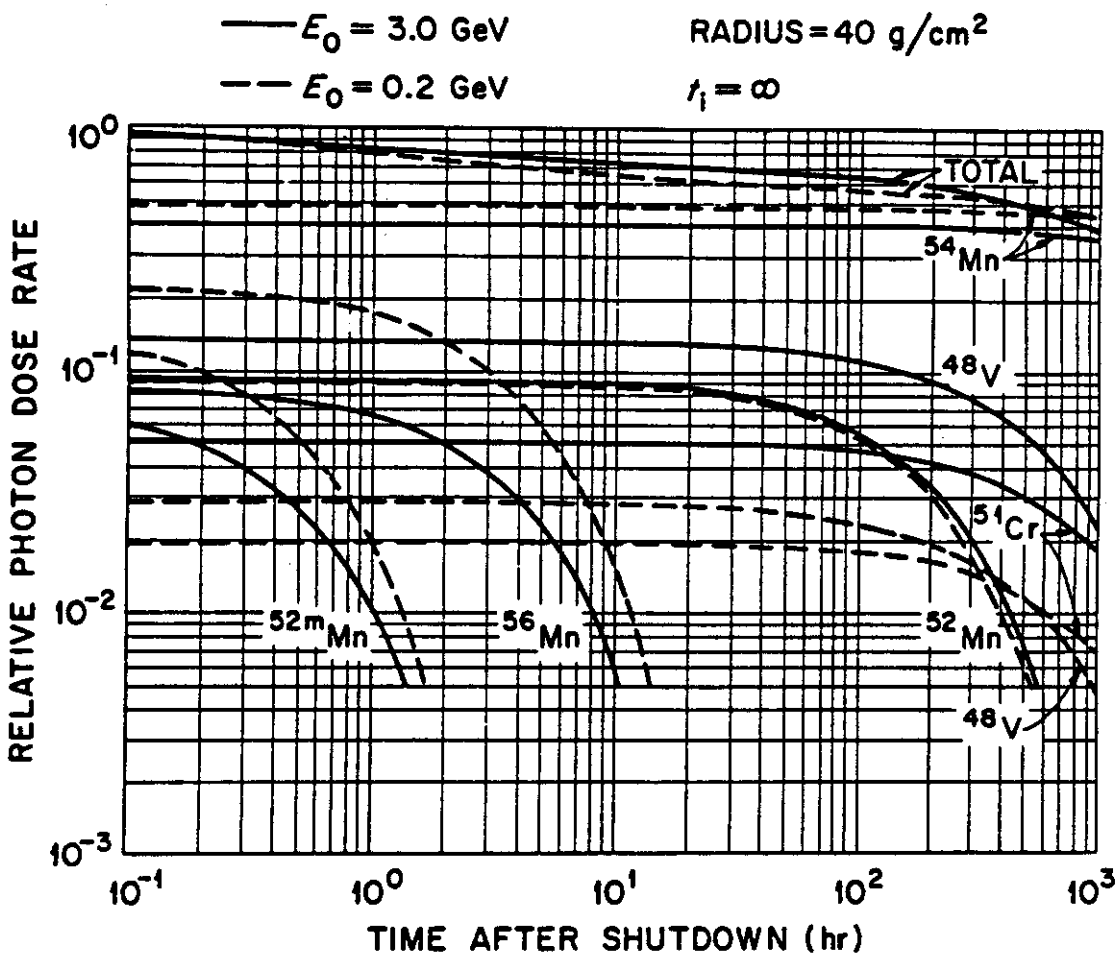
E_0 = 3.0 GeV
E_0 = 0.2 GeV
RADIUS = 40 g/cm²
$t_i = \infty$
RELATIVE PHOTON DOSE RATE
TIME AFTER SHUTDOWN (hr)
TOTAL
^{54}Mn
^{48}V
^{51}Cr
^{52m}Mn
^{56}Mn
^{52}Mn
^{48}V
10^{0}
10^{-1}
10^{-2}
10^{-3}
10^{-1}
10^{0}
10^{1}
10^{2}
10^{3}

2.15

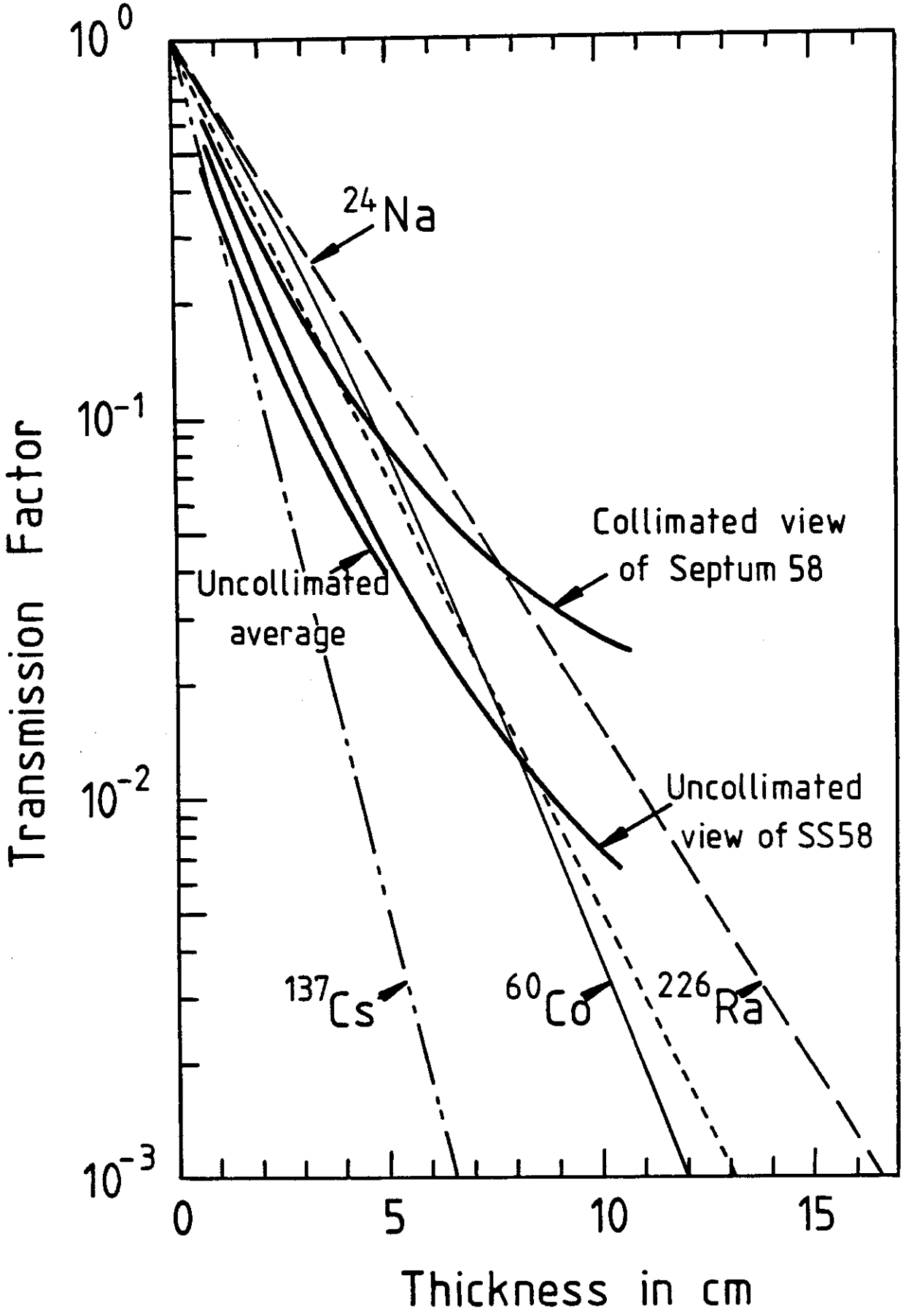
10^0
10^{-1}
10^{-2}
10^{-3}
Transmission Factor
^{24}Na
Collimated view
of Septum 58
Uncollimated
average
Uncollimated
view of SS58
^{137}Cs
^{60}Co
^{226}Ra
0
5
10
15
Thickness in cm

2.16

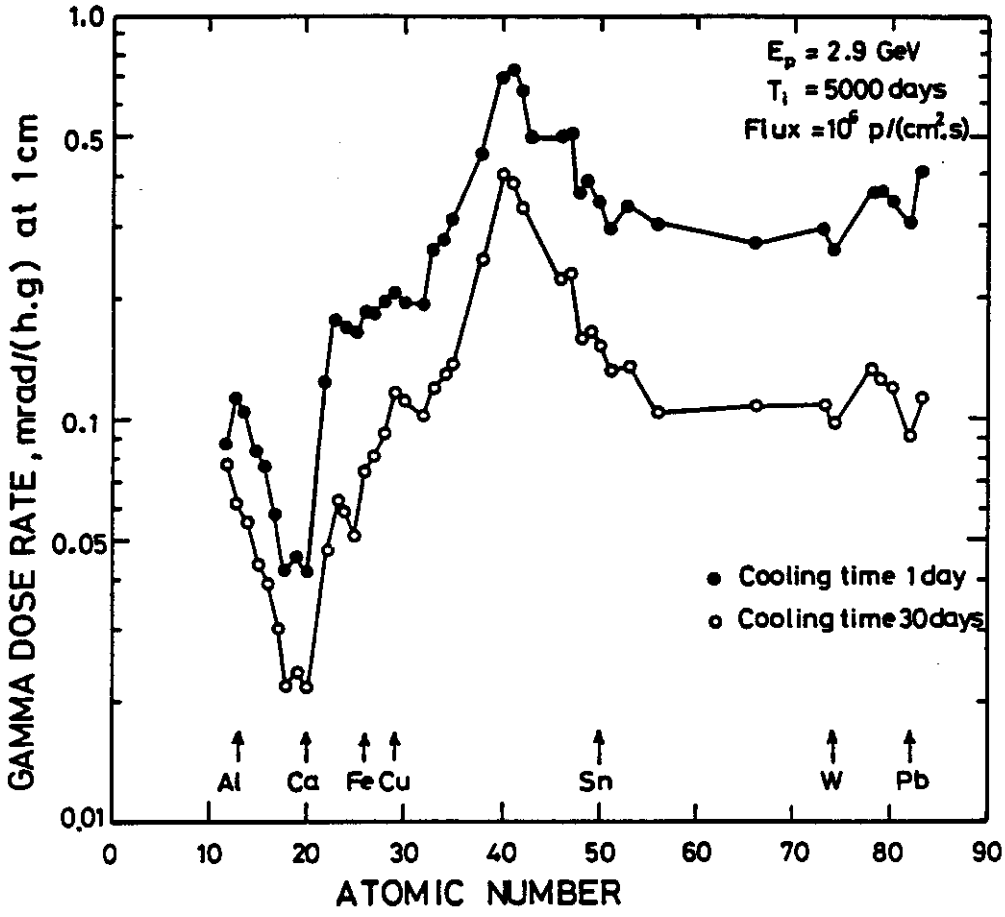
GAMMA DOSE RATE, mrad/(h.g) at 1cm
ATOMIC NUMBER
E_p = 2.9 GeV
T_i = 5000 days
Flux = 10^6 p/(cm^2.s)
Cooling time 1 day
Cooling time 30 days
Al
Ca
Fe
Cu
Sn
W
Pb
1.0
0.5
0.1
0.05
0.01
0
10
20
30
40
50
60
70
80
90

2.17

2.17

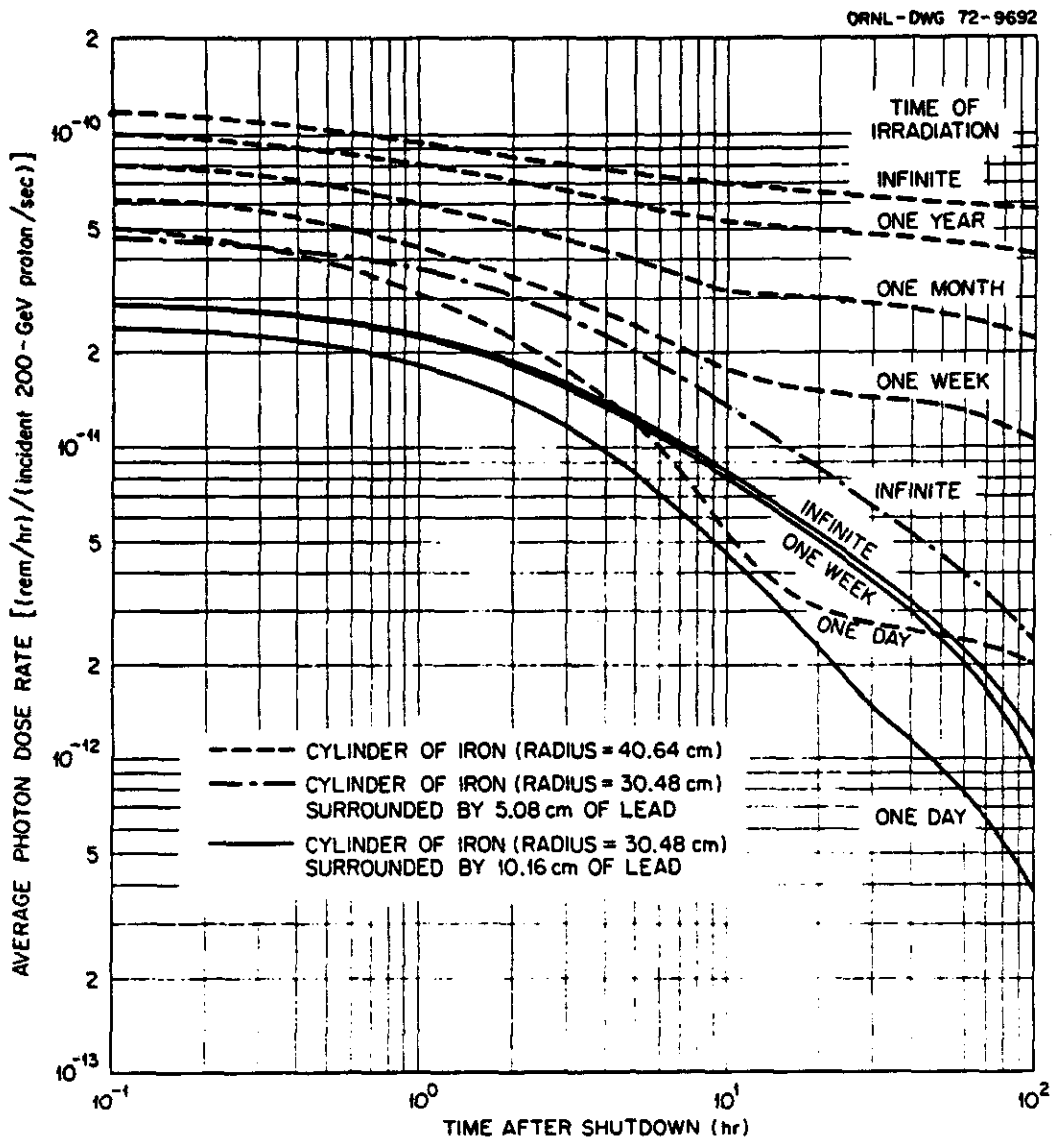
ORNL-DWG 72-9692
AVERAGE PHOTON DOSE RATE [(rem/hr)/(incident 200-GeV proton/sec)]
TIME AFTER SHUTDOWN (hr)
TIME OF IRRADIATION
INFINITE
ONE YEAR
ONE MONTH
ONE WEEK
INFINITE
INFINITE
ONE WEEK
ONE DAY
ONE DAY
CYLINDER OF IRON (RADIUS = 40.64 cm)
CYLINDER OF IRON (RADIUS = 30.48 cm) SURROUNDED BY 5.08 cm OF LEAD
CYLINDER OF IRON (RADIUS = 30.48 cm) SURROUNDED BY 10.16 cm OF LEAD

2.18

CHAPTER 3

Radiation Measurements at Accelerators

'With what measure ye mete, it shall be measured to you'.

from Gospel according to St. Mark
Chapter 4 Verse 24

CHAPTER 3 CONTENTS

3.1 Dosimetry at Particle Accelerators

3.2 Historical Background

3.3 Mixed Radiation Field Dosimetry
- Ionizion Chambers
- LET Spectrometer Instruments
- Ionizion Recombination Instruments
- Other Dose Equivalent Radiation Quality Instruments

3.4 Neutron Dosimetry at Accelerators
- Classification of Radiation Detectors
- Passive Detectors
- Active (Prompt) Detectors
- Threshold Detectors
- Activation Detectors
- Moderated Thermal Neutron Detectors
- Multisphere Techniques

3.5 Radiation Surveys
- Single Detector
- Two Detectors
- Three or More Detectors

3.6 Dose Equivalent Instruments Versus Physical Measurements

3.7 The Determination of Neutron Spectra at Accelerators
- Proton Recoil Spectrum Measurements

3.8 Interpretation of Accelerator Radiation Measurements
- Fluence to Dose-Equivalent Conversion Coefficients
- Intercomparison of Dose-Equivalent Determinations

References for Chapter 3

Figure Captions for Chapter 3

CHAPTER 3

RADIATION MEASUREMENTS AT ACCELERATORS

3.1. DOSIMETRY AT PARTICLE ACCELERATORS

Radiation dosimetry is, for our purposes here, taken to be the entire process of the acquisition of physical parameters of the radiation field and the interpretation of these measurements in terms of quantities needed for the purposes of radiological protection.

McCaslin and Thomas (McC 81) have defined six reasons for which radiation measurements are needed at particle accelerators.

- Routine radiation surveys for radiation protection purposes, at dose equivalent rates in the range 1-10 nSv s^{-1} (0.4 - 4 mrem h^{-1});
- Interpretation of the readings of personal dosimeters;
- Environmental monitoring;
- Accident dosimetry;
- Beam intensity measurements;
- Radiation measurements in regions of high radiation intensity, to enable an understanding of the radiation environment so that reductions in intensity may be made (e.g., by the addition of shielding or changes in operating conditions).

These various reasons for which dosimetric information is needed suggest three basic conditions under which measurements will be made:

- Beam Dosimetry-measurement in essentially pure, often monoenergic and non-divergent, particle beams. Such measurements may be made with great accuracy. Typical examples would be: nuclear physics experiments (e.g., the absolute determination of reaction cross-sections (Sm 76, Sm 83, St 71a); beam dose rate determinations for radiotherapy (Ne 76, Th 80a).
- Out-of-Beam Dosimetry-measurements close to beams, targets, magnets etc., to determine the parameters of the scattered radiation. Such measurements are very difficult to interpret. Typical examples would be: radiation damage studies to accelerator components (Be 82, Iz 80, Sc 79a,b); determination of absorbed dose to healthy tissues surrounding irradiated tumours (Sm 81) and accident dosimetry (HP 77, Mi 72).
- Radiological Protection-measurements usually at low average dose rates, although at instantaneous dose rates which may be high.

This chapter principally deals with the latter of these three conditions: dosimetry for the purposes of radiological protection. The first two conditions are largely beyond the scope of this chapter. Interested readers are referred to the literature for further information (La 69, Ra 69, Th 80a).

As we have seen in Chapter 2, the radiation fields around particle accelerators are often complex. In general the higher the particle energy the greater the complexity, and the health physicist should be prepared to make sophisticated measurements to define the prompt radiation field, even for the purposes of radiation protection for which dosimetry is often thought to be relatively crude (ICRU 68).

Because the relative terms high energy and low energy will be frequently used throughout this chapter it is convenient to define the term 'high energy'. It is a term which has taken on different meanings as the particle energies commonly available in the laboratory have changed. In the early fifties high energy was often taken to be greater than 3 MeV (by virtue of the definition of the roentgen [ICRP 64]). In ICRU Report 28 high energy was defined as greater than 100 MeV (ICRU 78), and this definition will often be used here. However, as we shall see later, it is often convenient for dosimetry purposes to make a breakpoint at 20 MeV as the position between low energy and high energy particles in accelerator radiation fields (McC 81, Th 85a).

High-energy particles interact with matter to produce copious numbers of lower energy particles in cascade processes. In radiological protection dosimetry it is the electromagnetic and hadronic cascades that are of greatest practical importance, and these have been extensively discussed in the literature [see for example ICRU 78, Pa 73]. In most cases the health physicist will be required to make measurements in situations where these cascades are well developed and uncharged particles (photons, neutrons) usually dominate the radiation field: practical high-energy dosimetry often then resolves itself into the measurement of these two components. Particle energies may extend up to the primary particle energy and down to thermal energies but typically, a large fraction of the absorbed dose is deposited by low-energy particles and there are thus important similarities between 'high-' and 'low-energy' dosimetry (Pa 73). The low energy particles that are observed are, however, produced quite locally by the interactions of high-energy particles and therefore appear to have the transport characteristics of their high-energy parents. As a consequence the dose-equivalent/depth-distribution characteristics of high-energy radiation fields are different from the more familiar low-energy situations (Sh 69).

Because of the importance of the low-energy particles in the deposition of absorbed dose it is often convenient and appropriate to use low-energy measurement techniques in radiation fields generated by high-energy particles. A word of caution is necessary here-the presence of high-energy particles may, in come instances, perturb the readings of low-energy detectors.* Furthermore, many of the current uncertainties in high-energy dosimetry arise from inadequate knowledge of the response of detectors to secondary radiations (see Section 3.6).

---

*A specific example would be where elastic scattering of neutrons above 1.02 MeV confuses the signals produced by the inelastic $(n + He^3) \rightarrow (p + T + 0.764\ MeV)$ reaction in a He^3 spectrometer system.

It is often convenient to consider two energy regions bounded at 20 MeV. The choice of 20 MeV is made because it roughly corresponds to the upper limit of moderated thermal neutron instruments and, more importantly, because it is the threshold of the $^{12}C(n,2n)^{11}C$ reaction (see Section 3.4). Table 3.1 shows how the 20 MeV boundary has been used to indicate differences in radiation fields at several accelerators.

Neutron dosimetry is better understood in the region below 20 MeV than at higher energies. This is largely due to the fact that the principal sources of exposure of people to neutrons arises from isotopic sources and considerable attention has therefore been devoted to this energy range. Other important sources of exposure to neutrons arise from nuclear power reactors and low-energy ion and electron accelerators. In all these cases the significant dose equivalent is produced by neutrons well below 20 MeV. An extensive and continuing study of these sources and the response of neutron detectors in well-understood environments has been made. As a result detector response functions have been adequately characterized and inter-laboratory comparisons established for a variety of instruments. Detector calibrations have been performed with monoenergetic neutrons from continuous and pulsed sources. (α,n) and spontaneous fission sources have also been extensively used in calibrations (Pa 73) and information of the neutron spectra emitted by such sources continue to be refined (He 59a, In 81). At energies above 20 MeV the calibration and test facilities available are much less reliable (Al 79a). Spatial and temporal variations of radiation intensity may impose severe limitations. In addition the qualitative features of the radiation field–for example particle energy spectra–may not be well defined (see Section 3.8).

Radiation dosimetry at particle accelerator laboratories has tended to develop almost independently of work in the mainstream of radiological protection. There are many reasons for this separate development, but it is principally due to the fact that health physicists at accelerator laboratories often have backgrounds in nuclear or particle physics and are thus familiar with techniques used to quantify the physical parameters of radiation fields, in addition to the standard techniques of dosimetry used in radiological protection.

One clear advantage of measurements that define the physical properties of the radiation field is that the parameters so determined are immutable. Quantities which are administratively defined, such as dose equivalent, are transient and may vary as changes in their definitions are brought about. While it is always possible to derive dose-equivalent quantities from appropriate field quantities, the converse is not true (see Sections 3.5 and 3.8).

3.2. HISTORICAL BACKGROUND

The first serious high-energy radiation studies around particle accelerators began to be reported in the literature in the middle and late fifties. Naturally enough they originated in those laboratories with significant radiation problems. The laboratories that built their early synchrocyclotrons underground were not particularly active in these studies because they had few problems.

Many of the early qualitative and quantitative data originate from the early proton synchrotrons operated at Brookhaven National Laboratory (the Cosmotron) and the Radiation Laboratory* of the University of California (the Bevatron).

Experience at the 184-Inch Synchrocyclotron at Berkeley and the early proton synchrotrons-the Cosmotron and Bevatron-rapidly established the qualitative nature of their radiation environments outside thick shielding (Pa 65, Sm 58, Sm 62). A general rule emerged, showing that neutrons between 0.1 and 10 MeV contributed more than 50% to the dose-equivalent contribution of the radiation field; γ-rays and low-energy neutrons contributed about 10–20%, and the balance was made up by neutrons greater than 10 MeV in energy. These early studies have been reported by Lindenbaum (Li 57), Moyer (Mo 57) and Patterson (Pa 57), and summarized by Patterson and Thomas (Pa 73).

In order to understand the dosimetric problem in a qualitative manner, Moyer and his colleagues leaned heavily on analogy to cosmic radiation. They argued that the radiation environment outside high-energy accelerator shields must in many respects be similar to that which exists at the base of the earth's atmosphere produced by the interaction of the galactic cosmic radiation with the earth's atmosphere. In particular, the neutron spectrum was of great interest (He 59b). Patterson et al. used the analogy to suggest that neutrons between 0.1 and 20 MeV would dominate the contribution to the dose equivalent (Pa 59). This suggestion led to the strategy, subsequently found to be largely sound, of concentrating on neutron measurements in that energy range.

As early as 1954 Moyer, among others, identified the experimental techniques that would be of value in high-energy dosimetry at accelerators:

'(1) for the determination of the flux density and spectrum of unidirectional fast neutrons: proportional counters, scintillation counters, photographic emulsions;

(2) for the determination of thermal neutron flux densities, regardless of direction: counting techniques based on neutron capture in boron, activation foils;

(3) for the approximately absolute determination of energy flux density delivered by fast neutrons, independent of energy spectrum or angular direction: polyethylene-lined proportional counters;

(4) for the contribution to energy absorption in tissue due to neutrons, where the effects due to γ-rays are known and may be corrected for: cavity chambers or tissue-equivalent chambers' (Mo 54).

'Such a list, if written today, would look much the same. Sullivan (Su 69), in reviewing dosimetric techniques used at particle accelerators up to 1969, showed that, although there has been a

*Now the Lawrence Berkeley Laboratory.

steady improvement over the past 18 years in the techniques listed by Moyer, few basically new ideas have arisen. Perhaps the two most important new techniques absent from Moyer's list and mentioned by Sullivan were the use of ionization chambers to estimate the quality factors for mixed radiation fields and the development of activation detectors capable of yielding neutron spectra adequate for health physics purposes' (Th 73).

By 1972 the course for the future development for techniques of high-energy dosimetry seemed clear. Speaking of the period 1965–1971, it was possible to say:

'...the last six years have resulted in solid, if not spectacular, achievement in neutron dosimetry with threshold detectors at accelerators. Given this depth of understanding of radiation environments, the response of any detector(s) used to monitor accelerator radiation may be correctly interpreted. Several authors have examined the errors involved in using a routine monitoring system based on a small number of activation detectors (Gi 68, Ri 68, Sh 69).

For example, a moderated BF_3 counter, suitably calibrated, will almost always estimate dose-equivalent to about a factor of 2, in a wide range of accelerator spectra. If an additional measurement using the $^{12}C(n, 2n)^{11}C$ reaction is made, the accuracy can be improved to much better than 50% (usually 20% or better). Furthermore, since the measurements and their evaluation take quite a short time (typically one hour or less), threshold detectors may be used as the basis of a very practical routine monitoring system' (Th 73).

Since that time work has proceeded in the following areas:

- Classification of the definition of the concept of dose equivalent (Bu 81a, Pa 71, Ri 71, Ri 72, St 73a);
- Development of new activation detector techniques (Ch 66, Gi 68, Ro 69);
- Incorporation of Bonner spheres and activation detectors (Al 76, Aw 66, Aw 85, St 67);
- Improvement of neutron spectrum unfolding routines (Ro 80, Ro 85, St 67);
- Improvement in the interpretation of neutron spectra in terms of dose equivalent (ICRP 70, ICRP 73, NCRP 71, Sh 68, Sh 69).

During the thirteen years from 1966 to 1979 several comparisons of dosimetric methods and results were made by various groups at the CERN 28-GeV proton synchrotron (Ho 75a,b), the Stanford 20-GeV electron linac (McC 77), and the 70-GeV proton synchrotron of the Institute of High Energy Physics at Serpukhov (An 78). These intercomparisons have been summarised by McCaslin and Thomas (McC 81) who pointed out some important discrepancies. Intercomparisons are continuing at Serpukhov and will hopefully lead to important improvements in dosimetric techniques in the future (An 78, Ho 83).

As we have seen the basic key to our understanding of particle accelerator radiation environments was the realisation that in some respects they would be similar to that produced by the interaction of the galactic cosmic radiation with the earth's atmosphere. This was of particular value in the case of neutrons (He 59a) and led Patterson et al. (Pa 59) to conclude that neutrons between 0.1 MeV and 20 MeV would produce the largest component of dose equivalent around high energy accelerators. This prediction was borne out by observations around particle accelerators at Berkeley (Pa 65, Sm 58, Sm 62) and elsewhere (Bo 62, CERN 71, Pe 66, USAEC 57, USAEC 65, USAEC 67, USAEC 69) and is still valid.

As early as 1965, however, it became clear that, under certain conditions, as much as 90% of the dose equivalent could be contributed by high-energy particles (i.e., those above 20 MeV in energy (Ba 64, Ba 65, Ca 65). Such conditions are increasingly important at very high energy facilities (in the 100 GeV energy range) and it is thus important to improve techniques for the measurement of particles of energy above 20 MeV present in accelerator radiation environments (St 84, Th 85a).

3.3. MIXED RADIATION FIELD DOSIMETRY

In general the radiation fields around accelerators are complex, often consisting of many different ionizing radiations extending over a broad range of energies (Ba 69b).

Zielczynski has discussed the uncertainties in mixed radiation-field dosimetry (Zi 70) and cites two major difficulties:

- Determination of response functions of radiation detectors,
- Interpretation of measurements and determination of accuracy.

More specifically at particle accelerators dosimetric techniques that span the wide energy range of accelerator radiation environments suffer from all or some of the following drawbacks:

- Interference from radiations other than those to be measured.
- Response-rate dependence in intense radiation fields.
- Complexity.
- Incomplete instrument response function data.
- Uncertainties in instrument response interpretation.

Dosimetrists continue their quest for techniques by which a single dosimeter would permit direct accurate measurement to be made of the entire radiation field. We have the LET spectrometer of Rossi (Ro 55), the modified LET spectrometer of Kuehner et al. (Ba 69a, Ku 72, Ku 73a, b), the differential recombination chambers of Zielczynski (Zi 62, Zi 64) and Sullivan (Su 63) and the scintillation method of Pszona (Ps 71).

IONIZATION CHAMBERS

Perhaps the simplest experimental approach to the determination of dose equivalent, H, in accelerator radiation fields is to make a determination of absorbed dose, D, with a suitable ionization chamber and multiply the result by an appropriate quality factor, Q, according to the relationship:

$$H = QD \tag{3.1}$$

Many different means of determining absorbed dose by ionization chambers have been developed including paired ion chambers, high-pressure argon-filled chambers and cavity chambers (Bu 68, Go 68, Pa 73).

At accelerators the determination of absorbed dose is usually determined by a tissue-equivalent chamber, following the original work of Rossi and Failla (Fa 50, Ro 56).

Tissue-equivalent chambers have found wide application at the PPA, the Argonne ZGS, and at CERN, where they are in routine use and have even been used for beam dosimetry (Ba 65, Ba 69b, USAEC 65).

The conceptual difficulty with this technique lies in the fact that it provides no method for the determination of Q or Eq. (3.1) and provides only a measurement of D. A conservative approach is to assume a quality factor of about 10, but this is often unreasonably restrictive (experience shows typical value for Q of about 5 in accelerator radiation fields [Pa 73]). Either some detailed knowledge of the radiation environment is required to estimate Q or resort may be made to an empirical determination of Q using recombination chambers. Both methods require further measurements.

Practical problems that arise with use of ionization chambers in accelerator fields include:

- Radio-frequency interference-ion chambers are low-signal high-gain detectors that are sensitive to electromagnetic interference such as is caused by the stray fields from the tuned radio-frequency cavities used in particle accelerators.
- Pulsed radiation fields-the field strength may be insufficient to ensure complete charge collection in pulsed radiation fields of low duty cycle. Even though the average absorbed dose rates may be low, the rates during pulses may be extremely high. Fine structure (e.g., RF structure) in the beam spill may exacerbate this problem.

LET SPECTROMETER INSTRUMENTS

Nguyen et al. (Ng 85) have recently reviewed LET and event-size (Y) spectrometry in detail and the interested reader is referred to their article. Baum and others of Brookhaven National Laboratory have developed a more robust and improved ion chamber that also reduces the need for frequent gas-filling (Ba 69a, Ku 72, Ku 73a,b). Two signals are extracted: one is proportional to the dose rate, independent of LET; the other is processed by non-linear amplifiers to produce an amplitude dependence that varies with LET in the same manner as does quality factor.

LET spectrometer instruments are of limited value for dosimetry for radiological protection purposes in typical particle accelerator environments because of their low sensitivity. Such instruments are not therefore found in routine use (Fr 70).

Ionization Recombination Instruments

These instruments depend upon the fact that ions produced in the gas will recombine to some degree when the electrical gradient across an ionization chamber is not adequate to achieve saturation. This recombination, which occurs along primary and secondary charged particle tracks, will depend upon the local density of ionization in the tracks and thus has some relation to the linear energy transfer, L_∞, used to define the quality factor, Q, in radiological protection (Su 84).

This has led to attempts to produce an instrument that measures the dose equivalent due to any ionizing radiation field, independently of L_∞ or, alternatively, to determine the Q of any field. Such instruments would be extremely useful in the complicated mixtures of radiations that comprise the radiation field outside the shielding of particle accelerators.

Several techniques for measuring quality factor have been suggested. For example, the characteristics of columnar recombination in ionization chambers are dependent on the LET of the charged particles causing the ionization. One approach, due to Zielczynski, is to use a double ionization chamber in which one part is operated at saturation voltage and another at a lower voltage in which a certain amount of columnar recombination can occur (Zi 62). It was shown to be possible to adjust the lower voltage so that the ratio of the currents from the two parts of the chamber is a linear function of quality factor, which means that the difference in ionization current from the two parts of the chamber will be directly proportional to the dose equivalent.

Another method based on columnar recombination relies on the observation that over a large voltage range, the current is empirically related to the polarising voltage by a relation of the form:

$$i = kV^n \qquad (3.2)$$

The index n is approximately proportional to Q and so a determination of n in a neutron field can give an estimate of the average quality factor to be applied to a measurement of absorbed dose (Di 65, Su 63, Su 64).

OTHER DOSE EQUIVALENT OR RADIATION QUALITY INSTRUMENTS

Another effect that can be used to obtain an estimate of radiation quality is the light output from a plastic scintillator. The method devised by Pszona (Ps 69, Ps 71, Ps 77) relies on the simultaneous measurement of currents from an ionization chamber and a photomultiplier tube attached to a plastic scintillator. The ratio of the currents is a complex function of LET, but it can be used to give a measure of an average Q in an unknown field.

Yet another technique, described by Tesch (Te 70), is to use pulse-shape discrimination on the pulses coming from an organic scintillator to discriminate against photons and to choose a suitable discriminator threshold so that the pulse rate is proportional to dose equivalent.

All these techniques have given satisfactory estimates of quality factor and dose equivalent in near-laboratory conditions of exposure. However, as yet, there is no universal dose equivalent meter which is both sufficiently sensitive and robust enough to withstand the rigours of measurement in the field and give reliable results at occupational radiation levels. This is to be contrasted with the multiple detector systems described later in this section, which have been shown to be reliably consistent for more than 20 years.

3.4. NEUTRON DOSIMETRY AT ACCELERATORS

Special discussion of the measurement of neutrons is given here because it is neutrons that lead to the most important dosimetric problems outside the shielding at many, or most, proton accelerators. (Chapter 2)

Neutrons must be measured over a wide range of energies, often in pulsed fields and usually as one component of a mixed radiation field. Such conditions impose a stern test on the dosimetrists who must resort to all the dosimetric techniques normally available in radiological protection.

CLASSIFICATION OF RADIATION DETECTORS

There are many types of radiation detectors, which may be classified in almost any number of ways. To assist the reader in understanding the published literature a brief summary is given here. In the literature on accelerator neutron dosimetry one will find several ways of classifying radiation detectors:

- Passive detectors
- Active (prompt) detectors
- Threshold detectors
- Activation detectors
- Moderator devices

PASSIVE DETECTORS

Passive detectors yield their information after their irradiation has ended and often only after some technical processing of the detector itself or interpretation of data from it (Th 80b). Holt has given an alternative definition as 'detectors which do not require any electronics equipment to be connected during the irradiation; the irradiation induces some change in the detector material as a function of the fluence, and the change is measured after the end of the irradiation' (Ho 85).

Examples of passive detectors are:

- Activation detectors
- Fission-track detectors
- Nuclear emulsions
- Radioluminescent glasses
- Silicon diodes
- Thermoluminescent dosimeters

Detectors that are often thought of as prompt may be converted to the passive mode. For example a passive thermal neutron detector may be used in conjunction with a set of Bonner moderators (Br 60).

Passive detectors are best used to determine the intensity of radiation fields that are essentially invariant over the time of measurement.

ACTIVE (PROMPT) DETECTORS

Active (prompt) detectors give immediate information in real time about radiation intensity and may be used to make measurements in radiation fields that fluctuate with time (Pe 80). Examples are:

- Geiger counters
- Proportional counters
- Fission counters
- Scintillation counters
- Solid state detectors

THRESHOLD DETECTORS

Threshold detectors are those that require a finite, fixed radiation energy to initiate any response to ionizing radiation. Below the threshold they give no response; above it they have a response proportional to the excitation functions (response function) of the detector. Examples of threshold detectors used in accelerator radiation field dosimetry are: the thorium fission chamber, which utilizes the (n, fission) reaction in thorium and has a threshold of 1.6 MeV; the production of ^{11}C, a positron emitter with a half life of 20.3 min, by the ^{12}C $(n,2n)^{11}C$ reaction, which has a threshold of about 20 MeV (see Fig. 3.1). Threshold detectors may be either of the active (Pe 80) [e.g., bismuth fission chambers (He 57, Ke 48, McC 68)] or the passive type (Ho 85, Sm 65, Th 80b) (e.g., the production of ^{11}C from ^{12}C in a plastic scintillator) (Ba 57, McC 60, Sh 51, Sh 62, St 84). Suitable nuclear reactions, their thresholds and sample materials are indicated in Table 3.2. Care must be taken in the particular reactions selected because in the high-energy environments of accelerators multiple reactions may be possible with the resultant production of many radionuclides. This restriction to reactions that are both simple and readily detectable often eliminates some reactions for use in high-energy environments that are perfectly acceptable around lower-energy facilities.

ACTIVATION DETECTORS

These comprise a subset of passive detectors. They depend upon the determination of radioactivity induced in samples placed in the radiation field. Activation detectors have the advantage of not being susceptible to a rate dependence as are pulse counters, which often suffer counting rate losses at the high instantaneous fluence rates found at accelerators resulting from low duty cycles, and because of the radiofrequency structure superimposed on the beam current within a pulse. Significant experimental ingenuity is often required to achieve the sensitivities needed to measure radiation fields at the occupational exposure level with activation detectors. This has inhibited the development of some otherwise very interesting reactions such as, for example, ^{149}Tb production in gold or mercury (McC 67, Sh 70). As may be seen in Table 3.3, most feasible reactions have thresholds in the energy region from 3–50 MeV, and so activation detectors must be used in conjunction with other techniques if the entire energy spectrum of the accelerator environment is to be spanned. Because of the limited number of reactions available the use of activation detectors is necessarily of low resolution, limited to the determination of neutron spectra without detailed structure. The technique most frequently used to supplement activation detectors below 1 MeV is that of Bonner spheres or 'multispheres'.

Thermal neutrons are usually detected by (n,capture) reactions. The choice of the activation foil used will depend upon the thermal flux density to be measured and the time over which it is to be measured. There is no difficulty in finding an appropriate (n,γ) reaction with suitable half-life and absorption cross section (Ho 85). Table 3.4 from Holt (Ho 85) shows several slow neutron detectors in common use. Several of these reactions have been frequently used around accelerators and Table 3.5 summarizes the properties of these reactions for the measurement of thermal neutrons in common use at the Lawrence Berkeley Laboratory.

Higher-energy neutrons may be measured using threshold activation detectors. Again there is no shortage of suitable reactions. Table 3.3 (from Holt) summarizes a suitable threshold detectors, many of which are suitable for use at accelerators. Particular activation reactions that are routinely used at accelerators are ^{32}S (n,p) ^{32}P; ^{27}Al (n,α) ^{24}Na, ^{27}Al(n,2p4n) ^{22}Na; ^{12}C (n,2n) ^{11}C; ^{12}C(n,spall.) ^{7}Be; ^{198}Hg(n,spall.) ^{149}Tb. Table 3.6 summarizes the properties of some typical activation detectors in use at LBL.

The ^{12}C(n,2n)^{11}C reaction–the measurement of the ^{11}C radioactivity induced in carbon or plastic scintillator–has a special place in accelerator radiation dosimetry. The technique was first used to monitor the intensity of cyclotrons using the ^{12}C (p,pn) ^{11}C reaction but Sharpe and Stafford (Sh 51) suggested the use of the (n,2n) reaction to measure low neutron fluence. These authors showed that fluence rates as low as 13 n cm^{-2}s^{-1} could be detected by a 4.5 g anthracene crystal. Baranov et al (Ba 57) improved the sensitivity of the technique by using a liquid scintillator. McCaslin (McC 60) and Shaw somewhat later (Sh 62) made the technique even more convenient by using solid plastic scintillators both as targets and detectors. The use of large scintillators

(2.7 kg) facilitates the measurement of neutron fluence rates as low as 1 n cm^{-2} s^{-1} (Gi 68).

The experimental techniques have been described in great detail in the literature: (McC 60, McC 73, Pa 73, Sh 62). Briefly, the saturation activity in the crystal, A_{sat}, is simply related to the cross section σ, and the spectrum of the stray field, ϕ, by the formula

$$A_{sat} = k \int_{E_{thr}}^{E_p} \sigma(E)\ \phi(E)\ dE, \qquad (3.3)$$

where the integration over kinetic energy, E, is taken from the threshold energy, E_{thr}, to the accelerated proton energy, E_p. The constant k is related to the density of carbon nuclei in the detector and the detector mass.

In using the activation technique it has been customary to make the assumption that the greatest part of the activity is induced by neutrons, and that the contribution due to photons and charged particles is either negligible or adequately accounted for by the procedures adopted. A nominal fluence, ϕ_{nom}, is calculated from the saturated ^{11}C activity, using an effective cross-section σ_{eff}:

$$A_{sat} = k\sigma_{eff}\phi_{nom} \qquad (3.4)$$

Early interpretations of the measurement of the cross-section σ (E) suggested a step-like excitation function with the threshold at 20 MeV, rapidly rising to a constant value of 22 mb [see Figs. 3.2 and 3.3] (Gi 68). With such a simple excitation function a value for σ_{eff} could readily be identified and it became the universal practice at accelerator laboratories to use a value of 22 mb for the effective cross-section (St 84).

These conventions resulted in excellent agreement in the determination of effective neutron fluence (E > 20 MeV) at accelerator laboratories (Gi 68, St 84). There were, however, significant differences in the interpretation of these fluence measurements, leading to differences in the equivalent estimates of more than a factor of two (Ba 65, Gi 68, Go 67, Sh 68; see also Section 3.7).

Since the work of the sixties and early seventies several important improvements in our understanding have occurred:

- New cross-section data are available,
- Radiation transport calculations have made possible the study of the charged component of accelerator radiation fields,
- Dose equivalent concepts have been clarified.

Figure 3.1 shows a summary of $^{12}C \rightarrow {}^{11}C$ cross section data for neutrons, pions and protons. Charalumbus et al. have reviewed these cross-sections (Ch 66) and their data have been augmented in Fig. 3.1 by the work of Garber and Kinsey (Ga 76) for neutrons, Tobailem for protons (To 71), and Butler et al. for pions (Bu 82). The arithmetic mean of the charged pion cross sections is shown. It is clear that the original

assumption of a step-like excitation function for the (n, 2n) reaction was incorrect and the usual 'resonance' type excitation function is observed, with a peak in the cross section at about 100 MeV.

Radiation transport calculations now make it possible to study both the charged and uncharged hadron components of accelerator radiation fields (see Chapter 4). Stevenson has recently reported calculations of the neutron, pion and proton components outside the shielding of a 30-GeV proton beamline (St 84, see Chapter 2). He shows that for transverse shields the assumption that neutrons dominate the production of ^{11}C is adequate. Furthermore, the estimation of neutron fluence using the assumption of a step-like excitation is in error by less that 15%. However, in the forward direction the charged particles play an important role in ^{11}C production and more detailed analysis is necessary.

The difference between various groups in their interpretation of hadron fluence in terms of dose equivalent have already been mentioned and have led to discrepancies of as much as a factor of two. Examination of the literature shows that these differences were largely influenced by the choice of the fluence to dose-equivalent conversion coefficients (28 fSv m^2 to 60 fSv m^2) rather than any significant differences in fluence determination (Sh 68, St 84). In turn these differences in the fluence to dose-equivalent conversion coefficients are in part due to different choices of the dose-equivalent quantity to be determined (see Sections 2.2 and 3.8).

In 1973 Stevenson and his colleagues suggested that it would be helpful to agree on fixed depth in the human body (or phantom) at which dose-equivalent should be determined. They selected a depth of 1 cm in soft tissue as an appropriate depth and recommended determining dose equivalent in a tissue-equivalent phantom whose front face was perpendicular to the incident radiation (St 73a,b). [This dose-equivalent quantity is referred to as H_s or H_{10} in this report.]

However even with the use of the same dose-equivalent quantity some differences in the fluence to dose-equivalent conversion factors remain. Thus combining the definition of dose equivalent of Stevenson with the work of Shaw et al., based on neutron spectra measured around high-energy proton accelerators, would suggest that the dose equivalent per unit fluence should be 60 fSv m^2 (a neutron fluence rate of 1 $cm^{-2} s^{-1}$ being equivalent to 0.22 mrem/h) (Sh 68, St 73a,b). This value is in fair agreement with the latter work of Stevenson (St 71b) where a value of 50 fSv m^2 was proposed (a fluence rate of 1 $cm^{-2} s^{-1}$ equivalent to 0.18 mrem/h), but differs from the value of 28 fSv m^2 in current use at CERN (a fluence rate of 1 $cm^{-2} s^{-1}$ equivalent to 0.1 mrem/h) (Go 67). This latter value is based on measurements of dose equivalent in high-energy beams by Baarli and Sullivan (Ba 65).

Stevenson was able to show that the value of 28 fSv m^2 measured in neutron beams agreed with that calculated for the pure neutron leakage spectra calculated by O'Brien for a 3-GeV proton beam shielded by concrete (OB 68, OB 71). However, in spectra that contained a charged particle component (pions, protons) the calculated conversion coefficient was 45 fSv m^2 in good agreement with the value of 50 fSv m^2 proposed by

Stevenson (St 71b).

MODERATED THERMAL NEUTRON DETECTORS

Many accelerator laboratories use the Andersson-Braun counter (An 63a,b) as the standard instrument for the assessment of dose equivalent produced by neutrons below 20 MeV. This is true, for example, at CERN, where the REM/N proportional counter instrument produced by 20th Century Electronics Ltd, based on the original design of the group of AERE Harwell (Harwell type 1940 A), is regarded as the reference dose equivalent meter. For area monitoring the ionization chamber version of this instrument is routinely used at CERN.

The response as a function of energy of the REM/N instrument is shown in Fig. 3.4. There are two sets of calibrations at energies less than 20 MeV, the original work of Leake and Smith at AERE Harwell (Le 64a) and the more recent work of the PTB group at Braunschweig (Al 79a, Co 81). It will be seen that the more recent calibrations give a slightly higher response than the earlier work. The point at 280 MeV is derived from a calibration by Höfert of the ionization chamber version (Ho 80). The standard calibration reference normally used is 1.01 nSv per count from the detector, when exposed to an Am-Be neutron source. (The solid line shown in Fig. 3.4 is the curve used later in this chapter to calculate and determine the response of the instrument in typical accelerator spectra.)

Another commonly used detector of this type is an indium foil or other thermal neutron activation detector placed in a spherical (or cylindrical) hydrogenous neutron moderator first described by Stephens et al. (St 58). Many variations on the original design have been reported in the literature (Ba 67, Ca 70, Si 64, Sm 61, Sm 66, St 58). The specific detector chosen as an example for discussion here is the 7 in. diameter paraffin wax moderator in a cadmium can used at the Rutherford Laboratory. The indium foil placed at the centre of the sphere is beta-assayed by a thin end-window Geiger counter. This device was calibrated by Simpson (Si 64) and these calibrations can be related to the response of a 7 in. diameter polyethylene sphere with a ^{6}LiI crystal as detector (derived from the calculations of McGuire (McG 66) to give the response of the wax sphere over the whole energy range (Fig. 3.5). The detector is calibrated in terms of the apparent flux density of 2-MeV neutrons, but a dose equivalent per unit fluence of 15 fSv m^2 was found to be most appropriate for the determination of dose equivalent in typical accelerator spectra (St 71b).

Given the response functions for the Anderson-Braun detector and 7-in. diameter wax moderator (Figs. 3.4 and 3.5), their response in any particular neutron environment may be calculated. As an example Fig. 3.6 shows the response of each in a 1/E spectrum. The readings are normalised to the dose equivalent at 10 mm depth in soft tissue (H_s or H_{10}) proposed by Stevenson et al. (St 73a) and shown as a function of the maximum (cut-off) energy of the spectrum. Inspection of Fig. 3.5 reveals that at a cut-off energy of 1 GeV the Andersson-Braun detector underestimates the dose equivalent by 30%.

These two detectors are often used to specify the dose equivalent produced by neutrons of energy less than 20 MeV. Because there is

contribution to the total response from higher energy neutrons it is of interest to compare the reading of these instruments with the actual dose equivalent below 20 MeV. This is done in Table 3.7 for a variety of neutron spectra.

MULTISPHERE TECHNIQUES

Bonner spheres of different sizes may be used with a variety of thermal neutron detectors (Br 60). Suitable detectors in practice have been found to be: BF_3 or ^3He proportional counters; ^6LiI scintillation counters; indium or gold activation foils and ^6LiF–^7LiF thermoluminescence dosimeter pairs. The specific choice of the detector is determined by constraints of the temporal nature of the radiation field. As with the use of activation detectors, the multisphere method is of low energy resolution. It has the added disadvantage that the constraints built into unfolding techniques to prevent the generation of physically unreasonable spectra also inhibit the detection of real structure in the spectra. Furthermore the detector response functions which are shown in Fig. 3.7 have not been determined experimentally over the entire energy range for which the technique is used, and one is therefore dependent upon the theoretically generated response functions (Al 76, Aw 85).

3.5. RADIATION SURVEYS

Detailed measurements in complex accelerator radiation fields are necessary but it is very important to have available techniques that facilitate rapid measurements for routine surveys.

Rapid surveys may be made by sacrificing accuracy and because radiation protection practice demands that such measurements must be interpreted in a conservative manner (Ri 68). Rapid survey measurements can be made by:

- Making measurements of only the dominant component of the radiation field (e.g., neutrons).
- Limiting the number of radiation detectors that are used.

Because neutrons usually dominate the radiation field outside the shield of heavy-ion accelerators we will discuss neutron survey techniques in some detail.

There are significant differences in the neutron spectra outside accelerator shielding and no single detector can be expected to give a response that is proportional to dose equivalent under all circumstances.

However, in general we may approximate the actual dose-equivalent quantity required by

$$H \approx \sum_{i=1}^{n} a_i R_i \qquad (3.5)$$

where the a_i's are suitably chosen dose equivalent conversion coefficient and the R_i's are the detector responses. The precise values of the a_i's will depend upon many parameters. The greater the number of

detectors (n) the better the actual dose equivalent will be approximated and the errors in its determination appreciated.

SINGLE DETECTOR

The simplest (and usually least accurate) method of determining neutron dose equivalent in surveys is to use a moderated thermal neutron detector that has an approximate dose-equivalent response in the energy range from thermal to about 15 MeV. To compensate for neutrons above 15 MeV the measured response may be multiplied by a factor of 2 to 3. Moderated thermal neutron detector instruments designed by Leake (Le 67, Le 68) or by Andersson and Braun (An 63a,b) are in common use for this purpose.

An alternative survey method that has been used is to determine the observed dose using a tissue-equivalent ionization chamber and to assume a conservative value of quality factor. This has been taken to be between 5 and 10 in accelerator radiation fields (Co 53).

Other survey techniques using single instruments include the use of recombination chamber instruments of the type described by Zielczynski and the scintillator instruments of Tesch described previously (Te 70, Zi 64).

TWO DETECTORS

Techniques using two detectors already described are the combined use of a tissue-equivalent ionization chamber with a recombination chamber to estimate Q (Di 65, Su 63, Su 64, Su69) and the combined ionization chamber/scintillator instrument of Pszona (Ps 69, Ps 71, Ps 77).

At the Lawrence Berkeley Laboratory the average energy of neutron spectrum has been determined using a polyethylene-lined proportional counter. This knowledge combined with a determination of neutron fluence with an instrument of the long counter type facilitates the determination of dose equivalent due to neutrons. The Moyer polyethylene-lined argon-CO_2 gas proportional counter has a response that is proportional to energy fluence so that the ratio of the energy fluence (given by the polyethylene-lined chamber) to the fluence (given by the saturated BF_3 counter) gives the average neutron energy, $\bar{E}_n$. The fluence to dose-equivalent conversion coefficient corresponding to $\bar{E}_n$ can then be applied to the flux density measurement to estimate the dose equivalent (Mo 52, St 73c). How well this technique approximates the true dose equivalent will depend on the spectral distribution of neutrons. For example the data of Ing et al. (In 81) give the average neutron energy, $\bar{E}_n$, for a ^{238}Pu-Li source as 0.5 MeV with a corresponding fluence to dose equivalent conversion coefficient of 18.2 fSv m^2 (1.82×10^{-8} cm^2). The survey technique using a moderated BF_3 counter and a polyethene-lined counter would overestimate the dose equivalent by a factor of 1.4 by declaring the average dose equivalent (corresponding to $\bar{E}_n$ = 0.5 MeV) to be 25.7 fSv m^2 (2.57×10^{-8} rem cm^2).

Care must always be exercised when using the PE counter, especially at electron accelerators, to ensure that photon pile-up is not interfering with the measurement.

THREE OR MORE DETECTORS

Experience shows that three detectors are the minimum that may be used to determine dose equivalent in the environment of particle accelerators with sufficient accuracy for radiation protection purposes [in the terms of Eq. (3.5) $n \geq 3$].

Typically the three detectors used are:

(1) An air ionization chamber to determine the dose equivalent contribution from charged particles and photons.

(2) A 'low-energy' ($E < 20$ MeV) neutron detector-usually one of the many types of moderated thermal neutron detectors (An 63a, An 63b, Aw 66, Ha 47, Ha 62, Le 67, Le 68, Na 72, Si 64, St 58).

(3) A 'high-energy' ($E \geq 20$ MeV) neutron detector-most frequently based on the ^{12}C $(n,2n)$ ^{11}C reaction (Ba 57, McC 60, Sh 51, Sh 62).

Such a scheme has been the basis for measurements at Berkeley (LBL), CERN and the Rutherford Appleton Laboratory for many years.

At CERN the total dosimetry system consists of four instruments-the three specified above plus a tissue-equivalent ionization chamber to determine absorbed dose and give an indication of the average quality factor of the radiation field (Ho 72). This dosimetry system has somewhat whimsically been named 'Cerberus' after the many-headed monster of Greek mythology.

In what follows, to give the reader a feeling for the inaccuracies involved we will compare the determination of dose equivalent by two elements of the detector systems, used by CERN and the Rutherford Appleton Laboratory.

At CERN the low-energy ($E < 20$ MeV) neutron dose equivalent is determined using an Andersson-Braun instrument. The ionization chamber version of the detector is used and a correction is made to the recorded ionization current for the contribution due to photons and charged particles. Calibration is achieved using an Am-Be neutron source. The high-energy ($E < 20$ MeV) neutron dose equivalent is determined from the nominal ^{11}C fluence (see previous section) using a conversion coefficient of 28 fSv m^2.

At the Rutherford Laboratory the dose equivalent, H_A, is given by:

$$H_A = 15\phi_{IN} + 50\phi_C \qquad (3.6)$$

where the unit of dose equivalent is fSv and the unit of the neutron fluence is per m^2. ϕ_{IN} is the fluence determined by paraffin wax moderated detector and ϕ_C is the nominal ^{11}C fluence (previous section). The conversion coefficients used in Eq. (3.6) are appropriate to H_{10}. (See Sections 2.2 and 3.8.)

Comparison of the dose equivalents that could be obtained in a variety of accelerator spectra is shown in Table 3.8. The estimates of H_{10} by both laboratories are seen to be good and (with exception of the

theoretical O'Brien spectra) never worse than 25%.

This good agreement between the laboratories for dose-equivalent values does not, however, persist when the dose equivalents that would be determined for neutrons below and above 20 MeV are compared.

Table 3.9 shows the ratio of dose equivalent contributed by neutrons below 20 MeV to that contributed by neutrons above 20 MeV, as would be determined by the CERN and Rutherford Laboratory prescriptions, for the several accelerator spectra used here. In addition, the correct value of this ratio is given for comparison. The CERN recipe is seen systematically to overestimate this ratio whereas the RL recipe usually underestimates it. This state of affairs may be corrected by readjustment of the calibration coefficients-a matter of administrative rather than physical difficulty.

Table 3.10 summarises some of the methods available for radiation surveys.

3.6. DOSE-EQUIVALENT INSTRUMENTS VERSUS PHYSICAL MEASUREMENTS

Over the past 15 years there has been a continuing debate between those dosimetrists who wish to limit their measurements to what is required solely for health physics surveys and those who wish to utilize their data for additional purposes (Ri 71, Ri 72).

There can be no argument that instruments that roughly indicate dose-equivalent rate are of great value in radiation surveys, but even in this respect many so called rem-responding instruments show deficiencies. For example, many neutron 'rem-meters' over-respond to intermediate energy neutrons (La 70, Na 72, Ro 79). The size or sensitivity of survey instruments may be a disadvantage; thus, for example, the size of the Brookhaven National Laboratory universal dose-equivalent instrument (Ku 72, 73a,b), which is of suitable sensitivity for radiation protection measurements, makes it practical only for surveys in free air in which the radiation field is fairly uniform over distances of ~20 cm.

Many survey instruments have only limited design constraints placed upon them. For example, Tesch has described two counters that may be used for neutron dosimetry in the energy region 10–100 MeV (Te 70). The first instrument consists of a liquid scintillator with the pulse height selected to give the required dose-equivalent response functions. Pulses originating from particles other than neutrons are suppressed by pulse-shape discrimination. The second counter is a simple extension of the multisphere method (Br 60). In his paper Tesch discusses the limited need for accuracy in radiation protection:

'...it is, however, questionable whether there is any point in aiming at a sensitivity curve with deviations considerably smaller than 50% since the concept of a quality factor is only a very rough approximation.'

This comment correctly reveals the reasonably limited design constraints that may be placed upon 'rem-meters' when these instruments are to be used solely for radiation surveys.

If, however, measurements are to be applied to the variety of tasks listed in the introduction to Section 3.1, physical measurements of the radiation field are to be preferred. The need for a broad application of radiation measurements, coupled with the possibility that there will be continuing refinement in dosimetric concepts and quantities, makes a convincing argument for a physical specification of the radiation field. The case is supported by current practice at high-energy laboratories where particle fluence measurements are almost universally made.

One of the basic assumptions of radiation protection that could be challenged is the Q-L relationship, which is now about 20 years old (ICRP 63). Mole has questioned whether we should continue to use a single quality factor in radiation protection for a given LET, regardless of the tissues being irradiated and the particular biological end-point of concern (Mo 79). Rossi has gone so far as to propose a substantial increase in the quality factor for fission neutrons (Ro 77, Ro 78a) and further to suggest that linear energy transfer might better be replaced by another quantity (lineal energy) to describe radiation quality.

The general thrust of the arguments presented here is that most practical systems of dosimetry at high energies require physical measurements that define the radiation environment. The parameters that define the biological detriment to humans exposed at low doses and dose rates are still uncertain. We may expect the determination of the risk resulting from radiation exposure to be refined as our knowledge increases. Precise determination of the physical parameters of the radiation field, however, provides an immutable basis for the derivation of any physical quantities subsequently required for a risk determination. The converse is not so. Measurements specified in terms of dose-equivalent quantities may be invalidated if fundamental changes are made in our dosimetric systems for radiological protection (Ca 82, NCRP 82).

3.7. THE DETERMINATION OF NEUTRON SPECTRA AT ACCELERATORS

While radiation surveys in the field provide useful after-the-fact data, the goals of radiation protection may only be met when the origin, attenuation through shielding, and transport through the air of accelerator-produced radiation are fully understood. As we have seen in previous sections, the dominant radiation protection problem around high-energy accelerators is expected to be due to neutrons. Thus knowledge of the neutron spectra found around particle accelerators provides an essential starting point for an understanding of accelerator radiation protection.

Neutron spectra are also a fundamental starting point in the measurement of the dose equivalent, since they permit an optimum choice of radiation detector combinations; they enable LET distributions to be calculated in phantoms and, finally, they facilitate the calculation of dose-equivalent quantities from appropriate fluence to dose-equivalent conversion coefficients. The techniques available for the determination of neutron spectra around accelerators will be discussed in this section.

Accelerator neutron spectra have been measured at only a few laboratories. This is no doubt partly because the techniques are protracted and long periods of stable operation are required (not a usual feature of particle accelerators used in research), partly because spectrum unfolding requires some mathematical ability or familiarity with some of the many computer programs (and, as a corollary, access to a computer facility), but principally because sufficient resources have not been made available at any national laboratory or university for a systematic study of accelerator radiation environments.

The techniques used for spectrum measurement at particle accelerators are well established and have been extensively described in the literature (Pa 73, In 85). The basic techniques used or attempted at high energy accelerators are summarized in Table 3.11.

Threshold detectors, activation detectors and Bonner spheres have already been described, so we will discuss only nuclear emulsion and other techniques for proton-recoil spectrum measurement in what follows.

Proton recoil spectrum measurements. Nuclear emulsions can be used to record recoil proton spectra, but their evaluation is tedious and time-consuming (Ak 63, Le 64b). They also require techniques and equipment that are no longer in readiness at many laboratories. Proton spectra have also been measured using bulk plastic scintillation detectors (Th 85c). Both these techniques are only able to give neutron spectral information in the energy range 2–20 MeV. At higher energies star prong counting has been utilised to give crude information on spectrum slope (Re 65, Pa 69).

At higher energies special counter-telescope arrangements (Al 74, Al 75, Al 79b, Ma 73, Pe 68) or spark chamber arrays (Li 73, Ma 74, Ri 69, Ri 74) are required. These techniques both derive directly from high-energy physics detectors and require a complex infrastructure typically beyond the capabilities of small accelerator laboratories.

Examples of neutron and recoil-proton spectra determined at several particle accelerators have been given in Chapter 2.

There are several examples in particle accelerator dosimetry where a knowledge of neutron spectra has been crucial to the understanding of observations. Thus, for example, in 1965 Baarli and his colleagues noted that neutrons with energy above 20 MeV contributed a much larger fraction of dose equivalent outside earth shielding than had been observed outside concrete shielding at the CERN 28-GeV proton synchrotron (CPS) (Ba 64, Ba 65). It was possible to demonstrate by a determination of the neutron spectra that this effect was due to the increased effectiveness of wet earth in removing intermediate energy neutrons (Gi 68). A second example is the establishment of the presence of a significant high-energy neutron component to the radiation field outside the shielding of the Stanford 20-GeV Linac (McC 77). This observation had been predicted by De Staebler (deS 65), but there had been some controversy as to its magnitude prior to these measurements.

3.8. INTERPRETATION OF ACCELERATOR RADIATION MEASUREMENTS

We have seen (Section 2.2) how the interpretation of physical data that are in essentially good agreement may lead to dose-equivalent estimates that differ by a factor of two or more.

These discrepancies have historically arisen because of the use of different dose-equivalent quantities and, in the case of neutron measurements, different interpretation methods to assess the fluence to dose-equivalent conversion coefficients.

FLUENCE TO DOSE-EQUIVALENT CONVERSION COEFFICIENTS

Several steps of fluence to dose equivalent coefficients for neutrons were recommended in the seventies by advisory bodies such as ICRP and NCRP and also by governmental regulatory agencies (see for example CFR 78, ICRP 70, ICRP 73, NCRP 71).

Detailed differences exist between such recommended coefficients [which have been much criticized in the literature (Ei 81, Ro 78b, Ro 79, Si 83, Th 85b)], because of variation in the:

- Calculational models (phantoms; nuclear physics)
- Interpretation of basic calculated data
- Techniques of interpolation between recommended data points.

The conversion coefficients recommended by ICRP and NCRP in the seventies are largely derived from Monte Carlo calculations of the absorbed dose distributions in semi-infinite tissue equivalent slabs or tissue-equivalent cylinders (Al 70, Au 68, ICRP 70, ICRP 73, Ir 67, NCRP 71, Sn 50, Sn 67, Sn 71, Ze 65).

Chilton and his colleagues (Ch 78, Ch 79, Ch 81a, b, Sh 83) have subsequently reported calculations within an ICRU sphere up to neutron energies of 14 MeV.

By examining all these data Chilton has concluded that the shape of the phantom has little effect on the values of the maximum of absorbed dose or dose equivalent (Ch 81a). He also concluded that the conversion coefficients recommended by ICRP (ICRP 73) suffered from excessive smoothing in the region 10–100 MeV (see Fig. 3.8). Chilton recommended more calculations at smaller intervals than in the ICRP-NCRP data to study the influence of the complex structure of the cross sections at energies above about 0.4 MeV for some of the important constituents of tissue.

Cross and Ing have also reached conclusions generally similar to those of Chilton. They have compiled data on conversion coefficients from neutron fluence to dose-equivalent quantitites in different phantoms as a function of neutron energy. The phantoms used included a tissue-equivalent sphere, slab and cylinder and the dose-equivalent quantities considered included maximum dose equivalent, dose equivalent at a depth of 1 cm and effective dose equivalent (Cr 85).

Conversion coefficients for the calculation of the index quantities from selected data for neutrons up to 15 MeV in energy are shown in Fig. 3.9. The values of the deep dose equivalent indexes do not differ greatly from values of the maximum dose equivalent calculated in slab or

cylindrical phantoms. Values of $H_{I,d}$ are therefore adequate for determining the conversion coefficient given in NCRP Report 38 and ICRP Publication 21 (ICRP 73,2NCRP71). The calculations now available span the energy range from 10^{-2} to 15 MeV in some detail (see Fig. 3.9), much reducing the uncertainties in interpolation errors discussed in the section entitled "The Evaluation of Dose Equivalent Produced by Neutrons" of Chapter 2. Figure 3.9 shows the results of calculations of both the shallow and deep dose-equivalent indexes by two groups-by Chilton and his colleagues at Urbana-Champaign (Ch 78, Ch 81a,b) and by Burger and his colleagues at Neuherberg (Bu 81b, Wi 80). Agreement between the two sets of calculations is seen to be fairly good.

Effective dose equivalent, H_E, must be calculated in a humanoid phantom. Kramer et al. have described two sex-specific adult human phantoms, ADAM and EVA, derived from the original MIRD phantom, that have been used for extensive calculations of effective dose equivalent (Kr 82a, Na 81) (see Fig. 3.10).

Kramer and Drexler have drawn attention to one possible source of ambiguity in the definition of H_E (Kr 82b). As currently defined effective dose equivalent requires a weighting factor of 0.06 to be applied to each of five organs or tissue-'the remainder'-receiving the highest dose equivalent, and for this sum to be added to the sum of the weighted dose equivalents to the six principal organs. The organs and tissues that comprise 'the remainder' vary with radiation type, energy and radiation geometry. It is not therefore appropriate, as is done by some workers, to predetermine which organs or tissues comprise the remainder. Calculations of effective dose equivalent are phantom-dependent, and it will be important to reach general agreement on the model to be used.

Conversion coefficients from fluence to dose equivalent are now available from thermal energies to 14 MeV for several dose-equivalent quantities including: effective dose equivalent, the deep and shallow dose-equivalent indexes, and for $H_{0.07\ mm}$ (the dose equivalent on the principal axis, of the ICRU sphere at depths of 0.07 mm and 10 mm, irradiated by a broad parallel beam of neutrons, Fig. 3.11) (ICRP 86, Th 85b).

For higher energies (up to 10^{12} MeV) there is no single set of data that spans the entire energy range, and calculations of H_E or H_I have not yet been made. Conversion coefficients are therefore obtained from calculations in a 30 cm thick tissue-equivalent slab phantom. (These, however, should be a good approximation to $H_{i,d}$; see Fig. 3.12) (Al 70, Ar 73, Ch 81a, Go 78, Ir 67, Ze 65).

Certain dosimetric techniques may require the determination of special conversion coefficients. Thus at CERN where the production of ^{11}C is used to measure hadrons of energy greater than 20 MeV a correction is made for the primary ionization of the charged hadron (pions and protons) (St 84). The primary ionization produced by these particles is measured by ionization chambers but the normal fluence to dose-equivalent conversion coefficients take into account the primary ionization. Estimates of the dose equivalent based on fluence measurements using ^{11}C activation need to be reduced to avoid duplication of the contribution to the absorbed dose produced by the primary ionization

component. Figure 3.12 shows conversion coefficients for protons and pions reduced by the contribution from direct coulomb losses (Al 70, Al 71, Ar 73, Ne 66, Tu 64, Wr 69, Ze 65). Stevenson has compared these coefficients with the values determined for neutrons (Al 70, Al 71, Dm 71, Ir 67, Na 69, NCRP 57, Ne 66, Wr 69, Ze 65). [The mean of the conversion coefficients for negatively and positively charged pions is plotted in Fig. 3.13.] The values of dose equivalent for protons obtained in this way are indistinguishable from neutrons, but below 2 GeV dose equivalents for pions are significantly higher.

INTERCOMPARISON OF DOSE-EQUIVALENT DETERMINATIONS

An important way to establish confidence in the determination of dose equivalent is to compare measurements by various groups, using different experimental techniques.

Ideally such intercomparisons should be made under carefully controlled conditions. Thus, for example, the instruments used should make measurements at the identical locations in a radiation field that is spatially uniform. In addition it is essential that the same dose-equivalent quantity be compared.

Rarely, if ever, have these criteria been exactly met. Thus a large contribution to the discrepancies revealed in the CERN - Lawrence Berkeley Laboratory - Rutherford Laboratory intercomparison of Gilbert et al. was due to the fact that the CERN group determined H_{10} whereas the other two groups determined H_m (Gi 68). None of the participating groups fully understood this subtlety, which has become apparent in the past decade, at the time the measurements were made. As Table 3.12 shows, estimates of the ratio of H_m to H_s (or H_{10}) in accelerator environments lie in the range 1.15 to 1.41. In the two spectra in which measurements were made at CERN the ratio has the value 1.41 (RT) and 1.24 (PSB). Interestingly enough the ratio of the dose equivalents reported by LBL to those reported by CERN was 1.31 (Gi 68).

Similar reasons may possibly be invoked to explain the discrepancies between measurements made by the BNL Universal Dose Equivalent Meter and by the LBL Physics Group (McC 77). Here, McCaslin et al. reported that the ratio of the dose equivalent determined by the LBL group was a factor of 1.8 greater than that measured by the BNL instrument (which measures H_{10}). Table 3.12 gives a value for the ratio of 1.24. The hypothesis here is less satisfactory but it is not discounted for two reasons - firstly, the calculation summarised in Table 3.12 used a different 'Bevatron' spectrum than that used for the measurements reported by McCaslin et al., and secondly, the BNL Universal Dose Equivalent Meter suffered from instrumental difficulties during the measurements.

These two examples do, however, point out the great importance in any intercomparison of selecting the dose-equivalent quantities to be determined.

Extensive efforts have been made at CERN and Serpukhov to make intercomparisons where the same neutron dose-equivalent quantities are compared. In this case H_{10} was chosen. Höfert (Ho 75a,b) has described the first comparison made at CERN in 1975, where measurements

were made with the CERN Cerberus system, the BNL Universal Dose Equivalent meter and a commercially available version of the chamber developed by Zielczynski, the REM2 (Me 73). The results of the measurements are given in Table 3.13 and are divided into groups according to whether muons, low-energy, or high-energy neutrons dominate the radiation environment.

The overall agreement between the three measurement systems is fair. When intermediate and fast neutrons dominate the radiation field the Cerberus system gives a higher estimate of dose equivalent than the other two, almost certainly due to the known overreading of the REM2 ion chamber to intermediate energy neutrons. The situation cannot easily be explained since the dose-equivalent and absorbed-dose measurements by this instrument were both higher than for the other two systems. As would be expected, the agreement is much better in those situations where the dose equivalent is dominated by radiation of low LET.

Antipov et al. have reported on measurements made in three locations around the 70-GeV proton synchrotron at Serpukhov (An 78). The detectors used included an LET spectrometer, a recombination chamber device (SUKHONA-2) and various thermal neutron detectors in moderating spheres (called SNMO-5, SNMO-3, SNM-3 and ^{103}Rh) that are used in conjunction with ^{11}C measurements and measurements with an aluminium walled air ionization chamber. Different matrices were used to correct the response of one detector due to components of the radiation field other than the one expected to be measured (KM-1 and KM-2). A simplified summary of the results of the measurements is given in Table 3.14. The two matrix methods used to derive the Serpukhov Group values will provide estimates of the MADE and can thus be expected to be higher than the H_{10} estimate of the Cerberus system. Again, if intermediate and fast neutrons dominate then the Cerberus system gives a high result.

REFERENCES FOR CHAPTER 3

Ak 63 Akagi, H. and Lehman, R., 'Neutron Dosimetry in and Around Human Phantoms by the Use of Nuclear Track Emulsion', Health Phys. 9, 207 (1963).

Al 70 Alsmiller, R.G., Jr., Armstrong, T.W., and Coleman, W.A., 'The Absorbed Dose and Dose Equivalent from Neutrons in the Energy Range 60 to 3,000 MeV and Protons in the Energy Range 400 to 3,000 MeV', Nucl. Sci. Eng. 42, 367 (1970).

Al 71 Alsmiller, R.G., Jr., Armstrong, T.W. and Bishop, B.L., 'The Absorbed Dose and Dose Equivalent from Negatively and Positively Charged Pions in the Energy Range 10 to 2000 MeV', Nucl. Sci. Engng. 43, 257 (1971).

Al 74 Aleinikov, V.E., Gerdt, V.P. and Komochkov, M.M., 'Neutron Spectra outside the Shielding of High-Energy Proton Accelerators', Joint Institute of Nuclear Research, Dubna, U.S.S.R., Preprint JNIR P16-8176 (1974).

Al 75 Aleinikov, V.E., Gerdt, V.P. and Timoshenko, G.N., 'Measurement of the Spectra of High-Energy Protons from the Shielding of the 680-MeV Sychrocyclotron', Joint Institute of Nuclear Research, Dubna, U.S.S.R., Preprint JNIR P16-9400 (1975).

Al 76 Aleinikov, V.E., Gerdt, V.P. and Komochkov, M.M., 'Some Regularities of the Formation of Neutron Spectra outside the Shielding of Proton Accelerators', Joint Institute of Nuclear Research, Dubna, U.S.S.R., Preprint JNIR P16-9870 (1976).

Al 79a Alberts, W.G., Cosack, M., Kluge, H., Lesiecki, H., Wagner, S. and Zill, H.W., 'European Workshop on Neutron Dosimetry for Radiation Protection', Physikalisch-Technische Bundesanstalt Report PTB-ND-17 (1979).

Al 79b Aleinikov, V.E., Komochkov, M.M., Krilov, A.R., Timoshenko, G.H. and Hahn, G., 'The Energy-Angle Distributions of the Proton Component of the Radiation Field Behind the 660 MeV Synchrocyclotron Shielding', Joint Institute for Nuclear Research, Dubna, U.S.S.R., Preprint 16-12732 (1979).

An 63a Andersson, I.O. and Braun, J., 'A Neutron Rem Counter', Nucleonik 6, 237 (1963).

An 63b Andersson, I.O. and Braun, J., 'A Neutron Rem Counter with Uniform Sensitivity from 0.025 MeV to 10 MeV', in 'Neutron Dosimetry' Proc. Symp. Neutron Detection and Dosimetry Standards, Harwell (Dec. 1962), Vol. 2, p. 87, IAEA, Vienna (1963).

An 78 Antipov, A.V., Bajshev, I.S., Golovachik, V.T., Krupnyj, G.I., Kustarev, V.N., Lebedev, V.N., and Höfert, M., 'Comparison of Dose Equivalent Measurements Behind the IHEP Accelerator Shielding Using Different Methods', Institute of High-energy Physics Serpukhov Report IFVEORI 78-15, 1978 (In Russian). Available in English Translation CERN Trans. 78-01 (B.C. Hodge).

Ar 73 Armstrong, T.W. and Chandler, K.C., 'Calculation of the Absorbed Dose and Dose Equivalent from Neutrons and Protrons in the Energy Range from 3.5 GeV to 1.0 TeV', Health Phys. 24, 277 (1973).

Au 68 Auxier, J.A., Snyder, W.S., and Jones, T.D., 'Neutron Interactions and Penetration in Tissue', in Attix, F.H. and Roesch, W.D., Eds., Radiation Dosimetry, 2nd ed., Vol. 1, p. 275, Academic Press, New York (1968).

Aw 66 Awschalom, M., 'The Use of the Multisphere Neutron Detector for dosimetry of Mixed Radiation Fields', Princeton-Pennsylvania Accelerator Report PPAD 596E (1966).

Aw 85 Awschalom, M. and Sanna, R.S., 'Applications of Bonner Sphere Detectors in Neutron Field Dosimetry', Radiat. Prot. Dosim. 10(1-4), 89 (1985).

Ba 57 Baranov, P.S., Goldanskii, V.I. and Roganov, V.S., 'Dosimeter for High-Energy Neutrons', Rev. Sci. Instrum. 28, 1029 (1957).

Ba 64 Baarli, J., Private communication to W. Middelkoop, CERN Internal Report AR/INT/SG64-6 (1964).

Ba 65 Baarli, J. and Sullivan, A.H., 'Health Physics Survey Methods Around the CERN High-Energy Accelerators', in Proc. of the First Symposium on Accelerator Dosimetry and Experience, USAEC Report CONF 651109, p. 103 (1965).

Ba 67 Bathow, G., Freytag, E. and Tesch.K., 'Measurements on 6.3-GeV Electromagnetic Cascades and Cascade Produced Neutrons', Nucl. Phys. B2, 669 (1967).

Ba 69a Baum, J.W., Woodcock, R.C., and Kuehner, A.V., 'Factors Effecting Pulse Size in Sealed Tissue Equivalent Counters', Proc. 2nd Inter. Conference on Accelerator Dosimetry and Experience, USAEC Report No. CONF-691101, p. 648 (1969).

Ba 69b Baarli, J., 'Dosimetry of Very High Energy Radiation' in Health Physics, Vol. 2, A.M.F. Duhamel, Ed., Pergamon Press, Oxford (1969) p. 297.

Be 82 Beynel, P., Maier, P., and Shönbacher, 'Compilation of Radiation Damage Test Data, Part III: Materials Used Around High-Energy Accelerators', CERN internal report CERN 82-10 (1982).

Bo 62 Bonet-Maury, P., Duhamel, M. and Perrin, F., 'Premier Colloque International sur la protection auprès des Grands Accelératéurs', Paris, France, January 18-20, 1961, Presses Universitaire de France, 108 Bd. Saint-Germain, Paris (1962).

Br 60 Bramblett, R.L., Ewing, R.I., and Bonner, T.W., 'A New Type of Neutron Spectrometer', Nucl. Inst. and Meths. 9, 1 (1960).

Bu 68 Burlin, T. E., 'Cavity Chamber Theory' in Radiation Dosimetry, vol. 1, p. 332, E.H. Attix and W.C. Roesch, Eds., Academic Press, New York (1968).

Bu 81a Burger, G., Ebert, H.G., Harder, D., Kramer, R. and Wagner, S.R. (Eds.), 'Proceedings of the European Seminar on Radiation

Protection Quantities for External Exposures', Braunschweig, Fed. Rep. of Germany, 13-15 October 1980, Harwood Academic Publishers Chur, Switzerland, London, EUR 7101-EN (1981).

Bu 81b Burger, G., Morhart, A., Nagarajan, P.S. and Wittmann, A., 'Conversion Functions for Primary and Operational Quantities in Neutron Radiation Protection', Proc. Fourth Symposium on Neutron Dosimetry, Munich-Neuherberg, Germany, June 2-5, 1981, Vol. 1, p. 33, Commission of the European Community, Luxembourg EUR 7101-EN (1981).

Bu 82 Butler, G.W., Dropesky, B.J., Orth, C.J., Green, R.E.L., Korteling, R.G. and Lam, G.K.Y., 'Cross Sections for the $^{12}C(\pi^{\pm},\pi N)^{11}C$ Reactions from 20 to 100 MeV', Los Alamos National Laboratory, Los Alamos, New Mexico, LA-UR-82-1323 (1982).

Ca 65 Capone, T., et al., 'A Radiation Survey Inside and Outside the CPS Tunnel to Estimate the Effectiveness of the Roof Shielding', CERN Internal Report DI/HP/71 (1965).

Ca 70 Carter, T.G., Chakalian, V.M. and Thomas, R.H., 'Stanford Mark I Moderator Calibration Using Tantalum', Stanford University Internal Report RHT/TN/70-2 (1970).

Ca 82 Casarett, G.W., 'Scientific Committee on Basic Radiation Protection Criteria', Reports on Selected NCRP Activities, op. cit. Ref. NCRP 82, p. 272 (1982).

CERN 71 Proceedings of the International Congress on Protection Against Accelerator and Space Radiation, Geneva, April 1971, European Organization for Nuclear Research Report CERN 71-16 (2 Vols.) (1971).

CFR 78 Code of Federal Regulations Title 10, Energy: Part 20, Standards for Protection Against Radiation, U.S. Govt. Printing Office, Washington, D.C. (1978).

Ch 66 Charalambus, St., Dutrannois, J. and Goebel, K., 'Particle Flux Measurements with Activation Detectors', CERN Internal Report DI/HP/90 (1966).

Ch 78 Chen, S.Y., 'Calculation of Neutron Fluence-to-Dose-Index Conversion Factors for the Standard ICRU Tissue Phantom by the Monte Carlo Method', Ph.D. Thesis, Nuclear Engineering Dept., Univ. of Illinois at Urbana-Champaign (1978).

Ch 79 Chen, S.Y. and Chilton, A.B., 'Calculations of Fast Neutron Depth-Dose in the ICRU Standard Tissue Phantom and the Derivation of Neutron Fluence-to-Dose-Index Conversion Factors', Rad. Res. 78, 335 (1979).

Ch 81a Chilton, A.B., 'Calculated Index Quantities for Neutrons', in Proceedings of the European Seminar on Radiation Protection Quantities for External Exposure, Braunschweig, Federal Republic of Germany, 13-15 October 1980, EUR 7101-EN, p. 89, Harwood Academic Publishers, Chur, Switzerland (1981).

Ch 81b Chilton, A.B. and Shiue, Y-L., 'Progress Report on Studies Concerning Doses in the ICRU Sphere Resulting from Neutron Beams', in Proceedings of the Fourth Symposium on Neutron Dosimetry, Munich-Neuherberg, Germany, June 2-5, 1981, Vol. 1, p. 63, Commission of the European Committee, Luxembourg, EUR 7448-EN (1981).

Co 53 Cowan, F.P. and Handloser, J.S., 'Health Physics Program for the Brookhaven Cosmotron', Brookhaven National Laboratory Report BNL 264 (T-43) (Nov. 1953).

Co 81 Cosack, M., and Lesiecki, H., 'Dependence of the Response of Eight Neutron Dose Equivalent Survey Meters with Regard to Energy and direction of Incident Neutrons', in Proceedings of the Fourth Symposium on Neutron Dosimetry, EUR 7448-EN, CEC, Luxembourg, p. 407 (1981).

Cr 85 Cross, W.G. and Ing, H., 'Conversion and Quality Factors Relating Neutron Fluence and Dosimetric Quantities', Rad. Prot. Dosim. 10(1-4), 29 (1985).

deS 65 De Staebler, H., 'Similarity of Shielding Problems at Electron and Proton Accelerators', in Proc. of First Symposium on Accelerator Dosimetry and Experience, Brookhaven, November 1965, USAEC Report CONF-651109 p. 429 (1965).

Di 65 Distenfeld, C.H. and Markoe, A.M., 'Determination of Quality Factor Through the Utilization of a Balanced Tissue-Equivalent Ionization Chamber', in Proceedings of First Symposium on Accelerator Dosimetry and Experience, Brookhaven, November 1965, USAEC Report CONF-651109, p. 181 (1965).

Dm 71 Dmitrievsky, I.M., Kabakov, J.I., Potjomkin, E.L. and Frolov, V.V., 'High Energy Nucleon Tissue Doses', Proceedings of the International Congress on Protection against Accelerator and Space Radiation, Vol. 1, p. 328, CERN, Geneva, Switzerland, CERN 71-16 (1971).

Ei 81 Eisenhauer, C. and Schwartz, R. 'Difficulties in Calculating Spectrum-Averaged Values of Neutron Dose Equivalent,' Health Physics 41, 774 (1981).

Fa 50 Failla, G. and Rossi, H.H., 'Tissue Equivalent Ionization Chambers'. Am. J. Roent. Radium Therapy Nucl. Med. 64, 485 (1950).

Fr 70 Freytag, E. and Nachtigall, D., 'A Comparison of Health Physics Measuring Procedures at Accelerators', Deutsches Electronen Synchrotron Internal Report DESY/70/27 (1970).

Ga 76 Garber, D.I. and Kinsey, R.R., 'Neutron Cross Sections', 3rd Edn., Vol. 2, National Neutron Cross Section Center, Brookhaven National Laboratory, Upton, NY, BNL 325 (1976).

Gi 68 Gilbert, W., et al., 'CERN-LBL-RHEL Shielding Experiment at the CERN Proton Synchrotron', Lawrence Berkeley Laboratory Report UCRL-17941 (1968).

Go 67 Goebel, K., Rindi, A., Sullivan, A.H. and Baarli, J., 'The Purpose, Interpretation and Utilization of Area Monitoring Measurements near the CERN Accelerators', in Radiation Dose Measurements, their Purpose, Interpretation and Required Accuracy in Radiological Protection, p. 435, CONF-670621, (Paris: European Nuclear Energy Agency) (1967).

Go 68 Goodman, L.J. and Rossi, H.H., 'The Measurement of Dose Equivalent Using Paired Ionization Chambers', Health Phys. 14, 168 (1968).

Go 78 Golovachik, V.T., Potemkin, E.L., Lebedev, V.N. and Frolov, V.V., 'Doses from High-Energy Particles in a Tissue-Equivalent Phantom', cited in Atlas of Dose Characteristics of External Radiations, Bikrov, A.I., Dudkin, V.E., Kovalev, E.E. et al., Eds., Atomizat, Moscow (1978).

Ha 47 Hanson, A. O. and McKibben, J.L., 'A Neutron Detector Having Uniform Sensitivity from 10 keV to 3 MeV', Phys. Rev. 72, 673 (1947).

Ha 62 Hankins, D.E., 'A Neutron Monitoring Instrument Having a Response Approximately Proportional to the Dose Rate from Thermal to 7 MeV', Los Alamos Scientific Laboratory Report LA-2717 (1962).

He 57 Hess, W.N., Patterson, H.W. and Wallace, R.W., 'Delay-Line Chamber Has Large Area, Low Capacitance', Nucleonics 15 (3), 74 (1957).

He 59a Hess, W.N., 'Neutrons from (α, n) Sources', Ann. Phys. N.Y. 6, 115 (1959).

He 59b Hess, W.N., Patterson, H.W., Wallace, R.W. and Chupp, E.L., 'Cosmic Ray Neutron Energy Spectrum', Phys. Rev. 116, 445 (1959).

Ho 72 Höfert, M., 'Dose Equivalent and Quality Factor of Radiation from High-Energy Accelerators', First Symp. Neutron Dosimetry in Biology and Medicine, Munich Euratom. Vol. 2, p. 873, EUR 4896d-f-e (1972).

Ho 75a Höfert, M., 'A Comparison of Dose Equivalent Measurements Around a GeV Proton Accelerator', European Centre for Nuclear Research (CERN) Internal Report DI/HP/187, July 7, 1975.

Ho 75b Höfert, M. and Baarli, J., 'Dose Estimation of Very High Neutron Radiation for Protection Purposes', Proceedings of the IVth All-Union Congress on Charged Particle Accelerators, Vol. 2, p. 207, Nauka (Moscow) (1975).

Ho 80 Höfert, M. and Raffnsoe, Ch., 'Measurements of Absolute Absorbed Dose and Dose-Equivalent Response for Instruments Used Around High-energy Proton Accelerators', Nucl. Instrum. Methods 176, 443 (1980).

Ho 83 Höfert, M., 'On the Problem of Neutron Dosimetry Around High-energy Accelerators and Pragmatic Solutions', CERN Internal Report HS-RP/IR/83-22 (1983).

Ho 85 Holt, P.D., 'Passive Detectors for Neutron Fluence Measurement', Radiat. Prot. Dosim. 10(1-4), 251 (1985).

HP 77 Health Physics Group, Lawrence Berkeley Laboratory, 'Accidental Accelerator Beam Exposure Dosimetry Procedure', Lawrence Berkeley Laboratory Internal Report UCID-3905 (April 1977).

ICRP 63 RBE Committee, Report of the RBE Committee to the International Commission on Radiological Protection and on Radiological Units and Measurements, Health Phys. 9, 357 (1968).

ICRP 64 International Commission on Radiological Protection, 'Protection Against Electromagnetic Radiation above 3 MeV and Electons, Neutrons and Protons', ICRP Publication 4, Pergamon Press, Oxford (1964).

ICRP 70 International Commission on Radiological Protection, 'Protection against Ionizing Radiation from External Sources' (Adopted by the Commission in Nov. 1969), ICRP Publication 15, Pergamon Press, Oxford (1970).

ICRP 73 International Commission on Radiological Protection, 'Data for Protection Against Ionizing Radiation from External Sources: Supplement to ICRP Publication 15' (Adopted by the Commission in April 1971), ICRP Publication 21, Pergamon Press, Oxford (1973).

ICRP 86 International Commission on Radiolocial Protection, 'Data for Use in Protection against External Radiation', ICRP Publication 44, Pergamon Press, Oxford (1986).

ICRU 68 International Commission on Radiation Units and Measurements, 'Radiation Quantities and Units', ICRU Report 11, Washington, D.C. (1968).

ICRU 78 International Commission on Radiation Units and Measurements, 'Basic Aspects of High Energy Particle Interactions and Radiation Dosimetry', ICRU Report 28, Washington, D.C. (1978).

In 81 Ing, H., Cross, W.G. and Tymons, B.J., 'The Spectrum of Neutrons from a ^{238}Pu-Li Source', Health Phys. 40, 345 (1981)

In 85 Ing, H. and Piesch, E. (Eds.), 'Neutron Dosimetry in Radiation Protection', Radiat. Prot. Dosim. 10(1-4) (1980).

Ir 67 Irving, D.C., Alsmiller, R.G., Jr. and Moran, H.S., 'Tissue Current-to-Dose Conversion Factors for Neutrons with Energies from 0.5 to 60 MeV', Oak Ridge National Laboratory Report ORNL-4032 (1967).

Iz 80 Iżycka, A. and Schönbacher, H., 'High-Level Dosimetry for Radiation Damage Studies at High-Energy Accelerators'. Proc. Third ASTM-EURATOM Symposium on Reactor Dosimetry, ISPRA, 1979. Euratom Report, EUR 6813, Ispra (1980).

Ke 48 Kelly, E. and Weigand, C., 'Fission of Elements from Pt to Bi by High-energy Neutrons', Phys. Rev. 73, 1135 (1948).

Kr 82a Kramer, R., Zanke, M., Williams, G., and Drexler, G., 'The Calculation of Dose from External Photon Exposures Using

Reference Human Phantoms and Monte Carlo Methods. Part 1. The Male (ADAM) and Female (EVA) Adult Mathematical Phantoms', Gesellschaft für Strahlen und Umweltforschung m.b.H., Munchen, GSF Report S-885 (1982).

Kr 82b Kramer, R. and Drexler, G., 'On the Calculation of the Effective Dose Equivalent', Radiat. Prot. Dosim. 3 (1/2), 13 (1982).

Ku 72 Kuehner, A.V., Chester, J.D. and Baum, J.W., 'Portable Mixed Radiation Dose Equivalent Meter', Brookhaven National Laboratory Report BNL-17298 (1972).

Ku 73a Kuehner, A.V., Chester, J.D., and Baum, J.W., 'Portable Mixed Radiation Dose-Equivalent Meter for Protection Monitoring', p. 233, Proc. Symp. on Neutron Monitoring for Protection Purposes, IAEA Vienna, (1973).

Ku 73b Kuehner, A.V., and Chester, J.D., 'Dose Equivalent Meter Operating Instructions', BNL, Health and Safety Division, Informal Report, 1973.

La 69 Laughlin, J.S., 'Electron Beams', Chapter 19, in Radiation Dosimetry, Vol. III, p. 92 (ed. F.H. Attix and E. Tochlin), Academic Press, New York (1969),

La 70 Larson, H.V., 'An Intercomparison of the Characteristics of Beta/Gamma and Neutron Survey Instruments', Proc. Symp. Adv. Phys. Biol. Radiat. Detectors, IAEA Vienna, p. 533 (1971).

Le 64a Leake, J.W. and Smith, J.W., 'Calibration of a Neutron Rem Counter', Atomic Energy Research Establishment Report AERE-R 4524 (1964).

Le 64b Lehman, R. and Fekula, O.M., 'Energy Spectrum of Stray Neutrons from the Bevatron', Nucleonics 22(11), 35 (1964).

Le 67 Leake, J.W., 'Portable Instruments for the Measurement of Dose-Equivalent Rate in Steady State and Pulsed Neutron Fields', Proc. Symp. Neutron Monitoring Vienna, August 1966, IAEA (Vienna), p. 313 (1967).

Le 68 Leake, J.W., 'An Improved Spherical Dose Equivalent Neutron Detector', Nucl. Inst. and Meth. 63, 329 (1968).

Li 57 Lindenbaum, S.J., 'The Brookhaven National Laboratory Proton Synchrotron', in Proc. Conference on Shielding of High-Energy Accelerators, New York, April 1957, p. 28, USAEC Report TID-7545 (1957).

Li 73 Lim, C.B., 'The Development of a Neutron Spectrometer using Multi-Wire Spark Chambers,' Ph.D. Thesis, Nuclear Engineering Department, University of California at Berkeley, Lawrence Berkeley Laboratory Report LBL-1719 (1973).

Ma 73 Madey, R. and Waterman, F.M., 'Neutron Spectroscopy from 1 MeV to 1 GeV', Proc. Symp. on Neutron Monitoring for Radiation Protection Purposes, Vienna, December 1972, Vol. 1, p. 113, IAEA Vienna (1973).

Ma 74 Mamont-Čiesla, K. and Rindi, A., 'Spark Chamber Neutron and Proton Spectrometer—First Report on Performance', University of California, Lawrence Berkeley Laboratory Report, LBL-3343 (1974).

McC 60 McCaslin, J.B., 'A High Energy Neutron Flux Detector', Health Phys. 2, 399 (1960).

McC 67 McCaslin, J.B. and Stephens, L.D., 'High-Sensitivity Neutron and Proton Flux Detector with a Practical Threshold Near 600 MeV Using Hg(spallation)^{119}Tb', Lawrence Berkeley Laboratory Report UCRL-17505 (1967).

McC 68 McCaslin, J.B., Patterson, H.W., Smith, A.R. and Stephens, L.D., 'Some Recent Developments in Techniques for Monitoring High-Energy Accelerator Radiation', Proceedings of the First International Symposium of the International Radiation Protection Association, Pergamon Press, New York, p. 113 (1968).

McC 73 McCaslin, J.B., 'Detection of Neutrons Greater than 20 MeV from the Production of ^{11}C', in Laboratory Manual Experiment 8, Patterson, H.W. and Thomas, R.H., Accelerator Health Physics, Academic Press New York, p. 621 (1973).

McC 77 McCaslin, J.B., Smith, A.R., Stephens, L.D., Thomas, R.H., Jenkins, T.M., Warren, G.J. and Baum, J.W., 'An Intercomparison of Dosimetry Techniques in Radiation Fields at Two High-Energy Accelerators', Health Phys. 33, 611 (1977).

McC 81 McCaslin, J.B. and Thomas, R.H., 'Practical Neutron Dosimetry at High-Energies', Proceedings of a Seminar on Radiation Protection Quantities for External Exposure, Braunschweig, Federal Republic of Germany 13-15 October 1981, Eds. Burger, G., Harder, D., Kramer, R. and Wagner, S., Harwood Academic Press, EUR-7101-EN, p. 137 (1981).

McG 66 McGuire, S.A., 'A Dose-Monitoring Instrument for Neutrons from Thermal to 100 MeV', Los Alamos Laboratory Report LA-3435 (1966).

Me 73 Metronex Company, Recombination Chamber Type REM-2, Technical Manual, Warsaw, Poland (1973).

Mi 72 Miller, A.J. and Patterson, H.W., 'Measurement of Induced Activity to Estimate Personal Radiation Exposures Received from Accelerator Beams', Health Phys. 23, 671 (1972).

Mo 52 Moyer, B., 'Survey Methods for Fast and High-Energy Neutrons', Nucleonics 10(5) 14 (1952).

Mo 54 Moyer, B.J., 'Neutron Physics of Concern to the Biologist', Rad. Res. 1, 10 (1954).

Mo 57 Moyer, B.J., 'Build-Up Factors', Proc. Conference on Shielding of High-Energy Accelerators, New York, April 1957, USAEC Report TID-7545, p. 96 (1957).

Mo 79 Mole, R.H., 'RBE for Carcinogenesis by Fission Neutrons', Health Phys. 36, 463 (1979).

Na 69 Nagarajan, P.S., 'Neutron Dose Distributions in an Infinite Slab of Standard-Man Composition', Proc. Symp. on Radiation Protection Monitoring, Bombay, December 1968, pp. 61-78, IAEA, Vienna (1968).

Na 72 Nachtigall, D. and Burger, G., 'Dose Equivalent Determinations in Neutron Fields by Means of Moderator Techniques', Topics in Radiation Dosimetry, Supplement 1, Attix, R.H., Ed., p. 385, Academic Press, New York (1972).

Na 81 Nagarajan, P.S., Wittmann, A. and Burger, G.,'Fast Neutron Organ Dose Calculations Using a MIRD Phantom', Proc. Fourth Symposium on Neutron Dosimetry, Munich-Neuherberg, Germany, June 2-5, 1981, Vol. 1, p. 49, Commission of the European Community, Luxembourg, EUR 7448-EN (1985).

NCRP 57 National Council on Radiation Protection and Measurements, 'Protection against Neutron Radiation up to 30 Million Electron Volts', National Bureau of Standards Handbook 63, U.S. Dept. of Commerce, Washington, D.C. (1957).

NCRP 71 National Council on Radiation Protection and Measurements, 'Protection Against Neutron Radiation', NCRP Report 38, Washington, D.C. (1971).

NCRP 82 National Council on Radiation Protection and Measurements, 'Critical Issues in Setting Radiation Dose Limits', Proc. of the Seventh Annual Meeting of the NRCP, 8-9 April 1981, NCRP, Washington, D.C. (1982).

Ne 66 Neufeld, J., Snyder, W.S., Turner, J.E. and Wright, H., 'Calculation of Radiation Dose from Protons and Neutrons to 400 MeV', Health Phys. 12, 227 (1966).

Ne 76 Nelson, W.R., 'Accelerator Beam Dosimetry', IEEE Trans. Nucl. Sci. NS23, No. 4, p. 1376 (1976).

Ng 85 Nguyen, V.D., Luccioni, C. and Parmentier, N., 'Average Quality Factor and Dose Equivalent Meter Based on Microdosimetry Technique', Radiat. Prot. Dosim. 10 (1-4), 277 (1985).

OB 68 O'Brien, K. and McLaughlin, J.E., 'The Propagation of the Neutron Component of the Nucleonic Cascade at Energies Less Than 500 MeV: Theory and a Solution to the Accelerator Transverse Shielding Problems', Nucl. Instrum. Meth. 60, 129 (1968).

OB 71 O'Brien, K., 'Neutron Spectra in the Sideshielding of a Large Particle Accelerator', Health and Safety Laboratory Report, USAEC, New York, HASL-240 (Washington, D.C., USNRC) (1971).

Pa 57 Patterson, H.W., 'The University of California Radiation Laboratory Synchrocyclotron', in Proc. Conf. on Shielding of High-Energy Accelerators, New York, April 1957, USAEC Report TID-7545, p. 3 (1957).

Pa 59 Patterson, H.W., Hess, W.N., Moyer, B.J. and Wallace, R.W., 'The Flux and Spectrum of Cosmic-Ray Produced Neutrons as a Function of Altitude', Health Phys. 2, 69 (1959).

Pa 65 Patterson, H.W., 'Accelerator Radiation Monitoring and Shielding at the Lawrence Radiation Laboratory, Berkeley', in Proceedings of First Symposium on Accelerator Dosimetry, Brookhaven, Nov. 1965, USAEC Report CONF-651109, p. 3 (1965).

Pa 69 Patterson, H.W., Heckman, H. and Routti, J.T., 'New Measurement of Star Production in Nuclear Emulsions and Applications to High-Energy Neutron Spectroscopy', Proc. Second Conf. on Accelerator Dosimetry and Experience, Stanford, California, Nov. 1969, USAEC Report CONF-691101, p. 750 (1969).

Pa 71 Patterson, H.W., Routti, J.T., and Thomas, R.H., 'What Quality Factor?', Health Phys. 20, 517 (1971).

Pa 73 Patterson, H.W. and Thomas, R.H., 'Accelerator Health Physics, Academic Press (New York) (1973).

Pe 66 Perry, D.R., 'Neutron Dosimetry Methods and Experience on the 7 GeV Proton Synchrotron Nimrod', Proc. IAEA Symp. on Neutron Monitoring for Radiation Protection, p. 355, IAEA, Vienna (1966).

Pe 68 Penfold, J. and Stevenson, G.R., 'Preliminary Measurements of the Angular Distribution of the Stray Radiation Field', Rutherford Laboratory Internal Report RP/PN/29 (1968).

Pe 80 Perez-Mendez, V., 'Detectors for Radiation Dosimetry' in Advances in Radiation Protection and Dosimetry in Medicine, Edited by R.H. Thomas and V. Perez-Mendez, Plenum Press, New York, p. 143 (1980).

Ps 69 Pszona, S., 'A New Approach for Determining Quality Factor and Dose Equivalent in Mixed Radiation Fields', Health Phys. 16, 9 (1969).

Ps 71 Pszona, S., 'The NE 102A Organic Scintillation Detector as an Acceptable LET Dependent Detector for Quality Factor and Dose Equivalent Determination in Mixed Radiation Fields', International Congress on Protection Against Accelerator and Space Radiation, CERN Internal Report 71-16, Vol. 1, p. 388 (1971).

Ps 77 Pszona, S. and Höfert, M., 'A Rapid Method for the Determination of Dose Equivalent in Mixed Radiation Fields', Nucl. Instr. and Meth. 146, 509-512 (1977).

Ra 69 Raju, M.R., Lyman, J.T., Brustad, T. and Tobias, C.A., ' Heavy Charged-Particle Beams,' Chap. 20, in Radiation Dosimetry, Vol. III (F.H. Attix and E. Tochilin, eds.), p. 151, Academic Press (New York) (1969).

Re 65 Remy, R., 'Neutron Spectroscopy by the Use of Nuclear Stars from 20-300 MeV', M.S. Thesis, Dept. of Nuclear Engineering, University of California Berkeley, Lawrence Berkeley Laboratory Report UCRL-16325 (1965).

Ri 68 Rindi, A., 'Evaluation of Fluxes and Dose Equivalent Rates in Neutron Fields Around High-Energy Accelerators', Lawrence Berkeley Laboratory Report UCRL-18424 (1968).

Ri 69 Rindi, A., 'Present and Projected Uses of Multiwire Spark Chambers in Health Physics', in Proc. Second International Symposium on Accelerator Dosimetry, Stanford, Nov. 1969, USAEC Report CONF-691101, p. 660 (1969).

Ri 71 Rindi, A. and Thomas, R.H., 'Absorbed Dose—An Unfortunate Red Herring in Radiation Protection', in Proc. 6th Annual Health Physics Society Mid-Year Topical Symposium, Richland, Washington, Nov. 1971, Columbia Chapter, Health Physics Society, Richland, Washington (1971).

Ri 72 Rindi, A. and Thomas, R.H., 'Povera e Nuda Vai, Dosimetria', Health Phys. 23, 715 (1972).

Ri 74 Rindi, A., 'A Spectrometer for Measuring Charged Particles and Neutrons', Nucl. Inst. and Meth. 116, 471 (1974).

Ro 55 Rossi, H.H. and Rosenzweig, W., 'A Device for the Measurement of Dose as a Function of Specific Ionization', Radiology 64, 404 (1955).

Ro 56 Rossi, H.H. and Failla, G., 'Tissue Equivalent Ionization Chambers', Nucleonics 14(2), 32 (1956).

Ro 69 Routti, J.T., 'Mathematical Considerations of Determining Neutron Spectra from Activation Measurements', Proc. 2nd Inter. Conference on Accelerator Dosimetry and Experience', Stanford, CA, CONF-691101, p. 494 (1969).

Ro 77 Rossi, H.H., 'A Proposal for the Revision of Quality Factor', J. Envir. Biophys. 14, 275 (1977).

Ro 78a Rossi, H.H. and Mays, C.W., 'Leukemia Risk from Neutrons', Health Phys.34, 353 (1978).

Ro 78b Rogers, D.W.O., Letter to the Editor: 'Conversion of Neutron/cm^2 to rem,' Health Phys. 34, 395 (1978).

Ro 79 Rogers, D.W.O. 'Why Not to Trust a Neutron Remmeter,' Health Physics 37, 735 (1979).

Ro 80 Routti, J.T. and Sandberg, J.V., 'Unfolding Techniques in Activation Detector Analysis', Lecture No. 24 in Computer Techniques in Radiation Transport and Dosimetry, Eds., Nelson, W.R. and Jenkins, T.M., Plenum Press, New York and London (1980).

Ro 85 Routti, J.T. and Sanberg, J.V., 'Unfolding Activation and Multiphere Detector Data, Rad. Prot. Dosimetry 10(1-4), 103 (1985).

Sc 79a Schönbacher, H. and Stolarz-Iżycka, A., 'Compilation of Radiation Damage Test Data, Part I: Cable Insulating Materials, CERN Internal Report CERN 79-04 (1979).

Sc 79b Schönbacher, H. and Stolarz-Iżycka, A., 'Compilation of Radiation Damage Test Data, Part II: Thermosetting and Thermoplastic Resins', CERN Internal Report CERN 79-08 (1979).

Sh 51 Sharpe, J. and Stafford, G.H., 'The $^{12}C(n,2n)^{11}C$ Reaction in an Anthracene Crystal', Proc. Phys. Soc. (London) A64, 211 (1951).

Sh 62 Shaw, K.B., 'High-Energy Flux Measurements Using Plastic Scintillators', CERN Internal Report DI/HP/6 (1962).

Sh 68 Shaw, K.B., Stevenson, G.R. and Thomas, R.H., 'Evaluation of Dose Equivalent from Neutron Energy Spectra', Rutherford Laboratory Report RPP/R5 (1968).

Sh 69 Shaw, K.B., Stevenson, G.R. and Thomas, R.H., 'Evaluation of Dose Equivalent from Neutron Energy Spectra', Health Phys. 17, 459 (1969).

Sh 70 Shave, A.J., 'The Extraction of Terbium from Mercury by a Chemical Method', Rutherford Laboratory Internal Report RP/PN/43 (1970).

Sh 83 Shiue, Y-L. and Chilton, A.B., 'Calculation of Low-Energy Neutron Dose Indices and Depth Doses in the ICRU Tissue Sphere', Rad. Res. 93, 421 (1983).

Si 64 Simpson, P.W., 'The Measurement of Accelerator-Produced Neutron Flux by Activation of Indium, Gold and Cobalt', Rutherford Laboratory Report NIRL/M/70 (1964).

Si 83 Sims, C.S. and Killough, G.C. 'Neutron Fluence to Dose-Equivalent Conversion Factors: A Comparison of Data Sets and Interpolation Methods', Radiation Protection Dosimetry 5(1), 45 (1983).

Sm 58 Smith. A.R., 'The Stray Radiation field of the Bevatron', Lawrence Berkeley Report UCRL-8377 (1958).

Sm 61 Smith, A.R., 'A Cobalt Neutron Flux Integrator', Health Phys. 7, 40 (1961).

Sm 62 Smith, A.R., 'The Measurement of the Radiation-Field Around High-Energy Accelerators', in Proceedings of the First International Conference on Shielding Around High-Energy Accelerators, Paris 1962, Press Universitaires de France (Paris), p. 137 (1962).

Sm 65 Smith, A.R., 'Threshold Detector Applications to Neutron Spectroscopy at the Berkeley Accelerators', Proc. First Symposium on Accelerator Radiation Dosimetry and Experience, USAEC Report CONF. 651109, p. 224 (1965).

Sm 66 Smith, A.R., 'A Tantalum Fast Neutron Integrator', Lawrence Berkeley Laboratory Internal Report UCRL-17051 (1966).

Sm 76 Smith, A.R. and Thomas, R.H., 'The Production of ^{11}C by the Interaction of 376-MeV/amu Ne^{10+} Ions with Carbon', Nucl. Instr. Methods 137, 459 (1976).

Sm 81 Smith, A.R., Schimmerling, W., Kanstein, L.L., McCaslin, J.B. and Thomas, R.H., 'Neutron Flux Density and Secondary Particle Spectra at the 184-Inch Synchrocyclotron Medical Facility', Medical Physics 8, 668 (1981).

Sm 83 Smith, A.R., McCaslin, J.B., Geaga, J.V., Hill, J.C. and Vary, J.P., 'Cross Sections for the Production of ^{11}C in C Targets by ^{12}C at Relativistic Energies', Phys. Rev. 28, 1641 (1983).

Sn 50 Snyder, W.S., 'Calculations for Maximum Permissible Exposure to Thermal Neutrons', Nucleonics 6(2), 46 (1950).

Sn 67 Snyder, W.S., 'Depth Dose, in Protection Against Neutron Radiation up to 30 Million Electron Volts', NCRP Report 20, p. 39, National Council on Radiation Protection and Measurements, Washington, D.C. (1957). (Reprinted with corrections, April 1967.)

Sn 71 Snyder, W.S., 'Dose Distribution in a Cylindrical Phantom for Neutron Energies Up to 14 MeV', op. cit. NCRP 71, p. 46.

St 58 Stephens, L.D. and Smith, A.R., 'Fast Neutron Surveys Using Indium Foil Activation', Lawrence Berkeley Laboratory Report UCRL-8418 (1958).

St 67 Stevenson, G.R., 'Neutron Spectrometry from 0.025 eV to 25 GeV', Rutherford Laboratory Report RHEL/R 154 (1967).

St 71a Stapleton, G.B. and Thomas, R.H., 'The Production of ^{7}Be by 7-GeV Proton Interactions with Oxygen', Nucl. Phys. A 125, 124 (1971).

St 71b Stevenson, G.R., 'Evaluation of Neutron Dose Equivalent Around Nimrod', Rutherford Laboratory Internal Report RP/PN/56 (1971).

St 73a Stevenson, G.R., Höfert, M., Neufeld, J., Rindi, A., Routti, J.T. and Prêtre, S., 'Standardising the Fluence to Dose Equivalent Conversion Factors for Whole-Body Neutron Exposure in Neutron Monitoring for Radiation Protection Purposes', Vol. 1, p. 177, IAEA (Vienna) (1973).

St 73b Stevenson, G.R., Discussion in op. cit. Ref. St 73a p. 185 (1973).

St 73c Stephens, L.D., 'The Polyethylene-Lined Proportional Counter, Experiment in No. 4 in Laboratory Manual, Accelerator Health Physics, by H.W. Patterson and R.H. Thomas, p. 601, Academic Press, New York (1973).

St 84 Stevenson, G.R., 'The Estimation of Dose Equivalent from the Activation of Plastic Scintillators', Health Phys. 47, 837 (1984).

Su 63 Sullivan, A.H. and Baarli, J., 'An Ionization Chamber for the Estimation of the Biological Effectiveness of Radiation', CERN Report CERN 63-17 (1963).

Su 64 Sullivan, A.H., 'An Approach to a Rem Dosimeter Using Ionization Chambers', CERN Internal Report DI/HP/29 (1964).

Su 69 Sullivan, A.H., 'The Present Status of Instrumentation for Accelerator Health Physics', Proceedings of Second Accelerator Conference on Dosimetry and Experience, Stanford, Nov. 1969, USAEC Report CONF-691101, p. 625 (1969).

Su 84 Sullivan, A.H., 'The Use of Detectors Based on Ionisation Recombination in Radiation Protection', Paper presented at the Workshop for Practical Implementation of Microdosimeter Counters in Radiation Protection, 15-17 May 1984, Homburg/Saar, Radiat. Prot. Dosim. 9, 123 (1984).

Te 70 Tesch, K., 'Neutron Dosimetry in the Energy Range Between 10 and 100 MeV', Nucl. Inst. and Meths. 83, 295-299 (1970).

Th 73 Thomas, R.H., 'Neutron Dosimetry at High-Energy Particle Accelerators', in Neutron Monitoring for Radiation Protection Purposes, IAEA Vienna, p. 327 (1973).

Th 80a Thomas, R.H. and Perez-Mendez, V. (eds), 'Advances in Radiation Protection and Dosimetry in Medicine', Proceedings of the Third Course of the International School of Radiation Damage and Protection, Erice, September 1979, Plenum Press, New York (1980).

Th 80b Thomas, R.H., 'Passive Detectors', in Advances in Radiation Protection and Dosimetry in Medicine, (Eds. R.H. Thomas and V. Perez-Mendez), Proceedings of the Third Course of the International School of Radiation Damage and Protection, Erice, Italy, Sept. 1979, p. 181, Plenum Press, New York, p. 181 (1980).

Th 85a Thomas, R.H., and Stevenson, G.R., 'Radiation Protection Around High-Energy Accelerators', Rad. Prot. Dos. 10, (No. 1-4), 283 (1985).

Th 85b Thomas, R., 'Dosimetric Aspects', in Some Important Issues in Developing Radiation Protection Issues, Proc. 1984 Annual Meeting of the National Council on Radiation Protection and Measurements, Washington, D.C., NCRP, Washington, D.C., p. 182 (1985).

Th 85c Thorngate, J.H. and Griffith, R.V., 'Neutron Spectrometers for Radiation Monitoring at Lawrence Livermore National Laboratory', Radiat. Prot. Dosim. 10 (1-4), 125 (1985).

To 71 Tobailem, J., 'Cross Sections for the Nuclear Reactions Induced by Protons, Deuterons, and Alpha Particles. I. Monitor Reactions', Centre d'Etudes Nucléaires de Saclay, 91190 Gif-sur-Yvette, France, CEA-N-1466(1) (in French) (1971).

Tu 64 Turner, J.E., Zerby, C.D., Woodyard, R.L., Wright, H.A., Kinney, W.E., Snyder, W.S. and Neufeld, J., 'Calculation of Radiation Dose from Protons to 400MeV', Health Phys. 10, 783 (1964).

USAEC 57 Conference on Shielding of High Energy Accelerators, New York, April 1957, USAEC Report TID-7545 (1957).

USAEC 65 Proceedings of the First Symposium on Accelerator Dosimetry and Experience, Brookhaven, November 1965, USAEC Report CONF-651109 (1965).

USAEC 67 Proceedings of the Symposium on the Biological Interpretation of Dose from Accelerator Produced Radiation, Berkeley, March

1967, USAEC Report CONF-670305 (1967).

USAEC 69 Proceedings of the Second Symposium on Accelerator Dosimetry and Experience, Stanford, November 1969, USAEC Report CONF-691101 (1969).

Wi 80 Wittmann, A. and Burger, G., 'Organ Doses and Effective Dose Equivalent for External Neutron Beams derived by the Chord Method', Gesellschaft für Strahlen und Umweltforschung m.b.H., München, Internal Report GSF-Berichts 708 (1980).

Wr 69 Wright, H.A., Anderson, V.E., Turner, J.E., Neufeld, J. and Snyder, W.S., 'Calculation of Radiation Dose Due to Protons and Neutrons with Energies from 0.4 to 2.4 GeV', Health Phys. 16, 13 (1969).

Ze 65 Zerby, C.D. and Kinney, W.L. 'Calculated Tissue Current-to-Dose Conversion Factors for Nucleons below 400 MeV', Nucl. Instr. Methods 36, 125 (1965).

Zi 62 Zielczynski, M., 'Use of Columnar Recombination for Determination of Relative Biological Efficiency of Radiation', Nukleonika 7, 175 (1962).

Zi 64 Zielczynski, M., 'Instrument for Determination of Recommended Relative Biological Effectiveness of Radiation', Instrum. Exp. Tech. USSR 6, 1217 (1964).

Zi 70 Zielczynski, M., 'Comments in Radiation Dosimetry', Proceedings of the International Summer School on Radiation Protection, CAVTAT, Sept. 1970, Vol. 2, p. 34 (1970).

Table 3.1
Fraction of dose equivalent due to neutrons below 20 MeV.

Accelerator	Energy (GeV)	Beam particle	% of neutron dose equivalent less than 20 MeV	Reference
Bevatron				
Lateral shield	6.2	p^+	48	Gi 68
Above septum	6.2	p^+	35	McC 77
Nimrod	7	p^+	85	Pe 66
SLAC				
Experimental Area	19.5	e^-	32	McC 77
CERN				
Earth Shield	24	p^+	22	Gi 68
PS Bridge	24	p^+	32	Gi 68

Table 3.2
Threshold detector techniques.

Reaction	Sample material	Threshold (MeV)
^{32}S-^{32}P	Sulphur powder or pellets	3
^{27}Al-^{27}Mg	Aluminum discs or pellets	3
^{27}Al-^{24}Na	Aluminum discs or pellets	6
^{27}Al-^{22}Na	Aluminum discs or pellets	35
^{27}Al-^{18}F	Aluminum discs or pellets	35
^{19}F-^{18}F	Teflon cylinders	12
^{12}C-^{11}C	Polyethylene cylinders or plastic scintillators	20
^{12}C-^{7}Be	Polyethylene cylinders or plastic scintillators	35
Bi-fission	Fission Chamber	50

Table 3.3
Activation threshold detectors (after Holt, Ho 85).

Reactions	Half-life of product	Energy of γ ray (MeV)	Approximate threshold energy (MeV)
$^{7}Li(n,\alpha n')^{3}H$	12.3 a	0.019 (β)	3.8
$^{12}C(n,2n)^{11}C$	20.3 min	0.51	20
$^{12}C(n,spall)^{7}Be$	53.6 d	0.48	30
$^{19}F(n,2n)^{18}F$	109.7 min	0.51	13.1
$^{24}Mg(n,p)^{24}Na$	15.0 h	1.37,2.75	7.5
$^{27}Al(n,p)^{27}Mg$	9.5 min	0.84,1.01	3.8
$^{27}Al(n,\alpha)^{24}Na$	15.0 h	1.37,2.75	4.9
$^{27}Al(n,spall)^{22}Na$	262 a	0.51,1.28	25
$^{32}S(n,p)^{32}P$	14.3 d	1.71 (β)	3.3
$^{46}Ti(n,p)^{46}Sc$	83.9 d	0.89,1.12	2.9
$^{47}Ti(n,p)^{47}Sc$	3.43 d	0.16	2.4
$^{48}Ti(n,p)^{48}Sc$	1.83 d	0.98,1.13	7.1
$^{50}Cr(n,2n)^{49}Cr$	41.9 min	0.15	13.5
$^{52}Cr(n,2n)^{51}Cr$	27.7 d	0.32	12.4
$^{54}Fe(n,p)^{54}Mn$	303 d	0.84	2.2
$^{54}Fe(n,2n)^{53}Fe$	8.53 min	0.38	13.9
$^{56}Fe(n,p)^{56}Mn$	2.58 h	0.85	5.0
$^{58}Ni(n,p)^{58}Co$	71.3 d	0.51,0.81	1.3
$^{58}Ni(n,2n)^{57}Ni$	36.0 h	0.51,1.37	12.6
$^{59}Co(n,\alpha)^{56}Mn$	2.58 h	0.85	5.2
$^{59}Co(n,2n)^{58}Co$	71.3 d	0.51,0.81	10.3
$^{63}Cu(n,2n)^{62}Cu$	9.76 min	0.51,1.17	11.3
$^{64}Zn(n,p)^{64}Cu$	12.8 h	0.51,1.35	2.0
$^{65}Cu(n,p)^{65}Ni$	2.56 h	1.12	3.2
$^{65}Cu(n,2n)^{64}Cu$	12.7 h	1.35,0.51, 1.35	10.3
$^{90}Zr(n,2n)^{89}Zr^{g+m}$	78 h	0.91	12
$^{93}Nb(n,n')^{93}Nb^{m}$	13.6 a	0.019,0.017	0.03
$^{93}Nb(n,2n)^{92}Nb^{m}$	10.2 d	0.93	9
$^{103}Rh(n,n')^{103}Rh^{m}$	56.1 min	0.02	0.6

$^{115}In(n,n')^{103}Rh^{m}$	4.5 h	0.34	1.5
$^{127}I(n,2n)^{126}I$	12.8 d	0.39,0.67	9.3
$^{197}Au(n,2n)^{196}Au$	6.2 d	0.36	8.6
$^{197}Au(n,4n)^{194}Au$	39.5 h	0.33	24
$^{197}Au(n,spall)^{149}Tb$	4.1 h	0.17	600
$^{199}Hg(n,n')^{199}Hg^{m}$	42.6 m	0.16,0.37	0.53
$Hg(n,spall)^{149}Tb$	4.1 h	0.17	600
$^{209}Bi(n,f)$			50
$^{231}Pa(n,f)$			1.0
$^{232}Th(n,f)$			1.6
$^{236}U(n,f)$			
$^{237}Np(n,f)$			0.75
$^{238}U(n,f)$			

Table 3.4
Slow neutron detectors [after Holt (Ho 85)].

Reactions	Half-life of product	Energy of γ ray (MeV)	Resonance energy (eV)
$^{6}Li(n,\alpha)^{3}H$	12.3 a	0.019 (β)	
$^{23}Na(n,\gamma)^{24}Na$	15.0 h	1.37,2.75	2850
$^{55}Mn(n,\gamma)^{56}Mn$	2.58 h	0.85,1.81	337
$^{59}Co(n,\gamma)^{60}Co$	5.26 a	1.17,1.33	132
$^{63}Cu(n,\gamma)^{64}Cu$	12.8 h	0.51	580
$^{115}In(n,\gamma)^{116}In^{m}$	54 min	1.09,1.29	1.46
$^{181}Ta(n,\gamma)^{182}Ta$	115 d	1.12,1.22	4.3
$^{186}W(n,\gamma)^{187}W$	23.9 h	0.48,0.69	18.8
$^{197}Au(n,\gamma)^{198}Au$	2.70 d	0.41	4.9
$^{235}U(n,f)$			
$^{239}Pu(n,f)$			

Table 3.5
Activation reactions commonly used in the determination of thermal neutron flux densities.

Reaction	Decay products	Half-life	Detector	Sensitivity at saturation
$^{115}In(n,\gamma)^{116m}In$	β^- γ: 0.47 MeV (36%) 1.09 MeV (53%) 1.25 MeV (80%)	54 min	γ spectrometer β-particle detector	Four foils 7.6 × 15.2 cm total mass 46 g, have a sensitivity of 300 cpm/unit flux density.
$^{197}Au(n,\gamma)^{198}Au$	β^- γ: 0.42 MeV (95%)	64.8 h	β-particle detector (a) γ spectrometer (b)	(a) 2.54-cm diam foil, mass 0.5 g, has a sensitivity of 1.8 cpm/unit flux density (Typical G-M counter background: 10 cpm.) (b) 5.08-cm-diam foil, mass 2.0 g, has a sensitivity of 13.4 cpm/unit flux density. [NaI(Tl)] crystal background: 48 cpm].
$^{23}Na(n,\gamma)^{24}Na$	β^- γ: 1.37 MeV (100%)[a] 2.75 MeV (100%)	15 h	γ spectrometer	Used in form of Na_2CO_3 cylinder 4.5 cm diam × 2 cm high, mass 12 g Na. 3.0 cpm/unit flux.

Table 3.6
Important characteristics of various activation-detector techniques.

Detector	Reaction	Energy range (MeV)	Detector size	Response to unit flux	Background response
Sulphur	$^{32}S(n,p)^{32}P$	>3	1-in. diam 4 g disk	0.049 cpm	10 cpm
Plastic Scintillator	$^{12}C(n,2n)^{11}C$	>20	13 to 2700 g	88 cpm at 85% efficiency 1700 g scint	165 cpm 1700 g scint
Mercury	$Hg(spall)^{149}Tb$	>600	up to 500 g	0.03 cpm	0.1 cpm
Gold foils	$^{197}Au(spall)^{149}Tb$	>600	1-in. diam 0.5 g	2.7×10^{-6} cpm	0.1 cpm
Aluminum	$^{27}Al(n,\alpha)^{24}Na$	>6	16.9 to 6600 g	101 cpm 6600 g E_n = 14 MeV	111 cpm, 16.9 g 118 cpm, 6600 g NaI(Tl)
Aluminum	$^{27}Al(spall)^{22}Na$	>25	16.9 g	0.21 cpm	67 cpm NaI(Tl)
Plastic scintillator	$^{12}C(spall)^{7}Be$	>25	16.9g by 1 in. high	0.21 cpm	67 cpm Na(Tl)

Table 3.7
Ratio of the apparent dose equivalent read by the instrument to the actual dose equivalent produced by neutrons below 20 MeV for different accelerator spectra.[a]

Spectrum	Andersson-Braun counter	7-in. moderated indium
1/E	1.40	1.03
RT	1.54	0.32
PSB	1.37	0.74
BEV	1.38	0.76
X2	1.67	0.92
P1	1.14	1.25
PLA	1.10	1.18
CR	1.29	0.84
O'B	2.09	0.50

[a]For an explanation of the designations of the neutron spectra see Section 2.2.

Table 3.8
CERN and RL detector responses and dose-equivalent rates calculated for different spectra.[a]

Neutron spectrum	Detector responses			Dose-equivalent rates ($\mu Sv\ h^{-1}$)		
	Andersson-Braun counter ($counts\ s^{-1}$)	Φ_{IN} ($m^{-2}\ s^{-1}$)[b]	Φ_{C} ($m^{-2}\ s^{-1}$)[b]	CERN	RL	H_{10}
1/E	88.9	0.43	0.21	53	61	68
RT	20.1	0.28	0.70	142	138	143
PSB	11.9	0.43	0.26	69	69	67
BEV	15.5	0.57	0.27	82	78	81
X2	9.4	0.34	0.33	67	77	77
CR	18.4	0.80	0.08	74	54	66
P1	5.2	0.39	0.03	22	26	21
PLA	6.3	0.46	0.02	25	29	25
O'B	18.8	0.30	0.81	148	159	103

[a] Total fluence rate is normalized to $10^{6}\ m^{-2}.s^{-1}$.
[b] Value must be multiplied by 10^{0}.
For an explanation of the designations of the neutron spectra see Section 2.2.

Table 3.9
Ratio of apparent dose equivalent from neutrons E < 20 MeV to that from neutrons E ≥ 20 MeV.

Neutron spectrum	Ratio determined		True Ratio
	CERN	RL	
1/E	1.5	0.6	0.5
RT	1.0	0.1	0.4
PSB	1.6	0.5	0.8
BEV	2.1	0.7	0.9
X2	1.0	0.3	0.3
CR	8.8	3.0	4.1
P1	6.5	3.9	3.8
PLA	10.4	6.6	5.2
O'B	0.8	0.1	0.3

For an explanation of the designations of the neutron spectra see Section 2.2.

Table 3.10
Approximate dose equivalent determination methods for radiation surveys.

Technique	Description	References
Single Detectors		
1. Moderated thermal neutron detector only. Reading multiplied by a factor of 2-3	Typical detectors are: • Andersson-Braun rem counter which uses a BF_3 gas proportional counter and layered boron-loaded plastic moderator to shape response to fit the ICRP fluence to dose equivalent conversion curve, • Leake-type ^3He detector with spherical moderator, • Other moderated detectors which respond to flux density (the appropriate spectral flux to dose factor must be applied). • Suitably moderated indium, gold foils.	An 63a,b Le 68 St 58
2. Tissue-equivalent ion chamber. Reading multiplied by a factor of 5 to 10	This technique allows quick estimation of the upper limit of dose equivalent in unknown fields when a conservative value of quality factor was used.	Co 53
Two Detectors		
3. Scintillator method	A tissue-equivalent ion chamber is used in conjunction with an organic scintillator (response is dependent on LET) to estimate total dose equivalent in high-energy accelerator radiation fields.	Ps 71 Ps 77
4. Moderated thermal neutron detectors as shown above plus a high energy detector such as $^{12}C \rightarrow {}^{11}C$	The dose equivalent estimated from each of the detectors is added. Correction factors may be applied if prior spectral knowledge warrants doing so. Andersson-Braun or Leake rem-meter in conjunction with 18-in. spherical moderator.	McC 60 Gi 68 Te 70
More than Two Detectors		

5.	Method 4 with the addition of air and tissue-equivalent ionisation chambers	The addition of the ion chambers allows the dose equivalent contribution from gamma and charged particles to be included in the total dose equivalent determination. Dividing the total dose equivalent by the dose equivalent as determined from the tissue-equivalent ion chamber yields an 'effective quality factor' which may lend confidence to the validity of the measurement. (This is the Cerberus technique of Hofert, when a moderated BF_3 rem ion chamber is used).	Ho 72

Table 3.11
Major techniques for neutron spectrometry.

	Technique	Description	Principal use	References
1.	Threshold detectors	Active (e.g., Bi fission counter) and passive (e.g., $^{12}C(n,2n)^{11}C$) detectors may be used separately or combined along with an appropriate spectrum unfolding code. Low resolution technique but can be reliable for accelerator produced neutron spectra which is devoid of sharp structure. Activation detectors have the advantage of immunity to counting losses at high fluence rates.	High-energy mixed radiation fields.	Ro 69 Sm 65 Th 80b
2.	Nuclear Emulsion	1) Proton recoil spectrum measurements can give ±20% accuracy for 2-20 MeV neutrons for fluence of 10^7 cm^{-2} in 600μ emulsion. 2) Star prong production, 20-300 MeV. Both techniques yield reliable results; both are relatively insensitive, tedious, and time consuming, using techniques and equipment no longer in readiness at many laboratories.	High-energy mixed radiation fields.	Ak 63 Le 64b Pa 69 Re 65
3.	Spark chamber	Large array approximately 1m × 1m with alternating converters and spark counters, has anticoincidence shield for external charged particles. Track length and angle are measured and input to unfolding code. Useful range: 30 MeV at 15% efficiency to 300 MeV at 0.5% efficiency.	High-energy mixed radiation fields.	Li 73 Ma 74 Ri 69 Ri 74

4.	Multi-sphere	Hydrogenous spheres up to 18 in. diameter house thermal neutron detectors. Possibility of photon plus pile-up during high instantaneous fluence rates when LiI is used. This problem is lessened with ^{3}He detectors. Activation and track detectors may also be used. Response is from thermal to 50 MeV or higher. Response functions depend largely on calculation.	High energy mixed radiation fields.	Al 74 Al 76 Aw 66 Aw 85 Br 60 Na 72 St 67
5.	Proton-recoil telescope	Requires point source, lacks sensitivity required for personnel monitoring, high resolution method. Invaluable for research efforts.	High-energy radiation fields not in equilibrium.	Al 75 Al 79b Ma 73 Pe 68

Table 3.12
Comparison of calculated values of various dose-equivalent quantities in several typical accelerator neutron spectra.

Spectrum	H_m	H_s	H_p
RT	1.21	0.86	1.00
PSB	1.33	0.99	1.00
BEV	1.58	1.26	1.00
X2	1.23	0.96	1.00
P1	1.73	1.49	1.00
PLA	1.94	1.68	1.00
CR	1.73	1.53	1.00

For an explanation of the designation of the neutron spectra and the dose equivalent quantities H_m, H_s and H_p see Section 2.2.

Table 3.13
CERN 1975 dose-equivalent intercomparison data.

Radiation field	Detector system[a]					
	Cerberus		REM2		BNL	
	$\dot{H}$	Q	$\dot{H}$	Q	$\dot{H}$	Q
A. Muons important						
(a) Experimental area	17	1.7	14	2.1	17	1.7
(b) End stop	30	1.5	22	1.5	31	1.4
B. Intermediate and fast neutrons important						
(a) Labyrinth	230	3.4	150	3.4	220	4.5
(b) Normal shielding	320	6.1	220	7.5	240	4.2
(c) Linac area	450	8.6	330	9.7	350	7.6
C. High-energy cascade important						
(a) Lateral shield (1)	380	4.0	300	5.6	470	4.5
(b) Lateral shield (2)	180	4.6	120	5.1	220	4.6

[a] Dose-equivalent rates in $\mu Sv\ h^{-1}$.

Table 3.14
Simplified summary of Serpukhov dose equivalent intercomparison data.

	Method	Dose equivalent (nSv)	Q
A.	Muons dominate dose equivalent:		
	KM-1(^{103}Rh)	67 ± 6	1.1 ± 0.2
	KM-2(^{103}Rh)	66 ± 9	1.2 ± 0.2
	Cerberus	53 ± 3	1.0 ± 0.1
	LET spectrometer	65 ± 6	1.2 ± 0.1
B.	Intermediate and fast neutrons dominate dose equivalent:		
	KM-1 (SNMO-5)	390 ± 30	3.9 ± 0.3
	KM-1 (SNM-3)	210 ± 10	2.8 ± 0.3
	KM-2 (SNM-3)	190 ± 10	3.5 ± 0.4
	Cerberus	290 ± 20	6.1 ± 0.5
	Sukhona-2	180 ± 30	3.6 ± 0.2
	LET spectrometer	110 ± 10	2.0 ± 0.2
C.	Cascade particles dominate dose equivalent:		
	KM-1 (SNMO-5)	340 ± 20	3.2 ± 0.6
	KM-1 (SNM-3)	300 ± 20	3.0 ± 0.3
	KM-2 (SNM-3)	240 ± 20	3.4 ± 0.4
	Cerberus	270 ± 20	4.2 ± 0.3
	Sukhona-2	290 ± 30	4.2 ± 0.4
	LET spectrometer	200 ± 20	2.8 ± 0.3

FIGURE CAPTIONS

Figure 3.1. Excitation functions for the reactions $^{12}C \rightarrow ^{11}C$ induced by neutrons, pions and protons. The arithmetic mean of the positive and negative pions cross sections is shown as the pion curve [after Stevenson (St 84)].

Figure 3.2. Response functions for the high-energy neutron detectors used in the sixties and seventies by the LBL group.

Figure 3.3. Response functions for the high-energy neutron detectors used in the sixties and seventies by the LBL group.

Figure 3.4. Response of the REM/N neutron dose equivalent meter as a function of neutron energy measured by groups of AERE (O). PTB (×), and CERN (□) (see text for details).

Figure 3.5. Response function of 7 in. diameter paraffin wax moderated indium foil detector.

Figure 3.6. Response of the Andersson-Braun and 7 in. diameter moderated indium detectors in a 1/E spectrum, as a function of spectrum cut-off energy.

Figure 3.7. Response of Bonner spheres of various diameters as a function of neutron energy.

Figure 3.8. Comparison of the neutron fluence rate to dose equivalent rate conversion coefficients recommended by the ICRP in Publication 21 (solid line) and by the NCRP in Report 38 (open circles). Linearly interpolated values between NCRP 38 points are shown as a dashed line.

Figure 3.9. Dose-equivalent indexes per unit fluence for neutrons incident in a broad unidirectional parallel beam on the ICRU sphere.

Figure 3.10. Effective dose equivalent per unit fluence for neutrons incident in AP and PA geometry upon an anthropomorphic phantom.

Figure 3.11. Dose equivalent per unit fluence at depths of 0.07 mm and 10 mm on the principal axis of an ICRU sphere (broad unidirectional parallel beam).

Figure 3.12. Maximum dose equivalent per unit fluence for neutron incident on a 30 mm thick equivalent-tissue slab (broad unidirectional parallel beam).

Figure 3.13. Dose equivalent at a depth of 1 cm in tissue-equivalent material for monoenergetic protons and pions without the contribution from primary ionisation compared to the neutron data of Fig. 3.8; x = pions (Al 71), o = protons (Al 70, Ar 73, Ne 66, Tu 64, Wr 69, Ze 65), solid circles = neutrons (Al 70, Al 71, Dm 71 In 67, Na 69, NRCP 57, Ne 66, Wr 69, Ze 65) [after Stevenson (St 84)].

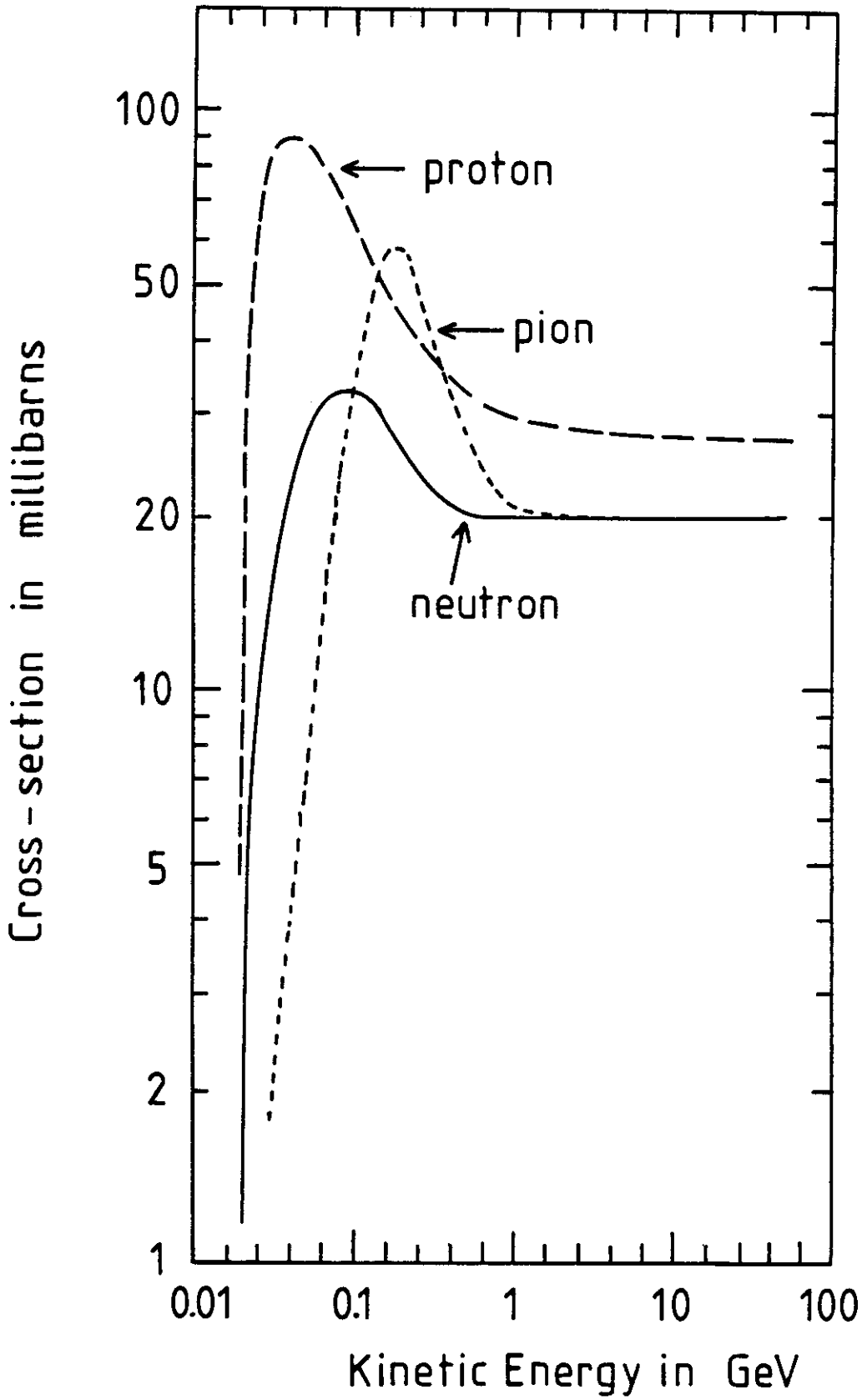
100
50
20
10
5
2
1
proton
pion
neutron
Cross-section in millibarns
0.01
0.1
1
10
100
Kinetic Energy in GeV

3.13 60

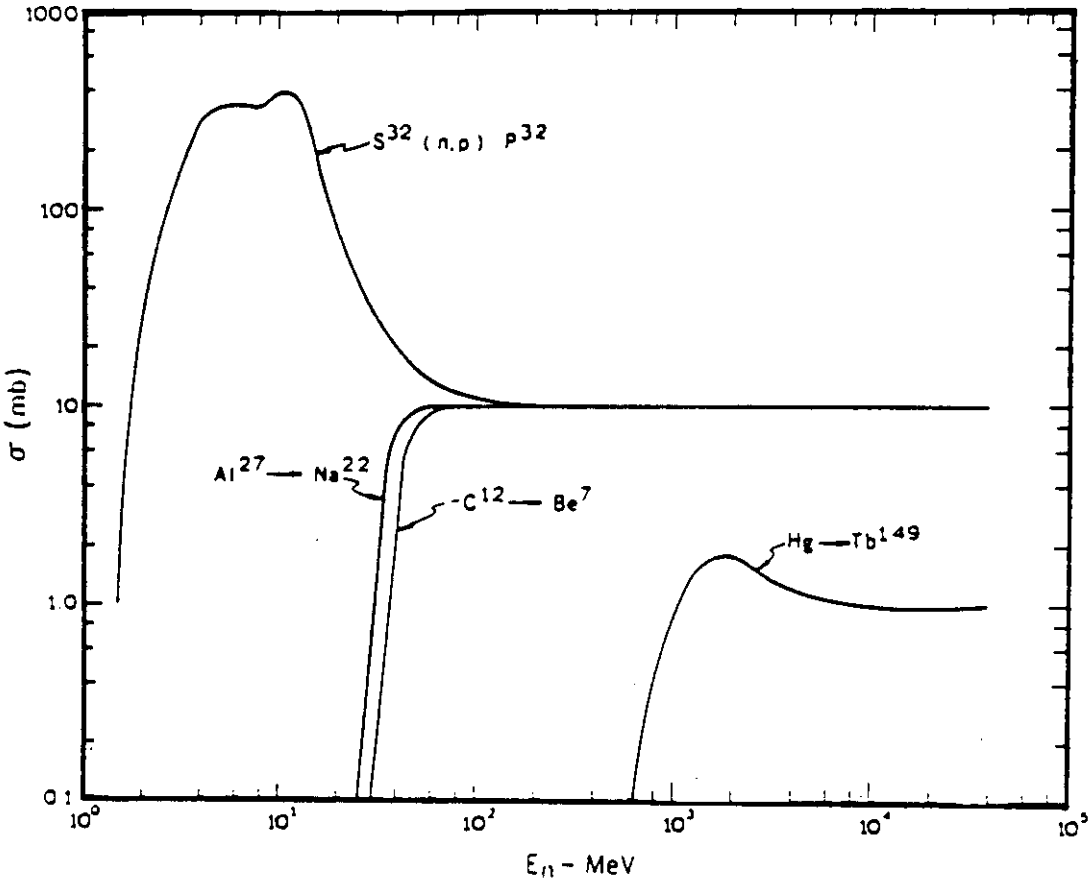

XBL 682 4492

3.2

3 61

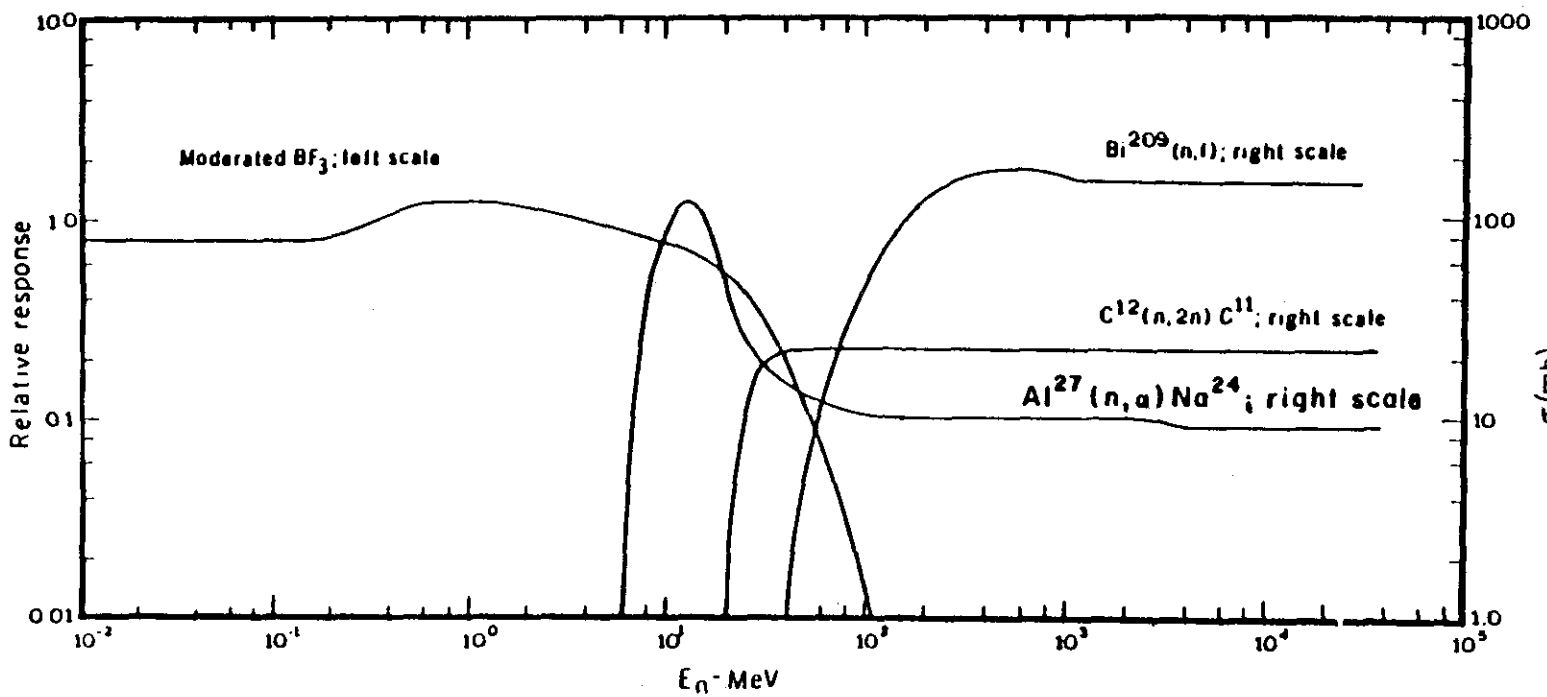

XBL 682 4491

3.3

3 G2

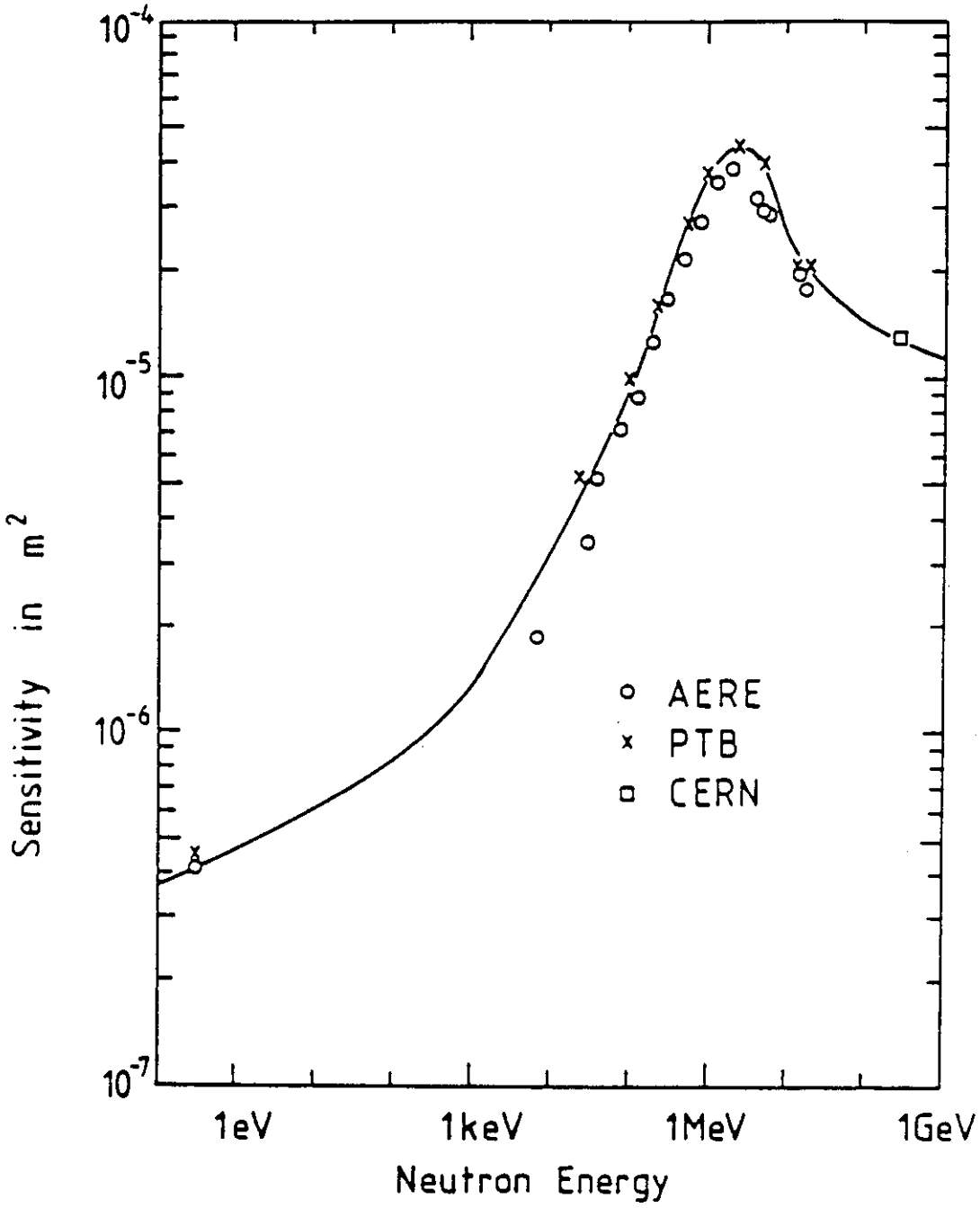

XBL 8412-5062

3.4

3 G3

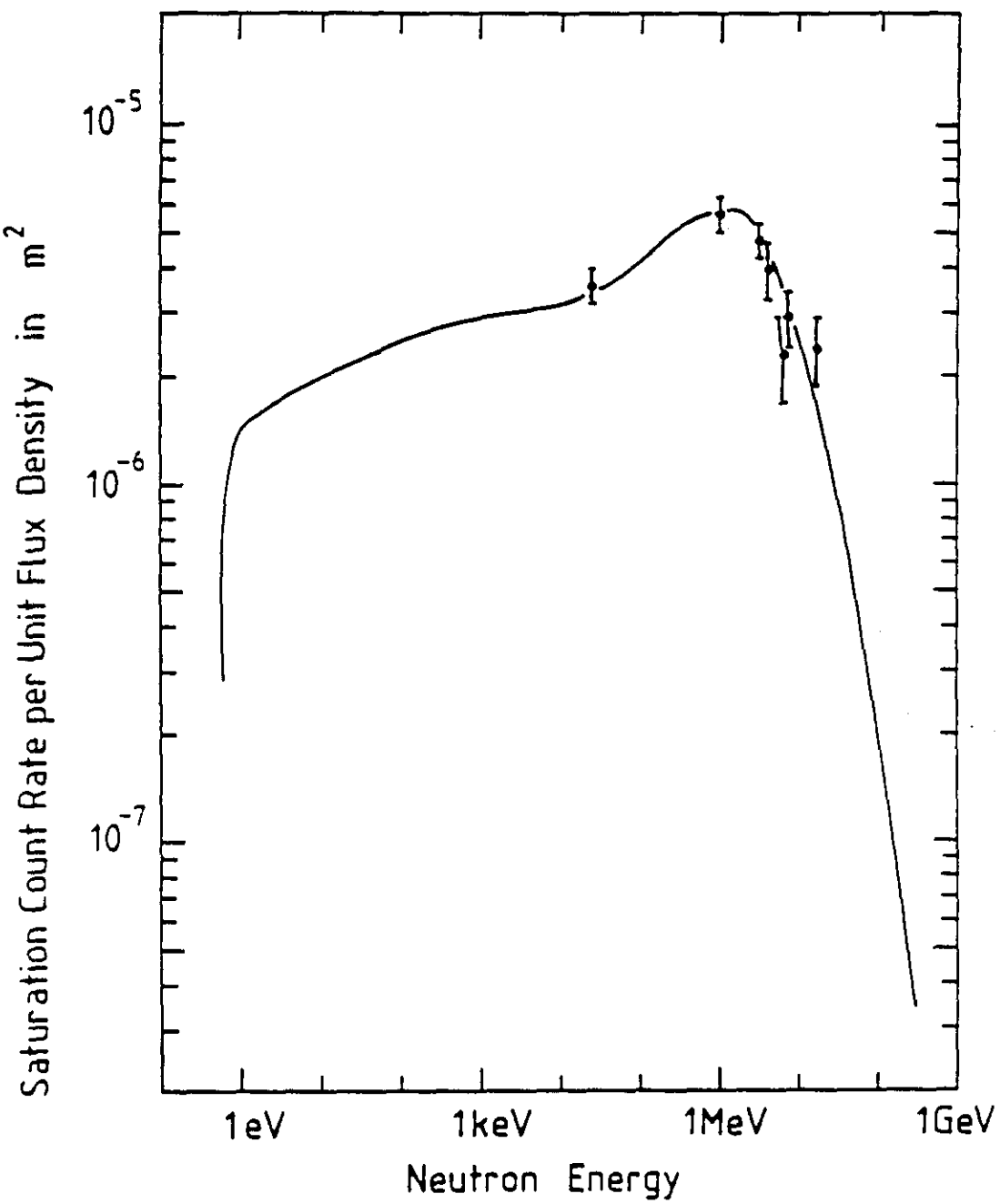

XBL 8412-5063

3.5

3 64

3.5

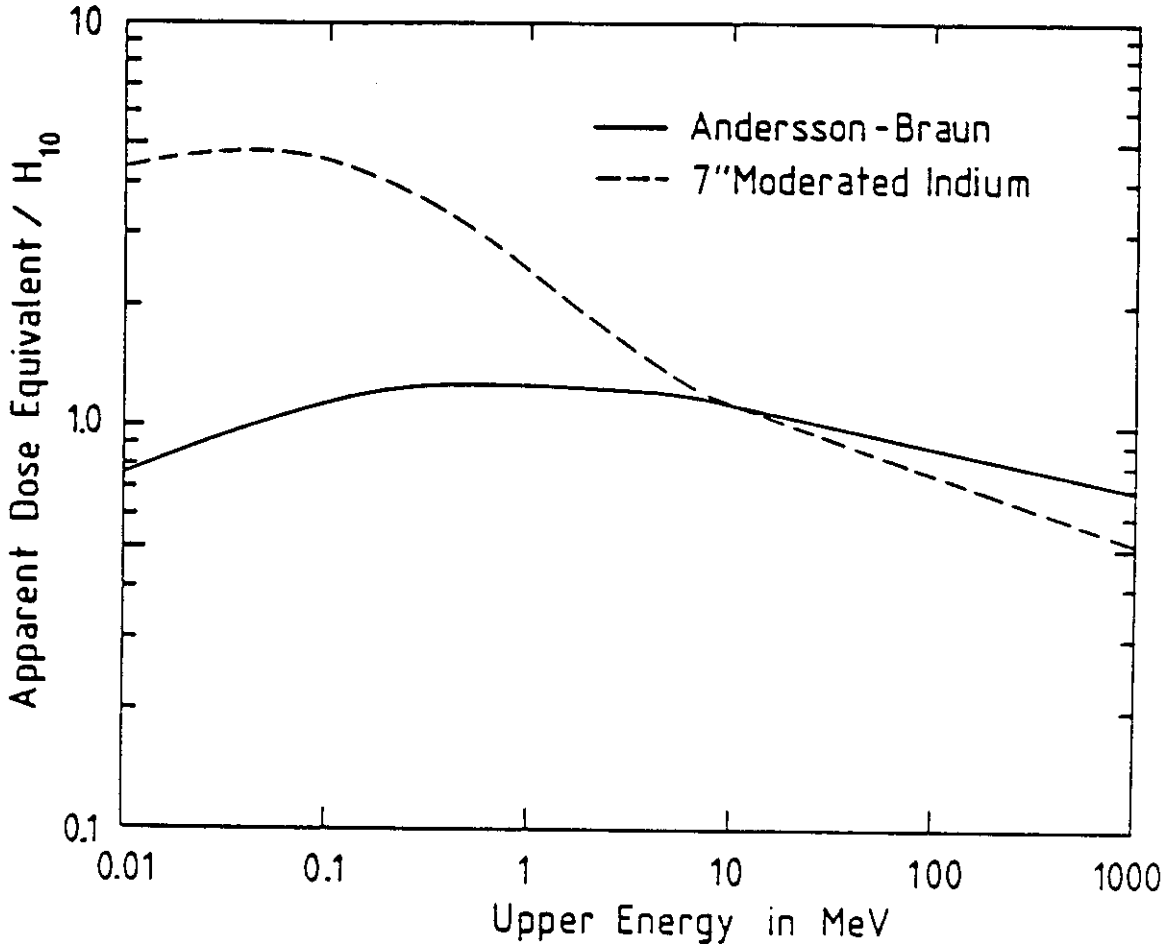

XBL 8412-5064

3.6

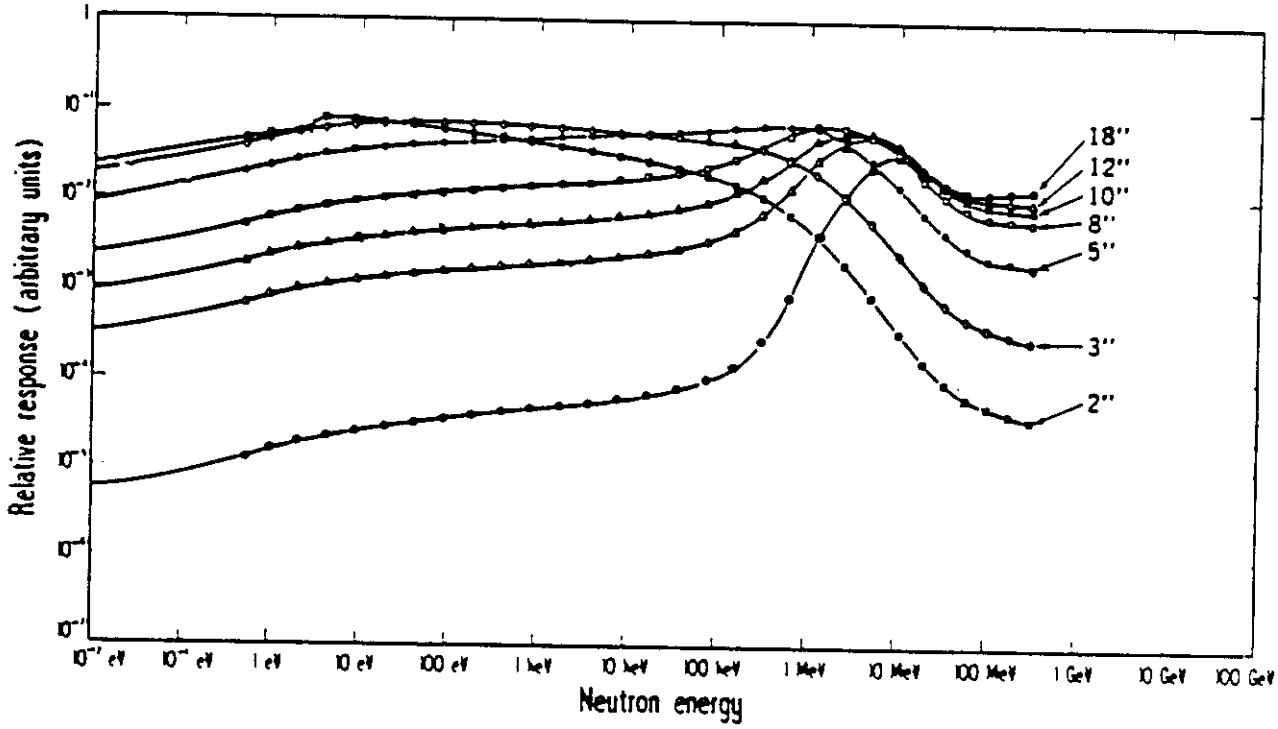

XBL 859-3784

3.7

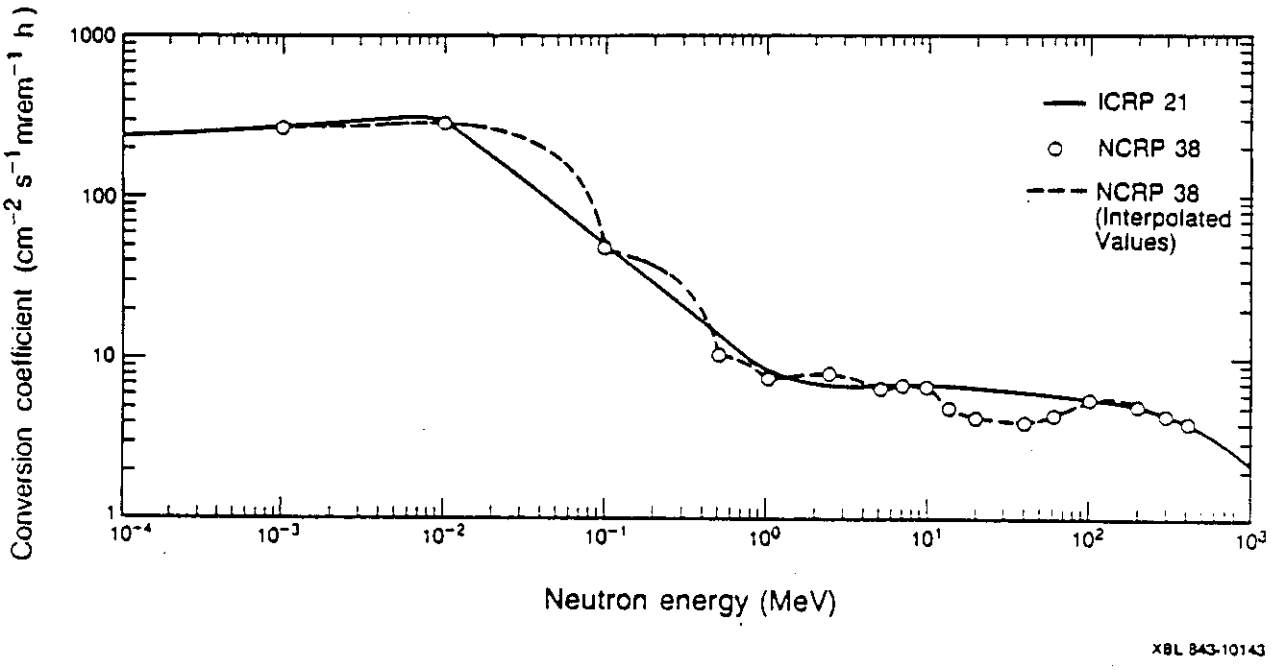
Conversion coefficient (cm^{-2} s^{-1} mrem^{-1} h)
1000
100
10
1
10^{-4}
10^{-3}
10^{-2}
10^{-1}
10^{0}
10^{1}
10^{2}
10^{3}
Neutron energy (MeV)
ICRP 21
NCRP 38
NCRP 38 (Interpolated Values)
XBL 843-10143

3.8

3 67

3.9

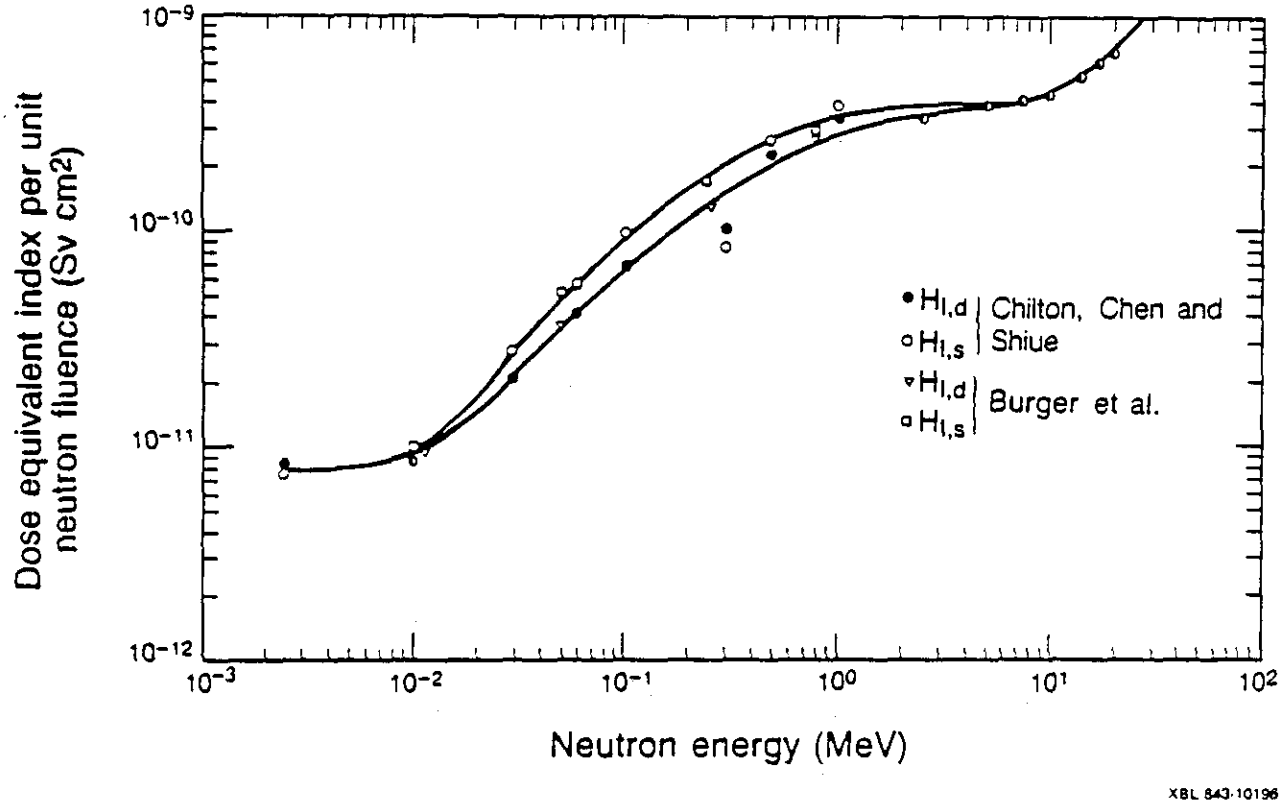
Dose equivalent index per unit neutron fluence (Sv cm²)
10⁻⁹
10⁻¹⁰
10⁻¹¹
10⁻¹²
10⁻³
10⁻²
10⁻¹
10⁰
10¹
10²
Neutron energy (MeV)
• H_I,d ○ H_I,s Chilton, Chen and Shiue
▿ H_I,d ▫ H_I,s Burger et al.
XBL 843-10196

3.9

3.

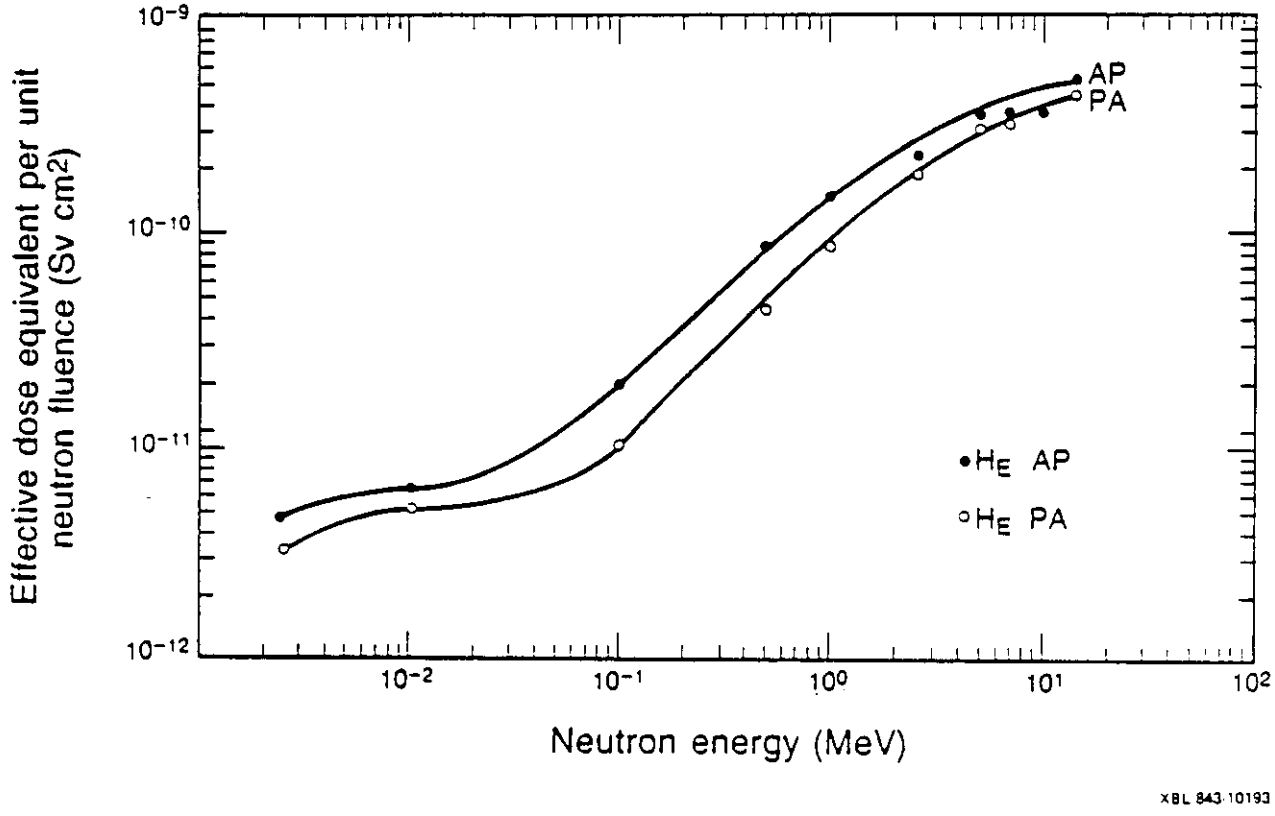
Effective dose equivalent per unit neutron fluence (Sv cm²)
10⁻⁹
10⁻¹⁰
10⁻¹¹
10⁻¹²
10⁻²
10⁻¹
10⁰
10¹
10²
Neutron energy (MeV)
AP
PA
•H_E AP
○H_E PA
XBL 843-10193

3.10

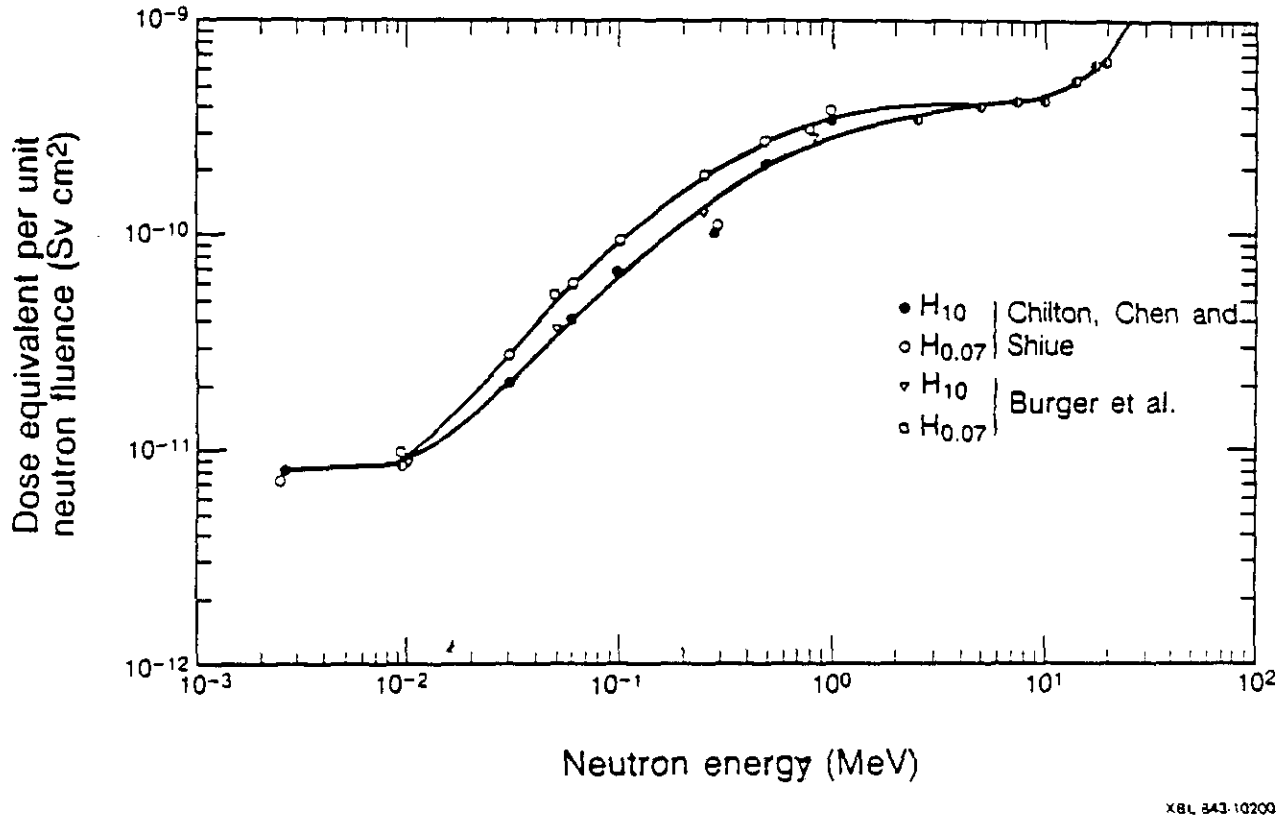
Dose equivalent per unit neutron fluence (Sv cm²)
10⁻⁹
10⁻¹⁰
10⁻¹¹
10⁻¹²
10⁻³
10⁻²
10⁻¹
10⁰
10¹
10²
Neutron energy (MeV)
• H10 | Chilton, Chen and
o H0.07 | Shiue
▿ H10 | Burger et al.
▫ H0.07
XBL 843-10200

3.11

3.1

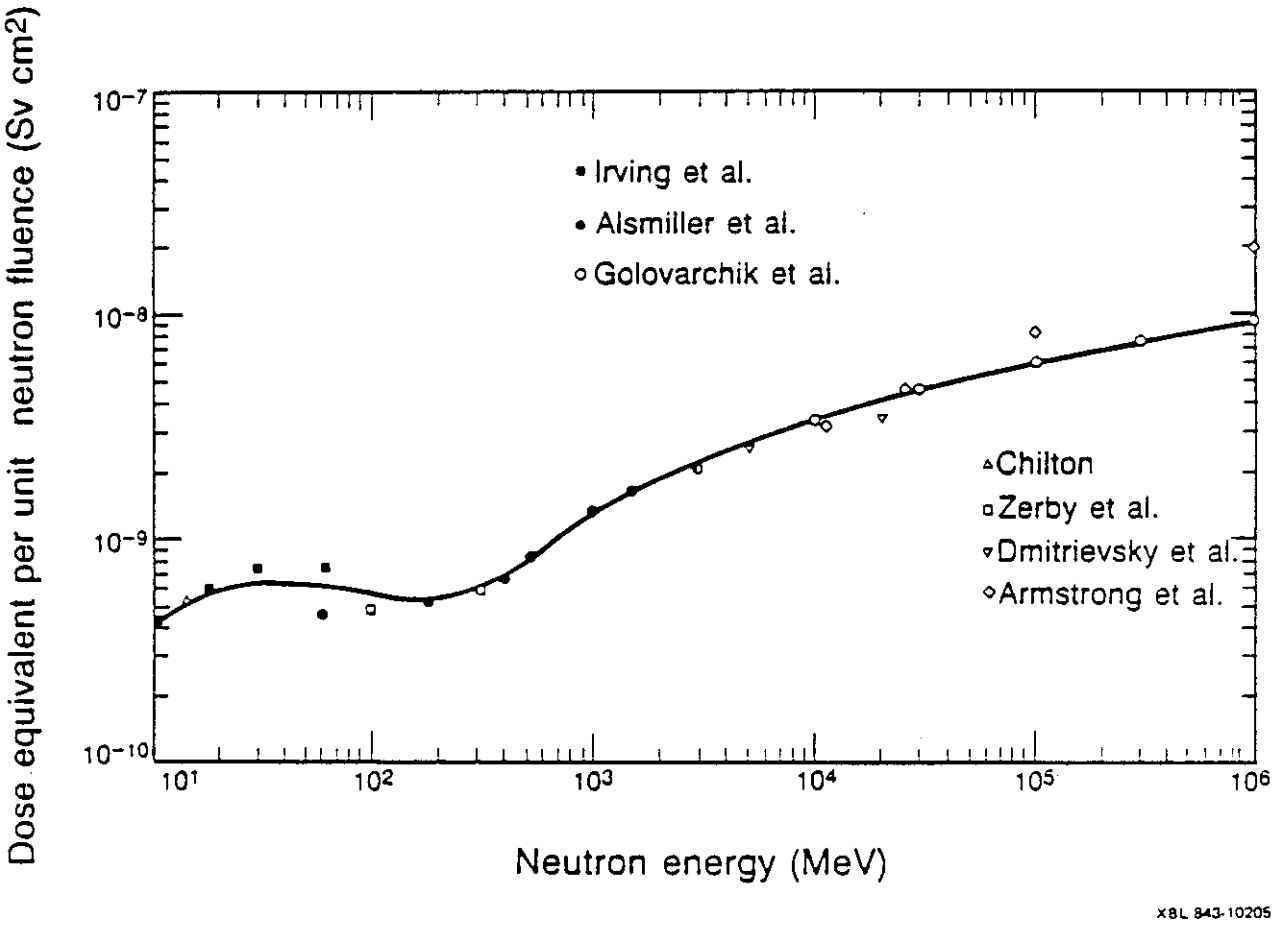
Dose equivalent per unit neutron fluence (Sv cm²)
10⁻⁷
10⁻⁸
10⁻⁹
10⁻¹⁰
10¹
10²
10³
10⁴
10⁵
10⁶
• Irving et al.
• Alsmiller et al.
○ Golovarchik et al.
△ Chilton
□ Zerby et al.
▽ Dmitrievsky et al.
◇ Armstrong et al.
Neutron energy (MeV)
X8L 843-10205

3.12

3 71

CHAPTER 4

Radiation Shielding

'Protection is not a principle, but an expedient'

Speech, House of Commons, 17 March 1845
Benjamin Disraeli, Earl of Beaconsfield (1804-1881)

CHAPTER 4 CONTENTS

4.1 Introduction

4.2 Shielding Criteria, Materials and Other Considerations

Shielding Criteria

Shielding Methods

Shielding Materials

4.3 The Shielding of Proton Accelerators at Energies between 50 MeV and 3 GeV

Introduction

Particle Yields from the Proton-Nucleus Interaction

The Transport of Monoenergetic Neutrons through Shielding

Shielding Calculations

4.4 The Shielding of Proton Accelerators at Energies Greater than 3 GeV

Introduction

The Design of Beam Stops (E > 3 GeV)

4.5 Ducts, Penetrations and Labyrinths

Introduction

Calculation of Radiation Transmission through Ducts and Labyrinths

Measurements of the Transmission of Straight Ducts

Measurements of Transmission in Labyrinths

Prediction of Transmission in Ducts and Labyrinths

Neutron Traps

Curved Tunnels

Appendix. Lateral Shielding Calculations—The Moyer Model

Historical Background

Generalised Formulation of the Moyer Model

The Variation of the Moyer Model Parameters with Energy

Point and Extended Source Calculations

Limitations of the Moyer Model

Conclusions

References for Chaper 4

Figure Captions for Chapter 4

4.1 INTRODUCTION

This chapter briefly discusses shielding criteria, the materials available for shielding and the factors determining the optimum choice. In addition the vast literature on the shielding of proton accelerators is reviewed. Because the number of papers is so large those discussed in detail here either deal with general techniques or contain data that may be incorporated as parameters in a generalized description used to specify shielding in simple geometries. The treatment of shielding in complex geometries or with several materials is not given here but reference is made to the literature in which techniques are given that are able to solve these problems.

In what follows it is important that the reader has an understanding of the basic physical processes involved in the interaction of ionizing radiations and particles with matter. These are concisely reviewed in Chapters 3 and 6 of 'Accelerator Health Physics' (Pa 73). These chapters also review the history of shielding studies at particle accelerators. For broader and more general discussions on radiation shielding the reader is referred to standard texts such as those by Price, Horton and Spinney (Pr 57), Chilton, Shultis and Faw (Ch 84), or the IAEA Engineering Compendium on Radiation Shielding (IAEA 68, 70, 75). [See also bibliography in Chapter 7.] Most of these texts primarily deal with radiation energies below about 20 MeV–much lower than the highest energies met with at particle accelerators. Nevertheless, they are relevant because, as we have seen in Chapters 2 and 3, much of the absorbed dose (and dose equivalent) from exposure to accelerator radiation environments is due to relatively low-energy radiations. The only text devoted entirely to particle accelerator shielding is by Zaitsev, Komochkov and Suchev (Za 71).

For convenience the treatment of shielding of proton accelerators is divided into two energy regions somewhat arbitrarily bounded at 3 GeV. The selection of this energy boundary may be justified by noting that below an energy of about 3 GeV the development of the hadronic cascade is relatively unimportant in determining the shield thickness.

A detailed discussion of the shielding of proton accelerators in a third energy region, below about 50 MeV, is not given here. The energy range below 100 MeV has been discussed in Report 51 of the National Council on Radiation Protection and Measurements (NCRP 77). This report gives Equilibrium Dose Equivalent Index tenth-value layers in concrete for neutrons of energy between 10^{-6} and 10^{2} MeV. NCRP Report 38 gives attenuation data for absorbed dose in a variety of materials (water, concrete, earth and polythene), for neutrons of energy 0.5, 1, 2, 3 and 5 MeV. Broad geometry is considered, but with angles of incidence to the shield varying between 0° to 70° (Al 63, NRCP 71). These data may be used in other geometries by the application of appropriate form-factors (Pa 73, Pr 57, Ro 56). For neutrons between 0.5 and 15 MeV the use of removal cross sections--an empirical approach to shielding developed for nuclear reactors–is applicable (Cl 71). For a discussion of the use of removal cross sections and details of measured values for fission neutrons see Chilton et al. (Ch 84). From an analysis of early shielding measurements made at accelerators Thomas has extended the concept of removal cross sections to 150 MeV (Mo 57, Pa 57, Pa 62a, Th 61).

For clarity it is important to define two terms that will frequently be used in connection with shielding in the discussions that follow. These are the 'longitudinal (or forward) direction' and the 'transverse (or lateral) direction'. The longitudinal direction is the direction along that of the incident proton beam, and the transverse direction is the direction orthogonal to the proton beam direction. Alternative terms sometimes used for the transverse direction will be the 'overhead' or 'sideways' directions.

The estimation of shielding for targets, both in the forward and lateral directions, and the design of beam-stops in which the entire accelerator beam may be dumped is first described for proton energies between 50 MeV and 3 GeV. Simple empirical formulae are developed for the calculation of shielding, with a discussion of the value of the parameters required and their variation with primary proton energy.

The subsequent section on shielding at proton energies greater than 3 GeV contains descriptions of the theoretical treatments that have been developed to describe the development of the extra-nuclear hadron cascade. Comparisons of these theoretical descriptions with experiment is made and guidance provided on the specification of shielding for extended and thin targets.

A limited discussion is given of muon shielding which becomes important at proton energies greater than 10 GeV and completely dominates the forward shielding requirements at very high energies.

Finally, the specific problems in the design of penetrations through a shield for access of personnel and the provision of services such as electrical power, air for ventilation and cooling water are briefly discussed.

An historical review of the development of an empirical approach to determining the lateral shielding required around targets bombarded by protons of energy greater than 3 GeV as an appendix to this chapter. Again the value and variation with primary proton energy of the parameters empirically derived is discussed. Comparison is made with values of these parameters derived from computer calculation of the hadron cascade.

4.2. SHIELDING CRITERIA, MATERIALS AND OTHER CONSIDERATIONS

SHIELDING CRITERIA

The goal of all efficient accelerator shielding designs is to attenuate the high radiation intensities produced by the accelerator and its associated equipment to levels that are acceptable outside the shielding, at minimum cost and without compromising the utility of the particle accelerator for its designed purposes. This is achieved in three stages:

- Determination of the source term.
- Specification of the required dose equivalent levels outside the shielding (dose equivalent limitations).

- Design of the shield with adequate attenuation to achieve the required dose equivalant limits, with sufficient flexibility to permit efficient accelerator operation, with readily available shielding materials and at optimum cost.

Determination of Source Term

The proton intensity to be utilised must be specified before any shield-design is attempted. In many cases this will be trivial–such as, for example, where a single proton beam utilises only one beam-stop. (Although even here it may be necessary to anticipate improved accelerator technology and an increasing beam intensity with time.) When multiple-beam operation is planned, either by developing several independent particle-beams or by diverting a single beam to several experimental areas, the specification of source-terms is more difficult. In the latter case it is prudent to assume that each target station must be built to receive the full proton intensity of the accelerator unless special beam-intensity interlocks can be provided as part of the safety system.

If it is assumed in the shield design that proton losses of less than full proton intensities can occur on beam splitters, extraction septa or at other loss points, then special interlocked monitors inside the shield or area radiation monitors outside the shield should be provided to maintain radiation intensities below the permitted maximum. Operational considerations may impose an upper limit to the source strength as, for example, when accelerator elements are destroyed or damaged when protons are incident at too high an intensity. In some cases such damage could be described as "catastrophic" as, for example, in the case of an accelerator using a superconducting magnet that is quenched due an an excessive power input during the beam loss, or in the case of the physical destruction of a target, or the piercing of the vacuum chamber where the time-averaging of proton intensities could take account of the time needed to repair the device. There are also "chronic" losses that will cause the degradation of magnet insulation by radiation damage and that will also cause down-time of the accelerator for necessary repairs.

It is worth-while reiterating that proton intensities and losses on which a shield design is based should be agreed upon by the laboratory management and any national or regional radiation control authority before shield specifications begin.

Dose Equivalent Limitation

The International Commission on Radiological Protection (ICRP) has recommended a system of dose limitation that has three interrelated components (ICRP 77):

- No practice shall be adopted unless its introduction produces a net benefit.
- All exposures shall be kept as low as reasonably achievable, economic and social factors being taken into account.
- The dose equivalent to individuals shall not exceed the limits recommended for the appropriate circumstances by the Commission.

These three components are often abbreviated by the terms:

- Justification
- Optimization of Radiation Protection
- Individual Dose Equivalent Limitation

Justification

The research worker may find the concept of justifying 'the practice' (i.e., his own research program) to be obscure. It is often taken to be a self-evident truth that scientific research will be of clear benefit to humanity. Nevertheless, when that research involves some possible detriment to health (as does work utilising ionizing radiations) and in an atmosphere of increasing public concern for nuclear installations, it may be necessary to present a reasonable argument justifying the construction and operation of particle accelerators to the surrounding community. In doing this the health physicist will often be assisted by the fact that research proposals of this magnitude are usually scrutinised by committees of the funding agency whether they be institutional or national in character. Nowadays expensive research, or even applied science, is rarely undertaken without a general consenus in the scientific community that beneficial results will follow.

The health physicist may find that while members of the community in which a particle accelerator is to be situated do not question the value of the research programme to be implemented, they do have concerns for the radiation exposures that may result. It is most important, therefore, that careful attention be given to clear explanation of the steps taken to optimize radiation protection.

Optimization of Radiation Protection

The optimization of radiation protection follows quite naturally from the Commission's recommendation that 'all radiation exposures shall be kept as low as readily achievable, economic and social factors being taken into account'. The significance of this recommendation is discussed in ICRP Publications 22 and 37 (ICRP 73a, 83). Publication 37, which discusses the use of cost-benefit analysis in radiation protection, will be particularly helpful. Because accelerator shielding is so massive (and therefore costly) optimization of shielding has long been practiced at accelerator laboratories as it has, for example, for nuclear reactors (Bu 70, Me 65, Th 76).

'A wide range of techniques is available to optimize radiation protection. Some of these techniques are drawn from operational research, some from economics and some from engineering. The techniques available include, but are not confined to, procedures based on cost-benefit analysis, although it is these procedures that have been discussed in detail in the ICRP report on optimization of protection (ICRP 83). It is important to recognize that other techniques, some quantitative, some more qualitative, may also be used in the optimization of radiation protection' (ICRP 84a).

Individual Dose Equivalent Limits

In the design of accelerator shielding we are usually concerned with limiting whole-body exposure to external ionizing radiations, but four different sets of dose limits must be used in minimizing exposure to:

- Radiation workers,
- Employees of the institution who are not radiation workers,
- Members of the general public,
- Scientific equipment and apparatus.

The ICRP has made recommendations of dose equivalent limits for both radiation workers and members of the general public. These are discussed in ICRP Publication 26 (ICRP 77) and in subsequent statements by the Commission (ICRP 80, 84b, 84c, 85). Because the detailed implementation of these recommendations and the philosophy behind them is rather sophisticated the reader is encouraged to study these ICRP reports carefully.

Radiation Workers and Nonradiation Workers. In the final analysis it is national or local regulations that prevail. An example of the detailed regulations and dose limits that apply at the Lawrence Berkeley Laboratory, which is regulated by the Department of Energy in the U.S.A., is given in Chapter 5. Other examples will be found in the radiation safety manuals listed in the Bibliography (Chapter 7). Because dose equivalent limits are frequently changed it is most important to review current regulations when accelerator installations are being planned.

The philosophy of the ICRP is that the primary dose equivalent limits applicable to radiation workers represent a ceiling that is rarely exceeded by individuals. Experience has shown that the implementation of programmes to maintain radiation levels as low and readily achievable produces in the irradiated population dose equivalents that are log-normally distributed. The average dose is almost an order of magnitude lower than the dose equivalent limit. It is not the intention of the ICRP that radiation workers should regularly be exposed to radiation levels at the limits. The simplest requirement of the ICRP for radiation workers is to maintain whole-body exposures below 50 mSv (5 rem) per year, but this would not be regarded as good practice: average exposures below 10 mSv (1 rem) should be aimed for, and in most cases can be achieved. This philosophy conforms with the design requirements of the American National Standards Institute (ANSI) that new accelerator installations should be designed with shielding sufficient to limit dose equivalent to one fifth of the applicable dose equivalant limits (ANSI 70). It will usually be too costly to design shielding that reduces the annual dose equivalent to less than 10 mSv (1 rem) at all locations: recourse is then usually made to administrative and physical controls. It is convenient to limit exposures by limiting the hourly or weekly dose equivalent rates in occupied areas, but because accelerator operation can be quite variable an average weekly dose equivalent limit will give greater flexibility. The policies of accelerator laboratories vary somewhat in this regard, what follows is an example of the practices to minimize radiation exposure adopted at CERN. Practices at other institutions, while similiar in principle, may differ in detail.

It is usual practice to consider the occupants of laboratories and offices not directly concerned with operation and utilisation of the accelerator as nonradiation workers. The annual dose equivalent limit for these personnel would then be the same as that for members of the general public (see next section). This is taken to be < 5 mSv/y (500 mrem/y). This annual dose equivalent rate can be taken to be the boundary that requires the estabilishment of a controlled radiation area, although in practice it is more convenient to use authorized limits of 100 μSv (10 mrem) in any one week but to permit dose equivalent rates to rise as high as 10 μSv in any one hour (see previous paragraph).

If areas outside the accelerator shield are classified as Controlled Radiation Areas higher levels are permissible because individual doses will be monitored and exposures limited by personal and area dosimeters, administrative controls and physical barriers. The greater the degree of the administrative and physical controls the higher the dose equivalent rate that may be tolerated (within limits). Thus, for example, in laboratories or workshops excursions as high as 50 μSv/h are permissible provided the integrated dose limit is maintained. In areas of very low occupation dose equivalent rates as high as 200 μSv/h might be permitted. If special measures are taken to control and restrict access (simple barriers), levels of up to 1 mSv/h are tolerable while in locked or interlocked areas up to 100 mSv/h may be permitted. However, the regions where these high dose equivalent rates are allowed must be strictly limited in number and extent because they contribute to the global source of skyshine neutrons and will increase site-boundary levels (see Chapter 6).

Members of the General Public (Environmental Levels). No consistent scheme of radiation limits for the public has yet been developed. In general the limits for members of the general population are taken to be an order of magnitude lower than those for radiation workers, i.e., 5 mSv per annum. This value had been adopted at many institutions where adequate radiation monitoring programs at the site boundary are in place. If perimeter monitoring is not carried out it is usual to introduce a safety factor of three and use 0.17 mSv per annum as the limit for an average member of the population. Variations of exposure conditions within the population as a whole should then ensure that the dose equivalent of any individual does not exceed 0.5 mSv per annum.

The ICRP has recently recommended that the principal limit on effective dose equivalent to members of the general public is 1 mSv (100 mrem) in a year (ICRP 85). It is permissible to use a subsidiary dose equivalent limit of 5 mSv in a year for some years, provided that the average annual effective dose equivalent over a lifetime does not exceed the principal limit of 1 mSv per year. Because the dose equivalents to the skin and the lens of the eye are not included in the computation of effective dose equivalent for the individual (ICRP 84b) separate organ limits are needed–the recommended dose equivalent limit for both the skin and lens is 50 mSv in a year for members of the public. This new interpretation is consistent with that for radiation workers and means that for planning purposes site boundary dose equivalents for individual members of the general population should be limited 1 mSv per annum.

The prime regulations that apply to the radiological protection of the general public are for determination by local or national authorities. It should not therefore be expected that there will be any consistency in authorized limits at various accelerator laboratories around the world. Thus, examples of site boundary dose equivalent limits currently in operation are:

> 50 μSv per annum (5 mrem per annum) at Fermilab, 1.5 mSv per annum (150 mrem per annum) at CERN, and 5 mSv per annum (1 mSv per annum lifetime average) at LBL.

Most regulations are expressed in terms of annual dose equivalent rates, i.e., upper limits to the dose equivalent to individuals. However, in some cases exposures from any particular radiation source may be limited by placing an additional limit on the contribution to population exposure from that source. For example, the Environmental Protection Agency of the U.S.A., in addition to specifying exposure levels of less than 250 μSv per annum, imposes a limit to collective dose equivalent of 1 man-Sv per annum. For control purposes, these limits are often translated into hourly dose-equivalent rates at the site boundry, taking acount of accelerator operating schedules. Thus in the case of CERN, one talks of normally limiting boundary dose rates to 150 nSv per hour with occasional allowed excursions up to 500 nSv/h.

In considering site boundary levels one must take into account the possible legal interpretations of the term 'site boundary'. The boundary of a laboratory is not a simple line drawn on the surface of the earth. Depending on national legislation in fields other than radiological protection, the boundary could in principle be taken as extending deep underground or outwards to some unspecified but high altitude. However, in relation to dose-rate limits at site boundaries where the underlying philosophy is the exposure of persons, the site could be reasonably deemed to extend as deep as the deepest local cellar or subway (10-20 m) and as high as local apartment blocks (30-100 m). This viewpoint must be agreed beforehand with local authorities before discussing, for example, the implications of a neutron beam coming from a diagonal hole in the roof-shield of an accelerator. Evidently due account must be taken of the diffusion (skyshine) of such beams into the occupiable height zone beyond the site boundary.

Scientific Equipment and Apparatus. In general scientific equipment is not particularly sensitive to ionizing radiation. Magnet insulation may fail at absorbed doses of the order of 10^7 grays, semiconductor devices may deteriorate at doses three orders of magnitude less (Be 82, Li 85, Sc 79a, Sc 79b, Va 72a). Such problems are usually solved by the location of the equipment away from any high intensity source in the accelerator-room or along beam lines. Patterson and Thomas have pointed out, however, that 'many radiation detectors are so sensitive that they operate in radiation levels one or two orders of magnitude below those allowed for personnel safety' (Pa 73).

SHIELDING MATERIALS

Because in the case of most particle accelerators the source intensity is large it is almost always necessary to interpose shielding material between the accelerator and working areas. Consequently the

determination of shield transmission factors for different materials as a function of shield thickness is the most important task in accelerator design.

The detailed computation of shield transmission factors is a complex process requiring, for the radiation of interest, a detailed knowledge of the atomic and nuclear interactions and their transport through the shield. Although, as we show in Chapter 3, the radiation environments outside accelerator shields are usually dominated by those radiations that have no electrical charge or interact weakly with nuclear matter-photons, muons and neutrons-it is often necessary to consider the production and transport of many other radiations such as, for example, kaons, pions and protons because they also will contribute to the photon, muon and neutron intensity outside the shield. [See, for example (Pa 73), Chapter 6.]

The number of radiations of interest increases with the energy of the accelerated particles. Below about 500 MeV it is sufficient to determine the production of neutrons and photons by the first interaction of the charged particle and the determine the transmission of both components through the shield. The combined influences of relative yield, absorption in the target and the greater attenuation result in a radiation field outside the shield in which photons are usually only a minor component (Chapter 3).

As we shall see in later sections, at energies above 500 MeV the development of the hadronic cascade becomes increasingly complex and the production of pions (and even kaons) must be taken in account. At energies above 10 GeV muons become of increasing concern until at energies in the 100 GeV region they can dominate some radiation environments.

The increasing complexity of the hadronic cascade with energy make it necessary that sophisticated computational methods be used to study the shield transmission.

Sources of Data in Shield Transmission

There are two principal sources of information on shield transmission:

- Experiment and Theory
- Transport Calculations

Experiment and Theory

The most direct approach to accelerator shield design is by the measurement of the transmission of the radiations of interest through shielding materials. In the subsequent section references to many such measurements are given. Although measurement has the appeal of apparent simplicity it is, by itself, of limited utility. The design of an accelerator shield is determined by many variables: type and energy of the incident radiation, target materials, shield composition and so on. It is extremely difficult to make a sufficient number of measurements of all the important variables to interpolate reliably to all situations of interest. Extrapolation of experimental data to new energy regions is even less reliable. It it therefore essential that interpretation of the experimental data be underpinned by our theoretical understanding of

particle and nuclear interactions and the subsequent generation of electromagnetic and hadronic cascades in matter. Our current theoretical understanding of these phenomena is such that it is now possible to calculate the transport of radiation through shielding. A very important role of measurement is therefore to confirm the results of these calculations by comparing experimental and calculated data determined under identical shielding conditions.

Transport Calculations

The two principal methods used to determine the transport of radiations through matter are:

- Analytical and Numerical Solutions of the Boltzmann Transport Equation
- Monte Carlo Simulation of Particle Interactions

The standard methods for analytical and numerical methods of solving the Boltzmann transport equation are described in the standard texts (see, for example, Ch 84, Da 57, IAEA 68). For example, below 400 MeV the transport of neutrons through material can be treated by the methods of spherical harmonics and discrete ordinates. O'Brien (OB 70) and Alsmiller (Al 69a) have shown that these two methods give essentially indentical results that are in agreement with those obtained by Monte Carlo methods.

The difficulty in obtaining numerical solutions to the Boltzmann equation in complex geometries has led to the widespread use of Monte Carlo methods. At energies above 3 GeV this need to use Monte Carlo methods is enhanced because the application of analytical and numerical methods require several approximations that severely limit the utility of the solutions obtained.

In the Monte Carlo approach the solution of the radiation transport equation is formulated as a succession of physical processes and the cascade is simulated by making a mathematical experiment.

Empirical Models.

Whatever the source of the radiation transmission data there is usually great practical convenience in summarising the data in the form of simplified empirical formulae. Such formulae provide a convenient means of interpolating between data and facilitate rapid and inexpensive shield estimates. In many cases, despite the approximations made by these empirical formulae, the results are of sufficient accuracy to proceed with shield construction. If not, the more sophisticated methods described later in this chapter may be employed to refine the estimates. These empirical formulae have the general form, for point sources, of combining the inverse square law, an exponential transmission factor and a virtual source term. They are used widely in shielding calculations (Th 60). It is important to add a note of caution: because the exponential transmission factor is an approximation empirical models should be used only within the range for which they are known to give results of acceptable accuracy. Considerable error may result from extrapolation beyond this range.

SHIELDING MATERIALS

Of the many possible materials available for the construction of accelerator shielding experience has shown that, principally for economic reasons, only three-concrete, earth and steel-are widely used. To a limited extent other materials such as polythene, lead, uranium, water and wood have also been used in special circumstances. In addition special techniques have been used to reduce the levels of induced activity in concrete by either the inclusion of low-sodium aggregrates or by the addition of boron components (see Chapter 2). Pa 73).

An excellent source of information on the properties of shielding materials is to be found in Volume 2 of the Engineering Compendium of Radiation Shielding sponsored by the IAEA (IAEA 75). Entitled 'Shielding Materials', this volume discusses materials to shield against both gamma rays and neutrons. Although primarily directed toward the design of reactor shields, the volume is also of great value to accelerator shielding. In the remainer of this section we shall restrict our remarks to the latter concern.

Earth

Many of the early cyclotrons were constructed underground, usually placing them in a concrete vault covered with earth (Li 52). Earth, in fact, has many admirable properties for the construction of accelerator shielding. The principal constituent of dry earth is SiO_2 so that it is an effective shielding material for both photons and neutrons. The neutron attenuating powers of earth are enhanced by its water content. The maximum water content of loosely packed water saturated soil is about 40% by weight (Sp 75): Gilbert et al. reported finding 20% water by weight in the earth shield of the CPS (Gi 68). The water content is extremely effective in reducing the dose equivalent contributed by intermediate and slow neutrons (see Chapter 2). Earth varies in density, depending upon the degree of compaction from about 1.7 g cm^{-3} to as high as 2.2 g cm^{-3}: to be compared with the density of 'light' concrete, which is 2.35 g cm^{-3} (Ca 67, Gi 68).

In circumstances where it is decided to place the accelerator underground, and space constraints are not severe, earth can thus be an extremely useful shield material. It is, however,-to make a bad pun-not 'dirt cheap'. During the construction of a large accelerator to be sited underground, earth will be readily available and costs can be minimized by placing the accelerator room at an optimum depth such that the volume of earth excavated equals that required for overhead shielding. Transporation of earth away from and to the accelerator site will significantly increase costs and is to be avoided wherever possible.

Concrete

'Ordinary concrete is an inexpensive, easily handled material whose nuclear properties are good enough, taken in conjunction with its excellent structural properties, to make it desirable as a shielding material' (Hu 75). Concrete may be used either in the form of modular blocks or as reinforced concrete to be poured in place to create an immobile and essentially inflexible structure. In the latter method, concrete is used to build accelerator rooms and tunnels. In many cases

the accelerator room is designed to be sufficiently strong to support an overburden of earth shielding (see Chapter 1). The use of concrete blocks to construct shield walls and roofs adds an essential degree of flexibility at accelerators, such as those engaged in research, where frequent changes in shield design and configuration are necessary. When mobile shielding blocks are used, they should be constructed to have agreed modular dimensions. At CERN, for example, the modular dimensions found to be convenient are 0.2 m, 0.4 m, 0.8 m, 1.6 m and 2.4 m. Block dimensions must coincide with one of these module sizes (see also section on steel).

Portland concrete is a relatively standard material whose density is nearly always in the range 2.3-2.4 g cm^{-3}, but obviously the composition of the aggregate used will influence this. Special aggregates such as barytes (barite) or iron ore are used to produce concretes of higher density (exceeding 4.5 g cm^{-3}) for special purposes, but at great increase in cost. Where space constraints are severe, rather than pay the extra cost for special concretes, it is usually more economical to specify a composite shield consisting of steel and ordinary concrete (see section on steel).

It is worthwhile to carefully select the aggregate and cement used in accelerator installations. Special low-sodium aggregates may be used to reduce thermal-neutron induced radioactivation of concrete and consequently residual radiation levels after the accelerator is turned off. The same result may be achieved by the addition of boron compounds such as boron frits or colemanite. The reader should consult the IAEA Engineering Compendium on Shielding for further details (IAEA 75).

The efficiency of both earth and concrete shields somewhat depends upon their water content, which may vary with time. O'Brien has calculated the magnitude of these effects for accelerator-produced neutron spectra (OB 68a, b, c).

Steel

The use of steel is particularly useful when space considerations require compact shielding. Its relatively high density, which is roughly three times that of ordinary concrete, facilitates great savings in space, which lead to greater flexibility and efficiency of the accelerator. As with the other two primary shielding materials the density can vary significantly. The density of low-grade cast iron barely attains a value of 7.0 g cm^{-3} while steel is generally taken to have a density of 7.8 g cm^{-3}. The density of 7.9 g cm^{-3} of elemental iron quoted in tables of physical constants such as for example, by Kay and Laby (Ka 72a) is only rarely attained.

Steel or iron for shielding is generally available in the form of blocks. Occasionally scrap steel becomes available from decommisioned warships or large accelerators. Such a source of steel is usually economically attractive, but there may be hidden costs, such as cutting the steel into blocks of suitable size, rough machining and transportation from source, that should be included in the cost analysis.

In any form iron poses significant handling difficulties because of its high density. The size of blocks will be limited by the weight

capabilities of cranes and other handling facilities. The consequent limitation in volume may then result in a large number of lifting operations in the construction or modification of shield walls.

Steel has one important deficiency in shielding neutrons: it contains no hydrogen and its lowest inelastic energy energy level is 600 keV. In consequence there is a buildup of neutrons below this energy. This fact explains the observation in the fifties of a very 'soft' neutron radiation field around the Bevatron when it operated without overhead shielding. Intermediate-energy neutrons streaming from the magnet yoke were thus an important component of the radiation field (Th 73). Somewhat later Perry and Shaw observed an increase in dose-equivalent rate at Nimrod when steel was used to replace concrete (Pe 65, 66). At the same accelerator Shaw et al. showed that the neutron operation spectrum outside shielding was richer in neutrons of energy less than 1 keV than the equivalent neutron spectra outside concrete or earth shielding (Sh 69a).

It is usual, then, to construct composite shields with the steel toward the source side: the intermediate-energy neutrons being removed by a hydrogenous shield (normally concrete) on the outside. Whereas for reactor shields extensive optimisation studies have been made for multi-media shields, such is not the case for particle accelerators. A useful rule of thumb is to ensure that at least one high-energy inelastic interaction mean free path thickness of hydrogeneous shielding lies on the outside. In practical terms this translates to about 60 cm of concrete.

Because both steel and concrete blocks will normally be used in modular shielding, it is a matter of common sense and convenience that the same basic modular dimensions for blocks of all materials be used.

Other Shielding Materials

Any departure from the three basic shielding materials, earth, ordinary concrete or steel, should only be undertaken after careful study. It will usually be expensive to use other materials. Nevertheless, special circumstances may demand special solutions. Examples of other materials used for accelerator shielding include lead, polyethylene, water, wood and depleted uranium.

Polyethylene

Polyethylene, $(CH_2)_n$, has often been used to shield neutrons produced by D-D and D-T generators. It is convenient for such a purpose because of its considerable hydrogen content (~ 5% by weight) and its density (0.92 g cm^{-3}). Neutron attenuation data for neutrons up to 5MeV may be found in NCRP 38 (Al 63, NCRP 71). The addition of boron carbide (~ 8% B_4C) is of value in reducing the buildup of 2.2-MeV γ rays produced by thermal neutron capture in hydrogen. The principal disadvantages of polyethylene lie in the fact that it is a fire hazard and relatively expensive. Its use is therefore limited to those situations where the volume of shielding required is small or cost is of minor concern.

Water

At first sight water appears to be an attractive material for neutron shielding. Like polyethylene it is rich in hydrogen but, in addition, it is plentiful and cheap. Many of the early neutron generators and cyclotrons were shielded with walls constructed of water-filled cans. More ambitious schemes have used water that could be pumped into or out of space sealed off by water-tight doors. Experience has shown, however, that water is not as convenient a shielding material for accelerators as might be thought. The integrity of 'water-can' walls was breached by the rusting of cans and the development of leaks. Maintenance of even such simple shields became inconvenient and expensive. Like polyethylene, water can act as a source of 2.2-MeV photons (Ma 70) but boration is more difficult than for polyethylene because boron salts are rather insoluble in water. It is often therefore necessary to design a composite shield, with a high-Z shield material (such as steel or lead) outside the water shield. As a consequence of this experience water is no longer widely used as a shielding material at particle accelerators.

Wood

During the early years of operation of the Bevatron wood was found to be as effective on a linear basis as concrete for neutron shielding-despite the difference in density of a factor of about 2.5 (Pa 57). This high efficiency of wood was due to the depletion of the intermediate-energy region of the neutron leakage spectrum from the magnet steel (see section on steel). Since wood is often considerably cheaper than concrete it may thus serve as an economical shielding material. However, its use at the Bevatron was effective only under the special conditions that obtained in the fifties. Knowledge of the neutron spectrum to be attenuated is essential before deciding whether wood may effectively replace concrete. One major disadvantage of wood is that it represents a major fire hazard.

Uranium

The use of uranium as a shield material is discussed by Hamer and Mc Arthur (Ha 75). Its principal advantage lies in its very high density (19 g cm^{-3}). Depleted uranium (^{238}U) is available in many countries, thus reducing the production of fission products in the irradiated material. Uranium has been used in accelerator shields where space problems are severe (for example above the straight sections sections of the Bevatron [Ev 70]). Special precautions must be taken with uranium to prevent the spread of low-level contamination by the abrasion of the surface oxide layer. Many practical solutions are available: painting, lacquering or electroplating the surface, or containment in metal boxes (Ha 75).

Other Heavy Materials-Lead, Tungsten

Heavy materials will have uses where space problems are severe or where photons are to be attenuated. Lead shielding in the form of thin sheets is widely used to attenuate the x rays produced, for example, by the injectors at large accelerator complexes. Lead has poor physical properties for the construction of massive shielding and when so used has been contained in steel boxes. Tungsten is of value in the construction of beam dumps when large quantities of heat must be

dissipated. Thus tungsten is usually placed in front of a depleted uranium back-stop to absorb the peak of the energy dissipation curve and so avoid disruption of the uranium containment.

4.3. SHIELDING AT PROTON ENERGIES OF LESS THAN 3 GeV

INTRODUCTION

The principal concern in shielding proton accelerators of less than about 3 GeV in energy is to attenuate to an acceptable level the neutrons produced by the interaction of the high-energy protons with experimental targets, beam-transport components, the accelerator structure and the shield itself. Most of the relevant published experimental and theoretical data in this energy range is for neutrons of energy less than 400 MeV. Consequently principal consideration will be given in this section to proton accelerator shielding below that energy.

The energy region between 400 MeV and 3 GeV is difficult to treat theoretically because hadron cascade processes have not stabilised. Experimental data are meagre. It is convenient to resort to interpolation between 400 MeV and the 'high-energy limit' that is achieved at proton energies of several GeV (Pa 73).

The estimation of shielding for proton accelerators requires a detailed understanding of the production of particles by the interaction of the primary protons, their transport through the shield and the determination of the energy spectrum of the radiations that penetrate the shield.

At proton energies above 3 GeV the lateral shielding (at 90° to the proton beam), and to some extent the longitudinal shielding (i.e., in the direction of the proton beam), may be determined by means of simple models. (See for example the discussion of the Moyer model in the appendix to this chapter.) At these higher energies (above 3 GeV) simplifications are possible because the attenuation length of high-energy neutrons is independent of neutron energy above about 100 MeV and the yield of high-energy neutrons is roughly proportional to primary proton energy, E_p (St 82). Below 1000 MeV both these simplifications may not be made: hadron cross sections change rapidly with energy and particle yields are no longer even approximately proportional to E_p (Te 85).

This section discusses, firstly, the particle yields from the proton nucleus interaction, the nuclear processes involved and the angular and energy distributions of the neutrons produced. Secondly, the transport of neutrons through the shield is described and, finally, methods of calculating shielding both in the transverse and longitudinal directions are summarised.

PARTICLE YIELDS FROM THE PROTON-NUCLEUS INTERACTION

Tesch has recently reviewed the literature that provides information on the total number of neutrons produced per proton interacting in various target materials (C, Al, Cu, Fe, Sn, Ta and Pb) over the energy range from 10 MeV to 1.45 GeV (Te 85). His summary is given in Table 4.1, together with references to the original sources.

The data presented in Table 4.1 were obtained, for the most part with targets thick enough to completely stop the incident protons. The values of neutron yields given are therefore maximal and, at energies above about 300 MeV, may include some multiplication effects because of the large targets used (Te 85).

For all target materials at primary proton energies, E_p, between 50 MeV and 500 MeV the neutron yield is roughly proportional to E_p^2; beyond 1000 MeV the yield is directly proportional to E_p.

The data summarised by Tesch suggest that, with sufficient accuracy, the ratios of the neutron yields from different target materials is independent of E_p in the range 20 MeV to 1 GeV and are given by:

C:Al:Cu-Fe:Sn:Ta-Pb = 0.3 ± 0.1:0.6 ± 0.2:1.0:1.5 ± 0.4:1.7 ± 0.2

For a detailed calculation of accelerator shielding more information than the total number of neutrons produced is required: in particular the energy and angular distribution of the neutrons must be known. Two nuclear processes are of importance in determining the yield of particles following proton-nucleus interactions:

- Nuclear Evaporation, and
- Intranuclear Cascades.

Nuclear Evaporation

At proton energies below 10 MeV the interaction of a proton with a nucleus is best explained by a compound-nucleus model, where the incident particle is absorbed into the target nucleus to create a new compound nucleus. This compound nucleus is in an excited state with a number of allowed decay channels; the preferred decay channel is the entrance channel. As the energy of the incident particle increases, the number of levels available to the incident channel becomes very large; there are no longer discrete levels in the quasi-stationary states of the compound nucleus but rather a complete overlapping of levels inside the nucleus. Under these circumstances the emission of particles is best described by an evaporation process analogous to the evaporation of a molecule from the surface of a liquid. For example the energy distribution of emitted neutrons, can be described by an equation of the form:

$$n(E)dE = \text{const} \times E \exp(-E/\tau), \qquad (4.1)$$

where τ is a so-called nuclear temperature and has the dimensions of energy, which is usually ≃ 2–10 MeV. Similar equations describe the emission of protons, deuterons and heavier particles. The evaporated particles are emitted isotropically and the energy distribution of the evaporated neutrons extends up to about 8 MeV. The evaporated particles are emitted isotropically and the energy distribution of the neutrons extends up to about 8 MeV. If the evaporated particles are charged the Coulomb barrier suppresses the emission of low-energy particles.

Intranuclear Cascade

At higher energies (> 50 MeV) the development of an intranuclear cascade becomes important. The intranuclear cascade develops through the interaction of individual nucleons inside the nucleus; the

probability of these interactions is determined by the interaction cross sections that apply in free space and by the Pauli exclusion principle (Be 63a, Ch 68, Me 58).

Tesch has evaluated three measurements (Br 83, Ci 81, Na 83) and two calculations (Al 82, Fu 72) of the neutron spectra emitted from thick targets.

> 'In all calculated and measured spectra both production processes can be distinguished: neutron emission by evaporation from the compound nucleus, and the neutrons of higher energy from the intranuclear cascade. The angular distribution of the "evaporation neutrons" is isotropic. Their energy distribution reaches to about 8 MeV. In the interesting angular interval from 75° to 105°, the "cascade neutrons" defined as neutrons with energy above 8 MeV, are only a few per cent of the total neutron yield. Their contribution to the dose at 90° with respect to the proton beam rises with increasing proton energy from 5% to about 20%'. (Te 85).

Bertini has reported calculations of the production of particles from protons interacting with several target nuclei: C, O, Al, Cr, Cu, Ru, Ce, W, Pb and U. Protons of energy 25 MeV and 50-400 MeV were selected and both evaporation and intranuclear cascades were included in the calculations. The particle yields were determined for four angular ranges: 0°-30°, 30°-60°, 60°-90° and 90°-180° (Be 63a). Alsmiller et al. (Al 67) have conveniently summarised the calculated spectra of Bertini by fitting them by fifth and sixth order polynomials. The number of neutrons per MeV per steradian per interaction of a proton of kinetic energy E_0 MeV may then be represented by:

$$n(E) = \frac{1}{E_0} \exp\left|\sum_{i=0}^{5} a_i \left(\frac{E}{E_0}\right)^i\right| + \frac{1}{4\pi}\frac{1}{25} \exp\left|\sum_{j=0}^{4} a_j \left(\frac{E}{25}\right)^j\right| , \qquad (4.2)$$

the first term referring to to yield from the intranuclear cascade, and the second from evaporation. Values of the coefficients a_i and a_j are given so that the energy distributions, for both evaporation and cascade neutrons produced at each of the incident energies and for each angular region, may be calculated. At the present time this parameterized version of yield data due to Alsmiller et al. is the most amenable form for calculation of shielding by computer. Although Haenssgen et al. have proposed a new parameterization of the existing yield data, they have not published parameters that give acceptable fits to the experimental data over the energy required here (Ha 80).

The data of Alsmiller et al. have been compared with experimental data around C, Al and Cu targets by Fasso and Hoefert (Fa 76) and with extensive intranuclear cascade calculations made at Brookhaven (Be 74). These comparisons show good agreement, giving confidence in the use of the yield data from Oak Ridge.

The Transport of Monoenergetic Neutrons through Shielding

Below 400 MeV, neutron transport in the shield can be treated by the standard methods of solving the Boltzmann diffusion equation, especially using the method of spherical harmonics, the method of discrete ordinates, and the Monte Carlo method. Studies by O'Brien and Alsmiller et al. have shown these methods to give essentially equivalent results (OB 70, Al 69a).

Discrete-ordinate calculations of the penetration of neutrons in broad-beam geometry through concrete in the energy range from 50 to 400 MeV have been reported by Alsmiller et al. (Al 69b) and from 1 to 100 MeV by Wyckoff and Chilton (Wy 73). In the former case the contributions to the total dose equivalent from neutrons and photons are given separately, whereas the Wyckoff and Chilton calculations give only the total dose equivalent. (This is of little practical significance because photons contribute less than a few percent of the total dose equivalent.) The latter calculations are used as a basis for the NCRP recommendations for shielding low-energy accelerators (NCRP 77). Comparison of these two sets of calculations shows essential agreement in their common energy regions and both sets agree with calculations of O'Brien using spherical harmonics (OB 70).

These three sets of calculations may be conveniently parameterized using an exponential function of the form:

$$H(z) = k_0 \exp(-x/\lambda) \quad , \tag{4.3}$$

where H(z) is the dose equivalent at depth z in the shield,
λ is the attenuation length, and
k_0 is the extrapolated dose equivalent at zero depth.

Figures 4.1 and 4.2 show the variation of the parameters λ and k_0 with neutron energy. The values of λ and k_0 shown have been selected to give a satisfactory representation of the Alsmiller data and the Wyckoff and Chilton data at depths greater than 1 metre in concrete. The values of these parameters used for subsequent analysis in this section are indicated by the solid line in Figs. 4.1 and 4.2 and are compared with the calculated values. For convenience some values are listed in Table 4.2. The value of λ at energies above 200 MeV has been chosen so as to agree with the limiting value of 1170 kg m^{-2} found at high energies [(Pa 73), see also the appendix to this chapter, which describes the Moyer model].

Shielding Calculations

Over fairly wide range of shield thicknesses it has been found sufficiently accurate to estimate shielding with simple formulae of the form:

$$H(d,\theta) = r^{-2} H_\theta \exp(-d(\theta)/\lambda_{eff}) \tag{4.4}$$

This formula applies to a point source with the symbols having the following meaning (see Figs. A4-1, and A4-3):

$H(d,\theta)$ is the dose equivalent at depth d, angle θ in the shield.

H_θ is a constant that may be described as the dose equivalent extrapolated to zero depth in the shield, and corresponding to angle θ, and at unit distance from the point source.

r is the distance from the source to the shield surface (or other point of interest outside the shield).

λ_{eff} is the effective attenuation length for dose equivalent through the shield.

Experience has shown that, over a limited range of shield thicknesses, the approximation of the radiation transmission by an exponential function works well: it fails for shield thicknesses less than about 100 g cm^{-2} and the value of λ_{eff} changes with increasing depth in the shield. Nevertheless, in the range of practical interest, 200–1200 g cm^{-2}, a single value of λ_{eff} will suffice.

In principle, values of H as a function of both angle and depth are needed for shield design. However it is often only necessary in practice to design shielding in the longitudinal ($\theta = 0$) and transverse ($\theta = \pi/2$) directions. Table 4.3 summarises values of the corresponding values H_0 and $H_{\pi/2}$ for proton energies in the range 20–1000 MeV. These values were obtained as described in the following section.

Tesch has described an empirical approach for the determination of the parameters $H_{\pi/2}$ and λ_{eff} (Te 85). By reviewing published data he was able to generate graphs showing the variation of both parameters up to a photon energy of 1000 MeV. Comparison between calculations using Tesch's empirical approach and those by Braid et al. (Br 71) and Alsmiller et al. (Al 75) shows agreement to within a factor of better than three.

A somewhat different approach has been adopted here, following the earlier work of Braid et al. (Br 71) and Stevenson (St 80). The entire spectrum of neutrons emitted from the target is transported through the accelerator shield: both the particle production and their transport were calculated by the methods described earlier in this section. The resultant emerging neutron spectrum is then converted to dose equivalent using the fluence to dose-equivalent conversion coefficients (ICRP 73b, NCRP 71).

One particular advantage of the method described in this section is that any arbitrariness is the interpolations for λ_{eff} is avoided–the value to be used is derived naturally from the calculation.

Thin Targets

A thin target is one in which the incident protons lose an insignificant amount of energy in the target. The kinetic energy available for neutron production is therefore the full incident proton energy.

Figure 4.3 shows the results of calculations made for a thin copper target. The dose equivalent at given depths in the concrete shield was obtained in two stages: by integrating over energy the product of the neutron yield at a distance of 1 metre at a given energy, from the Alsmiller et al. parameterization, with the dose equivalent at the depth

in question determined from the parameterization of Eq. (4.1).

Table 4.3 summarises values of $H_{\pi/2}$ and λ_{eff} so obtained, which can be used with Eq. (4.4) for the estimation of transverse shielding for thin targets.

Thick Targets

Here is assumed that the incident proton is completely stopped in the target. Figure 4.4 shows the results of calculations of dose equivalent as a function of depth in a concrete shield (ρ = 2.4 g cm^{-3}) with a copper target bombarded by protons.

The curves of Fig. 4.4 were calculated in the following manner: At a given depth in the shield the product of the dose equivalent (at that depth) and the cross section for interaction per unit distance at that energy, divided by the rate of energy loss per unit distance, dE/dx, is integrated with respect to proton energy. The dose equivalent at the required depth is obtained by interpolating the data of Fig. 4.3. The integral is evaluated from the proton energy down to 25 MeV. The contribution of neutrons produced by the remaining 25 MeV protons was estimated by using the yield of 10^{-2} neutrons per proton given by Nakamura et al. (Na 83); assuming the neutron spectrum produced by the 25 MeV protons given by the parametrization by Alsmiller et al. (Al 67) and carrying out the integration described in the case of thin targets.

Figure 4.4 also indicates calculations made by Braid et al. [Br 71] (dashed line) and Alsmiller et al. [Al 75] (dotted line). Both sets of calculations used the Alsmiller parameterizations for particle production but they differ in their treatment of neutron transport. Braid et al. used the method of spherical harmonics whereas Alsmiller et al. used the method of discrete ordinates. The calculations by Braid et al. are for 100-MeV, 200-MeV, 300-MeV and 400-MeV protons incident on a thick copper target and the Alsmiller calculations are for 200-MeV protons incident on aluminium: the data shown have been scaled by the appropriate target yield factor for a copper target.

Table 4.3 summarises values of the $H_{\pi/2}$ and λ_{eff} to be substituted with Eq. (4.4) to estimate the transverse shielding of thick targets.

Forward Shielding

There are suprisingly few published data on the attenuation of neutrons in the forward direction (i.e., along the direction of the proton beam) at energies below 1 GeV.

Some early shielding studies for 90 MeV neutrons have been described by Patterson (Pa 57). These suggested that the attenuation length, λ, was approximately given by the well known relation (Pa 73):

$$\lambda = \frac{1}{N\sigma_{inel}} \qquad (4.5)$$

where σ_{inel} is the inelastic cross section of the shield material.

Theoretical considerations suggested that, at least for high-energies, the effective attenuation length λ_{eff} would in fact be somewhat greater than that predicted by Eq. (4.5) [Fi 63]. Experience of

Sychev et al. (Sy 66a, Sy 66b) at Dubna suggested that in the case of broad beam geometry in the energy range between 350 MeV and 660 MeV the attenuation length was given by:

$$\lambda_{att} = (1.3 \pm 0.1)\lambda_{inel} \qquad (4.6)$$

Ban et al. were able to confirm this suggestion at higher energies by making measurements of transverse attenuation in various materials of neutrons produced by 12-GeV protons incident upon a steel target (Ba 80).

The most convenient data available are those of Braid et al. (Br 71) which are based on the same data use for transverse shield calculations but use as a source term the 0°–30° yield data from Alsmiller et al. (Al 67). The authors of that work expressed their results using a formula similar to that proposed here for the lateral shielding case, and from which the parameters H_0 and λ for use in the present formula can be derived. These parameters are given in Table 4.3. Braid et al. warn that these parameters should not be used for thin shields (<1000 kg/m^2) nor for shield thicknesses of greater than about 7 metres.

Table 4.3 Parameters for use in calculating shielding. [here]

Parameters for Simple Shielding Formulae

The result of the thin and thick copper target calculations for a concrete (ρ = 2.4 g cm^{-3}) shield are summarised in Figs. 4.5 and 4.6.

Figure 4.5 shows λ_{eff} as a function of proton energy: the values of λ_{eff} for the neutrons from a thick target are somewhat smaller than those for the thin target. This is to be expected because of the slightly softer neutron spectrum emitted from thick targets compared with thin targets. The limiting value of λ_{eff} at high energies (1170 kg m^{-2}) is indicated and permits rough interpolation between 400 MeV and 3 GeV indicated by the dotted lines. [A measurement of λ_{eff} in concrete for 500-MeV protons incident upon iron by Ban et al. (Ba 81) is seen to be in quite good agreement with the recommended value.] It is evident that transverse shielding measurements in the energy region 500 MeV to 1 GeV would be extremely helpful.

At proton energies below 500 MeV the recommended values of λ_{eff} given here are seen to be intermediate between values published in the literature (Te 85).

Figure 4.6 summarises values of $H_{\pi/2}$, the dose equivalent extrapolated to zero depth in the shield and at 1 metre from the target as a function of proton energy. Values of $H_{\pi/2}$ for proton energies below 400 MeV are taken from Figs. 4.3 and 4.4.

The thin target data (open circles) lie above the corresponding thick target values for proton energies below 400 MeV because of absorption within the target. At higher energies the thick target values will, however, exceed the thin target values because of cascading in the target and will approach values appropriate to shielding of an end-stop. The thin-target values for $H_{\pi/2}$ approach the Moyer-model parameter value given by:

$$H_{\pi/2} = 7.6 \times 10^{-15} E_p^{0.8} \text{ Sv m}^2 \text{ *}$$

Although the Moyer approximation no longer holds below 3 GeV, the trend is continued downwards to guide the eye.

These two figures should allow one to obtain the necessary parameters for shielding design of targets bombarded by lower energy protons. It should be remembered that the approximations made only make this simple formula accurate for shield thicknesses above 1 metre and below 4 metres. Outside this range the simple formula may over-estimate the dose equivalent.

Table 4.3 summarises values of $H_{\pi/2}$ and λ_{eff} for the calculation of transverse shielding for thin and thick targets.

4.4. THE SHIELDING OF PROTON ACCELERATORS AT ENERGIES GREATER THAN 3 GeV

INTRODUCTION

As we have seen, at proton energies above about 3 GeV the development of the hadronic cascade is important in determining the shield thickness of proton accelerators, while above about 10 GeV consideration of the production of muons must be taken into account for shield specification in the forward direction.

As late as the early sixties surprisingly little information can be found in the literature to guide the shield designer in the GeV energy region. The summary of our knowledge at that time may be found in the published proceedings of a symposium held in New York in April 1957 (So 57). The two great stimuli to improving our understanding of radiation phenomena in the GeV energy region were, firstly, the difficulties that resulted from excessive radiation levels around the early synchrotrons and, secondly, the desire to design and construct second generation weak-focussing and the first generation strong-focussing proton synchrotrons with energies up to 30 GeV (So 57, Pa 73).

These accelerator construction programmes stimulated an extensive series of both experimental and theoretical studies of the hadronic cascade in matter with a view to more efficient shield design. Two pressing problems emerged as needing attention:

- At the weak-focussing proton synchrotrons increased intensities and the development of extracted proton beams led to the need to design beam-stops and shielding around components of the extraction systems and beam transport elements (Mo 61b, Mo 62, Th 68, Th 70).
- At the strong-focussing proton synchrotrons initially designed for use only with secondary scattered beams, the more urgent consideration was for an efficient shield design above the accelerator tunnel. Because of the large circumference of these accelerators great savings in cost could result if shields were designed without the need for safety factors imposed by uncertainties in shielding

---

* $H_{\pi/2} = H_0 e^{-2.3\pi/2}$ (St 82)

$H_0 = 2.8 \times 10^{-13} E_p^{0.8}$ Sv m^2 (Th 84)

data. These concerns became enhanced as accelerator energies advanced into the hundred GeV range (CERN 64, LBL 65, URA 68). Furthermore as the design of beam extraction systems advanced it became necessary to design beam-stops for the strong-focussing accelerators as well as for the weak-focussing synchrotrons.

Fairly detailed reviews of the early shielding studies in the GeV energy region have been given elsewhere and will not be repeated here. The interested reader is referred to the summaries for further information (Li 61, Pa 71, Pa 73, Ri 73).

THE DESIGN OF BEAM-STOPS (E > 3 GeV)

When considering the specifications of the forward shielding of end-stops, two separate contributions must be taken into account. The first is that from the hadron cascade itself; this process is always dominant at proton energies less than 10 GeV. The second is that from muons generated by the decay of pions and kaons in the cascade and from the processes of direct production in proton-nucleus interactions. Muons dominate shielding specifications at the higher proton energies (Th 66) and their attenuation has been considerd in the design studies of several high energy accelerators (CERN 64, LBL 65, Th 71, Ti 83, URA 68).

The earliest theoretical and experimental studies began with the study of the longitudinal development of the hadronic cascade in the forward (incident particle) direction, in an attempt to obtain a definitive value for the effective attenuation length to be used in the shield design. Many such experimental studies were performed and their results published in the literature during the decade of the sixties (Be 71b, c, Be 73, Ch 65, Ci 61, Ci 65, Ho 63, Pa 71, Pa 73, Sh 64, Sm 64, Sm 65, Th 63, Th 64a,b). Because of an incomplete understanding of the differences in effective attenuation lengths under narrow-beam and broad-beam conditions the values of attenuation lengths reported in some of the earlier papers are quite disparate (Th 68).

Lindenbaum (Li 61) explained these early experiments in terms of the neutron inelastic cross sections and showed that for narrow-beam geometries the attenuation length is identical to the inelastic mean free path and has limiting value given by:

$$\lambda_{inel} = \frac{1}{N\sigma_{inel}} \tag{4.5}$$

where N is the number of atoms cm^{-3} and σ_{inel} is the inelastic cross section at high energies (approximately equal to the geometric cross section of the nucleus). [See Pa 73, Chapter 6.]

Sychev et al. found that for broad neutron beams normally incident on plane walls, that the attenuation length, λ_a, for neutrons in the energy range 350–660 MeV was given by:

$$\lambda_a = (1.3\pm0.1)\lambda_{inel} \tag{4.6}$$

a result confirmed at substantially higher energies by Ban et al. (Ba 80, Sy 66a,b).

Two of the series of experiments have provided sources of data with which to test modern computer programmes used to design beam stops. Details of these experiments are given by Patterson and Thomas (Pa 73). They were made in somewhat idealized geometries and in the current jargon of the computer world are referred to as 'bench-mark experiments'. The first of these experiments utilised nuclear emulsions to study the generation of the nuclear cascade through steel by 9- and 18-GeV protons (Ci 65, Ch 65, Ho 63, Th 63), while the second used activation detectors and nuclear emulsions to study the cascade generated in concrete by 6.2-GeV protons (Sm 64, Sm 65, Th 64a,b).

Recent experimental studies of the development of the hadron cascade in extended shields include: 500-MeV protons on an iron shield by Arakita et al. (Ar 79), 18-GeV protons on an iron beam-stop by Goebel and Ranft (Go 70a), 28-GeV protons on an iron beam-stop by Bennet et al. (Be 73), 29.4-GeV protons on a steel shield by Volynchikov et al. (Vo 83), 200-GeV protons on an aluminium beam-stop by Stevenson et al. (St 86a), 300-GeV protons on aluminium, iron and lead beam-stops by Gollon et al. (Go 81), 400 and 800 GeV protons on an iron beam-stops on an iron beam-stop by Cossairt et al. (Co 85a).

The design of beam-stops is complicated by the fact that the radiation source is extended, being not simply the products resulting from the first interaction of the primary beam, but including high-energy forward-going interaction products from particles that may have undergone many interactions in the shield. As the hadron cascade develops the average energy of particles decreases and the cone of cascade-propagating particles widens with depth in the shield. In the transverse direction, as we shall see, this extension of the radiation source is of no great consequence and, in fact, empirical models based on point-sources often serve to adequately define transverse shielding. In the longitudinal direction the initial build-up and equilibration of the hadron cascade has important consequences for the specification of the shield.

Both analytical and Monte Carlo methods have been used to study the longitudinal and transverse development of the hadron cascade.

Analytical Solutions

The simple one-dimensional description of Lindenbaum (Li 61) provides a qualitative but instructive analytical treatment of the development of the hadron cascade in a shield. Although limited in its practical application, this treatment is of great value in understanding the main features of the cascade.

Suppose we have an incident high-energy primary particle that after a collision continues in its original direction at a reduced energy but with the same mean free path, λ, or generates one or more secondary particles with the same λ, until it has undergone a sufficient number of collisions, n, so as to degrade its energy to the point at which the absorption cross-section increases rapidly with decreasing energy (about 150 MeV as may be seen in Fig. A4.2). At its next interaction it will be incapable of producing any secondary particles that continue the generation of the hadron cascade, and it is said to be 'removed from the cascade'. In reality there will be some distribution function in the

value of n, but for simplicity we will assume that a specific integral value may be ascribed to n and to calculate it we will proceed as follows: Referring to Fig. 4.7a, the number of particles that reach the plane Z having made no collisions is $N_0 \exp(-z/\lambda)$, where N_0 is the number of particles in the primary beam. We call this number ν_1. Suppose that there is one collision between 0 and Z. The number of particles that reach Z is given by the product of the number that reach dr multiplied by the probability of subsequently reaching Z times the probability of interacting in dr times the multiplicity, m_1, in the first interaction:

$$\int_0^z N_0 \exp(-r/\lambda)\exp[-(z - r)/\lambda]m_1(dr/\lambda) = (N_0 m_1 z/\lambda)\exp(-z/\lambda) = \nu_2 \quad (4.7)$$

Referring to Fig. 4.7b, suppose that there are two collisions. The number of particles that reach Z is the product of those that reach s having made one collision multiplied by the probability of subsequently reaching Z times the multiplicity in the second interaction, m_2, times the probability of interacting in ds:

$$\int_0^z (N_0 m_1 s/\lambda)\exp(-s/\lambda)\exp[-(z - s)/\lambda]m_2(ds/\lambda)$$

$$= (N_0 m_1 m_2/\lambda^2)\exp(-z/\lambda) \int_0^z sds$$

$$= (N_o m_1 m_2 z^2/2\lambda^2)\exp(-z/\lambda) = \nu_3 \quad (4.8)$$

We can therefore write, with n as defined above:
$N_n(x) = N_0 \beta_n(z/\lambda)\exp(-z/\lambda)$, where β is a build-up factor,

for n = 1 $N_1 = \nu_1$ $\beta_1 = 1$

for n = 2 $N_2 = \nu_1 + \nu_2$ $\beta_2 = 1 + (m_1 z/\lambda)$

for n = 3 $N_3 = \nu_1 + \nu_2 + \nu_3$ $\beta_3 = 1 + (m_1 z/\lambda) + (m_1 m_2 z^2/2\lambda^2)$

Therefore the build-up factor does not approach a constant value but is a monotonically increasing function of z. If $mz/\lambda \gg n$ ($m_1 = m_2 = \ldots = m$), approximately exponential absorption takes place with a mean free path equal to $\lambda + \Delta\lambda$, where $\Delta\lambda = n\lambda/zm$. This correction becomes small as mz/λ increases, so that the true equilibrium mean free path of the cascade is not attained except at large depths in the endstop. Figure 4.8 gives an example with m = 2 and n = 3, where the exponential region is not achieved until $z/\lambda = 10$. In concrete this would correspond to a depth of about 1200 g cm^{-2}.

Passow provided a more complete analytical description of the hadron cascade, which included differentiation between hadrons but was still of necessity one-dimensional (Pa 62b). More general discussions

were published by Fisher (Fi 63), Riddell (Ri 65) and Alsmiller and Barish (Al 65). Fisher's analysis is treated in detail in Patterson and Thomas (Pa 73). Alsmiller and Barish aimed at reproducing the experimental data of Childers et al. (Ch 65) and Citron et al. (Ci 65). Another form of solution was provided by Barbier and Hunter (Ba 71). In a study by O'Brien (OB 69), Passow's approximation was reparameterized to force the secondary production spectra to correctly reproduce the partial inelasticities and multiplicities up to energies of 30 GeV or so. The resulting solutions were then compared with the above experimental data at 19.2 GeV/c and with the data of Shen at 1 and 3 GeV (Sh 64). Figure 4.9, taken from O'Brien, shows reasonable agreement between the experimental data of Citron et al., Monte Carlo calculations by Ranft and calculations using Passow's approximation (Ci 65, OB 69, Pa 62b, Ra 67). The congruence between experiment and the early calculations was not always so good, as may be seen in the next figure (Fig. 4-10), also taken from O'Brien (which shows considerable divergence between experiment and calculation). Here the data of Shen are compared with a Monte Carlo calculation by Armstrong and Alsmiller and calculations using Passow's approximation. O'Brien has shown that the discrepancies were due to limitations of the one-dimensional cascade approximation when applied to the case of a shield of finite lateral dimensions (OB 69).

It is obvious that one-dimensional cascade approximations will not provide solutions to the transverse shielding problem.

Monte Carlo Solutions

The analytical methods just described require severe approximations, including:

- restriction to a one-dimensional geometry
- neglect of ionization energy losses
- neglect of elastic and multiple Coulomb scattering
- assumption that all secondary particle production is in the forward direction
- assumption that particle production is represented by rather simple analytic expressions.

In the Monte Carlo approach to the solution of the radiation transport equations the problem is formulated as a succession of individual processes rather than in terms of global physical quantities. The cascade is simulated by making a mathematical 'experiment' akin to the real physical situation. Particles in the cascade are tracked from interaction to interaction: these 'events' may be, for example, elastic or Coulomb scattering events, or inelastic nuclear events in which any variety of secondary particle may be produced. The processes and particle production are selected at random from their appropriate probability distributions which are either known, or may be well approximated. These probability distributions are usually either expressed in the form of empirical formulae or generated by Monte Carlo simulation. At any point in the cascade simulation any required macroscopic physical quantity, such as, for example, particle fluence, energy fluence, absorbed dose, and density of inelastic interactions may be 'scored'. That is to say that the individual contribution to required physical quantity from the particle being followed may be computed and stored. When a sufficient number of particles have been followed and scored the expectation values of the required global macroscopic quantities may be evaluated to the required statistical accuracy.

None of the restrictions imposed by the analytical solutions apply to the Monte Carlo solutions. In particular any three-dimensional geometrical configuration containing many different media may be considered. While it is simpler if the surfaces of the media can be represented in a regular Cartesian or cylindrical geometry, this is not a fundamental constraint. The main disadvantage of the Monte Carlo method is that the tracking of a sufficient number of particles to give good statistical accuracy may require considerable time. This is so, even if special techniques of biassed selection are used so that the followed particles are mainly those that contribute to the quantities of interest. Limited computational resources may therefore lead to data of poor precision.

In any event the shield designer must never forget that Monte Carlo methods are inevitably limited by the quality of the theoretical and experimental data used in their encoding. In this respect they do not differ from either analytical methods or experiment and their results should be evaluated just as critically.

The following sections give a brief summary of three of the Monte Carlo simulations available from the Radiation Shielding Center at Oak Ridge. Both the strong points and limitations of the codes are

discussed, and some comparison with experimental data on hadron cascade development in extended targets is made.

This brief description is in no way comprehensive. Many other computer simulations of the hadron cascade exist-for example that by Barashenkov et al. (Ba 72). The codes described here have the advantage of being readily available.

The High-Energy Transport Code (HETC)

HETC has for many years been a benchmark for hadron cascade codes used in radiation physics and radiation protection. It originates from the Neutron Physics Group of the Oak Ridge National Laboratory. Descriptions of the code have been given by Armstrong (Ar 80) and Gabriel (Ga 85). Operating instructions are given by Chandler and Armstrong (Ch 72).

The main feature of HETC is its use of an intranuclear cascade plus evaporation model to determine the products (energy and angular distributions and multiplicities) from non-elastic collisions. The earliest version of HETC was developed by Coleman (Co 68); the code, referred to at that time as NMTC, was essentially limited to the calculation of cascades induced by protons of energies less than 3 GeV. A description of nuclear collision products was obtained by employing the intranuclear cascade code of Bertini (Be 63a, Be 67). Below 25 MeV, charged particle interactions were neglected and neutrons transported using the O5R Monte Carlo program of Irving et al. (Ir 65). The calculations of Armstrong and Alsmiller (Ar 68) referred to in Fig. 4.10 were made using this version of the code. Another comparison with experimental data is given in Fig. 4.11, taken from Armstrong (Ar 69a), where radial variations at different depths in iron of ^{54}Mn produced from Fe are plotted for incident proton energies of 1 and 3 GeV.

In a revised version of the code the upper energy was extended beyond 3 GeV using an extrapolation model by Gabriel et al. (Ga 70, Ga 71a,b). The earlier intranuclear cascade code of Bertini was replaced by his newer MECC-7 code (Be 69) and the evaporation part replaced by EVAP-4 code of Guthrie (Gu 70). This is the version of the code that is currently available and that was compared by Armstrong et al. (Ar 72) with the experimental data of Childers et al. (Ch 65), Citron et al. (Ci 65) and Van Ginneken and Borak (Va 71). Figures 4.12 and 4.13, taken from (Ar 72), indicate the comparisons with the last-two mentioned experiments.

Although an extremely powerful and flexible code, there is one major weakness and one operational inconvenience in HETC. The weakness is in its treatment of collisions above 3 GeV by the extrapolation model. It would be preferable to incorporate a more fundamental treatment of such high-energy interactions and this modification is currently in progress. The extrapolation model is being replaced by the EVENTQ event generator of FLUKA82 (described in the following section). The inconvenience is a direct consequence of the flexibility on the code in which each event in the cascade is written to a tape that must subsequently be analysed for the physical quantity of interest. Although this means that many more physical quantities may be scanned, it also means that those of particular interest are not immediately available as

output from the programme. User-written programmes must be prepared for analysis of the event tape.

The Hadron Cascade Code (FLUKA)

The FLUKA series of hadron cascade codes are based on the work of J. Ranft of CERN and the University of Leipzig, DDR. The first code was operational in 1965. These codes do not treat the intranuclear cascade and evaporation stages of the inelastic hadron-nucleus interaction as separate entities. Because the intranuclear cascade mostly contains particles below 1 GeV, it does not significantly affect the growth of the extranuclear hadron cascade for high-energy incident particles. Additionally, particles below a cut-off energy of 50 MeV are not transported but their energy is deposited locally. The codes are designed to rapidly reproduce the high energy characteristics of the cascade, representing the low energy part in only an approximate way. Macroscopic physical quantities such as the density of inelastic interactions or the density of deposited energy as a function of position in the cascade are available as standard output options. Other physical quantities are available through user-written subroutines. The earliest versions of the program were restricted to single medium problems in cylindrical geometry. The latest versions allow multimedia and a variety of geometry options.

In the earliest version, called TRANSK (Ra 67), the products of the inelastic hadron-nucleus interactions were generated from the Trilling representation of the inclusive production cross-sections (Tr 66). Kaon production in these interactions was ignored. In addition particle splitting was introduced in an attempt to improve the statistical accuracy of deep penetration problems. Figure 4.14 shows a comparison of a TRANSK calculation with data from Citron et al. (Ci 65, Ra 67).

In a parallel development to study the development of cascades in calorimeter detectors for physics experiments, the system for maintaining energy balance in inelastic interactions was improved and the particle splitting option removed, giving rise to the program FLUTRA (Ra 70a). Van Ginneken and Borak compared their measurements of the production of ^{18}F in aluminium samples placed in a steel beam-stop irradiated by 29.4-GeV protons with values calculated using FLUTRA. Figure 4.15 show this comparision for various depths and radial distances (Va 71).

Ranft introduced a new formulation of the inclusive particle production cross-sections, leading to the programs TRANKA and FLUKA (Ra 74). Results from TRANKA were compared to measurements taken outside an iron beamstop of 75 cm radius (Go 70a) and satisfactory agreement obtained. A summary of the status of the programs in 1972 is given by Ranft (Ra 72a). Sampling of intranuclear cascade particle from simplified analytic fits was also introduced (Ra 72b).

In recent years FLUKA has been completely rewritten but with most of the physics characteristics being maintained (Aa 84, Ra 85). The new program is called FLUKA82. The program works with a multiregion, multimaterial geometry. Cylindrical, Cartesian, spherical and combinatorial geometry options are available. The old inelastic event generator from the earlier programs has been maintained as an option (EVENTI),

but a new event generator (EVENTQ) is now the standard default option. This new generator is based on measured exclusive particle production cross-sections below 5 GeV and on a dual multistring fragmentation model for particle production above 5 GeV to about 10 TeV. Figure 4.16 shows part of the comparison of the present FLUKA calculations with data of Stevenson et al. in an aluminium beamstop (St 86a).

The Cascade Simulation Program (CASIM)

The Monte Carlo programme CASIM has been developed by A. Van Ginneken at the Fermi National Accelerator Laboratory. Details of the program are to be found in three articles by the author (Va 72b, Va 75a, b, and Va 80). CASIM was written to simulate the average behaviour of cascades developed by high energy hadrons (10–1000 GeV) in targets of large dimensions. It is a Weighted Monte Carlo program: only one high-energy secondary is generated per collision, but this carries with it a weight related to its probability of production. Path-length stretching and particle splitting have also been introduced. High-energy secondary particle production uses the Hagedorn-Ranft Thermodynamical Model (Ra 70b); the production of intranuclear cascade particles is based on the same formulae as used in FLUKA (Ra 72b). The macroscopic physical quantities available as standard output from the program include inelastic interaction (star) density and energy density as a function of position in the cascade. Particle fluxes, etc., can also easily be made available by the programme.

There have been no published systematic tests of CASIM against the experimental data used to test both HETC and FLUKA. However, in the development of CASIM it was shown that it gave essentially similar results to FLUTRA in an iron block bombarded by 29.4 GeV/c protons in regions where FLUTRA could be expected to give reliable results (Va 72b). CASIM also gave excellent agreement with experimental results around a medium-sized target bombarded by 300 GeV protons and embedded in a magnet (Aw 76). Recent comparisons by Cossairt et al. (Co 82, Co 85a) have shown agreement of CASIM calculations with experimental data obtained for complex extended shields and at energies up to 800 GeV.

Hadron Cascade Development Studies and Beam-Stop Design

The Monte Carlo methods just described may be used to generate the data required for the specification of shielding, even in the most complex geometries. For simple geometries it is possible to undertake a systematic study of the development of the hadron cascade and summarize a large body of data in the form of simple empirical models.

Such systematic studies of the development of the hadron cascade in shields of iron and concrete using the CASIM program have been undertaken by Van Ginneken and Awschalom (Va 74). The authors give contours of the density of inelastic nuclear interactions ('stars') produced by hadrons above a momentum of 0.3 GeV/c for incident protons having momenta of 30, 100, 300 and 1000 GeV/c. An example of such a contour map taken from that report is given in Fig. 4.17 for 30-GeV/c protons incident upon steel. The data derived from these and similiar calculations may be used in the specification of shielding both in the

longitudinal and transverse direction by relating the calculated star density to dose equivalent. Some care must be taken in determining the appropriate conversion coefficients because there are significant differences in the radiation spectrum in the transverse and longitudinal cases. In the former, neutrons are of primary concern, whereas in the latter both the high-energy hadrons and the products of the electromagnetic cascade must additionally be taken into account.

Forward Shielding for Beam-Stops

Figures 4.18 and 4.19 show the variation of dose equivalent along the proton beam axis calculated using the CASIM, FLUKA82 and TRANKA codes (Fr 71, St 86b, Va 74). Data are presented in concrete and steel for proton momenta from 1 GeV/c to 1 TeV/c. In the case of concrete (Fig. 4.19) there appears to be reasonable agreement between the data calculated by the FLUKA82 and CASIM codes at the depth were there is overlap (about 5 metres) and moderate agreement between the CASIM and TRANSK data (to within about a factor of four) at a depth of 14 metres. However, in steel a serious discrepancy is evident. The CASIM data are a factor of four higher than those from FLUKA82 but the CASIM and TRANSK data differ by more than three orders of magnitude. Similar discrepancies between the results of the calculations will also be evident when the transverse shielding case is discussed. No reasons have yet been suggested for these discrepancies. Consideration of Fig. 4.18 would suggest that in the case of steel the CASIM data are in error and that the TRANKA data might link smoothly to the FLUKA82 data. However, these data are separated by more than four orders of magnitude, and extrapolation of either set of data is extremely inaccurate. This comparison does, however, reveal the current limitations of the Monte Carlo techniques described here and should serve as a warning against extrapolation of their data beyond regions of known reliability.

In order to convert from the star density obtained from the Monte Carlo calculations to dose equivalent, the presence of pions and protons of about 50 MeV was taken into account. The 'forward' spectrum taken from the work of Stevenson (St 84) normalized between 50 and 100 MeV to the O'Brien spectrum (OB 71) was used to determine these conversion factors. Account was also taken for the contribution of electrons from the π^0 induced electromagnetic showers. The conversion coefficients obtained were 1.9×10^{-8} Sv cm^3/star for iron and 5.4×10^{-8} Sv cm^3/star for concrete.

Because of the complex longitudinal development of the cascade it is not possible, as is the case for transverse shielding, to specify a virtual source strength that is independent of the thickness of the shield. It is possible, however, to use an empirical formulation:

$$H(z) = S(z)\exp(-z/\lambda) \qquad (4.9)$$

for the dose equivalent at depth z in the shield.

Figures 4.20 and 4.21 show the value of S(z) as a function of depth in steel and concrete respectively over the energy range from 2 GeV to 1 TeV. The values of attenutation length λ are the same as those determined for the lateral shield case described in the following section

(viz., 1700 kg m^{-2} for iron and 1170 kg m^{-2} for concrete). With the approximation of the complex transmission curve by the simple exponential form of Eq. (4.9) the required value of the virtual source strength, S(z), approaches plateau values at large depths for the highest proton momenta, is nearly constant at momenta around 10 to 30 GeV/c and decreases with depth at the lowest proton momentum illustrated, perhaps because an equilibrium spectrum is never achieved at these low energies.

Transverse Shielding for Beam Stops and Targets

In many respects the problem of calculating transverse (overhead and lateral) shielding for targets operating in accelerator tunnels is similar to that of determining the lateral dimension of beam-stops. The calculations of the longitudinal development of the hadronic cascade described in the previous section and shown in Figs. 4.18 and 4.19 show that in concrete, even in the highest energies, the length of the radiation source along the incident proton direction is comparable or less than the lateral dimensions of the shielding. Under such conditions the radiation source may often be regarded as point-like (see appendix to this chapter).

In operating accelerators the longitudinal dimensions of the radiation source in may also be comparable with the lateral shield dimensions. Thus, for example, Gilbert et al. found that with a thin target operating in the 28 GeV CERN proton synchrotron the apparent radiation source had a relaxation length of about 6 metres (Gi 68). Interactions in the accelerator magnets of secondary particles emitted in the forward direction from the target resulted in the development of a hadron cascade similar to that generated in a beam-stop. Such conditions are often typical of those at operating accelerators, and represent those for which many transverse shielding measurements have been made.

Several experiments to study transverse shielding have been reported in the literature. One of the earliest studies was reported by Hoffmann and Sullivan, who measured the attenuation through steel of particles produced by the interaction of 20-GeV protons with a thin beryllium target (Ho 65). A series of measurements through the steel shield of the Brookhaven AGS (Di 65, Ca 67) was followed by an extensive series of measurements at the CPS (Gi 68, Gi 69). Bennett et al. have reported attenuation studies in a steel side shield above a thin tungsten target bombarded by 28-GeV protons (Be 71a). Other measurements are mentioned in the appendix to this chapter.

The transverse shielding problem for a target may be quite well treated by semi-empirical methods. The appendix to this chapter gives a detailed discussion of the Moyer model, which expresses the dose equivalent, $H(\theta)$, above a target as:

$$H(\theta) = \frac{N\psi(E_p)\ \exp(-\beta\theta)\ \exp(-\ell\ \mathrm{cosec}\ \theta)}{R^2\ \mathrm{cosec}^2\theta} \qquad (4.10)$$

where N is the number of protons interacting in the target and the other symbols are explained in the appendix. Appropriate values for the parameters $\psi_0(E_p)$, the source strength in forward direction, and β, the

angular relaxation parameter, are:

$$\psi_0(E_p) = 2.8\times10^{-13}\ E_p^{0.8} \quad \text{Sv m}^2 \quad (E_p \text{ in GeV})$$

$$\beta = 2.3 \text{ radians}^{-1}$$

The approximate value of the source strength parameter orthogonal to the beam direction, $\psi_{\pi/2}(E_p)$, is related to the value in the forward direction, $\psi_0(E_p)$, by the equation:

$$\psi_{\pi/2}(E_p) = \psi_0(E_p)\ \exp(-\beta\pi/2) \qquad (4.11)$$

with $\beta = 2.3$ radians, then:

$$\psi_{\pi/2}\ (E_p) = 2.70\times10^{-2}\ \psi_0(E_p) = 7.6\times10^{-15}\ E_p^{0.8} \quad \text{Sv m}^2 \qquad (4.12)$$

The computer calculations described in the previous section may also be used to determine transverse shielding. They have the advantage of being able to make computations for complex geometries inaccessible to the Moyer model. It is nevertheless interesting to compare the results of the conputer calculations with those of the Moyer model for several reasons, not the least of which is because the Moyer model is based on measured data.

The contours of star density in concrete and steel calculated for incident protons of energy between 30 GeV and 1 TeV using the CASIM programme are shown in Fig. 4.17. As in the case of the forward cascade, the star density can be related to the dose equivalent. There is considerable uncertainty in this conversion (see, for example, Th 85, St 86c). Van Ginneken and Awschalom used the following method (Va 74). The CASIM computer programme gives an indication of the hadron spectrum down to about 50 MeV. This is too high an energy cut-off to permit a reasonable estimate of dose equivalent and it is necessary to make some reasonable assumption as to the slope of the neutron spectrum below 50 MeV. Van Ginneken and Awschalom normalized their CASIM spectrum to that of neutron spectra determined by Gabriel and Santoro (Ga 71a). [There was overlap between the two calculated spectra between 50 MeV and 300 MeV.] By assuming the hadron spectrum was entirely composed of neutrons (see Chapter 2) and using the maximum dose equivalent (MADE) conversion coefficients (see Chapters 2 and 3), Van Ginneken and Awschalom obtained conversion factors of 3.5×10^{-8} Sv cm^3/star in iron and 9.0×10^{-8} Sv cm^3/star in concrete. These conversion factors are conservative for two reasons: first, conversion coefficients for the MADE are used, and second, the neutron spectrum used for the normalization was determined inside a concrete shielded cavity in the forward direction from a target and so contains neutrons reflected from the concrete as well as low energy evaporation neutrons from the target which will not be present in the equilibrium cascade. A more appropriate spectrum to use is that determined by O'Brien (OB 71) for a concrete side shield which is given in Fig. 2.4. When the H_s conversion factors are used to relate dose equivalent to neutron fluence for the O'Brien spectrum normalized to the FLUKA82 spectrum in iron (see Chapter 2) and adding the contribution

from electrons generated in the electromagnetic shower arising from the decay of π°-mesons, as calculated from FLUKA82, conversion coefficients of 1.2×10^{-8} Sv cm^3/star in iron and 4.5×10^{-8} Sv cm^3/star in concrete are obtained. These are the conversion coefficients used in the subsequent analysis described here.

From the contour plot of Fig. 4.17 it will be seen that the longitudinal position of the maximum star density does not vary strongly with radius. One could reasonably assume that, as far as the radial development of these maxima are concerned, the core of the cascade acts as a point source. In this case the maximum star density should vary as the inverse square of the radius multiplied by some exponential term. Figures 4.22 and 4.23 indicate the dose equivalents corresponding to the longitudinal maxima of the star density contours of Van Ginneken and Awschalom, multiplied by the square of the radius, as a function of radius for iron and concrete shields respectively. Also shown in these figures are the results of recent calculations by Stevenson using the FLUKA82 cascade program. There is excellent agreement between the results of the CASIM and FLUKA82 programs except in regions where poor statistics play an important role. The FLUKA82 calculations cover a wider range of incident proton momenta that the CASIM calculations. It will be seen that the empirical approximation described above can be considered as justified. The apparent absorption mean free paths are 1700 kg m^{-2} for iron and 1170 kg m^{-2} for concrete, the latter being identical to the absorption mean free path found appropriate for use in the Moyer model (see appendix to this chapter).

For completeness the results of calculations using the TRANKA programme are also included in Figs. 4.22 and 4.23. As in the case of the longitudinal cascade there are puzzling discrepancies. In the case of steel, the FLUKA82 and CASIM data do not seem to join smoothly with the TRANKA calculations and the absorption mean free paths differ. In the case of concrete the absorption mean free paths appear the same but the TRANKA calculation are some two orders of magnitude higher than the FLUKA82 and CASIM calculations would suggest. No reasons can be given for these discrepancies, but they do indicate the need for increased vigilance when using computer codes in shield design and for comparison with measurements wherever possible.

The intercepts of the exponentials at zero depth in Figs. 4.22 and 4.23 give the constant $\Psi_{\pi/2}$ for use in the empirical formula

$$H = \psi_{\pi/2}(E_p)\ \exp(-x/\lambda)/r^2 \qquad (4.13)$$

where the variables have their usual meaning. These constants $\Psi_{\pi/2}$ have been plotted against energy in Fig. 4.24. The points at an energy above about 1 GeV can be well fitted by an $E^{0.8}$ power law giving the following relationship:

$$\psi_{\pi/2}(E_p) = 6.6 \times 10^{-15}\ E_p^{0.8}\ \text{Sv m}^2 \qquad (4.14)$$

for a concrete shield, where E_p is the energy of the incident proton energy. The point at a proton momentum of 1 GeV/c (energy of 400 MeV) is low probability due to the failure of the concept of an equilibrium

spectrum for relating star densities to dose equivalent. Equation (4.14) is in good agreement with that derived from a composite set of measurements at accelerators, made under a variety of experimental conditions at accelerators (see appendix to this chapter):

$$\psi_{\pi/2}(E_p) = 7.6 \times 10^{-15} E_p^{0.8} \quad \text{Sv m}^2$$

Comparison between these two estimates of $\psi_{\pi/2}$ is difficult firstly because the target conditions at the accelerators were diverse and the computation of dose equivalent is subject to considerable variability (Th 85). It seems most likely that the accelerator measurements were made with radiation sources that were effectively 'thick targets' because of secondary interactions with accelerator components and beam transport elements. In this case the two estimates of $\psi_{\pi/2}$ are comparable and the agreement is gratifying.

As an indication of the uncertainties involved two sources of variability may be explored:

- Dose equivalent estimation
- Target thickness

The value of $\psi_{\pi/2}$ strongly depends upon the conversion coefficients from star density to dose equivalent used. If the Van Ginneken and Awschalom conversion coefficient is used the value of $\psi_{\pi/2}$ doubles compared to the values given above. However the Van Ginneken and Awschalom conversion coefficients are generally believed to be very conservative.

In attempt to understand the effect of target thickness the programme FLUKA82 was used to simulate the geometry of the target situation used to derive the constants for the Moyer model. The results are given in Table 4.4.

The results show that, as expected, the value of $\psi_{\pi/2}$ increases with target thickness. If it is assumed that the accelerator measurements were made with sources that were effectively infinitely thick the calculations of Table 4.4 suggest reasonable agreement with the empirical data. It would be interesting to establish a series of measurements under well controlled target situations in simple geometries to compare calculations and measurements (Th 78). Whatever these studies reveal, it is clear that the present agreement in estimates of $\psi_{\pi/2}$ is perhaps better than could be expected considering the uncertainties in dose equivalent estimation.

Muon Shielding

It is usually only at proton accelerators with energies above 10 GeV that the specification of shielding against muons is needed. For completeness a brief discussion is given here with references to the scientific literature that enable the interested reader to find further details. (See also the section of Chapter 2 entitled The Charged Particle Environment outside High-Energy Proton Accelerator Shields.)

Muons were first identified as a significant problem during the initial operation of the 30-GeV AGS of the Brookhaven National Laboratory (Co 62) and are commonly observed at the very high energy

accelerators at CERN, Fermilab and Serpukhov (Be 71b, Co 83, Ka 72b, Ni 74, Th 71). Examples where muons have dominated the radiation environments around such accelerators have been given in Chapter 3 in the section entitled 'Intercomparison of Dose Equivalent Determinations'.

At high energy physics laboratories sophisticated radiation-transport programmes are usually available and are routinely used to specify shielding against muons. In many (or most) practical situations the physical configuration of the accelerator components, beam transport systems and shielding together with the presence of magnetic fields make the calculation of muon transport extremely complicated. Resort to transport codes based on Monte Carlo techniques, such as those available at high-energy physics laboratories, is usually necessary. In consequence muon shielding is routinely specified using such methods and particular shielding problems have been solved as needed. There has been little attempt [save in the work of Keefe and his colleagues (Ke 64, LBL 65, Th 64c)] to develop simple empirical formulae containing a few derived parameters for the specification of muon shielding in simple geometries as there has been, for example, in the case of neutron shielding. Analytical techniques are severely limited because of the complexities we have just described. Nevertheless, an attempt is made here to summarise the muon shielding problem in analytic terms, so that the reader may understand the essential points.

In what follows the development of muon source terms, the radial diffusion of muons as they pass through the shield, the experimental verification of Fermi-Eyges theory and practical shield design will be described.

Source Terms

As we have suggested, the diffusion of muons through shielding materials can be treated by analytical or Monte Carlo techniques; both methods have their advantages and limitations. In either case the first step required is to describe the source term. Analytical representation of the source term is possible when, for example, the muons are produced by the decay of kaons or pions collimated in a beam (Ke 64). However, when the muons are created more diffusely, for example, by the decay of pions resulting from proton interactions in a thick shield, an analytical representation requires a very simplified empirical description of the pion production-which may result in errors. Alternatively, more complex particle-production models may be used requiring Monte Carlo techniques. When the muons produced have to be transported through regions of a shield that contain magnetic fields the use of Monte Carlo techniques becomes essential.

The Muon Distribution Function

The spatial and angular distributions of a beam of particles that on passing through a layer of matter undergoes multiple scattering are described in a theory developed by Rossi and Greisen (Ro 41, Ro 52) following the treatment of Fermi (Fe 40), and extended by Eyges (Ey 48) to include the slowing down of particles while passing through the layer. From the results of Eyges, it can be shown that the radial distribution of particle fluence at a given depth in the scattering material,

independent of angle to the beam axis, is given by:

$$\phi(r) = N_o \exp[-r^2/(4A_2)]/(4\pi A_2) \quad , \tag{4.15}$$

where r is the radial distance off-axis, N_0 is the number of particles incident in the pencil beam and A_2 an area given by the following integral:

$$A_2 = \int_0^z \chi^2(t)\ (z - t)^2 dt \quad , \tag{4.16}$$

where z is the depth of the plane of interest in the shielding or scattering material and χ^2 is one-quarter of the mean square scattering angle per unit distance. The dependence of χ^2 on the position in the shield, t, is given through the momentum of the particle at that position. In the Fermi-Eyges theory, all range-straggling is ignored and the range-momentum relationship is considered to be monotonic. All scattering is considered to be the sum of many individual small-angle scattering processes. It was shown by Alsmiller et al. (Al 71) that the integration in Eq. (4.16) rigorously holds true for shielding consisting of slabs of different materials, even vacuum.

Scattering and Energy Loss

An essential part in the use of the Fermi-Eyges distribution function is the determination of the mean square angle of scattering per unit distance. There are four principal scattering processes for high energy muons:

(i) Coulomb scattering from the nuclei of the medium, and to a lesser extent from the orbital electrons,

(ii) bremsstrahlung from muon-nucleus collisions,

(iii) pair production from muon-nucleus collisions, and

(iv) muon-nucleus non-elastic collisions.

An approximate expression for Coulomb scattering is (Ro 52):

$$\chi_c^2 = \pi(m_e/p\beta)^2/(\alpha X_0) \quad , \tag{4.17}$$

where α is the fine structure constant, m_e is the mass of the electron, p is the muon momentum in units corresponding to m_e, β is the relativistic velocity of the muon and X_o is the radiation length of the material. Alsmiller et al. (Al 71) used the formulation of Hofstadter (Ho 56) to obtain values for the Coulomb differential scattering cross-section and showed that the values of χ_c so obtained did not significantly differ from those given by Eq. (4.16) for use in muon transport calculations.

The remaining three scattering processes differ from multiple Coulomb scattering in that, although of low probability, they have the potential for large-angle scattering, coupled with significant energy loss of the muon. The cross-sections for these processes only become important at muon energies above about 200 GeV, and they are discussed in detail by Alsmiller et al. (Al 71) to which the interested reader is referred. Monte Carlo programs that divide the track of a muon into

many small segments and calculate the scattering in each segment can treat these phenomena adequately. Analytical calculations treat these single-event processes in the same approximate manner as is used to treat Coulomb scattering, calculating mean square angles of scattering for each process and then summing the different processes in a Gaussian manner (Al 71).

The energy loss of muons from the ionization and excitation of atomic electrons is well established and may be computed from the Bethe-Bloch formula (Be 63b) with the density effect correction given by Sternheimer (St 71a). Muons also lose energy by bremsstrahlung production, direct pair production and inelastic nuclear collisions (Ko 67, Th 64c). The continuous slowing down approximation is used in most muon transport calculations, i.e., straggling is ignored, single large energy loss processes are averaged and a single value of the range is assumed for any momentum value.

Justification of Fermi-Eyges Theory

Until quite recently the calculation of muon transport depended entirely upon theoretical studies. No direct experimental verification of Fermi-Eyges theory, upon which these calculations heavily depend, was obtained until 1983 (Ne 83). In fact one measurement at the Stanford Linear Accelerator suggested a muon fluence at large angles much larger than predicted by Fermi-Eyges theory (Ne 68). This difference was further supported by a number of comprehensive experimental and theoretical studies of the production and transport of muons at electron accelerators (Al 69c, d, Ne 68, Ne 74a, b). In order to resolve this discrepancy, measurements of muon fluence were made in the shielding behind the CERN muon beam (Ne 83). Measurements were made of the fluence of muons as a function of radial distance at a distance of about 350 m in the earth shield, at muon energies from 200 to 280 GeV and with different measurement techniques: a scintillator telescope, a semiconductor detector telescope and nuclear emulsions (Ne 83). The fluence measurements made by these different techniques were in agreement. The experimental data were compared with transport calculations based on the Fermi-Eyges theory. Two codes were used: the analytic code TOMCAT (St 81) and the muon section TRANMU of the Monte Carlo hadronic cascade code CASIM (Va 75). The predictions of TOMCAT and TRANMU were in general agreement with each other [see Fig. 4.25 taken from (Ne 83)], and, except near the end of the muon range where straggling effects become important, there was also good agreement between the predictions of TOMCAT and the measured fluences [see Fig. 4.26 (Ne 83)]. One may conclude that the Fermi-Eyges theory can be used with some confidence for the estimation of shielding around proton accelerators where the transport of muons has to be combined with muon source terms arising from direct production and the decay of pions and kaons.

Practical Shield Design

One convenient approach to shielding muon beams is to place sufficient material in the forward direction so that the muons are completely stopped. This may be done by determining the mean range from the graph of range versus energy in Fig. 2.6 and adding about 20% to allow for straggling (St 76). This approach will usually be extremely

conservative.

An improved technique is to determine the radial width of muon distribution at different depths in the shield using Eq. (4.16). (For most purposes Eq. (4.17) gives a sufficiently accurate estimate of χ^2.) Contours of equal muon fluence may then be determined to guide the shield design. If one assumes a constant energy loss per unit distance in the shield then Eq. (4.16) is analytically integrable (Ke 68). Since the muon energy spectrum from pion decay is also flat (see for example Ke 64 and St 76) it is simple to integrate Eq. (4.15) over muon energy to derive the appropriate radial distribution in the case of muons from a pion beam. In practice, however, pion beams have finite momentum spread, divergence and spot size, which make direct integration difficult. The program TOMCAT was designed to ease the calculation in cases of real pion, kaon and muon beams (St 81). One important parameter in these calculations is the distance available for decay of pions and kaons into muons, Δ. While the radial profile does not greatly depend upon Δ, unless the divergence of the beam is large, the number of muons produced is strongly directly dependent on this distance. For short distances and high momenta the decay probability is directly proportional to Δ. The decay probability of a pion can be expressed in terms of a decay length whose value expressed in metres is 55.9 times the pion momentum in GeV/c (Ke 64): for kaons the multiplication constant is 7.51 (St 76).

Muon production from the decay of pions produced in proton interactions was treated by Keefe and Noble (Ke 68). Their program was slightly modified by Stevenson and Routti by removing unnecessary iterations to determine fluence contours, improving the pion production formulae and making the input to the programme more flexible. This revised version is available as the MUSTOP program (St 79). MUSTOP has been successfully compared against experimental data for proton momenta between 10 and 23 GeV/c (Ho 80, Li 80). Typical attenuation curves in both the longitudinal and radial directions for shields of steel (density 7.8 g/cm^3) and concrete (density 2.4 g/cm^3) are given in Figs. 4.27 to 4.30. In the case of the radial direction (Figs. 4.29 and 4.30) the maximum of the muon fluence that occurs at a given radius (independent of the longitudinal depth at which it occurs) is plotted as a function of that radius–as was done for the hadron end-stop case. Curves are given for proton energies of 10 to 1000 GeV and assume an available decay length of 1 m. In the longitudinal direction care should be taken when scaling to very much larger available decay lengths to include an inverse square law factor. These curves can also be used for muons coming from proton induced cascades in end-stops since the most energetic pions (and hence muons) will be produced in the first proton interaction. For an end-stop situation, Keefe and Noble showed that an effective length available for decay was 1.8 times the hadron absorption length (Ke 68); thus the values of dose-equivalent per proton given in Figs. 4.27 to 4.30 would have to be multiplied by a factor of 0.3 for steel and 0.8 for concrete. Care should also be taken not to use these data at shallow depths in the end-stop situation since many more low-energy muons will come from decays of cascade particles. A correct treatment of the cascade case is given by Van Ginneken in the CASIM program (Va 75).

It will be noted from the longitudinal attenuation curves of Figs. 4.27 and 4.28 that the attenuation at energies of less than 50 GeV is approximately exponential. This was noted experimentally by Drugachenok et al. (Dr 71), and Sullivan (Su 85) was able to theoretically justify the exponential shape. Sullivan showed that the muon flux at a distance x behind the point of interaction of a proton of energy E GeV and where pions have a path length of Δ metres in which to decay is:

$$\phi = 8.5 \times 10^{-2} \, E\Delta \exp(-\alpha t/E)/x^2 \qquad (4.18)$$

where t is the shield thickness in metres and α is an effective muon energy loss rate which has a value of 22 GeV/m for iron and 7.8 GeV/m for concrete. It was further shown that the effective muon attenuation mean free path is equivalent to 1/16 of the range of a muon with the energy of the interacting proton. This simple formula gives satisfactory predictions in the energy range 10 to 30 GeV.

4.5 TUNNELS, DUCTS AND LABYRINTHS

INTRODUCTION

In the construction of an accelerator installation some importance must be attached to the adequate design of

- Tunnels through the main biological shield for access of personnel and equipment.
- Ducts to allow the connection of essential services such as water, air, radiofrequency power and cryogenic cooling lines for the accelerator.

These ducts and tunnels act as leakage paths for radiation, especially low energy neutrons. They also remove absorber from the shield, reducing the effectiveness of the shield, particularly in the region of the penetrations. Thus they must be carefully designed such that their presence does not impair the efficiency of the main shield.

The streaming of neutrons along ducts is an important aspect of shield design for fission reactors (IAEA 68), and because of recent interest in fusion reactors, there have been several experimental and theoretical studies of the attenuation of 14 MeV neutrons in ducts (see for example Ha 83, Sa 82, Sa 83). However, in reactors the ducts are generally only for utilities and are rather small (of the order of 0.5 m × 0.5 m). At accelerator installations, in addition to such service-ducts, much larger passages are required both for the entry of personnel and for the movement of equipment. The width of personnel entries may be quite large (1.2 m or more), particularly if emergency fire and medical services are to be permitted efficient access and egress. Equipment access may require even larger ducts. For example, at the CERN SPS equipment access ducts with diameters up to 9 m are provided. In ducts of such large cross section the scattering of neutrons around corners by collisions in the air as well as by collisions at the duct wall may become important. At the largest accelerators where tunnels and ducts may be as long as tens, or even hundreds of metres, the scattering and attenuation in the air may become a significant factor.

The major theoretical and experimental studies of the transmission of radiation by tunnels have concentrated on neutrons produced by reactors. An excellent summary of the state of knowledge up to the mid-fifties is given by Price, Horton and Spinney (Pr 57). Early work is also reviewed in Chapter 8 of the Engineering Compendium on Radiation Shielding (Vol. 1) (IAEA 68). The more recent book by Chilton et al (Ch 84) also contains a summary of ideas useful in calculating the transmission of neutrons and photons in ducts. Russian experience is summarised in a book by Zolotukhin et al. (Zo 68) [see also (Bo 71)].

CALCULATION OF RADIATION TRANSMISSION THROUGH DUCTS AND LABYRINTHS

There are several types of Monte Carlo techniques that are applied to duct and labyrinth transmission problems. One of these is the strictly analogue Monte Carlo calculation that simulates the most important interactions occuring as the neutrons traverse the duct system. The calculations are based on interactions at the nuclear level. Particle tracks are sampled from probability distributions corresponding to microscopic elemental cross-sections. One such analogue Monte Carlo programme that has been applied to labyrinth calculations at accelerators is SAM-CE (Co 72, Co 73). This programme was used by Vogt in its analogue mode to study access-ways at the CERN SPS (Vo 75).

Because of the enormous computer time required in the execution of purely analogue programmes that track particles in regions of space that may be of little interest to the problem in hand, weighted Monte Carlo codes such as MORSE (Em 75) can be much more efficient for duct-attenuation calculations. Although differential cross-sections at the nuclear level are again used, various techniques of variance reduction can be employed to 'point' particle tracks to low probability regions of interest, e.g., down the tunnel and around the bends, rather than tracking particles for long times in the tunnel walls. An example of the use of the MORSE code in the tunnel attenuation problem around accelerators is given by Ye (Ye 82).

One way of making duct calculations even more efficient uses the albedo concept in which the reflecting properties of the tunnel walls are parametized in great detail. The total effect of an interaction with a duct wall is assumed to be either absorption in the wall or a reflection back into the duct at the point of incidence, with a probability equal to the total albedo. The direction and energies of the reflected neutrons are determined from probabilities derived from the double-differential albedos, which are functions of the angle of incidence and the initial energy of the neutron, as well as of the reflected polar and azimuthal angles, and the energy of the reflected neutron. The albedo concept is based on the assumption that when a neutron enters the wall of a tunnel, the area from which the neutron may re-emerge around the entry point is small compared with the cross-sectional area of the duct. It was shown by Maerker and Muckenthaler (Ma 67a) that this concept was valid in multilegged ducts provided that the lateral dimensions of the duct exceeded 0.3 m. The multi-group transport code AMC (Ma 67b) is based on this albedo technique, and was used by Alsmiller and Solomito (Al 69e) in a duct study at the Princeton PPA and by Routti and van der Voorde (Ro 72a) to study tunnels in the shielding of the CERN ISR.

It is also possible to run the MORSE programme in the albedo mode, the limitation being the availability of albedo data. In the middle 1970s double-differential albedos with respect to angle of incidence and neutron energy had been measured and calculated only for concrete (Ma 65, Ma 66, Co 67). At the present time, calculated albedo data is available for four materials (water, ordinary concrete, carbon steel, and steel-over-concrete) and can be prepared for use in the MORSE programme (Em 78, Ca 79); to date no comparison of experimental data with predictions made using this option of MORSE have been made for tunnels leading to accelerator enclosures.

A simplification of the multi-group albedo concept can be made by assuming that attenuation of absorbed dose, or dose equivalent, along a multilegged duct can be described by the albedo properties of a single energy group of neutrons. The ZEUS code of Gervaise and d'Hombres (Ge 68) makes use of this assumption. d'Hombres et al. found that the energy group between 3 and 4 MeV most closely approximated dose in its transmission properties along tunnels of the CERN PS (d'H 68). The ZEUS program was used systematically by Gollon and Awschalom in designing the access-ways of the Fermilab accelerator (Go 71) and by Routti and van der Voorde in the CERN ISR studies (Ro 72a).

MEASUREMENTS OF THE TRANSMISSION OF STRAIGHT DUCTS

There have been many measurements of the transmission of accelerator-produced radiation through tunnels in recent years. In one of them, reported by Gilbert et al. (Gi 68), several radiation radiation detectors were used to provide some information on the dose spectrum. Table 4.5 summarizes the detectors used and their important characteristics. The data presented here were obtained with 14-GeV protons hitting a clipper-target, providing an intense well-localized source just opposite and 3.2 m from a tunnel entrance. The tunnel was 2.8 m high by 1.8 m wide and 100 m long. Detectors were suspended approximately at its geometric centre and along its length. Figure 4.31 summarizes the transmission data obtained using the different detectors. Because of the varied accelerator operating conditions during which these data were obtained it was not possible to normalize them in terms of circulating beam intensities. For convenience therefore the data were normalized to unity at a depth of 0 m. A systematic trend may be seen in Fig. 4.31 in that the higher the threshold of the neutron detector, the larger the flux transmission. Thus the difference in overall transmission between thermal and ^{11}C neutrons is more than a factor of 10 at 80 m.

It was concluded from these data that the flux transmission T of a tunnel could be expressed as a function of depth z along the tunnel, the effective tunnel radius a and the energy response E of the detector:

$$T = \Gamma(z/a,E)\ \exp[-z/\lambda(E)], \qquad (4.19)$$

where $\Gamma(z/a,E)$ is the transmission of the tunnel uncorrected for neutron-absorption processes and $\exp[-z/\lambda(E)]$ is a correction factor which takes account of neutron interactions in the air along the tunnel. The mean-free-path, $\lambda(E)$, was assumed to be related to the neutron total cross-section in air. At large values of (z/a) it is to be expected (Pr 57) that

$$\Gamma(z/a,E) \rightarrow (a/z)^2 \qquad (4.20)$$

for z /a> 10, and thus a semi-log plot of z^2T should give a straight line with negative slope $\lambda(E)$. Figure 4.32 shows such semi-log plots of $z^2\phi$ (proportional to z^2T), against z for the bare-gold, film badges and TLD, aluminium and carbon detectors. For depths greater than 20 m in the tunnels, the attenuations are nearly exponential. Table 4.6 lists the estimated removal mean free paths and the corresponding removal cross-sections, assuming an atmosphere of nitrogen. At neutron energies between 1 and 20 MeV, the inelastic cross-section for nitrogen is 200 mb and the total cross-section 2 b, generally smaller than the values listed in Table 4.6

In another experiment, Stevenson and Squier (St 73) measured neutron transmission along a shorter tunnel (2.3 × 2.3 m^2 cross-section by 18 m length). The copper target providing the source of the radiation was bombarded by 7 GeV protons and was exactly on the tunnel axis, 1.9 m from its mouth. In addition to the detectors listed in Table 4.5, teflon cylinders (in which the $^{19}F(n,2n)^{18}F$ reaction with an 11 MeV neutron threshold was measured) were exposed. The data from the aluminium, teflon and plastic scintillator detectors were well fitted by an inverse-square dependence on distance from the target modified by an exponential attenuation with a mean free path of 60 m, identical to the value found for the aluminium detectors by Gilbert et al. (Gi 68), see Figure 4.33. The transmission curves for the moderated indium detectors and the various dosimeters used were similar to those of the higher energy threshold detectors. However, as is seen in Figure 4.33, the thermal neutron detectors indicated considerable enhancement of the fluence by wall-scattering.

The apparent exponential attenuation reported in these two experiments is difficult to explain in terms of interactions in the air. A mean free path of 60 m implies a removal cross-section of 3.2 b, which is considerably higher than the 1 to 2 b total cross-sections for nitrogen and oxygen in the 1–50 MeV neutron energy region. The presence of water vapour cannot give rise to an effect of this magnitude since the proportion by weight of water in the atmosphere is of the order of a percent, while the total absorption cross-section of hydrogen in the 1 MeV region is about 1 b. A possible explanation was provided by Ye (Ye 81) who was unable to match the experimental transmission curves in the MORSE calculations reported in (Ye 82) unless he included scattering of neutrons from the walls of the target enclosure in front of the tunnel entrance. This enhanced the response of the detectors near the mouth of the tunnel but, because these neutrons were not transmitted down the tunnel the responses of detectors deeper in the tunnel were not correspondingly increased. This enhancement of detector response at the tunnel entrance was greater for the neutrons of lower energy and naturally leads to a somewhat steeper than inverse-square dependence when the data are normalized to the response of the detector at the tunnel mouth.

MEASUREMENTS OF TRANSMISSION IN LABYRINTHS

Experiments reported by Shaw (Sh 66) showed that at the exit of both curved and multi-legged straight ducts (labyrinths) the dose equivalent is dominated by the contribution from low and intermediate

energy neutrons. In one of the first detailed experiments in labyrinths at accelerators, Schimmerling and Awschalom (Sc 69) used activation detectors similar to those listed in Table 4.5 to measure fluxes in a four-legged labyrinth. The radiation source at the labyrinth entrance was produced by 3 GeV protons interacting in a lead target. Alsmiller and Solomito used the AMC code to reproduce these measurements by calculation (Al 69e). Good agreement was obtained between the numerical predictions and the transmission as measured by the thermal neutron fluence and the integrated neutron fluence when the target was directly opposite the tunnel mouth. With the target in an off-axis position, the calculated flux densities were consistently lower, by a factor of two or three, than those measured.

Stevenson and Squier (St 73) also reported measurements of the change in spectrum at a right-angled bend in a labyrinth and of attenuation in the second leg of a concrete-lined tunnel. Figure 4.34 shows the experimental arrangement for these labyrinth measurements and Figure 4.35 shows the experimental data obtained in the first and second legs with the detectors discussed previously. In the second leg, all detectors show a more rapid attenuation than would be obtained for the same centre-line distance along a straight tunnel: an extra transmission factor of about 10^{-2} was achieved only 5 m inside the second leg of the tunnel compared with about 0.3 in 10 m for the corresponding section of the straight tunnel. The effect is most marked for the detector with the highest threshold energy: $^{12}C(n,2n)^{11}C$ in a plastic scintillator.

The data for the aluminium and moderated indium detectors taken from the second leg, normalized to unity at the mouth of this leg, are shown in Fig. 4.36. Also shown in this figure is a prediction from the 'universal curve' of Gollon and Awschalom using the ZEUS program (Go 71), where albedo coefficients corresponding to neutrons in the energy range 3–4 MeV were used. This universal attenuation curve is so-called because it has the depth in the tunnel measured in units of $z/\sqrt{A}$, where z is the physical depth in the tunnel and A is the cross-sectional area, and it may thus be applied to tunnels of different radius. This scaling behaviour of transmission in tunnels is suggested by the original analytical work of Simon and Clifford (Si 56). The ZEUS 'albedo' curve lies between the two experimental curves in Fig. 4.36 for aluminium detectors with a neutron threshold of 6 MeV and for the moderated indium detectors which respond mainly to neutrons of below 1 MeV (Sh 67). Thus the albedo properties used in determining the transmission in the second leg are consistent with the experimental data as far as neutron energy is concerned (3-4 MeV). In addition Fig. 4.36 shows the calculations of Ye using the MORSE code (Ye 82) for different energies of source neutrons, where the known detector cross-sections were folded with the calculated neutron spectra at the measurement points. It can be seen that there is excellent agreement between the measured and calculated data and that the transmission in the second leg, within the neutron energy range from 1.5 to 20 MeV, is essentially independent of the energy assumed for the neutron source. The data of a transmission experiment in a multi-legged duct by Borodin et al. (Bo 71) are in good agreement with the data described here.

From the fluence rate measurements, Stevenson and Squier evaluated the resultant neutron dose-equivalent rates by the method suggested by Shaw et al. (Sh 69a). In their work, Stevenson and Squier used the factors to convert the fluence measured by the ^{11}C and moderated indium detectors based on the dose-equivalent quantity practical dose equivalent, H_p, as discussed in Chapters 2 and 3. The two theoretical calculations using MORSE and ZEUS used the maximum dose equivalent (MADE) concept, H_m. It therefore seems more appropriate to convert the fluence data of Stevenson and Squier to maximum dose equivalent using the conversion factors to be found in Shaw et al. (Sh 68). Figure 4.37 shows a comparison between these dose equivalent rates and those calculated from the ZEUS-albedo 'universal curve' (Go 71) and the MORSE calculations of Ye (Ye 82). The measured transmission is considerably higher than the albedo calculation and is closer to the MORSE calculation using a source energy of 1.5 MeV. This confirms the conclusion of Stevenson and Squier (St 73) that the use of albedo coefficients corresponding to a neutron energy somewhat lower than 3–4 MeV in calculations of the ZEUS programme type would give results in better agreement with measurements in accelerator-radiation environments.

PREDICTION OF TRANSMISSION IN DUCTS AND LABYRINTHS

One can conclude from measurements of the transmission of ducts and labyrinths made for accelerator radiation environments described in the previous sections that the overwhelming proportion of the dose equivalent transmitted is contributed by source neutrons in the energy range from 1 to 20 MeV.

Calculations by Vogt using the SAM-CE code (Vo 75) and by Gollon and Awschalom with ZEUS (Go 71) both show a dependence with distance along the first tunnel which is faster than that expected from the inverse square law. As we have already suggested in the section describing the measurement of straight duct transmission, this is probably due to the scattering and reflection of low and intermediate energy neutrons into the tunnel entrance from the accelerator room. Goebel et al (Go 75) have derived a composite curve from the SAM-CE and ZEUS calculations which may be used to design straight tunnels or the first leg of multi-legged tunnel (or labyrinth). Their curve, which is shown in Fig. 4.38 (indicated by the label 'point'), may be used when the dose equivalent produced by neutrons between 1 and 20 MeV at the entrance to the tunnel is known.

If the tunnel is to be designed from known or expected beam losses, instead of a defined dose equivalent rate at the tunnel entrance, the neutron yield in the 1–20 MeV range from the effective source must be determined. This may then be converted to dose equivalent using a conversion coefficient. When the point-source is in full view of the back end of the duct, a simple inverse square law can be used to determine the neutron fluence at the end of the duct. It is suggested that an appropriate coefficient to convert the apparent neutron fluence to dose equivalent is 20 fSv m^2 (1 neutron/(cm^2 s) is equivalent to 0.07 mrem/h). Both thin and thick target neutron yield data are available. The experiments of Stevenson and Squier (St 73) allow one to obtain a source term for those neutrons detected by a moderated thermal neutron detector which are produced in a copper target: giving a figure of one

neutron produced per 1.6 GeV of proton energy lost from the beam at 7 GeV (at 90° to the incident proton beam). The yield experiments of Stevenson et al. at proton energies from 7 to 400 GeV (St 71b, St 83) suggest that since the neutron multiplicity scales as $E^{0.25}$, the energy required to produce a neutron scales as $E^{0.75}$ above an energy of 7 GeV. Below this energy the thin-target curve of Fig. 4.6 may be used to scale the neutron yield. For a thicker target there is evidently an optimum size of block in which the cascade develops to produce the maximum number of neutrons. It was suggested by Routti (Ro 72a), based on the HETC calculations of Armstrong and Alsmiller (Ar 69b) and Armstrong and Barish (Ar 69c), that one neutron would be produced per 0.25 GeV of energy from a proton beam at 25 GeV. This thick-target yield is expected to scale as $E^{0.8}$ (see the section on high-energy shielding) leading to a scaling law of $E^{0.2}$ for the energy required to produce a neutron. This scaling law is expected to be valid above a proton energy of 3 GeV. Below this energy, scaling according to the 'thick target' curve of Fig. 4.6 should be used.

Figure 4.38 also summarizes the first-leg transmission for source conditions other than the point source on the tunnel axis. These curves are again composites from SAM-CE, ZEUS and AMC calculations. The values of the dose equivalent at the tunnel mouth should either be known from measurements or estimated using the inverse-square law approximation and the source strengths discussed in the previous paragraphs.

We have already suggested that the transmission of tunnels of different size might be compared by using a 'universal curve' in which length along the tunnel is measured in units of $z/\sqrt{A}$. The studies of Vogt (Vo 75) show that there strictly could be no such 'universal curve' describing transmission in the second leg of a tunnel if the height:width ratio were allowed to vary outside the range 0.5–2.0. Nevertheless, Goebel et al. (Go 75), by summarizing SAM-CE, AMC and ZEUS calculations, and taking into account the available experiment data, suggested that in most cases the transmission would lie close to the solid line in Figure 4.39. Generalized AMC calculations and the data from the NIMROD experiment lie close to this solid line; some SAM-CE calculations showed a higher transmission and their upper limit is shown by the upper dotted line in Figure 4.39. The ZEUS-albedo calculation (the Gollon and Awschalom "universal" curve) is the most optimistic, giving the lower bound shown by the other dotted line in Figure 4.39. It was proposed (Go 75) that the solid line should give a satisfactory way of obtaining the transmission in the second leg of a multi-legged, concrete-lined tunnel, with the dotted lines indicating appropriate confidence limits. Both Gollon and Awschalom and Goebel et al. from theoretical arguments (Go 71, Go 75) and Stevenson and Squier from an experimental stand-point (St 73) suggest that the 'second-leg curve' can be used to predict transmission in subsequent legs of multi-legged ducts.

An alternative approach to the prediction of tunnel transmission was proposed by Tesch (Te 82). Based on the similarity of the spectrum of neutrons from an Am-Be source to the spectrum of neutrons due to beam losses at high-energy electron accelerators, and on experimental data for the transmission of Am-Be neutrons in concrete-lined labyrinths, he

presented two empirical formulae for describing the transmission of dose-equivalent in a labyrinth. The first equation is an inverse-square law, modified by a simple in-scattering factor of two, in the section of the labyrinth in direct view of the source:

$$H(r_1) = 2\ H_o(a)\ a^2\ r_1^{-2}. \qquad (4.21)$$

In this expression $H(r_1)$ is the dose equivalent at a depth r_1 in the first leg, a is the distance from the source to the mouth of the first leg and $H_o(a)$ is the expected dose equivalent at a distance a from a point source. For the subsequent transmission in the i'th leg, Tesch presents a simple sum of two exponentials:

$$H(r_i) = \frac{[\exp(-r_i / 0.45) + 0.022 A_i^{1.3} \exp(-r_i / 2.35)]}{[1 + 0.022\ A_i^{1.3}]} \qquad (4.22)$$

where A_i m^2 is the cross-sectional area and r_i m is the depth in the i'th leg.

A comparison of three procedures, that of Gollon and Awschalom (Go 71), Tesch (Te 82) and Goebel et al. (Go 75), for predicting tunnel attenuation is given in Fig. 4.40, based on an experiment by Cossairt et al. (Co 85b). It will be seen that there is generally good agreement between the three procedures and the experimental data but that of Goebel et al. is closest to the data. It is to be expected from the previous discussions that the ZEUS-albedo procedure will give a lower value of the expected transmission. It should also be noted that the procedure of Tesch, even though it fairly reproduces that experimental data, does not have the $1/\sqrt{A}$ scaling behaviour expected of transmission models. It does however have the benefit that the equations can be conveniently programmed into a pocket-calculator. On the other hand many persons prefer to work from graphical representations and so find the transmission curves more convenient. Within the observed limitations, both procedures appear to be sufficiently accurate for estimating the transmission of dose equivalent in labyrinths.

NEUTRON TRAPS

Several proposals have been made to reduce the transmission around the right-angled bend linking two legs of a labyrinth. These are indicated schematically in Figure 4.41. Type A is a continuation of the first leg of the tunnel beyond the mouth of the second leg, Type B has the second leg crossing the first leg in the form of a T and Type C attempts to combine both A and B in enlarging the region around the junction.

There are conflicting reports in the literature as to the efficacy of these various schemes. Gollon and Awschalom (Go 71) find that a trap of type A, of depth ~ $\sqrt{A}$ where A is the cross sectional area, reduces the neutron fluence in the subsequent leg by about a factor of three. Shallow Type A traps had a smaller effect and traps of Type B and Type C produced no discernable effect on the transmission. These conclusions are in contradiction to those of Perret (Pe 71) who, while agreeing with the extra attenuation of a Type A trap, concluded that a Type B trap was

even more efficient. On the other hand, Ban and Hirayama (Ba 84) measured no difference in attenuation at all between a normal right-angled bend and traps of either Type A or Type B. Clearly these differences need to be resolved by further study.

CURVED TUNNELS

Penetrations that permit the movement of large vehicles or equipment frequently cannot utilise sharp bends. Long curved tunnels have been used in such cases. Here the design parameters such as tunnel radius of curvature and cross section are constrained by the size of the equipment to pass along the tunnel. Even the length of the tunnel may be limited by civil engineering considerations. Under such conditions it is necessary to be able to predict the transmission of proposed designs to guide the correct location of such accesses. Unfortunately, information in the literature is scant.

Shaw (Sh 66) reported measurements of the transmission along a curved tunnel at the NIMROD accelerator. Similar measurements were made by Gilbert at al. (Gi 68) in a tunnel at the CERN PS accelerator. They showed that, as for a right-angled bend, the higher energy neutrons are attenuated more rapidly than neutrons of lower energies. The decrease in flux with depth in the tunnel as measured by moderated indium detectors in both experiments was approximately exponential. Rindi and Tardy-Joubert measured dose transmission in the same tunnels as Gilbert et al. and also obtained an exponential attenuation (Ri 67). These measurements by Rindi and Tardy-Joubert facilitated the development of the ZEUS program discussed previously.

Patterson and Thomas (Pa 73), based on ZEUS calculations reported by Gollon and Corrigan (Go 70b), suggested that the effective attenuation length, λ, is a function of the radius of curvature only of the tunnel, R, given by

$$\lambda = 0.7 \sqrt{R}, \qquad (4.19)$$

where R is measured in metres and lies in the range 4 - 40 m. Gollon and Awschalom (Go 71), based on more systematic ZEUS studies, proposed that λ was more closely linearly dependent on R with the constant of proportionality lying between 0.13 and 0.16. Both formulae predict the correct λ for the CERN and NIMROD experiments. They both also give satisfactory agreement with the limited data of Ban and Hirayama (Ba 84). There is an evident need here for more experimental and theoretical studies.

REFERENCES FOR CHAPTER 4

Aa 84 Aarnio, P.A., Ranft, J. and Stevenson, G.R., 'A Long Writeup of the FLUKA82 Program', CERN Divisional Report TIS-RP/106-Rev (1984).

Al 63 Allen, F.J. and Futterer, A.T., 'Neutron Transmission Data', Nucleonics 21(8), 120 (1963).

Al 65 Alsmiller, R.G., Jr. and Barish, J., 'Calculation of the Nuclear Cascade in Steel Initiated by 10 and 19.2 GeV/c Protons and Comparison with Experiment', Nucl. Instrum. and Meth. 36, 309 (1965).

Al 67 Alsmiller, Jr., R.G., Leimdorfer, M. and Barish, J., 'Analytic Representation of Non-Elastic Cross-Sections and Particle Emission Spectra from Nucleon-Nucleus Collisions in the Energy Range 25-400 MeV', Oak Ridge National Laboratory Report ORNL-4046 (1967).

Al 69a Alsmiller, Jr., R.G., Mynatt, F.R., Barish, J. and Engle, Jr., W.W., 'High Energy (<400 MeV) Neutron Transport Using the Method of Discrete Ordinates', Nucl. Sci. Eng. 36, 251 (1969).

Al 69b Alsmiller, Jr., R.G., Mynatt, F.R., Barish, J. and Engle, Jr., W.W., 'Shielding against Neutrons in the Energy Range 50 to 400 MeV', Nucl. Instrum. Meth., 72, 213 (1969).

Al 69c Alsmiller, Jr., R.G. and Barish, J., 'High-Energy (< 18 GeV) Muon Transport Calculations and Comparison with Experiment', Nucl. Instrum. and Meth. 71, 121 (1969).

Al 69d Alsmiller, Jr., R.G. and Barish, J., 'High-Energy (< 18 GeV) Muon Transport Calculations and Comparison with Experiment, II., Nucl. Instrum. and Meth. 75, 344 (1969).

Al 69e Alsmiller, R.G., Jr. and Solomito, E., 'The Transport of Neutrons produced by 3 GeV Proton-Lead Collisions through a labyrinth and Comparison with Experiment', Nucl. Instrum. Meths. 73, 280 (1969).

Al 71 Alsmiller, Jr., R.G., Alsmiller, F.S., Barish, J. and Shima, Y., 'Muon Transport and the Shielding of High-Energy (< 500 GeV) Proton Accelerators', Proc. Int. Congr. on Protection against Accelerator and Space Radiation, CERN Report CERN 71-16, Vol. 2, p. 601 (1971).

Al 75 Alsmiller, Jr., R.G., Santoro, R.T. and Barish, J., 'Shielding Calculations for a 200 MeV Proton Accelerator and Comparisons with Experimental Data', Particle Accelerators 7, 1 (1975).

Al 82 Alsmiller, R.G., Barish, J., Barnes, J.M. and Santoro, R.T., 'Calculated Neutron Production by 190 to 268 MeV Protons in a Water Cooled Tantalum Target', Nucl. Sci. Eng. 80, 452 (1982).

ANSI 70 American National Standards Institute, Radiological Safety in the Design and Operation of Particle Accelerators, NBS Handbook 101 (1970).

Ar 68 Armstrong, T.W. and Alsmiller, R.G., Jr., 'Monte-Carlo Calculations of the Nucleon-Meson Cascade in Iron Initiated by 1 and 3 GeV Protons and Comparison with Experiment', Nucl. Sci. Eng. 33, 291 (1968).

Ar 69a Armstrong, T.W., 'Monte-Carlo Calculations of Residual Nuclei Production in Thick Iron Targets Bombarded by 1 and 3 GeV Protons and Comparison with Experiment', J. Geophys. Res. 74, 1361 (1969).

Ar 69b Armstrong, T.W. and Alsmiller, R.G., Jr., 'Calculation of the Residual Photon Dose Rate around High-Energy Proton Accelerators', Nucl. Sci. Eng. 38, 53 (1969).

Ar 69c Armstrong, T.W. and Barish, J., 'Calculation of the Residual Photon Dose Rate Due to Activation of Concrete by Neutrons from a 3 GeV proton Beam on Iron', Nucl. Sci. Eng. 38, 265 (1969).

Ar 72 Armstrong, T.W., Alsmiller, Jr.,R.G., Chandler K.C. and Bishop B.L., 'Monte Carlo Calculations of High-Energy Nucleon-Meson Cascades and Comparison with Experiment', Nucl. Sci. Eng. 49, 82 (1972).

Ar 79 Arakita, Y., Hirayama, H., Inagaki, T. and Miyajima, M., 'Study of an Iron Beam Stop for 500 MeV Protons', Nucl. Instrum. and Meth. 164, 255 (1979).

Ar 80 Armstrong, T.W., 'The HETC Hadronic Cascade Code', in Computer Techniques in Radiation Transport and Dosimetry, W.R. Nelson and T.M. Jenkins (Eds.), Plenum Press, New York and London, p. 373 (1980).

Aw 70 Awschalom M., 'Lateral Shielding for the 8 GeV and 200 GeV Synchrotrons', Fermi National Accelerator Laboratory Internal Report, FNAL TM-241(1970).

Aw 76 Awschalom, M., Baker, S., Moore, C., Van Ginneken, A., Goebel, K. and Ranft, J., 'Measurements and Calculations of Cascades Produced by 300 GeV Protons Incident on a Target inside a Magnet', Nucl. Instrum. and Meth. 138, 521 (1976).

Ba 71 Barbier, M. and Hunter, R., 'Systematics of Extra-Nuclear Hadron Cascades in Shields', CERN Report CERN 71-13 (1971).

Ba 72 Barashenkov, V.S., Sobolevskii, N.M. and Toneev, V.D., 'The Penetration of Beams of High-Energy Particles through Thick Layers of Material', Atomnaya Energiya 32, 217 (1972).

Ba 80 Ban, S., Hirayama, H., Kondo, K., Miura, S., Hozumi, K., Taino, M., Yamamoto, A., Hirabayashi, H. and Katoh, K. 'Measurement of Transverse Attenuation Lengths for Paraffin, Heavy Concrete and Iron around an External Target for 12 GeV Protons', Nucl. Instrum. and Methods 174, 271 (1980).

Ba 81 Ban, S., Hirayama, H. and Katoh, K., 'Measurement of Secondary Neutron Fluxes around a Beam Stop for 500 MeV Protons', Nucl. Instrum. Meth. 184, 409 (1981).

Ba 84 Ban, S. and Hirayama, H., 'The Attenuation of Neutrons in a Labyrinth at an Accelerator', Proc. 5th Symp. on Accelerator Science and Technology, Sept. 1984, KEK, Tsukuba, Japan, p. 378 (1984).

Be 63a Bertini, H.W., 'Low Energy Intranuclear Cascade Calculation', Phys. Rev. 131, 1801 (1963).

Be 63b Bethe, H.A. and Ashkin, J., 'Passage of Radiations through Matter', in Experimental Nuclear Physics, Vol. 1 (Ed., E. Segre), Wiley and Sons, New York, p.166 (1963).

Be 67 Bertini, H.W., 'Preliminary Data from Intranuclear Cascade Calculations of 0.75, 1 and 2 GeV Protons on Oxygen, Aluminium and Lead, and 1 GeV Neutrons on the Same Elements', Oak Ridge National Laboratory Report ORNL-TM-1996 (1967).

Be 69 Bertini, H.W., 'Intranuclear Cascade Calculation of the Secondary Nucleon Spectra from Nucleon-Nucleus Interactions in the Energy Range 340 to 2900 MeV and Comparison with Experiment', Phys. Rev. 188, 1711 (1969).

Be 71a Bennett, G.W., Foelsche, H., Lazarus, D., Levine, G., Moore, W. and Toohig, T., 'Flux Attenuation in a Steel Side Shield at the AGS', IEEE Trans. Nucl. Sci. NS18 (3), 778 (1971).

Be 71b Bertel, E., de Séréville, B., Freytag, E. and Wachsmuth, H., 'Shielding against Muons', Chapter VI in Radiation Problems Encountered in the Design of Multi-GeV Facilities (Ed. K. Goebel), CERN Report 71-12 (1971).

Be 71c Bennett, G.W., Foelsche, H., Lazarus, D., Levine, G., Moore, W., Toohig, T., Thomas, R.H., and Koustoulas, J., 'Study of a Uniform Steel Beam Stop at 28 GeV', IEEE Trans. Nucl. Sci. NS18 (2), 776 (1971).

Be 73 Bennet, G.W., et al., 'Particle Distribution in a Steel Beam Stop for 28 GeV Protons', Particle Accelerators 4, 229 (1973).

Be 74 Bertini, H.W., Harp, G.D. and Bertrand, F.E., 'Comparisons of Predictions from Two Intranuclear Cascade Models with Measured Secondary Proton Spectra at Several Angles from 62 and 39 MeV Protons on Various Elements', Phys. Rev. C 10, 6, 2472 (1974).

Be 82 Beynel, P., Maier, P. and Schönbacher, H., 'Compilation of Radiation Damage Test Data: Part III, Materials Used around High-Energy Accelerators', CERN Report CERN 82-10 (1982).

Bo 71 Borodin, V.E., Obryashikova, L.P. and Chimankov, M.N., 'On Radiation Passing through the Labyrinth of the IHEP 70 GeV Synchrotron', Serpukhov Report IHEP.71-84 (1971).

Br 71 Braid, T.H., Rapids, R.F., Siemssen, R.H., Tippie, J.W. and O'Brien, K., 'Calculations of Shielding for Large Cyclotrons', IEEE Trans. Nucl. Sci. NS-18, 821 (1971).

Br 83 Broome, T.A., Perry, D.R., Stapleton, G.B. and Duc, D., 'Particle Distribution around a Copper Beam Stop for 72 MeV Protons', Health Phys. 44, 487 (1983).

Bu 70 Bünemann, D. and Enginol, T.B., 'Shield Optimization' in Section 10.11, Shielding of Ship Propulsion Reactors, IAEA 70, p. 425.

Ca 67 Casey, W.R., Distenfeld, C.H., Levine, G.S., Moore, W.H. and Smith, L.W., 'Sand as a Side Shield for 30 GeV Protons Stopping in the Brookhaven AGS', Nucl. Instrum. and Meth. 55, 253 (1967).

Ca 79 Cain, V.R. and Emmett, M.B., 'BREESE-II: Auxiliary Routines for Implementing the Albedo Option in the MORSE Monte-Carlo Code', Oak Ridge National Laboratory Report ORNL/TM-6807 (1979).

CERN 64 CERN Study Group on New Accelerators. Report on the Design Study of a 300 GeV Proton Synchrotron. (2 Vol.) European Center for Nuclear Research Report CERN-563 (Nov. 1964).

Ch 65 Childers, R.L., Zerby, C.D., Fisher, C.M., and Thomas, R.H., 'Measurement of the Nuclear Cascade at 10 GeV/c with Emulsions', Nucl. Instrum. and Meth. 32, 53 (1965).

Ch 68 Chen, K., Fraenkel, Z., Friedlander, G., Grover, J.R., Miller, J.M. and Shimamoto, Y., 'VEGAS: A Monte Carlo Simulation of Intranuclear Cascades', Phys. Rev. 166, 949 (1968).

Ch 72 Chandler, K.C. and Armstrong, T.W., 'Operating Instructions for the High-Energy Nucleon-Meson Transport Code HETC', Oak Ridge National Laboratory Report ORNL-4744 (1972).

Ch 80 Chu Yu-Cheng, 'The Estimation of Transverse Shielding Thickness for the BPS', CERN Internal Technical Memorandum HS-RP/TM/80-14 (1980).

Ch 84 Chilton, A.B., Shultis, J.K., and Faw, R.E., Principles of Radiation Shielding, Prentice-Hall, Inc., Englewood Cliffs, N.J. (1984).

Ci 61 Citron, A., Hoffmann, L. and Passow, C., 'Investigation of the Nuclear Cascade in Shielding Materials', Nucl. Instrum. Methods 14, 97 (1961).

Ci 65 Citron, A., Hoffmann, L., Passow, C., Nelson, W.R., and Whitehead, M., 'A Study of the Nuclear Cascade in Steel Initiated by 19.2 GeV/c Protons', Nucl. Instrum. and Meth. 32, 48 (1965).

Ci 81 Cierpackis, S., Raupp, F., Howe, S.O., et al., 'High Energy Particle Spectra from Spallation Target', in Proceedings of the 5th Meeting on Advanced Neutron Sources, Jülich (1980), p. 215.

Cl 71 Clark, B.K., Shielding Data, Appendix E in NCRP 71.

Co 62 Cowan, F.P., 'A Preliminary Report on Health Physics Problems at the Brookhaven Alternating Gradient Synchrotron', Premier Colloquel International sur la Protection auprès des Grandes Accélérateurs, Presses Universitaires de France, Paris (1962).

Co 67 Coleman, W.A., Maerker, R.E., Muckenthaler, F.J. and Stevens, P.N., 'Calculation of Doubly-Differential Current Albedos for Epicadmium Neutrons Incident on Concrete and Comparison of the Reflected Sub-Cadmium Component with Experiment', Nucl. Sci.

Eng. 27, 411 (1967).

Co 68 Coleman, W.A., 'Thermal-Neutron Flux Generation by High-Energy Protons', Oak Ridge National Laboratory Report ORNL-TM-2206 (1968).

Co 72 Cohen, M.O., Guber, W., Lichtenstein, H., Steinberg, H.A. and Troubetzkoy, E.S., 'SAM-CE, A Three Dimensional Monte-Carlo Code for the Solution of the Forward Neutron and Forward and adjoint Gamma-Ray Transport Equations, Revision A', Defense Nuclear Agency, Washington, D.C., Report DNA 2830-F (Rev.A) (1972).

Co 73 Cohen, M.O., Guber, W., Troubetzkoy, E.S., Lichtenstein, H., and Steinberg, H.A., 'SAM-CE, A Three Dimensional Monte-Carlo Code for the Solution of the Forward Neutron and Forward and adjoint Gamma-Ray Transport Equations, Revision B', Defense Nuclear Agency, Washington, D.C., Report DNA 2830-F (Rev.B) (1973).

Co 82 Cossairt, J.D., Mokhov, N.V. and Murphy, C.T., 'Absorbed Dose Measurements External to Thick Shielding at a High Energy Proton Accelerator: Comparison with Monte Carlo Calculations', Nucl. Instrum. and Meth. 197, 465 (1982).

Co 83 Cossairt, J.D., 'Recent Muon Fluence Measurements at Fermilab', Health Physics 45, 651 (1983).

Co 84 Cossairt, J.D. and Elwyn, A.J., 'Shielding Considerations for Fixed Target Usage of the SSC', Proc. SSC Fixed Target Workshop, The Woodlands, Texas, January 1984, p. 19.

Co 85a Cossairt, J.D., Butala, S.W. and Gerardi, M.A., 'Absorbed Dose Measurements at an 800 GeV Proton Accelerator; Comparison with Monte-Carlo Calculations', Nucl. Instrum. and Meth. A 238, 504 (1985).

Co 85b Cossairt, J.D., Couch, J.G., Elwyn, A.J. and Freeman, W.S., 'Radiation Measurements in a Labyrinth Penetration at a High-Energy Proton Accelerator', Health Physics 49, 907 (1985).

Da 57 Davison, B., Neutron Transport Theory, Clarendon Press, Oxford (1957).

DeS 62 de Staebler, H., 'Transverse Radiation Shielding for the Stanford Two-Mile Accelerator', USAEC Report SLAC-9 (1962).

d'H 68 d'Hombres, M.M., Devillers, C., Gervaise, F., de Séréville, B. and Tardy-Joubert, P., 'Propagation des Neutrons dans las Tunnels d'Accès a un Accélérateur de Haute Energie à Protons', Centre d'Etudes Nucléaires de Saclay Report CEA-R-3491 (1968).

Di 65 Distenfeld, C. and Colvett, R.D., 'AGS Conversion— A Summary', Proc. First Symp. on Accelerator Radiation Dosimetry and Experience, Brookhaven November 3-5, 1965, USAEC Report CONF-651109, p. 490 (1965).

Dr 71 Drugachenok, S.A., Kimel, L.R., Krupny, G.I., Lebedev, V.N. and Sidorin, V.P., 'Passing of High-Energy Muons through Steel

Shielding', Sepukhov Report IHEP 71-25 (1971).

Em 75 Emmett, M.B., 'The MORSE Monte-Carlo Radation Transport Code System', Oak Ridge National Laboratory Report ORNL-4972 (1975).

Em 78 Emmett, M.S. and Rhoades, W.A., 'CARP, a Computer Code and Albedo Data Library for Use by BREESE, the MORSE Albedo Package', Oak Ridge National Laboratory Report ORNL/TM-6503 (1978).

Ev 70 Everette, W., private communication, Lawrence Berkeley Laboratory, 1970.

Ey 48 Eyges, L., 'Multiple Scattering with Energy Loss', Phys. Rev. 74, 1534 (1948).

Fa 76 Fasso, A. and Hoefert, M., 'Distributions of Secondary Particles around Various Targets Exposed to 50 MeV Protons', Nucl. Instr. Meth. 133, 213 (1976).

Fe 40 Fermi, E., unpublished lecture notes quoted by Rossi and Greissen (Ro 41) (1940).

Fe 72 Feinberg, E.L., 'Multiple Production of Hadrons at Cosmic Ray Energies (Experimental Results and Theoretical Concepts)', Phys. Rev. 5C, 237 (1972).

Fi 63 Fisher, C.M., 'Note on the Nuclear Cascade in Shielding Materials', in Report of the Shielding Conference held at the Rutherford Laboratory on September 26 and 27, 1962, R.H. Thomas, (Ed.), Rutherford Laboratory Report NIRL/R/40 (1963).

Fr 71 Freytag, E. and Ranft, J., 'Hadronic and Electromagnetic Cascades', Chapter III of Radiation Problems Encountered in the Design of Multi-GeV Research Facilities (Ed., K. Goebel), CERN Report CERN 71-21 (1971).

Fu 72 Fullwood, R.R., Cramer, J.D., Haarmann, R.A., Forrest, R.P. and Schmidt, R.G., 'Neutron Production by Medium-Energy Protons on Heavy Metal Targets', Los Alamos Scientific Laboratory Report LA-4789 (1982).

Ga 70 Gabriel, T.A., Alsmiller, R.G., Jr., and Guthrie, M.P., 'An Extrapolation Method for Predicting Nucleon and Pion Differential Production Cross-Sections from High-Energy (>3 GeV) Nucleon-Nucleus Collisions', Oak Ridge National Laboratory Report ORNL-4542 (1970).

Ga 71a Gabriel, T.A. and Santoro, R.T., 'Calculation of the Long-Lived Activity in Soil Produced by 500 GeV Protons', Nucl. Instrum. and Meth. 95, 275 (1971).

Ga 71b Gabriel, T.A., Santoro, R.T. and Barish, J., 'A Calculational Method for Predicting Particle Spectra from High-Energy Nucleon and Pion Collisions (>3 GeV) with Protons', Oak Ridge National Laboratory Report ORNL-TM-3615 (1971).

Ga 85 Gabriel, T.A., 'The High Energy Transport Code HETC', paper presented at the CERN Workshop on Shower Simulation for LEP Experiments, 29-31 January 1985, Oak Ridge National Laboratory Report ORNL-TM-9727 (1985).

Ge 68 Gervaise, F. and d'Hombres, M.M., 'Variante du Programme ZEUS Appliquée a des Problèmes de Tunnels: Programmes ZEUS ALB.5 et Programmes Auxiliaires', Centre d'Etudes Nucléaires de Fontenay-aux-Roses Report CEA-N-933 (1968).

Gi 68 Gilbert, W.S., Keefe, D., McCaslin, J.B., Patterson, H.W., Smith, A.R., Stephens, L.D., Shaw, K.B., Stevenson, G.R., Thomas, R.H., Fortune, R.D., and Goebel, K., '1966 CERN-LRL-RHEL Shielding Experiment at the CERN Proton Synchrotron', Lawrence Berkeley Laboratory Report UCRL-17941 (1968).

Gi 69 Gilbert, W.S., 'Shielding Measurements at the CERN 25 GeV Proton Synchrotron', in Proc. 2nd Int. Conf. Accel. Dos., held at Stanford Linear Accelerator Center, 5-7 November 1969, USEAC Report CONF-601101, p. 323 (1969).

Go 70a Goebel, K. and Ranft, J., 'Radiation Measurements around a Beam Stopper Irradiated by 19.2 GeV/c Protons, and Neutron Energy Spectra from Monte Carlo Nucleon-Meson Cascade Calculations', CERN Report CERN 70-16 (1970).

Go 70b Gollon. P.J. and Corrigan, R.A., 'Design of Personnel and Vehicle Access Labyrinths', Fermilab Internal Report TM-239 (1970).

Go 71 Gollon, P.J. and Awschalom, M., 'Design of Penetrations in Hadron Shields', Proc. Internat. Congress on Protection against Accelerator and Space Radiation, CERN Report CERN 71-16, Vol. 2, p. 697 (1971).

Go 75 Goebel, K., Stevenson, G.R., Routti, J.T. and Vogt, H.G., 'Evaluating Dose Rates due to Neutron Leakage through the Access Tunnels of the SPS', CERN Internal Report LABII-RA/Note/75-10 (1975).

Go 81 Gollon, P.J., Awschalom, M., Baker, S.I., Coulson, L., Moore, C. and Velen, S., 'Measurements of Radial and Longitudinal Hadron Shower Development at 300 GeV', Nucl. Instrum. and Meth. 189, 387 (1981).

Gu 70 Guthrie, M.P., 'EVAP-4: Another Modification of a Code to Calculate Particle Evaporation from Excited Compound Nuclei', Oak Ridge National Laboratory Report ORNL-TM-3119 (1970).

Ha 75 Hamer, E.E. and Mc Arthur, A.E., 'Uranium', Section 9.1.3 in IAEA 75, p. 20 (1975).

Ha 80 Haenssgen, K., Kirschner, R., Ranft, J. and Wetzig, H., 'Monte-Carlo Simulation of Inelastic Hadron-Nucleus Reactions: Description of the Model and of the Computer Code NUCRIN', Karl-Marx University, Leipzig, Report KMU-HEP-80-07 (1980).

Ha 83 Hashikura, H., Fukumoto, H., Oka, Y., Akiyama, M. and An, S., 'Neutron streaming through a Slit and Duct in Concrete Shields and Comparison with a Monte-Carlo analysis', Nucl. Sci. Eng. 84, 337 (1983).

Ho 56 Hofstadter, R., 'Electron Scattering and Nuclear Structure', Rev. Mod. Phys. 28, 214 (1956).

Ho 63 Hoffmann, L., 'A Summary of the Shielding Experiments Using 20-GeV Protons of the CERN PS', NIRL/R40, p. 3 (1963).

Ho 65 Hoffmann, L. and Sullivan, A.H., 'Shielding Studies in Steel with 10- and 20-GeV Protons, Part V: Studies of the Shielding Required for the Secondary Radiation Produced by a Target in a High-Energy Proton Beam', Nucl. Instr. Methods 75, 130 (1965).

Ho 66 Howe, H.J., Oldfield, G.V., Sreniawski, D.J. and Wheeler, R.V., 1956, 'On the Shielding of the External Proton Tunnel Area of Argonne's Zero Gradient Synchrotron', Argonne National Laboratory Internal Report ANL-7273 (1966).

Ho 79 Hoefert, M., Chu Yu-Cheng, Hamer, J.M., and Sanchez, J., 'Radiation Protection Calculations and Measurements around the e 18 Beam in the PS East Experimental Hall', CERN Divisional Report HS-RP/044 (1979).

Ho 80 Hoefert, M., and Yamaguchi, Ch., 'Measurements of Muons at 10, 15 and 19 GeV/c and Comparison with Calculations', CERN Technical Memorandum HS-RP/TM/80-42 (1980).

Hu 75 Hungerford, H.E., Hönig, A., Desov, A.E., du Bois, F. and Davis, H.S., 'Concretes, Cements, Mortars and Grouts', Section 9.1.12 in IAEA 75, p. 75 (1975).

IAEA 68 International Atomic Energy Agency, Engineering Compendium on Radiation Shielding, Jaeger, R.G., Blizard, E.P., Chilton, A.B., Grotenhuis, M., Hönig, A., Jaeger, T.A. and Eisenlohr, H.H. (Eds.), Vol. 1., 'Shielding Fundamentals and Methods', Springer Verlag, Berlin [under the auspices of the International Atomic Energy Agency], (1968).

IAEA 70 International Atomic Energy Agency, Engineering Compendium on Radiation Shielding, Jaeger, R.G., Blizard, E.P., Chilton, A.B., Grotenhuis, M., Hönig, A., Jaeger, T.A. and Eisenlohr, H.H. (Eds.), Vol. 3., 'Shield Design and Engineering', Springer Verlag, Berlin [under the auspices of the International Atomic Energy Agency], (1970).

IAEA 75 International Atomic Energy Agency, Engineering Compendium on Radiation Shielding, Jaeger, R.G., Blizard, E.P., Chilton, A.B., Grotenhuis, M., Hönig, A., Jaeger, T.A. and Eisenlohr, H.H. (Eds.), Vol. 2., 'Shielding Materials', Springer Verlag, Berlin [under the auspices of the International Atomic Energy Agency], (1975).

ICRP 73a International Commission on Radiological Protection, Publication 22, 'Implications of Commission Recommendations that Doses Be Kept as Low as Readily Achievable', Pergamon Press, Oxford (1973).

ICRP 73b International Commission on Radiological Protection, Publication 21, 'Data for Protection against Ionizing Radiation from External Sources, Supplement to ICRP Publication 15', Pergamon Press, Oxford (1973).

ICRP 77 International Commission on Radiological Protection, Publication 26, 'Recommendations of the International Commission on Radiological Protection', Annals ICRP 1 (No. 3), Pergamon Press, Oxford (1977).

ICRP 80 International Commission on Radiological Protection, 'Statement and Recommendations of the 1980 Brighton Meeting of the ICRP', Annals of the ICRP 4 (3/4), 1 (1980).

ICRP 83 International Commission on Radiological Protection, Publication 37, 'Cost Benefit Analysis in the Optimization of Radiological Protection', Annals of the ICRP 10, (No. 2/3) (1983), Pergamon Press, Oxford.

ICRP 84a International Commission on Radiological Protection, Publication 42, 'A Compilation of the Major Concepts and Quantitites in Use by the ICRP', Annals of the ICRP 14, (4), para. 42, 43, p. 10 (1984).

ICRP 84b International Commission on Radiological Protection, Statement from the 1983 Washington Meeting, Annals of the ICRP 14 (1), 1 (1984).

ICRP 84c International Commission on Radiological Protection, Statement from the 1984 Stockholm Meeting of the Commission, Annals of the ICRP 14, (2) (1984).

ICRP 85 International Commission on Radiological Protection, Statement from the 1983 Paris Meeting, Radiat. Prot. Dosimetry 11 (2), 134 (1985).

Ir 65 Irving, D.C., Freestone, R.M., Jr. and Kam, F.B.K., '05R, A General Purpose Monte Carlo Neutron Transport Code', Oak Ridge National Laboratory Report ORNL-3622 (1965).

Ka 71 Kaye, G.W.C. and Laby, T.H., 'Tables of Physical and Chemical Constants', Longman, London (1971)

Ka 72 Kang, Y. et al., 'Design of a Magnetized Iron Muon Shield for a High Energy Neutrino Laboratory', Part. Accel. 4, 31 (1972).

Ke 64 Keefe, D. 'Mu-Meson Shielding Problems at 200 GeV: Approximate Calculations', Lawrence Berkeley Internal Note UCID-10018 (1964).

Ke 68 Keefe, D. and Noble, C.M., 'Radiation Shielding for High-Energy Muons: The Case of a Cylindrically Symmetrical Shield and No Magentic Fields', Nucl. Instrum. and Meth. 64, 173 (1968).

Ko 67 Kobayakawa, K., 'Fluctuations and Nuclear Interactions in the Energy Loss of Cosmic-Ray Muons', Nuovo Cimento XLVIIB, 156 (1967).

LBL 65 '200 BeV Design Study', Lawrence Berkeley Laboratory Internal Report UCRL-1600 (2 vols.) (1965).

Le 72 Levine, G.S., Squier, D.M., Stapleton, G.B., Stevenson, G.R., Goebel, K. and Ranft, J., 'The Angular Dependence of Dose and Hadron Yield from Targets in 8 GeV/c and 24 GeV/c Extracted Proton Beams,' Particle Accelerators 3, 91 (1972).

Li 52 Livingston, M.S., 'High Energy Accelerators— Standard Cyclotron', Ann. Rev. Nucl. Sci. 1, 157 (1952), 'High-Energy Accelerators— Synchrocyclotron', Ann. Rev. Nucl. Sci. 1, 163 (1952), 'High-Energy Accelerators— Proton Synchrotron', Ann. Rev. Nucl. Sci. 11, 213 (1952).

Li 61 Lindenbaum, S.J., 'The Shielding of High-Energy Accelerators', Ann. Rev. Nucl. Sci. 11, 213 (1961).

Li 80 Liu, Kuei-Lin, 'Calculation of Muon-Shielding Using the MUSTOP Program and Comparison with Experimental Data', CERN Internal Report HS-RP/IR/80-19 (1980).

Li 84 Liu, Kuei-Lin, Stevenson, G.R., Thomas, R.H. and Thomas, S.V.,'Variance and Regression Analyses of Moyer Model Parameter Data and their Variation with Primary Proton Energy', Health Physics 46, 674 (1984).

Li 85 Lipták, G., Schuler, R., Maier, P. Schönbacher, H., Haberthür, B., Müller, H. and Zeier, W., 'Radiation Tests on Selected Electrical Insulating Materials for High-Power and High-Voltage Application', CERN Report CERN 85-02 (1985).

Lo 83 Lone, M.A., Jones, R. and Ozaki, A. et al., 'Total Neutron Yields from 100 MeV Protons on Pb and Li Targets', Nucl. Inst. and Methods 214, 333 (1983).

Ma 65 Maerker, R.E. and Muckenthaler, F.J., 'Calculation and Measurement of the Fast Neutron Differential dose Albedo for Concrete', Nucl. Sci. Eng. 22, 455 (1965).

Ma 66 Maerker, R.E. and Muckenthaler, F.J., 'Measurements and Single-Velocity Calculations of Differential Angular Thermal-Neutron Albedos for Concrete', Nucl. Sci. Eng. 26, 339 (1966).

Ma 67a Maerker, R.E. and Muckenthaler, F.J., 'Monte-Carlo Calculations, Using the Albedo Concept, of the Fast-Neutron Dose Rates along the Center Lines of One- and Two-Legged Square Concrete Open Ducts and Comparison with Experiment', Nucl. Sci. Eng. 27, 423 (1967).

Ma 67b Maerker, R.E. and Cain, V.R., 'AMC, a Monte-Carlo Code Utilizing the Albedo Approach for Calculating Neutron and Capture Gamma-Ray Distributions in Rectangular Concrete Ducts', Oak Ridge National Laboratory Report ORNL-3964 (1967).

Ma 70 Marshall, T.O., 'The Attenuation of 14-MeV Neutrons in Water', Health Phys. 19, 571 (1970).

Ma 79 Marchal, H., private communication, CERN, Geneva, Switzerland (1979).

McC 84 McCaslin, J.B., La Plant, P.R., Smith, A.R., Swanson, W.P., and Thomas, R.H., 'Neutron Production by Ne and Si Ions on a Thick Cu Target at 670 MeV.A with Application to Radiation Protection', Proceedings of Particle Accelerator Conference, Vancouver, B.C., May 1985, IEEE Trans. Nucl. Sci. (in press).

McC 85 McCaslin, J.B., Swanson, W.P. and Thomas, R.H., 'Moyer Model Approximations for Point and Extended Beam Losses', Lawrence Berkeley Laboratory Report LBL-14699 (1985).

Me 58 Metropolis, N., Bivins, R., Storm, M., Turkevitch, A., Miller, J.M. and Friedlander, G., 'Monte Carlo Calculations on Intranuclear Cascades', Phys. Rev. 110, 185 (1958).

Me 65 Meuser, R.B., 'Shielding: Beam Transport Sections', Advanced Accelerator—Experimental Areas Project, Lawrence Berkeley Laboratory Mechanical Engineering Department Note AS/Experimental/01 M3563, May 17, 1965.

Mo 57 Moyer, B.J., 'Build Up Factors', Proc. Conf. on Shielding of High-Energy Accelerators, New York, April 11-13, 1957, USAEC Report TID 7545, p. 96 (1957).

Mo 61a Moyer, B.J., (Lawrence Berkeley Laboratory), 'Data Related to Nuclear Star Production by High Energy Protons', private communication, June 20, 1961, quoted in Pa 73, p. 128. (1961).

Mo 61b Moyer, B.J., 'Evaluation of Shielding Required for the Improved Bevatron', Lawrence Berkeley Laboratory Report UCRL-9769 (1961).

Mo 62 Moyer, B.J., 'Method of Calculation of the Shielding Enclosure for the Berkeley Bevatron', in Proc. 1st Int. Conf. Shielding around High Energy Accelerators, Presses Universitaires de France, Paris, p. 65 (1962).

Na 83 Nakamura, T., Fujii, M. and Shin, K., 'Neutron Production from Thick Targets of Carbon, Iron, Copper and Lead by 30 and 52 MeV Protons', Nucl. Sci. Eng. 83, 444 (1983).

NCRP 71 National Council on Radiation Protection Measurements, 'Protection against Neutron Radiation', Report 38, Washington, D.C. (1971).

NCRP 77 National Council on Radiation Protection and Measurements, 'Recommendations of the National Council on Radiation Protection and Measurements, Radiation Protection Design Guidelines for 0.1-100 MeV Particle Accelerator Facilities', NCRP Report No. 51, Washington, D.C. (1977).

Ne 68 Nelson, W.R., 'The Shielding of Muons around High-Energy Electron Accelerators: Theory and Measurement', Nucl. Instrum. and Meth. 66, 293 (1968).

Ne 74a Nelson, W.R. and Kase, K.R., 'Muon Shielding around High-Energy Accelerators. Part I. Theory', Nucl. Instrum. and Meth. 120, 401 (1974).

Ne 74b Nelson, W.R., Kase, K.R. and Svensson, G.K., 'Muon Shielding around High-Energy Accelerators. Part II. Experimental Investigation', Nucl. Instrum. and Meth. 120, 413 (1974).

Ne 83 Nelson, W.R., Jenkins, T.M., Stevenson, G.R., Nielsen, M., Heijne, E.H.M., Jarron, P., Lord, J., and Anderson, S., 'Transport of High-Energy Muons in a Soil Shield', Nucl. Instrum.

and Meth. 215, 385 (1983).

Ni 74 Nielsen, B., 'Muon Measurements for Radiation Protection', CERN Internal Report HP-74-135 (1974).

OB 67 O'Brien, K., 'The Neutron Shielding of the Los Alamos Meson Physics Facility', USAEC Health and Safety Laboratory Report HASL-188 (1967).

OB 68a O'Brien, K. and McLaughlin, J. 'The Propagation of the Neutron Component of the Nucleonic Cascade at Energies Less than 500 MeV: Theory and a Solution to the Accelerator Transverse Shielding Problem', Nucl. Instrum. and Methods 60, 129 (1968).

OB 68b O'Brien, K. 'Transverse Shielding Calculations for Components of a 1/2-TeV Proton Synchrotron', USAEC Health and Safety Laboratory Report HASL-199 (1968).

OB 68c O'Brien, K., 'Tables for the Determination of the Lateral Shielding Requirements of High-Energy Accelerators', USAEC Health and Safety Laboratory Report HASL-203 (1968).

OB 69 O'Brien, K., 'Extra-Nuclear Hadron Cascade Calculations Using Passow's Approximation', Nucl. Instrum. and Meth. 72, 93 (1969).

OB 70 O'Brien, K., 'Shielding Calculations for Broad Neutron Beams Normally Incident on Slabs of Concrete', USAEC Health and Safety Laboratory Report HASL-221 (1970).

OB 71 O'Brien, K., 'Neutron Spectra in the Side Shielding of a Large Particle Accelerator', USAEC Health and Safety Laboratory Report HASL-240 (1971).

Pa 57 Patterson, H.W., 'The University of California Synchro-Cyclotron', in So 57, p. 3 (1957).

Pa 62a Patterson, H.W., 'The Effect of Shielding on Radiation Produced by the 730 MeV Synchrocyclotron and the 6.3 GeV Proton Synchrotron at the Lawrence Radiation Laboratory', in Proc. Premier Colloque International sur la Protection auprès des Grandes Accélérateurs, Presses Universitaires de France, Paris (1962).

Pa 62b Passow, C., 'Phönomenologische Theorie zur Berechnung einer Kaskade aus schweren Teilchen (Nukleonenkaskade) in der Materie', DESY Report DESY-Notiz A 2.85 (1962).

Pa 71 Patterson, H.W. and Thomas, R.H., 'Experimental Shielding Studies—A Review', Particle Accelerators 2, 77 (1971).

Pa 73 Patterson, H.W. and Thomas, R.H., Accelerator Health Physics, Academic Press, New York and London, in particular pp. 386-400 (1973).

Pe 65 Perry, D.R. and Shaw, K.B., 'Radiation Levels in and around Nimrod', Proc. First Symposium on Accelerator Radiation Dosimetry and Exposure', USAEC Report CONF-651109, p. 20 (1965).

Pe 66 Perry, D.R., 'Neutron Dosimetry Methods and Experience on the 7 GeV Proton Synchrotron, Nimroc', Proc. Symp. on Neutron Monitoring for Radiological Protection, IAEA, Vienna, STI/PUB/136, p. 355 (1966).

Pe 71 Perret, C.S., 'Dosisverteilung schneller Neutronen in Betonlabyrinthen in abhängigkeit der Neutronenenergie und der Geometrie', Proc. Internat. Congress on Protection against Accelerator and Space Radiation, CERN Report CERN 71-16, Vol. 2, p. 714 (1971).

Pr 57 Price, B.T., Horton, C.C. and Spinney, K.T., Radiation Shielding, Permagon Press, Oxford (1957).

Ra 67 Ranft, J., 'Improved Monte Carlo Calculation of the Nucleon-Meson Cascade in Shielding Material, I and II', Nucl. Instrum. and Meth. 48, 133 and 48, 261 (1967).

Ra 70a Ranft, J., 'Monte Carlo Calculation of Energy Deposition by the Nucleon-Meson Cascade and Total Absorption Nuclear Cascade (TANC) Counters', Nucl. Instrum. and Meth. 81, 29 (1970).

Ra 70b Ranft, J., 'Secondary Particle Spectra According to the Thermodynamical Model. A Fit to Data Measured in p-Nucleus Collisions', Karl Marx University Leipzig Report TUL-36 (1970).

Ra 72a Ranft, J., 'Estimation of Radiation Problems around High Energy Accelerators Using Calculations of the Hadronic Cascade in Matter', Particle Accelerators 3, 129 (1972).

Ra 72b Ranft, J. and Routti, J.T., 'Hadronic Cascade Calculations of Angular Distributions of Integrated Secondary Particle Fluxes from External Targets and New Empirical Formulae Describing Particle Production in Proton-Nucleus Collisions', Particle Accelerators 4, 101 (1972).

Ra 74 Ranft, J. and Routti, J.T., 'Monte Carlo Programs for Calculating Three-Dimensional High-Energy (50 MeV - 500 GeV) Hadron Cascades in Matter', Comput. Phys. Commun. 7, 327 (1974).

Ra 85 Ranft, J., Aarnio, P.A. and Stevenson, G.R., 'FLUKA82', CERN Divisional Report TIS-RP/156/CF, paper presented at the CERN Workshop on Shower Simulation for LEP Experiments, 19-31 January 1985.

Ri 65 Riddell, R.J., Jr., 'High-Energy Nuclear Cascades in Matter', Lawrence Radiation Laboratory Report UCRL-11989 (1965).

Ri 67 Rindi, A. and Tardy-Joubert, P., 'Contribution to the Experimental Study of the Transmission of Radiation through Service Tunnels in the Shielding of High-Energy Accelerators', Industries Atomiques 3/4, 53, (in French) (1967). English translation available as Lawrence Berkeley Laboratory UCRL Transl. 350.

Ri 73 Rindi, A. and Thomas, R.H., 'The Radiation Environment of High-Energy Accelerators', Ann. Rev. Nucl. Sci. 23, 315 (1973).

Ro 41 Rossi, B. and Greisen, K., 'Cosmic Ray Theory', Rev. Mod. Phys. 13, 240 (1941).

Ro 52 Rossi, B., High Energy Particles, Prentice-Hall, Inc., Englewood Cliffs, N.J. (1952).

Ro 56 Rockwell, T., Reactor Shielding Design Manual, Office of Technical Services, U.S. Department of Commerce, Washington, D.C. (1956).

Ro 69 Routti J.T. and Thomas R.H., 'Moyer Integrals for Estimating Shielding of High-Energy Accelerators,' Nucl. Instrum. and Methods 76, 157 (1969).

Ro 72a Routti, J.T. and Van de Voorde, M., 'Monokinetic and Multi-Group Monte-Carlo Albedo Estimates of Neutron Leakage through Penetrations of the ISR Shielding', CERN Internal Report CERN ISR-MA/72-27 (1972).

Ro 72b Routti, J.T. and Van de Voorde, M.H., 'Dose Estimates outside the Shielding of the CERN Intersecting Storage Rings by the Moyer Method', Nucl. Eng. Design 21, 421 (1972).

Ry 82 Ryder, R., 'Neutron Production from Protons and Deuterons', Daresbury Laboratory DL/NUC/TM60A (compilation) (1982).

Ry 83 Ryabov, Y.V., Matushko, G.K. and Slastnikov, V.M., 'Measurement of the Average Neutron Yield from 250 MeV Protons Absorbed in a Lead Target', Z. Phys. A311, 363 (1983).

Sa 82 Santoro, R.T., Alsmiller, R.G., Jr., Barnes, J.M., Chapman, G.T. and Tang, J.S., 'Comparison of Measured and Calculated Neutron and Gamma-Ray Energy Spectra behind an In-Line Shielded Duct', J. Fusion Energy 2, 403 (1982).

Sa 83 Santoro, R.T., Barnes, J.M., Alsmiller, R.G., Jr. and Soran, P.D., 'Streaming of 14 MeV Neutrons through an Iron Duct—Comparison of Measured Neutron and Gamma-Ray Energy Spectra with Results Calculated Using the Monte-Carlo MNCP Code', Nucl. Sci. Eng. 84, 260 (1983).

Sc 69 Schimmerling, W. and Awschalom, M., '3 GeV Protons on Pb Neutrons Streaming through a Labyrinth', IEEE Trans. Nucl. Sci. NS-16, 604 (1969).

Sc 79a Schönbacher, H. and Stolarz-Izycka, A., 'Compilation of Radiation Damage Test Data: Part I. Cable Insulating Materials', CERN Report CERN 79-04 (1979).

Sc 79b Schönbacher, H. and Stolarz-Izycka, A., 'Compilation of Radiation Damage Test Data: Part II. Thermosetting and Thermoplastic Resins', CERN Report CERN 79-08 (1979).

Sh 64 Shen, S.P., 'Passage of High-Energy Particles in Matter: Nuclear Cascades Induced in Dense Media by 1 and 3 GeV Protons', Brookhaven National Laboratory Report BNL-8721 (1964).

Sh 66 Shaw, K.B., 'Neutron Studies in Shields and Tunnels with the 7 GeV Proton Synchrotron NIMROD', Proc. Conf. Rad. Meas. in Nucl. Power, Berkeley, Glos, U.K., Inst. Phys. and Phys. Soc., London

(1966).

Sh 67 Shaw, K.B. and Stevenson, G.R., 'Interpretation of Results from the Activation in Indium, Gold and Cobalt Disks in Wax Moderators', Rutherford Laboratory Internal Report RP/A/1 (1967).

Sh 68 Shaw, K.B., Stevenson, G.R. and Thomas, R.H., 'Evaluation of Dose Equivalent from Neutron Energy Spectra', Rutherford Laboratory Report RPP/R5 (1968).

Sh 69a Shaw, K.B., Stevenson, G.R. and Thomas, R.H., 'Evaluation of Dose Equivalent from Neutron Energy Spectra', Health Phys. 17, 459 (1969).

Sh 69b Shaw, K.B. and Stevenson, G.R., 'Radiation Studies around Extracted Beams at Nimrod', Proc. 1969 Particle Accelerator Conference, Washington, D.C., March 1969, IEEE Trans. Nucl. Sci. NS-16 (3), Part 1, 57 (1969).

Si 56 Simon, A. and Clifford, C.E., 'The Attenuation of Neutrons by Air-Ducts in Shields', Nucl. Sci. Eng. 1, 156 (1956).

Sm 64 Smith, A.R., McCaslin, J.B. and Pick, M.A., 'Radiation Field inside a Thick Concrete Shield for 6.2 BeV Incident Protons', Lawrence Radiation Laboratory Report UCRL-11331 (1964).

Sm 65 Smith A.R., 'Some Experimental Studies at the 6.2 BeV Berkeley Bevatron,' in: Proc. 1st Symp. Accel. Radiat. Dos. and Exp., at Brookhaven National Laboratory, 3-5 November, 1965, USAEC Report CONF-651109, p. 224 (1965).

So 57 Solon L.R. (ed.), Conference on Shielding High-Energy Accelerators, New York, 11-13 April, 1957, USAEC Report TID-7545 (1957).

Sp 75 Spielberg, D., 'Soil', Section 9.1.8 in IAEA 75, p. 31 (1975).

St 69 Stevenson, G.R., Shaw, K.B., Hargreaves, D.M., Lister, L.P. and Moth, D.A., 'Measurements of the Radiation Field Around the X2 Extracted Proton Beam, Rutherford Laboratory Report RHEL/M 148 (1969).

St 71a Sternheimer, R.M. and Peierls, R.F., 'General Expression for the Density Effect for the Ionization Loss of Charged Particles', Phys. Rev. B3, 3681 (1971).

St 71b Stevenson, G.R., Squier, D.M. and Levine, G.S., 'Measurements of the Angular Dependence of Dose and Hadron Yield from Targets in 8 GeV/c and 24 GeV/c Extracted Proton Beams', Rutherford Laboratory Report RHEL/MR 7 (1971).

St 73 Stevenson. G.R. and Squier, D.M., 'An Experimental Study of the Attenuation of Radiation in Tunnels Penetrating the Shield of an Extracted Beam of the 7 GeV Proton Synchrotron NIMROD', Health Physics 24, 87 (1973).

St 76 Stevenson, G.R., 'The Radiation Environment of Proton Accelerators and Storage Rings', CERN Report CERN 76-04 (1976).

St 79 Stevenson, G.R., 'A User Guide to the MUSTOP Program', CERN Technical Memorandum HS-RP/TM/79-37 Rev. (1979).

St 80 Stevenson, G.R., 'Shielding of Low Energy Accelerators (<100 MeV): Part I', CERN Internal Report, HS-RP/IR/80-51 (1980).

St 81 Stevenson, G.R., 'A Description of the TOMCAT Muon Transport Program', CERN Internal Report HS-RP/IR/81-28 (1981).

St 82 Stevenson G.R., Liu, Kuei-Lin and Thomas, R.H., 'Determination of Transverse Shielding for Proton Accelerators Using the Moyer Model'. Health Physics 43, 13 (1982).

St 83 Stevenson, G.R., Fasso, A., Sandberg, J., Regelbrugge, A., Bonifas, A., Muller, A., and Nielsen, M., 'Measurements of the Dose and Hadron Yield from Copper Targets in 200 GeV/c and 400 GeV/c Extracted Proton Beams. An Atlas of the Results Obtained', CERN Divisional Report TIS-RP/112 (1983).

St 84 Stevenson, G.R., 'The Estimation of Dose Equivalent from the Activation of Plastic Scintillators', Health Physics 47, 837 (1984).

St 86a Stevenson, G.R., Aarnio, P.A., Fasso, A., Ranft, J., Sandberg, J.V. and Sievers, P., 'Comparison of Measurements of Angular Hadron Energy Spectra, Induced Activity and Dose with FLUKA82 Calculations', Nucl. Instrum. and Methods A245, 323 (1986).

St 86b Stevenson, G.R., 'Shielding of Extended Targets at Proton Energies of Greater than 3 GeV', CERN Internal Report TIS/IR/86-04 (1986).

St 86c Stevenson, G.R., 'Dose Equivalent per Star in Hadron Cascade Calculations', CERN Divisional Report TIS-RP/173 (1986).

Su 85 Sullivan, A.H., 'A Method for Estimating Muon Production and Penetration through a Shield', Nucl. Instrum. and Meth. A239, 197 (1985).

Sy 66a Sychev, B.S., Mal'kov, V.V., Komockhov, M.M. and Zaitsev, L.N., Atomnaya Energiya 20, 23 (1966).

Sy 66b Sychev, B.S., Mal'kov, V.V., Komockhov, M.M. and Zaitsev, L.N., Atomnaya Energiya 20, 355 (1966).

Te 82 Tesch, K., 'The Attenuation of the Neutron Dose Equivalent in a Labyrinth through an Accelerator Shield', Particle Accelerators 12, 169 (1982).

Te 83 Tesch, K., 'Comments on the Transverse Shielding of Proton Accelerators, Health Physics 44, 79 (1983).

Te 85 Tesch, K., 'A Simple Estimation of the Lateral Shielding for Proton Accelerators in the Energy Range 50 to 1000 MeV', Rad. Prot. Dosim. 11 (3), 165 (1985).

Th 60 Thomas, R.H., 'Rough Estimates of Shielding Requirements in the Nimrod Experimental Area', Rutherford Laboratory Internal Report NIRL/M/10 (1960).

Th 61 Thomas, R.H., 'Neutron Shielding Properties of Various Materials in the Energy Region 1-100 MeV', Rutherford Laboratory Internal Report NIRL/M/13 (1961).

Th 63 Thomas, R.H. (Ed.), 'Report of the Shielding Conference Held at the Rutherford Laboratory 26-27 September 1962', Rutherford Laboratory Report NIRL/R/40 (1963).

Th 64a Thomas, R.H., 'Shielding Experiment at 6 GeV—I.', Lawrence Berkeley Laboratory Internal Report UCID-10023 (1964).

Th 64b Thomas, R.H., 'Shielding Experiment at 6 GeV—II.', Lawrence Berkeley Laboratory Internal Report UCID-10021 (1964).

Th 64c Thomas, R.H., 'Energy Loss of High-Energy Muons', Lawrence Berkeley Laboratory Internal Report UCID-10100, February 1964.

Th 66 Thomas, R.H., 'Radiation Hazards of the New Generation of Accelerators', Nucleonics 24 (4), 64 (1966).

Th 68 Thomas, R.H., 'Proton Synchrotron Accelerators', in IAEA 68, p. 56 (1968).

Th 70 Thomas, R.H., 'The Bevatron', in part of Section 10.7.3, Proton Synchrotrons: Shield Designs, in IAEA 70, p. 165 (1975).

Th 71 Theriot, D., Awschalam, M. and Lee, K., 'Muon Shielding Calculations: Heterogeneous Passive and Active Shields, Applications to Experimental Beams and Areas', in Proc. Int. Congress Radiation Protection, Accelerator and Space Radiation, Geneva, CERN Internal Report 71-16, Vol. 2, p. 641 (1971).

Th 73 Thomas, R.H., 'Neutron Dosimetry at High-Energy Particle Accelerators', Proc. Symp. on Neutron Monitoring for Radiation Protection Purposes', IAEA, Vienna, STI/PUB/318 (1973).

Th 76 Thomas, R.H., 'Implementing the Requirement to Reduce Radiation Exposure to "...As Low as Practicable" at the Lawrence Berkeley Laboratory', Health Phys. 30, 271 (1976).

Th 78 Thomas, R.H., 'High-Energy Accelerator Shielding—The Present Situation and Future Needs', Proc. Symp. on Shielding Design of Accelerators. Tsukuba, Japan, 7-8 November 1977, National Laboratory for High-Energy Physics Report KEK-77-31 (1978).

Th 81 Thomas, R.H., 'The Variation of the Moyer Model Parameter, H_0, with Primary Proton Energy', Lawrence Berkeley Laboratory Health Physics Note HPN-115, July 13, 1981.

Th 83 Thomas, R.H. and McCaslin, J.B., 'General Shielding for the 20 TeV Hadron Collider Facility: Hadron Considerations', in Report of the 20-TeV Hadron Collider Technical Workshop, Cornell University, April 1983.

Th 84 Thomas, R.H. and Thomas, S.V., 'Variance and Regression Analyses of Moyer Model Parameter Data—A Sequel.' Health Physics 46, 954 (1984).

Th 85 Thomas, R.H., 'Some Important Issues in Developing Radiation Protection Recommendations: Dosimetric Aspects', Proc. 20th

Annual Meeting of the NCRP, April 4-5, 1984, National Council on Radiation Protection and Measurements Proceedings No. 7, Washington, D.C. (1985).

Ti 83 Tigner, M. (Ed.), Report of the 20-TeV Hadron Collider Technical Workshop, Cornell University, April 1983.

Tr 66 Trilling, G.H., 'Pion and Proton Fluxes from High Energy Proton Collisions', Lawrence Berkeley Laboratory Report UCRL-16830 (1966).

URA 68 Universities Research Association, 'National Accelerator Laboratory Design Report', January 1968 (Rev. July 1968), Batavia, IL

Va 68 Vasil'kov, R.G., Gol'danskii, V.I. and Grishkevich, T.V. et al., 'Neutron Yields in a Lead-Water System by High Energy Protons', Sov. At. Energy 25, 1307 (1968).

Va 71 Van Ginneken, A. and Borak, T., 1971, 'Beamstop Experiment at 29.4 GeV', IEEE Trans. Nucl. Sci. NS-18, 3, 746 (1971).

Va 72a Van de Voorde, M.H. and Restat, C., 'Selection Guide to Organic Materials for Nuclear Engineering', CERN Report CERN 72-7 (1972).

Va 72b Van Ginneken, A., 'Weighted Monte Carlo Calculations of Hadronic Cascades in Thick Targets', Fermilab Report FN-250 (1972).

Va 74 Van Ginneken, A. and Awschalom, M., 'High-Energy Particle Interactions in Large Targets: Volume I. Hadronic Cascades, Shielding, Energy Distribution', Fermilab report (unnumbered, 1974).

Va 75 Van Ginneken, A., 'CASIM, Program to Simulate Hadronic Cascades in Bulk Matter', Fermilab Report FN-272 (1975).

Va 80 Van Ginneken, 'Calculation of the Average Properties of Hadronic Cascades at High Energies (CASIM)', in Computer Techniques in Radiation Transport and Dosimetry, W.R. Nelson and T.M. Jenkins, Eds., Plenum Press, New York and London, p. 323 (1980).

Vo 75 Vogt, H.G., 'Monte-Carlo Calculations of the Neutron Transmission through the Access Ways of the CERN Super Proton Synchrotron', CERN Report CERN 75-14 (1975).

Vo 83 Volynchikov, A.I., Getmanov, V.B., Kuznetsov, A.A., Krupnyi, G.I., Lukanin, V.S., Rastsvetalov, Ya.N. and Tatarenko, V.H., 'Secondary Radiation Field Measurements in a Steel Block Absorbing 69 GeV/c Proton Beams', Serpukhov Inst. for High Energy Physics Preprint (in Russian) IFVE 83-86; translated by I. Schulz-Dahlen in DESY Internal Report DESY L-Trans-284 (1983).

We 63 Wenzel, W.A., 'Bevatron External Proton Beams', Proc. Int. Conf. on High-Energy Accelerators, Dubna, 21-27 August 1963', p. 698, Atomizdat, Moscow (1964).

We 71 West, D. and Wood, E., 'Neutron Yield from Protons and Deuterons of Momenta between 0.85 and 1.7 GeV/c Totally Absorbed in Lead', Can. J. Phys. 49, 2061 (1971).

Wy 73 Wyckoff, J.M. and Chilton, A.G., 'Dose Due to Practical Neutron Energy Distributions Incident on Concrete Shielding Walls', Proc. 3rd Int. Cong. of the IRPA, Ed. W.S. Snyder, CONF-730907-P1, p. 694 (1973).

Ye 81 Ye Sizong, private communication to G.R. Stevenson (1981).

Ye 82 Ye Sizong, 'The Calculation of the Neutron Transmission through the Access Way of a High-Energy Accelerator Installation (Using the MORSE Code)', Part. Acc. 12, 65 (1982).

Za 71 Zaitsev, L.N., Komochkov, M.M. and Sychev, B.S., 'Fundamentals of Shielding for Accelerators', (in Russian), Atomizdat, Moscow (1971).

Zo 68 Zolotukhin, V.G., Klimanov, V.A., Leipunskii, O.I., Mashkovich, V.P., Sakharov, V.K., Sinitsyn, B.I. and Tsypin, S.G., 'Radiation Transmission through Inhomogeneities in Shields', Atomizdat (Moscow), in Russian (1968). English translation published by Israel Program for Scientific Publications (Jerusalem) (1971).

Table 4.1.
Number of neutrons produced per proton for different target materials.
Some values have been slightly adjusted by interpolation. [From Tesch (Te 85).]

	Neutrons per incident proton									
E_p (MeV)	C	Ref.	Al	Ref.	Cu, Fe	Ref.	Sn	Ref.	Ta, Pb	Ref.
10					1.2×10^{-3}	Ry 82	1×10^{-3}	Ry 82	2×10^{-4}	Ry 82
20	1.1×10^{-3}	Ry 82	2×10^{-3}	Ry 82	4×10^{-3}	Ry 82	1.3×10^{-2}	Ry 82a	2.4×10^{-3}	Ry 82
30	1.1×10^{-3}	Na 83			1.1×10^{-2}	Na 83			2×10^{-2}	Ry 82
					1×10^{-2}	Mo 61			1.7×10^{-2}	Ne 83
40	6×10^{-3}	Ry 82	1.5×10^{-2}	Ry 82	4.3×10^{-2}	Ry 82	4×10^{-2}	Ry 82		
50	7.6×10^{-3}	Na 83	2×10^{-2}	Mo 61	2.2×10^{-2}	Na 83			3×10^{-2}	Na 83
					3.3×10^{-2}	Mo 61			6.6×10^{-2}	Mo 61
60	1.6×10^{-2}	Ry 82	3×10^{-2}	Ry 82	8×10^{-2}	Ry 82	9×10^{-2}	Ry 82	1.2×10^{-1}	Ry 82
70					5.5×10^{-2}	Br 83				
100	3.6×10^{-2}	Ry 82	1.0×10^{-1}	Ry 82	1.8×10^{-1}	Ry 82	2.3×10^{-1}	Ry 82	2.1×10^{-1}	Ry 82
	3×10^{-2}	Mo 61	1.1×10^{-1}	Mo 61	1.6×10^{-1}	Mo 61			3×10^{-1}	Mo 61
									3.4×10^{-1}	Lo 83
200	1.9×10^{-1}	Ry 82	4×10^{-1}	Ry 82	1.0	Ry 82	1.2	Ry 82	1.6	Ry 82
	2×10^{-1}	Mo 61	4×10^{-1}	Mo 61	6.5×10^{-1}	Mo 61			1.2	Mo 61
									1.5	Al 82
250									2.3	Al 82
									2.5	Ry 83
300									3.0	We 71
400									6.0	Va 68
500	1.0	Mo 61	1.6	Mo 61	2.7	Mo 61			4.7	Mo 61
									7.0	We 71
									8.5	Va 68
550			1.8	Pa 73					10	Fu 72
									7.4	Fu 72
700							7.5	Fu 72	14	Fu 72
									11	We 71
800			3.1	Pa 73					16	Fu 72
									14	We 71
									13	Va 68
1000	2.0	Mo 61	3.2	Mo 61	6	Mo 61	11	Fu 72	11	Mo 61
			3.1	Pa 73					20	Fu 72
									17	Ne 71
1450							17	Fu 72	32	Fu 72

Table 4.2
Values of neutron broad-beam attenuation parameters.

Neutron energy (MeV)	Attenuation length, ℓ (kg/m^2)	Dose equivalent per unit fluence at zero depth k_0 ($Sv\ m^2$)
5	292	1.05×10^{-13}
10	292	1.52×10^{-13}
15	303	2.4×10^{-13}
20	325	5.4×10^{-13}
25	345	1.16×10^{-12}
30	372	1.33×10^{-12}
35	404	1.30×10^{-12}
40	437	1.19×10^{-12}
45	488	9.4×10^{-13}
50	534	7.6×10^{-13}
55	581	6.1×10^{-13}
60	625	5.0×10^{-13}
65	663	4.3×10^{-13}
70	695	4.1×10^{-13}
75	725	4.0×10^{-13}
80	753	3.9×10^{-13}
85	782	3.9×10^{-13}
90	810	3.9×10^{-13}
95	836	3.9×10^{-13}
100	860	3.9×10^{-13}
150	1064	4.2×10^{-13}
200	1150	4.6×10^{-13}
250	1165	5.6×10^{-13}
300	1169	6.9×10^{-13}
350	1170	8.2×10^{-13}
400	1170	9.7×10^{-13}
450	1170	1.10×10^{-12}
500	1170	1.25×10^{-12}
600	1170	1.59×10^{-12}
700	1170	1.89×10^{-12}
800	1170	2.2×10^{-12}
900	1170	2.6×10^{-12}
1000	1170	3.0×10^{-12}

Table 4.3
Values of the parameters to be used in the empirical shielding formulae.

Neutron energy (MeV)	Effective attenuation length λ_{eff} (kg/m^2)	Dose equivalent at 1 m and zero depth per interacting proton (Sv m^2)
Thin target, lateral shielding:		
25	290	5.8×10^{-15}
50	320	6.6×10^{-15}
100	460	7.6×10^{-15}
200	720	8.6×10^{-15}
300	870	9.3×10^{-15}
400	950	9.8×10^{-15}
600	1060	1.0×10^{-14}
800	1120	1.1×10^{-14}
1000	1150	1.2×10^{-14}
Thick target, lateral shielding:		
25	290	7.0×10^{-17}
50	230	1.8×10^{-16}
100	460	4.8×10^{-16}
200	690	1.3×10^{-15}
300	810	2.3×10^{-15}
400	890	3.2×10^{-15}
600	1000	4.8×10^{-15}
800	1070	6.4×10^{-15}
1000	1100	7.6×10^{-15}
Thick target, forward shielding (Br 71):		
50	470	1.4×10^{-15}
100	770	1.8×10^{-15}
200	880	7.4×10^{-15}
300	1010	1.2×10^{-14}
400	1270	1.3×10^{-14}

Table 4.4.
Effect of target thickness on estimate of $\Psi_{\pi/2}$. E_p = 9.1 GeV.

Target	$\Psi_{\pi/2}$ (10^{14} Sv m^2)
1 cm copper	1.3
15 cm copper	2.1
Concrete beam stop	3.8
Moyer value	4.4

Table 4.5
Detectors and their characteristics.

Detector	Reaction	Energy range (MeV)
bare gold foils	$^{197}Au(n,\gamma)^{198}Au$	thermal
large bare indium foils	$^{115}In(n,\gamma)^{116m}In$	thermal
moderated gold foils	$^{197}Au(n,\gamma)^{198}Au$	0.02 to 20
Kodak Type-B neutron films	proton recoil	0.5 to 25
sulphur	$^{32}S(n,p)^{32}P$	3 to 25
aluminium	$^{27}Al(n,\alpha)^{24}Na$	6 to 25
plastic scintillator	$^{12}C(n,2n)^{11}C$	> 20
$\beta\gamma$ film and LiF TLD	Gamma & charged particles	

Table 4.6
Mean free paths and removal cross-sections
for tunnel transmission.

Detector	Mean free path metres	Removal cross-section barns
Plastic scintillator	100	1.9
Aluminium	60	3.2
Film and TLD	55	3.3
Bare gold	30	6.2

FIGURE CAPTIONS FOR CHAPTER 4

Figure 4.1. The variation of the attenuation length, λ, for monoenergetic neutrons in concrete as a function of neutron energy. Full circles indicate the data of Alsmiller et al. (Al 69b), open circles that of Wyckoff and Chilton (Wy 73). The solid line shows recommended values of λ and the dashed line shows the high-energy limiting value of 1170 kg m^{-2}.

Figure 4.2. The variaton of the parameter k_0 as a function of monoenergetic neutron energy. k_0 is the value of the dose equivalent per unit neutron fluence extrapolated from deep in the shield back to zero depth. Full circles indicate values calculated by Alsmiller et al. (Al 69b), open circles indicate values calculated by Wyckoff and Chilton (Wy 73). The solid line indicates recommended values of k_0.

Figure 4.3. Dose equivalent as a function of depth in concrete for protons of the energies indicated incident on thin targets of copper. The solid lines have been used to determine the parameters λ_{eff} and $H_{\pi/2}$ used in Figs. 4.5 and 4.6.

Figure 4.4. Dose equivalent as a function of depth in concrete for protons of the energies indicated incident on thick targets of copper. The solid lines have been used to determine the parameters λ_{eff} and $H_{\pi/2}$ in Figs. 4.5 and 4.6. The dashed lines are from Braid et al. (Br 71) at 100, 200, 300, and 400 MeV; the dotted line is from Alsmiller et al. (Al 75) at 200 MeV.

Figure 4.5. Effective attenuation length in concrete as a function of proton energy. Open circles are the thin-target data from Fig. 4.3; closed circles are the thick-target data from Fig. 4.4; x — calculations of O'Brien (OB 68); + — data from Braid et al. (Br 71); * — the calculation of Alsmiller et al. (Al 75); Δ — the data of Ban et al. (Ba 81); $\square$ — data of Allen and Futterer reported by Patterson and Thomas (Pa 73).

Figure 4.6. The parameter $H_{\pi/2}$ as a function of proton energy. Open circles are the thin-target data from Fig. 4.3; closed circles are the thick-target data from Fig. 4.4. The solid line above 3 GeV indicates the high-energy Moyer parameter given by the equation

$$H_{\pi/2} = 7.6 \times 10^{-15} E_p^{0.8} \quad \text{Sv m}^2 \quad .$$

The dashed line, where the Moyer model is no longer valid is indicated merely to guide the eye.

Figure 4.7. a) Single-collision geometry for Lindenbaum approximation. b) Two-collision geometry for Lindenbaum approximation.

Figure 4.8. Development of a one-dimensional cascade in the Lindenbaum approximation with n = 3 and m = 2.

Figure 4.9. The laterally integrated star density in nuclear emulsions

produced by a 19.2 GeV/c proton beam incident on an iron slab as a function of depth in the slab. The measurements were made by Citron et al. (Ci 65), the Monte Carlo Calculations were performed by Ranft (Ra 67).

Figure 4.10. The thick-target cross-section for ^{18}F production for 1 and 3 GeV protons incident on an iron block as a function of depth in the block. The measurements were made by Shen (Sh 64), the Monte Carlo calculations were performed by Armstrong and Alsmiller (Ar 68).

Figure 4.11. Comparison of calculated (histograms) and experimental (solid circles) radial variations of the production of ^{54}Mn at various depths in iron for 1 and 3 GeV incident protons (Ar 69a).

Figure 4.12. Calculated and measured track intensity at various depths as a function of lateral distance from the beam axis. Both the calculated and measured results are normalized to give a laterally integrated track intensity of unity at zero depth. The error bars without the air gaps have approximately the same magnitude as those shown with air gaps present (Ar 72).

Figure 4.13. Comparison of calculated and measured lateral distribution of ^{18}F production in aluminium foils at various depths in iron for 19.4 GeV/c incident protons (Ar 72).

Figure 4.14. The longitudinal development of the total track density (sum of proton, pion and muon track densities) for a cascade initiated by a well-collimated proton beam of cross-section 10 × 10 mm^2 and momentum 20 GeV/c in steel. The curves are normalized to unit proton track density at $r = 0$ and $z = 0$. The points represent the track densities along the beam axis ($r = 0$ cm) and 8 and 32 cm outside the beam axis ($r = 8$, 32 cm) which were measured by Citron et al. (Ci 65). The change in the slope of the curve near the depth $z = 2000$ g cm^{-2} arises from the muon track density (Ra 67).

Figure 4.15. ^{18}F production from aluminium versus radial distance at various depths in the beamstop (Va 71). (a) zero depth, (b) 5.08 cm Fe + 2.54 cm air, (c) 10.16 cm Fe + 5.08 cm air, (d) 20.32 cm Fe + 7.62 cm air, (e) 30.48 cm Fe + 10.16 cm air, (f) 40.64 cm Fe + 12.70 cm air, (g) 71.12 cm Fe + 20.32 cm air, (h) 101.60 cm Fe + 27.94 cm air, and (i) 132.08 cm Fe + 35.56 cm air.

Figure 4.16. Hadron fluence using star densities in an aluminium cylinder for 200 GeV incident protons at a depth of 83.6 cm. The open circles are the experimental data based on ^{18}F measurements. The histogram is the FLUKA82 calculation.

Figure 4.17. 30-GeV/c protons incident on a solid iron cylinder. Contours of equal star density (stars/cm^3 per incident proton). The beam of 0.3 × 0.3 cm^2 cross-section is centred on the cylinder axis and starts to interact at zero depth. The star density includes only those due to hadrons above 0.3 GeV/c momentum. Contours of higher star density are not shown for clarity of the plot, those of lower star density are not included due to the statistical uncertainty.

Figure 4.18. Variation of the dose equivalent on the longitudinal axis as a function of depth in the shield for proton induced cascades in steel of density 7.88 g cm^{-3}. The FLUKA82 calculations are for incident proton momenta of 1 GeV/c (+), 3 GeV/c (solid square), 10 GeV/c (open triangle), 30 GeV/c (solid circle), 100 GeV/c (x), 300 GeV/c (solid inverted triangle), and 1 TeV/c (open square). The solid lines correspond to the results of CASIM calculations at the marked proton momenta. The dashed lines are fits by eye through the TRANKA points for proton momenta of 20 GeV/c (o) and 300 GeV/c (open inverted triangle) respectively.

Figure 4.19. Variation of the dose equivalent on the longitudinal axis as a function of depth in the shield for proton induced cascades in concrete of density 2.4 g cm^{-3}. The FLUKA82 calculations are for incident proton momenta of 1 GeV/c (+), 3 GeV/c (solid square), 10 GeV/c (open triangle), 30 GeV/c (solid circle), 100 GeV/c (x), 300 GeV/c (inverted solid triangle), and 1 TeV/c (open square). The solid lines correspond to the results of CASIM calculations at the marked proton momenta. The dashed lines are fits by eye through the TRANKA points for proton momenta of 20 GeV/c (o) and 300 GeV/c (inverted open triangle).

Figure 4.20. Variation of the effective source strength S(z) with depth in a steel shield of density 7.88 g cm^{-3} for cascades initiated by protons of the marked momenta.

Figure 4.21. Variation of the effective source strength S(z) with depth in a concrete shield of density 2.4 g cm^{-3} for cascades initiated by protons of the marked momenta.

Figure 4.22 Variation of the dose equivalent at the position of the longitudinal maximum multiplied by the square of the radius as a function of radius off-axis for proton induced cascades in steel of density 7.88 g cm^{-3}. The FLUKA82 calculations are for incident proton momenta of 1 GeV/c (+), 3 GeV/c (solid square), 10 GeV/c (open triangle), 30 GeV/c (solid circle), 100 GeV/c (x), 300 GeV/c (inverted solid triangle), and 1 TeV (open square). The solid lines correspond to the results of CASIM calculations at the marked proton momenta. The dashed lines are the extensions of the CASIM lines of 30 GeV/c and 300 GeV/c through the TRANKA points for proton momenta of 20 GeV/c (o) and 300 GeV/c (open inverted triangle) respectively.

Figure 4.23. Variation of the dose equivalent at the position of the longitudinal maximum multiplied by the square of the radius as a function of radius off-axis for proton induced cascades in concrete of density 2.4 g cm^{-3}. The FLUKA82 calculations are for incident proton momenta of 1 GeV/c (+), 3 GeV/c (solid square), 10 GeV/c (open inverted triangle), 30 GeV/c (solid circle), 100 GeV/c (x), 300 GeV/c (inverted solid triangle), and 1 TeV (open square). The solid lines correspond to the results of CASIM calculations at the marked proton momenta. The dashed lines are best fits by eye using an effective absorption mean free path of 1170 kg m^2 through the TRANKA points for proton momenta of 20 GeV/c (o) and 300 GeV/c (open inverted triangle) respectively.

Figure 4.24 Variation of the constant $\Psi_{\pi/2}$ with incident proton energy for the side-shielding of end-stops. The solid circles are for the steel shield and the open circles are for the concrete shield.

Figure 4.25. Comparison between TOMCAT (solid line) and TRANMU (histogram): Radial distribution for 240 GeV/c incident muons [from (Ne 83)].

Figure 4.26. Comparison between TOMCAT and scintillation counter data for 240 GeV/c incident muons [from (Ne 83)].

Figure 4.27. Longitudinal attenuation curves in steel of density 7.8 g cm^{-3} for muons produced by pions of both signs from proton interactions in a copper target. The numbers against the curves correspond to the proton energy in GeV.

Figure 4.28. Longitudinal attenuation curves in concrete of density 2.4 g cm^{-3} for muons produced by pions of both signs from proton interactions in a copper target. The numbers against the curves correspond to the proton energy in GeV.

Figure 4.29. Radial attenuation curves in steel of density 7.8 g cm^{-3} for muons produced by pions of both signs from proton interactions in a copper target. The numbers against the curves correspond to the proton energy in GeV.

Figure 4.30. Radial attenuation curves in concrete of density 2.4 g cm^{-3} for muons produced by pions of both signs from proton interactions in a copper target. The numbers against the curves correspond to the proton energy in GeV.

Figure 4.31. The relative transmission of neutron flux density and γ dose rate along a large straight tunnel [from (Gi 68)].

Figure 4.32. Approximate exponential absorption of neutron flux density and γ dose rate in a large straight tunnel for a variety of detectors [from (Gi 68)].

Figure 4.33. Relative variation of particle flux density (as determined by several activation detectors) with distance along a straight tunnel [after (St 73)].

Figure 4.34. Experimental layout used to study the transmission of neutrons around right-angled bends [from (St 73)].

Figure 4.35. Relative transmission of particle flux density along the tunnel layout shown in Fig. 4.34 [after (St 73)].

Figure 4.36. Calculated and measured transmission in the second leg of the layout of Fig. 4.34. All data normalized to unity at the mouth of the second leg [from (Ye 82)].

Figure 4.37. Comparison of transmission around a right-angled bend in the NIMROD experiment for the ZEUS-albedo model, MORSE calculations and

neutron dose equivalent [after (St 73) and (Ye 82)].

Figure 4.38. Universal transmission curves for the first leg of a labyrinth [from (Go 75)].

Figure 4.39. Universal transmission curves for the second and subsequent legs of labyrinths [from (Go 75)].

Figure 4.40. Measurements and predictions of transmission in a tunnel at Fermilab [after (Co 85b)].

Figure 4.41. Various types of neutron-trap configuration.

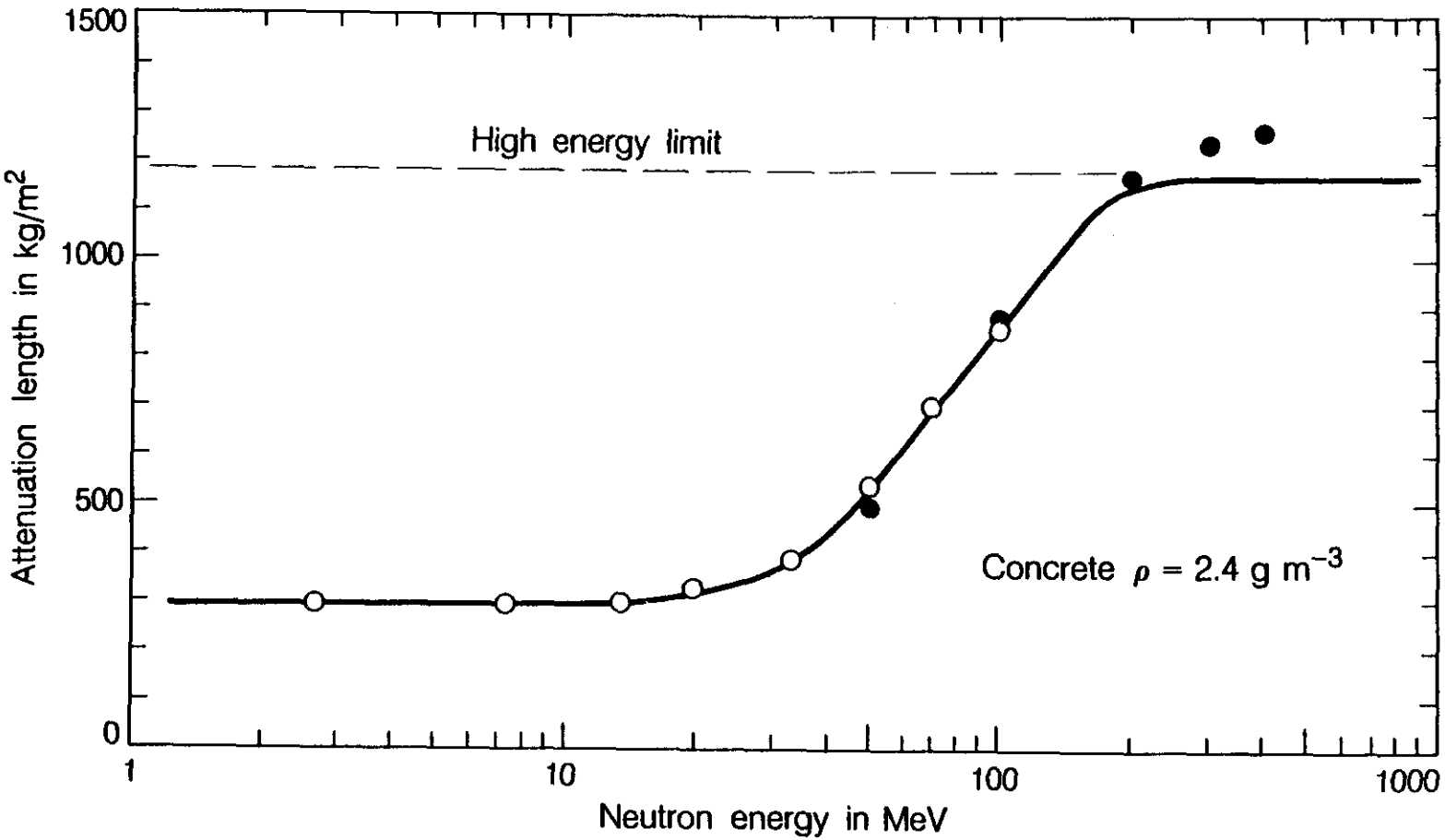

XBL 855-9985A

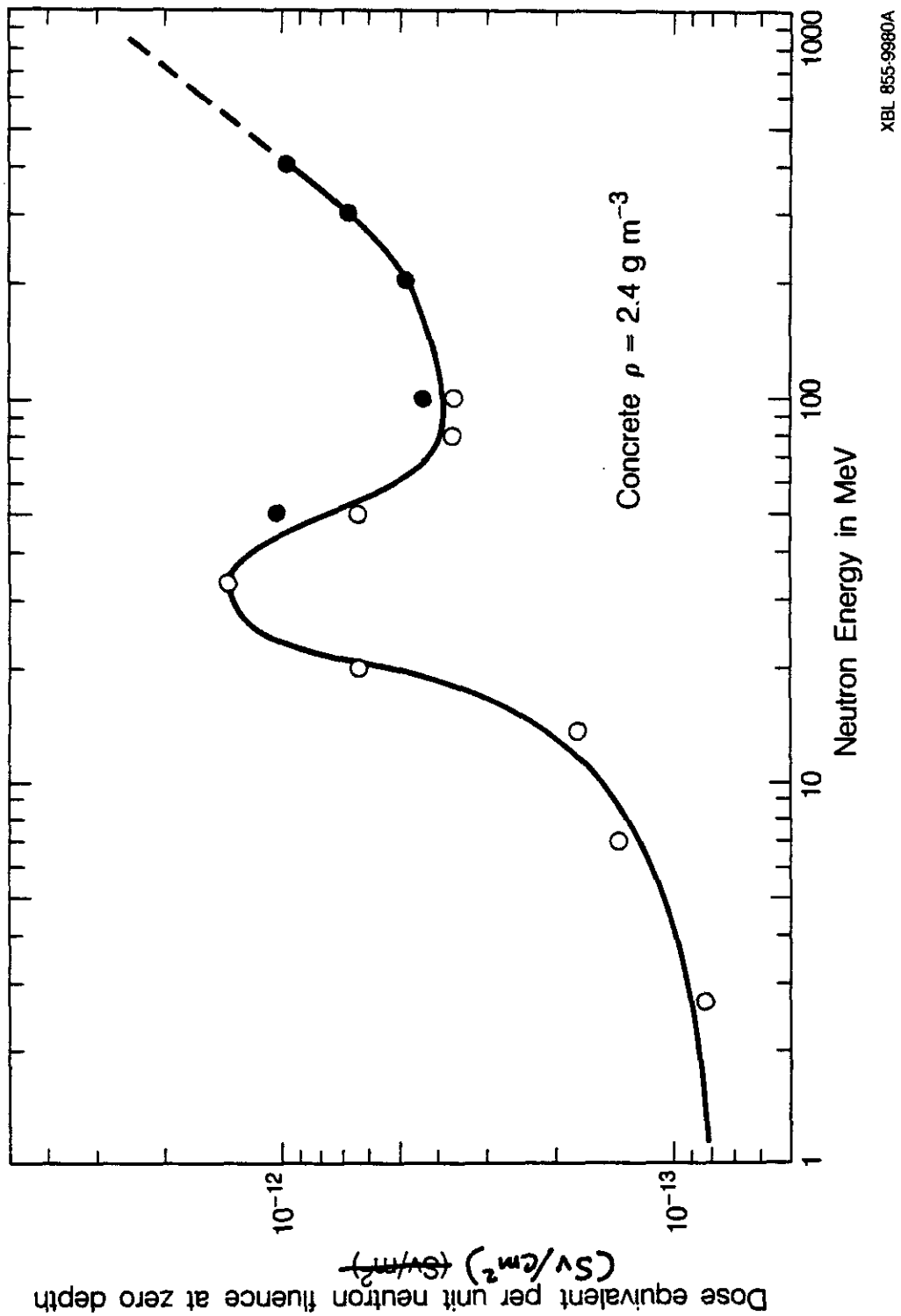

4.2

Rev: GRS 5/87

4.2

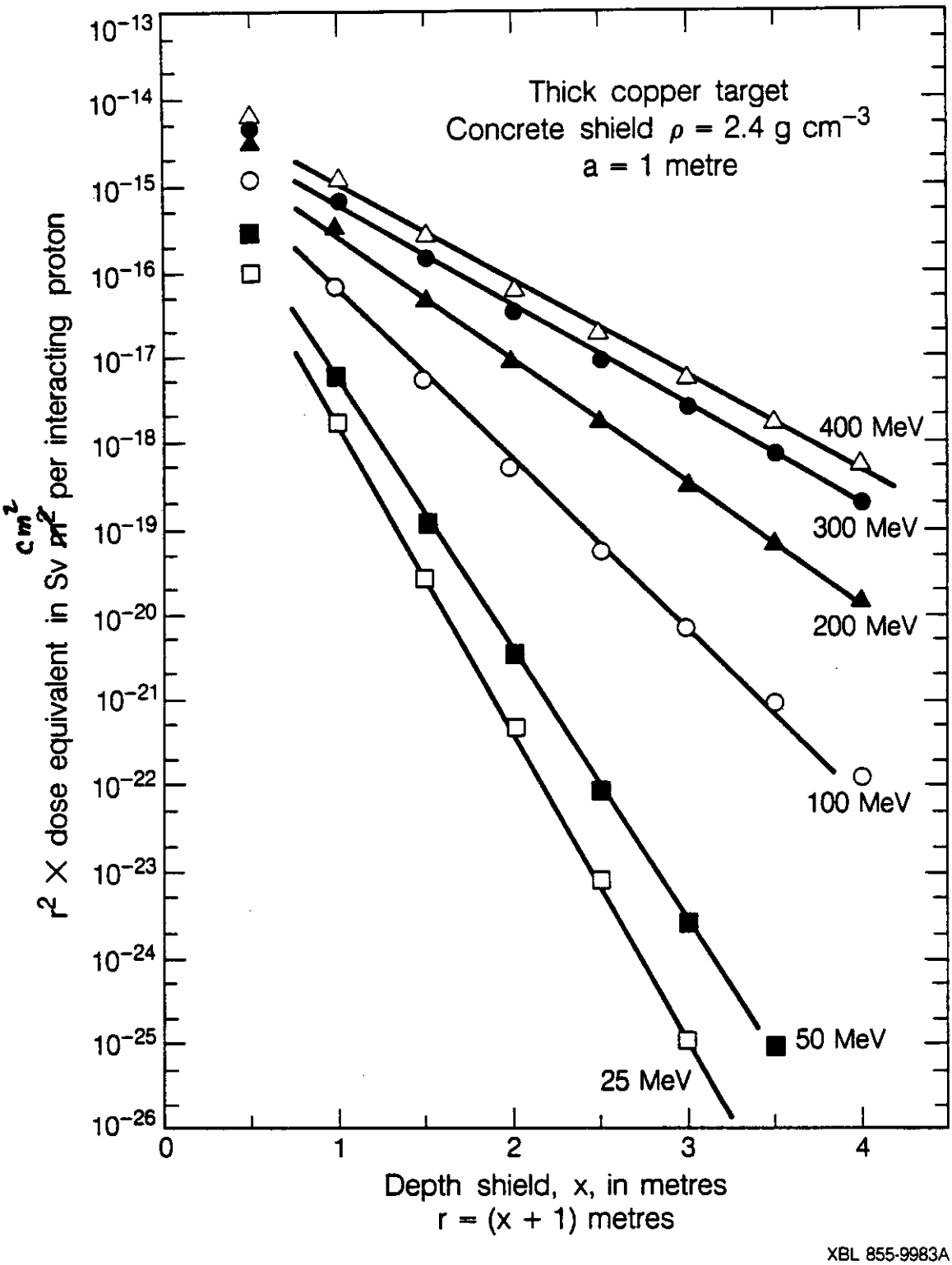

4.3

Rev: GRS 5/87

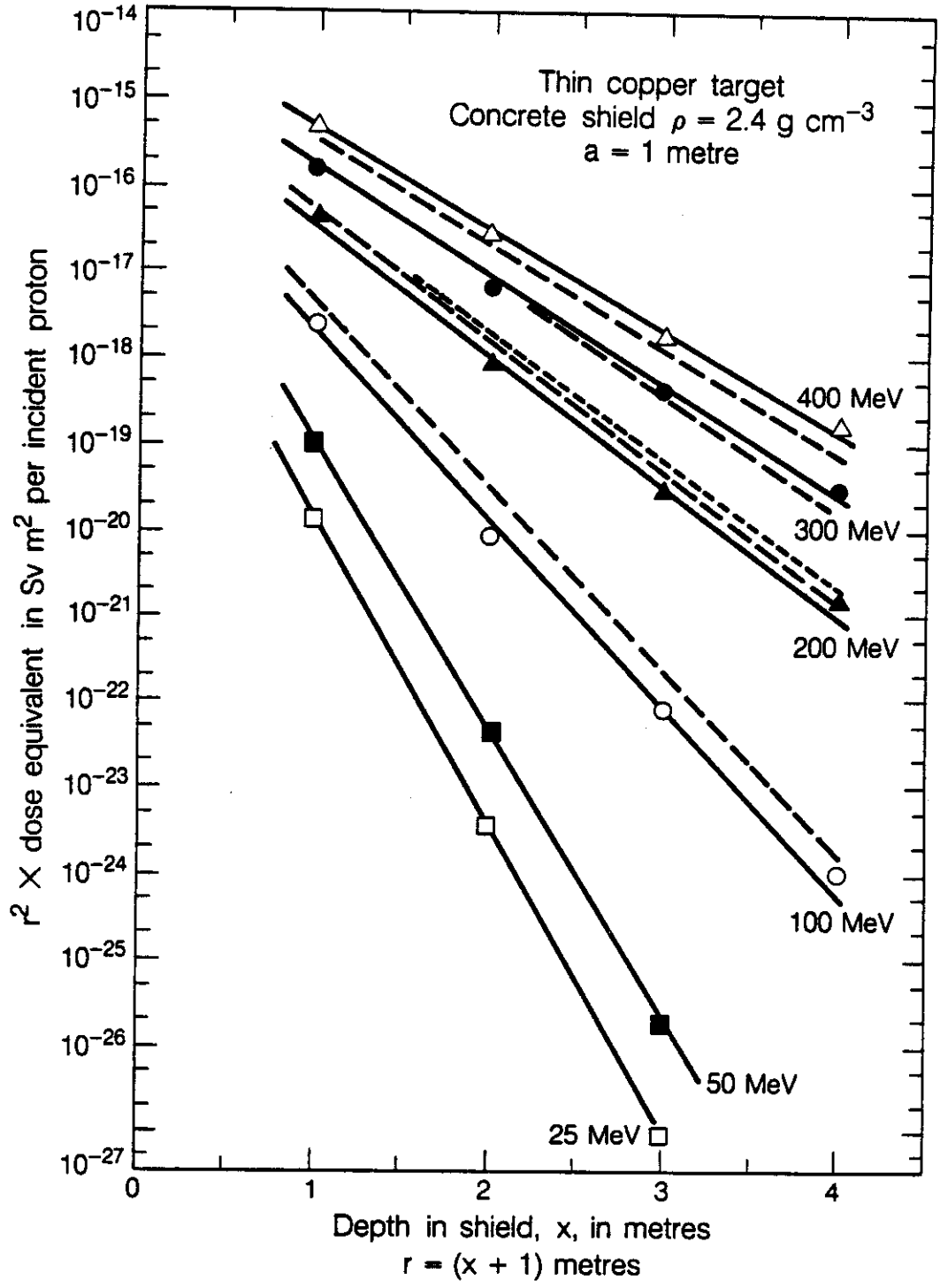
Thin copper target
Concrete shield ρ = 2.4 g cm⁻³
a = 1 metre
400 MeV
300 MeV
200 MeV
100 MeV
50 MeV
25 MeV
r² X dose equivalent in Sv m² per incident proton
Depth in shield, x, in metres
r = (x + 1) metres
XBL 855-9982A

4.4

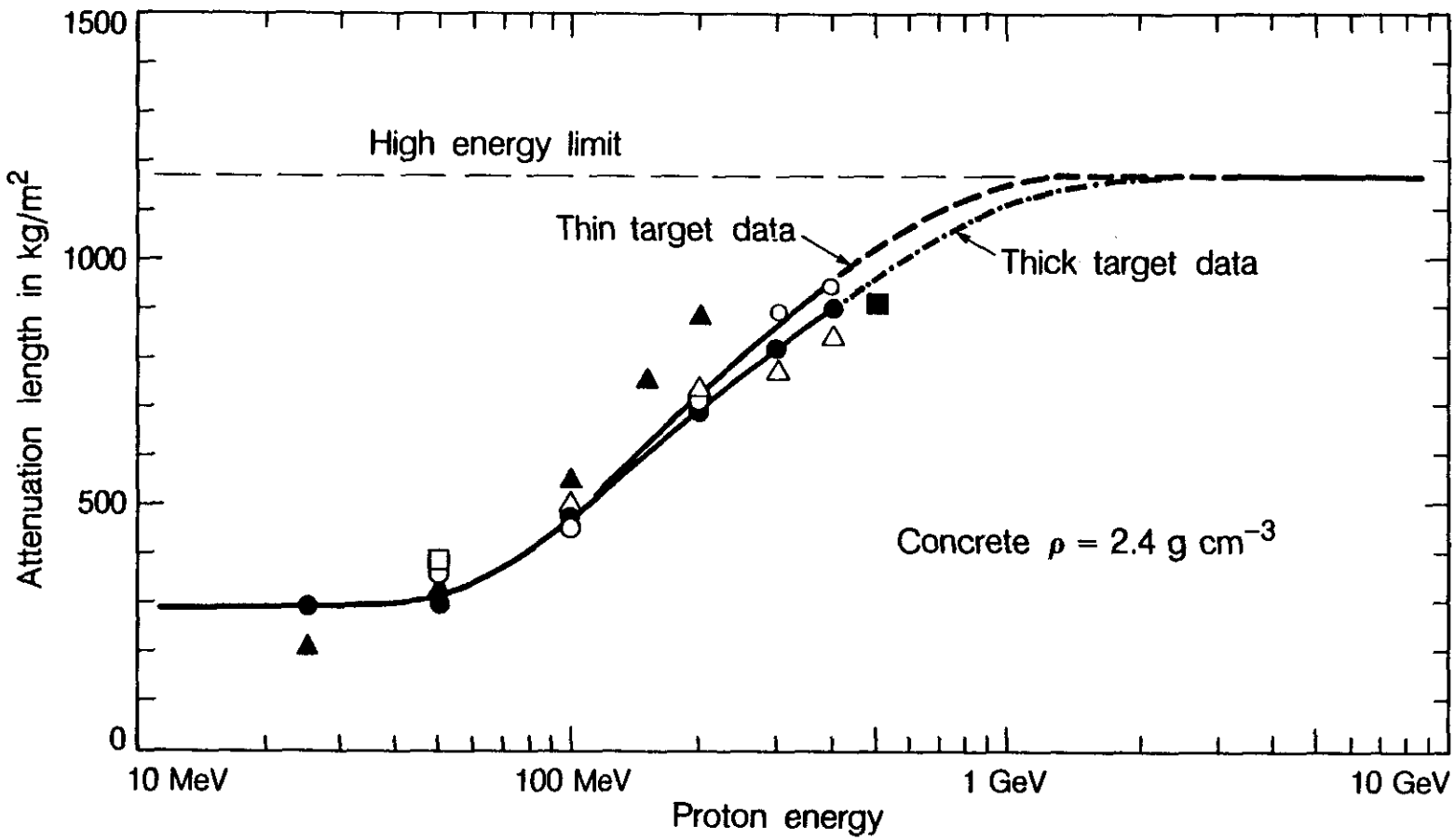

XBL 855-9981A

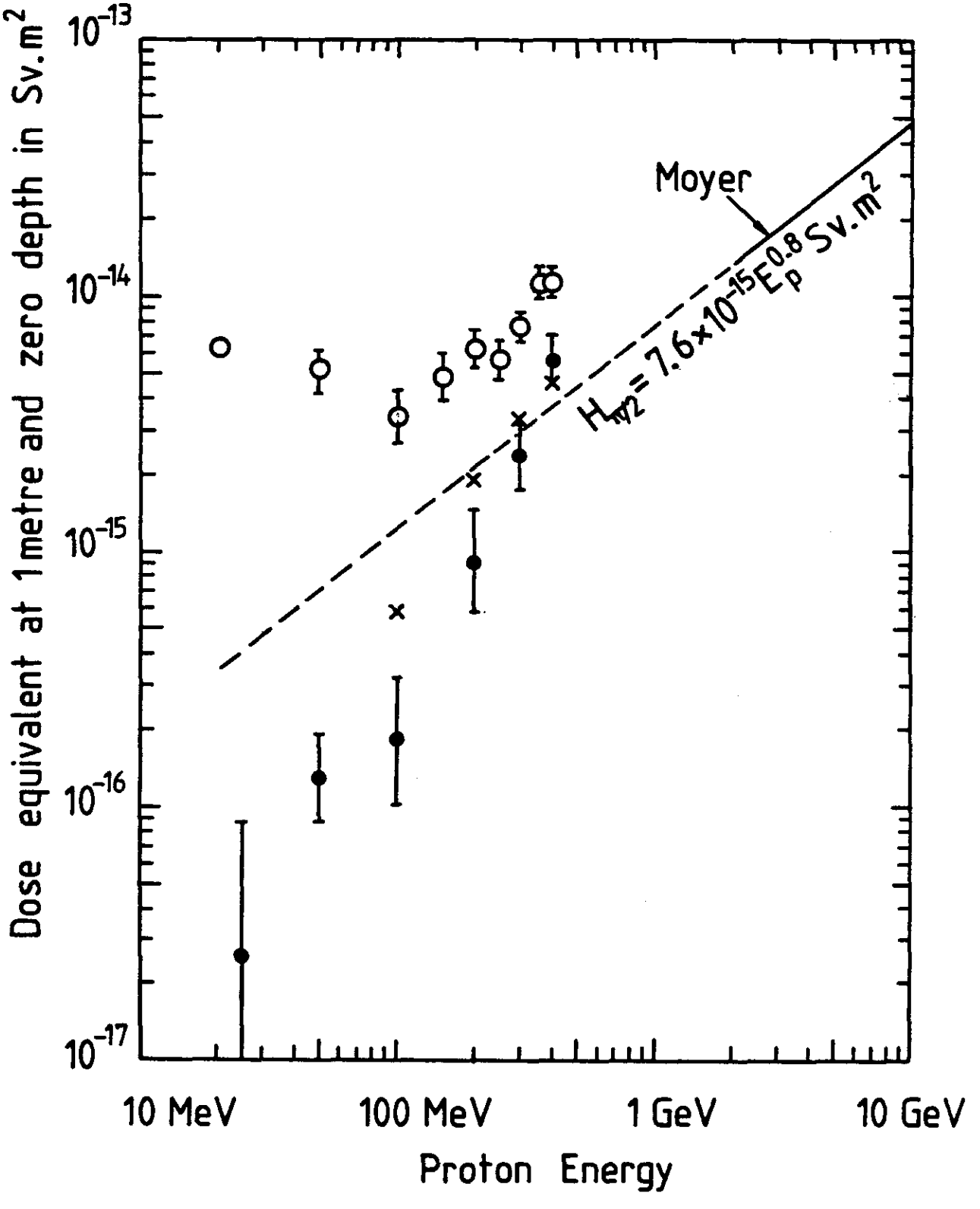
Dose equivalent at 1 metre and zero depth in Sv.m^2
10^{-13}
10^{-14}
10^{-15}
10^{-16}
10^{-17}
Moyer
$H_{m2} = 7.6 \times 10^{-15} E_p^{0.8}$ Sv.m^2
10 MeV
100 MeV
1 GeV
10 GeV
Proton Energy

4.6

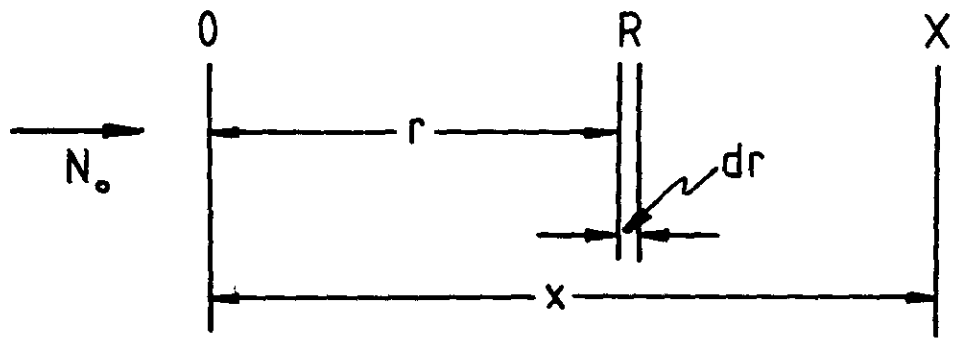

a)

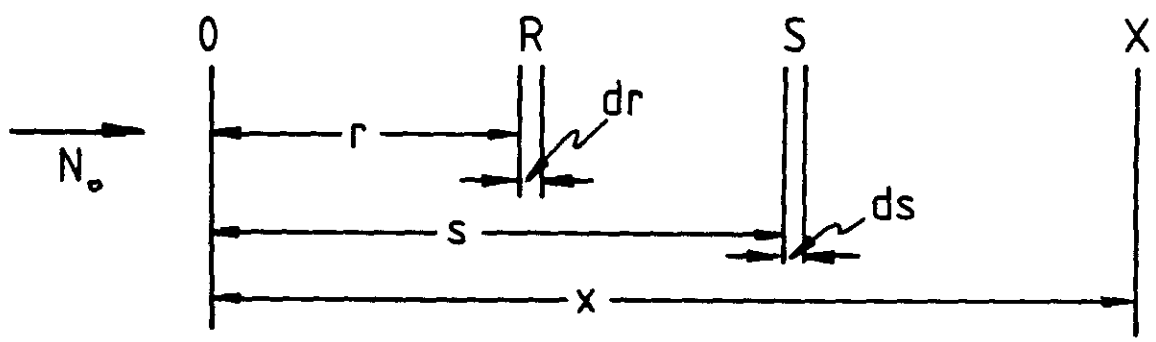

b)

4.7

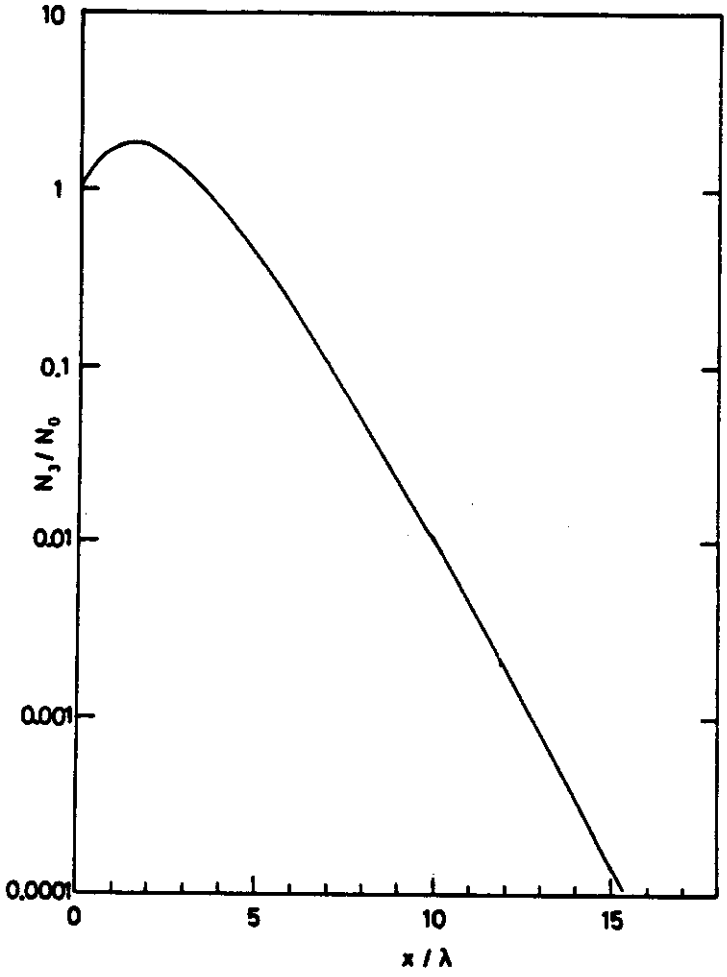

4.8

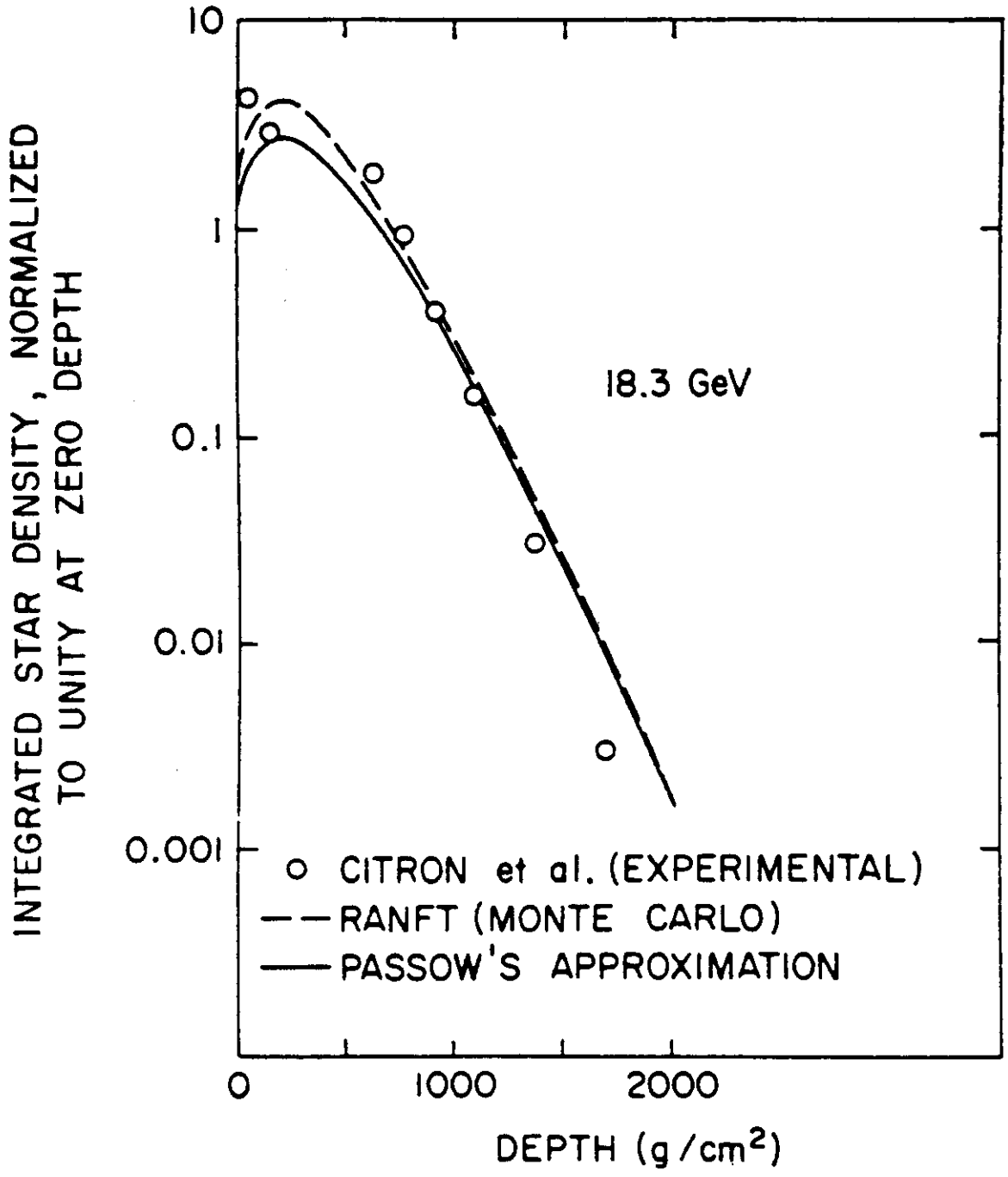
INTEGRATED STAR DENSITY, NORMALIZED TO UNITY AT ZERO DEPTH
10
1
0.1
0.01
0.001
18.3 GeV
o CITRON et al. (EXPERIMENTAL)
— — RANFT (MONTE CARLO)
—— PASSOW'S APPROXIMATION
0
1000
2000
DEPTH (g/cm²)

4.9

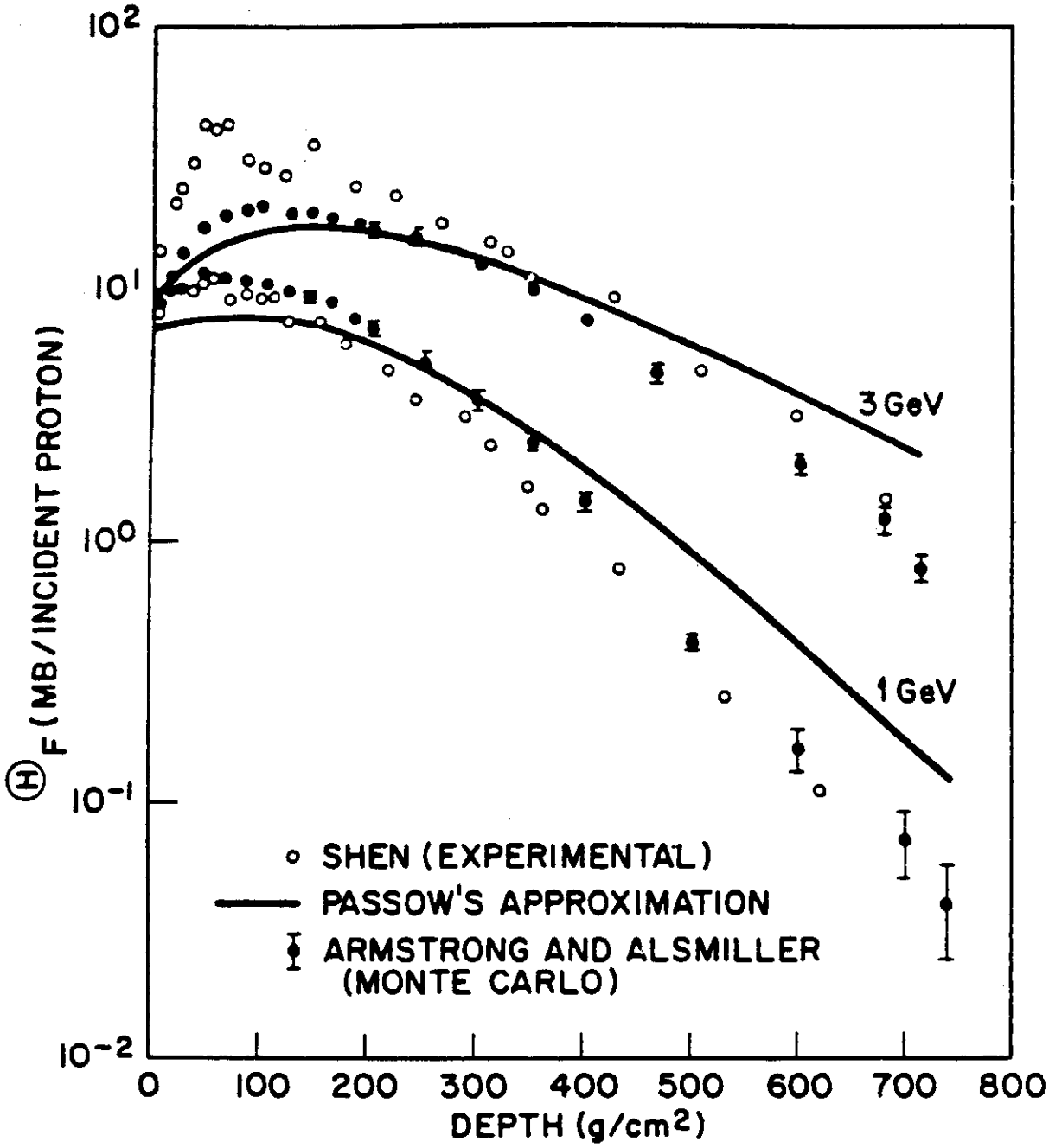
10^2
10^1
10^0
10^{-1}
10^{-2}
$\textcircled{H}_F$ (MB/INCIDENT PROTON)
3 GeV
1 GeV
SHEN (EXPERIMENTAL)
PASSOW'S APPROXIMATION
ARMSTRONG AND ALSMILLER (MONTE CARLO)
0
100
200
300
400
500
600
700
800
DEPTH (g/cm^2)

4.10

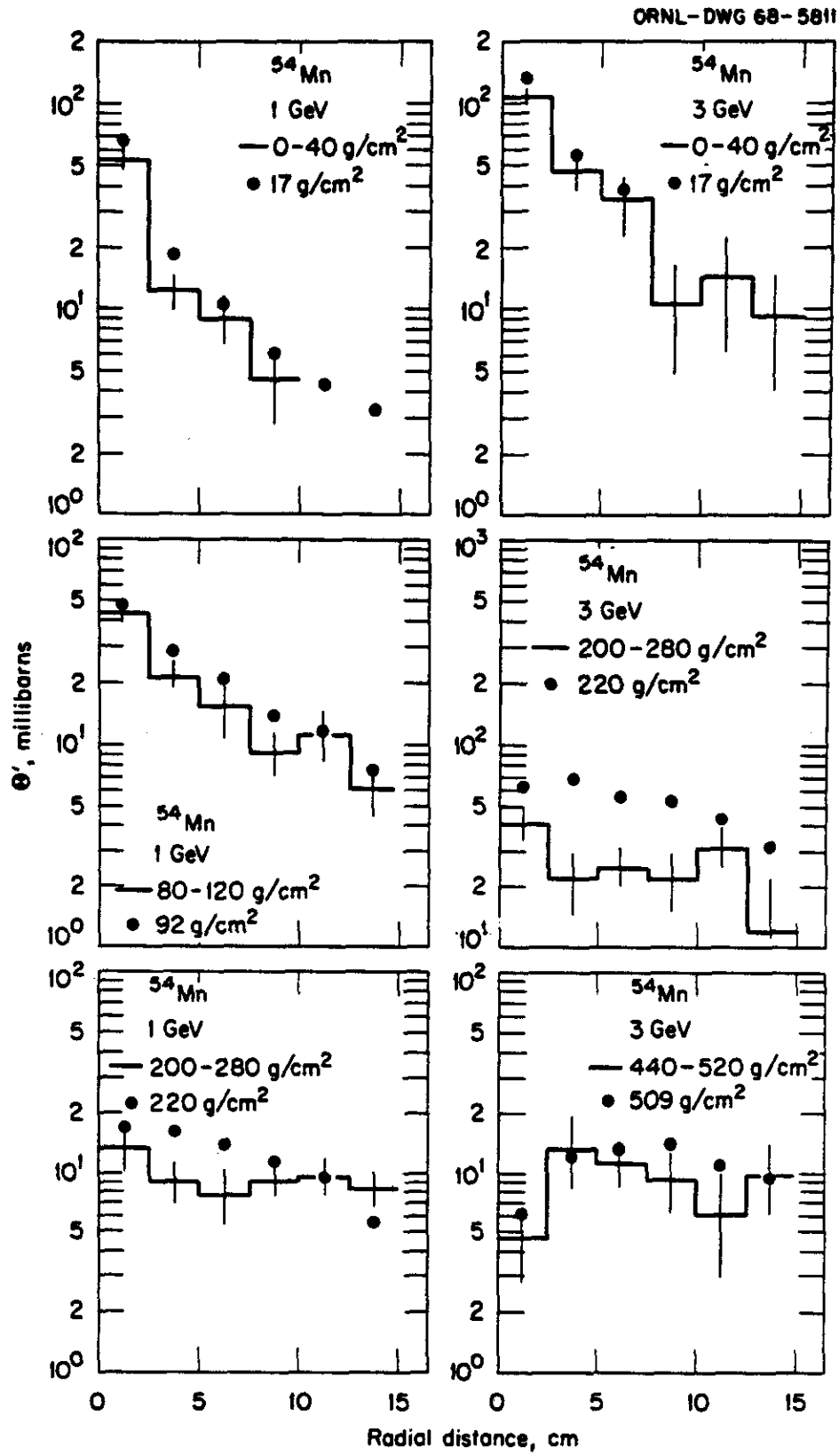
ORNL-DWG 68-5811
^{54}Mn
1 GeV
0-40 g/cm^2
17 g/cm^2
^{54}Mn
3 GeV
0-40 g/cm^2
17 g/cm^2
^{54}Mn
1 GeV
80-120 g/cm^2
92 g/cm^2
^{54}Mn
3 GeV
200-280 g/cm^2
220 g/cm^2
^{54}Mn
1 GeV
200-280 g/cm^2
220 g/cm^2
^{54}Mn
3 GeV
440-520 g/cm^2
509 g/cm^2
θ', millibarns
Radial distance, cm

4.11

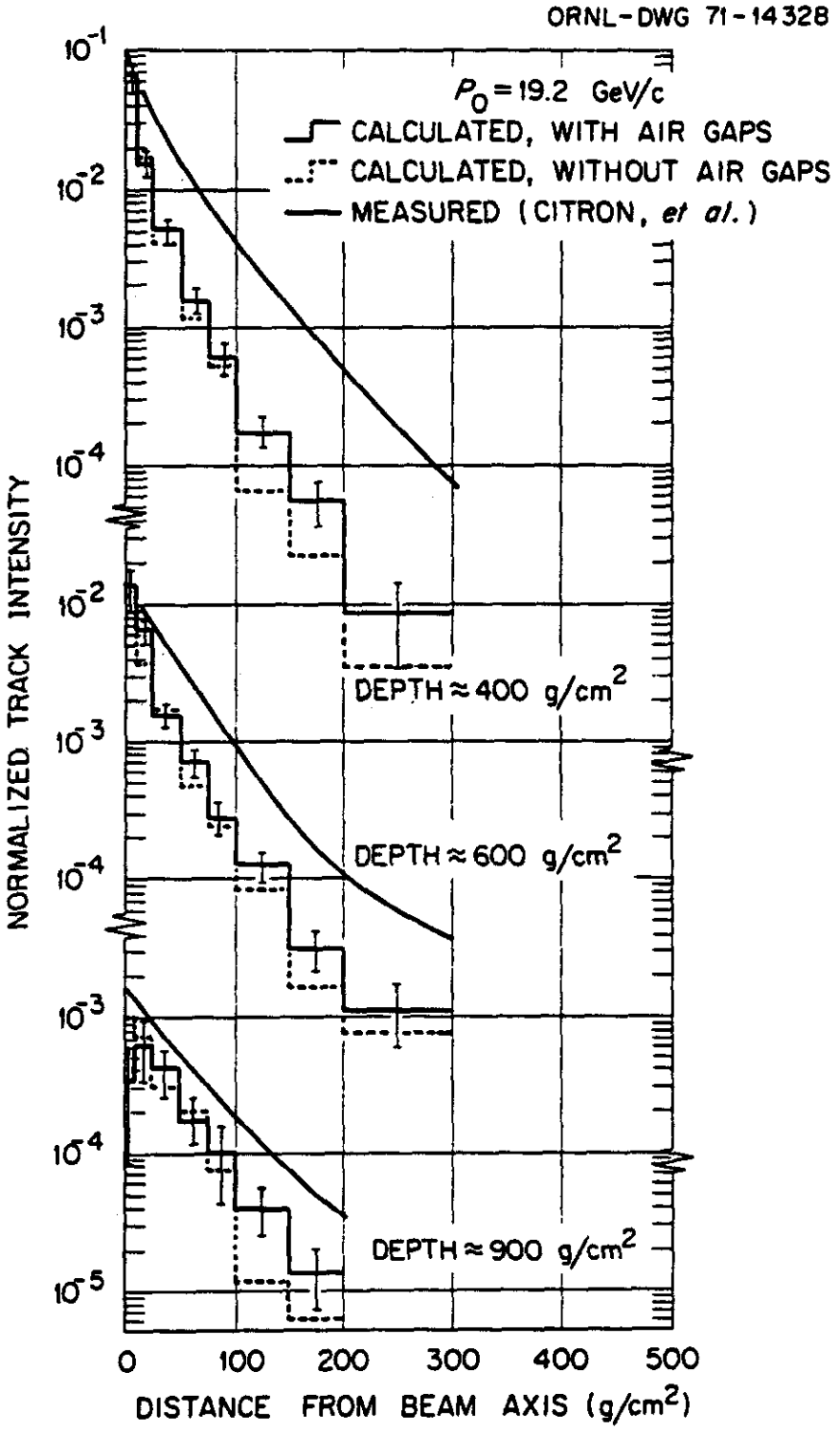
ORNL-DWG 71-14328
$P_0 = 19.2$ GeV/c
CALCULATED, WITH AIR GAPS
CALCULATED, WITHOUT AIR GAPS
MEASURED (CITRON, *et al.*)
DEPTH ≈ 400 g/cm²
DEPTH ≈ 600 g/cm²
DEPTH ≈ 900 g/cm²
NORMALIZED TRACK INTENSITY
10^{-1}
10^{-2}
10^{-3}
10^{-4}
10^{-2}
10^{-3}
10^{-4}
10^{-3}
10^{-4}
10^{-5}
0
100
200
300
400
500
DISTANCE FROM BEAM AXIS (g/cm²)

4.12

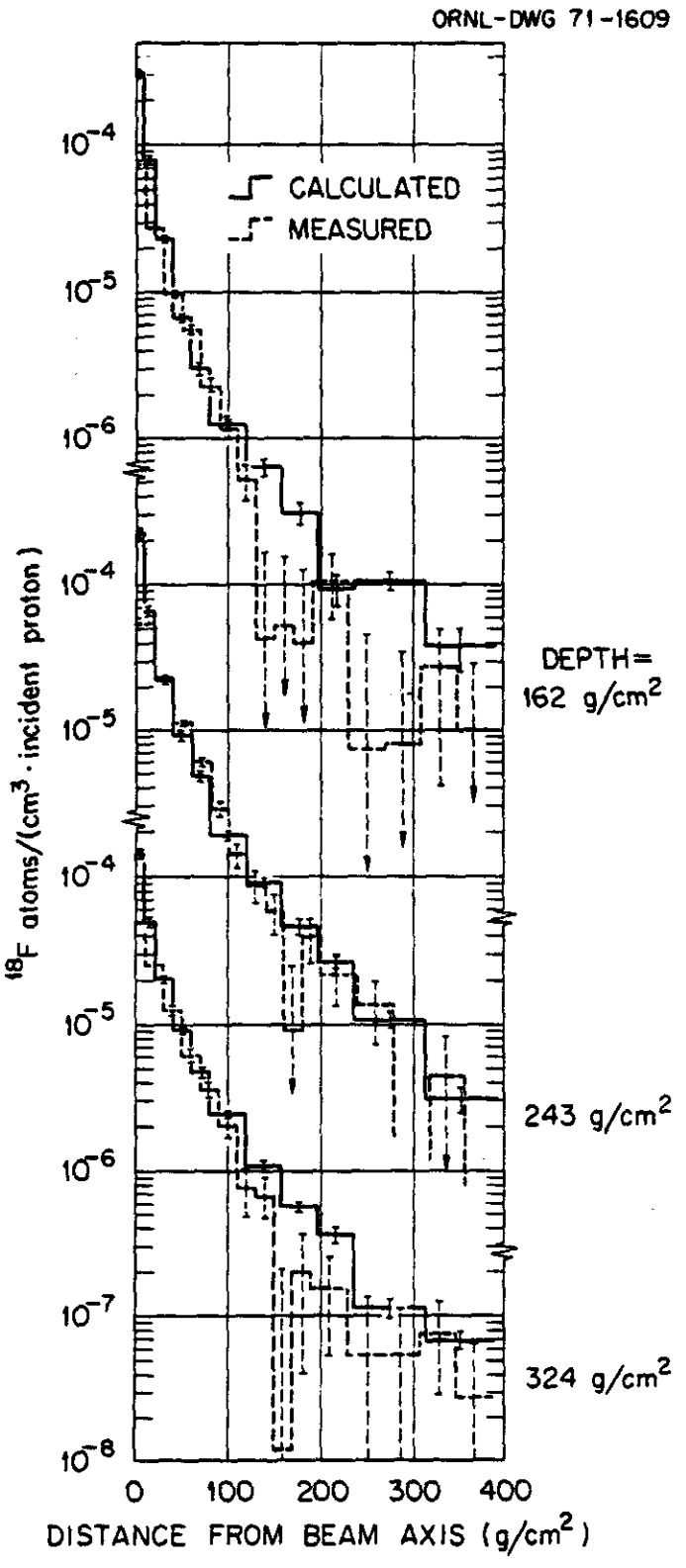
ORNL-DWG 71-1609
CALCULATED
MEASURED
DEPTH=
162 g/cm2
243 g/cm2
324 g/cm2
18F atoms/(cm3 · incident proton)
DISTANCE FROM BEAM AXIS (g/cm2)
10-4
10-5
10-6
10-4
10-5
10-4
10-5
10-6
10-7
10-8
0
100
200
300
400

4.13

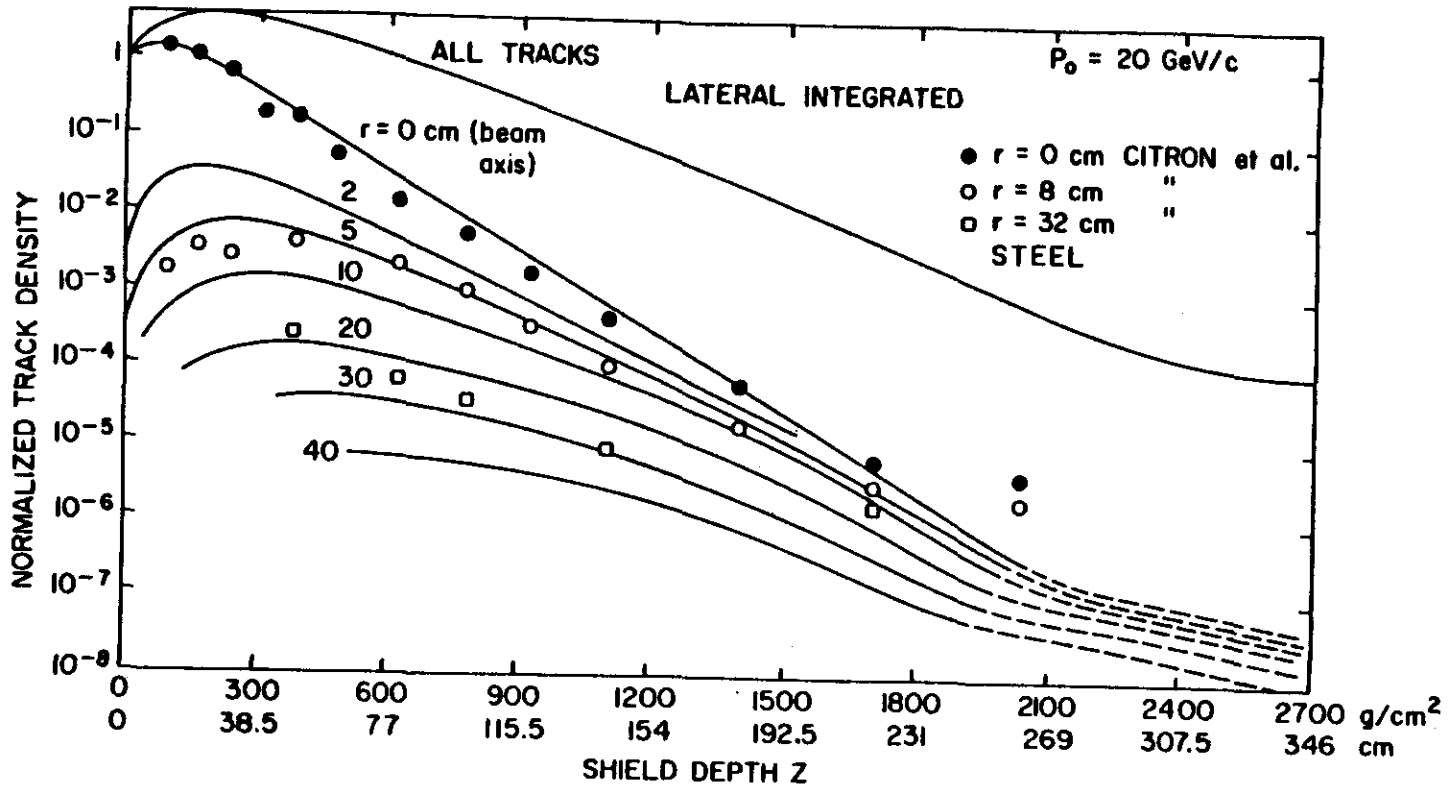
ALL TRACKS
LATERAL INTEGRATED
P_o = 20 GeV/c
r = 0 cm (beam axis)
2
5
10
20
30
40
● r = 0 cm CITRON et al.
o r = 8 cm "
□ r = 32 cm "
STEEL
NORMALIZED TRACK DENSITY
1
10^{-1}
10^{-2}
10^{-3}
10^{-4}
10^{-5}
10^{-6}
10^{-7}
10^{-8}
0 300 600 900 1200 1500 1800 2100 2400 2700 g/cm^2
0 38.5 77 115.5 154 192.5 231 269 307.5 346 cm
SHIELD DEPTH Z

No. of Atoms/(cm³)(Incident Proton)
Radial Distance (in)
(a)
(b)
(c)
(d)
(e)
(f)
(g)
(h)
(i)

4.15

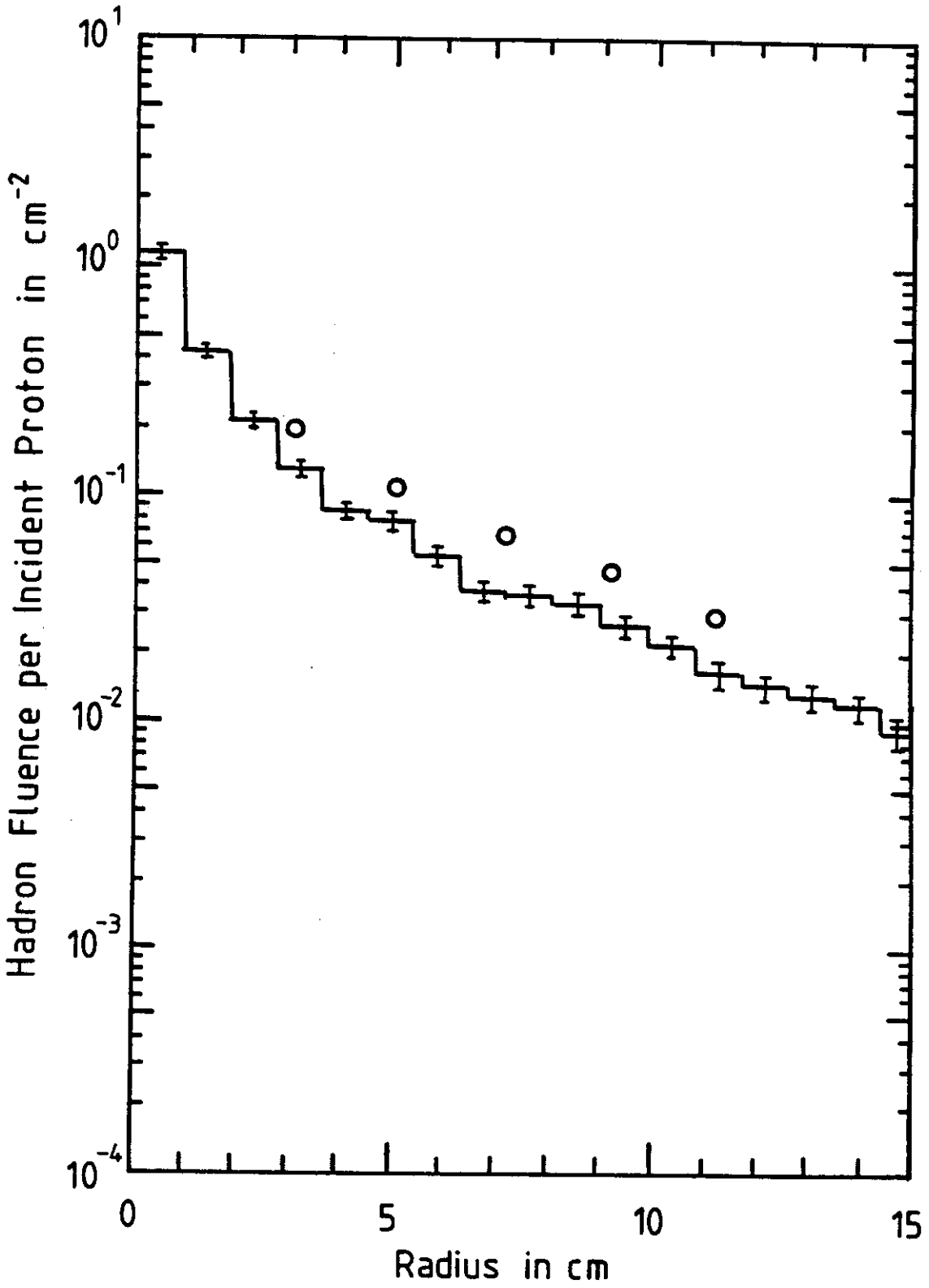
Hadron Fluence per Incident Proton in cm^{-2}
10^{1}
10^{0}
10^{-1}
10^{-2}
10^{-3}
10^{-4}
0
5
10
15
Radius in cm

4.16

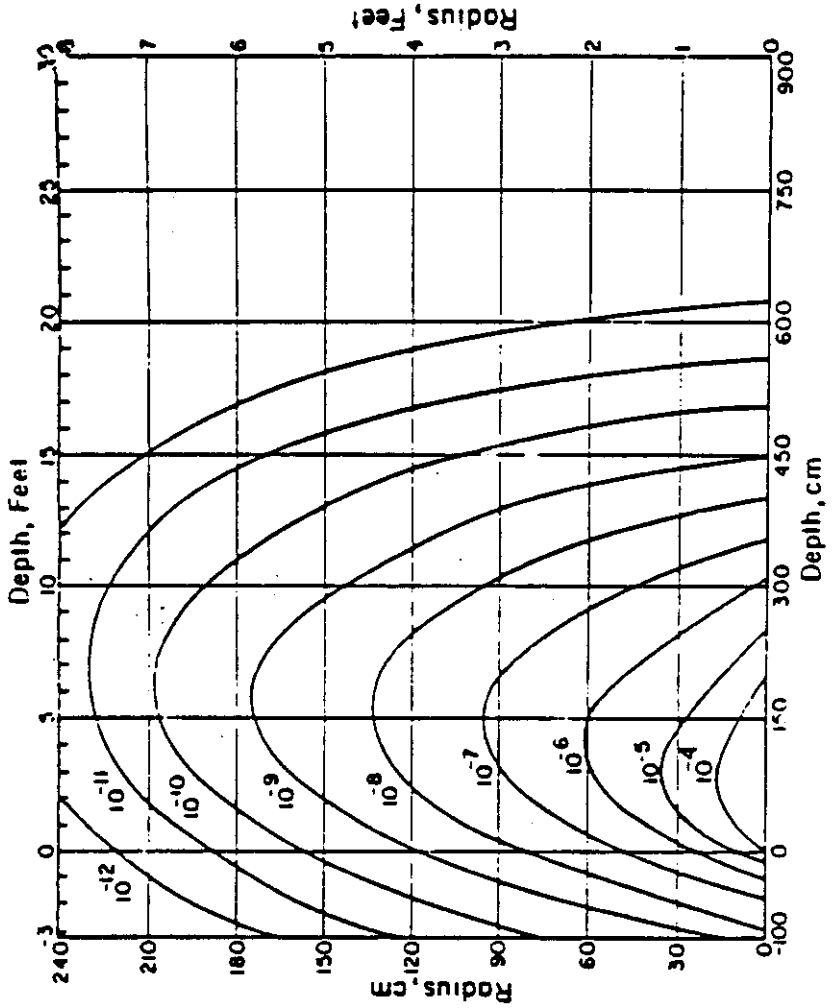
Radius, Feet
Depth, Feet
Depth, cm
Radius, cm
10^{-4}
10^{-5}
10^{-6}
10^{-7}
10^{-8}
10^{-9}
10^{-10}
10^{-11}
10^{-12}

4 LL7

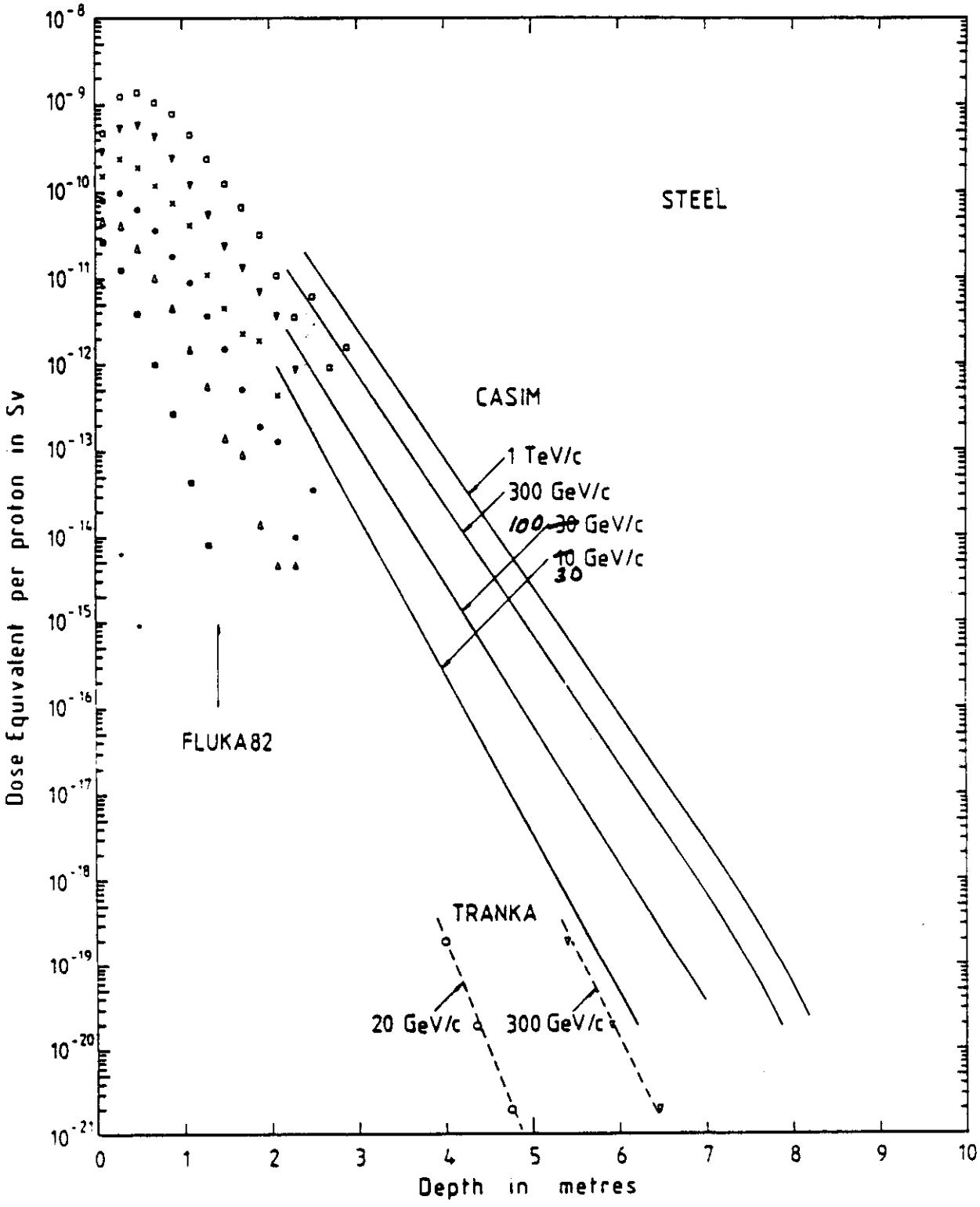

Rev: GRS 5/87

4.18

4 LLB

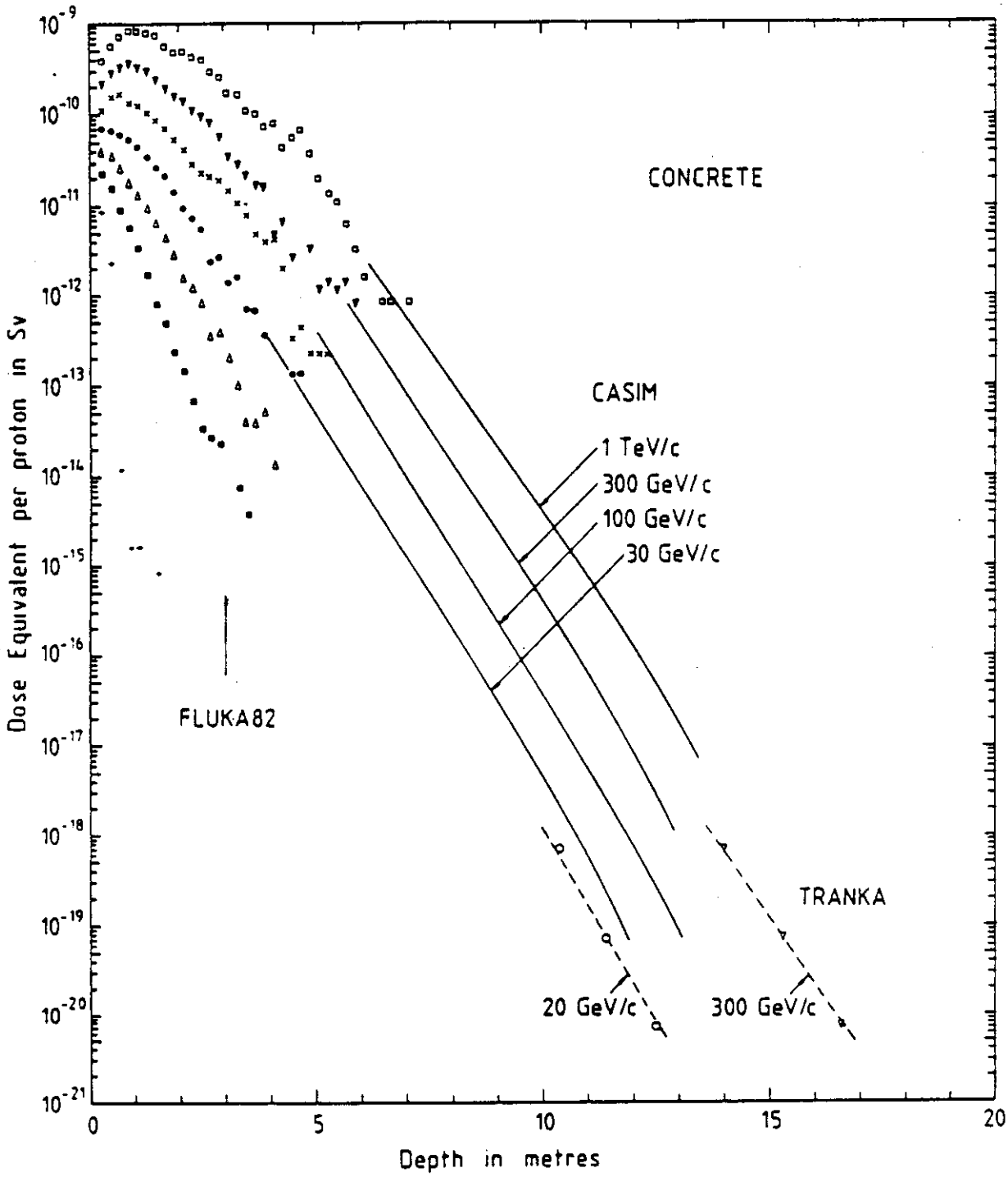
CONCRETE
CASIM
1 TeV/c
300 GeV/c
100 GeV/c
30 GeV/c
FLUKA82
TRANKA
20 GeV/c
300 GeV/c
Dose Equivalent per proton in Sv
Depth in metres
10^-9
10^-10
10^-11
10^-12
10^-13
10^-14
10^-15
10^-16
10^-17
10^-18
10^-19
10^-20
10^-21
0
5
10
15
20

4.19

4.19

4.19

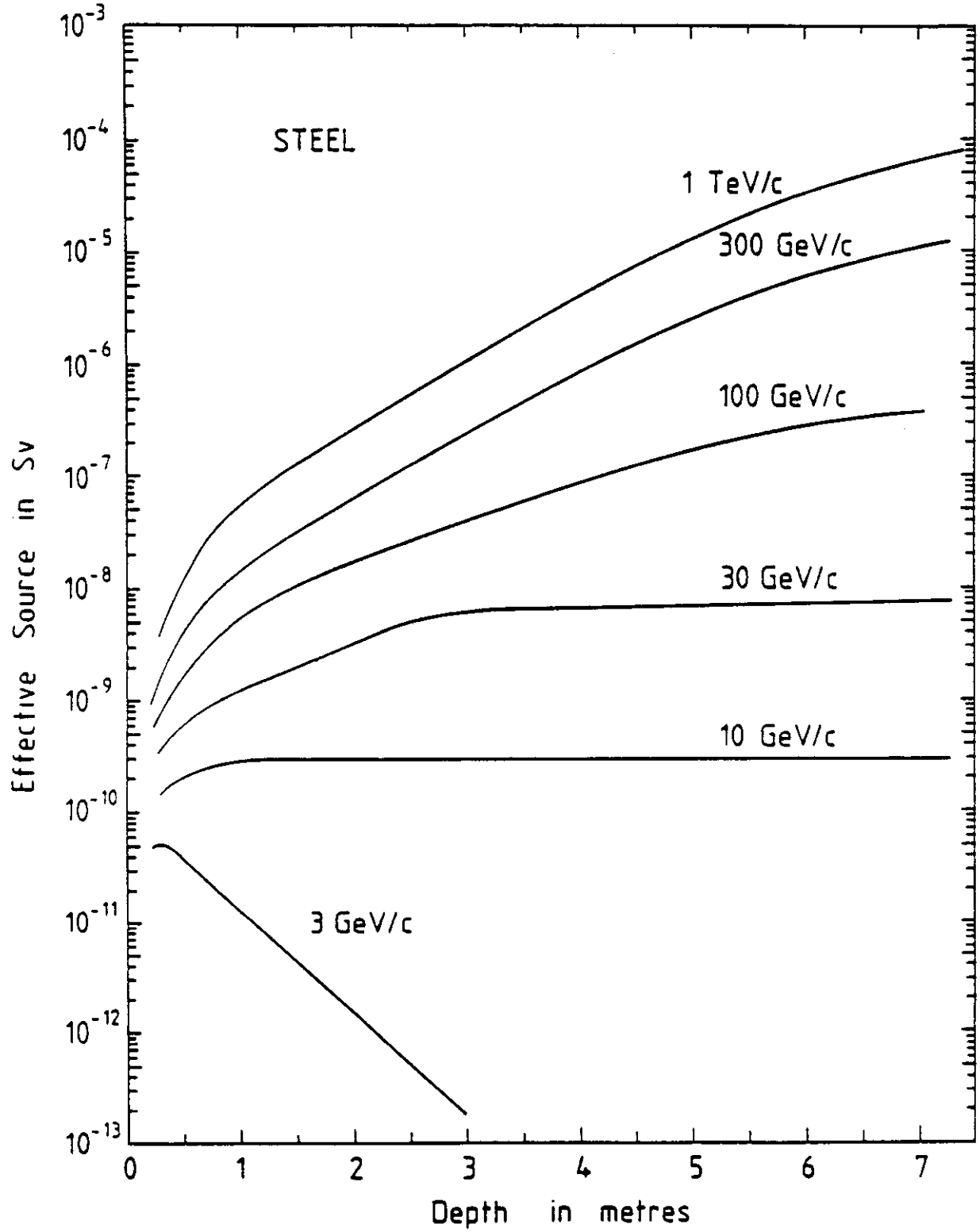
STEEL
1 TeV/c
300 GeV/c
100 GeV/c
30 GeV/c
10 GeV/c
3 GeV/c
Effective Source in Sv
Depth in metres
10^{-3}
10^{-4}
10^{-5}
10^{-6}
10^{-7}
10^{-8}
10^{-9}
10^{-10}
10^{-11}
10^{-12}
10^{-13}
0
1
2
3
4
5
6
7

4.20

4 120

4 20

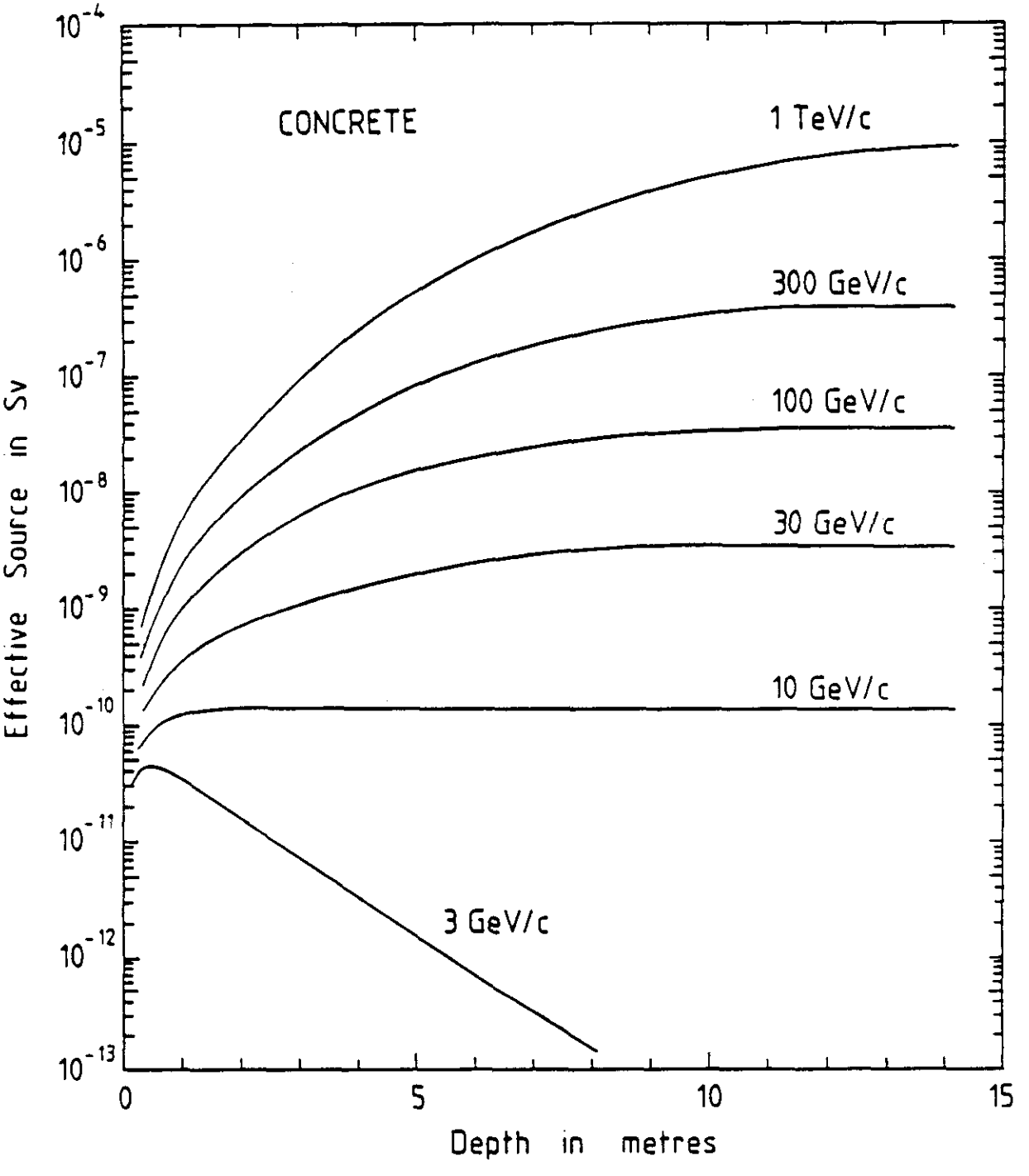
CONCRETE
1 TeV/c
300 GeV/c
100 GeV/c
30 GeV/c
10 GeV/c
3 GeV/c
Effective Source in Sv
Depth in metres
10^-4
10^-5
10^-6
10^-7
10^-8
10^-9
10^-10
10^-11
10^-12
10^-13
0
5
10
15

4.21

4 L2L

4.21

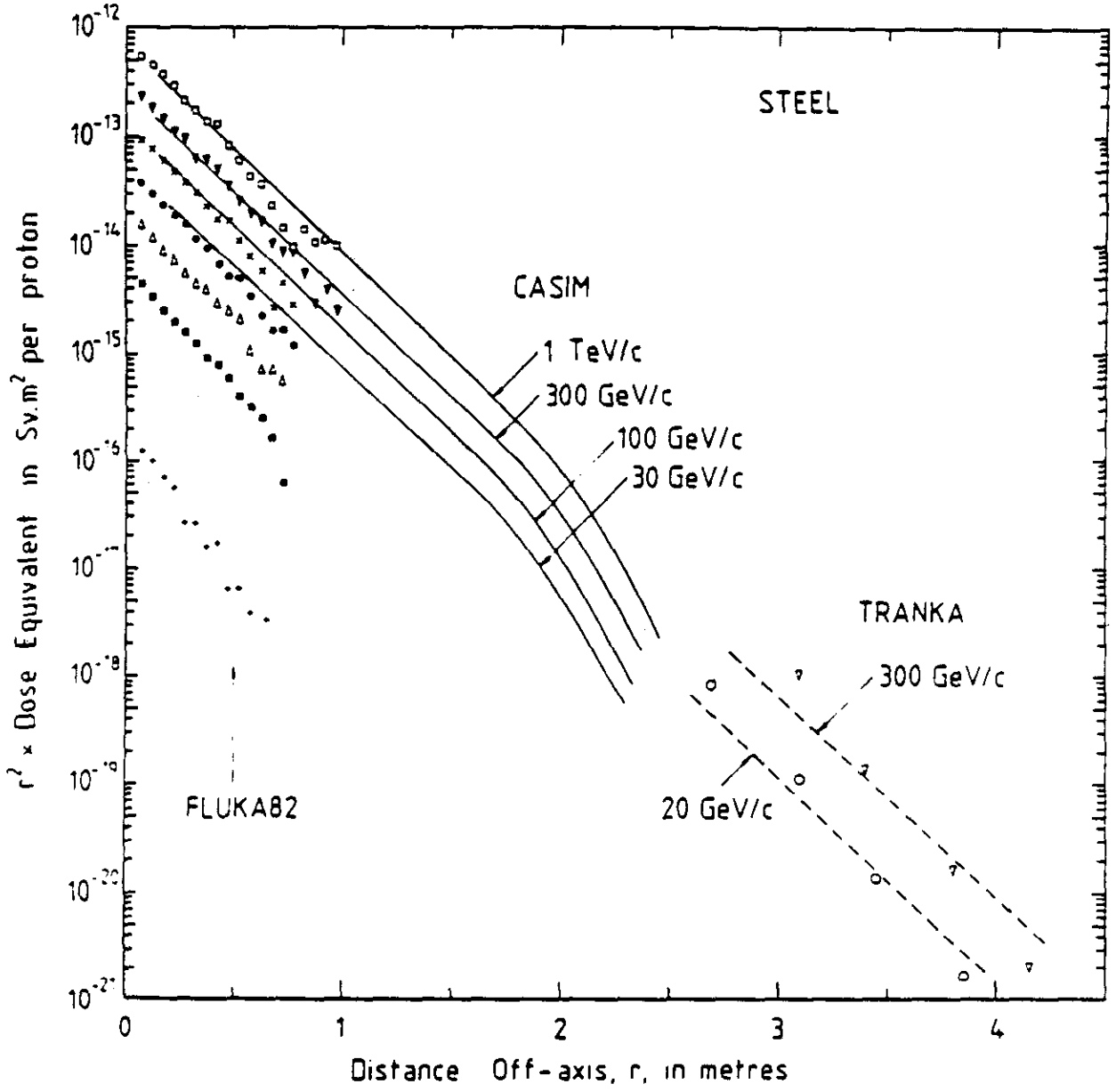
STEEL
CASIM
1 TeV/c
300 GeV/c
100 GeV/c
30 GeV/c
TRANKA
300 GeV/c
20 GeV/c
FLUKA82
$r^2 \times$ Dose Equivalent in Sv.m^2 per proton
Distance Off-axis, r, in metres

4.22

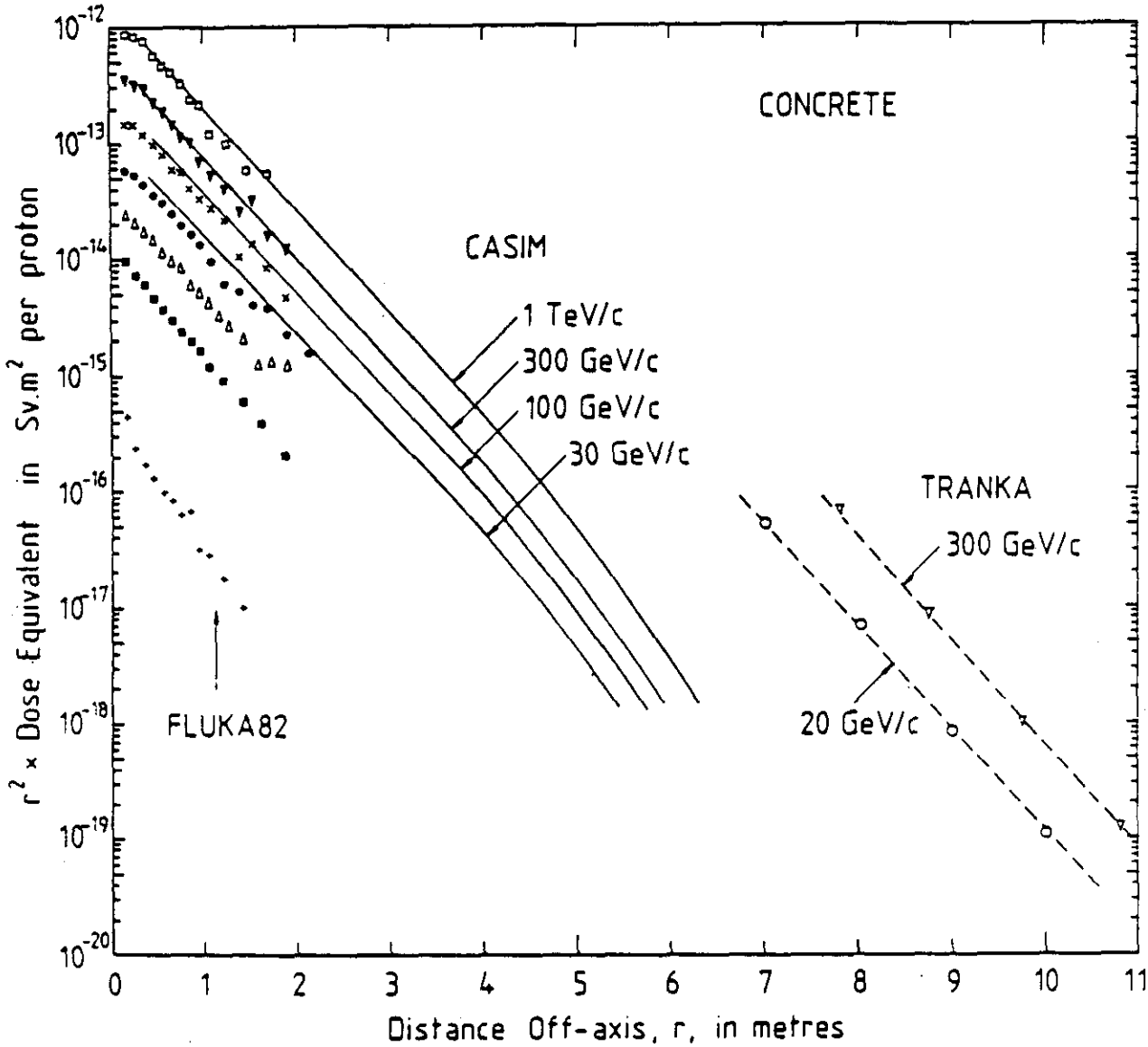
CONCRETE
CASIM
1 TeV/c
300 GeV/c
100 GeV/c
30 GeV/c
TRANKA
300 GeV/c
20 GeV/c
FLUKA82
$r^2 \times$ Dose Equivalent in Sv.m^2 per proton
Distance Off-axis, r, in metres
10^{-12}
10^{-13}
10^{-14}
10^{-15}
10^{-16}
10^{-17}
10^{-18}
10^{-19}
10^{-20}
0 1 2 3 4 5 6 7 8 9 10 11

4.23

4 123

4.22

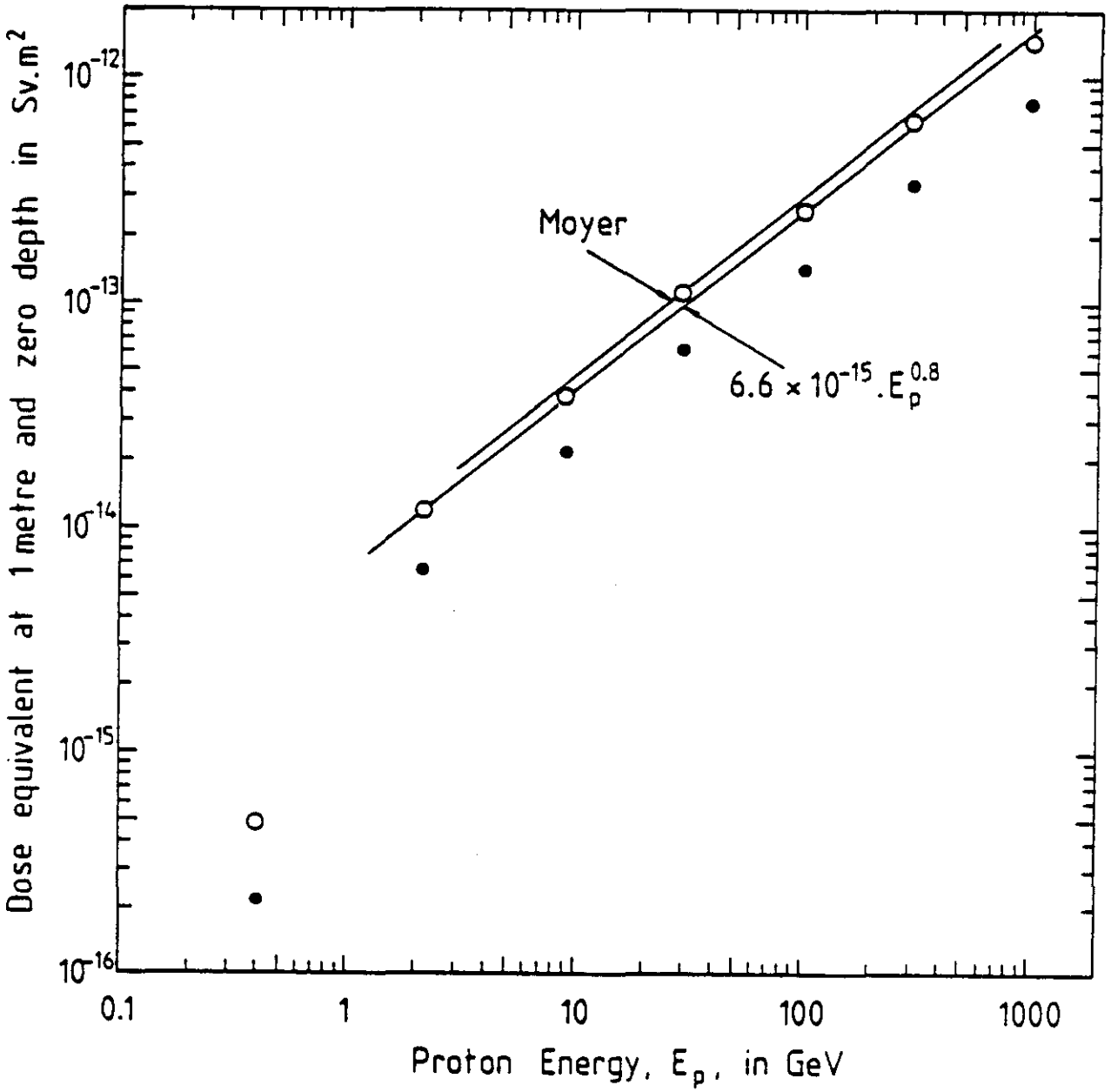
Dose equivalent at 1 metre and zero depth in Sv.m^2
10^{-12}
10^{-13}
10^{-14}
10^{-15}
10^{-16}
Moyer
$6.6 \times 10^{-15} . E_p^{0.8}$
0.1
1
10
100
1000
Proton Energy, E_p, in GeV

4.24

4 124

240 GeV/c
Relative Vertical Distance in metres
0
1
2
3
4
5
6
10^{0}
10^{-1}
10^{-2}
10^{-3}
10^{-4}
Fluence per incident Muon in m^{-2}

4.25

4 125

4.25

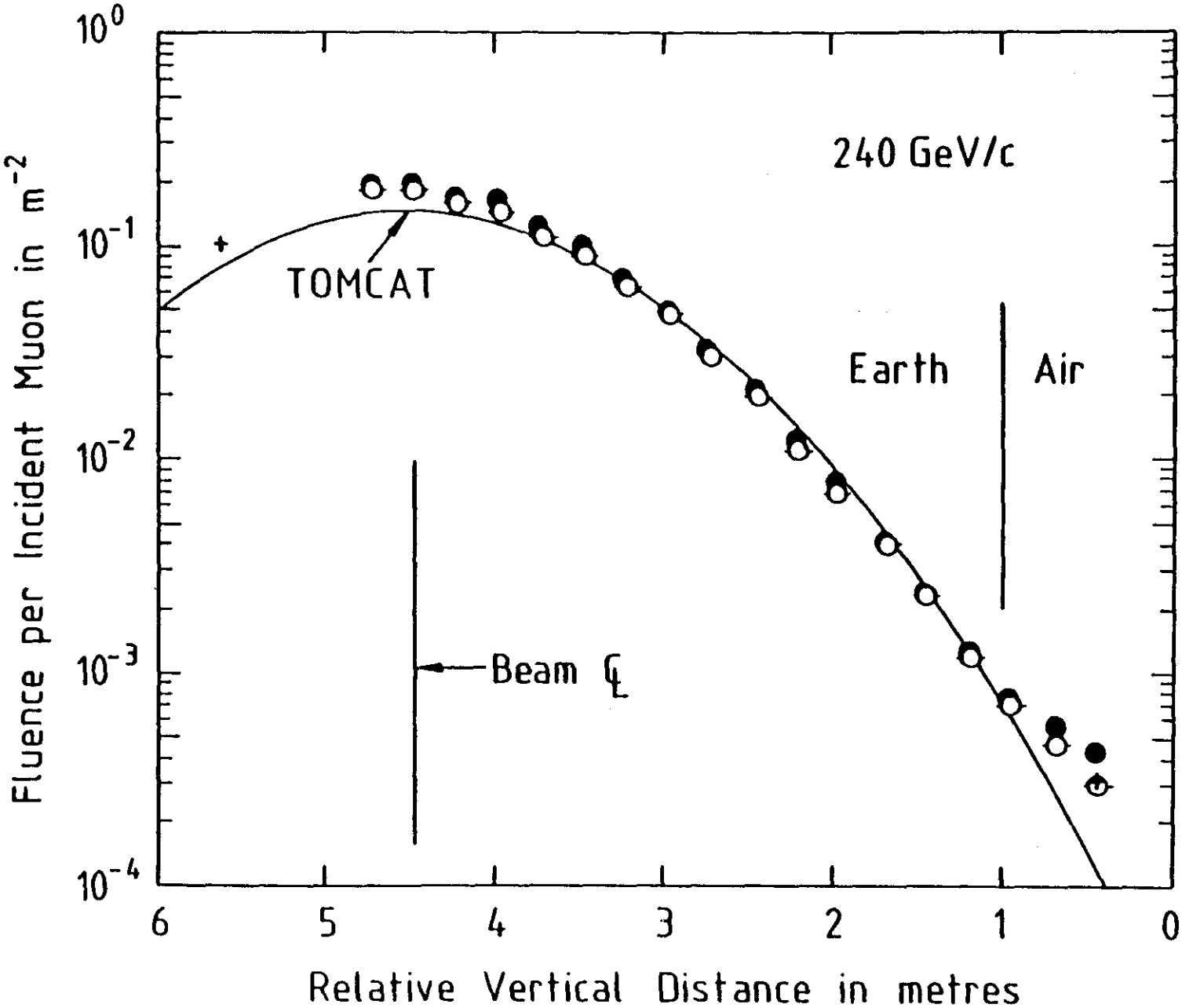
240 GeV/c
TOMCAT
Earth
Air
Beam ℄
Fluence per Incident Muon in m^{-2}
Relative Vertical Distance in metres
10^0
10^{-1}
10^{-2}
10^{-3}
10^{-4}
6
5
4
3
2
1
0

Fig. 2a & 12b

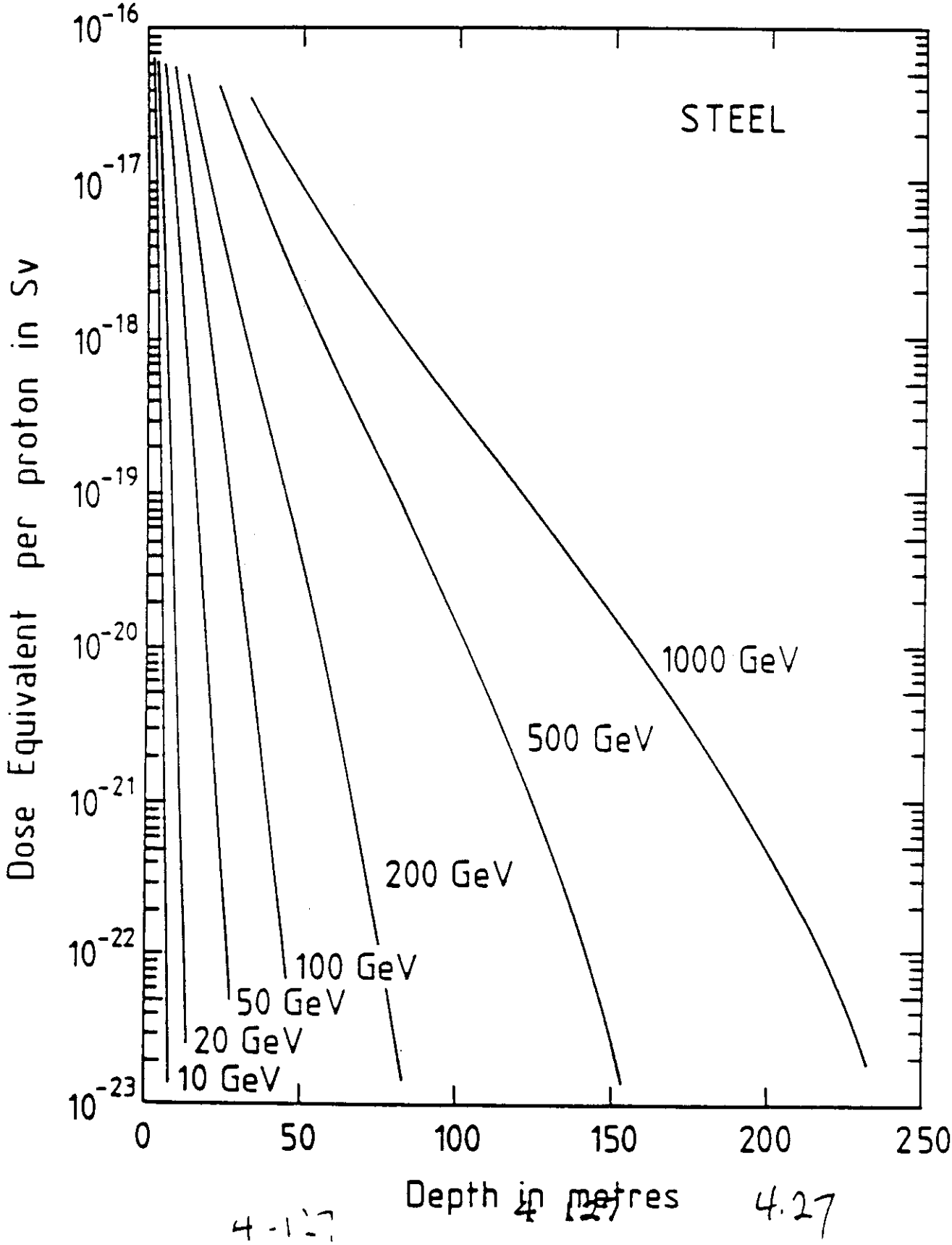
STEEL
Dose Equivalent per proton in Sv
10^{-16}
10^{-17}
10^{-18}
10^{-19}
10^{-20}
10^{-21}
10^{-22}
10^{-23}
1000 GeV
500 GeV
200 GeV
100 GeV
50 GeV
20 GeV
10 GeV
0
50
100
150
200
250
Depth in metres

4-127

4.27

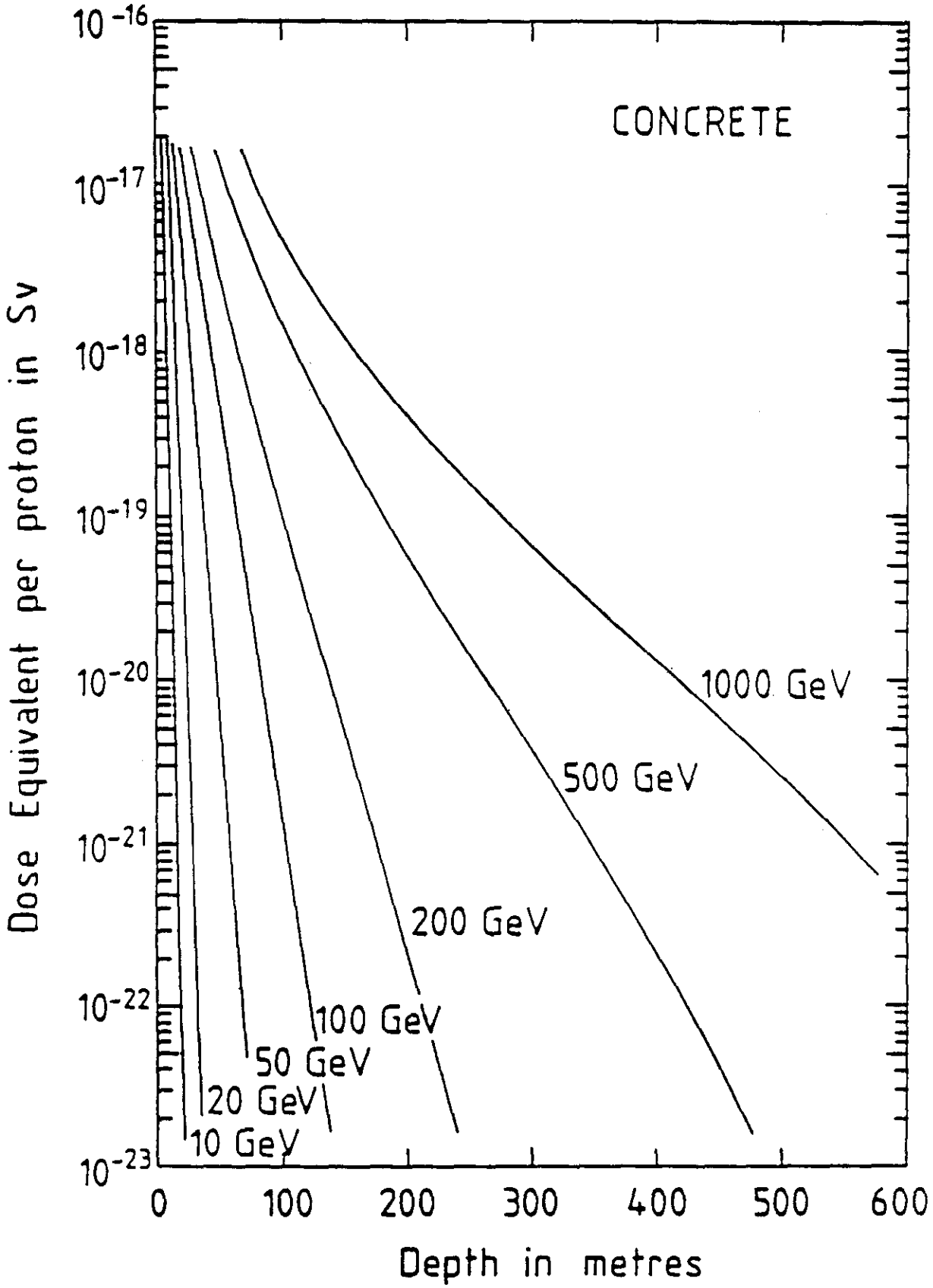
CONCRETE
Dose Equivalent per proton in Sv
10 -16
10-17
10-18
10-19
10-20
10-21
10-22
10-23
0
100
200
300
400
500
600
Depth in metres
1000 GeV
500 GeV
200 GeV
100 GeV
50 GeV
20 GeV
10 GeV

4.28

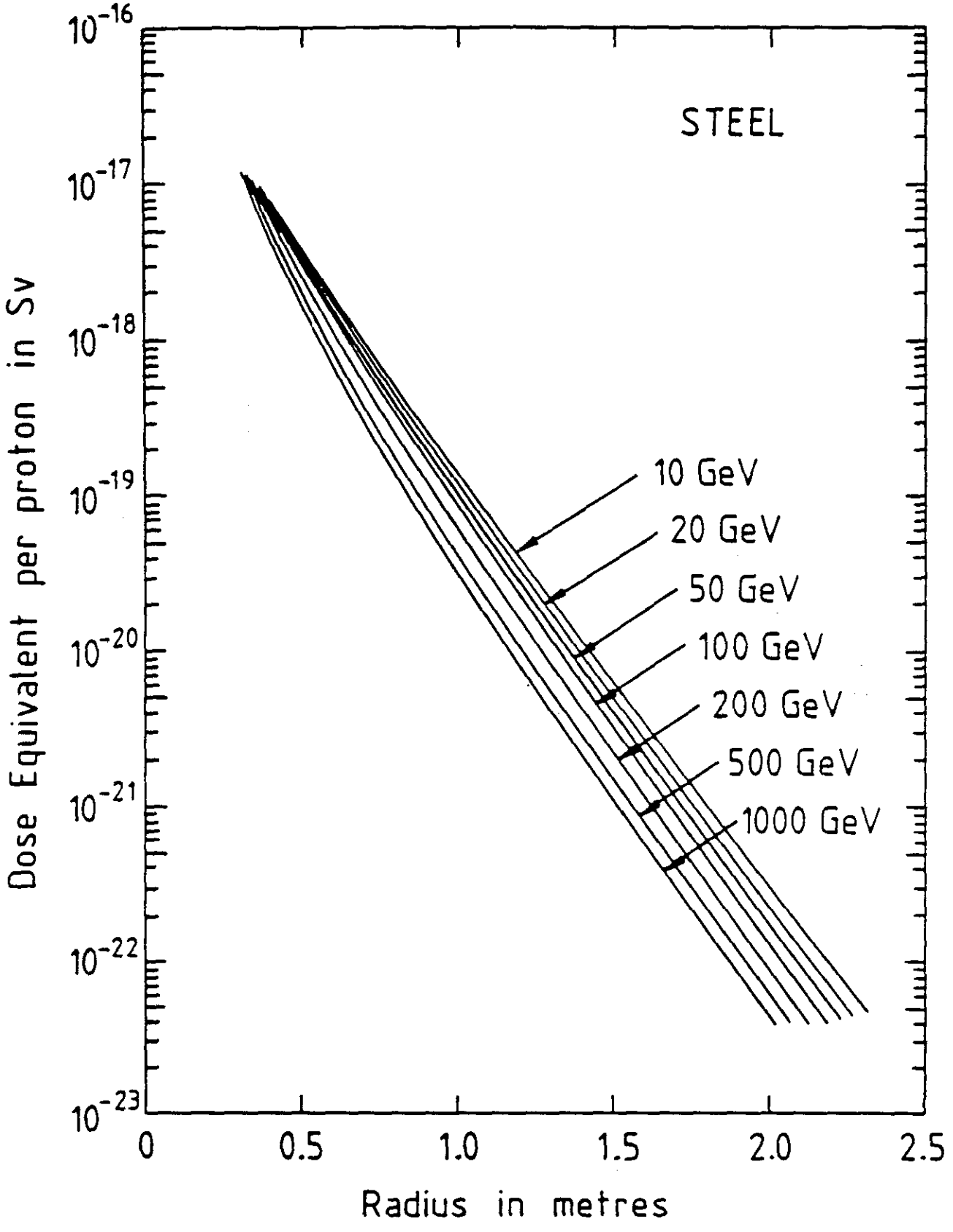
STEEL
10 GeV
20 GeV
50 GeV
100 GeV
200 GeV
500 GeV
1000 GeV
Dose Equivalent per proton in Sv
Radius in metres
10^{-16}
10^{-17}
10^{-18}
10^{-19}
10^{-20}
10^{-21}
10^{-22}
10^{-23}
0
0.5
1.0
1.5
2.0
2.5

4.29

4 129

4.29

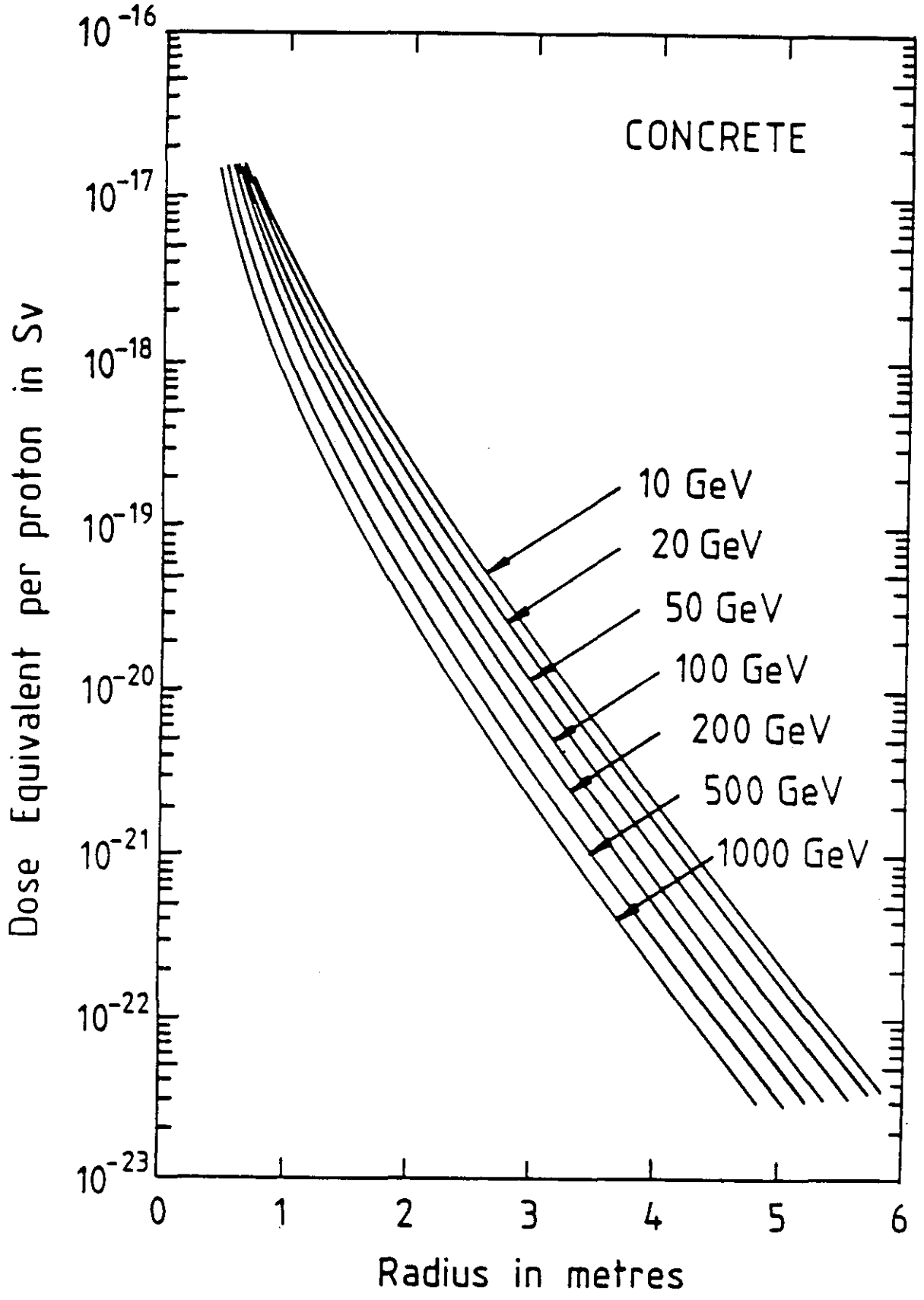
CONCRETE
10 GeV
20 GeV
50 GeV
100 GeV
200 GeV
500 GeV
1000 GeV
Dose Equivalent per proton in Sv
Radius in metres
10^{-16}
10^{-17}
10^{-18}
10^{-19}
10^{-20}
10^{-21}
10^{-22}
10^{-23}
0
1
2
3
4
5
6

4.30

4.30

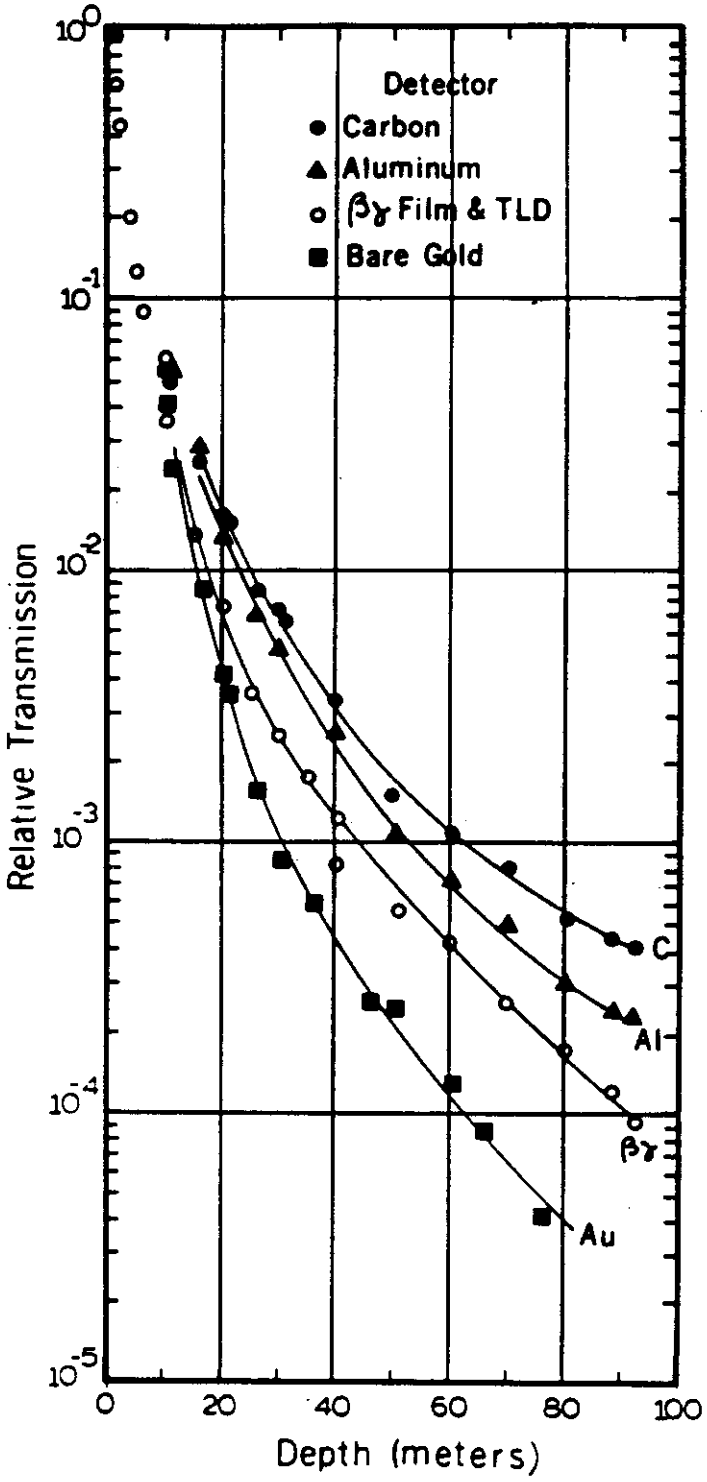

XBL 681 4415

4.31

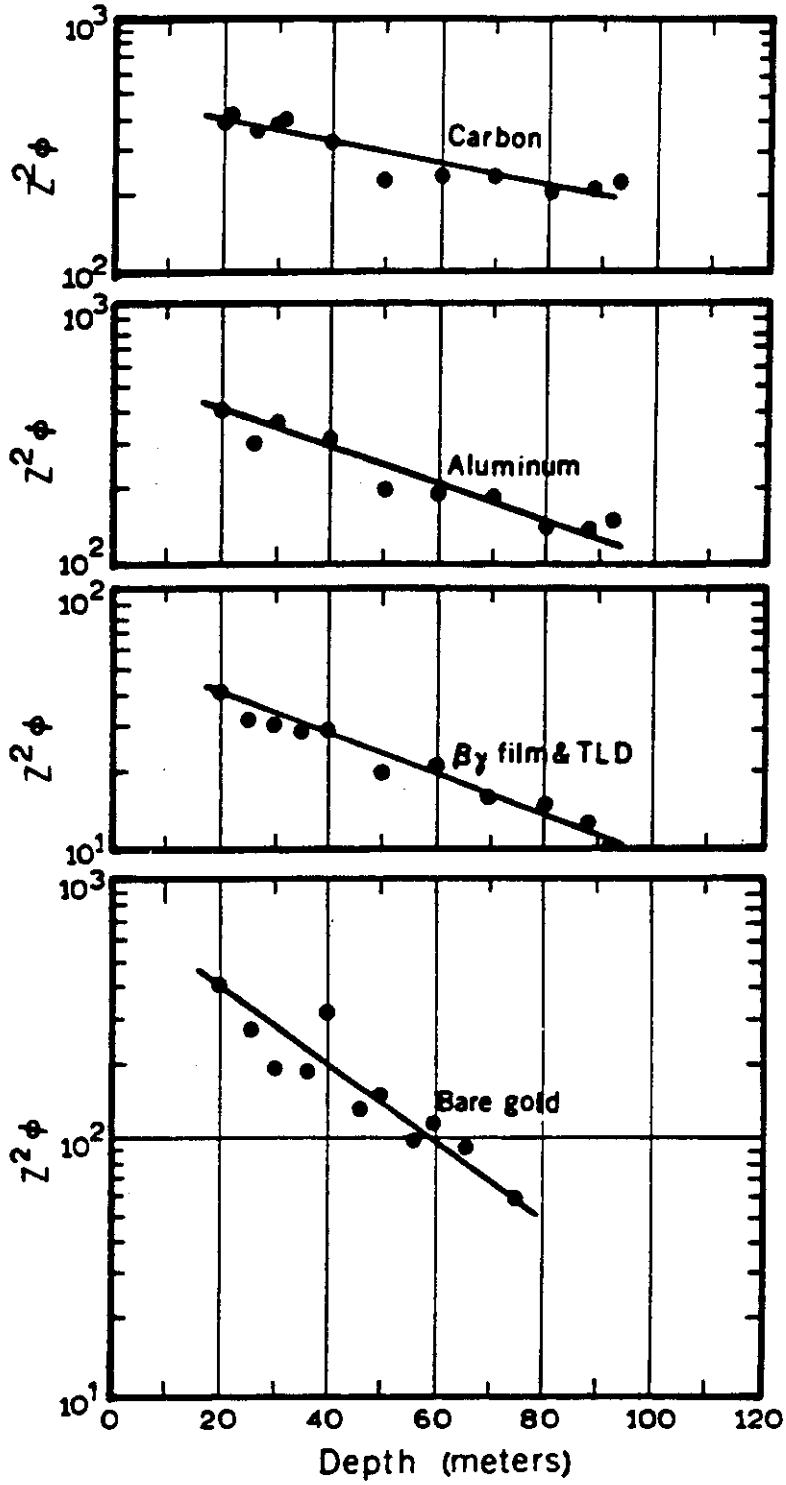

XBL 681 4428

4.32

4.32

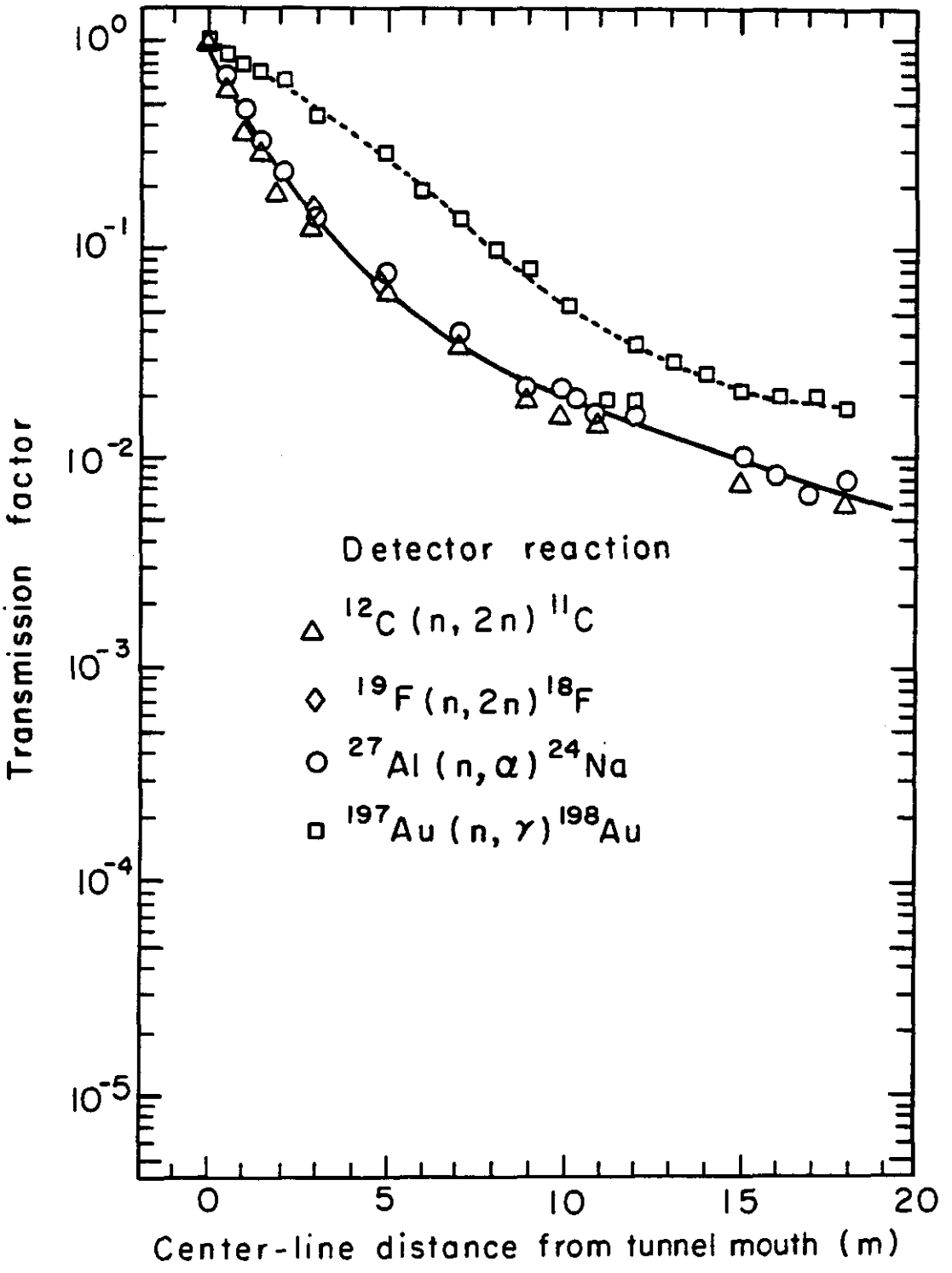

XBL7112-4835

4.33

4.33

Plan view

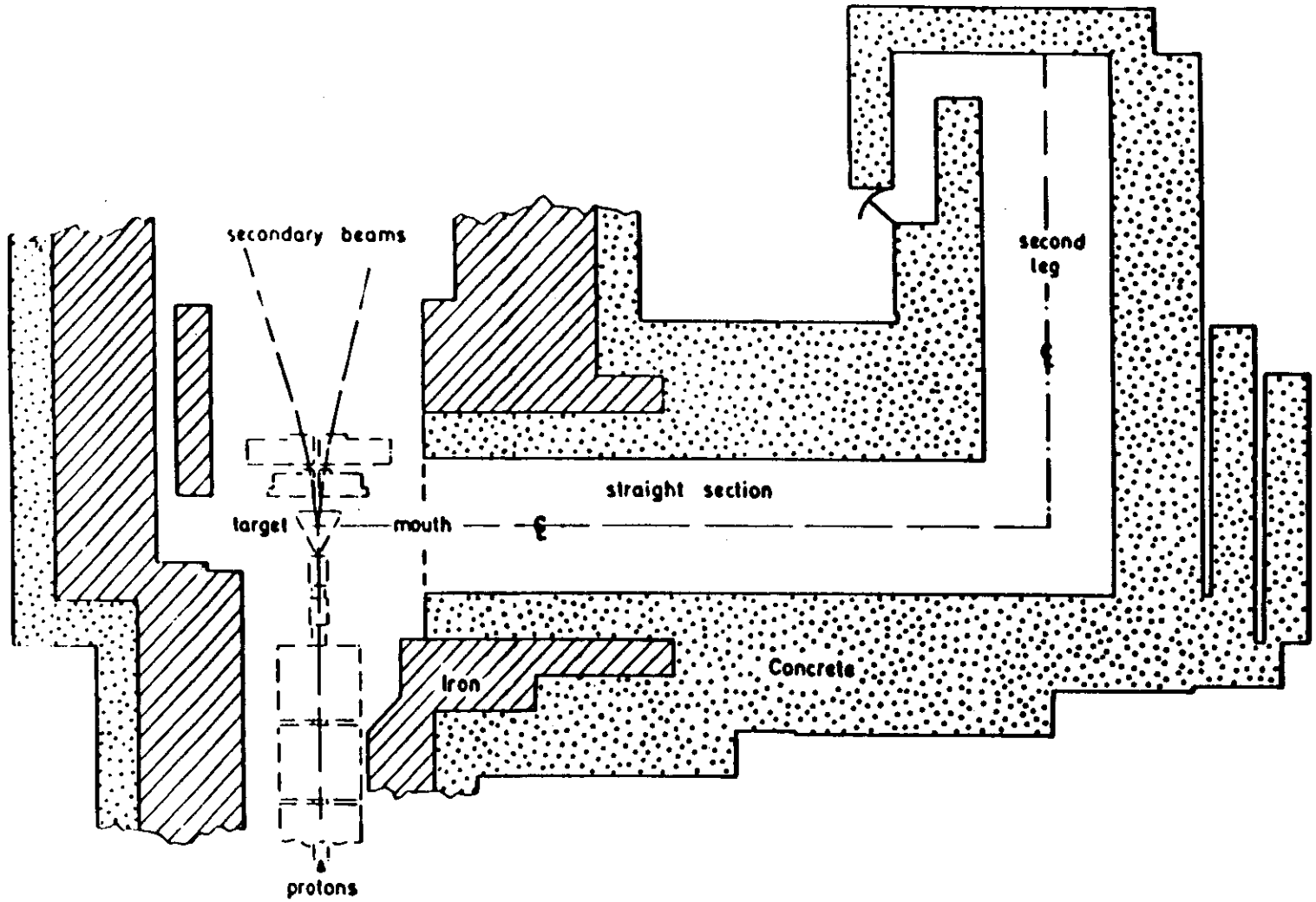

XBL 7111-1756

4.34

4.34

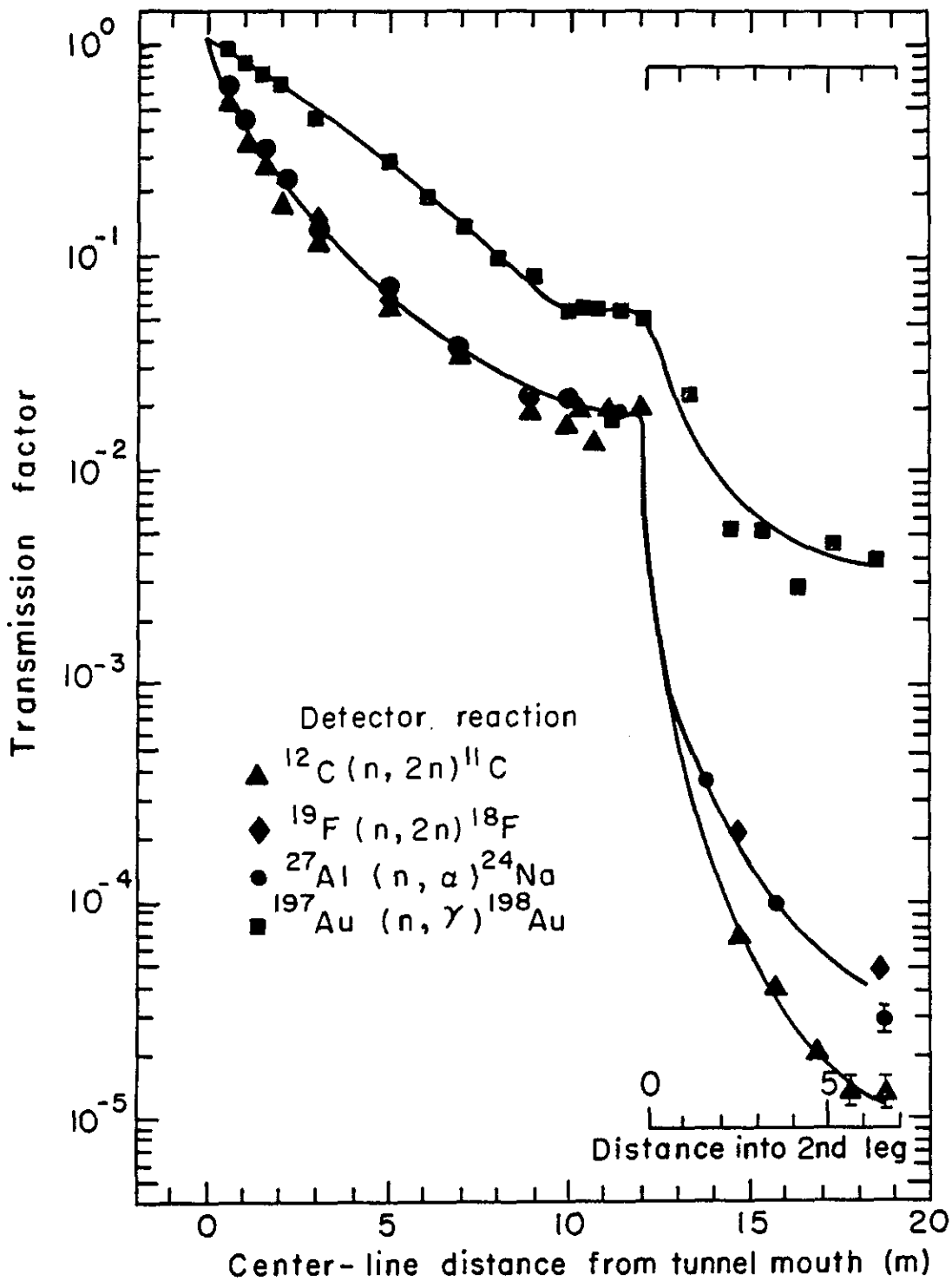

XBL7112-4834

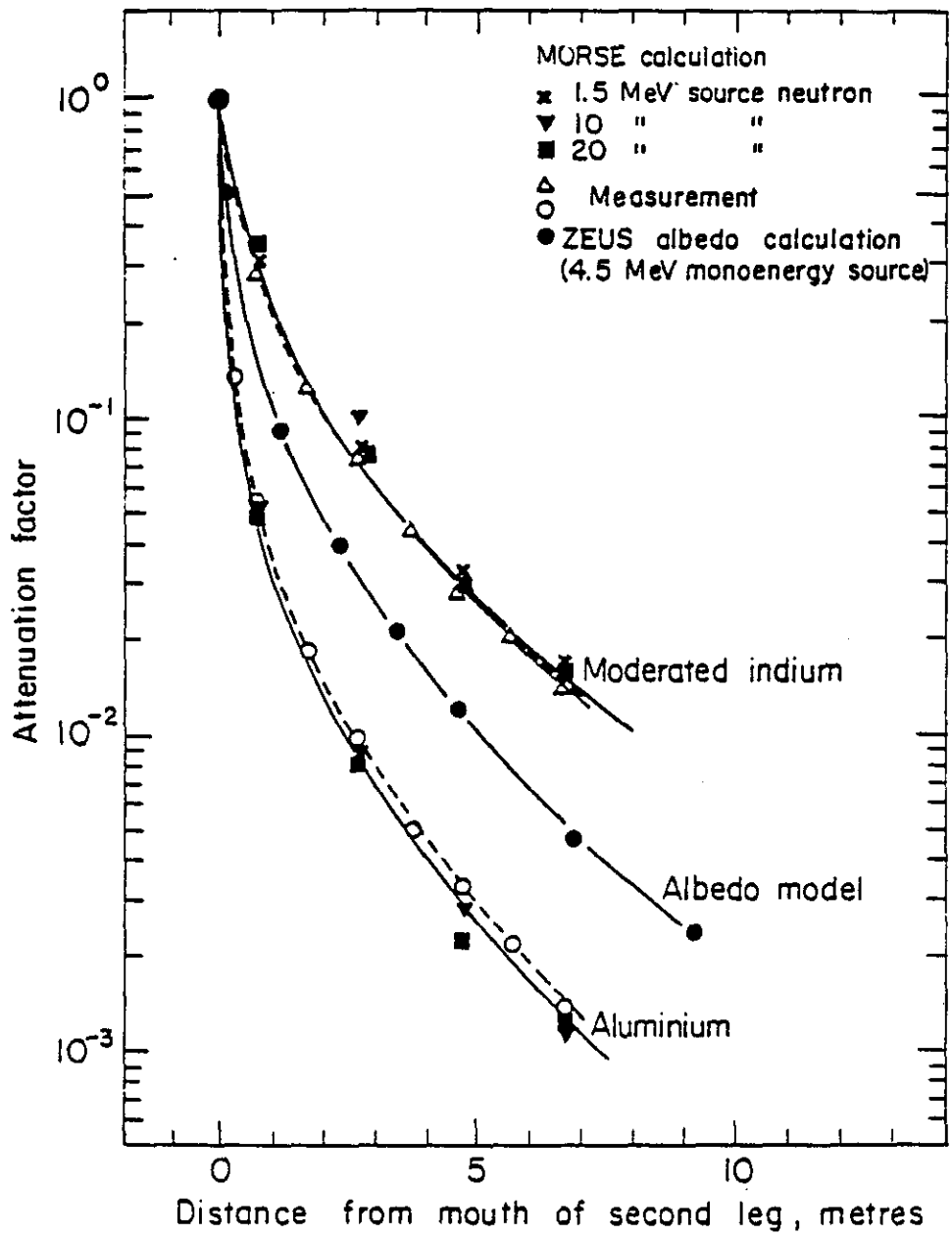
MORSE calculation
1.5 MeV source neutron
10 " "
20 " "
Measurement
ZEUS albedo calculation
(4.5 MeV monoenergy source)
Moderated indium
Albedo model
Aluminium
Attenuation factor
10^0
10^{-1}
10^{-2}
10^{-3}
0
5
10
Distance from mouth of second leg, metres

4.36

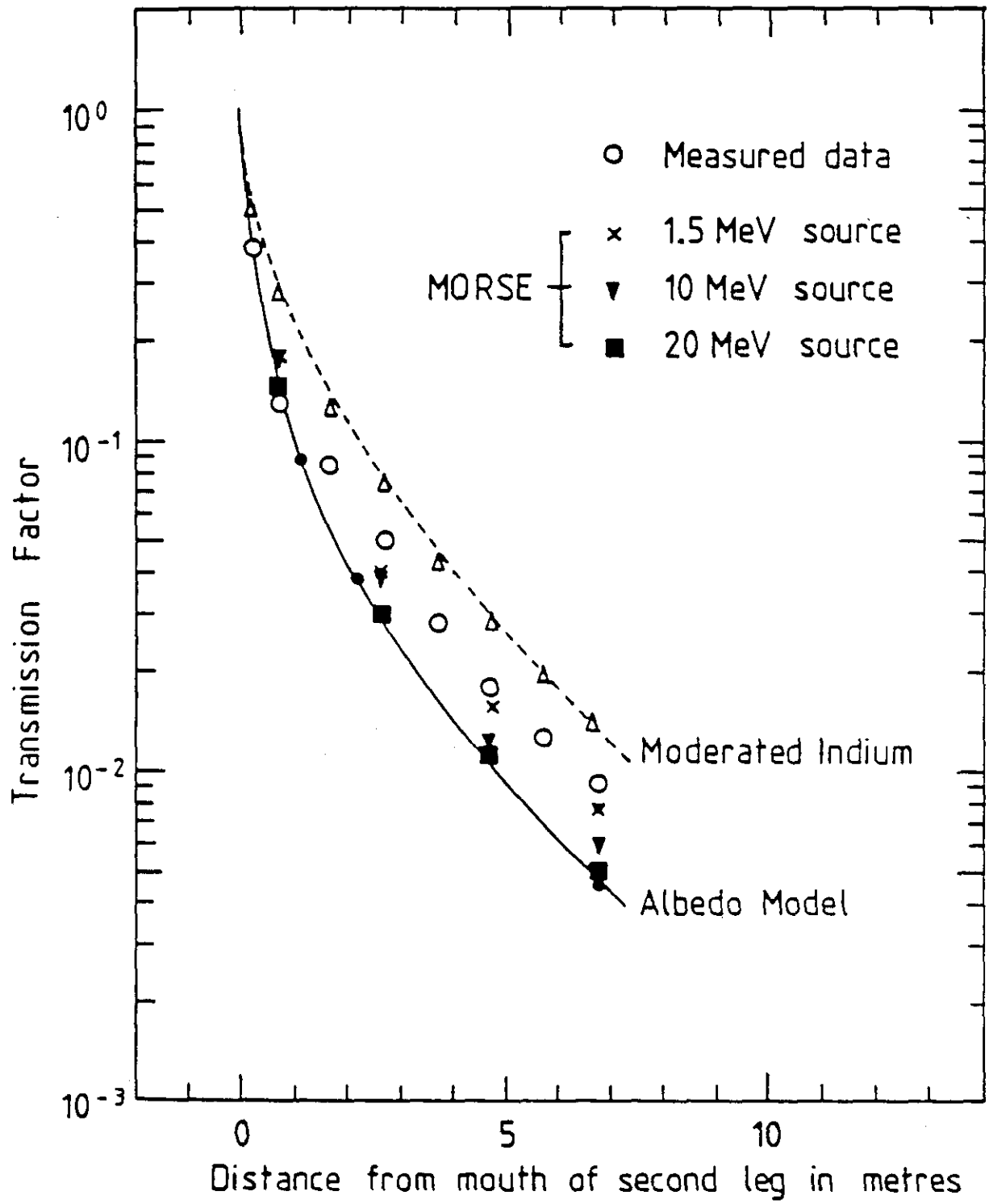
Measured data
1.5 MeV source
MORSE
10 MeV source
20 MeV source
Moderated Indium
Albedo Model
Transmission Factor
10^0
10^{-1}
10^{-2}
10^{-3}
0
5
10
Distance from mouth of second leg in metres

4.37

4 137

4.37

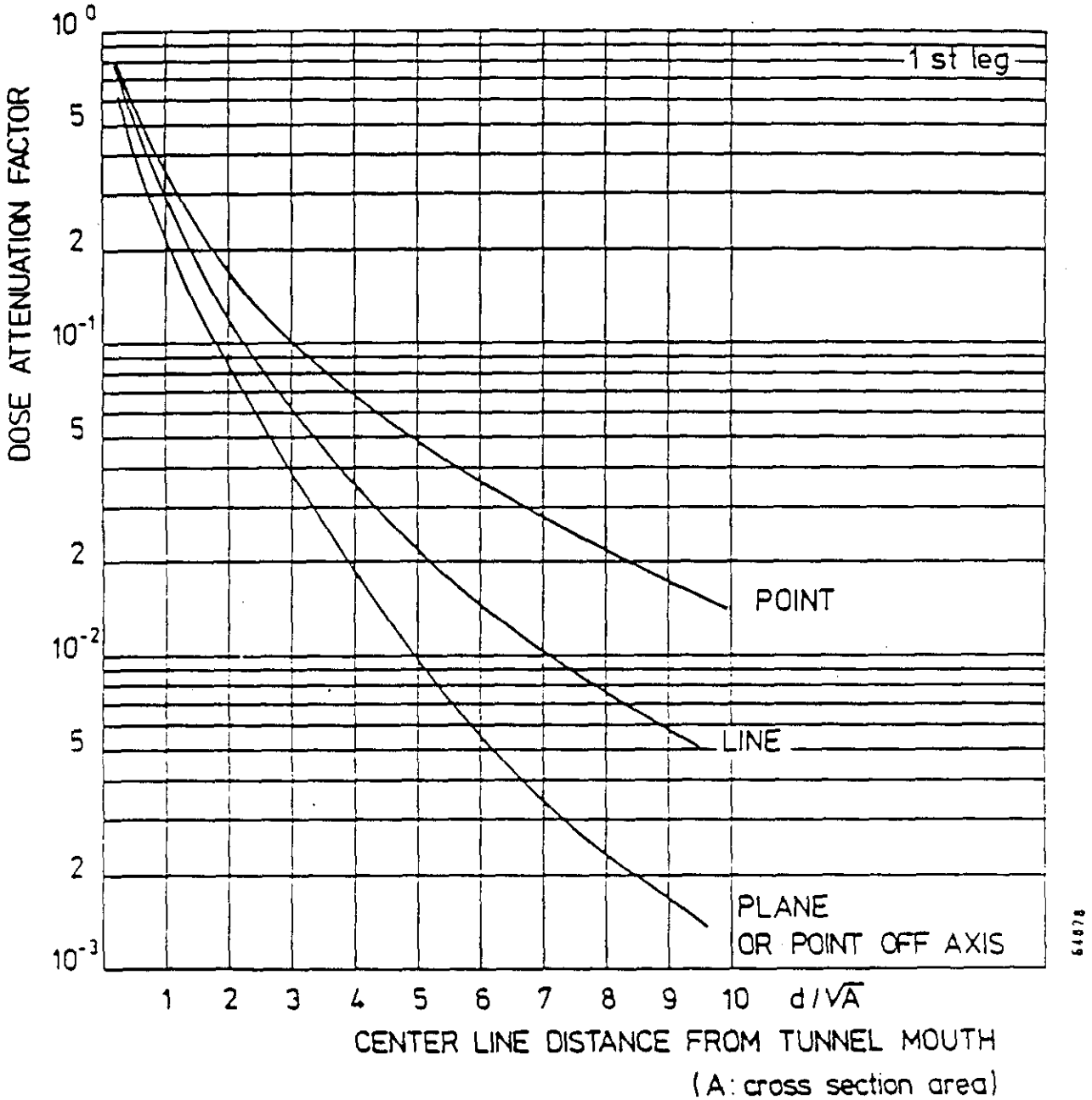
DOSE ATTENUATION FACTOR
10 0
5
2
10-1
5
2
10-2
5
2
10-3
1 st leg
POINT
LINE
PLANE
OR POINT OFF AXIS
1 2 3 4 5 6 7 8 9 10 d/√A
CENTER LINE DISTANCE FROM TUNNEL MOUTH
(A: cross section area)

4.38

4 138

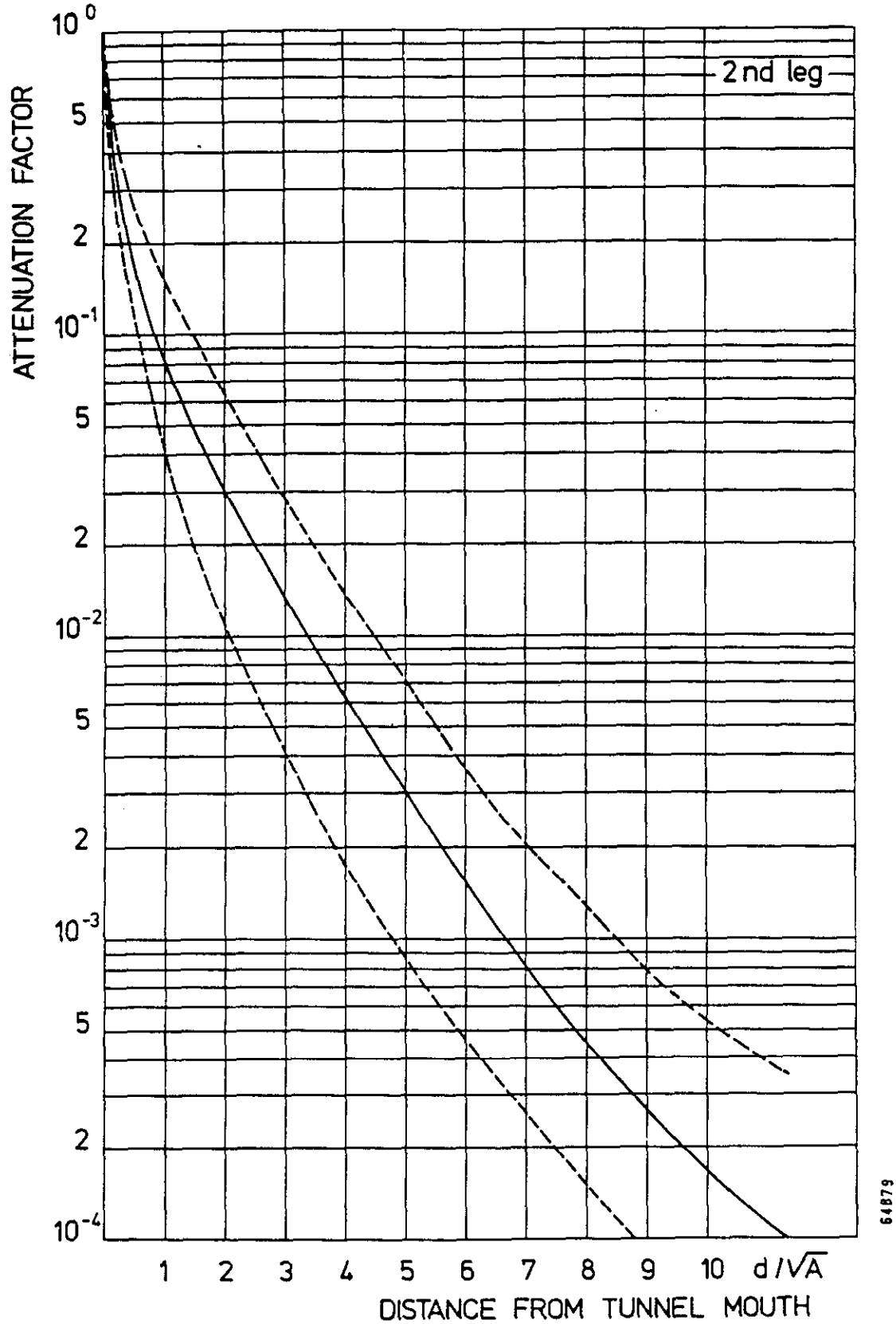
ATTENUATION FACTOR
10^0
5
2
10^{-1}
5
2
10^{-2}
5
2
10^{-3}
5
2
10^{-4}
2nd leg
1 2 3 4 5 6 7 8 9 10 $d/\sqrt{A}$
DISTANCE FROM TUNNEL MOUTH
64879

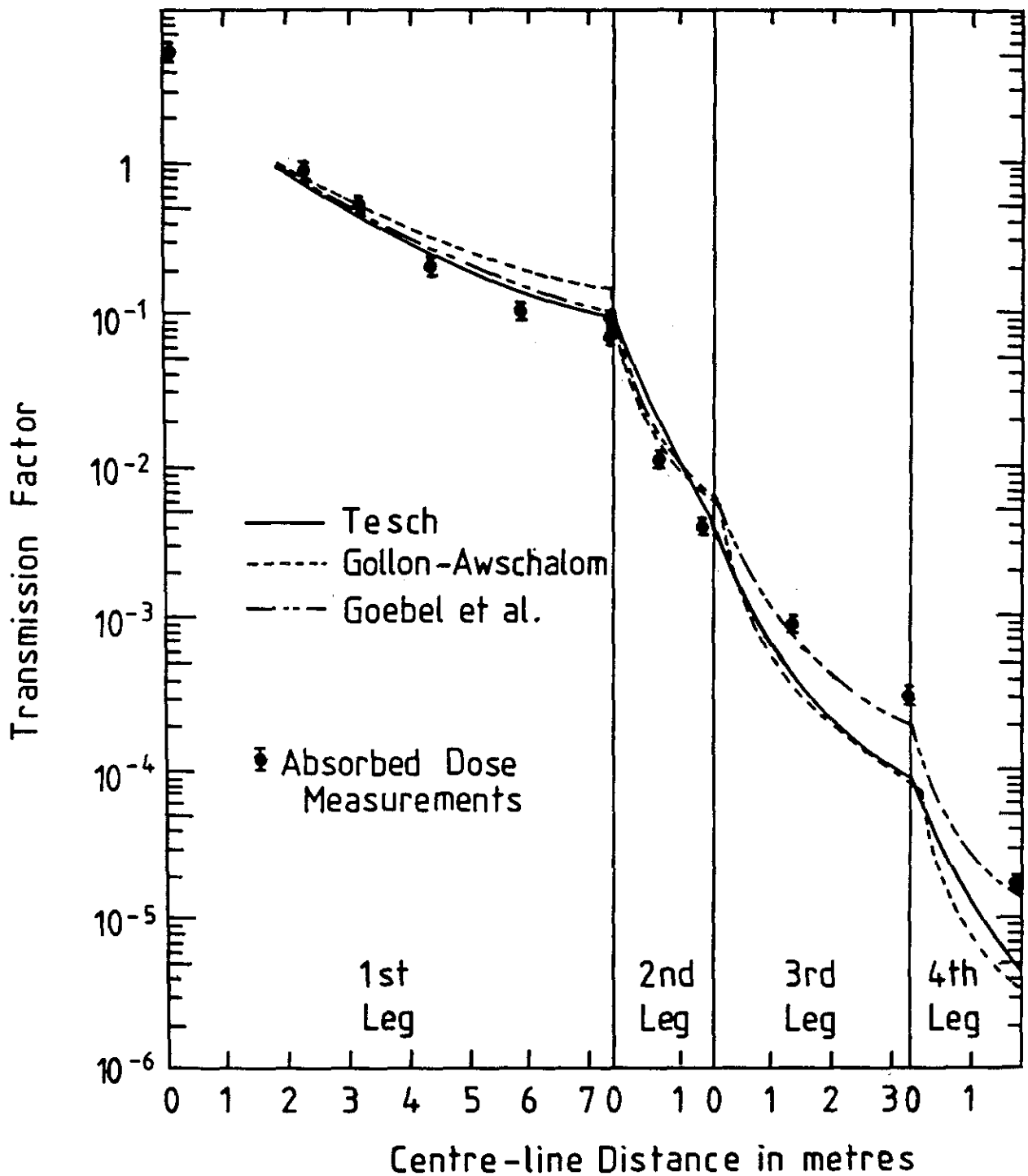
Transmission Factor
1
10^{-1}
10^{-2}
10^{-3}
10^{-4}
10^{-5}
10^{-6}
Tesch
Gollon-Awschalom
Goebel et al.
Absorbed Dose Measurements
1st Leg
2nd Leg
3rd Leg
4th Leg
0 1 2 3 4 5 6 7 0 1 0 1 2 3 0 1
Centre-line Distance in metres

Normal

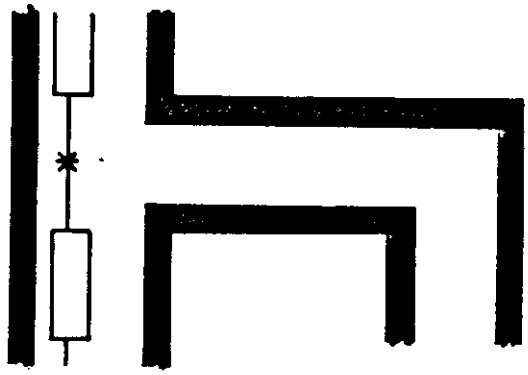

Type A

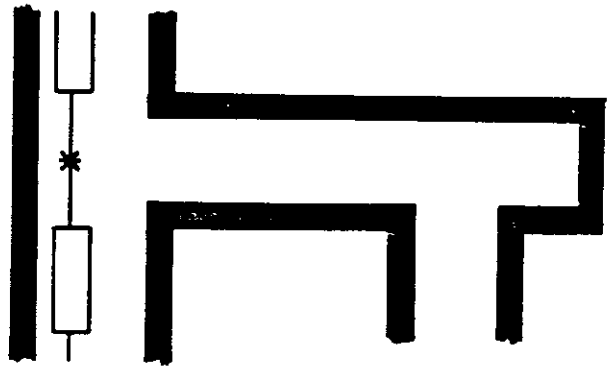

Type B

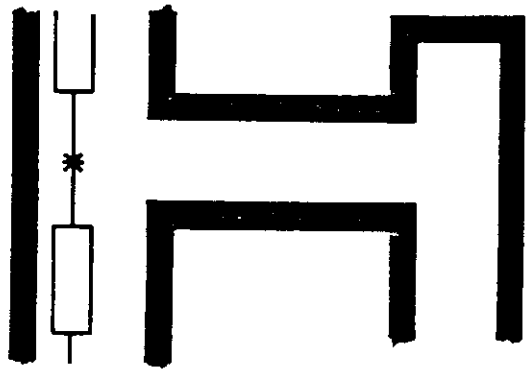

Type C

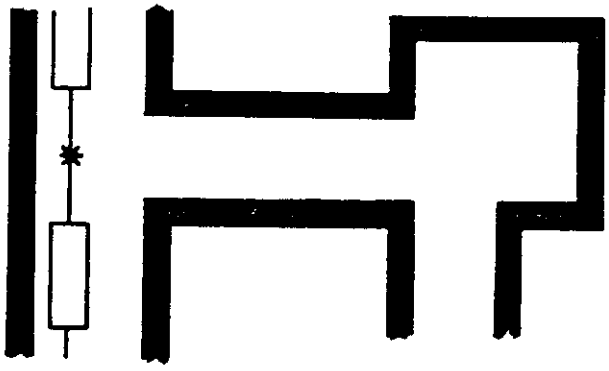

Appendix
Lateral Shielding Calculations--The Moyer Model

Introduction

As we have seen (in Chapter 4) the increasing intensities of weak-focussing synchrotrons in the late fifties generated a need for efficient shield design, particularly in the transverse direction. This is a problem particularly amenable to solution by the use of empirical methods and one of the best known of these was developed for the design of the shielding of proton synchrotrons in the 10 GeV energy region. It has become know as the "Moyer model" and, despite its limitations is still in use today. Its development is described here in some detail because it gives good physical insight into shielding phenomena.

In 1961 Moyer described a semi-empirical method for determining the shielding required for the Bevatron, the 6-GeV proton synchrotron of the (then) University of California Radiation Laboratory (Mo 61b, Mo 62), whose intensity was to be substantially increased (We 63). This model 'Provides a formalism to evaluate the high energy neutron fluxes and associated biological dose-rates outside the main shield of the accelerator, in places where the nucleon-meson cascade is well-developed and essentially in equilibrium' (Ro 72b).

The design and construction of the first proton accelerators in the GeV energy region during the fifties and early sixties demanded an increased understanding of high-energy particle accelerators' radiation environments (Pa 73). Control of the intensity of the radiation field around these accelerators-to permit safe and efficient operations-by the design of radiation shielding became an urgent task following experience obtained with the early operation of the Cosmotron and Bevatron (So 57).

At that time there was no firm theoretical basis for designing accelerator shielding and, in consequence, semi-empirical methods were developed of which, as we have suggested, the most useful and widely known is the Moyer Model (Mo 61b, Mo 62).

Moyer's procedure was to "find the best available data on total neutron production, angular distribution and spectrum of the neutrons created by the Bevatron [and to] consider a target in different positions characteristic of Bevatron operation and evaluate the necessary shielding to accomodate the situation within the bounds of the radiation guide rules" (Mo 61b). Because "the most severe requirements on local sheilding will occur when a target of considerable thickness effects a concentrated creation of neutrons and secondary particles in its immediate vicinity" Moyer calculated shielding for a target whose dimension in the beam direction was about 100 g cm^{-2}. Shielding thick enough for this condition would "be easily capable of accomodating the distributed production of neutrons and secondary particles from the machine in general".

The numerical values of the parameters used by Moyer may be found in his original papers and review articles (Mo 61b, Mo 62, Th 70). He made calculations for four situations representative, for the most part, of familiar operating conditions at the Bevatron.

This appendix discusses the historical background; the generalized formulation of the Moyer model; the derivation of numerical values for the parameters of the model and the variation of these values with proton energy; and, finally, the application of the model to point source and extended source calculations.

Historical Background

Moyer designed a shield for the 6-GeV proton synchrotron of the Lawrence Radiation Laboratory (the Bevatron) to reduce dose equivalent rates by a factor of 100. Measurements showed that in practice the overall effect on the recommended shield was to reduce neutron flux densities (proportional to dose equivalent) by a factor between 90 and 100 (Sm 65a, Th 70).

This success naturally stimulated an interest in generalizing Moyer's method so that it could be applied to shield design over a wide range of energies, in particular to the 100 GeV region.

Our understanding of the Moyer model was greatly improved during the mid sixties when the proton synchrotrons at the Fermi National Accelerator Laboratory (Batavia, Illinois) and the SPS (CERN, Geneva) (Aw 70, CERN 64, Gi 68, LBL 65, URA 68) were designed.

These design studies led first to a more precise formulation of the Moyer equation, studies of the angular distribution function, determination of values for the parameters of the Moyer equation and their variation with proton energy. The following discussion is based on the paper by Stevenson et al. (St 82).

Generalised Formulation of the Moyer Model

Many descriptions of the Moyer model have been published in the literature (Pa 73). In these earlier descriptions the authors have concentrated on a discussion of the neutron component of the radiation field. This was principally because neutrons make the dominant contribution to dose equivalent outside well-shielded proton accelerators (Pe 66). Although high-energy neutrons are not the only particles that play an important role in propagating the hadronic cascade in matter, it was sufficiently accurate at that time to treat all hadronic cascade propagators as neutron-like.

The fact that the neutrons that largely contribute to the dose equivalent ($E < 50$ MeV) are not those that propagate the hadronic cascade ($E > 150$ MeV) has led to some confusion in understanding the early literature.

Consider an effective point source produced by protons interacting in a thin target (Fig. A4.1). Assuming that neutrons are the only secondary particles to be considered the radiation level on the outside of a shield may be written by

$$H = \frac{1}{r^2} \int F(E) \cdot B(E,\theta) \exp[-d(\theta)/\lambda(E)] \frac{d^2n(E,\theta)}{dE d\Omega} dE \qquad (A4.1)$$

where r is the distance from the source, E is the neutron energy, F is a factor that converts fluence to dose equivalent, d is the shield

thickness, λ is the effective removal mean free path, B is a buildup factor, and $d^2n/dEd\Omega$ is the yield of neutrons per unit solid angle, at angle θ, per unit energy interval at E.

Following technique used in other branches of neutron shielding (e.g., nuclear reactors), de Staebler (deS 62) wrote Eq. (A4.1) as:

$$H = r^{-2} \sum_i B_i F_i \exp(-d(\theta)/\lambda_i) \ (dn/d\Omega)_i \qquad (A4.2)$$

where the subscript i denotes a range of neutron energies for which B, F, and λ are fairly constant and the definition of $(dn/d\Omega)$ is obvious.

Moyer, in his original formulation, recognized that Eq. (A4.2) may be approximated by a single energy group. This is possible because of the characteristic variation of neutron attenuation lengths as a function of energy (Fig. A4.2).

Neutron attenuation lengths above 150 MeV are roughly independent of energy, but diminish rapidly with energy below about 100 MeV. Consequently the greater yields of low-energy, as compared to high-energy, neutrons at the primary interaction will be more than compensated for by the greater attenuating action of the shield for these neutrons. The actual variation of attenuation length with energy may be approximated by a step function (see Fig. A4.2) where:

$$\lambda \ (E > 150 \text{ MeV}) = \lambda \quad .$$

$$\lambda \ (E \leq 150 \text{ MeV}) = 0 \quad . \qquad (A4.3)$$

Consideration of only the high-energy (E > 150 MeV) group of neutrons is not strictly accurate because the lower-energy particles do have a small but finite attenuation length. Some allowance therefore has to be made for these lower energy particles.

Moyer recognized that the nature of the radiation field outside the shield of a high-energy proton accelerator will be determined by neutrons with energy greater than about 150 MeV. In fact, because high-energy pions and protons in the hadronic cascade have very similar cross sections to neutrons, we may talk of 'cascade propagators' rather than just 'high-energy' neutrons. Deep in the shield these high-energy (E > 150 MeV) hadrons regenerate the cascade but are present in relatively small numbers. At a shield interface the radiation field observed consists of these 'propagators', born close to the primary radiation source, accompanied by many particles of much lower energy, mainly neutrons, born near the interface.

The total neutron flux density (and consequently the dose-equivalent rate) will be proportional to the high-energy hadron flux density. Because the low-energy components are produced by interaction of the high-energy propagators, their intensity decreases through the shield in an exponential manner with effectively the same attenuation length for all directions through the shield.

The essence of the Moyer model, therefore, is that the dose equivalent at any point outside the accelerator shield is largely governed by the simple 'line-of-sight' propagation of the cascade-generating particles produced at the first interaction (target) and a multiplication factor may be used to account for particle build-up. The cascade-generating particles have an attenuation length that is independent of energy.

Several experimental verifications of Moyer's basic assumptions have been reported in the literature. In a series of measurements in concrete irradiated by protons with energy between 2.2 and 6.2 GeV, Smith et al. demonstrated the essential independence of radiation attenuation length with angle to the incident proton beam direction, and with a threshold of the neutron detector used (Sm 64). Smith has described the excellent agreement between measured radiation levels around the Bevatron and those predicted by Moyer (Sm 65). In that series of measurements the development of radiation field equilibrium was also demonstrated.

Gilbert et al. showed that it was possible to account for neutron flux densities in the earth shielding of the CERN 25 GeV proton synchrotron with good accuracy using a Moyer-type equation with empirically determined parameters (Gi 68, Gi 69). Over a range of 10^5 in flux density and up to a distance of 40 m from an internal target in the accelerator, which was the principal source of radiation during the measurements, typical results gave an accuracy in neutron flux density estimation of 20 percent or better (Gi 68).

In practical shield configurations the combined influence of angular distribution and attenuation results in the fact that hadrons emitted at angles between 60° and 120° determine the thickness of the transverse shield. $B(E,\theta)$ then loses its angular dependence because the spectrum can be assumed to be invariant over this limited angular range. Since now one is dealing with the global fluence of particles above 150 MeV, $B(E)$ can be replaced by $m(E_p)$, which is constant for a given target material and primary proton energy, E_p.

One can also write

$$\int_{E>150\ \mathrm{MeV}}^{E_{max}} \frac{d^2n(E,\theta)}{dEd\Omega}\, dE = g(\theta) \qquad \text{(A4.4)}$$

where $g(\theta)$ is the angular distribution function for hadrons with energy greater than 150 MeV.

Thus

$$\phi(E > 150\ \mathrm{MeV}) = g(\theta)r^{-2}\exp(-d/\lambda)m(E_p) \qquad \text{(A4.5)}$$

For an equilibrium cascade the total dose equivalent is proportional to the fluence of hadrons with energy above 150 MeV:

$$H = km(E_p)g(\theta)r^{-2}\exp(-d(\theta)/\lambda) \qquad \text{(A4.6)}$$

As we shall show in the following section, the angular distribution function, $g(\theta)$, may be approximated by an exponential of the form:

$$g(\theta) = c \exp(-\beta\theta) \tag{A4.7}$$

Combining equations (A4.6) and (A4.7) and writing the product of the constants as $\Psi(E_p)$ the source strength parameter we have:

$$H = \frac{\Psi(E_p) \exp(-\beta\theta) \exp(-d(\theta)/\lambda)}{r^2} \tag{A4.8}$$

and in the geometry of Fig. A4.3 this becomes

$$H = \frac{N \Psi(E_p) \exp(-\beta\theta) \exp(-d\,\mathrm{cosec}\,\theta/\lambda)}{R^2 \mathrm{cosec}^2\theta} \tag{A4.9}$$

where N is the number of protons interacting at a point.

The Variation of the Moyer Model Parameters with Primary Proton Energy

The Source Strength Parameter, $\Psi(E_p)$

During the period in which the Moyer model was formulated there was considerable discussion in the literature concerning the variation of Ψ with primary proton energy, E_p. Lindenbaum suggested that if the variation be written in the form

$$\Psi(E_p) = H_o E_p^m \tag{A4.10}$$

the value of m was bounded between the values $0.25 \le m \le 1.0$ (Li 61). The basis for this argument was that the production of shower particles varied as $E_p^{0.25}$, while the production of low-energy (thermal) neutrons varied as $E_p^{1.0}$ (Pa 73). As a compromise Lindenbaum suggested that the actual value of m should be the geometric mean of the extreme values, giving $m = 0.5$ (Li 61).

The actual value of m will depend upon the equipartition of energy in the hadron cascade. Feinberg's calculations of the hadron cascades generated in matter by high-energy protons suggested a value $m = 0.75$ (Fe 72). The fact that m has a value less than 1 may be understood by remembering that at high energies an increasing proportion of the total energy in the cascade processes is transmitted through the electromagnetic cascade. Thus the total production of hadrons—and ultimately the neutrons of concern in accelerator shielding—will vary less rapidly than a direct proportionality to primary proton energy.

With the accumulation of a limited number of experimental determinations of Ψ as a function of E_p in the energy range 7.4–30 GeV, Stevenson et al. were able to show that a value of $m = 1$ was consistent with the available data and with the assumption that Ψ varies linearly with E_p. H_o of Eq. (A4.10) had the value $(1.61 \pm 0.19) \times 10^{-13}$ Sv m^2 GeV^{-1} (St 82, Th 81).

More recent statistical analyses of a somewhat larger data base (Li 84, Th 84) (Table A4.1) with values of Ψ determined up to energies

of 350 GeV have shown that when E_p is in GeV, the best values of the parameters of Eq. (A4.10) are

$$H_o = (2.84 \pm 0.14) \times 10^{-13}$$

$$m = 0.80 \pm 0.10 \quad .$$

A Student's t-test applied to the data rejects the hypotheses m = 0.5 (p = 1 percent, two-tail test) and m = 1.0 (p = 3 percent, one-tail test). Figure A4.4 shows the results of regression analysis of the data together with the 95 percent confidence limits to the regression line.

Cossairt et al. (Co 85a) and Stevenson (St 86b) have extended the energy region over which the parameter proposed by Thomas and Thomas applies (Th 84).

Cossairt et al. made a detailed comparison of measured values of absorbed dose with values calculated using the Monte Carlo simulation code CASIM in both steel and composite (steel, concrete, earth) absorbers. Incident proton energies of 200, 400, 600 and 800 GeV were assumed. Agreement of the measurements (of absorbed dose) with the calculations was quite good (within 20%) at small distances from the beam axis (d < 0.5 cm) in steel, while for even a thick earth shield (d ~ 5 m) the agreement was acceptable for radiation protection purposes (within a factor of 2). For the two cases studied the energy exponents for the absorbed dose (which may be assumed to be proportional to dose equivalent) were 0.84 ± 0.02 and 0.61 ± 0.08 respectively. Cossairt et al. conclude that the energy scaling determined in their study is consistant with that suggested earlier (Li 84, Th 84).

Stevenson has derived values of $H_{\pi/2}$* from cascade calculations in concrete for protons of energy from 400 MeV to 1 TeV (St 86b). His data confirm an energy variation as $E^{0.8}$:

$$H_{\pi/2} = 6.6 \times 10^{-15} E_p^{0.8} \quad \text{Sv m}^2$$

The value of the constant 6.6×10^{-15} Sv m^2 is in agreement within 20% of the value derived by Thomas and Thomas for thick targets (Th 84). For a complete discussion see Section 4.3.

In summary, at the time of writing (1986), the magnitude and variation with energy of the Moyer model source strength parameter, Ψ, within the energy range 5 GeV $\leq E_p \leq$ 500 GeV, and possibly as high as 1000 GeV, is best summarized by the equation

$$\Psi (E_p) = 2.8 \times 10^{-13} E_p^{0.8} \qquad \text{(A4.11)}$$

with $\Psi (E_p)$ in Sv m^2 when E_p is in GeV.

---

* $H_{\pi/2}$ is related to H_0 by the equation $H_{\pi/2} = H_0 \exp(-\beta\pi/2)$. With $\beta = 2.3$ radians^{-1}, $H_{\pi/2} = 2.70 \times 10^{-2} H_0$.

There is a clear need for more accurate experimental determination of Ψ over the entire energy range of concern to improve both our knowledge of its magnitude and its variation with energy.

The Angular Relaxation Parameter, β

In the practical determination of transverse shielding for proton accelerators in this energy range, we are concerned with the combined effects of angular distribution and attenuation of neutrons above about 150 MeV through shields sufficiently thick that several interactions will take place.

Ranft and his colleagues were able to show that the shape of the angular distribution of protons greater than 150 MeV produced in primary interactions was nearly independent of primary proton energy in the range $1 < E_p < 300$ GeV (Ra 67, Ro 69). For angles around $\pi/2$ radians the angular distribution has a simple experimental form:

$$g(\theta) \propto e^{-\beta\theta} \qquad \text{(A4.7a)}$$

For the primary interaction the predicted value of β was 4.0 radians^{-1} (Ro 69).

More recent experimental studies of the angular distributions around accelerator targets using threshold detectors have been made by Levine et al. (Le 72). Figure A4.5 summarizes these data and shows values of β as a function of detector threshold (E_{th}). A linear relationship between β and E_{th} is evident. The value of β corresponding to E_{th} = 150 MeV extrapolated from these data is 2.3 ± 0.3. The values of β, in the angular range 60–120°, were independent of target material (Al, Cu, W) and did not differ for proton energies of 3.7 and 23 GeV. Experiments at 225 and 400 GeV have confirmed this independence of proton energy (St 83). No adequate explanation of the difference between the originally calculated and measured values of β have been given. However more recent models of the proton-nucleus interaction contained in the FLUKA82 hadron cascade program (Aa 84) are able to reproduce the experimental data of Levine et al. (Le 72) and Stevenson et al. (St 83) [see Stevenson et al. (St 86a)]. It is therefore probable that the earlier calculations (Ro 69) were based on an inadequate model of the proton-nucleus interaction.

In the practical determination of transverse shielding for proton accelerators in the 1 -100 GeV range we are concerned with the combined effects of the angular distribution and attenuation through shields in which several interactions have occurred. We are thus interested more in the apparent angular distribution of the 'virtual source' of neutrons which control the transverse shielding, rather than the angular distribution close to accelerator targets.

Stevenson et al. (St 82) have summarized determinations of β derived from several target and shielding measurements. These values are summarized in Table A4.2. There is no indication of any large variation of and with primary proton energy and assuming invariance. The mean of these values of β is 2.3 ± 0.1 radians^{-1} -in good agreement with the value extrapolated from the data of Levine et al. (Le 72).

Measurements of angular distributions of high-energy neutrons around targets bombarded with heavy ions of about 500 MeV/amu have also confirmed values of β close to 2.3 radians^{-1} (McC 84).

It may be concluded that the best value of β that may be determined from existing data is 2.3 $\pm$ 0.1 radians^{-1} and that β is either independent of, or only weakly dependent upon, incident proton energy.

The Attenuation Parameter, λ

The attenuation length (parameter), λ, appropriate for use in the Moyer model is determined by the neutron inelastic cross section of the constituents of the shield. At high energies the attenuation, λ_A, for material of mass number, A, is given by:

$$\lambda_A = \frac{k}{\rho} A^{1/3} \qquad \text{(A4.12)}$$

where λ_A is in units of mass per unit area, ρ is the density of the shield material (mass per unit volume) and k is a constant. Theoretical considerations suggest that k has a value of 380 kg m^{-2} (Pa 73).

Perhaps the best empirical determination of attenuation length was made in earth by Gilbert et al. (Gi 68). A value of:

$$\lambda_E = 1170 \pm 20 \text{ kg m}^{-2}$$

was obtained. Assuming that the earth in which this measurement was made consists of 95 percent SiO_2 (by weight) and 5 percent H_2O (by weight) the effective mass number for earth A_E, is 20.4 (McC 85).

Substituting into Eq. (A4.12) we obtain:

$$k = \frac{\rho_E \lambda_E}{A_E^{1/3}} = \frac{1170}{(20.4)^{1/3}} = 428 \text{ kg m}^{-2}$$

a result in reasonable agreement with that predicted on theoretical grounds.

Use of the empirically determined value, k, will lead to somewhat thicker shields than by using the theoretical value of 380 kg m^{-2} and is thus, perhaps, conservative.

In summary, for the Moyer model a value of

$$\rho\lambda_A = 428\ A^{1/3} \text{ kg m}^{-2} \qquad \text{(A4.13)}$$

independent of energy is recommended.

Point Source Calculations

Although beam losses at high-energy particle accelerators are usually of an extended nature it is often the case that the region of high beam loss occurs over lengths small or comparable with the thickness of the accelerator shields and tunnel radius (the distance R in Fig. A4.3). Under such conditions the assumption of point loss may be used to determine the dose equivalent at the shield surface.

Substitution into Eq. (A4.9) enables the dose equivalent at the shield surface, H_θ, to be calculated as a function of θ (Fig. A4.3).

Figure A4.6 summarises calculation of H_θ, normalized to the value at $\theta = \pi/2$, as a function of θ for values of shield thickness, ℓ, between 1 and 20 (McC 85). The figure shows values of the function $F(\theta)$ defined by the equation:

$$F(\theta) = \frac{H(\theta)}{H(\pi/2)} = \frac{\exp(-\beta\theta)\exp[(1 - \operatorname{cosec}\theta)]}{\exp(-\beta\pi/2)\operatorname{cosec}^2\theta} \quad \text{(A4.14)}$$

Substituting the value $\beta = 2.3$ radians^{-1} we obtain:

$$F(\theta) = 37.1 \sin^2\theta \exp(-2.30\theta)\exp[\ell(1 - \operatorname{cosec}\theta)] \quad \text{(4.19a)}$$

Figure A4.6 clearly indicates that for thin shields errors of as much as a factor of two can be made by using the assumption that the maximum dose equivalent occurs directly above the point source ($\theta = \pi/2$ radians), but for $\ell \geq 5$ the errors are less than 40%.

The maximum dose equivalent, H_m, can be calculated (exactly) by substituting the appropriate value of θ_m into Eq. (A4.9). By differentiating this equation and setting the result to zero the following equation for θ_m is obtained:

$$[\cot\theta_m \operatorname{cosec}\theta_m - \beta + 2\cot\theta_m] = 0 \quad \text{(A4.15)}$$

Figure A4.7 summarizes the results of solving Eq. (A4.15) with $\beta = 2.3$ and shows values of θ_m as a function of shield thickness ℓ. The exact value of H_m is then given by:

$$H_m = \frac{\Psi(E_p)\, N \exp(-\beta\theta_m)\exp(-\ell \operatorname{cosec}\theta_m)}{R^2 \operatorname{cosec}^2\theta_m} \quad \text{(A4.16)}$$

McCaslin et al. (Mc 85) have shown that a good approximation for H_m is given by:

$$H_m = \frac{5.93\times10^{-2}\,\Psi(E_p)\, N \exp(-\ell)\,\ell^{-0.245}}{R^2} \quad \text{(A4.17)}$$

with R in metres, and $\Psi(E_p)$ in Sv m^2, H_m is in Sv.

Infinite Uniform Line Source

Using the Moyer model expression of Eq. (A4.9) it may be simply shown (Ro 69) that for an infinite uniform line source of S protons per unit length the dose equivalent on the shield surface, H_∞, is given by

$$H_\infty = \frac{\Psi S}{R}\int_0^\pi \exp(-\beta\theta)\exp(-\ell \operatorname{cosec}\theta)\, d\theta \quad \text{(A4.18)}$$

The integral of Eq. (A4.18) has been designated by $M(\beta,\ell)$ and is known as a Moyer integral (Ro 69).

$$M(\beta,\ell) = \int_0^{\pi} \exp(-\beta\theta)\ \exp(-\ell\ \mathrm{cosec}\ \theta)\ d\theta \qquad (A4.19)$$

The Moyer integral may be regarded as a generalized form of the Sievert integral used in the calculation of shielding of extended sources of γ-emitting radioactive materials. Values of Moyer integrals have been tabulated for arguments in the range $0 \leq \beta \leq 10$; $0 \leq \ell \leq 40$ (Ro 69, Pa 73).

For the design of the shielding of proton accelerators in the GeV energy region we have seen that the value of β has been empirically determined to be 2.3. The Moyer integral $M(2.3,\ell)$ therefore takes on special significance. Table A4.3 summarizes calculated value of the integral.*

McCaslin et al. have written a computer program that facilitates computation of the particular integral by Simpson's rule. The program is suitable for use by small programmable calculators such as the Hewlett Packard HP-97 (McC 85).

As an example of the use of Eq. (A4.18): with E 10 GeV, Ψ has the value 1.79×10^{-12} Sv m^2. Then with R in metres and S in protons per metre Eq. (A4.18) and (A4.19) give:

$$H_{\infty} = \frac{1.79\times10^{-12}\ S\ M(2.3,\ell\ )}{R} \qquad (A4.20)$$

Substituting the value R = 5 m and using the value of $M(2.3,\ell)$ given in Table A4.3 we can calculate the dose equivalent at a point 5 metres above the infinite uniform line source as a function of shield thickness. Table A4.4 summarizes several values.

Finite Uniform Line Source

Here we consider the more practical case of the dose equivalent produced at a shield surface by a finite, but uniform, beam loss.

If we consider that the beam spill strength has a value S protons per unit length over a distance of length L (the 'beam spill length') along the beam axis and that beam loss is zero elsewhere it is convenient to define a parameter,

$$\eta = \frac{L}{a + d} = \frac{L}{R} \qquad (A4.21)$$

where a, d and R have previously been defined (Fig. A4.3). It is also convenient to measure distance along the beam axis Z in units of R and place the origin Z = 0 at the start of the beam spill. (Figure A4.8 illustrates this for a spill length L = 4R, i.e., $\eta = 4$.)

The dose equivalent at the source point on the shield surface $H_L(z,R)$ for a given spill length L is given by:

---

*Tesch (Te 83) has shown that for most purposes in shielding calculations $M(2.3,\ell)$ may be approximated by the expression: $M(2.3,\ell) = 0.065 \exp(-1.09\ \ell)$, $2 \leq \ell \leq 15$.

$$H_L(z,R) = \frac{\Psi\ S}{R} \int_{\alpha_1}^{\alpha_2} \exp(-\beta\theta)\ \exp(-\ell\ \ \mathrm{cosec}\theta)\ d\theta \qquad \text{(A4.22)}$$

where the angles α_1, α_2 limiting the integral are given by (see Fig. A4.9):

$$\alpha_1 = \tan^{-1}\ (R/Z) \qquad \text{(A4.23a)}$$

$$\alpha_2 = \tan^{-1}\ [(R/(Z - L)] \qquad \text{(A4.23b)}$$

If we define a restricted Moyer integral, designated as $M_{\alpha_1,\alpha_2}(\beta,\ell\ )$, by the equation:

$$M_{\alpha_1,\alpha_2}(\beta,\ell\ ) = \int_{\alpha_1}^{\alpha_2} \exp(-\beta\theta)\ \exp(-\ell\ \ \mathrm{cosec}\theta)\ d\theta \qquad \text{(A4.24)}$$

Equation (A4.18) may be more conveniently written as:

$$H_L(z,R) = \frac{\Psi\ S\ M_{\alpha_1,\alpha_2}(\beta,\ell\ )}{R} \qquad \text{(A4.22a)}$$

or, remembering that $S = \frac{N}{L} = \frac{N}{\eta R}$, in the alternative form:

$$H_L(z,R) = \frac{N}{\eta R^2}\ M_{\alpha_1,\alpha_2}(\beta,\ell\ ) \qquad \text{(A4.22b)}$$

As with the case of Moyer integrals, the integrals of Eq. (A4.22) may be evaluated by numerical means (McC 85).

In shielding calculations the primary interest lies in the maximum value of $H_L(z,R)$. In the case of finite uniform extended line sources it is not possible to write down an explicit analytical expression for $H_L$max–as it was in the case of a point loss [Eq. (A4.16)]. However, numerical methods may be used to determine $H_L$max by calculating $H_L(z,R)$ as a function of z. Specimen calculations have been carried out by McCaslin et al. (Mc 85). Calculations were made of $H_L(z,R)$ as a function of z using Eq. (4.22a) and (4.22b) with the following parameters substituted:

$\Psi = 1.79 \times 10^{-12}$ Sv m^2 (corresponding to E = 10 GeV)

R = 1 metre

N = 1 proton or S = 1 proton metre^{-1}

$0.002 < \eta < 4$.

(The choice of R = 1 m was made for convenience, facilitating easy scaling to different transverse distances by use of the inverse square law). These calculations are summarized in Figs. A4.10 and A4.11.

Summary-Point and Extended Source Calculations

In Fig. A4.10 since N = 1 proton is assumed for all spill lengths the area under the curves is constant (independent of η). In Fig. A4.11 since S is held constant at S = 1 proton per metre the area under the curves is proportional to the beam spill parameter η. Inspection of Figs. A4.10 and A4.11 shows that for short spill lengths ($\eta \ll 1$) the source is nearly point-like. Under these conditions substitution of the appropriate value for H into Eq. (A4.16) will yield a good estimate of H_m. For longer spill lengths ($\eta > 1$) the source behaves more like an infinite uniform line source. In this case substitution of the appropriate value of S into Eq. (A4.18) will provide an acceptable estimate of H_m.

For these specimen calculations McCaslin et al. summarised their conclusions in Fig. A4.12. Values of H_m for a finite uniform line source were calculated as a function of beam spill length η and are shown as a solid line. The actual value of dose equivalent will, in fact, depend upon the exact nature of the beam loss distribution but is bounded by (a) the assumption of point loss-shown as a rising straight line to the left of the diagram-and (b) the assumption an infinite uniform beam loss-shown as a horizontal line in the figure. All other physically possible values of H_m lie within the approximately triangular cross-hatched area. The shaded area shows the degree of over-estimation in H_m that may be made by assuming the minimum of either point loss or by substituting the value of S = N/L into the infinite uniform loss equation. In Fig. A4.12 η_p is shown and defined as the value of η at which H would equal 0.9 of the value obtained, assuming all the loss occurred at a point. Similarly η_∞ is defined as the value of η at which H would equal 0.9 of the value obtained if the source were infinite and uniform of strength S = N/L.

Figure A4.13 summarizes the over-estimation that may result from the use of either of the two limiting assumptions (point loss or infinite uniform line sources). The percentage overestimation ϵ, is defined by:

$$\epsilon = \frac{H_A - H_m}{H_m} \times 100 \text{ percent} \qquad \text{(A4.25)}$$

where H_m is the maximum dose equivalent and H_A is the dose equivalent estimated using either of the limiting assumptions. Taking an error of 10 percent as a criterion we see from Fig. A4.13 that:

- For short spills ($\eta \leq 0.6$) H_m may be calculated by substitution of the value N = SL into Eqs. (A4.16) and (A4.17).
- For long spills ($\eta \geq 1.4$) may be calculated by substituting the value S = N/L into Eq. (A4.18).
- For intermediate spills ($0.6 \leq \eta \leq 1.4$) the maximum dose equivalent must be calculated using Eqs. (A4.22a) or (A4.22b) which contain limited Moyer integrals. Figure A4.13 shows the error incurred in adopting either of the simplifying assumptions for 'short' or 'long' spills.

It is important at this point to emphasize that these conclusions apply only to the specimen cases calculated by McCaslin et al. (McC 85). Similar calculations over a wider range of the parameters ℓ and R are desirable before general conclusions are to be drawn.

A general relationship between H_m (point source) and H_∞ may be obtained by combining Eq. (A4.16), (A4.18) and (A4.19) whence:

$$\frac{H_m}{H_\infty} = \frac{N}{SR} \times \frac{\exp(-\beta\theta_m)\ \exp(-\ell\ \mathrm{cosec}\theta_m)}{M(\beta,\ell)} \qquad \text{(A4.26)}$$

Substituting $N = LS$ and $\eta = L/R$, Eq.(A4.26) reduces to:

$$\frac{H_m}{H_\infty} = \eta \times \frac{\exp(-\beta\theta_m)\ \exp(-\ell\ \mathrm{cosec}\theta_m)}{M(\beta,\ell)} \qquad \text{(A4.27)}$$

McCaslin et al. have defined a function,

$$B(\ell) = \frac{\exp(-\beta\theta_m)\ \exp(-\ell\ \mathrm{cosec}\theta_m)}{M(\beta,\ell)} \qquad \text{(A4.28)}$$

whence Eq. (A4.27) reduces to:

$$\frac{H_m}{H_\infty} = \eta B(\ell) \qquad \text{(A4.27a)}$$

Figure A4.14 shows values of $B(\ell)$ calculated as a function of η. McCaslin et al. have shown that $B(\ell)$ may be approximated by a second order polynomial:

$$B(\ell) = 0.44 + 0.12\ \ell\ - 0.0028\ \ell^2 \qquad \text{(A4.29)}$$

Equation (A4.27a) facilitates the use of the Moyer model for shielding calculations.

Limitations of the Moyer Model

The Moyer model as described in the preceeding sections may be used to determine the intensity of the radiation outside the transverse shielding of accelerators under appropriate conditions to probably within a factor of 2. Stevenson et al. have suggested that the model may be used in the energy range 1-50 GeV, but some of the more recent developments have suggested it might be used under limited circumstances up to as high as 1 TeV (Co 84, St 82, Th 83). However, it is important to understand the limitations of the model.

Stevenson et al. (St 82) have given two examples where significant errors might result from use of the value of H_0 given in the earlier sections. The recommended value of H_0 (2.8×10^{-13} Sv m^2) was determined with small target to shield distances ($a \leq R$) and normal to thick targets ($\theta \simeq 90°$). Any large departure from these conditions ($\theta \simeq 0°$ or $a \simeq R$) may result in error (see St 82).

Conclusions

The Moyer model for high-energy neutron shielding has proved itself a very durable instrument since it was first developed in the early 1960s and has been utilized in the design of several important high-energy accelerator facilities. It has recently been used to estimate shielding for a 50 GeV proton synchrotron and for the transverse shielding of a 20 TeV collider facility (Ch 80, Co 84, Th 83). Its advantage over 'sophisticated' methods lies in its simplicity; the algorithm contains only three parameters whose values are now well established. The figures presented and the sample codes for use with desk-top or hand-held computers demonstrate the ease with which the Moyer model can be applied to many shielding problems. The procedure, which requires very modest computational power, is useful in its own right besides serving as a check on more elaborate, but less transparent, methods of shielding calculation.

References

The references for this appendix are incorporated in Chapter 4.

Table A4.1
Summary of experimentally determined values of source strength of Moyer model parameters $\Psi(E_p)$, as a function of proton energy, E_p (Th 84).

Primary proton energy, E_p (GeV)	Moyer parameter, $\Psi(E_p)$ (Sv m^2)	Source
7.4	1.4	Sh 69b, St 69
7.4	2.1	Sh 69b, St 69
10.0	0.96	Ho 66
13.7	2.5	Gi 68
13.7	3.1	Gi 68
21.0	1.6	Ho 79
23.0	3.5	Ma 79
25.5	3.3	Gi 68
25.5	5.0	Gi 68
25.5	6.6	Ro 69, St 82
30.0	3.4	Aw 70
350	21.2	Co 82
350	44.6	Co 82

Table A4.2
Summary of measured values of the angular relaxation parameter, β

Laboratory	Incident proton energy (GeV)	β (radians^{-1})
CERN-LBL-Rutherford	13.7	
Laboratory Collaboration	13.7	
(Gi 68)	25.5	2.1 - 2.4[a,b]
Rutherford Laboratory	7.4	2.3 ± 0.4[a]
(St 69)	7.4	2.4 ± 0.2[b]
Argonne National Laboratory	10.0	2.0 ± 0.3[c]
(Ho 66)	10.0	2.5 ± 0.2[d]

Detector: (a) Aluminium Activation
(b) Carbon Activation
(c) Film
(d) Tissue Equivalent Ionization Chamber

Table A4.3
Value of the Moyer integral M(2.3,ℓ) as a function of shield thickness ℓ.

ℓ	M	ℓ	M	ℓ	M	ℓ	M
0.10	0.26570E+00	5.10	0.23505E-03	10.10	0.10211E-05	15.10	0.53891E-08
0.20	0.19690E+00	5.20	0.20997E-03	10.20	0.91833E-06	15.20	0.48751E-08
0.30	0.15221E+00	5.30	0.18762E-03	10.30	0.82593E-06	15.30	0.43779E-08
0.40	0.12158E+00	5.40	0.16768E-03	10.40	0.74287E-06	15.40	0.39460E-08
0.50	0.98960E-01	5.50	0.14991E-03	10.50	0.66821E-06	15.50	0.35568E-08
0.60	0.81623E-01	5.60	0.13404E-03	10.60	0.60109E-06	15.60	0.32061E-08
0.70	0.68008E-01	5.70	0.11989E-03	10.70	0.54075E-06	15.70	0.28900E-08
0.80	0.57123E-01	5.80	0.10725E-03	10.80	0.49649E-06	15.80	0.26052E-08
0.90	0.48301E-01	5.90	0.95964E-04	10.90	0.43770E-06	15.90	0.23485E-08
1.00	0.41070E-01	6.00	0.85883E-04	11.00	0.39383E-06	16.00	0.21172E-08
1.10	0.35089E-01	6.10	0.76876E-04	11.10	0.35437E-06	16.10	0.19087E-08
1.20	0.30101E-01	6.20	0.68827E-04	11.20	0.31889E-06	16.2	0.17207E-08
1.30	0.25915E-01	6.30	0.61632E-04	11.30	0.18697E-06	16.30	0.15514E-08
1.40	0.22380E-01	6.40	0.55199E-04	11.40	0.25826E-06	16.40	0.13986E-08
1.50	0.19381E-01	6.50	0.49446E-04	11.50	0.23244E-06	16.50	0.12610E-08
1.60	0.16825E-01	6.60	0.44300E-04	11.60	0.20921E-06	16.60	0.11370E-08
1.70	0.14638E-01	6.70	0.39696E-04	11.70	0.18831E-06	16.70	0.10251E-08
1.80	0.12761E-01	6.80	0.35576E-04	11.80	0.16951E-06	16.80	0.92435E-09
1.90	0.11145E-01	6.90	0.31888E-04	11.90	0.15259E-06	16.90	0.83347E-09
2.00	0.97496E-02	7.11	0.28587E-04	12.00	0.13736E-06	17.00	0.75154E-09
2.10	0.85418E-02	7.10	0.25632E-04	12.10	0.12367E-06	17.10	0.67769E-09
2.20	0.74941E-02	7.20	0.22985E-04	12.20	0.11134E-06	17.20	0.61110E-09
2.30	0.65834E-02	7.30	0.20611E-04	12.30	0.10024E-06	17.30	0.55108E-09
2.40	0.57902E-02	7.40	0.18490E-04	12.40	0.90260E-07	17.40	0.49695E-09
2.50	0.50982E-02	7.50	0.16588E-04	12.50	0.81274E-07	17.50	0.44815E-09
2.60	0.44936E-02	7.60	0.14882E-04	12.60	0.73185E-07	17.60	0.40416E-09
2.70	0.39644E-02	7.70	0.13354E-04	12.70	0.65904E-07	17.70	0.36449E-09
2.80	0.35007E-02	7.80	0.11984E-04	12.80	0.59350E-07	17.80	0.32872E-09
2.90	0.30939E-02	7.90	0.10756E-04	12.90	0.53450E-07	17.90	0.29647E-09
3.00	0.27365E-02	8.00	0.96548E-05	13.00	0.48139E-07	18.00	0.26738E-09
3.10	0.24221E-02	8.10	0.86673E-05	13.10	0.43357E-07	18.10	0.24116E-09
3.20	0.21454E-02	8.20	0.77817E-05	13.20	0.39051E-07	18.20	0.21751E-09
3.30	0.19015E-02	8.30	0.69872E-07	13.20	0.35175E-07	18.30	0.19618E-09
3.40	0.16864E-02	8.40	0.61745E-05	13.40	0.31684E-07	18.40	0.17695E-09
3.50	0.14965E-02	8.50	0.56350E-05	13.50	0.28541E-07	18.50	0.15961E-09
3.60	0.13288E-02	8.60	0.50613E-05	13.60	0.25710E-07	18.60	0.14397E-09
3.70	0.11814E-02	8.70	0.45463E-05	13.70	0.23162E-07	18.70	0.12986E-09
3.80	0.10492E-02	8.80	0.40841E-05	13.80	0.20866E-07	18.80	0.11714E-09
3.90	0.93297E-03	8.90	0.36693E-05	13.90	0.18799E-07	18.90	0.10567E-09
4.00	0.83000E-03	9.00	0.32968E-05	14.00	0.16937E-07	19.00	0.95317E-10
4.10	0.73972E-03	9.10	0.29625E-05	14.10	0.15360E-07	19.10	0.85984E-10
4.20	0.65775E-03	9.20	0.26622E-05	14.20	0.13750E-07	19.20	0.77567E-10
4.30	0.58588E-03	9.30	0.23926E-05	14.30	0.12389E-07	19.30	0.69975E-10
4.40	0.52206E-03	9.40	0.21505E-05	14.40	0.11164E-07	19.40	0.63126E-10
4.50	0.46536E-03	9.50	0.19330E-05	14.50	0.10060E-07	19.50	0.56949E-10
4.60	0.41497E-03	9.60	0.17376E-05	14.60	0.90650E-08	19.60	0.51378E-10
4.70	0.37015E-03	9.70	0.15621E-05	14.70	0.81690E-08	19.70	0.46352E-10
4.80	0.33208E-03	9.80	0.14045E-05	14.80	0.73619E-08	19.80	0.41818E-10
4.90	0.29179E-03	9.90	0.12628E-05	14.90	0.66346E-08	19.90	0.37729E-10
5.00	0.26319E-03	10.00	0.11355E-05	15.00	0.59794E-08	20.00	0.34039E-10

Table A4.4
Sample calculations of H as a function of shield thickness ℓ [E = 10 GeV; S = 1 proton metre^{-1}; R = 5 metres]. From (McC 85).

Attenuation lengths, ℓ	Dose equivalent (Sv proton^{-1} metre)
0	—
1	1.47×10^{-13}
2	3.49×10^{-15}
5	9.42×10^{-17}
10	4.07×10^{-19}
15	2.14×10^{-21}
20	1.22×15^{-23}

FIGURE CAPTIONS FOR APPENDIX TO CHAPTER 4

Figure A4.1 Schematic diagram of shielding geometry for the generalized formulation of the Moyer model.

Figure A4.2 Neutron attenuation length as a function of energy. The step-like function assumed in Moyer Model calculations is shown by a dashed line.

Figure A4.3 Diagram showing the accelerator geometry assumed in Moyer Model calculations and defining the symbols used. (a) longitudinal section; (b) cross section.

Figure A4.4 Ψ (E_p) as a function of primary proton errors. (Summary of Regression Analyses of the experimental data in Table 1). The regression line Ψ (E_p) = 2.8×10^{-13} E_p (0.80) is shown as a heavy solid line. Experimental points are shown as a solid circle. The 95% confidence limits are shown by a light solid line (after Thomas and Thomas, Th 84).

Figure A4.5 The angular distribution parameter, β, as a function of detector energy-threshold (after Levine et al., Le 72).

Figure A4.6 Dose equivalent on the shield outer surface as a function of angle with respect to beam direction (point source loss is assumed) relative to the same quantity at $\pi/2$ (90°). Parameter ℓ is shield thickness in units of the attenuation length.

Figure A4.7 Angle θ_m, at which maximum dose equivalent, H_m, on the shield outer surface occurs, as a function of shield thickness, = d/λ. Point source loss is assumed.

Figure A4.8 Schematic diagram showing beam spill length L and its relationship to the parameters η and R.

Figure A4.9 The definition of the angles α_1 and α_2.

Figure A4.10. Specimen calculations of the dose equivalent on the shield surface resulting from a finite uniform beam loss as a function of position along the beam direction, for different spill lengths $10.002 \leq \eta \leq 4$. The origin is chosen to be at the start of the beam spill. A uniform beam loss, S, of one proton per metre is assumed and the other parameters used are: E = 10 GeV R = 1 m

Figure A4.11. As for Fig. 4A.10 but with a point source (N = 1 proton) assumed.

Figure A4.12. The maximum dose equivalent, H_m, on the shield surface for a finite uniform beam loss as a function of beam spill length parameter η. Values of parameters: S = 1 proton metre^{-1}, ℓ = 5, E = 10 GeV, R = 1 metre, and were calculated using restricted Moyer integrals. The rising straight line to the left is the asymptote obtained if it is assumed that all beam loss occurs at a point. The horizontal line is the limit set by as infinite uniform beam loss. The cross hatched region

shows where the dose equivalents due to intermediate beam losses may occur and enable the error that may arise from incorrect assumptions as to beam loss. The shaded region shows the overestimate that arises by assuming the minimum of either the point source (N = SL) or the infinite uniform line source (S = N/L) assumptions.

Figure A4.13. Overestimation of the maximum dose equivalent on the outer shield surface, H_m, as a function of spill length, η, when either the point-source or infinite uniform line source is assumed. The values η_p, η_∞ indicate where a 10 percent overestimation occurs.

Figure A4.14. The function $B(\ell) = H_m/\eta H_\infty$ as a function of shield thickness, ℓ. The function $B(\ell)$ relates the actual maximum dose equivalent, H_m, to that given by a infinitely extended uniform source having the loss rate S = N/L. The dashed curve shows a second degree polynomial approximation to the actual function.

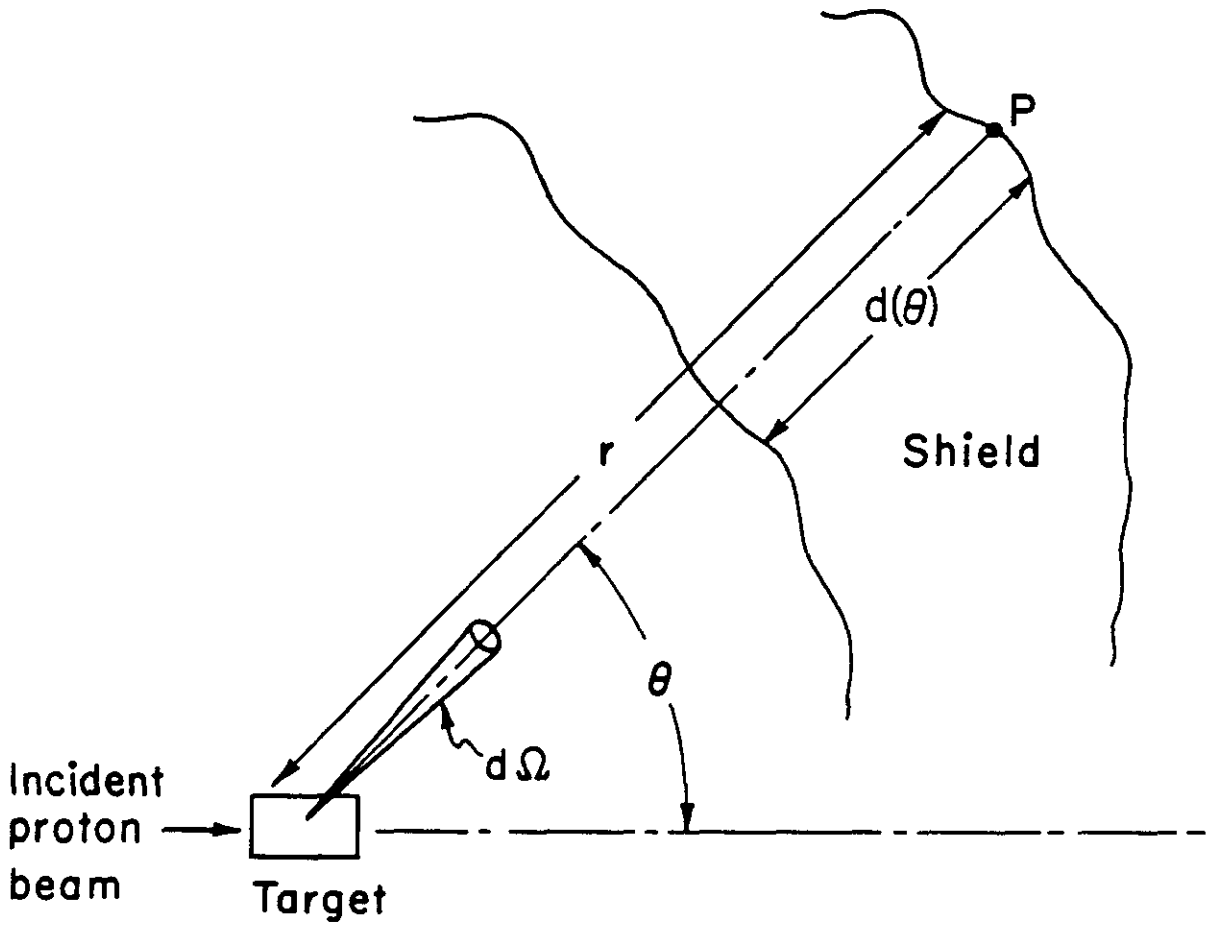

XBL 853-8045

A4.1

A4.1

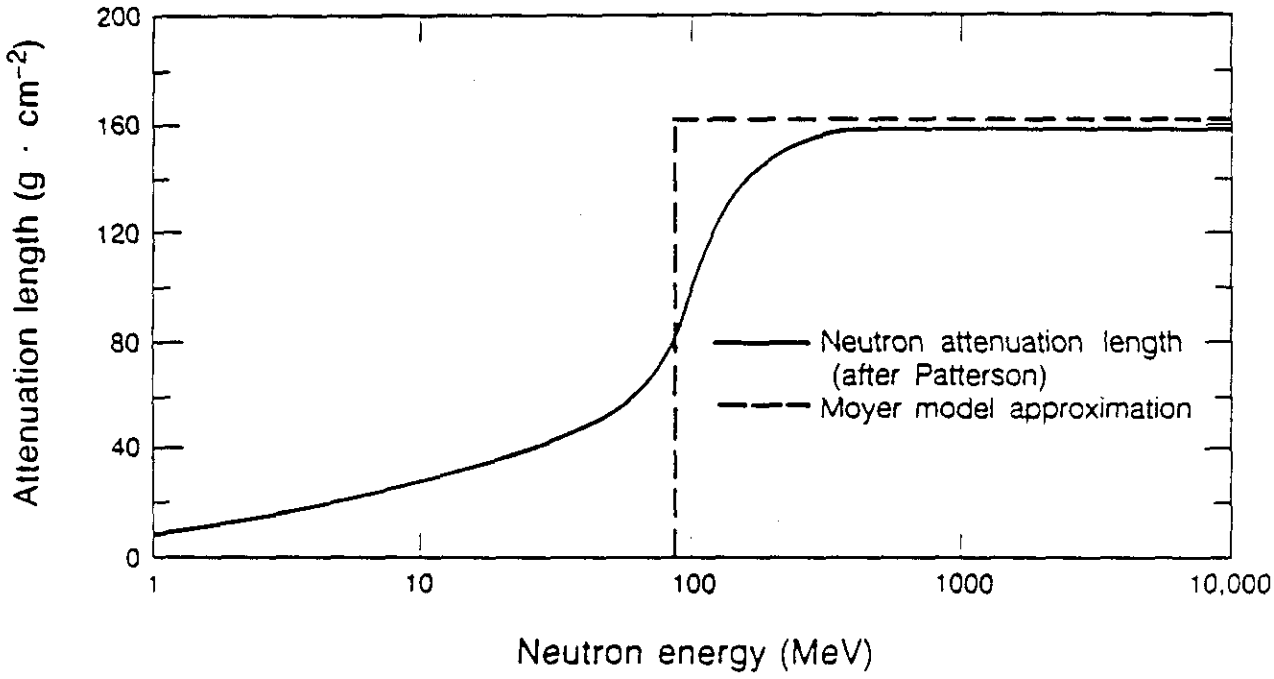

XBL 852-6953

A4.2

A4.2

(a)

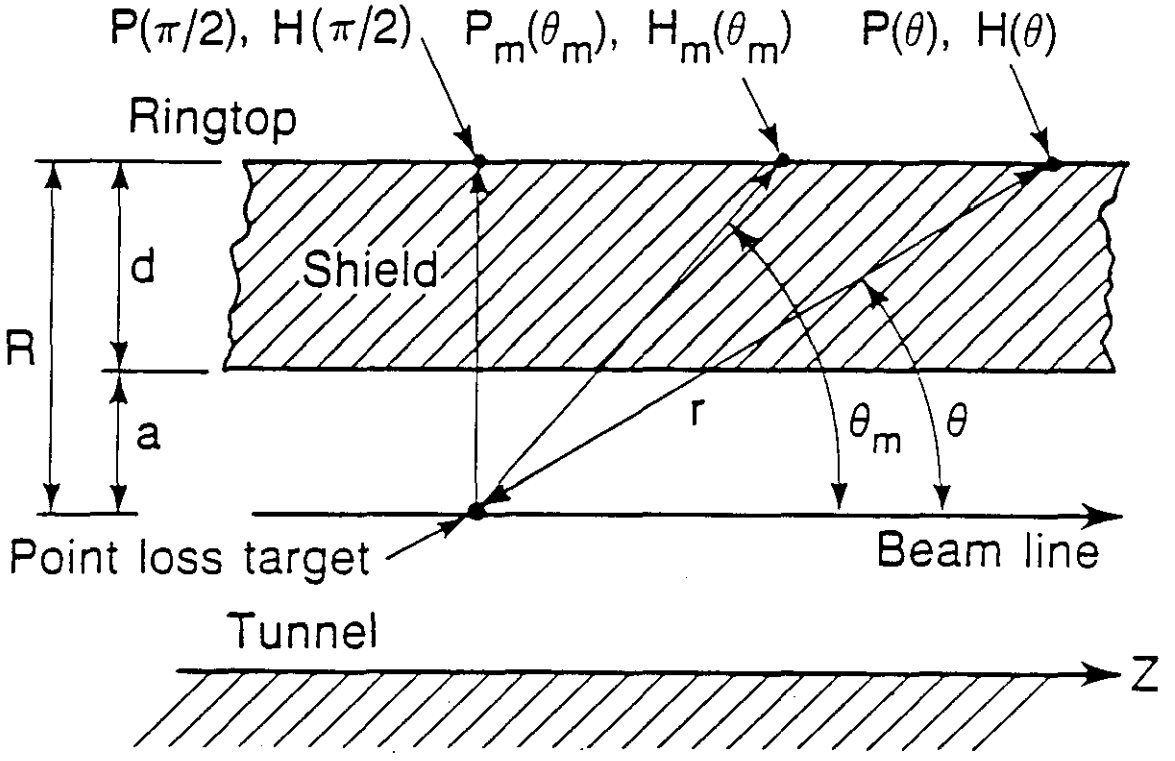

(b)

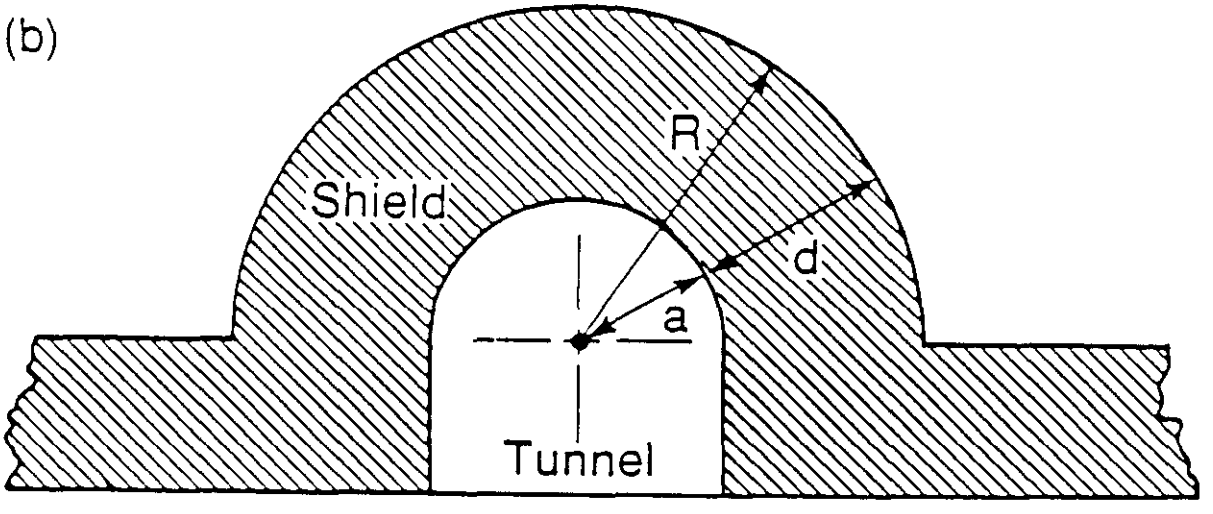

X8L 8411-6346

A4.3

A4.3

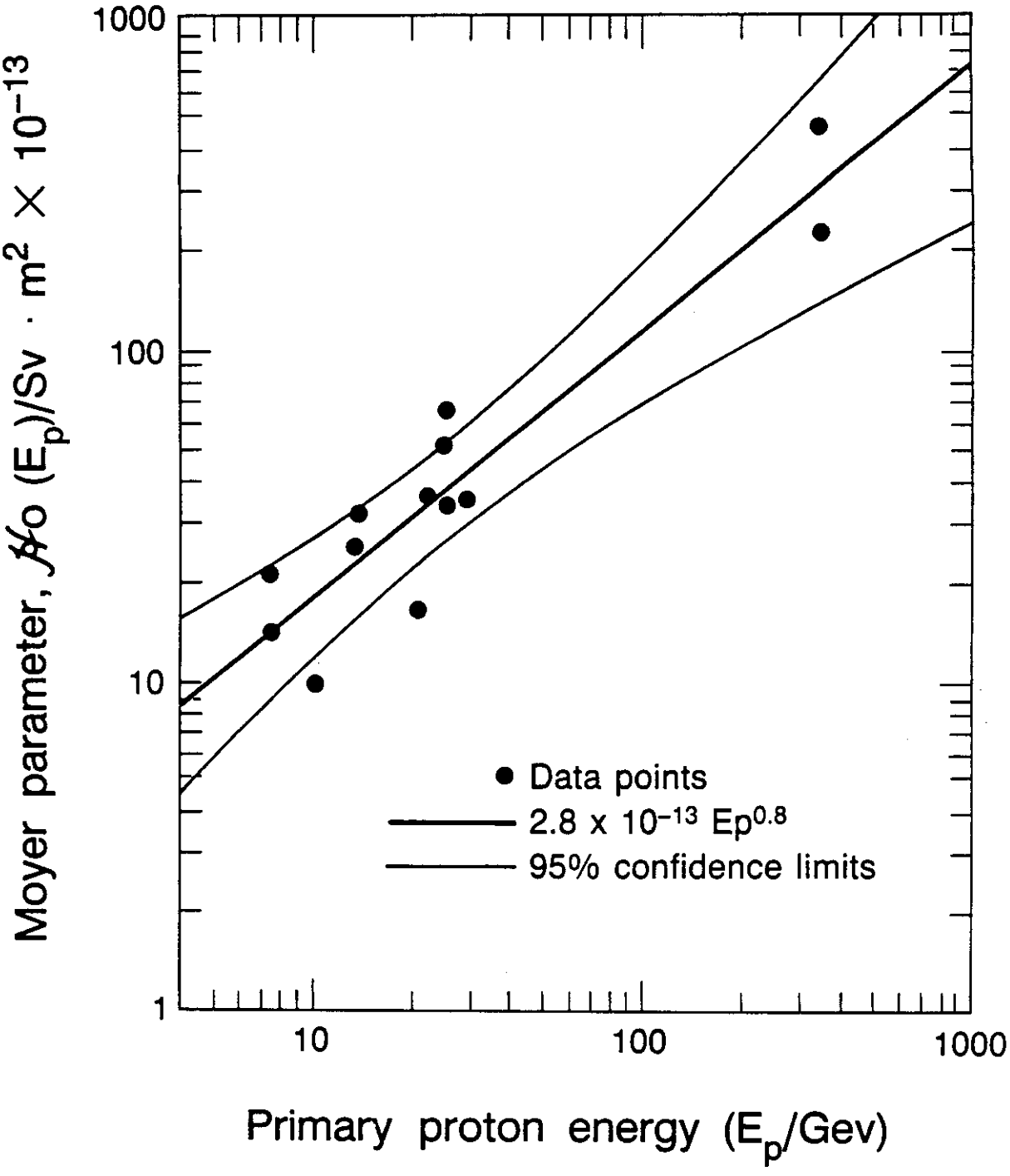

XBL 852-6954

A4.4

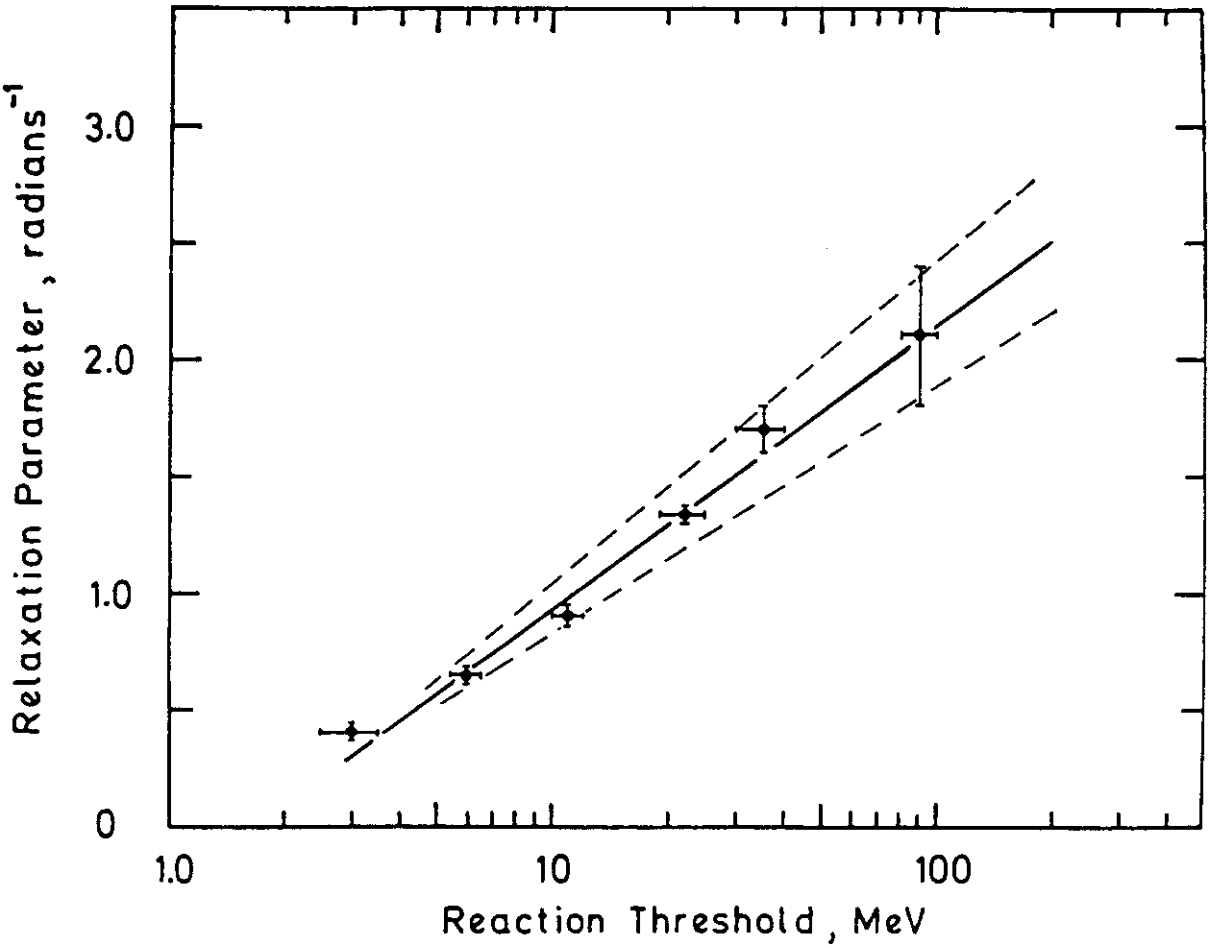

XBL 732-211

A4.5

A4.5

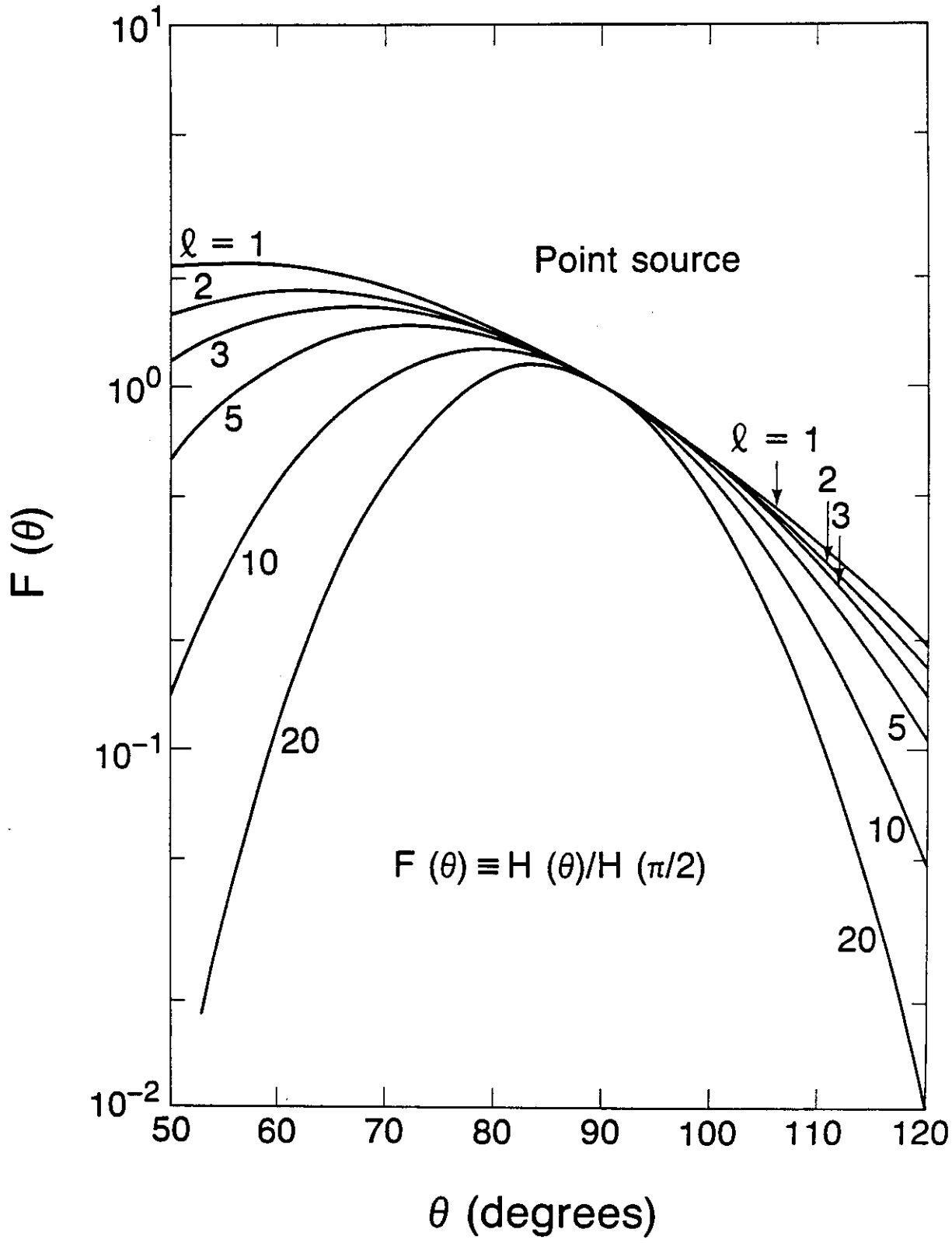

A4.6

XBL 8411-6352

A4.6

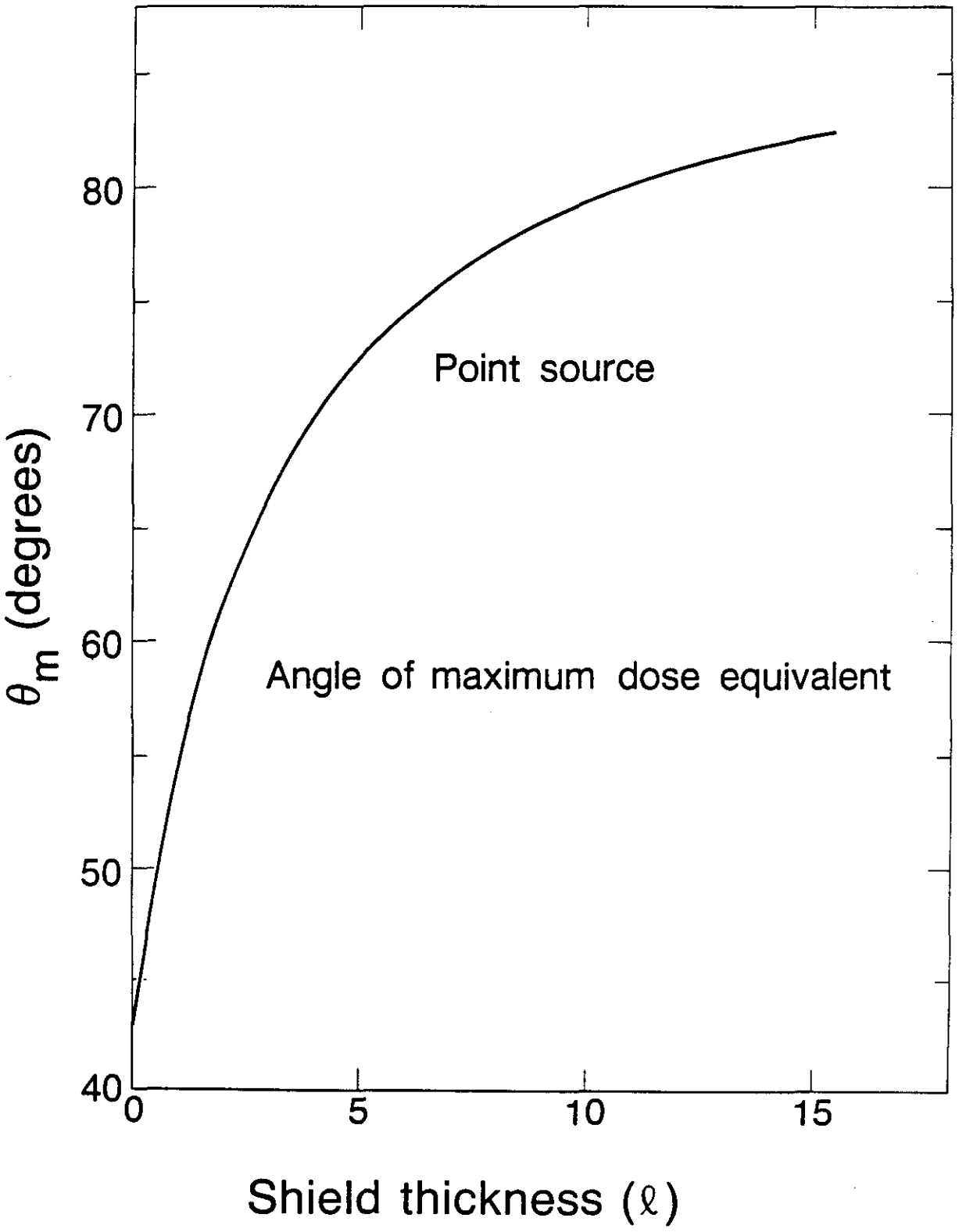

XBL 8411-6348

A4.7

A4.7

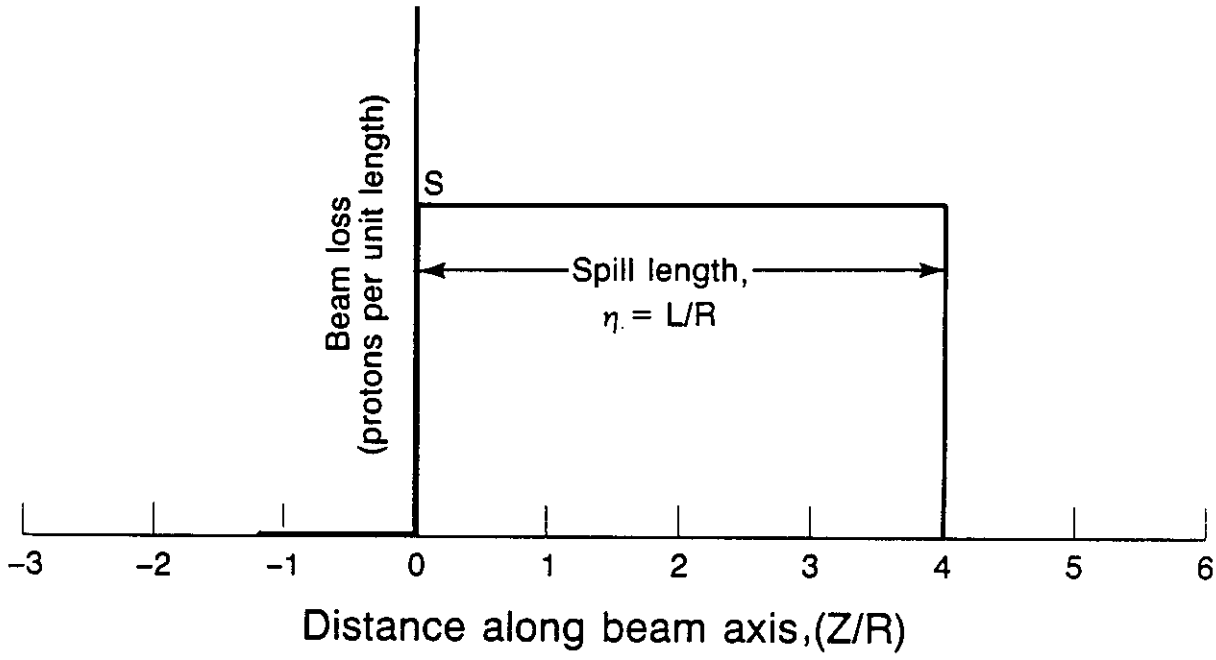

XBL 853-8042

A4.8

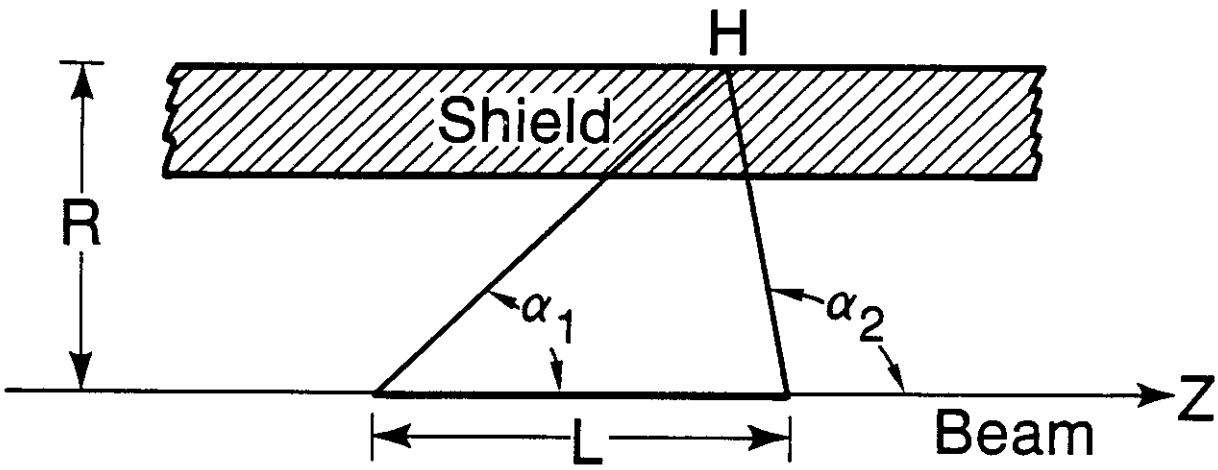

Finite uniform line source

XBL 8411-6355

A4.9

A4.9

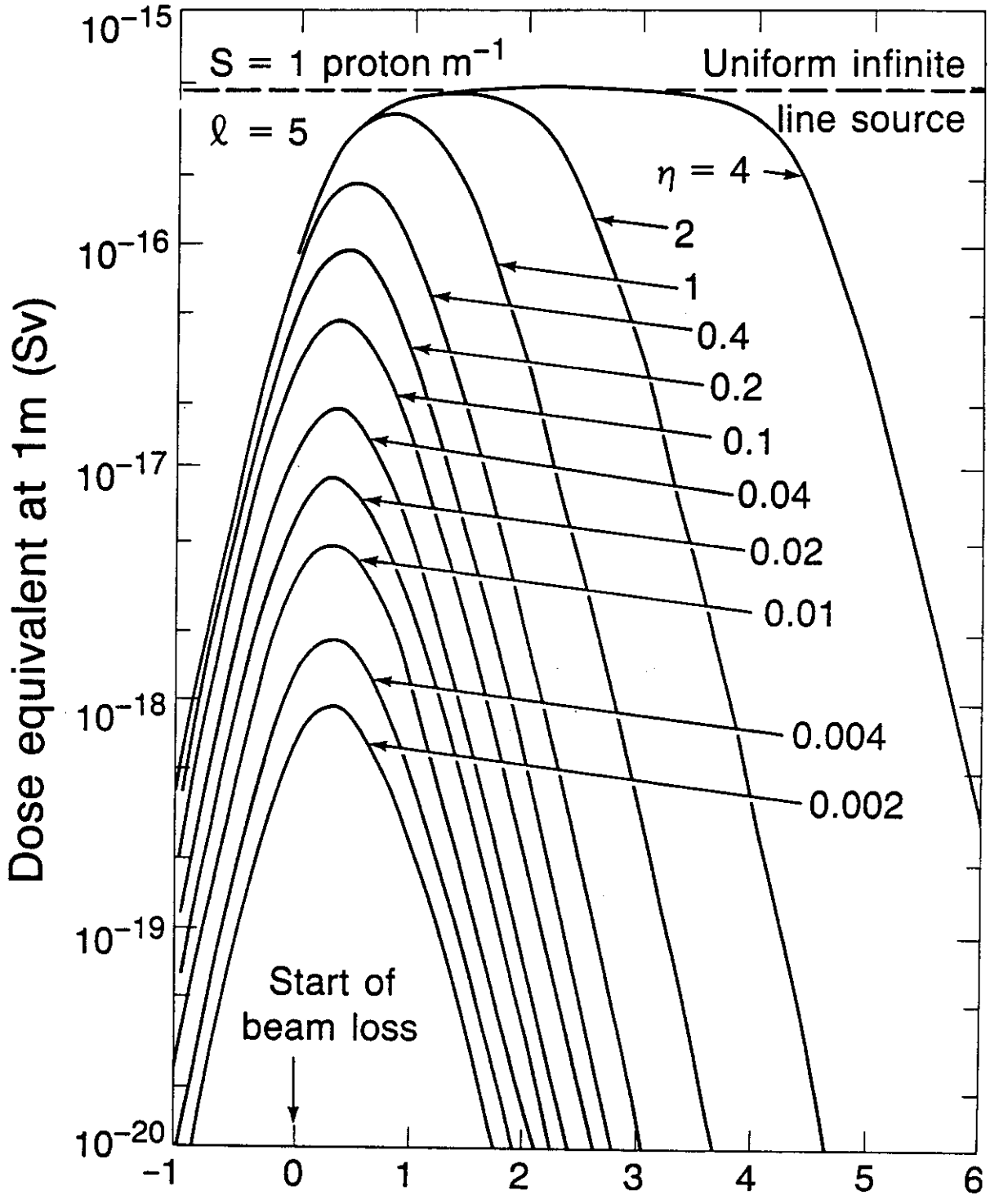

A4.10

XBL 8411-6342

A4.10 4.10

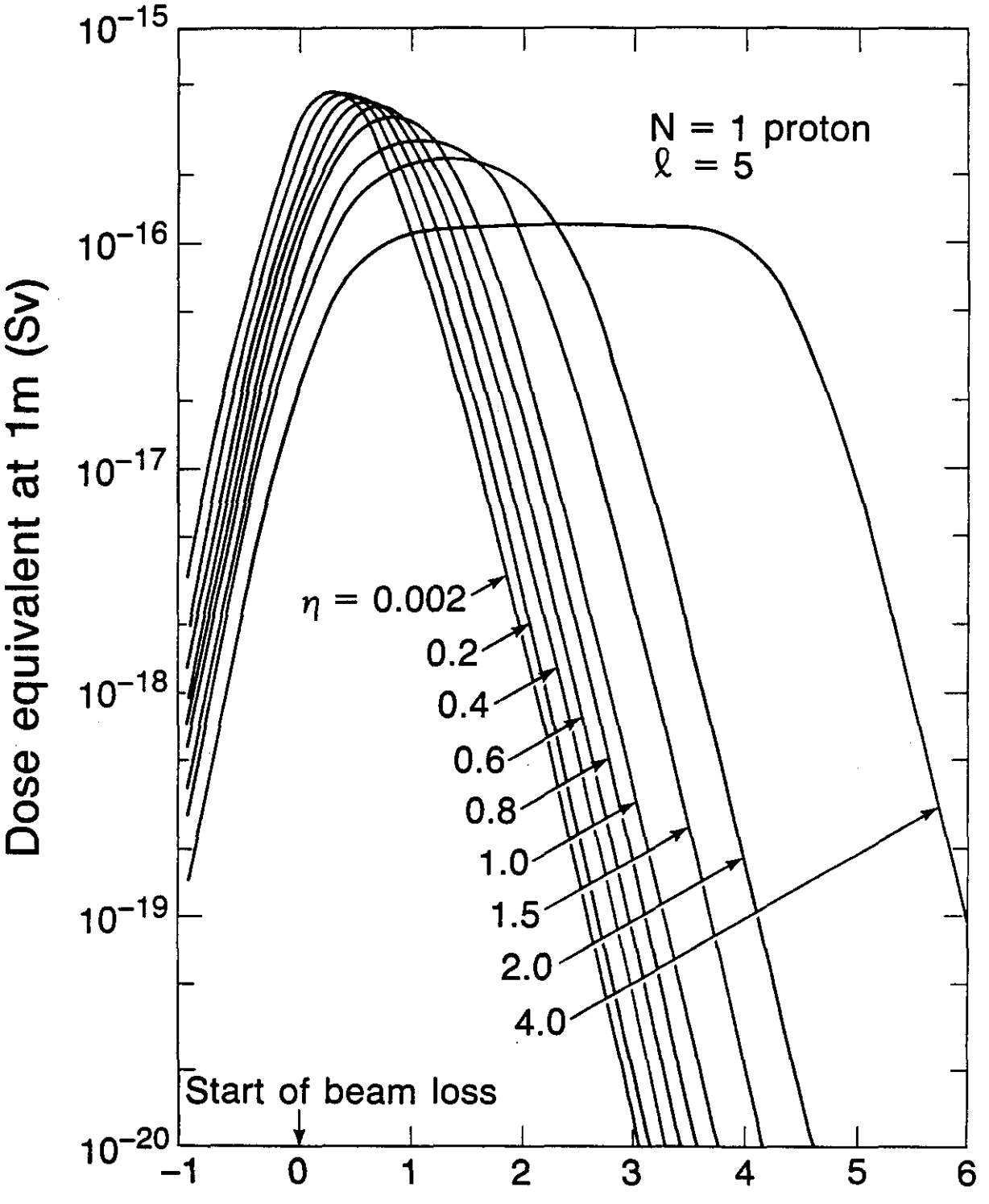

A4.11

XBL 8411-6345

A4.11

4.11

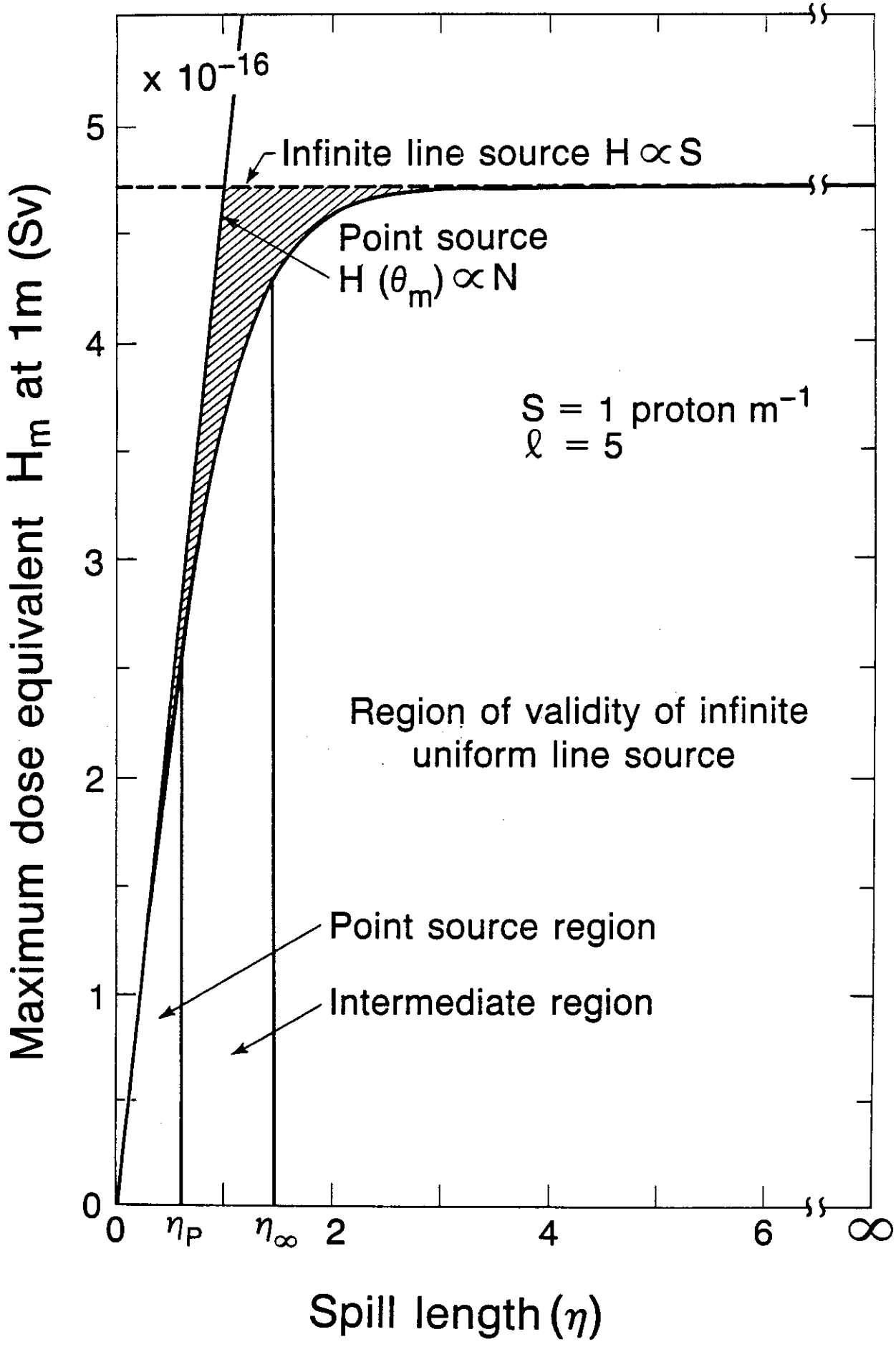

A4.12

XBL 8411-6358

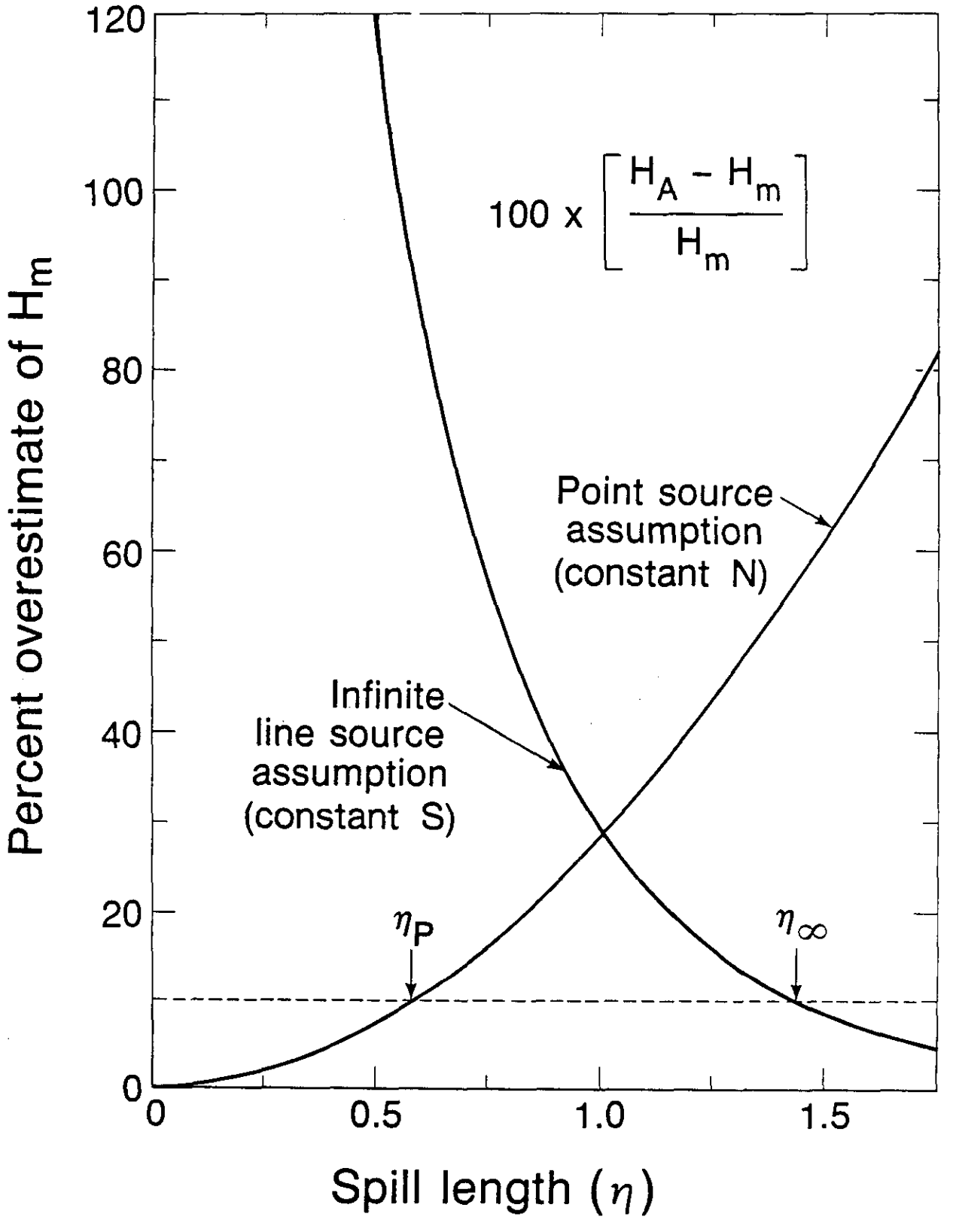

XBL 8411-6357

A4.13

A4.13

4.13

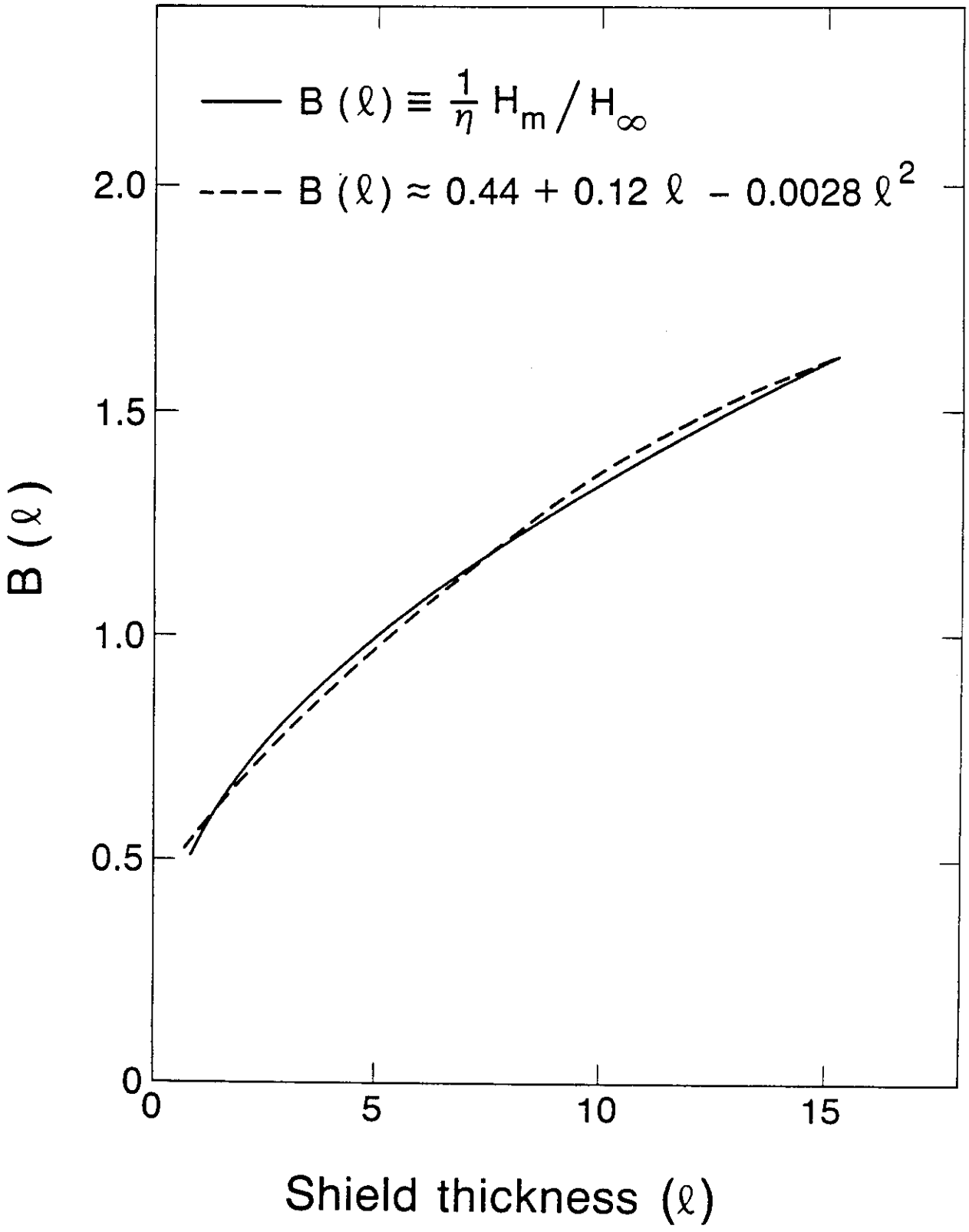

XBL 8411-6353

A4.14

A4.14

Chapter 5
Accelerator Radiation Safety Programme

'For forms of government let fools contest;

Whatever is best administered is best'.

from 'An Essay on Man'

Alexander Pope (1688-1762)

CHAPTER 5 CONTENTS

5.1 Introduction

5.2 Safety Organization
- Line Organization
- Professional Safety Department
- Health and Safety Committee

5.3 The Health and Safety Programme
- Health and Safety Policy
- Safety at Industrial and Research Installations
  - Extract from Technical Report No. 188

5.4 The Radiation Safety Programme
- Radiation Safety Committee
- Radiation Safety Officer
- Radiation Protection Group
- Qualified Expert
- A Sample Radiation Safety Programme

5.5 The Accelerator Radiation Safety Programme

References for Chapter 5

Figure Captions for Chapter 5

Appendix 5.1. Employee Rights and Obligations.

Example: Lawrence Berkeley Laboratory

Appendix 5.2. The Functions and Organization of a Laboratory Safety Committee.

Example: Lawrence Berkeley Laboratory

Appendix 5.3. Statement of Health and Safety Policy.

Example: Lawrence Berkeley Laboratory

5. ACCELERATOR RADIATION SAFETY PROGRAMME

5.1. INTRODUCTION

As we have seen from the examples of typical accelerator facilities given in Chapter 1 there is a great diversity among accelerator institutions and each radiation safety programme must be designed to facilitate the safe and effective operation of accelerators according to the needs of the operating institution. Although there is no standard organization suitable for all institutions, experience suggests some general principles that should be considered in establishing an accelerator radiation safety programme. These general principles will be discussed in this chapter.

There have been profound changes over the past twenty-five years in general attitudes to health and safety in the work place. It is increasingly recognized that we all have a right to a safe and healthy working environment. This realization has led in many countries to the enactment of legislation that specifies both the rights and obligations of individual workers.

For example in the United States of America the passage of the Williams and Steiger Occupational Safety and Health Act in 1970 requires that employees be informed of their rights under this legislation. Appendix 5.1 shows how this requirement is implemented at the Lawrence Berkeley Laboratory of the University of California, which is regulated by the Department of Energy, a Department of the government of the United States of America.

It is most important to recognize that an accelerator radiation safety programme should not be developed in isolation from the institution's health physics programme or indeed from its own overall health and safety programme. On the contrary, a good accelerator radiation safety programme is integrated with all the disciplines involved in a comprehensive safety programme.

This integration of safety disciplines into a comprehensive programme is especially necessary at accelerator laboratories because some desirable aspects of the radiological safety programme may conflict with other safety needs. Seldom, if ever, are safety requirements absolute. The success of an occupational safety and health programme will depend upon the successes of the compromises it can make between conflicting requirements and the balance it makes among them, keeping in mind that the overall goals are the protection of human life, prevention of injuries and the minimization of property damage.

Three typical examples of such conflicts in safety requirements at accelerator laboratories are given below:

- At physics research laboratories explosive gas mixtures are used in some thin-walled particle detectors. The room in which such detectors are used may require special ventilation, but it may not be possible to release the air from this room

during accelerator operation because of its radioactivity.

- Escape routes from an accelerator vault should ideally be sufficiently wide and straight to permit the removal of injured persons without undue difficulty: this is in direct conflict with good maze design for minimum photon and neutron leakage.
- Good access control to a radioactive accelerator vault requires only one entry; while emergency escape from the vault requires many exits.

A comprehensive occupational health and safety programme must ensure that no unsafe compromises are made.

This chapter will briefly discuss the occupational safety and health organization; the safety programme and its relation to the radiation safety programme; and, finally, give a specific example of an occupational health programme suitable for a large multi-disciplinary research institution (national laboratory) utilizing ionising radiations, including those produced by several types of particle accelerators.

5.2. SAFETY ORGANIZATION

The responsibility for the safe operation of accelerator facilities, for the protection of personnel, the public and the environment rests with management. Experience shows that an efficient safety organization has three branches (see Fig. 5.1):

(i) The normal line organization

(ii) A professional occupational health and safety department

(iii) A health and safety committee

Line Organization

The normal line organization is responsible, by delegation from the director*, for the detailed implementation of safety policy and procedure. To every level of management is delegated authority commensurate with the responsibilities for safety assigned to them. In this respect, safety is treated no differently from other functions of the organization. Every member of management is responsible for ensuring that employees under their supervision are provided a safe and healthy working environment, free from undue hazards. Supervisors at all levels should aggressively promote the safety programme of their organization. It is incumbent on those in charge of departments or groups to ensure that their work areas are safe and that all operations under their care are performed safely. The responsibility for safe working conditions extends downwards to all employees. It should be a condition of employment or participation that employees are familiar with and implement the organization's health and safety policy.

*In what follows the word 'director' is used to describe the head of the organization operating particle accelerators. Readers will be able to substitute the appropriate description in their own particular case.

Professional Occupational Health and Safety Department

The size of the occupational health and safety department must depend upon the size of the accelerator facility and the resources available, but typically the total number of personnel involved may be about 2% to 3% of the total complement of permanent staff and visitors. In the smallest organizations, the occupational health and safety department may consist of only one member of the staff who devotes part of his or her time to health and safety matters; alternatively the organization may engage the part-time services of a consultant. At larger research laboratories, the total personnel involved with health and safety may exceed 100. Of this total, some 25 will be professionals with varied training in the physical and biological sciences, engineering and the healing arts. The exact composition of the professional staffing of the occupational health and safety department must clearly depend upon the nature of work performed. Advice may be obtained from standard texts on safety (Ch 81, NSC 78, PE 75, PE 78, St 76; see also the bibliography in Chapter 7). At a minimum, all organizations that operate particle accelerators should obtain the services of what the American National Standards Institute describes as a 'qualified expert' during the early planning stage or installation phase of any new particle accelerator (ANSI 70).

Health and Safety Committee

A health and safety committee should be appointed by the director (or equivalent) to advise top management on all aspects of health and safety practice and policy. Its terms of reference should be clearly specified and include monitoring the safety performance of the line organization and of the professional safety group. As an example of the scope of such a committee, Appendix 5.2 gives the charter for the Safety Review Committee of the Lawrence Berkeley Laboratory (LBL 80a). The policy statement of other research institutions will, of course, reflect their own functions and needs.

Membership of the safety committee should be determined on the basis of scientific activity, balance of technical knowledge and expertise in safety matters. Membership may be made up of two types of persons-first, professional health and safety experts (e.g., health physicist, industrial hygienist, fire-protection officer, physician, safety engineer, etc.) and second, responsible members of the line organization. Particularly in research laboratories, participation by active experimental scientists is most important because, in some cases, no applicable safety codes may exist for research operations or equipment. Without such a diverse composition of the health and safety committee, it would be extremely difficult to operate an efficient health and safety programme at a research institution.

Appendix 5.2 gives an example of the function and organization of the safety ommittee of a large national laboratory. Several important points should be made about this committee. It is:

- Appointed by top management
- Advisory

- Balanced in membership (scientists, safety experts, administrators)

Such a system of peer review has been found to work well at the Lawrence Berkeley Laboratory of the University of California (LBL), a multidisciplinary national laboratory.

At large institutions the review of safety policies and practice can be an extremely large task. There may be important economic, political, or institutional issues related to health and safety matters, so that it may be necessary to separate the review of day-to-day safety practice from the fundamental consideration of safety policy, forming two distinct but evidently linked committees. On the other hand, smaller institutions may require a single, small committee consisting of the director, the accelerator operator and the qualified expert. However, what ever the different needs and preferences, the same general principles outlined in this section apply.

5.3. THE HEALTH AND SAFETY PROGRAMME

Analysis of health and safety programmes in a wide variety of facilities shows that seven basic elements are necessary for satisfactory safety performance:

- Management leadership
- Assignment of responsibilities
- Maintenance of safe working conditions
- Safety training
- Accident recording and investigation system
- Professional health and safety staff
- Acceptance of personal responsibility

Health and Safety Policy

The responsibility for the specification, provision and enforcement of a safe working environment rests with management. Management in turn may delegate authority and assign responsibility for the implementation of the safety policies and programme but retains accountability for oversights and errors that lead to injury, illness or damage to property.

Management leadership begins with a clear statement of policy. Such a statement should be issued by top management and contain the following elements:

- Concise statement of health and safety policy.
- Acceptance of primary responsibility by top management and a statement or the source of their authority.
- Delegation of health and safety responsibilities to middle management, the health and safety staff, and all employees.
- Statement of health and safety performance required of all employees.
- Description of the safety resources and organization.

Appendix 5.3 gives as an example, the health and safety policy statement of the Lawrence Berkeley Laboratory, which includes all the elements listed above (LBL 82). The policy statements of other research institutions will, of course, reflect their own function and needs.

Safety at Industrial and Research Installations

Details of the requirements of health and safety programmes may be found in the copious literature available. Only a few references can be given here (see also the bibliography in Chapter 7).

In the United States, general safety standards have been codified under the Occupational Safety and Health Act (OSHA) of 1970 (OSH 83). Similar regulations exist for other countries.

Occupational medicine is addressed in standard texts (Hu 80, La 80, La 81, Sc 82 Ze 75, Ze 80). Electrical safety is discussed in the

National Safety Council Accident Prevention Manual (NSC 74) and the Laboratory Safety Handbook (St 76). Industrial hygiene is dealt with in the standard texts by Patty (Pa 79, Pa 81a, Pa 81b, Pa 82) and those issued by the National Institute of Occupational Safety and Health and the National Safety Council (NIOSH 78, NSC 79) and in the bibliography of Chapter 7. Toxicology and the dangers of hazardous materials are discussed in Cassarett and Doull (Do 80), Sax (Sa 75), the Laboratory Safety Handbook (St 76), monographs published by the U.S. National Academy of Sciences (NAS 81, NAS 83) and other standard texts (An 81, Pr 78). In the United States, fire protection is dealt with in publications of the National Fire Protection Association (NFPA nd); it is also discussed in the Accident Prevention Manual of the National Safety Council (NSC 78). For the special problems in fire fighting at installations where radioactive materials are used the monograph by Purington and Patterson (Pu 77) should be consulted.

The safety programme should be developed in accordance with local and national regulations, but the advice of national advisory bodies (such as, for example, the National Council on Radiation Protection and Measurements in the USA) and international organizations such as the ICRP, ICRU, and IAEA should also be carefully considered. (See Chapter 7, General Bibliography).

As a general example the Occupational Health Programme of the Lawrence Berkeley Laboratory (LBL) will be briefly described. This programme is specified in a safety manual (LBL 80b), the table of contents of which is given below so that the reader can visualize how the components of the safety programme fit together. Other institutions will make variations appropriate to their own functions.

Health and Safety Manual of the Lawrence Berkeley Laboratory

University of California

Table of Contents

Preface x
Acknowledgements x
Emergency Actions x
Chapters:
1 General Policies and Administration x
2 The Environmental Health and Safety Department x
3 The Medical Services Department x
4 Biological Hazards x
5 Chemical Safety x
6 Confined Space Entry x
7 Cryogenic Safety x
8 Electrical Safety x
9 Emergency Plans x
10 Engineering and Construction x
11 Excavations, Trenching, and Shoring x
12 Fire Safety x
13 Gases, Flammable and Compressed x
14 Guarding, Mechanical x
15 Ladders, Scaffolds, Work Surfaces, and Elevated Work Stations x
16 Laser Safety x
17 Materials Handling and Storage x
18 Noise x
19 Personal Protective Equipment x
20 Pressure Safety x
21 Radiation Safety, Ionizing and Non-ionizing x
22 Sanitation x
23 Seismic Safety x
24 Training, Environmental Health and Safety x
25 Tools, Power and Hand Operated x
26 Traffic and Transportation x
27 Warning Signs and Devices x
28 Miscellaneous x
29 Boating and Diving x

In IAEA Technical Report No. 188, Radiological Safety Aspects of the Operation of Electron Linear Accelerators, Swanson has given a good brief summary of safety problems at industrial and research installations; this discussion is reproduced below, for the convenience of the reader (IAEA 79).

Extract from Technical Report No. 188

Safety at Industrial and Research Installation

The following safety areas are particularly relevant to industrial and research facilities. The suggestions given may be developed to meet the particular needs of the installation.

Emergencies. Notices of emergency procedures should be conspicuously posted. Emergency telephone numbers should be posted at every telephone (fire, emergency paramedical services, ambulance). Periodic instruction should be given in emergency procedures, including resuscitation techniques.

Electrical Safety. Because of the variety of unusual circuitry found at research facilities, electrical safety should be given very careful attention. A fundamental aspect of electrical safety is the thorough training of personnel in the operation and safety provisions of thee equipment used. All pertinent electrical codes should be well understood by responsible personnel and every attempt made to ensure compliance with them. The physical planning should allow convenient access to electrical equipment the is to be installed in dry, well-lighted locations. The provisions for enclosure, interlocking and grounding of circuits should be adequate. A grounding hook or preferably an automatic mechanical discharging device should be provided for high-voltage power supplies and particularly for capacitor banks. Only connectors approved by the safety organization should be installed, and they should be maintained in good repair at all times. Metal ladders should not be used for electrical work. The equipment should be turned off in an obvious and positive manner before working on it. (This is best accomplished by means of multiple padlocks, one for each person who wishes to lock out the circuit.) Work on energized high-voltage circuits should be undertaken only as a last resort and then only by persons having complete understanding of the equipment, and with cognizance of the responsible authorities. In such cases a standby person is essential.

Fire and Explosion. Fire protection should be planned in terms of prevention, provision for prompt detection and containment. Unnecessary sources of ignition should be eliminated and unnecessary combustible loading should be removed. Flammable substances such as solvents, oils, acetylene, propane and hydrogen should be carefully stored, handled and properly disposed of. Cabling is susceptible to fire and is particularly capable of propagating an existing fire. A smoke detector and automatic

sprinkler system is advisable for most areas. Adequate fire extinguishers should be maintained and conveniently available. Adequate means of egress should be provided, particularly for the accelerator and target room(s).

Hydrogen. Liquid hydrogen is frequently used in experiments in nuclear and elementary particle physics. The precautions should include a committee review of each new experiment using hydrogen, ventilation to prevent dangerous accumulations, grounding to prevent electrostatic built-up, sealed wiring and switches, enclosure of necessary nearby electrical equipment in inert atmosphere at positive pressure, elimination of other sources of ignition, mechanical protection of thin target windows, and access control. Although emphasis must be placed on prevention, consideration must also be given to provisions for damage limiting, such as walls or partitions that are swung open by excess pressure. Electrical equipment used in the area should be of a type approved by national or regional authorities for the particular class of hazard.

Gas cylinders should be properly labelled, carefully handled, stored upright and secured to prevent overturning. Proper regulators and other fixtures should be used.

Hazardous Materials. A variety of unusual materials may be used at large research institutions. They should be properly labelled, using words such as CAUTION, WARNING, DANGER, POISON, together with a brief explanation of the hazard (such as 'do not machine', etc.), as appropriate. An inventory should be kept of dangerous materials and they should be locked up until released to responsible persons for use. Among the materials sometimes found in laboratories are mercury, beryllium metal, lithium hydride, asbestos, polychlorinated byphenyls (PCBs), epoxy resins, acids, caustic fluids, ether and solvents. Where volatile materials are used, adequate ventilation should be available. Where acids, caustics or strong chemicals are used, emergency eye wash facilities and showers are advisable.

Solvents. Protection against harmful solvent should include breathing protection (ventilation, complete enclosure or respirators) and skin protection (avoidance, gloves or creams), in addition to precautions against fire. Extremely toxic solvents (e.g., carbon tetrachloride and carbon disulphide) should not be used.

Microwaves. Where microwave components, including klystrons, magnetrons, RF separators, RF cavities and connecting waveguides, are operating in accessible areas, there is a possibility of exposure to unsafe microwave intensities from openings in the system. Operating systems should remain entirely shielded and flanges and joints examined for integrity. An instrument, preferably one that does not distort the field appreciably, should be available to ensure that microwave intensities

at frequencies between 10 MHz and 100 GHz do not exceed 10 mW cm^{-2} when averaged over any possible 0.1-hour period (there may be other limitations imposed by government authorities).

Rigging and Handling of Heavy Objects. The handling of shielding blocks, large objects to be radiographed, and accelerator and beam-transport equipment gives rise to chance of accidents. Crane and forklift operators should be properly trained and provided with adequate equipment.

Magnetic Fields. Magnets should bear a warning sign and, when energized, be marked by a flashing light. There should be positive means of ensuring that they are off for personnel working nearby. There is a risk that tools and other ferrous objects may be pulled into magnetic fields, causing injury or damage. Personnel should not be permitted to enter areas where their bodies are immersed in high magnetic fields, such as between the pole faces or in fringing fields of large magnets.

Noxious Gases. Ozone and oxides of nitrogen formed in the air by radiation should be assessed. If necessary, steps should be taken to mitigate this health hazard.

Noise. In rooms containing large motor-generators, compressors or boilers the limits of noise levels allowed by local standards may be exceeded. When engineering or administrative controls cannot bring the exposure of personnel down to the levels allowed, hearing protectors should be worn.

Vacuum Safety. A special hazard is presented by large vacuum systems with thin windows such as, for example, the long, large-diameter pipes used in neutron time-of-light facilities. The rupture of a window can result in a serious, even fatal, accident to a nearby person. There is danger of objects or persons being drawn into a system through a large window, and some possibility of ear damage, even with a small window, if the vacuum system is large enough. When the system is not in use, thin windows to large vacuum systems should be protected by temporary covers capable of withstanding atmospheric pressure. Alternatively, a gate valve near each end of a large vacuum pipe should be provided which can be closed to isolate the largest volume. Warning signs at the window should be used to alert personnel to this peculiar hazard and remind them to implement these protective measures. Unessential occupancy of the vicinity should be discourage.

Radiation Doors. The heavy, motor-operated doors that are used at many research facilities should be designed to permit safe operation. The operating switch should be designed such that continual manual activation is required for motion of the door to continue. A warning bell should sound while the door is in motion. Limit switches should prevent motion beyond the proper range, and the closing edge should be equipped with a

pressure-sensitive safety plate which will disconnect power if a person or object is caught. Each door should also be capable of manual operation in case of power failure.

General provisions for safety should also include the provision and maintenance of emergency lighting and power, ventilation systems, respirators, emergency showers and eye wash facilities, self-contained breathing apparatus, air sampling equipment, safety glasses and safety shoes. Proper walking surfaces should be provided and liquid spills should be cleaned up promptly. Care should be exercised when climbing ladders and on equipment. Neatness, cleanliness, and, order provide an environment conducive to good safety habits.

Figure 5.2 shows a suggested organization chart for an occupational health and safety programme at a large research laboratory. One extremely important function that should be included is an internal, independent audit office that monitors compliance with applicable legislation and regulations. This internal audit function should be provided in addition to the institutional audit function which reports to the Director of the laboratory (provided by the health and safety committee shown in Fig. 5.1)

5.4. THE RADIATION SAFETY PROGRAMME

The radiological safety programme is properly one part of a comprehensive occupational health programme. The emphasis given to each of the separate disciplines will depend upon the operations and functions fo the particular laboratory or institution.

The basic elements of a radiation protection programme are

a) The definition of exclusion areas, high-radiation areas, controlled areas and noncontrolled areas.

b) The categorisation of personnel into professionally exposed and nonradiation worker groups.

c) The provision of an area- and personnel-monitoring programme.

Element a) defines the requirements for shielding and other barriers designed to prevent access to areas where sometimes lethal doses could be received in a matter of minutes. It also defines the need for locked and/or interlocked doors to control access to these areas. This is particularly important at accelerator laboratories where in order to allow the accelerator to be switched on there must be mechanisms to ensure that all doors are closed, all movable shielding and barriers are in place and that no person is present inside the exclusion area. Administrative procedures play an important role in this process. The machine elements that must be 'made safe' in order that access to the exclusion area is possible must also be determined and signals from these linked correctly into the access authorization procedure.

The requirements of element b) are administrative in character and require compliance with national and local regulations.

Element c) takes on particular importance at accelerator laboratories where it depends on the shielding philosophy adopted in the design of the accelerator. The requirements for monitoring could be minimal if the accelerator is so heavily shielded and the configuration so stable that any dose rates in accessible areas are insignificant. On the other hand, radiation monitors could be part of an interlock chain to prevent the escape of beams into occupied areas, and personal monitors could be necessary to prove that small excursions in dose rate due to unwanted operation have not given rise to unacceptable exposures. More usually the monitoring programme is an economic and operational balance between these two extremes.

In organizing the radiological safety programme the NCPR Report 59 entitled 'Occupational Radiation Safety Programme' will be found to be extremely helpful (NCRP 78).

Any organization using ionising radiations should form a radiation safety committee and appoint a radiation safety officer. The advice of qualified experts should be obtained as needed.

Radiation Safety Committee

All organizations that use ionising radiations should form a committee dealing with radiation safety. If the institution is large enough, the committee may be devoted solely to matters concerning

radiation safety; alternatively, radiation safety may be one of the concerns of a general safety committee (see Section 5.2). The functions of the radiation safety committee should include:

- Advising management on radiation safety policy and procedures.
- Monitoring radiation safety performance.
- Reviewing unusual procedures or operations and requests for variances from established policies.

It is imperative that members of the radiation safety committee keep themselves informed of the recommendations of advisory organizations and of the appropriate legal requirements for radiation safety.

Radiation Safety Officer

A radiation safety officer (RSO) should be appointed. In a large organization this would normally be the head of the operational health physics group. In a small organization the duties of the RSO may not require full-time attention and may undertaken on a part-time basis. The qualifications of the RSO will depend upon the operations of the institution but should include a thorough understanding of both technical operations and radiation protection.

Radiation Protection Group

The size and composition of the radiation protection group will clearly depend upon the nature of the work being carried out, the size of the institution and the technical complexity of its operations. At a minimum, all organizations that operate particle accelerators should obtain the services of a qualified expert as defined below. Figure 5.3 shows a suggested organization chart for the radiological protection group in an organization using particle accelerators.

Qualified Expert

The definition of a qualified expert in radiation protection is necessarily imprecise because such people come from a variety of backgrounds and experience. The American National Standards Institute defines a qualified expert as:

> 'A person having the knowledge and training to measure ionizing radiation, to evaluate safety techniques, and to provide advice on radiation protection needs'.

Such persons generally will have studied the physical or biological sciences at the baccalaureate level and often will have some postgraduate experience in nuclear physics, radiobiology or perhaps occupational health or industrial hygiene. In addition to the experience required for a health physicist, it is essential that a qualified expert in accelerator health physics have several years experience in the design and operation of particle accelerators.

Several countries have systems for the registration of those personnel that have relevant qualifications and experience in the radiological sciences. In the United States, there are three national boards

that register professionals in the radiological sciences- the American Board of Health Physics, the American Board of Industrial Hygiene and the American Board of Radiology (ABHP 80). In addition many states - for example the State of California,-also register engineers qualified in safety disciplines, including health physics. The detailed requirements for such registration are continually changing and the interested reader should make direct contact with the organization of interest for current information.

A Sample Radiation Safety Programme

As a sample radiation safety programme, we here reproduce the Ionizing and Non-Ionizing Radiation Safety chapter of the Lawrence Berkeley Laboratory Health and Safety Manual (LBL 80b). A few modifications have been made to clarify its meaning and usefulness for the reader who will be using it only as an example.

There is, of course, no unique way of organizing a radiation safety programme and the interested reader should study several typical accelerator radiation safety programmes. (See the section on Accelerator Radiation Safety Manuals in the Bibliography - Chapter 7.)

The Radiation Safety Program of the Lawrence Berkeley Laboratory is, as we have already seen, is one component of a complete Occupational Health Program described in its Health and Safety Manual (LBL 80b). Chapter 21 of this manual sets forth the Ionizing and Non-ionizing Radiation Safety Program and is given below as an example for the reader.

Health and Safety Manual, Lawrence Berkeley Laboratory

University of California

Ionizing and Non-Ionizing Radiation Safety

CONTENTS

I. IONIZING RADIATION

A. BASIC POLICY x

B. PROTECTION GUIDES FOR IONIZING RADIATION x

B.1. General x

B.2. Protection guides for internal radiation x

B.3. Protection guides for off-site environment x

B.4. Employees under 18 years of age x

B.5. Women employees x

B.6. Nonemployees x

C. PERSONAL RADIATION MONITORING x

C.1. General x

C.2. External radiation exposure x

C.3. Internal radiation exposure x

D. MONITORING OF THE WORKING ENVIRONMENT x

D.1. On-site monitoring x

D.2. Off-site monitoring x

D.3. Portable radiation detecting instruments x

D.4. Protective equipment x

E. EXPOSURE TO RADIATION IN AN EMERGENCY x

F. ACCELERATOR HEALTH PHYSICS x

G. RADIOACTIVE MATERIALS x

G.1. General x

G.2. Training in radioisotope safety procedures x

G.3. Engineering controls x

G.4. Proper preparation of radioactive waste x

G.5. Radioactive waste disposal x

G.6. Transportation and shipment of radioactive material x

G.7. Storage of radioactive materials x

G.8. Decontamination of radioactive equipment x

G.9. Contaminated precious metals x

G.10. Monitoring and movement of materials x

G.11. Radioactive sources x

H. EMERGENCY PROCEDURES FOR RADIOACTIVE SPILLS x

I. X-RAY SAFETY x

I.1. Introduction x

I.2. Scope x

I.3. Definitions x

I.4. Responsibility x

I.5. Warning x

I.6. Procedures x

I.7. Interlocks and indicators x

I.8. Posting x

I.9. Records x

I.10. Property management x

I.11. Personnel monitoring x

I.12. Radiation safety surveys x

I.13. Routine safety maintenance x

I.14. Modifications x

I.15. User training x

I.16. Use control x

I.17. Instrumentation x

I.18. Shielding x

I.19. New installations x

I.20. Notification of suspected accidents or injuries x

I.21. Standards and recommendations x

I.22. Unusual occurrence review critique x

I.23. Safety systems analysis x

I.24. X-ray machine-type classification x

I.25. Variances x

II. NON-IONIZING RADIATION x

A. ULTRAVIOLET x

B. MICROWAVES x

B.1. General x

B.2. Microwave ovens x

C. MAGNETIC FIELDS x

APPENDIX. RADIOISOTOPE PROCEDURES x

I. IONIZING RADIATION

A. Basic Policy

All Laboratory operations must be planned to prevent exposure of personnel to ionizing radiation in excess of the limits stated in the following Standards for Radiation Protection: Department of Energy Order DOE 5480.1 Chapter XI (DOE nd) and Occupational Safety and Health Standards 29 CFR 1910.96 (OSHA 83). These documents give radiation dose equivalent limits for both radiation workers and nonradiation workers.

In addition to these basic regulations, it is also Laboratory policy that exposure to ionizing radiation associated with Laboratory operations be as low as is reasonably achievable. This policy means that, subject to programmatic requirements and economic limitations, radiation dose equivalents to employees and radiation levels at the perimeter fence should be the minimum attainable. Implementation of this policy requires that each operation involving the use of radioactive material or the production of radiation be evaluated individually to ensure that the associated personnel exposures are as low as is reasonably achievable.

For external radiation, protection is provided by time and distance restrictions source intensity (beam current limitations for accelerators) and adequate shielding. For internal radiation, protection is normally provided by preventing the escape of radioactive material into the working environment. Work with radionuclides must be restricted to certain locations that are designed specifically for such work. Furthermore, persons under 18 years of age are restricted from working in certain areas. (See section entitled 'Employees under 18 years of age')

B. Protection Guides for Ionizing Radiation

B.1. General

The protection guides for the control of external and internal dose equivalents are based on the standards listed in the DOE 5480.1 Ch XI and are shown in Table 5.1a.* Supervisors are primarily responsible for assuring that employee's exposures to ionizing radiation are kept as low as is reasonably achievable and within the standards shown in the table. Assistance in that regard is available from the Environmental Health and Safety Department.

It is recommended that whole body dose equivalent increments in excess of 150 mrem over a short period of time be avoided. Consult with EH&S Dept. personnel when it appears likely that certain procedures can lead to a dose equivalent accumulation in excess of 150 mrem in a single exposure or in a series of exposures encompassing only a few days.

B.2. Protection Guides for Internal Radiation

---

*At the time of writing the US Department of Energy had not fully adopted the International System of Units or the recommendations of ICRP Publication 26 (ICRP 77). Discussions were underway to prepare for their adoption in the future.

The protection guides for the control of internal dose equivalents at LBL are based on the Concentration Guides (CG's) of radionuclides in air and water above natural background listed in DOE Order 5480-1, Ch. XI Attachment 1, Table 1. The maximum permissible body burdens (MPBB's) are published in the National Bureau of Standards Handbook No. 69. (NBS 63). These documents are available from the Environmental Health and Safety Department.

Table 5.1
Individuals in Controlled Areas: Radiation Protection Standards for External and Internal Exposures

Type of Exposure	Exposure Period	Dose Equivalent (Dose or Dose Commitment[a] (rem))
Whole body, head and trunk, gonads, lens of the eye[b], red bone marrow, active blood forming organs	Year	5[c]
	Calendar Quarter	3
Unlimited areas of the skin (except hands and forearms). Other organs, tissues, and organ systems (except bone)	Year	15
	Calendar Quarter	5
Bone	Year	30
	Calendar Quarter	10
Forearms[d]	Year	30
	Calendar Quarter	10
Hands[d] and feet	Year	75
	Calendar Quarter	25

[a]To meet the above dose commitment standards, operations must be conducted in such a manner that it would be unlikely that an individual would assimilate in a critical organ, by inhalation, ingestion, or absorption, a quantity of a radionuclide(s) that would commit the individual to an organ dose which exceeds the limit specified in the above table.

[b]A beta exposure below a maximum energy of 700 keV will not penetrate the lens of the eye; therefore, the applicable limit for these energies would be that for the skin (15 rem/year).

[c]In special cases with the approval of EP-30, a worker may exceed 5 rem/year provided his/her average exposure per year since age 18 will exceed 5 rem per year. This does not apply to emergency situations.

[d]All reasonable effort shall be made to keep exposures of forearms and hands to the general limit for the skin.

The concentration guides were established at levels that present knowledge indicates will not result in significant injury after continual exposure at that level for many years. Nevertheless, personnel must not be exposed for extended periods at the limit values while reasonable avenues exist for avoiding such exposure.

When the concentration guide value (which is based on continuous exposure at 40 hours per week) is exceeded, the exposure time must be limited so that the total intake during a calendar quarter does not exceed the intake permitted. If external radiation is present, the permissible internal concentration values must be reduced to bring the whole body or a particular organ to the total dose within the basic dose limits.

The control of airborne radioactivity below CG's often involves sophisticated enclosure systems and careful experimental planning. Failure of a control system for an experiment involving a large amount of radioactivity could result in exceeding the CG's both on and off-site. Therefore, it is mandatory that operations involving large quantities of unencapsulated radioactive material be planned with EH&S Dept. assistance.

Protection Guides for Off-Site Environment

The off-site protection guide for external and internal radiation as established by DOE Order 5480.1 Ch. XI is that no person outside the fence receives a whole body dose equivalent exceeding 0.5 rem in year.

The specific protection guide values to be used at the Lawrence Berkeley Laboratory for concentrations of radionuclides in air and water are to be those stated in DOE Order 5480.1, Ch. XI, Attachment 1, Table II (with the exception of discharge to the sanitary sewer). In the case of releases to sanitary sewers, the concentration values are to be those stated in DOE Order 5480.1, Ch XI, Attachment 1, Table I.

The Laboratory policy regarding off-site radiation and radioactivity is that the levels be reduced to the lowest reasonably achievable amounts within the DOE guidelines consistent with economic and programmatic considerations.

B.4. Employees Under 18 Years of Age

Employees under 18 years old must be limited to a total body dose equivalent of 0.5 rem in any calendar year and a dose equivalent no greater than 0.3 rem in any calendar quarter.

The following guidelines are to be followed for all employees and participating guests under age 18 who work in radiation areas.

- Each case is to be handled individually.
- The programme for each person is to be outlined in writing with a listing of the proposed work areas and time schedule.
- A supervisor for each person is to be designated.
- Access to the proposed work area must be evaluated by the EH&S Dept. personnel for possible radiation hazards or exposures above background. In general, persons under 18 years of age are restricted from working in certain buildings and areas, such as accelerators, areas adjacent to accelerators, parts of buildings that contain large quantities of radioisotopes, and machines producing ionizing radiation. At the present time the following buildings are in this category:

[HERE FOLLOWS A LIST OF BUILDINGS AND AREAS IN WHICH PERSONS UNDER THE AGE OF 18 MAY NOT WORK.]

NOTE: this list is correct as of the date of publication of this page; it is updated whenever conditions change. Consult the EH&S Dept. for current status.

- All new employees or participating guests must attend the safety orientation sessions presented by the EH&S Dept.

B.5. Women Employees and Pregnancy

The National Council on Radiation Protection in their Report No. 53 (NCRP 77a, see also NCRP 77b) has recommended that during the entire gestation period, the maximum permissible dose equivalent to the embryo-fetus from occupational exposure of the expectant mother should be 0.5 rem. It is Laboratory policy that fertile women who work in radiation areas, as well as their supervisors, should be aware of this recommendation and the reasons for it. As in all cases, occupational radiation exposure of fertile or pregnant women should be kept as low as is readily achievable. It is DOE policy, however, that no woman be denied a job or work assignment solely because of this recommendation.

As soon as an employee learns that she is pregnant, she is required to inform Medical Services of the expected date of childbirth (see RPM, Sec. 2.09, D, 3 [LBL nd]). A physician will discuss her work environment with her and will determine whether or not any changes in the environment should be made to ensure her good health and that of her baby. All new employees are given a copy of the booklet, 'Pregnancy and Radiation'. (LBL 78)

B.6. Nonemployees

The radiation protection rules and guides for non-LBL personnel are the same as for employees. Non-LBL personnel includes visitors and contractor workers.

Contractor personnel are the responsibility of their employer who is obligated by contract to comply with all pertinent DOE and LBL safety and health regulations and requirements. [See section on Contractor Safety in Chapter 10, LBL 80]

Non-LBL personnel under 18 years of age must be limited to the dose equivalents specified for employees under the age of 18.

C. Personal Radiation Monitoring

C.1. General

Certain employees and participating guests who work at the Laboratory are defined to be radiation workers. A radiation worker is an individual whose regular job duties involve, or potentially involve, exposure to ionizing radiation. Such work is subject to appropriate radiological protection controls and is usually performed in controlled areas.

All radiation workers at LBL are required to participate in the Laboratory's bioassay program, its personal dosimetry program, or both.

Most radiation workers who are exposed to external ionizing radiation will be issued a personal dosimeter (usually film badge/badges) to record their exposure to radiation. Radiation workers exposed to internal emitters will be required to participate in the bioassay program. The U.S. Department of Energy require monitoring of individuals who have the potential to receive a dose equivalent in any calendar quarter which is 10% of the applicable radiation protection standard. (For whole body external exposure this guideline translates to a potential exposure of 300 mrem per quarter.)

C.2. External Radiation Exposure

Personal Dosimetry Program. Dosimeters which are issued to employees who work with ionizing radiation are the primary personal detectors used to monitor the amount of radiation dose equivalent to employees from Laboratory and non-Laboratory exposure.

The plastic dosimeter holder contains a large pocket to hold the Laboratory identification card and two smaller pockets to hold the monitoring films. One of these smaller pockets has two circular metal filters and holds the beta-gamma film used for all radiation workers. The other holds a neutron film for those employees who may be exposed to significant neutron radiation, e.g., persons working in accelerator areas.

Radiation workers are issued two holders. One has a blue identification tag; the other, a yellow tag. The tags contain the employee's name and dosimeter number. Holders are alternated monthly by the wearer at exchange points located throughout the Laboratory. New employees must check with their supervisors for their exchange location.

Film packets must be carried at all times in areas where a radiation exposure might be received. Employees working in induced radioactivity areas, in radioisotope areas, or with machines must clip the dosimeter to the front of their chest. Clips are available at the Personnel Dosimetry Office on request. Dosimeters must be stored in natural background areas when not worn by radiation workers.

The dosimeter is relied on to provide accurate information about the wearer's exposure to radiation, so it must not be misused. Each individual's record of exposure to Laboratory-produced ionizing and particulate radiation is carefully maintained at the Personal Dosimetry Office. It is important that non-Laboratory exposures, such as those that might be received through medical or dental procedures, be reported to the Personal Dosimetry Office. Employees may request extra film to monitor non-Laboratory exposures and in that way make the task of record keeping easier.

Criteria for issuance of personal dosimeters:

- Gamma film dosimeters will be issued monthly to employees who work directly with the following radiation-producing items:

a) particle accelerators, 10 hours or more per month
b) x-ray generators
c) irradiators
d) radioisotopes, except exclusive users of the radionuclides ^{14}C and/or ^{3}H
e) anyone having the potential for significant exposure (such as experimenters, radiation therapy personnel, etc.)

- Firemen, certain Protective Services personnel, and other selected individuals will also be issued personal gamma dosimeters.
- Neutron dosimeters will be issued monthly to a limited number of personnel who work at accelerator sites; these fall in the following categories:
  a) operations and maintenance personnel who work 35 hours or more per month at any of the accelerators
  b) users (experimenters, radiation therapy personnel)
  c) special cases as determined by EH&S on an individual basis.
- Employees whose work only occasionally falls in one of the above categories will be issued dosimeters to cover those time intervals.

Questions concerning the need for neutron film packets may be directed to the Personal Dosimetry Office, Ext. xxxx.

Finger dosimeters are worn on the finger by experimenters whenever they handle concentrated amounts of radioisotopes. They are used only for short intervals and then sent to the EH&S Dept. for evaluation and record keeping. Finger dosimeters are normally issued and collected by the EH&S Dept. monitors.

Pocket dosimeters are a self-reading beta-gamma-indicating type and are worn in areas where the radiation levels are high or unpredictable. Usually these are areas of induced activity within the accelerator shielding. The purpose of the dosimeter is to provide the wearer with a means of keeping a running check on the approximate radiation dose equivalent received while working in a high radiation field. When the wearer is finished using the pocket dosimeter, he must record the amount of radiation he received in the logbook that is kept with the dosimeters. The pocket dosimeter is not a substitute for the film badge, which must be worn concurrently.

Thermoluminescent dosimeters (TLDs) are a supplementary means of measuring the dose received on the extremities such as the hands and forearms. The TLDs may be obtained from the EH&S monitors.

Wearing of Personal Dosimeters

It is mandatory that radiation workers wear their personal dosimeters in posted areas.

It is recommended that radiation workers wear their personal dosimeters at all times when at the Laboratory.

When a single dosimeter is used, the preferred location for wearing it is the upper torso, where it will give the best measure for estimating the whole body dose equivalent. When wearing the dosimeter on the upper torso is impracticable and the whole body radiation exposure is from omnidirectional, penetrating radiation (as for example, when working around operating particle accelerators) it is sufficient that the dosimeter be carried on the person. In certain work areas it is mandatory that the dosimeter be worn on the upper torso-these areas are so posted.

During off-hours, the dosimeter may be taken home or stored in the Laboratory in areas having relatively low background radiation intensities. Most office areas at the laboratory meet this requirement. the Environmental health and Safety Coordinator in your area can advise you as to appropriate dosimeter storage locations. The dosimeter must not be work during medical or dental x-rays, nuclear medical procedures, or radiation therapy. It is important that you notify the Personal Dosimetry Office should such exposures to your dosimeter occur.

Monitoring Responsibility

Each radiation worker is responsible to wear an issued dosimeter in accordance with this policy.

Line management is responsible to:

- determine which employees should be designated as radiation workers.
- ensure compliance with the DOE radiation monitoring order.
- ensure that dosimeters are properly worn in posted areas, substantiated by periodic audits of record.
- ensure compliance with bioassay monitoring programme requirements.

Penalty for Nonreturn of Dosimeter

Each month anyone who does not return his/her dosimeter during the prescribed month will receive a reminder indicating this fact; the person's supervisor will also receive this notice. It is the individual's responsibility to follow laboratory procedure and return the dosimeter at the prescribed time. The supervisor's responsibility is to enforce this procedure.

If the dosimeter is not returned after two months, the person's Division Head will be notified of this fact. After three months delinquency, the individual will be subject to removal from any radiation work.

C.3. Internal Radiation Exposure

The programme to monitor internal radiation dose equivalent to LBL employees is administered by the Medical Services Department, with the advice of the EH&S Dept. The EH&S Dept. provides the Medical Services Dept. with a list of LBL personnel working with radioactive

material (exclusive of some encapsulated material, such as sealed sources; see Radioactive Sources, Section G.10). This bioassay list is reviewed every six months by the EH&S Dept. Area Coordinators. Everyone on the list is required by the Medical Services Dept. to provide appropriate bioassay samples.

The bioassay programme consists of in vivo counting at the Donner Laboratory whole-body counter and radiochemical analysis of urine samples. Employees submit urine samples and have whole-body counts once a year, or more frequently as appropriate. Persons working only with low energy beta-emitters (e.g., ^{3}H, ^{14}C) are not included in the whole-body counter program. Results of all bioassay tests are kept in the employee's medical file and by the Medical and EH&S Departments.

In all cases of known exposure to internal radiation by ingestion, inhalation, or puncture wound, the absorbed dose equivalent must be estimated by the most appropriate methods available. Elimination rates must be followed as long as they are relevant to the exposure.

Those employees who have worked in areas where internal deposition of radionuclides is possible must have a bioassay examination included in their terminal physical examination.

D. Monitoring of the Working Environment

The EH&S Dept. maintains a working environment monitoring programme to assure that dose equivalent rates and the concentration of radioactivity in areas inhabited by people do not exceed the radiation protection guide values.

D.1. On-Site Monitoring

Where radiation-producing machines are operated, external radiation intensity must be measured at least every 6 months and whenever a significant change is made in equipment or mode of operation, or on the schedule stated in the operating procedure.

In areas containing radioactive material:

- External radiation intensity must be measured at least every 3 months, and whenever a significant change is made in equipment, quantity of material, or mode of operation, or on the schedule stated in the operating procedure.
- At the onset, during and upon completion of an operation, surveys must be made. Area contamination surveys must be made at least monthly when work is in progress, once every three months when an experiment is inactive, and whenever there is reason to believe that radioactive material may have escaped from its enclosure.
- Air sampling must be performed on a continuous basis in the areas of actual operations with radioactive material that can potentially release airborne contamination and in exhaust systems serving the radioactive material handling areas.
- Certain areas at the Laboratory are designated Restricted Areas due to the presence of radiation or radioactive materials in

amounts above the levels set by DOE regulations. These areas are identified by signs bearing the universal radiation symbol and the words 'Caution Radiation Area' (Fig. 5.4), 'Caution High Radiation Area' (Fig. 5.5) or 'Caution Radioactive Materials' (Fig. 5.6).

'Radiation Area' means any area, accessible to personnel, in which a major portion of the body could receive in any 1 hour a dose equivalent in excess of 5 millirem, or in any 5 consecutive days a dose equivalent in excess of 100 millirem.

'High Radiation Area' means any area, accessible to personnel, in which a major portion of the body could receive in any 1 hour a dose equivalent in excess of 100 millirem.

The 'Caution Radioactive Materials' warning sign is to be used in areas and rooms where radioactive material is present and on containers in which radioactive material is being transported, stored, or otherwise used.

To enter these areas, persons must find out from the local area supervisors or EH&S Dept. representative where and what radiation hazards are and proceed as appropriate.

The radiation warning signs are posted at the advice of the EH&S Dept.

Radiation of a level high enough to cause possible injury exists in certain areas of the Laboratory: For example the large gamma irradiators; many vaults and experimental caves associated with particle accelerators. These areas are identified by warning signs and, when in operation, by flashing magenta or red lights. All of these areas are equipped with various types of entry interlocks and run-safe switched. Never attempt to enter one of these areas unless you have permission and unless you are fully familiar with the operational safety rules of that particular facility. These rules are printed in the facility's Operational Safety Procedures, which can be obtained from the facility's Building Manager. For further information, call the EH&S Dept.

D.2. Off-Site Monitoring

A programme of sampling air, water, and sewage as well as ionizing radiation is maintained by the EH&S Dept. to evaluate:

- the effect of the Laboratory's operations on the environment.
- the effectiveness of on-site control measures in meeting the radiation protection guide restrictions on concentrations of radioactivity that may be released to the area around the site.

External radiation is monitored at the boundary fence to establish the Laboratory's control of the external radiation reaching the off-site environment. This monitoring programme is described in 'The Environmental Surveillance Program of the Lawrence Berkeley Laboratory' [LBL-4678], (LBL 76). The EH&S Dept. prepares an annual summary of off-site surveillance which is contained in 'The Annual Environmental Monitoring Report of the Lawrence Berkeley Laboratory'.

D.3. Portable Radiation Detecting Instruments

The Laboratory provides and maintains radiation detection and measuring instruments. Instruments are issued to employees or groups when their use is clearly of value in monitoring and controlling exposure of personnel. The EH&S Dept. selects, obtains, and distributes the portable instruments. The Instrument Techniques Support group provides maintenance. These instruments are delicate and expensive, and the employees who use them must be trained to operate and interpret them and be familiar with their limitations.

D.4. Protective Equipment

The primary control of unencapsulated radioactive material is through confinement in a suitable enclosure provided with appropriate ventilation. The enclosure is designed to provide control of airborne radioactivity commensurate with the hazard.

E. Exposure to Radiation in an Emergency

Specific dose criteria and judgment factors are set forth for the three categories of risk-benefit considerations, i.e., actions involving the saving of human life, the recovery of deceased victims, and the protection of health and property. Details are found in DOE Order 5481.1, Chapter XI.

F. Accelerator Health Physics

The accelerator health physics safety programme of the EH&S Dept. consists of the following functions:

- Consultation with operations personnel, experimenters and monitoring personnel.
- Training for operations and monitoring personnel.
- Radiation monitoring.
- Shielding evaluation and design and other safety systems, such as interlocks, area monitors, etc.
- Personal radiation monitoring.

It is recommended that experimenters, operations and monitoring personnel consult with an accelerator health physicist for help in planning new or unusual beams, beam lines, targets, unusual requirements for rapid access to a target or target area, or for special shielding.

Prior to the use of a new or unusual operation at any of the LBL accelerators or ion sources, monitoring must be requested from the EH&S Dept.

Each of the accelerators must have a current Operational Safety Procedure (OSP) manual prior to operations. These manuals detail accelerator health physics and safety programs. Help in reviewing the OSP is available from the EH&S Dept. Operations as detailed in the OSP must be followed.

Interlocks and warning device operation must be checked and serviced for proper functioning at intervals not to exceed a months review of the system requirements must be made on a regular basis.

Requirements for personal radiation monitoring must be met by all employees and participating guests. Contact the EH&S Dept. Personal Dosimetry Office, Ext. xxxx, for the necessary dosimeters.

G. Radioactive Materials

G.1. General

Operations During Regular Hours

The handling of, or working with any radioisotope (except sealed sources) is prohibited unless an EH&S monitor is present, or the person is trained in a specific procedure which has been approved by the EH&S Department. Radiological assistance normally is available during the following hours: Monday through Friday, 8:00 AM to midnight.

Off Hour Assistance

Assistance during the hours not listed above is available; however, arrangements must be made at least one week in advance. Call EH&S Department, Ext. xxxx.

G.2. Training in Radioisotope Safety Procedures

All employees newly working with radiation or radioactive materials are required to attend specific EH&S Training Courses (see Chapter 24, LBL 80). Supervisors are responsible for seeing that this requirement is met by employees in their groups.

G.3. Engineering Controls

Key card locks are mandatory on doors to rooms where radioactive material in large quantities are present. The maintaining of logbooks on the current inventory of radioactive materials in the area is also mandatory.

To provide for maximum safety and economy, the EH&S Dept. reviews plans for all new facilities involving radioactive materials (and for alterations to existing facilities) at the earliest possible opportunity. Operations involving radioactive materials are restricted to those buildings (or areas within buildings) which are designated by the EH&S Dept. as adequate for such usage.

All chemical, physical, and mechanical operations on materials containing radioisotopes must be performed in a manner that will limit the spread of radioactive contamination. Each proposed use of enclosures or of fume hoods is reviewed with respect to the type of operation and the amount of the radioactive materials to be used. The EH&S Dept. must be consulted prior to the initial use or significant change in use of radioisotopes.

Fume hoods are designed and intended to protect the operator by providing an air barrier. For operations that might release

radioactive contamination to the atmosphere, enclosures such as glove boxes must be used. Fume hoods are not adequate for use in operations that generate radioactive aerosols.

Storage of radioactive material in hoods for periods of time exceeding a month or more-even though well packaged and well shielded-is discouraged. Instead, the material should be given to the EH&S Dept. for storage in its Pit Room facilities to minimize the possibility of dispersal of aerosols to the environment and to reduce the radiation level from gamma emitters. If radioactive material must be kept in a hood for short periods, it must be safely packaged and well shielded, and the EH&S Dept. must be notified of its location. A warning tag or sticker identifying the radioactive isotope, level of activity, chemical form, etc., must be affixed in a prominent location outside the hood. The EH&S Dept. can help in achieving proper shielding of gamma emitters.

Flammable or explosive liquids and pyrophoric material must never be stored in large quantities in hoods but in approved storage lockers. These materials, in any quantity, must never be stored in hoods containing radioactive materials.

Acids, solvents, and heat sources can damage the inside surfaces of hoods, making any needed decontamination difficult. Always use protective coverings such as sheet plastic, absorbent paper or heat-resistant materials as working surfaces.

The sliding front window that most hoods have performs two functions:

- Protection against splashing chemicals and unexpected reactions.
- Control of air face velocity at the front of the hood.

The recommended face velocity of 100 fpm is achieved by matching the arrow on the side of the vertical sash with the arrow on the frame.

Periodic maintenance and repair of the hood blowers located on the roofs of the chemistry laboratories necessitates the shut-down of the hoods' ventilating system. When this condition exists, the individual wishing to turn off any hood must contact the occupants in the room and inform the EH&S Dept. representative in the area. The EH&S Dept. representative must place a sign reading, CAUTION-HOOD OUT OF SERVICE-DO NOT USE, on the front of the hood. The sign must remain in place until service is restored, at which time the occupants of the room must be notified. Because of poor hood ventilation, the hood sash must be in its lowest position during shut-down conditions.

Sanitary waste drains are located in or near most hoods. Do not pour liquid radioactive waste (LAW) into this drain. If this is done by accident, notify the EH&S Dept. immediately.

Air sampling devices (Filter Queens) must be located next to any work station where potentially dispersible radioactive materials is being handled or where radioisotopes are stored. When leaving any radioisotope work areas employees must check for personal contamination by using the hand and foot counter.

Safe Glove-Box Practices. The basic glove box consists of a plywood enclosure whose volume is maintained at a negative pressure with respect to the room by a manifold system. A variety of glove boxes are used at the Laboratory: basic boxes ('Berkeley boxes'), lead-shielded boxes ('junior caves'), vacuum-line boxes ('piano boxes'), and inert atmosphere boxes.

Adequate ventilation of glove boxes must be maintained at all times. This is assured if the ball indicator in the flow meter, mounted to the cold side of the high-efficiency filter on every box, is never below the black line inscribed on the face of the flow meter. Exhaust manifold control box alarms occasionally go off owing to an interruption in power or a malfunction. Should this occur, notify the EH&S Dept., Ext. xxxx, immediately. Never turn the control box off and never disconnect a glove box from an exhaust manifold.

Box gloves and glove O-rings must be checked for holes and deterioration before entering the box. If they need replacing, call the EH&S Dept. Surgeons' gloves must be donned before entering the box. Sharp objects used inside the glove box must be kept in protected containers to prevent accidental puncture of gloves.

Radioisotope contents and approximate level of radioactivity inside the glove box must be posted in a prominent location on the front of the box. Box "pass-outs" and "pass-ins" must be done with the assistance of an EH&S Dept. monitor unless the operator has been properly trained.

Flammable liquids or gases used in ordinary glove boxes must be in volumes small enough to prevent the buildup of explosive concentrations. Spark-proof glove boxes are available for experiments requiring large volumes of flammable liquids or gases. Special fire extinguishers for use on glove box fires are available from the EH&S Dept. and must be located near any glove box containing flammable material.

Never enter a shielded glove box ('junior cave' until the radiation level inside the cave has been checked with a portable survey meter. Check hands and feet for contamination after working in a glove box, and when leaving the work area.

Glove boxes are designed with consideration for resistance to earthquake damage and are secured to prevent tipping.

G.4. Proper Preparation of Radioactive Waste

EH&S Dept. representatives are available for advice and assistance whenever radioactive material is to be discarded (Ext. xxxx). Dry active waste (DAW) must contain no liquids greater than several milliliters. Liquid active waste (LAW) must be clearly identified by chemical name or formula (HNO_3, toluene, etc.) or by group (organics, aqueous, etc.).

Scintillation vials can be received unopened if packaged in 30 or 55 gallon steel drums containing enough absorbent material to absorb at least twice the total volume of liquid in the vials and if the concentration of liquid does not exceed 0.02 microcuries per milliliter.

G.5. Radioactive Waste Disposal

New employees intending to work with radioactive material must contact an EH&S Dept. representative for instruction in the proper handling and disposal of such material. When radioactive material is to be discarded, it must be given to the EH&S Dept., which provides active waste collection containers for:

- Dry waste
  [16 gallon galvanized waste cans
  55 gallon steel drums (shielded and unshielded)
  Ice cream cartons, plastic bags, cement sacks]
- Liquid waste
  [5 gallon carboys
  Plastic or glass containers]

Accidental release of radioactive waste into the sanitary or storm sewer system must be reported to the EH&S Dept. immediately (Ext. xxxx).

Alpha-emitting waste must be identified by isotope and segregated from beta-gamma waste whenever possible. Mixed waste containing both alpha- and beta-gamma is to be treated as alpha waste. Explosive, flammable, or highly toxic radioactive chemicals must not be discarded in DAW cans. Sharp objects such as hypodermic needles, spitzers, and scalpels must be put in a protective container, such as an ice cream carton, before they are placed in DAW cans.

DAW cans must not be used for non-radioactive waste.

G.6. Transportation and Shipment of Radioactive Material

IMPORTANT

REMOVAL OF ANY RADIOACTIVE MATERIAL FROM THE LABORATORY PREMISES IS PROHIBITED WITHOUT WRITTEN PERMISSION. THE DIRECTOR'S OFFICE HAS GIVEN THE ENVIRONMENTAL HEALTH AND SAFETY DEPARTMENT (AND THE PROPERTY MANAGEMENT GROUP AS APPROPRIATE) THE AUTHORITY TO GRANT SUCH PERMISSION.

Shipment of radioactive material or equipment must be handled in the following manner:

- The person wishing to ship radioactive materials from the Laboratory must fill out a Hazardous Materials Request for Shipment (Form RL-3634) available from the EH&S Department Operations Group. The completed form is to be returned to the EH&S Dept., which forwards a copy to Property Management for approval, if indicated.
- After receiving approval for the shipment, the material must be turned over to the EH&S Transportation Section, EXT. xxxx, for proper packaging, paperwork, and shipment.

Inter-building transferral of radioactive material or equipment must be done by the EH&S Dept. Transportation Section. Exception to this rule to allow hand-carrying of certain low-level, well-contained

items, can be requested from the EH&S Dept.

G.7. Storage of Radioactive Materials

General

Radioisotopes and radioactive material that are not being used (exclusive of material that has become radioactive by bombardment with neutrons or charged particles, called 'induced radioactive material', covered separately below), must be stored in a secure environment such as:

- the Pit Room storage operated by the EH&S Dept., Ext. xxxx.
- lockable, fire retardant Berkeley Boxes or air-filtered cabinets, designed with consideration for earthquake resistance.

Radioactive research equipment that is too large to be stored at the Laboratory can be stored at the Laboratory Warehouse provided that

- the level of radiation at the surface of the package does not exceed 2 mr/hr.
- the only alpha emitters present are fixed, low-level (100 dpm/cm^2) alpha emitters such as ^{226}Ra, ^{232}Th, or ^{238}U.
- the package has been monitored and tagged by an EH&S Dept. representative.

Unsafe storage areas include: bench tops, desk drawers, fume hoods, and wooden cabinets or lockers.

Storage of Induced Radioactive Materials

'Induced radioactive material' is the term used to describe material that has been made radioactive by bombardment with neutrons or charged particles produced by accelerators.

Any item is called 'induced radioactive materials' if, when monitored with a partable thin-window Geiger-Muller count-rate survey instrument in a low background area (0.05 to 0.1 mr/hr), a definite reading above background is indicated.

Guidelines regarding induced radioactive material:

- The proper disposal of induced radioactive material is encouraged.
- All equipment, furniture, and material that is to be moved from the accelerator buildings and accelerator areas must be monitored, and, if found free of activity, tagged with a NO ACTIVITY DETECTED tag (Fig. 5.7).
- With the exception of material within the accelerator operational area*, induced radioactive material falls into two general categories-portable items that are easily hand-carried, and heavy and/or bulky items. The storage of these items is to be as follows:

  Portable items: store in locked areas identified by radiation

warning signs. (See Figs. 5-4, 5-5, and 5-6).

Heavy items: store in areas clearly identified by radiation warning signs; those reading greater than 100 mr/hr must be inventoried.

- If items in either category are not stored as described above (and are not within the accelerator operational area*), they must be tagged with radiation warning signs; those reading over 100 mr/hr at the surface with a portable ion chamber survey meter or that can cause radioactive contamination are to be inventoried.
- Inventory number, description, location, Area Coordinator, and owner of the material are assigned and records maintained by the EH&S Dept., which must make an annual inventory.

G.8. Decontamination of Radioactive Equipment

Articles that are of sufficient value to make recycling economical are to be given to the EH&S Dept., Ext. xxxx, for decontamination. Proper packaging and identification of these items must be done by an EH&S Dept. representative. Glove boxes, hoods, and other enclosed work areas can be cleaned in place by EH&S Dept. personnel. Contaminated clothing and other personal items must be decontaminated by the EH&S Dept. before they can be removed from the Laboratory premises. Contaminated lab coats must be given to an EH&S Dept. representative.

Decontaminated equipment will be released to the owner when any radioactive residue cannot escape into the air, be transferred by contact, or when there is no hazard from external radiation levels.

G.9. Contaminated Precious Metals

Radioactively contaminated precious metals must be kept separate from noncontaminated precious metals. The EH&S Dept. is responsible for the monitoring of all radioactive precious metals to be returned to stock, for providing proper disposition of contaminated metals, and for the maintenance of a secured repository for radioactive precious metals.

Return of contaminated precious metal to the Property Accounting Office is done in the following manner:

- The user, with the assistance of an EH&S Dept. representative and in the presence of a Property Accounting representative (Bldg. xxx, Ext. xxxx), must load a tared weight ice cream carton with the contaminated metal. The carton is given to the EH&S Dept.
- The ice cream carton is then sealed, surveyed for radioactivity, and reweighed for the true weight of the metal.

*Accelerator operational area: area inside the shielding, beam line, etc.

- The identification of the metal, its weight, contaminating isotope, survey meter readings in mr/hr or dpm, and its ownership is put on the carton.
- The material is sent to the Lawrence Livermore National Laboratory, for decontamination and the proper account is credited.

G.10. Monitoring and Movement of Material

All equipment and furniture that is not radioactive must be tagged with a NO ACTIVITY DETECTED tag (Fig. 5-7) before being removed from the following buildings:

[HERE FOLLOWS A LIST OF BUILDINGS IN WHICH CONTAMINATED EQUIPMENT OR FURNITURE MIGHT POSSIBLY BE LOCATED.]

Material that is to be scrapped, regardless of its point of origin must be monitored and then tagged with a NO ACTIVITY DETECTED tag (Fig. 5-7) before it is sent to the Salvage Department for reclamation.

Gas cylinders do not require a tag if they are located in the designated cylinder collection areas for each building.

Waste collected from certain buildings [here specified] must be certified free of radioactivity before it is released to waste collectors. Waste from all other buildings needs no special delineation.

G.10. Radioactive Sources

WARNING:

WILLFUL VIOLATIONS OF THE FOLLOWING REGULATIONS OR NEGLIGENCE IN HANDLING AND STORAGE OF RADIOACTIVE SOURCES ARE GROUNDS FOR DISCIPLINARY ACTION (REGULATIONS AND PROCEDURES MANUAL (RPM), PUB-201, PARAGRAPH 2.05B) AND MAY ALSO RESULT IN THE CANCELLATION OF FURTHER PRIVILEGES TO DRAW OR USE SUCH MATERIALS AND/OR IMMEDIATE RECALL OF SUCH MATERIALS, (LBL nd).

A radioactive source is defined as a radioisotope of a known amount of activity that has been encapsulated in such a manner that the radioisotope will not be released under conditions likely to be encountered by the source. Serial numbers must be assigned, by the EH&S Department, to all radioactive sources whether they are purchased from an outside vendor or fabricated at LBL.

Procurement of radioactive sources is handled through EH&S, which also maintains a supply of used sources of various types. Arrangements can be made to purchase new sources from commercial vendors.

Responsibility for the location and condition of the source belongs to the person in whose name the source is assigned. This rule remains in effect even if the source is loaned by the assignee to another person. Sources not in use must be stored in a locked storage area, room, or container bearing the sign: CAUTION-RADIOACTIVE MATERIAL (Fig. 5-6). Sources left unattended in an unsecured or unauthorized area will be confiscated by the EH&S Department. A

confiscated source will not be released to it a former assignee without authorization from the Director's office.

Periodic inventory and inspection of all serially numbered sources is conducted by the EH&S Department. The user of a serially numbered source must produce the source for inspection when requested by EH&S. The inventory schedule is as follows:

Three Classifications of Inventory

Class A - Up to 10 body burdens	Inventoried annually
Class B - 11 body burdens or over	Inventoried semiannually
Class C - High hazards sources that require special care and handling	Inventoried semiannually with special instructions given to assignee

Missing sources must be reported to the EH&S Department immediately. If, after a thorough search, the source is not found, a memo stating when and where the source was last seen must be sent to EH&S. Destruction of, or tampering with, a serially numbered source without the approval of the EH&S Department is prohibited. Removal of any radio-active source from the Laboratory premises without written authorization is prohibited; see Sections G.1 to G.6 for instructions.

Sources no longer needed or sources that may not be used for long periods of time are to be given to the EH&S Department for safe keeping. Employees terminating from the Laboratory must turn in all radioactive sources assigned to them. Termination processing will not be complete until all sources have been accounted for.

Violations of any of the preceding rules and regulations will be reported by EH&S Department to the Director's office.

H. Emergency Procedures for Radioactive Spills

The following procedures must be followed whenever a spill has occurred or is suspected to have occurred:

- Immediately notify the EH&S Dept. representative, EXT. xxxx or xxxx, or emergency EXT. xxxx, and evacuate all personnel from the immediate area.
- Retain personnel in a safe area until the EH&S Dept. can monitor them for contamination.
- Quarantine the spill area to prevent further personnel contamination.
- Give as many details of the incident as possible to the EH&S Dept. person in charge of the clean-up operation. This information will be used for reports and accident analysis.
- Never attempt to clean up a spill without the assistance of an EH&S Dept. representative.

I. X-RAY SAFETY

I.1. Introduction

The bulk of this section determines general requirements for all x-ray equipment at LBL. Specific requirements are given for x-ray machines that are classified into analytical (open and enclosed beam), portable, therapy, diagnostic and photoemission types. Safety requirements for these x-ray machines are based on ANSI Standards and the appropriate sections of NCRP Reports 33 and 49. (ANSI 78, NCRP 68, NCRCP 76)

This section determines responsibilities, specific authorization of users, and requirements for x-ray machine operation and maintenance. Logbooks are to be used to keep records of operation and maintenance. Double interlocks are required for all x-ray machines. An Operational Safety Procedure is to be included in all operating instructions for x-ray machines.

Exceptions to the general safety standards for specific operational cases are to be handled on a variance basis. This will require the operator to evaluate and explain his need for a variance. The X-Ray Safety Officer, an appointee of the Director's Office, is to review the standards at least annually and revise as necessary and to continually review the quality of the x-ray safety program.

I.2. Scope

This section establishes requirements and recommendations pursuant to radiation safety aspects of the design and operation of electronic equipment designed to produce x rays and to be used under the administrative control of Lawrence Berkeley Laboratory (LBL).

I.3. Definitions

controlled items: The Laboratory's Property Management designation of items which must be kept under inventory control regardless of value.

dead-man switch: A switch so constructed that a circuit closing contact can be maintained only by continuous pressure on the switch.

bistable indicator: An indicator which is either on or off and has no normal metastable state.

fail-safe design: One in which all failures of indicators or safety components that can reasonably be anticipated cause the equipment to fail in such a manner as to maintain personnel safe from exposure to radiation. For example: (a) if a light indicating "X-RAY ON" fails, the production of x rays must be prevented, and (b) if a shutter status indicator fails, the shutter shall close.

must: See "shall."

shall: Where "shall" and "must" are used for a provision specified herein, that provision is intended to be a requirement.

techniques: Instrument-use parameters employed during an x-ray exposure, i.e., kV, mA, mAs, sec, filter, distance, field size, etc. (all parameters are, of course, not applicable to all types of x-ray machines).

x-ray generator: That portion of an x-ray system which provides the accelerating voltage and current for the x-ray tube.

x-ray accessory apparatus: Any portion of an x-ray installation which is external to the radiation source housing and into which an x-ray beam is directed for making x-ray measurements or for other uses.

NOTE: The following terms are equivalent to an x-ray system: x-ray equipment, x-ray generating equipment, x-ray generating unit, x-ray machine, x-ray unit.

x-ray system supervisor: A person having administrative control over an x-ray machine and so designated in the Operational Safety Procedure for that machine.

I.4. Responsibility

The x-ray system supervisor is charged with the prime responsibility of ensuring that all requirements are completely and continuously applied. The responsibilities of the individual worker are detailed in Section 7.1 of the American National Standards Institute (Report N43.2) as follows:

> "7.1.2 Each worker shall, upon the instruction of a qualified expert or responsible supervisor, follow the recommendations and instructions which have been drawn up in the interest of radiation protection.
>
> 7.1.3 Each worker shall use the protective devices provided.
>
> 7.1.4 Each worker shall bring to the attention of those in charge any defect or deficiency in radiation protection devices and procedures."

I.5

WARNING

WILLFUL VIOLATIONS OF THE FOLLOWING REGULATIONS OR NEGLIGENCE IN THE USE AND SECURING OF X-RAY SYSTEMS ARE GROUNDS FOR DISCIPLINARY ACTION (RPM, PAGE 2-10, PARAGRAPH 2.03) AND MAY ALSO RESULT IN THE CANCELLATION OF FURTHER PRIVILEGES TO USE SUCH EQUIPMENT AND/OR IMMEDIATE REMOVAL FROM SERVICE OF THE X-RAY SYSTEMS INVOLVED.

I.6. Procedures

Each x-ray generating unit must have an Operational Safety Procedure (OSP) located near the unit. It must contain at least:

1. Diagram of facility.
2. Name of person responsible for the unit (system supervisor).
3. List of authorized users.
4. List of authorized instructors.
5. Emergency or problem call list.
6. Description of safety features (prepared by the X-Ray Safety Officer).
7. Specific operating procedures (submitted by the systems supervisor for approval by the X-Ray Safety Officer).
8. Specific alignment procedures as applicable (submitted and approved as 7 above).
9. Emergency instructions.
10. Copies of appropriate standards and policies.

These Operational Safety Procedures are to be prepared from the latest OSP preparation guide filled out initially by the X-Ray Safety Officer and the x-ray system supervisor, and sent at least annually to the x-ray system supervisor for review and, if necessary, revision.

I.7. Interlocks and Indicators

All x-ray generating equipment is to have interlocks and indicators as specified in applicable standards (NCRP 33 and ANSI N43.2) and by the X-Ray Safety Officer.

In addition, all x-ray generating equipment is to have the following, with the exception that medical diagnostic type equipment is exempt from items 1 and 2.

1. Redundant interlock chains or mechanical shutters, either of which may prohibit the emission of x rays from the x-ray tube. It is recommended that a signal from a fail-safe area radiation monitor be part of one of these interlock chains.
2. A bistable indicator which gives a positive indication that high voltage is applied to the x-ray tube. It is required that either this indication be incorporated into an interlock chain in a fail-safe manner or that a bistable indicator be used which gives a positive indication that high voltage is not applied to the x-ray tube.
3. A key-controlled switch which controls the main power to the entire x-ray unit. Furthermore, actuation of this switch must not in and of itself cause high voltage to be applied to the x-ray tube. Also, it must not be possible to remove the key while the switch is in the "ON" position. Access to this key must be controlled. It is recommended that there should be as few copies of this key as possible and those copies must be serialized and assigned. When not in

use, this key must be secured. This requirement may be exempted where access to the room in which the x-ray generating unit is located is both limited and controlled at all times.

In addition, it is recommended that each x-ray generating unit have an audible, attention catching, reliable or fail-safe indication when high voltage is applied to the x-ray tube and one or the other interlock chain has not been satisfied.

I.8. Posting

Posting must be in accordance with the standards listed in the standards section of this document (Secion I. 21), and according to the recommendations of the X-Ray Safety Officer.

I.9. Records

All x-ray machines are to be considered controlled items, requiring complete property management accountability records. All x-ray machines are to have a user's log located near the machine. This logbook is to be used to record the following information:

1. User's name.
2. Experiment or procedure performed.
3. Number of exposures and techniques used.
4. Approximate time of use.
5. Date of use.
6. Any suspected anomalies noted in machine operation.
7. Name of responsible person notified of above anomaly.
8. Frequent user leakage surveys are to be noted in the user's log.

All notifications of suspected machine anomalies must be answered in the maintenance logbook. All maintenance work on x-ray generating equipment is to be considered a use of that equipment and must be entered in the user's logbook with a reference to the location of a more detailed entry in the maintenance logbook.

All x-ray generating equipment must have a maintenance log. This logbook is to be used to record the following information:

1. Maintenance person's name and employer (if other than LBL).
2. Reason for maintenance (may refer to user's log entry of noted nomaly).
3. Specific problems noted during maintenance (need not be entered in user's log).

4. Repairs performed (if modification is performed, reference date of approval note from X-Ray Safety Officer).

5. Time and date of maintenance operation.

6. Signature of maintenance person (signature indicates a certification that the machine is in normal working order, including all interlocking and fail-safe devices, and that circuitry and construction is in strict accordance with original manufacture plus approved modifications).

The user's logbook and maintenance logbook may be combined if deemed appropriate by the x-ray system supervisor. This combined logbook is to be located near the machine, as is a user's logbook, and it must contain all information required for both logbooks.

All records of any recorded radiation exposure to users are to be maintained by the EH&S Dept.

I.10. Property Management

All requisitions for x-ray generating equipment must be reviewed by the X-Ray Safety Officer. Such equipment is to be considered a controlled item and must not be removed from Laboratory inventory while still under Laboratory authority. Removal from inventory for purposes of disposal, transfer of ownership, or any other reason must have prior approval of the X-Ray Safety Officer. Any suspected loss of inventory accountability of x-ray generating equipment must be reported to the X-Ray Safety Officer who will assist in a prompt investigation. All movements of x-ray generating equipment is to be recorded by means of an Equipment Movement Record and have prior approval of the X-Ray Safety Officer.

All x-ray generating equipment inventory information (including that for electron microscopes) is to be available in the form of an annual computer readout and upon request of the X-Ray Safety Officer. In addition, the computer search information must be complete and exclusive of superfluous items.

I.11. Personal Monitoring

All users of x-ray equipment and people working in the vicinity of that equipment must properly and continuously wear appropriate personal monitoring devices as supplied by the EH&S Dept.

I.12. Radiation Safety Surveys

With the exception of medical diagnostic equipment, all x-ray generating equipment is to have a radiation safety survey performed by the X-Ray Safety Officer or his designate at intervals not to exceed six months for machines in active use and at the start of use for machines which have not been used for longer than six months.

Medical diagnostic equipment is to receive a radiation safety survey and machine performance survey at least annually. Such equipment must also receive a machine performance survey after any repair

or maintenance operation which may affect machine performance.

In addition, all x-ray generating equipment is to receive a radiation safety survey:

1. Upon installation but before regular use.
2. After a repair operation which could have caused a change in condition of shielding or safety protection devices.
3. Upon request.

The safety survey must be recorded in the user's log. To supplement these major surveys the x-ray system supervisor for analytical equipment must survey the x-ray machine at least weekly to spot check for radiation leakage.

I.13. Routine Safety Maintenance

All x-ray machines are to have their safety systems checked by the x-ray system supervisor or his designate at intervals not to exceed six months. This must include at least:

1. Check of the operation of all interlocking switches and devices.
2. Verification of the condition and performance of all failsafes.
3. Check for general electrical and mechanical deterioration.
4. Check to assure that no unapproved modifications have been made.
5. Appropriate entries and signatures in applicable logbooks.
6. Prior notification to the X-Ray Safety Officer that this maintenance is to be done so that he may witness and certify that the above items have been completed.

I.14. Modifications

All modifications to any x-ray generating equipment must have the prior approval of the X-Ray Safety Officer. In considering the approval of a proposed modification, the X-Ray Safety Officer must concern himself only with that modification's bearing on safety and reliability.

I.15. User Training

Each user must be personally trained by an approved instructor as named in the Operational Safety Procedure. This training must include machine operation, introduction to the function and meaning of each safety feature and to basic radiation hazards and cautions. Additional courses may be added as available or appropriate. Written certification of training signed by both student and instructor must be submitted to the X-Ray Safety Officer before this person is added to the

list of approved users.

I.16. Use Control

Use of each machine is to be controlled as specified under paragraph 3 of Section I.7, Interlocks and Indicators.

I.17. Instrumentation

All analytical and portable x-ray generating equipment must have in the immediate area a working radiation monitor, of appropriate energy response characteristics, which must be used to monitor frequently for leaks. In addition, a fixed Geiger or ionization type monitor of fail-safe design is strongly recommended. This monitor may also be incorporated into the safety interlock chain as noted under the sections on interlocks and indicators.

I.18. Shielding

All x-ray generating equipment is to be shielded for stray radiation according to the direction of the X-Ray Safety Officer with reference to prescribed standards and within the prescribed practice of "as low as readily achievable."

I.19. New Installations

New installations of x-ray generating equipment must not be operated without prior approval of the X-Ray Safety Officer. For this reason it is strongly advised that this officer be consulted while the installation is still in the planning stage so that requirements such as shielding, interlocks and fail-safes may be reviewed.

I.20. Notification of Suspected Accidents or Injuries

In case of suspected accidents or injury relating to the use of a piece of x-ray equipment, the persons named in the Operational Procedure Guide shall be immediately notified.

I.21. Standards and Recommendations ANSI N43.2. NCRP No. 33. NCRP No. 49.

I.22. Unusual Occurrence Review Critique

A review critique is to be called by the x-ray system supervisors within one week following any unusual occurrence involving possible x-ray exposure. The following personnel must be in attendance:

1. Any personnel involved and their immediate supervisors
2. X-ray system supervisor
3. Department head
4. Building manager
5. X-Ray Safety Officer or his designate

6. Head of the EH&S Dept. or his designate

7. Other persons who might be helpful to the proceedings.

Exceptions to the above requirements may be made by the EH&S Dept. head if deemed necessary.

The critique shall cover: the incident, causal factors, responsibilities, dosimetry, and corrective action.

A summary of this critique must be sent to the LBL Safety Review Committee. An additional copy is to be sent to the Department of Energy, San Francisco Operations Office (DOE SAN) as a follow-up to the initial report made to DOE SAN at the time of the occurrence as required by the terms of the contract between DOE and the Laboratory.

I.23. Safety Systems Analysis

Safety Systems Analysis for x-ray machines is provided for in Laboratory procedures. These procedures are covered in Pub. 3001, "Rules and Procedures for the Design and Operation of Hazardous Research Equipment."

I.24. X-Ray Machine Type Classification

Analytical X-Ray Equipment. Analytical x-ray machines are classified into two types: Open beam x-ray systems Enclosed beam x-ray systems

The definitions of these terms are contained in ANSI N43.2, paragraphs 5.2.1.1, 5.2.1.2 and Section 5.2.2.3.

Contained in the classification of enclosed beam x-ray systems are x-ray diffraction and x-ray fluorescence equipment which meet the specifications in ANSI N43.2. In addition, all cabinet x-ray units are considered as an enclosed beam x-ray system.

Contained in the classification of open beam x-ray systems are all x-ray diffraction and x-ray fluorescence equipment not meeting the requirements for an enclosed beam x-ray system.

In all cases first consideration and effort must be given to making a system meet the requirements of an enclosed system. Approval to use an open beam x-ray system is to be handled as a variance.

An operable portable survey meter must be used with this equipment to check for stray radiation periodically and whenever any changes are made to the experimental setup which could compromise shielding effectiveness.

Portable X-Ray Equipment. Portable x-ray equipment presents particular hazards due to its flexibility of use and must be used more carefully. The output of such units is, with a few exceptions, generally low and will usually overload before a serious x-ray exposure can occur.

The following requirements are to be applied specifically to portable generators:

1. Fail-safe visual indication that x rays are being generated. This is to be located in a prominent place and its meaning obvious.
2. Reliable audio indication that x rays are being generated.
3. Circuitry must be such that exposure can be ultimately controlled by a dead-man-type switch.
4. Extra caution and awareness must be given to beam orientation and the location of other persons in the vicinity of the x-ray machine.
5. Interlocks are recommended to be used if possible; however, the nature and use of these machines often precludes such considerations.
6. An operable portable survey meter must be used with this equipment to check for stray radiation periodically and whenever any changes are made to the experimental setup which could compromise shielding effectiveness.
7. A key switch must be on each unit.

All NCRP standards applicable to portable x-ray machines are required.

Therapy Type X-Ray Equipment. Medical therapy x-ray equipment safety is detailed in the appropriate sections of NCRP No. 33 and 49. Because of the moderate to high output of these machines and their ability to maintain a continuous exposure, the shielding of their location is a prime concern.

The Operational Safety Procedure for this equipment will state whether or not the x-ray machine is known to meet state and federal regulations for use on human subjects. Any x-ray machine to be used on human subjects must be found by the X-Ray Safety Officer to be in compliance with these regulations before such use commences, unless specifically exempted on the responsibility of the Human Use Committee.

Diagnostic Type X-Ray Equipment. Medical diagnostic equipment safety is detailed in NCRP No. 33 and 49. Since long exposures at high outputs are generally impossible with such units, interlocking is deemed inappropriate. All such equipment is to have a reliable audible indicator which signals the production of x rays.

The Operational Safety Procedure for this equipment is to state whether or not the x-ray machine is known to meet state and federal regulations for use on human subjects. Any x-ray machine to be used on human subjects must be found by the X-Ray Safety Officer to be in compliance with these regulations before such use commences, unless specifically exempted on the responsibility of the Human Use Committee.

All these installations are to have a light outside the room that must indicate when the x-ray control unit is energized and when x rays are being produced (a "rotor on" indication will suffice for the "X-

ray on" indication). These lights are to be fail-safe or redundant in nature. Furthermore, they are to be positioned and labeled so that their meaning and presence is obvious.

Photoemission X-Ray Spectrometers. These x-ray systems do not, by design, emit x rays beyond the contiguous internal vacuum. They are therefore not within the scope of these regulations and must be considered exempt from them. The X-Ray Safety Officer must, however, survey them for x-ray leakage on a perennial basis and maintain records of their location and existence.

I.25. Variances

When the x-ray system supervisor feels that it is impossible or highly impractical to adhere to this standard, he may request, in writing, a variance. This request is to be directed to the LBL Safety Review Committee for approval.

All requests for variances are to be evaluated on an individual basis and for approval must demonstrate:

- A definite need for variance.
- Alternate safety devices and/or procedures which ensure an equivalent degree of safety.

All requests for variances from DOE-prescribed regulations must, in addition, require specific DOE approval.

II. NON-IONIZING RADIATION

A. ULTRAVIOLET LIGHT

The effects of exposure to ultraviolet radiation are similar to sunburn. Since there is a measurable period of time between exposure and development of injury, deep burns may be caused without immediate discomfort. The severity of the burn depends upon the spectral distribution of energy in the ultraviolet region, the intensity, and the time of exposure.

Considerable discomfort can be produced in the eye by exposure to radiation below about 3100 Å. The absorption of this radiation by the outer layers of the eye (cornea and conjunctiva) produces conjunctivitis, which occurs 4 to 8 hours after exposure and may last several days.

Most lamps used for general lighting purposes emit little or no ultraviolet radiation so that in typical lighting installations there are no harmful effects. On the other hand, there are certain special-purpose lamps that are designed to emit shorter-wave radiation. Some industrial processes, such as welding, also produce considerable amounts of such radiation. In these cases it is necessary to take certain precautions.

It is recommended that protective glasses be worn by all personnel when they may be exposed to ultraviolet radiation. Furthermore, opaque shielding is recommended to be used around welding areas to Protect other persons. Measurement of UV radiation can be obtained from Industrial Hygiene, EXT. xxxx.

B. MICROWAVES

B.1. General

Microwaves are electromagnetic radiations which occur in the electromagnetic spectrum between radiowaves and infrared radiation. They cover a frequency range of approximately 30 megahertz to 300,000 megahertz with the corresponding wavelengths of 10 meters to 1 millimeter.

Typical sources of microwave radiation are klystrons, magnetrons, backward wave oscillators, and semiconductor transit time devices. Some of these sources, when operated at high voltages, also generate x rays.

At LBL the most common application of microwave energy is in cooking with microwave ovens. Additional information on microwave ovens is given below. Microwaves may also be associated with diathermy equipment, induction and dielectric heaters, and accelerators.

The primary effect of exposure to microwave energy is thermal. The depth of heating is frequency-dependent. Above 3,000 megahertz, heating occurs primarily within the skin. Frequencies below 3,000 megahertz can penetrate the skin and heat the underlying tissues. Serious damage may occur in these tissues without warning because this area of the body has fewer nerve endings to sense overheating. In

general, the higher the frequency the lower the potential health hazard.

The exact biologic effects of microwave radiation at low power levels has not been established. However, at high power levels there is substantial evidence linking microwave exposures to eye cataracts and gonadal damage. In addition to biologic effects, flammable gases and vapors, confined inside metallic objects, may ignite when exposed to microwave radiation.

Based on thermal damage to tissue, the maximum permissible exposure limit for all microwave frequencies has been established at 10 milliwatts per square centimeter as averaged over any 0.1-hour (six minute) period. A safety factor of 10 has been applied to this limit. For more information see the American National Standard C95.1, Safety Levels with Respect to Human Exposure to Radiofrequency Electromagnetic fields, 30 kHz to 100 GHz (ANSI 82), available in building B75B.

The use of engineering controls is the preferred method for limiting exposures to microwave radiation. Typical engineering measures involve either completely enclosing the source or shielding the source from personnel.

B.2. Microwave Ovens

The microwave oven is a convenient tool which cooks food on the inside and outside simultaneously by means of microwave radiation. Most general-use ovens operate at a frequency of 2,450 megahertz.

The hazards involved are commonly due to leakage of microwave energy by warped or misaligned doors, through defective seals around the door or viewing window, or failure of door interlocks to shut off the oven when the door is opened. While present-day ovens are built so well that leakage at a density of radiation high enough to cause injury is unlikely, faulty interlocks could expose personnel in the vicinity of the oven to densities of a hundred-fold above safe levels.

The following precautions must be taken to reduce the possibility of injury from microwave radiation:

- Do not operate the oven when empty.
- Do not use metallic containers.
- Do not leave food residue in oven.
- Never tamper with oven.
- Keep door gaskets clean.

The Industrial Hygiene Group of the EH&S Dept. is responsible for evaluating each oven once a year, as well as any new ovens when initially placed in service.

C. MAGNETIC FIELDS

Very little information is available on the biological effects of magnetic fields, both varying and steady-state. The meager literature indicates that while actual survival is not threatened by exposure to high magnetic fields, these fields can influence humans to a degree sufficient to cause a number of disturbances (e.g., headache, fatigue, low blood pressure, decreased red blood cell count, etc.). For this reason. appropriate control measures must be taken by those working in magnetic fields greater than background. Precautions applicable to both varying and steady-state magnetic fields are as follows:

- Employees and visitors with pacemakers must be excluded from all areas where they could be exposed to magnetic fields.
- Personnel must not linger unnecessarily in magnetic fields greater than background.

APPENDIX A

LBL RADIOISOTOPE SAFETY PROCEDURES

EMERGENCIES

1. In case of suspected area or personnel contamination or abnormal exposure to penetrating radiation, evacuate all personnel and quarantine the area; avoid tracking contamination; retain all personnel in a safe area; do not attempt decontamination; and immediately notify Environmental Health and Safety Department (EH&S Dept.) at EXT. xxxx.
2. DOE requires notification of accidents for the purpose of investigating and identifying causes and corrective action. Immediate notification and preservation of the scene are necessary in the case of a serious accident. If you are in doubt about severity, preserve the scene.

PROCUREMENT AND TRANSPORTATION

1. Employees intending to work or make significant changes in experiments with radioisotopes must review their operations with the area EH&S Dept. representative before procurement and/or possession of radioactive materials. Holders of radioactive materials must maintain a logbook and a current inventory.
2. Purchase must be through the EH&S Dept. representative and/or the local business office, by requisition form sent to the Purchasing Department.
3. All incoming and outgoing radioisotope shipments and interbuilding transferral of radioisotopes must be done by the EH&S Dept. Transportation Group.
4. Removal of any radioisotopes from Laboratory premises is prohibited without permission; see p. xx. Fill out a Hazardous Materials Request for Shipment (form RL-3634) available from the EH&S Dept.

LABORATORY USE

1. Employees presently working with radioisotopes must be encouraged to take the EH&S Dept. Radiation Orientation courses, and all new employees who will work with radioisotopes must attend.
2. Radioisotope operations (except sealed, low-level sources) must not be performed without an EH&S Dept. radiation representative being present on the Laboratory site. Normal assistance is during the hours between 8:00 AM to midnight, Monday through Friday. Arrangements for off-hour assistance must be made with the EH&S Dept. at least one week in advance.
3. Ventilated glove boxes must be used for all radioactive operations that can generate aerosols, or the possible spread of contamination; fume hoods are not adequate for use in operations

that generate radioactive aerosols.

4. Glove box pass-outs and pass-ins must be done with the assistance of an EH&S Dept. monitor.

5. Lab coat and disposable gloves must be worn at all times when working in a glove box, or where chance of contamination exists. All working surfaces must be covered with absorbent paper.

6. Radiation detection equipment is available from the EH&S Dept.

7. Storage areas, glove boxes, and contaminated or radioactive items must be labeled with a "CAUTION, RADIOACTIVE MATERIAL" sticker.

8. Mouth pipetting, eating, drinking, and smoking when working with radioisotopes are prohibited.

9. All radioactive sources (encapsulated radioisotopes) must be assigned a serial number for inventory by the EH&S Dept. Responsibility for the location and condition of the source belongs to the person assigned the source.

10. All equipment and furniture from areas containing radioisotopes, and all items going to reclamation must be tagged by the EH&S Dept. with a "NO ACTIVITY DETECTED" tag before removal.

11. All employees working with those radioisotopes which emit penetrating radiation must wear film packets and be on the Medical Bioassay Program.

DISPOSAL AND DECONTAMINATION

1. Contact an EH&S Dept. representative for all radioactive materials requiring decontamination or discard.

2. Accidental release of radioactive waste into the sanitary or storm sewer system must be reported to the EH&S Dept.

3. Dry active waste (DAW) must contain no liquids, and liquid active waste (LAW) shall be identified by chemical name.

4. Liquid scintillation vials can be submitted unopened, either in 16 gallon drums, or in delivery carton.

5. Animals and tissue must be kept frozen until an EH&S Dept. pick-up for waste disposal.

LBL Environmental Health & Safety Department
Building B75B - EXT. xxxx

Off-hours - EXT. xxxx

April, 1980

1.1. THE ACCELERATOR RADIATION SAFETY PROGRAMME

Any organisation that has an effective occupational health programme with appropriate emphasis on radiological safety will have no difficulty in coping with the special problems presented by the operation of particle accelerators. In fact with few exceptions accelerators present radiological protection problems that are qualitatively similar to those found in many institutions using ionising radiations. The principal differences that do exist lie in the energy and variety of the radiations and in their production in pulsed modes that may demand special techniques for measurement.

There is a large diversity among accelerators and the hazards they present. It is not necessary, or even desirable, for all accelerators to have identical physical and administrative safety controls. The controls recommended here represent the minimum necessary for accelerator operation.

In large multipurpose laboratories the accelerator radiation safety programme will administratively be a part of a larger radiological protection group (as, for example, obtains at the Lawrence Berkeley Laboratory). In single-purpose laboratories solely dedicated to particle accelerator research (such as, for example, CERN) all necessary aspects of radiological protection will be contained within the accelerator health physics group.

Whatever the precise administrative arrangement might be the necessary tasks remain the same.

The basic elements of an accelerator radiation protection programme are:

- Administrative procedures
- Shielding and physical barriers
- Interlocked access
- Area monitoring
- Personnel monitoring
- Environmental monitoring

The specific requirements of the LBL Accelerator Health Physics Programme are given in Part I, Subsection F of the Ionizing and Non-Ionizing Radiation Safety chapter of the LBL Health and Safety Manual.

Accelerator Radiation Safety Checklist

The Lawrence Berkeley Laboratory has used the following checklist as an aid in assessing accelerator radiation safety programmes (Pa 73); it is reproduced here in slightly modified form for the convenience of the reader.

Accelerator Radiation Safety Checklist

[extracted from 'Accelerator Health Physics' (Pa 73)]

> Following is a checklist of a number of areas found to be important in many accelerator radiation-safety programmes. The list, though not applicable to all accelerators, should prove useful in many circumstances. The reader may wish to add items or put greater emphasis on some, but probably nothing should be omitted.

I. Shielding

a. Design and calculations. Are the calculations available on which shielding design is based? What is the source of the input data for the calculations?

b. Measurements. Have measurements been made to check the accuracy of the calculations and the efficacy of the shield?

II. Radiation Damage Estimates for Sensitive Components.

Are sensitive components of the radiation-monitoring system or the interlock system so located that their function cannot be impaired by exposure to very high radiation doses?

III. Accelerator Controls

Is access to the accelerator controls restricted to those persons who are authorised to operate the accelerator or can the accelerator controls be locked to prevent unauthorised use?

IV. Interlocks

a. Manual reset. Can tripped interlocks be reset only manually at the location of the interlock, rather than remotely from the control console?

b. Run-safe switches. Are there switches in the radiation and high-radiation areas that make it impossible for the accelerator to operate or beam to be admitted to the area when the switch is in the "safe" position or is each person entering the zone forced to take a key or other token with him that cuts accelerator operation until all keys (tokens) are returned to their distribution point?

c. Regular tests. Is the function of the entire interlock system tested at regular intervals and are the results recorded?

d. up-to-date circuit diagrams. Are up-to-date circuit diagrams maintained?

V. Exclusion Areas and High-Radiation Areas

a. Have all areas that must be cleared of personnel before the accelerator can be allowed to operate been properly marked and interlocked? Have the responsibilities of the persons who will effect the search and secure procedure been set down in writing? Has special attention been paid to the possibilities of holes in the enclosures of exclusion areas?

b. Can all areas where high radiation levels could occur be locked, or has a visible and audible alarm system been provided to warn of the presence of radiation? Have staff working in such areas been instructed concerning the correct course of action should alarms occur?

c. Is an audible warning or other suitable indication given to alert personnel that the accelerator is about to be turned on, or that beam is about to be admitted to a specific area?

d. Are suitable radiation monitors available to indicate the presence of radiation in areas where personnel may have access?

1. Are these monitors calibrated at regular intervals?

2. Is the functioning of the monitors and any associated alarms checked regularly?

3. Is the readout from these monitors and alarms conveniently available to the operators?

4. Are the suitable records maintained concerning calibration, testing and radiation levels?

e. Is there a need to carry a portable instrument to monitor for unsuspected radiation upon entry to a shut-down accelerator (induced radioactivity or x rays from high-voltage equipment) or into a shut-down beam area (beam in an adjacent area)?

VI. Procedures

a. Widespread understanding. Are procedures posted, read, and familiar to operators and support personnel and to visitors?

b. Validity. Are procedures reviewed and updated at suitable intervals?

c. Inclusiveness. Do procedures include

1. A clear statement of responsibilities of management, accelerator operators, and radiation safety officers?

2. Standard operating procedures and procedures for emergency situations?

3. Access rules and regulations and search procedures to be used before turning on the accelerator?

4. Instructions for the proper handling of radioactivity and disposal of radioactive waste?

5. Descriptions of the facility and the accelerator giving enough information so that people unfamiliar with it can make some estimate of the relative hazard that prevails? Are any special problems described?

VII. Personnel Monitoring

a. Requirement. Is suitable personnel monitoring required?

b. Calibration. Is the calibration correct for the circumstances under which the monitors are used?

c. Interpretation. Is there adequate justification for the interpretation of results and assumptions made in deriving dose equivalent?

d. Records. Are adequate monitoring records maintained and are they available to the supervisor and employees?

VIII. Area Monitoring and Surveys

a. Instruments

1. Calibration. Is their calibration correct for the circumstances under which monitoring or survey instruments are used?

2. Interpretation. Is there adequate justification for the interpretation of results and assumptions made in deriving dose equivalent?

b. Repetition. Are area radiation surveys performed at regular intervals?

c. Records. Do the records of radiation surveys include

1. Date and time and person doing?

2. Particle, energy, and current?

3. Target?

4. Collimator and magnets?

5. Purpose and detector used?

6. Location?

7. Results and recommendations?

d. Induced Activity

1. Accelerator. Have suitable measurements been made of the radioactivity induced in the accelerator itself, in targets, and in shielding? Are suitable methods used to reduce personnel exposures from this source?

2. Atmosphere. Have suitable measurements or estimates been made of radioactivity induced in air? If this is a problem, is ventilation adequate, and where does the exhausted air go?

3. Water. Have measurements been taken to ensure pipes carrying radioactive water do not pass through occupied areas, or are adequately shielded? Have suitable measures been taken for the storage and regeneration or disposal of deionising resins? Is a programme for monitoring the release of radioactivity in water necessary?

4. Workers. Are bioassay and whole-body counting procedures used occasionally to check for ingested or inhaled radioactivity?

IX. Education and Training of Operators, Support Personnel, and Others

Is there a regular programme of education training available? Does it include at least the following topics?

a. Radiation Safety

1. Interaction of radiation with matter
2. Units of dose and radioactivity
3. Biological hazards
4. Methods of control of exposure
5. Procedures

b. Radiation Detection

1. Use of instruments and personnel monitors
2. Survey and measurement techniques

c. Equipment

1. Accelerator
2. Remote handling devices
3. Interlocks

X. Relations Between Health Physics, Accelerator Operators, and Experiments.

Are the technical and personal relations between Health Physics, accelerator operators, experiments, and management good? Are there frequent interchanges of views and positions? Is there a radiation safety committee? If not, what takes its place?

REFERENCES FOR CHAPTER 5

ABHP 80 American Board of Health Physics, 'General Requirements of Certification' (1980).

ANSI 70 American National Standards Institute, 'Radiological Safety in the Design and Operation of Particle Accelerators', National Bureau of Standards, NBS Handbook 107 (1970).

ANSI 77 American National Standards Institute, Standard 43.2, Radiation Safety for X-Ray Defraction and Fluorescence Analysis Equipment, (1977).

ANSI 78 American National Standards Institute, Standard N43.2, Radiation Safety for X-Ray Diffraction and Fluorescence Analysis Equipment (1978).

ANSI 82 American National Standards Institute, Standard C95-1, Safety Levels with Respect to Human Exposure to Radiofrequency Electromagnetic Fields, 30 kHz to 100 GHz (1982).

An 81 Anderson, K. and Scott, K., Fundamentals of Industrial Toxicology, Ann Arbor Science Publishers, Ann Arbor, MI (1981).

CERN 75 European Organization for Nuclear Research (CERN), 'Radiation Safety Manual' (May, 1975).

Ch 81 Chissick, S.S. and Derricot, R. (Eds.), Occupational Health and Safety Management, John Wiley and Sons, Chichester (1981).

DEHW 68 U.S. Dept. of Health, Education and Welfare, Public Health Service, 'Particle Accelerator Safety Manual', MORP 68-12. Rockville, MD (October 1968).

Do 80 Doull, J., Klaassen, C.D. and Amdur, M.O. Casarett and Doull's Toxicology, MacMillan, New York, (1980).

DOE nd U.S. Dept. of Energy, DOE Order 5480.1, Chapter XI, Requirements for Radiation Protection (no date, continually revised).

IAEA 79 Swanson, W.P., Radiological Safety Aspects of the Operation of Electron Linear Accelerators, International Atomic Energy Agency, Technical Report Series No. 188, Vienna (1979).

ICRP 77 International Commission on Radiological Protection, 'Recommendations of the ICRP', Publication 26, Pergammon Press, Oxford (1977).

Hu 80 Hunter, D., The Diseases of Occupations, Hodder and Stougham, London (1980)

La 80 Last. J.M. (Ed), Maxcy - Rosenau, Public Health and Preventive Medicine, Appleton Century Crofts, New York (1980).

La 81 LaDou, J., Occupational Health Law - A Guide for Industry, Marcell Dekker, New York (1981).

LBL 76 Thomas, R. H. (Ed), 'The Environmental Surveillance Program of the Lawrence Berkeley Laboratory', Lawrence Berkeley Laboratory Report LBL-4678 (1976).

LBL 78 Lawrence Berkeley Laboratory, 'Pregnancy and Radiation', Lawrence Berkeley Laboratory Publication 105 (May 1978).

LBL 80a Lawrence Berkeley Laboratory, 'Charter for the Safety Review Committee, Lawrence Berkeley Laboratory, University of California' (Dec. 12, 1980).

LBL 80b Lawrence Berkeley Laboratory, 'Health and Safety Manual', Lawrence Berkeley Laboratory Publication 3000 (1980 and subsequent revisions).

LBL 82 Lawrence Berkeley Laboratory, 'Health and Safety Policy', Lawrence Berkeley Laboratory (June 1982).

LBL nd Lawrence Berkeley Laboratory, 'Regulations and Procedures Manual', Lawrence Berkeley Laboratory Publication 201, revised frequently (no specified date).

Ma 72 Martin, T.C. (Ed.), 'Accelerator Radiation Protection', Technical Report TR-73-7, U. S. Army Natick Laboratories, Natick, MA (1972).

NAS 81 National Academy of Science, Prudent Practice for Handling Hazardous Chemicals in Laboratories, National Academy Press, Washington, DC (1981).

NAS 83 National Academy of Science, Prudent Practice for the Disposal of Chemicals from Laboratories, National Academy Press, Washington DC (1981).

NBS 63 National Bureau of Standards, Maximum Permissible Body Burdens and Maximum Permissible Concentrations of Radionuclides in Air and in Water for Occupational Exposure, Handbook 69, U.S. Dept. of Commerce, Washington, DC (1963).

NCRP 68 National Council on Radiation Protection and Measurements, Medical X-Ray and Gamma-Ray Protection for Energies up to 10 MeV—Equipment Design and Use, Report 33, Washington, DC (1968).

NCRP 76 National Council on Radiation Protection and Measurements, Structural Shielding Design and Evaluation for Medical and Allied Health Personnel, Report 49, Washington, DC (1976).

NCRP 77a National Council on Radiation Protection and Measurements, Review of NCRP Radiation Dose Limit for Embryo and Fetus in Occupationally Exposed Women, Report 53, Washington, DC (1977).

NCRP 77b National Council on Radiation Protection and Measurements, Medical Radiation Exposure of Pregnant and Potentially Pregnant Woman, Report 56, Washington, DC (1977).

NCRP 78 National Council on Radiation Protection and Measurements, 'Operational Radiation Safety Program', Report 59, Washington DC (1978).

NFPA nd National Fire Protection Association, National Fire Codes, Boston, MA (published periodically).

NIOSH 78 National Institute of Occupational Safety and Health, The Industrial Environment—Its Evaluation and Control, U.S. Department of Health Education and Welfare, U.S. Government Printing Office, Washington DC (1973).

NSC 78 National Safety Council, Accident Prevention Manual for Industrial Operations, 7th Ed., NSC Chicago IL (1978).

NSC 79 National Safety Council, Fundamentals of Industrial Hygiene, 2nd Ed., National Safety Council, Chicago IL (1979).

OSHA 83 Occupational Safety and Health Administration, U.S. Department of Labor, OSHA Safety and Health Standards (29 CFR 1910), General Industry, Occupational Safety and Health Administration OSHA-2206 (Rev. March 11, 1983).

Pa 73 Patterson, H. W. and Thomas R. H., Accelerator Health Physics, Academic Press, New York (1973).

Pa 79 Patty's Industrial Hygiene and Toxicology (Third Revised Edition), Vol III. Theory and Rational of Industrial Hygiene Practice, L.J. Cradley and L.V. Cradley (Eds.), John Wiley and Sons, New York (1979).

Pa 81 Patty's Industrial Hygiene and Toxicology (Third Revised Edition), Vol I. General Principles, G.D. Clayton and F.E. Clayton (Eds.), John Wiley and Sons, New York (1981).

Pa 81a Patty's Industrial Hygiene and Toxicology (Third Revised Edition), Vol IIa Toxicology. G.D. Clayton and F.E. Clayton (Eds.), John Wiley and Sons, New York (1981).

Pa 81b Patty's Industrial Hygiene and Toxicology (Third Revised Edition), Vol IIb. Toxicology, G.D. Clayton and F.E. Clayton (Eds.), John Wiley and Sons, New York (1981).

Pa 82 Patty's Industrial Hygiene and Toxicology (Third Revised Edition), Vol IIc. Toxicology, G.D. Clayton and F.E. Clayton (Eds.), John Wiley and Sons, New York (1982).

Pe 75 Petersen, D., Safety Management, Aloray, Fairview, NJ (1975).

Pe 78 Petersen, D., Techniques of Safety Management, McGraw-Hill, New York (1978).

Pl 76 Plunkett, E.R., Handbook of Industrial Toxicology, Chemical Publishing Co. New York (1976).

Pr 78 Proctor, N.H. and Hughes, J.P., Chemical Hazards in the Work Place, J.P. Lippincott, Philadelphia (1978).

Pu 77 Purington, R.G. and Patterson, H.W., Handling Radiation Emergencies, National Fire Protection Association, Boston, MA (1977).

Sa 75 Sax, N.I., Dangerous Properties of Industrial Materials, Van Nostrand Reinhold (1975).

Sc 82 Schilling, R.S.F. (Ed), Occupational Health Practice, Butterworths, London (1982).

St 76 Steete, N.V.(Ed), Handbook of Laboratory Safety, Chemical Rubber Company, Cleveland, OH (1976).

Ze 80 Zenz, C. (Ed.), Developments in Occupational Medicine, Year Book Medical Publishers, Inc., Chicago, IL (1980).

FIGURE CAPTIONS FOR CHAPTER 5

Fig. 5.1. The three elements of a safety organization.

Fig. 5.2. An example for the organization of an occupational health programme at a large research laboratory.

Fig. 5.3. An example for the organization of a radiological safety group at an accelerator laboratory.

Fig. 5.4. A 'Caution Radiation Area' sign.

Fig. 5.5. A 'Caution High Radiation Area' sign.

Fig. 5.6. A 'Caution Radioactive Materials' sign.

Fig. 5.7. A 'No Activity Detected' tag.

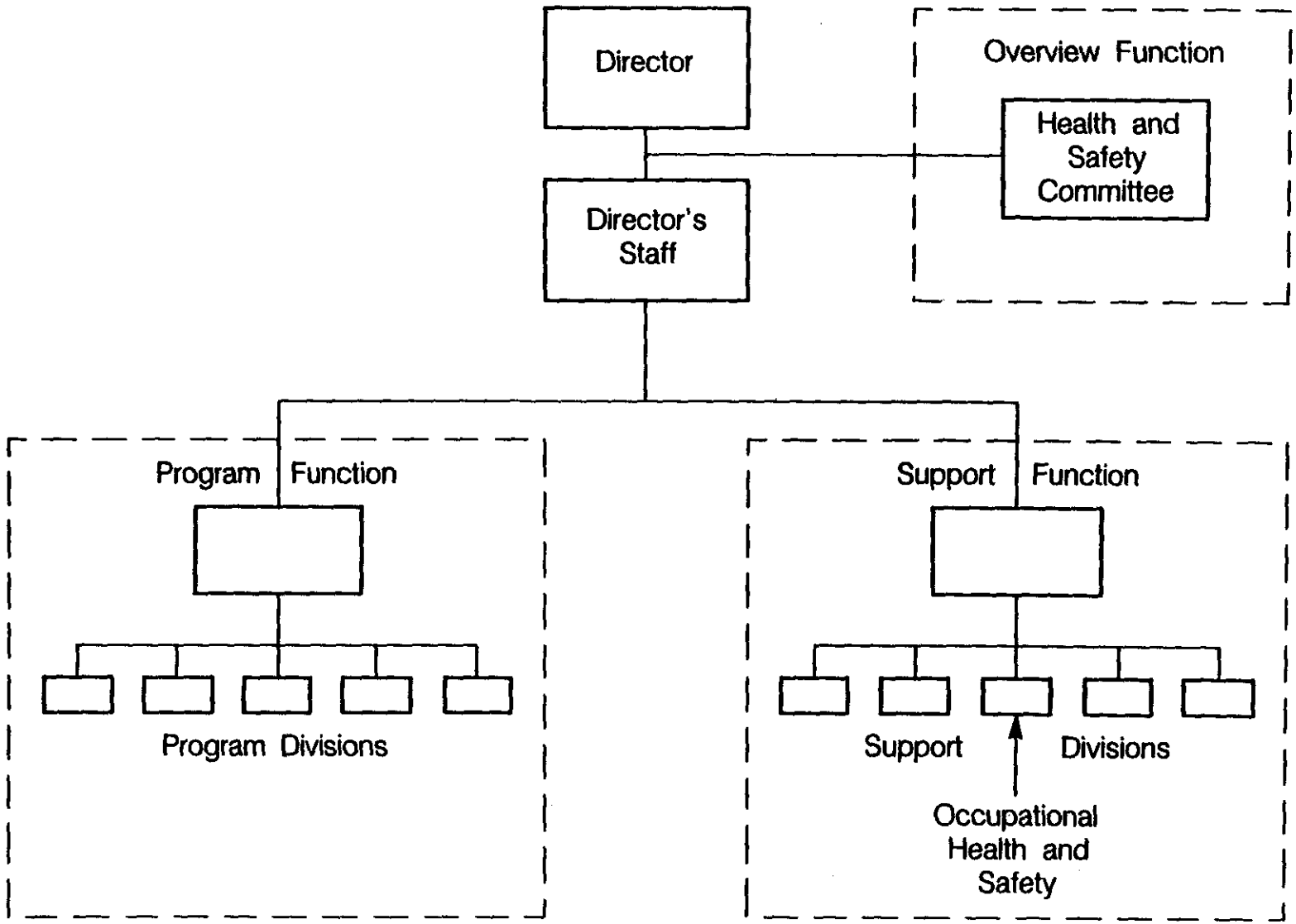
Director
Overview Function
Health and Safety Committee
Director's Staff
Program Function
Program Divisions
Support Function
Support Divisions
Occupational Health and Safety
XBL 858-9887

Fig. 5.1

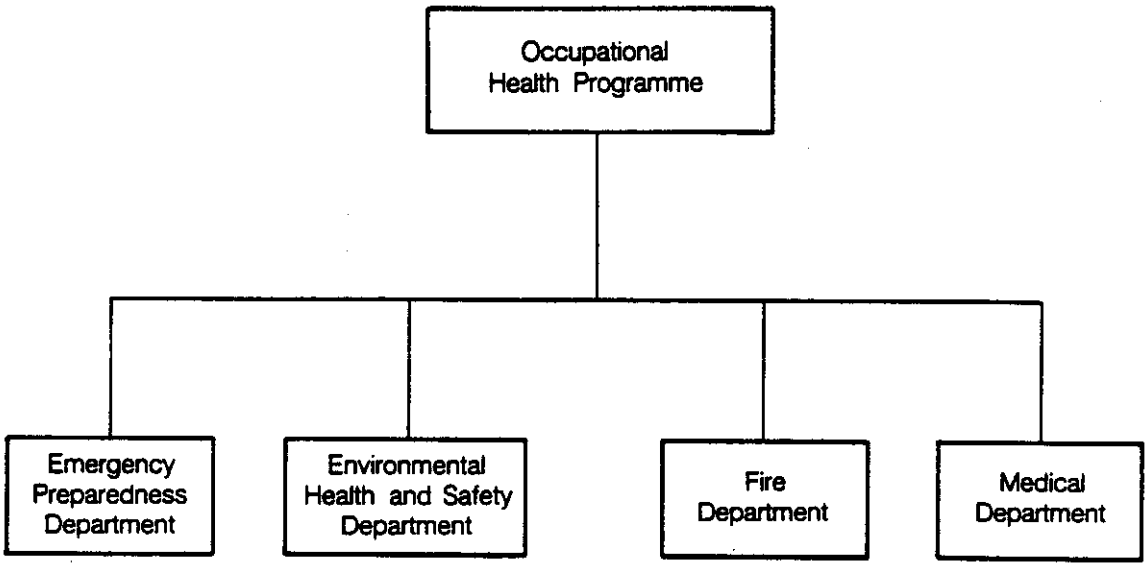
Occupational Health Programme
Emergency Preparedness Department
Environmental Health and Safety Department
Fire Department
Medical Department
XBL 859-3855

Fig. 5.2

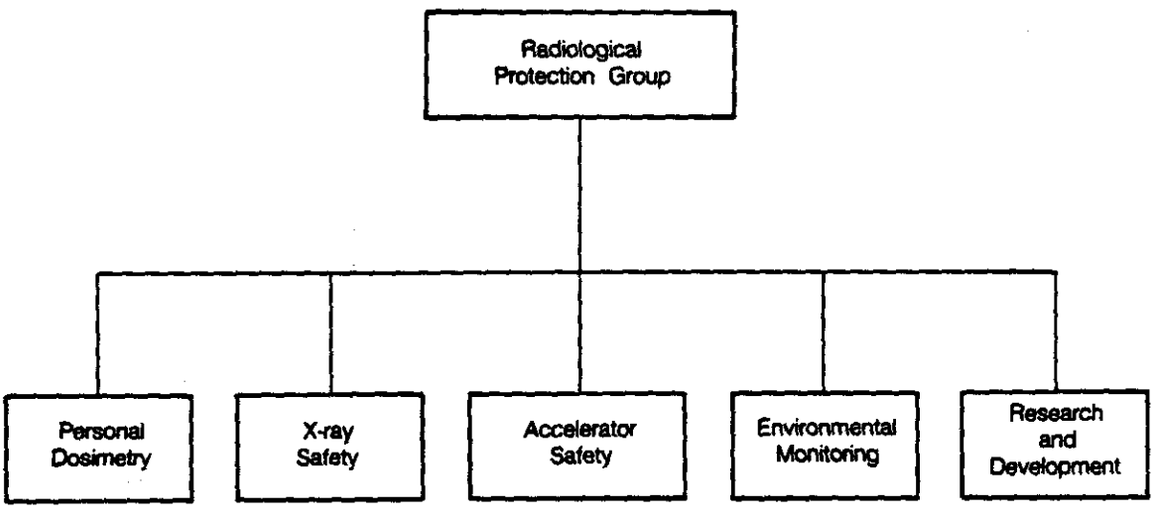
Radiological
Protection Group
Personal
Dosimetry
X-ray
Safety
Accelerator
Safety
Environmental
Monitoring
Research
and
Development
XBL 859-3854

Fig 5.3

Fig. 5.4

Fig. 5.5

Fig. 5.6

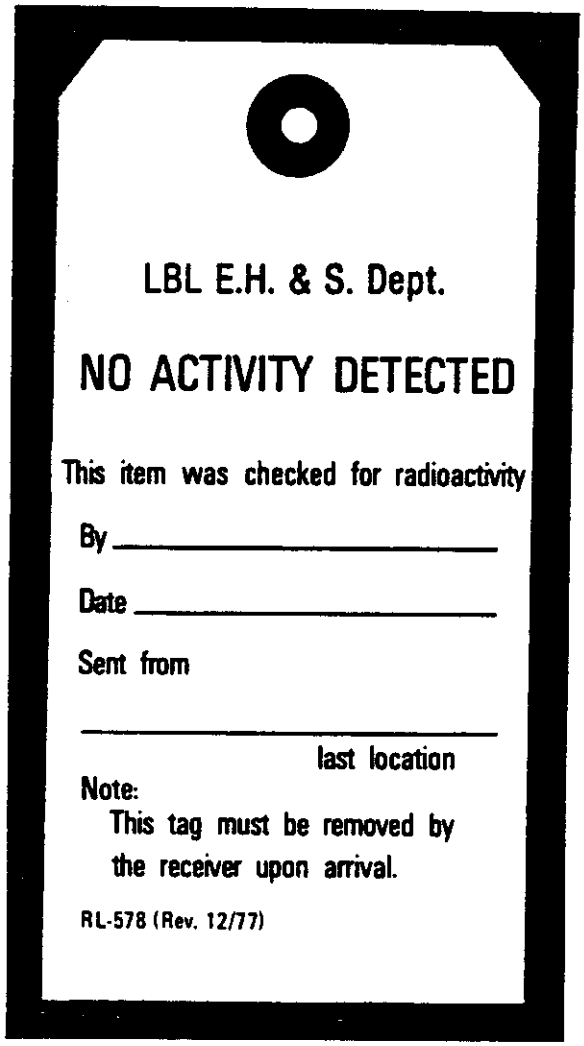
LBL E.H. & S. Dept.
NO ACTIVITY DETECTED
This item was checked for radioactivity
By _____
Date _____
Sent from
_____
last location
Note:
This tag must be removed by the receiver upon arrival.
RL-578 (Rev. 12/77)

Fig. 5.7

LAWRENCE BERKELEY LABORATORY
ADMINISTRATIVE MEMO

POLICY AND PROCEDURE

April 22, 1985 Volume XI, No. 21

EMPLOYEE RIGHTS AND OBLIGATIONS
(Update of Vol. X - No. 16)

Attached to this memorandum is a copy of the DOE poster on occupational safety and health protection, which is widely displayed around the Laboratory.

Please read this notice carefully since it summarizes both your rights and obligations under DOE Order 5483. Copies of this Order are available in Building B75B (Environmental Health and Safety Department).

This memo is being sent to all employees and guests as our annual reminder of your rights and obligations relating to health and safety.

Laboratory management is committed to providing safe and healthful working conditions. Please do your part toward achieving this goal.

David A. Shirley
Director

DAS:RHT:es
0878C

Attachment: 1

Distribution: Level I

Occupational Safety and Health Protection

Policy:

U.S. Department of Energy contractor employees shall be provided with safe and healthful working conditions in accordance with the standards prescribed pursuant to the Atomic Energy Act of 1954, as amended, the Energy Reorganization Act of 1974, and the Department of Energy Organization Act of 1977, which standards shall be at least as effective as those promulgated under the Occupational Safety and Health Act of 1970.

DOE Contractors:

DOE has determined that

University of California
Lawrence Berkeley Laboratory

is subject to DOE Procurement Regulation 9-50.704-2(a) and is required to comply with DOE safety and health standards. These standards are listed in DOE Order 5483.1 and are available for employee review at

Building B75B
U. C. Lawrence Berkeley Laboratory

The DOE contractor is required to:

1. Furnish to each employee employment and a place of employment which are free from recognized hazards that are causing or are likely to cause death or serious physical harm to employees.

2. Establish a program to monitor the workplace for known toxic materials and harmful physical agents which are used or produced at the facility, and maintain records of the data. As part of this program:

(a) Advise employees or their authorized representative that they are to be provided with an opportunity to observe monitoring or measuring for toxic materials or harmful physical agents and have access to the results thereof.

(b) Provide to each employee or former employee, within 45 days of the receipt of a written request, a written summary of any monitoring or bioassay records relevant to potential exposure to toxic materials or harmful physical agents during employment.

(c) Notify the employee promptly of any information indicating that an exposure to toxic materials or harmful physical agents may have exceeded DOE standards.

(d) Provide to each employee or former employee, within 45 days of the receipt of a written request, a written summary of the employee's cumulative recorded occupational radiation dose during employment.

(e) Notify the employee promptly of any radiation dose which exceeds the limits of DOE standards.

Employees:

All employees are required to:

1. Observe the DOE safety standards applicable to their work.

2. Report promptly to the contractor any condition which may lead to a violation of these standards.

3. Respond to warning signals which may be activated in the event of fire, radiation, or other possible emergencies.

4. Report emergencies using established procedures.

Inspections:

All activities under this contract are subject to inspection by DOE. When an inspection under DOE Order 5483.1 is conducted, a contractor representative and a representative authorized by the employees will be given an opportunity to accompany the DOE inspector during the inspection.

Where there is no representative authorized by the employees the DOE inspector will consult with a reasonable number of employees concerning safety and health conditions in the workplace.

Complaints:

Employees may file a complaint with the local DOE office using Form EV-628 to request an inspection of the workplace. Form EV-628 is available from

Environmental Health and Safety
Building B75B, U. C. L. B. L.

When the employee requests anonymity from the employer, DOE shall honor this request.

Nondiscrimination:

No contractor shall discharge or in any manner discriminate against any employee by virtue of the filing of a complaint, or in any other fashion exercising on behalf of himself or herself or others any action set forth in DOE Order 5483.1.

Inquiries:

Inquiries should be addressed to the contractor; however, additional inquiries may be addressed to the following local DOE official.

Director
Safety and Health Division
U. S. Department of Energy
1333 Broadway
Oakland, California 94612

Posting Requirements:

Copies of this notice must be posted in a sufficient number of places in Government-owned plants and facilities operated by DOE contractors subject to DOE PR 9-50.704-2(a) to permit employees working in or frequenting any portion of the plant to observe a copy on the way to or from their workplace.

U.S. Department of Energy

DOE F 5480.2 (11-81)

LAWRENCE BERKELEY LABORATORY
ADMINISTRATIVE MEMO

POLICY AND PROCEDURE

April 4, 1983 VolIX- No. 9

SAFETY REVIEW COMMITTEE

For many years the Laboratory has had a Safety Review Committee which reports to the Director, independently of the Associate Directors who have the line responsibility for the implementation of the Laboratory Health and Safety Policies. The Safety Review Committee, with its seven Subcommittees - Electrical Safety, Emergency Preparedness, Mechanical Safety, Radiation Safety, Seismic Safety, Toxic Substances, Traffic Safety - draws widely for membership from expertise available throughout the Laboratory. The Committee performs a valuable oversight function for the Director.

The charter, revised from that prepared in December 1980, is attached. I should like to thank Dr. Rolf Muller, Chairman of the Safety Review Committee, for preparing this revision.

David A. Shirley

DAS:mc

Distribution: LEVEL I

FUNCTION AND ORGANIZATION OF THE SAFETY REVIEW COMMITTEE

Introduction

The Safety Review Committee advises the Director on all aspects of health and safety policy. Its members are appointed by, are responsible to and serve at the pleasure of the Director of the Laboratory.

Functions and Responsibilities

The functions and responsibilities of the Safety Review Committee are:

(I) To advise the Director on any policy matters that affect the health and safety of all employees, participating guests and visitors of the laboratory, or which may adversely affect the general public or the environment.

(II) To make recommendations to the Director as to the need for new policies, or modifications to existing policies, on health and safety.

(III) To appoint subcommittees to address specific health and safety matters.

(IV) To oversee the implementation of safety policy throughout the Laboratory and specifically to assess the safety programs of the Laboratory Divisions.

(V) To review hazardous operations and designs for equipment for which no applicable standard exists.

(VI) To appraise the performance of the Health and Safety Section and Emergency Preparedness Organization.

(VII) To review requests for variances from Laboratory safety guidelines and procedures.

(VIII) To submit an annual report to the Director, describing the activities of the Committee.

Membership

The Safety Review Committee is made up of a chairperson, deputy chairperson, secretary, divisional representatives, chairperson of subcommittees and ex officio members.

Members are selected on the basis of their scientific activity, balance of technical knowledge and safety expertise. Participation by active experimental scientists is important to the functioning of the Safety Review Committee.

Members are appointed by the Director for an indefinite term.

The secretary of the Safety Review Committee is responsible for maintaining records of activities of the committee.

Subcommittees

The Safety Review Committee forms subcommittees as necessary to deal with safety matters that require special expertise, and to develop safety standards and procedures for operations for which there are no existing codes.

The chairperson of each subcommittee is a member of and reports to the Safety Review Committee. These subcommittees are comprised of individuals with special expertise in appraising difficult technical situations which might result in safety hazards.

Chairpersons of the subcommittees are appointed by the Chairperson of the Safety Review Committee from the membership of the committee. Chairpersons of subcommittees have the authority with Department or Division Head approval to appoint members to their respective subcommittees and to assign tasks to subcommittee members.

The chairperson of each subcommittee is responsible for maintaining records of the activities of the subcommittee and will submit a written annual report to the Safety Review Committee.

The present subcommittees are:

- Electrical Safety Subcommittee
- Emergency Preparedness Subcommittee
- Mechanical Safety Subcommittee
- Radiation Safety Subcommittee
- Seismic Safety Subcommittee
- Toxic Substances Safety Subcommittee
- Traffic Safety Subcommittee

Their functions and responsibilities are described below:

Electrical Safety Subcommittee

This subcommittee reviews all electrical and electronic equipment and their installations at the Laboratory from the standpoint of personnel and equipment safety. It issues guidelines for the safe operation of such equipment and investigates electrical safety problems referred to it by the Environmental Health and Safety Department. Members of the subcommittee also conduct annual electrical safety inspections for most areas within the Laboratory.

Each member of the subcommittee has a specified area of responsibility where he or she is familiar with the operation of equipment. The member is responsible to see that the equipment is maintained and operated within published guidelines. Equipment that is found to deviate from Laboratory guidelines/or is felt to present a hazard to personnel or equipment shall be shut down. If a disagreement on the interpretation or implementation of the guidelines arises the matter shall be brought to the attention of the chairperson of the subcommittee for resolution. Any member can request an interpretation of the rules by the chairperson and one other member of the subcommittee. Any request for a variance to the rules shall be made to the Safety Review Committee.

Emergency Preparedness Subcommittee

This subcommittee collects, updates and refines the emergency plans for each area and building and the overall plan for the Laboratory. This subcommittee plans for the coordination of the Director's Office, Medical Services, Protective Services, Environmental Health and Safety, Construction and Maintenance, Plant Engineering, Stores and Transportation Departments during emergencies.

Mechanical Safety Subcommittee

The Mechanical Safety Subcommittee reviews the mechanical design, fabrication, testing, operation and emergency procedures of hazardous research equipment such as pressure vessels, cryogenic apparatus and equipment containing flammable gases or liquids. It also reviews experimental setups where unusual arrangements of equipment may result in a potential hazard.

The subcommittee develops design standards for hazardous research equipment, novel experimental arrangements and new or unusual mechanical safety problems. Hazardous research equipment is defined as special equipment for scientific or developmental experiments having unusual personnel hazards not covered by conventional safety codes.

Radiation Safety Subcommittee

This subcommittee defines Radiation Safety problems that arise from the operation of equipment such as particle accelerators, X-ray sets, high voltage equipment and electron microscopes. It has been charged with the tasks of:

- Establishing a uniform set of radiation safety guidelines for all our particle accelerators.

- Establishing guidelines for the safe handling, posting and storage of induced materials produced by the accelerators.

- Evaluating the current personal dosimetry system; developing guidelines for the use of dosimeters at LBL accelerators.

Seismic Safety Subcommittee

The Seismic Safety Subcommittee provides guidance for structures and special LBL equipment involving "state-of-the-art" seismic design problems, or for those cases where the codes may not apply directly, by conducting Seismic Design Review meetings. These meetings are convened at the request of the person in charge of the equipment or experiment, who has the primary responsibility for the proper design, for carrying out the required procedures, and for the safe operation of equipment (as defined in LBL Publication 3001, Sec. 1.C.-1).

In the Seismic Design Review meetings, the subcommittee determines whether dynamic structural analyses are required or whether a static structural analysis is sufficient. The subcommittee provides a Design Earthquake (with time-history and special response data) if dynamic analyses are required.

The subcommittee is responsible for being aware of state-of-the-art developments in the seismic response of structures and for utilizing this knowledge in the performance of its functions. The seismic-safety codes have been in a state of rapid evolutionary change in recent years. Therefore, it is important to recognize this rapid evolution and its impact on the functions of subcommittee and on the LBL seismic safety policy.

The statutory seismic codes are changed as seismic knowledge is developed and codified. However, current codes necessarily lag the state-of-art developments and are considered a minimum LBL standard. Accordingly, all structures and equipment at LBL, as a minimum requirement, shall be designed and constructed to be in accordance with: (1) The latest edition of the "Uniform Building Code" and all other applicable seismic safety codes; and (2) LBL Publication 3001, "Rules and Procedures for the Design and Operation of Hazardous Research Equipment".

Toxic Substances Safety Subcommittee

The Toxic Substances Safety Subcommittee is charged with reviewing existing policies and procedures for the use, accountability and control of carcinogens, radioactive materials, sources and toxic chemicals; it also prepares and recommends new policies and procedures as required.

Traffic Safety Subcommittee

The Traffic Safety Subcommittee reviews moving traffic violations, vehicle accidents and their related causes such as road layouts and conditions, and makes recommendations for the correction of traffic safety hazards. It reviews all accidents involving laboratory-furnished vehicles whether on site or off site.

The committee serves as the hearing board for drivers who are involved in vehicle accidents or who receive moving traffic violation warnings or citations. Such drivers may be requested to appear before the board to review such incidents.

Procedure to Obtain a Variance from Laboratory Safety Guidelines

A variance from Laboratory safety guidelines may be requested from the Safety Review Committee. The Chairperson of the Safety Review Committee may ask that the request for a variance be first studied by the appropriate subcommittee. Approval or denial for a variance may be given after the written request with documentation has been discussed by the Safety Review Committee. Denial of a variance may be appealed to the Laboratory Director.

LAWRENCE BERKELEY LABORATORY
ADMINISTRATIVE MEMO

POLICY AND PROCEDURE

June 1, 1982 Volume VIII - 19

HEALTH AND SAFETY POLICY

It is the policy of the Lawrence Berkeley Laboratory to provide a safe and healthful working environment for its employees, participating guests and visitors and to prevent any harm to the health and safety of the general public or to the environment as a result of the Laboratory's activities. It is also policy to protect Laboratory property from damage or loss from accidents or other causes.

The Director of the Lawrence Berkeley Laboratory exercises the authority to carry out this policy and interpret the requirements for health, safety and emergency preparedness placed upon the University of California as a consequence of its contract with the United States Department of Energy (DOE) under contract DE-AC03-76SF00098 for the operation of the Laboratory.

Responsibility and Authority

The Director has delegated to all levels of management the authority necessary to implement the health, safety and emergency preparedness policies of the Laboratory.

- Associate Directors are responsible for assuring that the Laboratory's health, safety and emergency preparedness policies are being observed within their own Divisions.

- Building Managers are responsible for preparing, updating and implementing the emergency plan for their jurisdiction; taking charge of emergency actions; organizing safety training programs as needed and acting as a point of contact for building residents with respect to health, safety and emergency preparedness. Building Managers have been given the authority to see that safe work spaces are provided within the areas of their jurisdiction. It is incumbent upon those persons actually in charge of various departments, groups, activities, or experiments to carry out their operations safely, and to cooperate fully with the Building Managers.

- Each member of the Laboratory management is responsible for ensuring that employees and participating guests under his or her supervision are properly trained in safety and emergency procedures and are provided a safe and healthful working environment, free from undue hazards. In exercising this responsibility, all members of management may delegate authority and assign responsibility for a particular operation, but they retain accountability for oversights and errors that lead to injury, illness, or damage to property within their jurisdiction.

- Supervisors at all levels shall aggressively promote the safety and emergency prepardeness programs of the Laboratory.

- The Environmental Health and Safety Department is responsible for independently auditing for compliance all Laboratory activities with the applicable safety rules and standards and for providing appropriate technical services.

- The Emergency Preparedness Coordinator is responsible for monitoring compliance with applicable emergency preparedness policies.

It is a requirement of employment and for the use of the Laboratory's facilities that every employee, visiting scientist, or person performing work at the Laboratory or at one of the Laboratory's off-site locations, be familiar with and implement the applicable Laboratory safety standards. This responsibility includes taking the initiative to consult with resource groups listed below when assistance or advice is needed to carry out safe operations.

Performance Requirements

To achieve its safety goal, the Laboratory's safety program requires that supervisors and employees:

Comply with DOE's fire, health, safety, emergency preparedness and environmental control policies.

Plan and perform experiments and supporting work with full consideration given to prevention of accidents.

Prepare Operational Safety Procedures for operations that involve potentially hazardous conditions and are not covered by health and safety regulations.

Proceed with work only after having implemented appropriate safety procedures.

Train employees and guests to perform all work safely and to be particularly aware of potentially hazardous operations.

Correct hazardous conditions promptly after they are discovered.

Assure that personal exposure to toxic chemicals, ionizing radiation and contaminants released to the environment be maintained as low as reasonably achievable.

Safety Resources

To aid supervisors and employees in establishing and maintaining an accident-free working environment, the Laboratory issues Pub. 3000, the Health and Safety Manual, for general guidance. The safe design and operation of hazardous experimental equipment is discussed in Pub. 3001, Rules and Procedures for the Design and Operation of Hazardous Research Equipment. Applicable rules and procedures extend to all Laboratory operations. These publications are available from the Environmental Health and Safety Department, which also issues manuals and reports discussing safety in specialized areas. It is the responsibility of every employee to be familiar with these publications, and to apply the rules and regulations that are applicable in planning and carrying out their work. In addition, the Laboratory makes available the services of the Environmental Health and Safety Department and Medical Services Department. These departments can provide specialized support skills and resources. The personnel of these groups evaluate operations for hazardous conditions, recommend methods of safe operations, and monitor the work environment for all groups at the Laboratory.

Safety Review Committee

Work at the Laboratory is often experimental in nature and involves several different areas of science and technology for which there are no published safety guidelines or applicable codes or regulations. Therefore the Safety Review Committee has been established and its members, who represent a broad range of scientific and safety experience, are appointed by the Director. The functions and responsibilities of this committee are described in its Charter.

The Safety Review Committee has formed several subcommittees to deal with specialized safety problems.

These subcommittees are:

Mechanical Safety Subcommittee

Electrical Safety Subcommittee

Emergency Preparedness Advisory Subcommittee

Seismic Safety Subcommittee

Toxic Substances Safety Subcommittee

Traffic Safety Subcommittee

Radiation Safety Subcommittee

The Chairman of each Subcommittee is a member of and reports to the Safety Review Committee. The Subcommittees comprise individuals with a wide variety of experience in appraising difficult technical situations which might result in safety hazards. They are a valuable Laboratory resource available to all who use the Laboratory's facilities.

David A. Shirley

David A. Shirley
Director
Lawrence Berkeley Laboratory

DAS:mc

CHAPTER 6

The Radiological Environmental Impact of Accelerators

And, as imagination bodies forth
The form of things unknown, the poet's pen
Turns them to shapes, and gives to airy nothing
A local habitation and a name.
Such tricks hath strong imagination,
...
And in the night, imagining some fear
How easy is a bush suppos'd a bear!

from 'A Midsummer Night's Dream',
Act 5, Scene 1
William Shakespeare (1564-1616)

CHAPTER 6 CONTENTS

6.1 The Radiological Impact of Accelerators

6.2 Skyshine

The Stray Radiation Field

Population Exposure from Accelerator Prompt Radiation

6.3 Radioactivity Produced in the Accelerator Structure and its Surroundings

Total Radioactivity

Quantity of Radioactivity in Earth and Groundwater

Summary of the Production of Radioactivy by High-Energy Accelerators

6.4 Radioactivity in Earth and Water

Radioactivity Produced in Earth

Radioactivity Produced in Cooling Water

Radioactivity Produced in Ground Water

6.5 The Environmental Impact of the Radioactivity Produced in the Earth and Ground Water

Radionuclide Production in Water

Radionuclides Resulting from Dissolved Solids in Water

Radionuclides Produced in the Earth

The Migration of Radionuclides through the Ground

Potential Contamination of Drinking Water Supplies

Population Exposure from Accelerator-Produced Nuclides in Ground Water

6.6 Radioactivity Produced in the Atmosphere

Radionuclides Produced in Air by Accelerator Operation

Radionuclides Produced in Dust

Gaseous Radionuclides Released from Water

Environmental Impact of Airborne Radionuclides

Population Exposure from Radioactivity in the Air

References for Chapter 6

Figure Captions for Chapter 6

Appendix 6.1. Neutron Importance Functions

Appendix 6.2. Photon Importance Functions

CHAPTER 6

THE RADIOLOGICAL ENVIRONMENTAL IMPACT OF ACCELERATORS

6.1 THE RADIOLOGICAL IMPACT OF ACCELERATORS

In assessing the radiological impact of an accelerator installation, attention must be given to the following exposure pathways:

- Prompt radiation fields during accelerator operation,
- Radionuclides and noxious chemicals (such as ozone and nitric oxide) in the air of the accelerator vault and their subsequent release,
- Radionuclides in the soil and ground water near the accelerator and possible subsequent migration from the accelerator site into wells or other sources of potable water,
- Radionuclides in the cooling water of the installation that may mix with, or be accidentally released into, the normal effluent,
- Long-lived radionuclides in accelerator components that may subsequently be recycled, with consequent transmission of the radionuclides into the general environment; this would be particularly true for valuable metals such as copper, brass, iron, or aluminum.

For prompt stray radiation, it is necessary to assess only external exposure; for radioactivity in air and water, both external and internal exposure pathways must be considered.

This chapter will not discuss the radiological impact of accelerators whose primary purpose is to produce radioisotopes. The impact of such accelerators depends mainly on the radiotoxicity and quantities of radioisotopes produced and on the separation procedures used (Bi 80, Ci 79). These problems must be treated individually with a full knowledge of each possible exposure pathway. Another problem that requires individual attention and will not be treated here is the introduction of radioisotopes into the accelerator as a target material; tritium gas, for example, could be released by a rupture or by absorption in vacuum-pump oil, or could be accelerated. These problems depend more on the quantity of the radioisotope introduced into the accelerator rather than on the operation of the accelerator itself.

The problems that will be treated in this chapter are:

- The spectrum of particles leaving the accelerator enclosure and the scattering and transport of these particles in the air/ground/building complex to the point where they can irradiate persons outside the accelerator laboratory,
- The radionuclides of importance created in the air of the accelerator enclosure and the release of this air into the environment,

- The radionuclides of importance created in cooling water and in ground water around the accelerator, together with their subsequent migration (with consideration, as well, of radioisotopes in surrounding soil that may be leached by rain or ground-water movement).

6.2 SKYSHINE

THE STRAY RADIATION FIELD

As it appears in the literature, the word skyshine refers to all the radiation reaching a point in the vicinity of an accelerator, whether unscattered (direct) or scattered by ground, air, or neighboring buildings (indirect). In this section, we will assume that the environmental point of interest is at least 50–100 metres from the accelerator enclosure and that it is shielded from a direct view of the outer surface of the enclosure, so that the radiation environment is dominated by particles that have undergone elastic and inelastic scattering in the air and, perhaps, in the ground before reaching the point of interest.

A summary of the skyshine phenomenon around accelerators was given by Rindi and Thomas, where experience up to 1975 was reviewed (Ri 75). Experience has shown that neutrons will be the dominant skyshine component, and Fig. 6.1 shows measurements of neutron flux density versus distance at several accelerators. It can be concluded from the data that the empirical relation

$$\phi(r) = \frac{Q \exp(-r/\lambda)}{4\pi r^2} \qquad (6.1)$$

is a simple but adequate expression for the skyshine intensity around most accelerators, where r is the distance from the accelerator enclosure, Q is an effective source strength of neutrons emitted from the shield surface, and λ is an effective absorption length.

The use of Eq. (6.1) requires knowledge of the two parameters λ and Q. The values of λ observed in practice vary between 267 m and 990 m (Ri 75). The lower value generally pertains to those conditions when low energy neutrons dominate the shield leakage spectra, and the higher value is more appropriate where the high-energy cascade in the shield may be considered as continuing in the air, giving rise to a diffuse source of evaporation neutrons, which then is subsequently scattered before arriving at the point of interest. In this latter case, λ should approximately correspond to the value of the high-energy absorption mean free path in air (100 g/cm^2 or 850 m for air at STP). The data summarized by Rindi and Thomas tend to confirm this hypothesis, but Katoh and his co-workers have reported a value of 1300 m from data obtained around the KEK proton synchrotron (Mi 77, Ka 78a). This value of λ, however, may have been elevated by the presence of multiple sources (Ka 77).

The practical use of Eq. (6.1) is also limited by the choice of the value of the effective source strength, which depends on the energy spectrum and angular distribution of particles leaving the enclosure surface. Effective neutron source strengths have appeared to be unique to each accelerator, because their value depended strongly on the amount

of local shielding and, to some extent, on the technique used to measure the leakage neutrons.

Any complete theoretical treatment of skyshine from accelerators must treat the transport through the air of neutrons with energies of up to hundreds of MeV. Much of the published work, however, is limited to neutrons of energy up to a few MeV.

In 1957, in one of the first theoretical studies of the subject, Lindenbaum (Li 57, Mo 57) formulated an expression to describe the propagation of low-energy neutrons (~few MeV) through the atmosphere. This work, which incidentally introduced the term skyshine for these phenomena at high-energy proton accelerators, was based on experience at the Brookhaven National Laboratory Cosmotron.

In essence, Lindenbaum used the expression for the neutron flux produced by a point source in an infinite isotropic scattering medium. This expression was derived by Case et al. (Ca 53) using diffusion theory. Lindenbaum wrote the scalar neutron flux density, ϕ (r), in the form:

$$\phi(r) = \frac{Qe^{-\Sigma_t r}}{4\pi r^2}\,\epsilon(c,r) + \frac{Qk(c)e^{-k_0 r}}{4\pi D r}, \qquad (6.2)$$

where Q = neutron source strength (neutrons s^{-1}),

Σ_t = macroscopic total cross section,

D = diffusion coefficient,

$1/k_0$ = diffusion length,

c = Σ_s/Σ_t, the ratio of the scattering cross section (Σ_s) to the total cross section, and $\epsilon(c,r)$ and k(c) are functions of c.

The assumptions made in the Case formulation are:

- One velocity group neutron diffusion, i.e., the source emits monoenergetic neutrons and neutrons arriving at points distant from the source have the same energy as those emitted at the source (they do not lose any kinetic energy in elastic collisions).
- The source is an isotropic point source.
- Neutrons diffuse in an infinite uniform absorbing medium (taken to be air by Lindenbaum).
- Scattering is isotropic in the center-of-mass system.

Given these assumptions, the general solution to the steady-state

problem (i.e., a source intensity constant with time) has for the flux density the familiar form Eq. (6.2) given by Lindenbaum.

For neutrons of a few MeV transported in air substitution of the appropriate numerical value for the parameters in Eq. (6.2) yields:

$$\phi(r) = Q \left\{ \frac{7.9 \times 10^{-2}}{r^2} \exp(-r/1.4 \times 10^4) + \frac{1.4 \times 10^{-5}}{r} \exp(r/2.5 \times 10^4) \right\} \quad (6.3)$$

where ϕ is in neutrons cm^{-2} s^{-1},

r is in cm,

Q is in neutrons s^{-1}.

The presence of the ground requires some modification of Eq. (6.2). Lindenbaum suggested this could be adequately achieved by changing only the value of c. Such a change limits the use of the equation to the transport of neutrons of few MeV. Lindenbaum pointed out that if higher-energy neutrons were to be considered, changes in both mean free path and c would be necessary.

The first term of Eq. (6.2) is almost identical with the equation describing propagation of radiation from a point source with absorption but without scattering. With the values of the parameters proposed by Lindenbaum, the first term of Eq. (6.3) becomes negligible in comparison with the second for distances larger than about 3 mean free paths in air (some 300 m). The second term of Eq. (6.3) represents the component of the radiation field scattered to the point of measurement from all directions. In practice, the component of the radiation field at a point arriving from the ground is much smaller than that arriving from the air.

Lindenbaum's equation was intended to describe those situations where the neutron-leakage spectrum into the air was composed of, or at least strongly dominated by, neutrons in a narrow band of energy in the MeV region. When neutrons in the MeV region are dominant–as for example when there is either no roof shielding or the shield is constructed of materials containing little or no hydrogen (e.g., steel or lead), Lindenbaum's equation can predict neutron flux densities to within a factor of three at distances out to ~200 m. In particular, reasonable agreement (within a factor of 2) was found between measurements within a range of 30 and 150 m at the Cosmotron and theoretical estimates using Eq. (6.3) (Li 61). Other workers have developed treatments of skyshine similar to those of Lindenbaum (Pa 57, Wi 57). For those cases where the accelerator is well shielded with earth or concrete, the radiation field is controlled by high-energy neutrons (E > 100 MeV), and Lindenbaum's equation cannot be expected to have great accuracy.

However, even under such conditions it can often predict neutron dose-equivalent rates with an accuracy adequate for the purposes of health physics.

More recently, Kinney (Ki 62) used the 05R Monte Carlo neutron transport code (Co 60, Ir 65) to study the transport of neutrons with source energies between 1 and 20 MeV at an air-earth interface. Kinney's calculations give the spectrum of neutrons at radial distances out to 4000 m for a source with an isotropic angular distribution for three cases: (1) at an air-ground (SiO_2) interface, (2) for an infinite air medium, and (3) on the interface between air and a totally absorbing black ground. The results can be interpreted in terms of flux density or dose equivalent since the neutron spectrum is given. It has been suggested (Ki 62) that for positions near the source the flux density values are higher (because of the moderating effect of the ground) for the air-ground than for the infinite air calculation for energies below the source energy; for locations far from the source, the ground lowers the flux density at all energies.

Ladu et al. (La 68) have also carried out Monte Carlo calculations for an isotropic point source of 5-MeV neutrons at an air-earth interface. They also studied the influence of lateral shielding by performing the calculations for various values of the solid angle subtended upward by the source, $\omega = 2\pi(1 - \cos\theta)$. Values of θ chosen were 30°, 60°, and 90°. The first two cases correspond to accelerators without roof shielding but with thick lateral shielding, and the last case corresponds to no shielding whatever.

Ladu et al. give two representations for the variation with distance of the total neutron fluence per neutron emitted, depending on the distance of the observer from the source r, given in Eqs. (6.4a) and (6.4b).

$$\phi(r) = A\, r^{-\alpha} \qquad 20\ \text{m} < r < 300\ \text{m} \qquad (6.4a)$$

$$\phi(r) = B \exp(-r/\lambda) \qquad r > 300\ \text{m} \qquad (6.4b)$$

The values of the constants A, B, α, and λ depend somewhat on the semivertical angle of the neutron emission cone θ (see Table 6.1).

Ladu et al. conclude that the transport of low-energy neutrons (few MeV) produced at air-earth interfaces is quite well understood—a view supported by the good agreement between various theoretical treatments of low-energy neutron and secondary γ-ray transport through air and between the calculations and experiments.

Nakamura et al. (Na 81a, 81b) have recently studied the accelerator skyshine problem by using a development (Ha 76) of the MORSE Monte Carlo neutron transport code (Em 75). Their calculations of neutron fluence per unit neutron emitted isotropically into the upward hemisphere (semivertical angle 85°) are shown as a function of distance from the source point in Fig. 6.2. For comparison, the results of the Kinney calculations (Ki 62) for the air/ground interface and the 'black-ground' conditions, the Lindenbaum/Ladu comparison taken from Ladu et al. (La 68), and a calculation by Nakamura and Kosako (Na 81a), all for a

semivertical angle of 90°, are also shown in Fig. 6.2.

There are many minor differences in the conditions for which the calculations shown in Fig. 6.2 were made. These differences may be summarized as follows:

- The Lindenbaum calculation (Li 57) is a monoenergetic diffusion calculation in an infinite medium with a very crude approximation for the presence of the ground.
- The data of Kinney (Ki 62) have only very limited statistics and the calculations use a special form of 'last-collision' estimator to obtain the fluence.
- The calculation by Ladu et al. (La 68) is for a neutron source energy of 5 MeV rather than 2 MeV.
- The calculations of Nakamura and Kosako (Na 81a) approximate ground scattering by using albedo data for concrete rather than attempting a full treatment of the scattering in earth.

However, upon examination, the agreement between these various calculations shown in Fig. 6.2 is seen to be quite good.

A calculation similar to those of Fig. 6.2 was made by Alsmiller et al. (Al 81) using the discrete ordinates transport (DOT) code in the adjoint mode (Rh 78). For selected distances from the skyshine source these authors calculated the dose equivalent at each distance as a function of the energy of the source neutron and as a function of the semivertical angle of the emission cone; the authors defined this quantity as the 'neutron importance' and it has the units of dose-equivalent/neutron. Appendix 6.1 tabulates these importance functions.

A comparison of the Nakamura and Alsmiller calculations for neutrons emitted into a cone with a small vertex angle is given in Fig. 6.3. Comparison is complicated by minor differences in the intrinsic assumptions of these two calculations. The Alsmiller calculations are for a semivertical angle of 37°, whereas the Nakamura data for 0° have been used in Fig. 6.3 [the latter calculations, however, showed very little dependence of dose equivalent on semivertical angle in this range. This difference in semivertical angle should not therefore result in serious differences.] Another difference is that the Alsmiller dose equivalent includes a photon contribution generated by the neutron interactions. Although Fig. 6.3 shows that the Nakamura calculations give somewhat lower values of dose equivalent per neutron emitted than those obtained by Alsmiller et al., as would thus be expected from the difference in dose equivalents calculated, this difference is also in the direction to be expected from any comparison between weighted Monte Carlo and discrete ordinates methods in a low-probability region.

The use of the importance functions calculated by Alsmiller et al. (Al 81) for the conditions of the Brookhaven Alternating Gradient Synchrotron (AGS) experiment (Di 66) of Fig. 6.1 was shown to give good agreement with the form of the experimental data (see Fig. 6.4), but the prediction differs from the experiment on an absolute basis by a factor of 2.5. The same importance functions were used by Stevenson and Thomas

(St 84a) under the conditions of the experiments reported by Nakamura et al. (Na 81a, Na 81b). The comparison by Nakamura et al. between their calculations and measurements is shown in Figs. 6.5 and 6.6. Also shown in these latter two figures are our own calculations of neutron dose equivalent as a function of distance using the spectra and neutron emission of Nakamura but folding these spectra with the importance functions of Alsmiller et al. (St 84a). It will be seen that the points calculated in this manner are as in good agreement with experiment as those of Nakamura et al. for the YAYOI reactor spectrum and are in better agreement with the experimental data for the accelerator spectrum. It would thus appear that the importance functions calculated by Alsmiller et al. form a reasonable basis for the estimation of dose equivalent from skyshine neutrons. However, in their present form they are too cumbersome and ill-adapted for similar desk-top calculations. The authors have therefore studied the way in which parameters for Eq. (6.1) may be obtained from the importance functions given by Alsmiller et al. (Al 81).

In order to derive a recipe for skyshine neutron calculations at proton accelerators, two simplifying assumptions were made:

- That the differential neutron energy spectrum has the form 1/E up to a neutron energy equal to the maximum proton energy of the accelerator and zero at higher energies. This maximum energy is called the upper energy of the neutron spectrum. Such an assumption has the effect of overestimating the more penetrating neutron component.
- That neutrons are emitted into a cone whose semivertical angle is about 75°. This may lead to an overestimation of the dose equivalent at large distances by as much as a factor of three for sources that emit into cones of very small semivertical angle.

The appropriate absorption length for insertion into Eq. (6.1) may be found in the following way:

The variation of dose equivalent with distance, as calculated using the response matrix from Al 81, is shown in Fig. 6.7, for various upper energies of the 1/E spectrum. Since the ordinate has been multiplied by distance squared, the graph gives the departure from an inverse square law. The points at 495 and 1005 m have been used to obtain an effective absorption length (which is shown plotted as a function of upper energy in Fig. 6.8).

Figures 6.7 and 6.8 also indicate data obtained from the measurements of Distenfeld and Colvett (Di 66), made at Brookhaven. The dose equivalent data reported (Fig. 6.7) have been normalized to total neutron emission from the accelerator shield. The total neutron emission was obtained using the measured emission for particles with energies above 20 MeV (Di 66) and Hack's observation that for typical spectra of neutrons leaving the shield of a multi-GeV proton accelerator such particles amount to one-half of the total emission (Ha 69).

The effective absorption lengths for energies of 30 MeV and 50 MeV determined from Fig. 6.8 are compared with the Rutherford Laboratory Proton Linear Accelerator data of Fig. 6.1 (Th 62, Si 62). This

comparison is shown in Fig. 6.9, where the slopes corresponding to the absorption lengths for the two proton energies are seen to be in reasonable agreement with the experimental data.

Finally a source term is required. This may be obtained by extrapolating the exponential through the data at 495 and 1005 m in Fig. 6.7 to zero distance from the source. The values of the source term so obtained range from 1.5 to 3×10^{-15} Sv m^2/neutron. The source term from the BNL experiment also falls within this range.

From the conservative upper bound of these values the neutron dose equivalent per neutron emitted from the source can be calculated as a function of distance from the source from a relation of the form

$$H(r) = 3 \times 10^{-15} \exp(-r/\lambda)/r^2 \text{ Sv/neutron} \quad , \qquad (6.2)$$

where r is measured in metres.

If the number of neutrons emitted is not known directly, it can be inferred from the dose equivalent and surface area of the skyshine source. Table 6.2 gives the average dose equivalent per unit neutron fluence of 1/E spectra for maximum energies ranging from 1 to 400 MeV, determined from the data of ICRP-21 (ICRP 73a). It should be noted that the dose equivalent per unit fluence for a neutron spectrum found outside a 50-MeV proton linear accelerator was approximately 8 fSv m^2 (Sh 69), which can be compared with 10 fSv m^2 from Table 6.2. The same reference gives values of between 30 and 50 fSv m^2 for neutron spectra outside the shielding of proton synchrotrons of 6–24 GeV energy, to be compared with 35–40 fSv m^2 deduced from Table 6.2.

As an approximate check on this procedure, even though the data of Nakamura et al. (Na 81b) pertain to an electron synchrotron, the given source spectrum was used to determine an average dose equivalent per neutron and, thus, an effective upper energy of a 1/E spectrum from Table 6.2. This allowed an appropriate λ to be deduced from Fig. 6.8. The values of dose equivalent obtained by using this value of λ and the given neutron emission in Eq. (6.6) are a factor of two higher than those obtained by the complete analysis indicated in Fig. 6.6 over the whole distance range.

The use of Eq. (6.2) will result in an overestimate of the dose equivalent for distances less than 400 m as will be seen from Fig. 6.7. The use of this procedure, which is derived from the data for a semivertical angle of nearly 90°, will also produce some overestimation of the resulting dose equivalent for sources that emit into cones of smaller semivertical angles, since the dose equivalent for smaller angles falls off faster with distance than does the data for 90°.

If the overestimation arising from any of these assumptions is not acceptable, then the full importance functions must be used with the full angular and energy spectrum of the source neutrons. However, it should also be noted that the dose equivalent calculated using the ICRP-21 (ICRP 73a) conversion coefficients as in Ref. Al 81 will overestimate the effective dose equivalent to a person exposed to low-energy neutron and photon skyshine because of the random orientation of the human body with respect to the incident radiation. This overestimate

can be as high as a factor of two (Bu 81).

Nakamura and colleagues have reported measurements of skyshine neutrons and photons produced by 52-MeV protons at the cyclotron of the Institute of Nuclear Study, Tokyo (Na 75). The authors showed that skyshine photons are transported in the atmosphere with approximately the same dependence on distance as both thermal and fast neutrons. These measurements support the hypothesis that the relative importance of photons will not increase with distance from high-energy accelerators. In fact, at accelerators where photons are initially dominant, the fraction of total dose equivalent contributed by neutrons will increase because photons will be absorbed more rapidly in the atmosphere. Ultimately, an equilibrium will be achieved with high-energy neutrons controlling the photon production. Measurements of the energy spectrum of scattered photons show a prominent 2.2-MeV peak resulting from the capture of thermal neutrons in hydrogen. At higher energies, the photon spectrum falls monotonically with a 'knee' at about 7 MeV (see Fig. 6.10).

The calculations of skyshine by Alsmiller et al. (Al 81) also gave the photon importance matrix (see Appendix 6.2), which can be used if it is thought that photon skyshine could be dominant.

Under certain shielding conditions, muons may be observed as a major component of the stray radiation field at the Brookhaven (Co 62) or the CERN Proton Synchrotron (PS). Hoefert and Baarli have described the use of a counter telescope to locate the source of muons and leakage in the shielding at the CERN PS (Ho 73).

At the 500-GeV proton synchrotron of the Fermi National Accelerator Laboratory (FNAL), muons are the dominant component of the radiation at the site boundary (Ba 76). This is in part due to the large distances from the accelerator to the site boundary. Neutrons produced at the accelerator are greatly reduced in intensity at the laboratory perimeter by inverse square law and air attenuation. Muons, on the other hand, as a consequence of experimental use of the accelerator, are produced in a highly collimated beam directed towards the site boundary. Because of their weak interaction with matter, they survive thick shielding and emerge into the air still well collimated. At the site boundary, a well-defined 'beam' ~50 m wide can be identified. The maximum dose equivalent at the site boundary was 2 mrem during 1974. At FNAL, as at CERN, a muon telescope is used to locate the origin of the more energetic muons.

POPULATION EXPOSURE FROM ACCELERATOR PROMPT RADIATION

Because the prompt radiation field dominates the radiation environment of high-energy accelerators (as we shall show in later sections) it is the dominant source of population exposure resulting from accelerator operations.

There is no generally accepted method of calculating the population exposure resulting from accelerator operation (Je 74, Ri 75). In the following discussion, a model suggested by Stephens et al. (St 75, 76) is described.

The population dose equivalent resulting from operation of a nuclear facility, M, is defined by the equation (ICRP 73b):

$$M = \int_{H_{MIN}}^{H_{MAX}} H\, N(H)\, dH \qquad (6.7)$$

where N(H)dH is the number of people receiving a dose equivalent H, and the subscripts refer to the minimum and maximum dose equivalent.

For accelerator laboratories, where M is averaged over an extended period such as a year, it has been suggested (St 75) that Eq. (6.7) be replaced by the equation:

$$M = \int_{R_{MIN}}^{R_{MAX}} H(r)\, N(r)\, dr \qquad (6.8)$$

where H(r) is the annual dose equivalent at a distance r from the accelerator, and R_{MAX} and R_{MIN} are the furthest and closest possible distance within which members of the public approach the accelerator.

It has been shown (St 76) that Eq. (6.8) may be numerically evaluated using the approximation:

$$M = \frac{2\pi r_0^2\, H_0 e^{r_0/\lambda}}{S_1 S_2} \sum_{i=0}^{i=n} \frac{N_i}{\pi(r_i^2 - r_{i-1}^2)} \int_{r_{i-1}}^{r_i} \frac{e^{-r/\lambda}}{r}\, dr \qquad (6.9)$$

where H_0 is the annual dose equivalent at the laboratory boundary; λ has previously been defined; N_i is the average number of people who may be considered permanently resident between distances r_{i-1} and r_i from the accelerator; $S_1 S_2$ are shielding factors for surrounding hills and buildings; and r_o, r_n correspond to R_{MIN} and R_{MAX} in Eq. (6.8).

The accuracy of the estimate of population dose equivalent obtained using Eq. (6.7) will depend upon whether the parameters λ and n are correctly chosen.

Values of λ may range from about 225 m to 850 m. Assuming a uniform population density around an accelerator laboratory the integral of equation 6.9 reduces to the exponential integral that is tabulated (Ka 78b). Under these conditions Stephens et al. (St 75) showed that the population dose equivalent was approximately proportional to $\lambda^{2/3}$. Thus, if a conservative value of λ is assumed (850 m), the population dose equivalent could be overestimated by as much as a factor of 2.5 if the leakage spectrum from the accelerator shield were rich in low-energy neutrons.

Typically, the population dose equivalent converges towards its ultimate value within a few kilometres from the accelerator. For example, at the Lawrence Berkeley Laboratory (LBL), the population dose equivalent reaches its ultimate value at about 5 km from the Laboratory (Figure 6.11). Thus, although in the United States it is conventional to quote the 80-km (50-mile) population dose equivalent, the value of r_n in Eq. (6.7) will, in general, be much smaller.

The extent of the radiological impact on the environment resulting from penetrating radiation produced by high-energy accelerators may be measured by the parameter M/H_0 (population dose equivalent per unit fence-post dose equivalent).

At LBL, numerical integration gave $M/H_0 = 1023$ (St 75). This value probably represents an upper limit to the value of M/H_0 likely to be found at accelerator laboratories, since LBL is situated adjacent to fairly densely populated areas of the San Francisco Bay Region (Th 76a). About 170,000 people live within 5 km of the laboratory, at an average population density ranging from 2000 to 3000 persons per square kilometre.

In calculating the population dose equivalent resulting from operations at the Stanford Linear Accelerator Center, the variation of dose equivalent with distance is assumed to be of the form (Je 74):

$$H(r) \propto \frac{e^{-r/\lambda}}{r} \qquad (6.10)$$

where $\lambda = 140$ m, and a value of $M/H_0 = 460$ man rem per fence-post rem was obtained (Bu 76a,b). This value is lower than that at LBL for two reasons. First, the population density around the Stanford accelerator is somewhat lower than that at Berkeley, and second, the evaluation of dose equivalent was only carried out to a distance of 1 mile (1.6 km) from the accelerator. Nevertheless, the values of the population dose equivalent produced by these two centres with similar locations–adjacent to a university campus and a large urban population–are seen to be comparable.

At CERN, where the average population density around the laboratory is considerably lower than at Berkeley (Table 6.3), M/H_0 has the value 160.

At laboratories such as Brookhaven National Laboratory (BNL), where the site boundaries are at considerable distances from the accelerator-produced radiation sources, the parameter M/H_0 has a low value. At BNL, the value of M/H_0 estimated from data contained in its environmental report for 1975, is 54 (Hu 76).

At the Fermi National Accelerator Laboratory (FNAL), the population dose equivalent was largely due to penetrating muons directed towards the northeast boundary of the laboratory. Baker (Ba 76) has estimated a population dose equivalent of 10 mSv resulting from a total equivalent of 10 μSv during 1975 over a region about 50-m wide at the FNAL site boundary.

When the fence-post dose equivalent resulting from accelerators is only a few tens of microsieverts per year, spatial and temporal variations in natural background and detector sensitivity place a limit on the accuracy to which the fence-post dose equivalent resulting from photons may be determined. These problems have been discussed in detail elsewhere (deP 74a, 74b).

6.3 RADIOACTIVITY PRODUCED IN THE ACCELERATOR STRUCTURE AND ITS SURROUNDINGS

TOTAL RADIOACTIVITY

The total quantity of radioactivity produced in an accelerator structure (including the shield) may be related to the total number of inelastic interactions produced by a proton in the materials of interest.

A simple approximate relationship between the total saturated activity, A_{sat} and the number of inelastic interactions per second N is:

$$A_{sat} = kN \qquad (6.11)$$

where k is a constant to be determined.

The number of inelastic interactions in various materials may be studied as a function of proton energy by using Monte Carlo simulations of the hadron cascade induced by the protons in a semi-infinite medium. The results of calculations using the program FLUKA (Aa 84) for protons of different energies incident on shields of oxygen and copper are given in Table 6.4. The data show that the total number of inelastic interactions (stars) produced is not greatly dependent on the target material but is approximately proportional to the incident proton energy. The mean number of stars per GeV will be taken to be 2.9 in what follows.

Equation (6.11) may be then be modified to:

$$A_{sat} = 2.9kE \qquad (6.11a)$$

with E in GeV.

The constant k may be determined from the work of Barbier (Ba 69) who suggests that one third to one half of all inelastic interactions give rise to a radioactive isotope with a half-life between several tens of minutes and a few years. Thus the saturation activity in Bq of these isotopes would be about one third of the numbers given in column 5 of Table 6.4 per interacting proton per second. Equation (6.11) may be further conveniently modified to read:

$$A_{sat} \approx E \qquad (6.11b)$$

when A_{sat} is in becquerels and E is in GeV. Convenient rules of thumb then are that the saturated activity for incident proton energies of more than 1 GeV are 1 Bq/GeV or 6.3×10^{12} Bq/kW.

Equation (6.11) would predict a saturated activity of 30 Bq per unit proton intensity for the Brookhaven National Laboratory AGS-in fair

agreement with the value of 24 Bq determined by Moore (Mo 66).

The total saturated activity produced by a 30-GeV proton accelerator operating at a proton intensity of 5×10^{12} s^{-1} would be 150 TBq (4000 Ci). Most of the induced radioactivity will be produced in the accelerator structure and shield and is therefore tightly bound in the constituent materials; it is thus not likely to migrate into the environment. It is, however, important to understand the quantities of radioactivity produced outside the accelerator shield, directly in the environment, which might be potential sources of radioactive contamination.

QUANTITY OF RADIOACTIVITY IN EARTH AND GROUNDWATER

Stapleton and Thomas (St 72) have estimated the total quantity of radionuclides produced in the earth, Q_E, and groundwater, Q_W, of an accelerator buried underground. If Q_W is known, the total activity in the earth shield, Q_E, may be estimated from the equation

$$\frac{Q_E}{Q_W} = \left(\frac{1 - f}{f}\right) \frac{\rho_E \sigma_E}{\rho_W \sigma_W} \frac{M_W}{M_E} \qquad (6.12)$$

where

f is the fraction of water by weight in the earth shield

ρ is density

σ is the inelastic reaction cross section

M is the molecular weight

and the subscripts E and W represent earth and water respectively.

Q_W was estimated using experimental data (Gi 68) to give:

$$Q_W = 2.2\times10^{-6} \text{ Bq mb}^{-1} \text{ GeV}^{-1} \text{ s}^{-1} \qquad (6.13)$$

Using a value of 290 mb for the total inelastic cross section of oxygen, we may estimate the total activity produced in groundwater to be $\sim 6.3 \times 10^{-3}$ Bq GeV^{-1} s^{-1} (1.7×10^{-13} Ci GeV^{-1} s^{-1}) which is less than 1% of the total activity produced (1 Bq GeV^{-1}).

Once Q_W is known, Q_E may be calculated using Eq. (6.12). In the case of an accelerator buried in chalk, considered by Stapleton and Thomas (St 72), assuming the earth contains 20% water by weight, the values to be substituted into Eq. (6.12) are:

$$f = 0.2$$

$$\frac{\rho_E}{\rho_W} = 2.0$$

$$\frac{M_N}{M_E} = \frac{1}{5.5}$$

$$\frac{\sigma_E}{\sigma_W} = 5.6$$

whence

$$\frac{Q_E}{Q_W} \approx 8.1 \quad .$$

Conditions will vary somewhat for other accelerators, but we see that typically the total radioactivity in the earth will be 5–10 times higher than the radioactivity in the water.

SUMMARY OF THE PRODUCTION OF RADIOACTIVITY BY HIGH-ENERGY ACCELERATORS

Table 6.5 summarizes the distribution of radioactivity produced by strong focussing accelerators such as the Brookhaven National Laboratory AGS or the CPS, operating at an energy of 30 GeV and a proton intensity of 5×10^{12} s^{-1}.

6.4 RADIOACTIVITY IN EARTH AND WATER

RADIOACTIVITY PRODUCED IN EARTH

The radioactivity produced in earth is discussed in Section 6.5.

RADIOACTIVITY PRODUCED IN COOLING WATER

One source of contamination of the environment arises from the possibility of accidental releases from the water circuit used to cool such machine elements as magnets, extraction septa etc. The circuits are normally closed but accidental rupture, possibly caused by the proton beam itself, could lead to an eventual release of radioactive water to the environment through the drainage system of the accelerator. Another problem that must be considered is the external dose rate from pipes containing radioactive cooling water should these pipes pass through uncontrolled areas outside the beam enclosure.

The radionuclides that can be produced by hadron-induced spallation interactions in the oxygen of the cooling water are given in Table 6.6 (Ch 78) together with their half-lives and estimated production cross-sections. The production of these radionuclides has been confirmed in several experimental studies (Di 64, Pa 73, Ro 58, St 67, Th 78, Th 79, Wa 69). Measurements have shown that ^{11}C is the dominant short-lived radionuclide 1 to 5 hours after irradiation and ^{7}Be is the only gamma-emitter with a half-life greater than 10 hours. However, the 0.511-MeV photon from positron annihilation should not be forgotten when estimating dose rates from the activity induced in water. Rindi (Ri 72b) made detailed calculations of the radioisotopes produced in the cooling water of the CERN 300-GeV proton synchrotron and showed that the presence of the large amounts of ^{7}Be can also cause external irradiation exposure from pipes and heat-exchangers. Komochkov et al. (Ko 72) and Borak

(Bo 72a) have reported gamma-spectroscopy measurements performed in the cooling waters of the Dubna 700-MeV synchrocyclotron and CERN 20-GeV proton synchrotron showing the presence of radioisotopes which were produced by the corrosion of machine parts. ^{60}Co, ^{58}Co, ^{57}Co, ^{56}Co, ^{59}Fe, ^{56}Mn, ^{54}Mn, ^{52}Mn and ^{22}Na were identified. These isotopes, like ^{7}Be, are absorbed in the ion exchange resins of the cooling water circuit, and this must be taken into account when determining the probability of finding them in water released to the environment, which is essentially nil.

The radioisotope production in water can be estimated, as in the case of the accelerator structure, from the density of inelastic interactions (stars) calculated using a Monte Carlo program such as FLUKA (Aa 83). Typical calculations, in geometries that simulated part of the accelerator structure, made for the CERN SPS have shown that about 0.3% of the inelastic interactions occur in the cooling water. Consequently a rule of thumb commonly used at CERN is to assume that 1% of the values given in column 2 of Table 6.4 represents an upper limit to the number of stars occuring in cooling water (St 84b). The ratio between the actual isotope production cross-section and the hadron cascade star production cross-section is given in column 4 of Table 6.6; this is numerically equal to the number of atoms of a given isotope produced per hadron star. These data, taken with a knowledge of the hydrodynamics of the water circuit, may be used to provide estimates of isotope concentrations and external dose rates as was done by Christensen et al. (Ch 78).

Table 6.7 shows values shows values calculated using the rule of thumb mentioned above for two irradiation conditions for isotopes whose lifetimes are longer than a few minutes (those likely to live long enough to reach the outside environment after the rupture of a cooling circuit). Column 2 gives the initial activity produced by a single pulse of 10^{13} protons at 30 GeV. Column 3 of Table 6.7 gives the activities resulting from a continuous loss of 10^{11} protons per second at 30 GeV for a total of 5000 hours. The activities of the longer-lived isotopes are naturally higher relative to the short-lived isotopes because of the build up over the year. The decay factor for a delay of 1 hour is also shown in column 4.

In order to assess the radiological impact of this isotope production on the outside environment, the pathway for the release of activity and the incorporation of the isotope into the human body must be specified. The following simple assumptions are made here:

- Single Pulse: A single proton pulse is assumed to be lost and to rupture the demineralised water circuit (total volume 100 m^3). At least 10 m^3 of this water would escape before fast shut-off valves close off the rest of the water circuit. The concentration is highest for the lowest quantity of water released; the volume of water released is therefore assumed to 10 m^3. No decay of activity is assumed to occur between the rupture of the water circuit and the release of the water into the environment. In these estimates it is assumed a person drinks 1 litre of this contaminated water.

- Continuous Loss: For this loss pattern in time the activity could be dispersed into the whole of the water circuit. The activity concentration is therefore estimated using a water volume of 100 m^3. As before, no decay of radioactivity is assumed to occur between rupture and release, and an ingestion of 1 litre is assumed.

The values of the quantities of radioisotopes ingested in this manner are compared with the annual limits of intake (ALI) taken from ICRP Publication 30 (ICRP 79) except in the case of ^{13}N where the ALI for ^{11}C has been assumed (Table 6.8). The impact of this ingestion can be crudely compared to that of external irradiation by assuming that 1 ALI is equivalent to 50 mSv. The equivalent external dose rates thus obtained are also given in Table 6.8.

Although these exposures are small, simple practical steps may be taken to reduce them even further. For example, the short-lived isotopes can be eliminated from any effluent by introducinig a simple time delay via storage tanks before any water can reach the uncontrolled environment. As a second example ^{7}Be is readily absorbed by any ion-exchange resin, and indeed by most surfaces over which spilled water may flow.

RADIOACTIVITY PRODUCED IN GROUNDWATER

The radioactivity produced in groundwater is discussed in Section 6.5, *Radionuclide Production in Water*.

6.5 THE ENVIRONMENTAL IMPACT OF THE RADIOACTIVITY PRODUCED IN THE EARTH AND GROUNDWATER

The radioactive nuclides induced in the accelerator structure or concrete of the accelerator room are relatively immobile. However, the radionuclides produced in the earth shield or groundwater are free to move.

The radioactive nuclides produced in the groundwater might pass into the general groundwater system and therefore potentially into the public water supplies extracted from the area. In addition, the possibility that activity induced in the earth may be leached into the groundwater system must also be considered.

It is important at the outset to remark that up to the present time no significant groundwater system contamination due to accelerator operation has been observed. However, it is good health physics practice that such a possibility be investigated.

An assessment of a potential contamination of drinking-water supplies falls into three stages:

(i) Consideration of the possible radionuclides that could be produced from a knowledge of the chemical composition of rock and water impurities.

(ii) Estimation of the yield of these radionuclides from the known production cross-section, radioactive half-life, particle flux densities and energy spectra.

Should the yield of radionuclides estimated at stage (ii) be sufficiently high, then a third stage follows:

(iii) Estimation of the final specific concentration of radionuclides in local water supplies must be made, taking into account site hydrology, dilution, radioactive decay and chemical sorption.

Several authors have reported the observation of radionuclide production in earth and water, either in laboratory simulations or directly in the accelerator shield. None of them is complete, but together they give a fairly comprehensive picture of the most important radionuclides of concern.

RADIONUCLIDE PRODUCTION IN WATER

The most obvious potential source of radioactive contamination of groundwater systems arises from the production of radionuclides directly in the water. Thermal neutron capture in hydrogen and spallation reactions in oxygen and dissolved substances in water may result in a large number of radionuclides. Because these radionuclides are produced directly in water which is mobile, there might be a possibility of their transfer from the site of activation (around the accelerator) and entry into local groundwater systems.

A review of studies prior to 1972 of the production of radionuclides in water around accelerators has been published by Stapleton and Thomas (St 72, Th 70) and more recent work has been discussed by

Patterson, Rindi and Thomas (Pa 73, Th 79).

Table 6.6 lists the possible spallation products from ^{16}O with half-lives longer than 10 sec that will be produced directly in water (listed in order of increasing half-life). Nelson (Ne 65) reported the first studies of possible groundwater contamination due to a high-energy accelerator, in estimating radionuclide production near beam dumps of the SLAC 20-GeV electron linac. Middlekoop (Mi 66), in a design study for a 300-GeV proton synchrotron, showed that spallation reactions in water could produce concentrations of ^{3}H and ^{7}Be many times greater than the maximum permissible concentrations recommended by the ICRP.

Measurements of the production of radionuclides in water irradiated in accelerator environments have identified ^{11}C as the dominant short-lived radionuclide 1 to 5 hours after irradiation. ^{7}Be was the only γ-emitter with half-life greater than 10 hours produced in measurable quantities, and was produced with a cross section of about 10 mb in a variety of experimental conditions. The production of tritium under these conditions was consistent with a production cross section of 30-35 mb (St 67, St 71, St 72). From this information and the data of Gilbert et al., (Gi 68) Stapleton and Thomas estimated that at saturation there are about 220 GBq (6 Ci) of ^{7}Be and 670 GBq (18 Ci) of tritium in the groundwater of the earth shield around a 300-GeV proton accelerator operating at an intensity of 3×10^{13} protons sec^{-1} (St 72).

RADIONUCLIDES RESULTING FROM DISSOLVED SOLIDS IN WATER

Middlekoop (Mi 66) was the first investigator to estimate the specific activity due to irradiation of the impurities dissolved in groundwater. His investigation was limited to those radionuclides produced by thermal neutron capture and to only a single example, the groundwater of a chalk region in the United Kingdom.

Middlekoop showed that no nuclides are produced in concentrations at saturation comparable to MPC, with the exception of ^{36}Cl. This radionuclide will be of no consequence, however, because its half-life of 3×10^{5} years will result in an extremely low production rate.

In the experiments of Stapleton and Thomas, (St 67, St 71, St 72) the presence of ^{32}P in the dissolved solids of irradiated groundwater taken from the chalk site was detected. However, ^{32}P is fixed in chalk in the form of calcium phosphate and would not be expected to be mobile in groundwater in chalk soil (Bl nd).

The special problems of corrosion products in cooling water have been discussed in Section 6.4.

RADIONUCLIDES PRODUCED IN THE EARTH

As in the case of groundwater, several studies of the production of radionuclides in earth have been made and the results are summarized in Table 6.9. From the chemical composition of the soil at the CERN site and measurements of particle flux densities in the CPS arth shield, Hoyer (Ho 68) calculated the specific activity of radionuclides to be expected in the soil. He concluded that only four radionuclides were produced in measurable quantities. To check his calculations, Hoyer compared his estimates with measured values of the specific activity of

^{45}Ca and ^{22}Na found in earth taken from several locations in the earth shield. Measured activities were, in general, lower by a factor of 3 than those calculated, which Hoyer attributed to leaching of these nuclides from the site by rain water. Hoyer took the rough agreement between his measured and calculated values to confirm his suggestion that only four radionuclides will be of significance. The production of tritium was not considered in this study.

In studying the radiological impact of the 500-GeV proton synchrotron of the Fermi National Accelerator Laboratory, Borak et al. (Bo 72b) irradiated glacial till and various clay soils in typical high-energy accelerator radiation fields. Table 6.9 summarizes the radionuclides identified in these soils.

Since operation of the Fermilab 500-GeV accelerator, an extensive program monitoring the radioactivity in earth and groundwaters at critical areas on the accelerator site has been developed (Ba 75a, Ba 75b). Water samples are collected from wells and creeks and no accelerator-produced radionuclides have been detected in such samples. However, in some sumps which collect water from the footings around accelerator tunnels and enclosures and from drains under targets and beam dumps tritium is routinely detected. Occasionally low concentrations of ^{45}Ca and ^{22}Na are also reported. Baker reports that predictions of radionuclide concentrations in the soil outside the accelerator are now generally reliable. Measurements of particle flux density inside the accelerator tunnels and calculations of the hadronic cascade in the earth shielding by Monte Carlo techniques to predict activities in the earth usually result in good agreement with measured values in the soil (Ba 76).

A similar study to that of Borak et al. (Bo 72b) was carried out for the design of a 300-GeV proton synchrotron (which might be located in a chalk site but was never constructed) (St 72). The radionuclides identified in chalk are shown in Table 6.9.

Finally, Thomas (Th 72) has reported measurements of radionuclides produced in an earth beam dump by 1-GeV electrons from the Mark III electron linear accelerator of Stanford University. The significant production of radioactivity in the earth beam dump was dominated by photo-nuclear reactions with the constituent elements of the soil. The data obtained in this series of measurements were in good agreement with electromagnetic cascade theory.

THE MIGRATION OF RADIONUCLIDES THROUGH THE GROUND

A large number of radionuclides may be produced in the earth and groundwater by high-energy accelerator production. However, the ultimate concentration of radionuclides in the groundwater will then be controlled by the half-life of the radioactive species, solubility of the radionuclide, its possible dilution and the site hydrology. Radionuclides with too short a half-life will decay so rapidly as to be of no potential hazard when they reach a public water supply. Conversely, if the half-life is too long saturation activities will not be approached.

Knowledge of the hydrology of the accelerator site being studied will indicate the range of radioactive half-lives that are of interest. It is reasonable to study radionuclides with half-lives T_H in the range:

$$10 \text{ hr} < T_H < 100 \text{ yr}$$

It should be noted that this general consideration limits the number of radionuclides that can appear in maximal quantities in groundwater systems. In practice, therefore, only a small number of radionuclides usually need to be studied in detail. Detailed investigation of site conditions will identify the appropriate range to be investigated. In particular, the production of ^{3}H, ^{7}Be, ^{22}Na, ^{54}Mn, and ^{45}Ca merit detailed study.

Not all the radioactivity produced will be in soluble chemical form. Thus, for example, less than 0.7% of the gamma-activity (principally ^{54}Mn and ^{22}Na) produced in the earth dump of the Mark III electron linac was soluble (Th 72). Borak et al. (Bo 72b) have made detailed studies of the solubility of the radionuclides produced in glacial till (Table 6.9). Of these radionuclides only ^{45}Ca, ^{54}Mn, ^{22}Na and ^{3}H were observed in leach waters. Of ^{45}Ca and ^{54}Mn, only a fraction of the activity (5% and 2% respectively) was readily soluble.

However, even the production of radionuclides in soluble form in the earth shield and the appearance of radioactive species in the groundwater is not necessarily indicative of environmental harm–the radionuclides may be immobile. In a review of the movement of radioactive wastes buried in the ground, Mawson reports that 'with few exceptions, absorption and exchange processes occur between the radionuclides and constituents of the soil. If the site is selected with care any radionuclides that enter the soil will progress quite slowly down the water table. Once in the groundwater they will move faster, but still at a rate one to several orders of magnitude less than the rate of movement of the groundwater. These statements apply to most cations–many anions move at about the same speed as the groundwater' (Ma 69).

The greater part of radioactivity induced in the soil is confined to regions of high radiation intensity and is typically confined to a few locations close to the accelerator. Stapleton and Thomas (St 72) estimate that 95% of the activity induced in earth is produced within 2 m from the outer wall of the accelerator tunnel of a proton synchrotron. In the absence of migration of any radionuclides from the activation zone, the radioactivity would increase to a final saturation determined by the accelerator intensity, the nuclear cascade process in the shield and the macroscopic cross sections for radionuclide production in rock and groundwater.

Migration of the radionuclides will be determined by the distribution coefficient, K, which is a measure of the relative affinity of the radionuclide for earth compared with water. It is defined as the ratio of the concentration of ions absorbed by the soil to those remaining in solution at equilibrium. A large value of K indicates that ions preferentially adhere to soil and their migration is retarded.

The average velocity of ions through the earth, v_i, is related to the velocity of the water, v_w, by the equation:

$$\frac{v_i}{v_w} = \frac{1}{1 + K(\rho/p)} \qquad (6.14)$$

where

K is the distribution coefficient,

ρ is the bulk density of the rock, and

P is the porosity of the rock (fraction of total volume of soil occupied by voids).

For large distribution coefficients equation (6.14) reduces to:

$$\frac{v_i}{v_w} = \frac{P}{K\rho} \qquad (6.15)$$

Table 6.10 summarizes measurements of the distribution coefficient, K, for some radionuclides in various soils.

If the distribution coefficient is high, the potential for contamination of public water supplies is much reduced. Thus Stapleton and Thomas point out that for ^{7}Be in chalk the beryllium ions move more slowly than the groundwater by a factor of about 15,000. Under these conditions migration rates would be so slow that radioactive decay will reduce the original activity to negligible levels (St 73). In the case of ^{22}Na there seems to be a significant difference between the observations of Hoyer, who determined a distribution coefficient of 100 at CERN, and those of Borak et al. at FNAL. The latter workers found that in the case of ^{22}Na, 10-20% of the activity is produced in a chemical form that is extremely soluble in water. In equilibrium the distribution coefficient was determined to be 0.20 and the ion velocity about 40% of that of the groundwater.

Of all the radionuclides produced in the earth and groundwater, it is likely that only tritium will move freely in groundwater, without significant holdup due to absorption on rock surfaces. In static measurements of distribution coefficient, Borak et al. report that the quantity of tritium found in leach waters was consistent with the quantity produced in the free water in the soil. The distribution coefficient measured was very small and thus the tritium will migrate with the same velocity as water through the aquifier.

It is therefore probable that tritium may be the radionuclide that should be most carefully studied in groundwater around accelerators.

POTENTIAL COMTAMINATION OF DRINKING WATER SUPPLIES

From what has gone before we can speculate that the possibility of significant contamination of drinking water supplies is extremely remote.

A detailed study of these phenomena would be extremely complex, but Thomas has proposed a simple model that may be used to understand their magnitude (Th 70). This model is schematically shown in Fig. 6.12, where an accelerator is buried underground. Radioactivity is induced in an activation zone close to the accelerator building. It is postulated that the radionuclides may be washed downward to the water table by

rainfall. When they reach the water table they are transported to the boundaries of the accelerator laboratory. In the movement they are mixed with and diluted in the groundwater. This water might be available for public use.

The specific activity, S, of this water available to the public is then given by

$$S = D \sum_i \frac{\epsilon_i Q_i \left[1 - e^{-T_i/\tau_i}\right] e^{-t_i/\tau_i}}{M_i} , \qquad (6.16)$$

where there are i radionuclides produced and

D is a dilution factor,

ϵ_i is the fraction of activity produced that migrates from the site of its production,

Q_i is the total quantity of the ith radionuclide produced at saturation,

T_i is the residence time of the ith radionuclide in the activation zone,

τ_i is the mean life of the ith radionuclide,

t_i is the transport time from leaving the activation zone to reaching the laboratory perimeter,

M_i is the MPC of the ith radionuclide, and

S is measured in units of maximum permissible concentration (MPC).

Equation (6.16) permits a crude assessment of the magnitude of the problem. The maximum rate of release of activity occurs at small residence times (T = 0), when all the activity produced migrates ($\epsilon = 1$) and the transport time to the site boundary is very short ($e^{-t_i/\tau_i} = 1$) when:

$$S_{MAX} = D \sum_i \frac{Q_i}{M_i \tau_i}$$

At an accelerator site where the water table is not disturbed by pumping, the outflow of water would equal the inflow from rainfall and the radioactivity released would be diluted in a volume of water equivalent to the rainfall on the site.

If, as we have seen, it is likely that tritium is the only radionuclide of significance, the value of S_{max} reduces to:

$$S_{MAX} = D \frac{Q_T}{M_T \tau_T} \qquad (6.17)$$

where the subscript T refers to tritium.

If we are considering a large accelerator site such as CERN or Fermilab the factor D can be quite small-typically 10^{-4} m^{-3} day-and substituting other typical values:

$1/D$ 10^4 m^3 day^{-1}

Q_T 750 Bq (20 Ci)

τ_T 17.6 yr

M_T 120 MBq m^{-3} (general population).

we obtain:

$$S_{max} \approx 1 \times 10^{-4} \text{ MPC} \quad .$$

Thomas has reported calculations for a 500-GeV proton synchrotron similar to the CERN 28-GeV proton synchrotron, losing 10^{12} protons per second to the shield. It was assumed that all the radionuclides produced in the earth and water in the shield were released directly to the groundwater, rapidly transported to the site boundary and diluted with a quantity of water equivalent to the net rainfall on the accelerator site (10^4 m^3 day^{-1}). Figure 6.13, which summarizes these calculations, shows that even under these extremely conservative assumptions the specific activity of the water would never exceed 0.03 MPC and that this value is rather insensitive to residence time up to periods of 1000 days. This crude treatment shows that the problem is not likely to be a serious one, and in actual practice the magnitude of radioactive contamination of drinking water supplies will be extremely small.

POPULATION EXPOSURE FROM ACCELERATOR-PRODUCED RADIONUCLIDES IN GROUND WATER

The arguments presented in this section show that the concentration of the accelerator-produced nuclides will be insignificant at existing accelerator intensities. The radioactivity from natural sources will in fact be higher by orders of magnitude than that from accelerator-produced nuclides.

There have been no reported observations of accelerator-produced radionuclides in public water supplies and experience shows the consequent population dose equivalent to therefore be effectively zero.

6.6 RADIOACTIVITY PRODUCED IN THE ATMOSPHERE

The second most important source of exposure resulting from accelerators is from radioactivity produced in the air. Typically, the magnitude of this exposure is many times smaller than that from 'prompt' radiation.

RADIONUCLIDES PRODUCED IN AIR BY ACCELERATOR OPERATION

The principal source of radioactivity in air is the interaction of primary and secondary particles directly with constituent target nuclei of the air. A secondary source of airborne radioactivity is dust, formed by natural erosion and wear, or by work on radioactive accelerator components. The third and final source of air-borne radioactivity results from the emission of gaseous radioactivity from liquids irradiated in the accelerator-produced radiation environment.

Radionuclides Produced Directly in Air

During accelerator operation, radioactive nuclides are produced by the interaction of primary and secondary particles with the air in the accelerator halls. In addition, spallation reactions in solid machine parts may also contribute to the formation of radioactive gases. If the air is confined in the accelerator hall there will be no release of radioactivity to the general environment during the operation of the machine. In such a case, a rather high concentration of radioactive gases may accumulate. In general, high-energy or high-intensity accelerators provide air circulation, mainly for cooling reasons. The residence time of air inside the accelerator room (and consequently the irradiation time of the air) is usually less than 30 minutes so that the production of high concentrations of radioactive gases with a long half-life is minimal.

Table 6.11 summarizes the target nuclei most abundant in air. A summary of the radionuclides with half-life greater than 1 second that may be produced from these by thermal neutron capture (n,γ), and spallation reactions with these target nuclei is given in Table 6.12.

With the exception of ^{3}H and ^{7}Be, the half-lives of most radionuclides are short, so that there will be some decay even during the short time they take to reach inhabited regions around the accelerator.

The radionuclides of significance for environmental contamination are ^{3}H, ^{7}Be, and perhaps ^{11}C, ^{13}N, and ^{15}O. The long ^{3}H half-life limits its environmental impact because its rate of production is rather small.

Among the first reported measurements of radioactive gases produced at accelerators are those of Russel and Ryan in 1965 who detected ^{15}O and ^{13}N in the air around a 70-MeV electron linac produced by (γ,n) reactions with ^{16}O and ^{14}N in the air (Ru 65). By calculating the maximum possible concentration for these radionuclides (which were not at that time available in the literature) and by estimating the diffusion of these radionuclides from the source, these authors concluded the concentrations around the accelerator to be much lower than MPC. Similar conclusions were reached by George et al. (Ge 65).

Over the years considerable effort has gone into identifying airborne radionuclides at accelerators. Table 6.13 summarizes some of the published data.

The Magnitude of Radionuclide Production in Air

Patterson and Thomas (Pa 73) have summarized estimates of the total specific activity, S, of an enclosed volume of radioactive air near an accelerator and show it to be given by:

$$S = C \sum_i \left[\sum_j \Phi_\gamma N_j \bar{\sigma}_{ij_\gamma} + \sum_j \Phi_{th} N_j \bar{\sigma}_{ij_{th}} + \sum_j \Phi_{HE} N_j \bar{\sigma}_{ij_{HE}} \right] \times (1 - e^{-\lambda_i T}) \, e^{-\lambda_i t} \quad , \qquad (6.18)$$

where Φ_γ, Φ_{th}, and Φ_{HE} are the average photon, thermal neutron, and

high-energy particle flux densities, and $\bar{\sigma}_{ij_\gamma}$, $\bar{\sigma}_{ij_{th}}$ and $\bar{\sigma}_{ij_{HE}}$ are the corresponding average cross sections.

Equation (6.18) gives results that are in agreement with observed values within a factor of two or better. Figure 6.14 compares calculated and measured values of activity around the accelerators at CERN (Ri 67).

Quite accurate estimates of the concentration of radioactivity in air may be made if the influence of air changes is considered. This may be done by substituting an effective decay constant λ_i' for λ_i in Eq. (6.18). λ_i' is given by:

$$\lambda_i' = \lambda_i + D/V \qquad (6.19)$$

Where D is the ventilation rate and V is the volume of the accelerator room.

Table 6.14 gives an example of the good agreement obtained by Peetermans and Baarli (Pe 74) between calculated and measured values of specific activity for four radionuclides, at the CERN 600-MeV synchrotron.

RADIONUCLIDES PRODUCED IN DUST

The most direct method of determining if any potentially serious internal contamination problem exists is to determine the body burdens of accelerator-produced radionuclides in accelerator workers and to study possible contamination pathways.

Experience at several large accelerators tends to show that the potential exposure to radioactive dust for maintenance crews working in the accelerator vault is negligible. This problem has been discussed at some length by Thomas and Rindi (Th 79b) and so will not be discussed here.

It is of interest to note that Busick and Warren (Bu 69) have concluded that chemical toxicity and external radiation exposure are the factors that limit the machining of radioactive accelerator components rather than the inhalation of radioactive dust.

GASEOUS RADIONUCLIDES RELEASED FROM WATER

In certain circumstances radionuclides produced in liquids irradiated at accelerators may be released to the environment. For example, tritium produced by spallation reactions in magnet cooling water may be released by the evaporation of water spills and losses during magnet maintenance or replacement.

Warren et al. (Wa 69) have studied the production of CO_2, which acts as a carrier for ^{11}C and ^{15}O produced in water beam-dumps at the Stanford Linear Accelerator Center.

ENVIRONMENTAL IMPACT OF AIRBORNE RADIONUCLIDES

In 1972, Prantl and Baarli (Pr 72) reported finding some small amounts of ^{7}Be in a creek at the CERN accelerators. However, due to the lack of systematic background measurements of ^{7}Be produced by cosmic

rays, no final conclusions as to its origin could be drawn at that time. The same year, Rindi (Ri 72a) made a detailed theoretical study of the production of radioisotopes in the air of a 300-GeV proton accelerator and of the dispersion of these isotopes in the environment. He concluded that, under some adverse atmospheric conditions coupled with some particular machine use, concentration of ^{7}Be and perhaps also of ^{3}H of the order of the MPC for the population at large could be detected at some 5 km from the air rejection shaft of the accelerator. In 1974 Peetermans and Baarli (Pe 74) reported some new calculations and measurements performed at the CERN 600-MeV proton synchrocyclotron to estimate the concentration of radioactive gases in surrounding region when the intensity of that accelerator was increased. ^{7}Be, ^{24}Na, ^{28}Mg, ^{31}Si, ^{32}P, and ^{33}P were identified in the ventilation air around an extracted beam by flow ionization chambers and γ-spectroscopy on filters. The measured concentrations were in good agreement with those calculated (Table 6.14). These authors concluded that the annual contribution to the dose equivalent at the CERN boundaries due to radioactive isotopes in air would be about 60 μSv (less than 10% of the dose equivalent due to stray radiation) and that the eventual ^{7}Be surface pollution at distances up to 1 km from the boundaries would be barely detectable. In fact measurements of the ^{7}Be content of rainwater around CERN show much larger fluctuations than at control sites (see Fig. 6.15). Air-sampler filters subjected to γ-spectrometry show that, while the activity of γ-emitting nuclides from nuclear weapons fallout shows similar trends at both laboratories, fluctuations in ^{7}Be activity in air at CERN are much larger than those found at Le Vesinet.* These data tend to suggest that accelerator operation at CERN produces detectable quantities of ^{7}Be close to the high-energy accelerators, corresponding to periods of high-intensity operation. At the Lawrence Berkeley Laboratory where several proton and heavy-ion accelerators are operated, a search for possible contamination from ^{7}Be was made by measuring the radioactivity of bracken ferns collected around the centre and at different locations several miles away. These studies show that the ^{7}Be contamination in air due to the presence of the accelerators at the Berkeley laboratory, if any, is within the variation of the background produced by cosmic rays (Sm 77).

The measurement of the concentration of ^{7}Be in air or in dust around accelerators may prove to be a valuable indicator of radioactive contamination. Further studies are needed, including measurements of the natural background fluctuation of ^{7}Be in rainwater.

POPULATION EXPOSURE FROM RADIOACTIVITY IN THE AIR

Four short-lived radionuclides–^{10}C, ^{11}C, ^{12}N and ^{15}O–typically account for the major portion of the total activity released. Of the longer lived radionuclides only ^{41}Ar, ^{7}Be, and ^{3}H are released in significant quantities.

---

*Le Vesinet is situated in the suburbs of Paris–more than 400 km from Geneva. The value of this station as a control for Geneva CERN is therefore somewhat suspect. However, the gross β-activity and γ-activity from known nuclear weapons fallout nuclides shows similar seasonal trends at many West-European stations.

The calculation of population exposure resulting from the release of these gaseous radionuclides is normally performed according to the following steps:

1) Measurement or calculation of the concentration of the different radioisotopes released at the ventilation stacks of the accelerators.

2) Calculation of the transport of the gases outside the boundaries of the Laboratory. This is generally done by applying the Sutton equation for some average meteorological conditions.

3) Conversion of the concentrations of radioactive gases to dose equivalent to an exposed individual by using the MPC values.

4) Summation of the total number of exposed individuals and their dose equivalent to give the total population dose.

Steps 2, 3 and 4 can be summarized in a general equation. Thomas (Th 76a) has described the use of the following expression to calculate the population dose equivalent resulting from the release of a given radionuclide that applies for the Lawrence Berkeley Laboratory, but which can be easily generalized.

$$M = \sum_{i=1}^{n} \left[\left(\frac{1}{2\pi}\right)^{1/2} \left(\frac{n}{2\pi}\right) \frac{f_i Q R}{\bar{u}} \int_{r_o}^{\infty} \frac{N_i(r)}{r\sigma_z(r)}\, dr \right] , \qquad (6.20)$$

where

n is the number of sectors into which the region surrounding the source is divided (this division is decided by the wind direction (frequencies);

f_i is the fraction of time in which the wind blows toward a given sector;

Q is the total quantity of radionuclide released (in Bq);

R is the dose equivalent conversion factor for the given radionuclide (Sv m^3 per Bq s);

$\bar{u}$ is the average wind velocity (in ms^{-1});

r is the distance from the rejection point;

$N_i(r)dr$ is the total number of people in the ith sector in the region between r and r + dr;

r_o is the distance of closest approach to the Laboratory; and

$\sigma_z(r)$ is the vertical dispersion coefficient (in m).

The integral can be simplified into a summation by subdividing each sector into m regions in which the population density may be assumed to be constant.

The number of residents at a distance r from the rejection point in the jth region of the ith sector is then given by

$$ {}_{j}N_{i}(r) = \frac{2\pi r}{n}\,\sigma_{ij}\,dr \quad , \tag{6.21} $$

where σ_{ij} is the population density.

The expression between square brackets in Eq.(6.20) can be expressed by

$$ {}_{j}M_{i} = (2/\pi)^{1/2}\,\frac{f_{i}QR\sigma_{ij}}{\bar{u}}\int_{r_{j-1}}^{r_{j}}\frac{dr}{\sigma_{z}(r)} \tag{6.22} $$

and the population dose equivalent is then expressed by

$$ M = \sum_{i=1}^{n}\sum_{j=1}^{m} {}_{j}m_{i} \quad . \tag{6.23} $$

From the meteorological statistics for the region under study, $\sigma_{z}(r)$ can be given an analytical expression as a function of r such that the integral in Eq. (6.22) can be evaluated.

It is customary at accelerator centres to report yearly on environmental monitoring results. Several centres perform continuous measurements of gaseous radioactivity in air, in addition to radioactivity deposited on filters, and also periodically investigate the radioactivity on ground, water and plants around the boundaries of the centre.

At the Fermi Laboratory in Batavia, where a 300-GeV proton synchrotron is located, the annual off-site exposure from airborne release was estimated to be about 91 mSv, 1/10 of the exposure from external radiation during 1975 (Ba 76).

At the Lawrence Berkeley Laboratory, where several proton and heavy-ion accelerators are located, the air monitoring systems detect releases of radioactive gas only from chemistry laboratories and not from accelerator operation (Th 76b).

REFERENCES FOR CHAPTER 6

Aa 84 Aarnio, P.A, Ranft, J. and Stevenson, G.R., 'A Long Write-Up of the FLUKA Program', CERN Divisional Report TIS-RP/106(Rev) (1984).

Al 81 Alsmiller, R.G., Jr., Barish, J. and Childs, R.L., 'Skyshine at Neutron Energies <400 MeV', Particle Accelerators, 11, 131 (1981) or ORNL/TM-7512 (1980).

Aw 65 Awschalom, M., Larsen, F.L. and Sass, R.E., 'The Radiation Measurements Group at the Princeton, Pennsylvania 3 GeV Proton Synchrotron', in Proceedings of the First Symposium on Accelerator Radiation Dosimetry and Experience, Brookhaven National Laboratory, CONF-651109, p. 57 (1965).

Ba 67 Bathow, G., Clausen, U., Freytag, E. and Tesch, K., 'Skyshine-Messungen und ihr Vergleich mit Abschätzungen, aus der Diffusionstheorie', Nukleonik 9, 14 (1967).

Ba 69 Barbier, M., 'Induced Radioactivity', in particular pp. 17-27, North Holland, Amsterdam (1969).

Ba 75a Baker, S.I., 'Fermi National Accelerator Laboratory Environmental Monitoring Report for Calendar Year 1974', Report ERDA-54, USERDA, 561 TID-26775 (1975).

Ba 75b Baker, S.I., 'Soil Activation Measurements at Fermi Laboratory', Proc. Third Environmental Protection Conference ERDA-92, Vol. 1, p. 329 (1975).

Ba 76 Baker, S.I., 'Environmental Monitoring Report for Calendar Year 1975', Fermi National Accelerator Laboratory, Internal Report (1976).

Bi 80 Biratarri, C., 'Radioisotope Production by Accelerators', in Advances in Radiation Protection and Dosimetry in Medicine', R.H. Thomas and V. Perez-Mendez, Eds., p. 269, Plenum Press, New York (1980).

Bl nd Blythe, H.J., 'Some Field Trials on Ground Disposal by the Industrial Chemical Group', AERE, Internal Report - AERE, GDF/P2 (undated).

Bo 72a Borak, T.B., 'Measurement of Induced Radioactivity in Cooling Waters for the CERN PS and External Beam Magnets', CERN H.P. Internal Report HP-72-112 (1972).

Bo 72b Borak, T.B., Awschalom, M., Fairman, W., Iwami, F. and Sedlet, J., 'The Underground Migration of Radionuclides Produced in Soil Near High-Energy Proton Accelerators', Health Physics 23, 679 (1972).

Br 70 Brodzinski, R.L. and Wogman, N.A., 'High-Energy Proton Spallation of Argon', Phys. Rev. C1, 1955 (1970).

Bu 69 Busick, D. and Warren, G.J., 'Operational Health Physics Associated with Induced Radioactivity at the Stanford Linear

Accelerator Center', in Proc. II, Int. Conf. on Accelerator Dosimetry and Experience, Stanford, November 1969, USAEC Rep. CONF-691101, p. 139 (1969).

Bu 76a Busick, D., 'Environmental Monitoring Report, 1975', Stanford Linear Accelerator Center, p. 194 (1976).

Bu 76b Busick, D., Stanford Linear Accelerator Center, private communication (1976).

Bu 81 Burger, G., Morhart, A., Nagarajan, P.S. and Wittman, A., 'Effective Dose Equivalent and its Relationship to Operational Quantities for Neutrons', in Proc.European Seminar on Radiation Protection Quantities for External Exposure, 13-15 October 1980, Braunschweig, Federal Republic of Germany, EUR 7101-EN, p. 117, Harwood Academic Publishers, Chur, Switzerland (1981).

Ca 53 Case, K.M., de Hoffmann, F. and Placzek, G., 'Introduction to the Theory of Neutron Diffusion', Vol. 1, Los Alamos Scientific Laboratory (1953).

Ch 78 Christensen, G.C., Fasso, A. and Stevenson, G.R., 'Radioactivity in the Cooling Water from the NAHIF Installation', CERN Internal Report HS-RP/IR/78-46 (1978).

Ci 79 Cimetière, C., Leger, J., Muxart, R. and Vernois, J., 'Utilisation de Cyclotrons pour la Préparation de Radionucléides a Usage Médicale', SFRP Séminaire sur les Accélérateurs de Particles, Utilisation et Radioprotection, Saclay, France (May 1979).

Co 60 Coveyou, R.R. and Sullivan, J.G., 'ORNL Neutron Physics Division Annual Progress Report', ORNL-3016, p. 193 (Sept. 1, 1960).

Co 62 Cowan, P.F., A Preliminary Report on Health Physics Problems at the Brookhaven Alternating Gradient Synchrotron', in Premier Colloque International sur la Protection auprès des Grands Accelerateurs, Presses Universitaire de France, Paris (1962) p. 143.

deP 74a de Planque Burke, G., 'Variations in Natural Environmental Gamma Radiation and its Effect on the Interpretability of TLD Measurements Made near Nuclear Facilities', Health and Safety Laboratory, New York, Report HASL-287 (1974).

deP 74b de Planque Burke, G., 'A Model for Estimating Variations in Terrestrial Radiation Exposures Based on Soil-Water Balance', in Second Workshop on the Natural Radiation Environment, W. M. Lowder (Ed.), Health and Safety Laboratory, New York (1974).

Di 64 Distenfeld, C., in 'A Proposal for Increasing the Intensity of the AGS at the Brookhaven National Laboratory', BNL-7956, May (1964).

Di 66 Distenfeld, C.H. and Colvett, R.D., 'Skyshine Considerations for Accelerator Shielding Design', Nucl. Sci. Eng., 26, 117 (1966).

Em 75 Emmett, M.B., 'The MORSE Monte Carlo Radiation Transport System', Oak Ridge National Laboratory Internal Report ORNL-4972

(1975).

Fa 76 Falk, R., Grobon, G., Renaud, C., Roubaud, G. and Tuyn, J.W.N., 'Environmental Radiation on the CERN Site During 1975', CERN Health Physics Group Internal Report HP-76-151 (1976).

Ge 65 George, A.C., Breslin, A.J., Haskins, Jr., J.W. and Ryan, R.R., 'Evaluation of the Hazard from Radioactive Gas and Ozone at Linear Electron Accelerators', Proceedings of the First Symposium on Accelerator Radiation Dosimetry and Experience, Brookhaven National Laboratory, CONF-651109, p. 513 (1965).

Gi 68 Gilbert, W.S., et al., '1966 CERN-LRL-RHEL Shielding Experiment at the CERN Proton Synchrotron', Lawrence Berkeley Laboratory Report, UCRL-19741 (1968).

Ha 69 Hack, R.C., 'Radiation Protection Group (Operations) Progress Report for 1968', Rutherford Laboratory Report RHEL/M 171 (1969).

Ha 76 Hayashida, Y., 'Study on the Production and Transport of Neutron-Induced Secondary Gamma Rays in Matter', Master's Thesis, Department of Nuclear Engineering, Kyoto University, in Japanese (1976).

Ho 68 Hoyer, F.E., 'Induced Radioactivity in the Earth Shielding on Top of High-Energy Particle Accelerators', CERN 68-42 (1968).

Ho 69 Hoefert, M., 'Radiation Hazard of Induced Radioactivity in Air as Produced by High-Energy Accelerators', Proceedings of the Second International Conference on Accelerator Dosimetry and Experience, SLAC, Stanford, CONF-691101, p. 111 (1969).

Ho 73 Hoeffert, M. and Baarli, 'Some Preliminary Investigations on the Contributions of Muons to the Stray Radiation Level around the CERN 28 GeV Proton Synchrotron', Proc. Third Int. Congress of IRPA, USAEC Report CONF-730907, p. 841 (1973).

Hu 76 Hull, A.P. and Ash, J.A., '1975 Environmental Monitoring Report', Brookhaven National Laboratory Internal Report BNL 21320 (1976).

ICRP 73a International Commission on Radiological Protection, 'Data for Protection against Ionizing Radiation from External Sources: Supplement to ICRP Publication 15', ICRP Publication 21, Oxford (1973).

ICRP 73b International Commission on Radiological Protection, 'Implications of Commission Recommendations that Doses Be Kept as Low as Readily Achievable', ICRP Publication 22, Pergamon Press, Oxford (1973).

ICRP 79 International Commission on Radiological Protection, 'Limits for Intake of Radionuclides by Workers', ICRP Publication 30, Part 1 (1979), Part 2 (1980), Part 3, including addendum to Parts 1 and 2 (1981), Supplement A to Part 3, Supplement B to Part 3 (1982), Index (1982), Pergamon Press, Oxford.

Ir 65 Irving, D.C., Freestone, R.M., Jr. and Kam, R.B.K., '05R, A General Purpose Monte Carlo Neutron Transport Code', Oak Ridge National Laboratory Internal Report ORNL-3622 (1965).

Je 74 Jenkins, T.M., 'Accelerator Boundary Doses and Skyshine', Health Physics, 27, 251 (1974).

Ka 77 Katoh, K., National Laboratory for High-Energy Physics, Tsukuba, Japan, private communication (1977).

Ka 78a Katoh K., 'Radiation and Safety Control Division', in KEK Annual Report 1978, National Laboratory for High Energy Physics (KEK), Oho-machi, Tsukuba-gun, Ibaraki-ken, Japan (1978).

Ka 78b Katoh, K. and Thomas, R.H., 'Population Dose Equivalent Due to Accelerator Operations at KEK', National Laboratory for High Energy Physics, Tsukuba-gun, Ibaraki-ken, Japan (June 1978).

Ki 62 Kinney, W.E., 'A Monte Carlo Calculation of Scattered Neutron Fluxes at an Air-Ground Interface due to Point Isotropic Sources on the Interface', Oak Ridge National Laboratory Internal Report ORNL-3287 (1962).

Ko 70 Komochkov, M.M., 'The Dubna Synchrophasotron', in Engineering Compendium on Radiation Shielding, Vol. 3, p. 171, R.G. Jaeger (Ed.), Springer-Verlag, Berlin (1970).

Ko 72 Komochov, M.M. and Teterev, Yu.G., 'Activation of Water Cooling the Synchrocyclotron Units', Joint Institute of Nuclear Research Report JNIR-P16-6314, Dubna (1972).

La 68 Ladu, M., Pelliccioni, M., Picchi, P. and Verri, G., 'A Contribution to the Skyshine Study', Nucl. Instrum. Meth. 62, 51 (1968).

Le 65 Lebedev, V.N., Zolin, L.S. and Salatskaya, M.I., 'Distribution of the Penetrating Radiation Field over the Protective Zone of the 10 GeV Synchrophasotron', Joint Institute for Nuclear Research, Dubna, USSR, Internal Report, JNIR-P-2177 (1965).

Li 57 Lindenbaum, S.J., 'Brookhaven National Laboratory Proton Synchrotron', in Proc. Conference on Shielding of High Energy Accelerators, New York, April 11-13, 1957, USAEC TID-7545, p. 28 (1957).

Li 61 Lindenbaum, S.J., 'Shielding of High Energy Accelerators', Ann. Rev. Nucl. Sci., 11 213 (1961).

Ma 69 Mawson, C.A., 'Consequences of Radioactive Disposal into the Ground', in Health Physics, Vol. 2, Part I (A.M.F. Duhamel, ed.), Pergamon Press, Oxford (1969).

Mi 66 Middlekoop, W.C., 'Remarks about Groundwater Activation by a 300 GeV Proton Synchrotron', CERN Internal Report ISR/INT BT/66-3 (1966).

Mi 77 Miyajima, M., Hirayama, H., Hozumi, K., Miura, S. and Katoh, K., 'Measurement of Stray Neutron Doses around KEK PS-Facility (1)', National Laboratory for High Energy Physics (KEK), Oho-machi, Tsukuba-gun, Ibaraki-ken, Japan, Internal Report KEK-77-17

(1977).

Mo 57 Moyer, B.J., 'University of California Radiation Laboratory Proton Synchrotron', in Proc. Conference on Shielding of High Energy Accelerators, New York, April 11-13, 1957, USAEC TID-7545, p. 38 (1957).

Mo 66 Moore, W.H., 'Source of High-Energy Particles from an Internal Target in the AGS', Brookhaven Laboratory Internal Report, AGSCD-62 (1966).

Mu 81 Mughabghab, S.F., Divadeenam, M. and Holden, N.E., 'Neutron Cross Sections: Neutron Resonance Parameters and Thermal Cross Sections', Vol. 1, Part A, Academic Press, New York (1981).

Na 75 Nakamura, T., Kawabata, H., Hayashi, K., Shin, K., Sugai, I., Hasegawa, T. and Ishizaki, Y., 'Skyshine of Neutrons and Photons from the INS FM-Cyclotron', Institute of Nuclear Study, Tokyo, Report 43 (1975).

Na 81a Nakamura, T. and Kosako, T., 'A Systematic Study on the Neutron Skyshine from Nuclear Facilities, Part I: Monte Carlo Analysis of Neutron Propagation in Air-over-Ground Environment from a Monoenergetic Source', Nucl. Sci. Eng., 77, 168 (1981).

Na 81b Nakamura, T., Kosako, T., Hayashi, K., Ban, S. and Katoh, K., 'A Systematic Study on the Neutron Skyshine from Nuclear Facilities, Part II: Experimental Approach to the Behavior of Environmental Neutrons around an Electron Synchrotron', Nucl. Sci. Eng., 77, 182 (1981).

Ne 65 Nelson, W.R., 'Radioactive Groundwater Produced in the Vicinity of Beam Dumps', Stanford Linear Accelerator Center Internal Note SLAC-TN-65-16 (1965).

Ol 64 Ollendorf, W., 'A Study of Radiation Levels at the CERN Site', CERN Internal Report DI/HP/66 (1964).

Pa 57 Panofsky, W. K. H., 'Shielding Work at Stanford University', in Proc. Conference on Shielding of High Energy Accelerators, New York, April 11-13, 1957, USAEC TID-7545, p. 199 (1957).

Pa 73 Patterson, H.W. and Thomas, R.H., 'Induced Radioactivity', in Accelerator Health Physics, Academic Press, New York, Chapter 7 (1973).

Pe 74 Peetermans, A. and Baarli, J., 'Radioactive Gas and Aerosol Production by the CERN High-Energy Accelerators and Evaluation of their Influences on Environmental Problems', Environmental Surveillance around Nuclear Installations, Vol. 1, p. 433 IAEA Vienna (1974).

Pr 72 Prantl, F.A. and Baarli, J., 'Control of Radioactive Pollution in the Environment of the CERN Accelerators', CERN Report CERN 72-15 (1972).

Rh 78 Rhoades, W.A., Simpson, D.B., Childs, R.L. and Engle, W.W., 'The DOT-IV Two-Dimensional Discrete Ordinates Transport Code with

Space-Dependent Mesh and Quadrature', Oak Ridge National Laboratory Technical Memorandum ORNL/TM-6529 (1978).

Ri 63 Rindi, A. and Baarli, J., 'Scattered Radiation at Large Distance from the CERN 600 MeV Synchrocyclotron', CERN Internal Report DI/HP/19 (1963).

Ri 67 Rindi, A. and Charalambus, S., 'Airborne Radioactivity Produced at High-Energy Accelerators', Nucl. Instrum. Methods 47, 227 (1967).

Ri 72a Rindi, A., 'La Radioactivé Induite dans l'Air de l'Accelerateur de Protons de 300 GeV du CERN', CERN Internal Report CERNLABII RA/72-5 (1972).

Ri 72b Rindi, A., 'Induced Radioactivity in the Cooling Waters of the 300 GeV SPS', CERN Internal Report Lab II-RA/Note/72-13 (1972).

Ri 75 Rindi, A. and Thomas, R.H., 'Skyshine—A Paper Tiger?' Particle Accelerators 7, 23 (1975).

Ro 58 Rose, B., Goddard, B.A., Loveridge, B.A., Salmon, L and Thomas, A.M., 'Radioactivity of Synchrocyclotron Cooling Water', Atomic Energy Research Establishment, Internal Report, Harwell, AERE NP/R 2768 (1958).

Ru 65 Russel, J.E. and Ryan, R.M., 'Radioactive Gas Production from the R.P.I. Electron Linear Accelerator', IEEE Trans. Nucl. Science NS-12; 3, 678 (1965).

Sh 67 Shaw, K.B., Thomas, R.H., 'Radiation Problems Associated with a High-Energy Extracted Proton Beam', Health Physics 13, 1127 (1967).

Sh 69 Shaw K.B., Stevenson, G.R. and Thomas R.H., 'Evaluation of Dose Equivalent from Neutron Energy Spectra', Health Physics 17, 459 (1969).

Si 62 Simpson, P.W. and Laws, D., Rutherford Laboratory Internal Report, Addendum to NIRL/M/30 (Th 62) (1962).

Sm 77 Smith, A.R., Lawrence Berkeley Laboratory (private communication, 1977).

St 67 Stapleton, G.B. and Thomas, R.H., 'Radioassay for ^{7}Be and ^{3}H of Nimrod Cooling Water', Rutherford Laboratory Internal Note RP/PN/45 (1967).

St 71 Stapleton, G.B. and Thomas, R.H., 'The Production of ^{7}Be by 7 GeV Proton Interactions with Oxygen', Nucl. Phys. A175, 124 (1971).

St 72 Stapleton, G.B. and Thomas, R.H., 'Estimation of the Induced Radioactivity of the Groundwater System in the Neighborhood of a Proposed 300-GeV High-Energy Accelerator Situated on a Chalk Site', Health Physics 23, 689 (1972).

St 73 Stapleton, G.B. and Thomas, R.H., 'The Effect of Sorption on the Migration of ^{7}Be from a High-Energy Accelerator Constructed on a Chalk Site', Water Research 7, 1259 (1973).

St 75 Stephens, L.D., Thomas, R.H. and Thomas, S.B., 'Population Exposure from High Energy Accelerators', Health Phys., 29, 853 (1975),

St 76 Stephens, L.D., Thomas, R.H. and Thomas, S.B., 'A Model for Estimating Population Exposures Due to the Operation of High Energy Accelerators at the Lawrence Berkeley Laboratory', Health Phys., 30, 404 (1976).

St 84a Stevenson, G.R. and Thomas, R.H., 'A Simple Procedure for the Estimation of Neutron Skyshine from Proton Accelerators', Health Phys. 46, 115 (1984).

St 84b Stevenson, G.R., 'Estimation of Star Densities in the Cooling Water of Certain SPS Machine Components', CERN Internal Report TIS-RP/IR/84-12 (1984).

Th 62 Thomas, R.H., Shaw, K.B., Simpson, P.W. and MacEwan, J.E., 'Neutron Surveys around the Rutherford Laboratory 50 MeV Proton Linear Accelerator', Rutherford Laboratory Internal Report NIRL/M/30 (1962).

Th 70 Thomas, R.H., 'Possible Contamination of Groundwater System by High-Energy Accelerators', Proc. Fifth Annual Health Physics Soc., Mid-Year Topical Symposium on the Health Physics Aspects of Nuclear Facility Siting, November 3-6, Idaho Falls, p. 93 (1970). Also published as Lawrence Berkeley Laboratory Internal Report UCRL-20131 (1970).

Th 72 Thomas, R.H., 'Radioactivity in Earth Induced by High-Energy Electrons', Nucl. Instrum. Methods 102, 149 (1972).

Th 76a Thomas, R.H. (Ed.), 'The Environmental Surveillance Program of the Lawrence Berkeley Laboratory', Lawrence Berkeley Laboratory Internal Report LBL-4678 (1976).

Th 76b Thomas, R.H. (ed.), 'Annual Environmental Monitoring Report of the Lawrence Berkeley Laboratory— 1975', Lawrence Berkeley Laboratory Report LBL-4827 (1976).

Th 78 Thomas, R.H., 'The Radiological Impact of High-Energy Accelerators on the Environment', Lawrence Berkeley Laboratory Report LBL-8101 (1978).

Th 79 Thomas, R.H. and Rindi, A., 'Radiological Environmental Impact of High-Energy Accelerators', Critical Reviews of Environmental Control 9(1), 51 (1979).

Tu 76 Tuyn, J W.N., CERN Health Physics Group, private communication (1976).

Vi 69 Vialettes, H., 'Gas and Dust Activation in the Target Room of the Saclay Electron Linac Identification of the Produced Radioactive Nuclei and Determination of the Rejected Activities', Proceedings of the Second International Conference on Accelerator Dosimetry and Experience, SLAC, Stanford, CONF-691101, p. 121 (1960).

Wa 69 Warren, G.J., Busick, D.D. and McCall, R.C., 'Radioactivity Produced and Released from Water and High Energies', in Proc. Second Int. Conf. in Accelerator Dosimetry and Experience, Stanford, November 1969, CONF-691101, p. 99 (1969).

Wi 57 Williams, R.W., 'Attenuation', in Proc. Conference on Shielding of High Energy Accelerators, New York, April 11-13, 1957, USAEC TID-7545, p. 92 (1957).

Table 6.1
Constants for Ladu skyshine formula (La 68).

	Θ	A	B	α	λ(m)
All Neutrons	30°	8.24×10^{-8}	4.75×10^{-11}	1.53	232
	60°	3.56×10^{-7}	1.50×10^{-10}	1.59	220
	90°	6.03×10^{-7}	5.25×10^{-10}	1.47	200
$E_n > 2.5$ eV	30°	8.45×10^{-8}	2.40×10^{-11}	1.67	215
	60°	2.33×10^{-8}	8.75×10^{-11}	1.63	200
	90°	5.17×10^{-8}	3.30×10^{-10}	1.57	180

Table 6.2
Dose equivalent per unit fluence for
1/E neutron spectra of various upper energies.

Upper energy (MeV)	Spectrum averaged dose equivalent [fSv m^2]
1.6	3.9
2.5	4.8
4.0	5.6
6.3	6.4
10	7.2
16	7.9
25	8.6
40	9.4
63	10.1
100	10.9
160	11.7
250	12.5
400	13.4
630	14.6
1000	16.2
1600	18.4
2500	21.2
4000	25.0
6300	30.0
10000	36.5

Table 6.3
Summary of population dose equivalent estimates for several high-energy accelerators.

Laboratory	M/H_0	Comments	Reference
Lawrence Berkeley Laboratory	1023	~170,000 people living within 5 km of the laboratory; average population density $2-3 \times 10^3$ persons per square kilometre	St 76
Stanford Linear Accelerator	460	Population dose equivalent calculated out to 1 km from the laboratory	Bu 76a, 76b
European Organization for Nuclear Research (CERN)	160	30,000 people living within 4 km of the laboratory; population density 35 persons per square kilometre <1 km, 640 persons per square kilometre >1 km from laboratory	Fa 76 Tu 76
Brookhaven National Laboratory	54	7,381 persons living within 5 km of the laboratory; 5.2×10^6 people living within 80 km of laboratory; population density of ~260 persons per square kilometre	Hu 76
Fermi National Accelerator Laboratory	1000	Dose resulting from collimated muon beam ~50-m wide at site boundary; ~100,000 people in irradiated zone	Ba 76

Table 6.4
Star production in various materials.

Kinetic energy	Material			Stars/GeV
	Oxygen	Copper	Mean	
300 MeV	0.57	0.52	0.55	1.8
1 GeV	3.8	3.1	3.5	3.5
3 GeV	11.6	9.1	10.4	3.8
30 GeV	93	78	86	2.9
300 GeV	780	660	720	2.4

Table 6.5
Distribution of radioactivity produced by the CPS or AGS.

Total radioactivity produced	150 TBq	(100%)
Total radioactivity produced in magnet, accelerator components, concrete room	140 TBq	(~93%)
Total radioactivity produced in earth	8 TBq	(~5%)
Total radioactivity produced in groundwater	1 TBq	(~1%)

Table 6.6
Spallation products from ^{16}O.

Isotope	Half-life $T_{1/2}$ (s)	Production cross-section σ (mb)	Ratio σ/σ_{inel} (%)	Atoms per star N	Beta decay	Gamma energies (MeV)	Gamma emission probability
^{10}C	19.1	4	1.4	5.4	100% β^+	0.717	1
						1.023	0.017
^{14}O	71.1	9	3.1	12.2	100% β^+	2.312	0.99
^{15}O	124	28	9.6	37.8	100% β^+	none	
^{13}N	600	5	1.7	6.8	100% β^+	none	
^{11}C	1220	10	3.4	13.5	100% β^+	none	
^{7}Be	4.60×10^{6}	9.3	3.2	12.6	100% EC	0.477	0.103
^{3}H	3.78×10^{8}	33	11.3	44.6	100% β^-	none	
^{14}C	1.76×10^{11}	1.9	0.65	2.6	100% β^-	none	
^{10}Be	7.88×10^{13}	0.9	0.31	1.2	100% β^-	none	

Table 6.7
Activities produced in cooling water by 30-GeV protons.

Isotope	Instantaneous loss of 10^{13} protons	Continuous loss of of 10^{11} protons/s for 5000 hours	1-hour decay factor
^{13}N	180 MBq	1.6 GBq	0.016
^{11}C	180 MBq	3.2 GBq	0.13
^{7}Be	45 kBq	2.8 GBq	1.00
^{3}H	1.9 kBq	330 MBq	1.00
^{14}C	230 mBq	42 kBq	1.00
^{10}Be	400 µBq	71 Bq	1.00

Revised 6-19-87 per GRS.

Table 6.8
Hazard estimation of activity in cooling water.

			Instantaneous loss [dilution factor = 10^{-4}]		Continuous loss [dilution factor = 10^{-9}]	
Isotope	ALI		Intake ALI	Equivalent µSv	Intake ALI	Equivalent µSv
^{13}N	20	GBq	9.1×10^{-7}	4.6×10^{-2}	7.9×10^{-7}	4.0×10^{-2}
^{11}C	20	GBq	9.0×10^{-7}	4.5×10^{-2}	1.6×10^{-6}	7.9×10^{-2}
^{7}Be	2	GBq	2.2×10^{-9}	1.1×10^{-4}	1.4×10^{-5}	7.0×10^{-1}
^{3}H	2	GBq	9.4×10^{-11}	4.7×10^{-6}	1.7×10^{-6}	8.3×10^{-2}
^{14}C	90	MBq	2.6×10^{-13}	1.3×10^{-8}	4.6×10^{-9}	7.3×10^{-4}
^{10}Be	40	MBq	9.9×10^{-16}	4.9×10^{-11}	1.8×10^{-11}	8.9×10^{-7}

Revised 6-19-87 per GRS.

Table 6.9
Radionuclides identified in earth or water at accelerator laboratories.

Laboratory	Accelerator	Soil type	Radionuclides identified		Reference
			In soil	In water	
CERN	28 GeV proton synchrotron	Molasse	^{7}Be, ^{45}Ca, ^{54}Mn, ^{22}Na	^{22}Na	Ho 72
Rutherford Laboratory	300 GeV proton synchrotron	Chalk	^{7}Be, ^{47}Ca, ^{43}K, ^{32}P, ^{47}Sc	^{7}Be, ^{11}C, ^{3}H	St 72
FNAL Batavia	500 GeV proton synchrotron	Glacial till, various clays	^{7}Be, ^{45}Ca, ^{60}Co, ^{51}Cr, ^{55}Fe, ^{59}Fe, ^{3}H, ^{22}Na, ^{46}Sc, ^{48}V	^{45}Ca, ^{3}H, ^{54}Mn, ^{22}Na	Bo 72a
Stanford SLAC	1 GeV electron linear accelerator	Sandstone	^{7}Be, ^{58}Co, ^{59}Fe, ^{54}Mn, ^{22}Na, ^{46}Sc	^{54}Mn, ^{22}Na	Th 72

Table 6.10
Values of the distribution coefficient, K (ml g^{-1})

Radionuclide	Soil type	Distribution coefficient	Reference
^{7}Be	Chalk	~4500	St 73
^{22}Na	Molasse*	100	Ho 68
^{22}Na	Glacial till	0.2	Bo 72b
^{32}P	Molasse*	100	Ho 68
	chalk	Very high	Bl nd
^{45}Ca	Molasse*	1000	Ho 68
^{54}Mn	Molasse*	100	Ho 68

*Arenaceous rocks, typical of alpine orogeny, related to the Flysch formation.

Table 6.11
Most abundant isotopes in the atmosphere.

Isotope	*Percentage by volume* in the atmosphere
^{14}N	78.1
^{16}O	21.2
^{40}Ar	0.46
^{15}N	0.28
^{18}O	0.04

Table 6.12
Radionuclides with half-life > 1 minute that can be produced in air at accelerators [after Rindi (Ri 72b)].

Radionuclide	Half-life	Emission	Parent element	Production reaction	Cross section (mb)
^{3}H	12.2 yr	β^-	N	spallation	30
			O	spallation	30
^{7}Be	53 days	γ,EC	N	spallation	10
			O	spallation	5
			Ar	spallation	0.6
^{11}C	20.5 min	β^+	N	spallation	10
			O	spallation	5
			Ar	spallation	0.7
^{14}C	5730 yr	β^-	N	(n,p)	1640
^{13}N	10 min	β^+	N	spallation	10
			N	(γ,n)	10
			O	spallation	9
			Ar	spallation	0.8
^{14}O	74 sec	β^+,γ	O	spallation	1
			Ar	spallation	0.06
^{15}O	2.1 min	β^+	O	spallation	40
			O	(γ,n)	10
			Ar	spallation	
^{18}F	1.85 h	β^+,EC	Ar	spallation	6
^{24}Ne	3.4 min	β^-,γ	Ar	spallation	0.12
^{22}Na	2.6 yr	β^+,γ	Ar	spallation	10
^{24}Mg	15 h	β^-	Ar	spallation	7
^{27}Mg	9.5 min	β^-,γ	Ar	spallation	2.5
^{28}Mg	21.3 h	β^-,γ	Ar	spallation	0.4
^{28}Al	2.3 h	β^-,γ	Ar	spallation	13
^{29}Al	6.6 min	β^-,γ	Ar	spallation	4
^{31}Si	2.6 h	β^-,γ	Ar	spallation	6
^{30}P	2.5 min	β^+,γ	Ar	spallation	4.4
^{32}P	14.3 days	β^-	Ar	spallation	25
^{33}P	25 days	β^-	Ar	spallation	9
^{35}S	87 days	β^-	Ar	spallation	23
^{34}Cl	32.4 min	β^-,γ	Ar	spallation	0.6[a]
^{38}Cl	37.3 min	β^-,γ	Ar	(γ,pn)	4
^{39}Cl	55 min	β^-,γ	Ar	(γ,p)	7
^{41}Ar	1.8 h	β^-,γ	Ar	(n,γ)	660[b]

[a] Ref. (Br 71).
[b] Ref. (Mu 81).

Table 6.13
Radionuclides identified in the air around several accelerators.

Laboratory	Accelerator	Radionuclides identified	Reference
RPI	50-MeV electron linac	^{15}O, ^{13}N	Ru 65
Saclay	330- to 560-MeV, electron linac	^{13}N, ^{15}O, ^{11}C, ^{41}Ar, ^{38}Cl, ^{7}Be	Vi 69
CERN	600-MeV proton synchrotron	^{11}C, ^{13}N, ^{41}Ar	Ri 67
PPA	3-GeV proton synchrotron	^{14}O, ^{15}O, ^{13}N, ^{11}C	Aw 65
RHEL	7-GeV proton synchrotron	^{16}N, ^{15}O, ^{13}N, ^{11}C	Sh 67
CERN	25-GeV proton synchrotron	^{13}N, ^{11}C, ^{41}Ar	Ho 69
BNL	30-GeV proton synchrotron	^{13}N, ^{11}C, ^{41}Ar	Di 64

Table 6.14

Measured and calculated specific activity in air of some long-lived isotopes leaving the CERN 600-MeV synchrocyclotron ISOLDE area (Pe 74) (in Bq/m^3).

Isotope	Half-life	Measured	Calculated
^{3}H	12.26 yr	---	0.59
^{7}Be	53.6 days	10.0	12.0
^{24}Na	15 days	1.3	1.8
^{32}P	14.5 days	0.22	0.31
^{33}P	25 days	0.074	0.17
^{41}Ar	1.83 h	---	930.0

FIGURE CAPTIONS FOR CHAPTER 6

Figure 6.1. Measurements performed around various accelerators. On the abscissa is the distance from the accelerator in metres; on the ordinate is the product of the measured neutron flux density and the square of the distance. In these coordinates, a $1/r^2$ variation is represented by a horizontal line.

(a) Measurements of fast-neutron flux density performed at the CERN 28-GeV Proton Synchrotron (Ol 64).

(b) Measurements of fast-neutron flux density performed at the Dubna 10-GeV Proton Synchrophasotron (Ko 70, Le 65).

(c) Measurements of dose-equivalent rate performed at the Brookhaven 30-GeV Proton AGS (Di 66).

(d) Measurements of the fast-neutron flux density performed at the CERN 600-MeV Proton Synchrocyclotron (Ri 63).

(e) Fast-neutron flux density measurements performed at the DESY 7.5-GeV Electron Synchrotron (Ba 67).

(f) Fast-neutron flux density measurements performed at the Rutherford Laboratory Proton Linear Accelerator (Si 62, Th 62).

(g) Measurements made at the 12-GeV Proton Synchrotron at KEK (Ka 77).

Figure 6.2. Absolute neutron fluence as a function of distance from the source for an opening angle of 90°, after (La 68). The dotted line gives the Lindenbaum curve, the solid line and histogram represent the (La 68) empirical relation and Monte Carlo calculation, respectively. The crosses and open diamonds represent the (Ki 62) calculations for the air-ground interface and the black ground, respectively. The open circles give the results from the (Na 81a) calculations.

Figure 6.3. Neutron skyshine importance functions for small semivertical angles. The histogram gives the results of the calculations of Alsmiller et al. (1981). The crosses, open circles, and closed circles are from Nakemura et al. (Na 81a) for distances of 100 m, 500 m, and 1000 m, respectively.

Figure 6.4. Dose equivalent per unit source neutron versus radial

distance from the source. Data taken from the experiment of (Di 66) and figure from (Al 81).

Figure 6.5. Absolute comparison of measured, calculated, and synthesized neutron dose distributions as a function of slant distance from the source of the YAYOI skyshine experiment [figure from (Na 81a)].

Figure 6.6. Absolute comparison of measured and calculated neutron dose distributions in the field as a function of distance from the centre of the synchrotron ring [figure from (Na 81b)].

Figure 6.7. Variation of dose equivalent with distance for 1/E spectra with various upper energies (St 84a).

Figure 6.8. Effective absorption length as a function of upper neutron energy for 1/E spectra (St 84a).

Figure 6.9. Comparison of the effective absorption length for 30 and 50 MeV with data from the Rutherford Laboratory Proton Linear Accelerator (Th 62, Si 62).

Figure 6.10. Spectra of skyshine photons taken at various distances from a 52-MeV proton cyclotron (Na 75).

Figure 6.11. The convergence of collective dose equivalent as a function of distance from the accelerator for various neutron attenuation lengths in air (St 75).

Figure 6.12. Simple model illustrates the mechanism by which accelerator-produced radioactivity may appear in ground water.

Figure 6.13. The specific activity of accelerator-produced radionuclide in ground water at a hypothetical 500-GeV accelerator site, as a function of water time, T, in the activation zone.

Figure 6.14. Typical decay curves of radioactive air as measured at two accelerators at CERN. The measurements are compared with the decay calculated assuming that the radioactive air consists of ^{41}A, ^{11}C, ^{13}N, ^{15}O and ^{14}O in the proportions 0.14:0.31:0.47:0.08:0.04.

Figure 6.15. Monthly variation of radioactivity in rainwater at CERN and Le Vesinet during 1975. The variation of beta activity with time is monitored at both locations and shows no correlation with accelerator activity. On the other hand the variation of ^{7}Be activity with time measured at CERN shows a significant departure from that measured at Le Vesinet. This departure may be correlated with accelerator operation at CERN (from Falk et al., Fa 76).

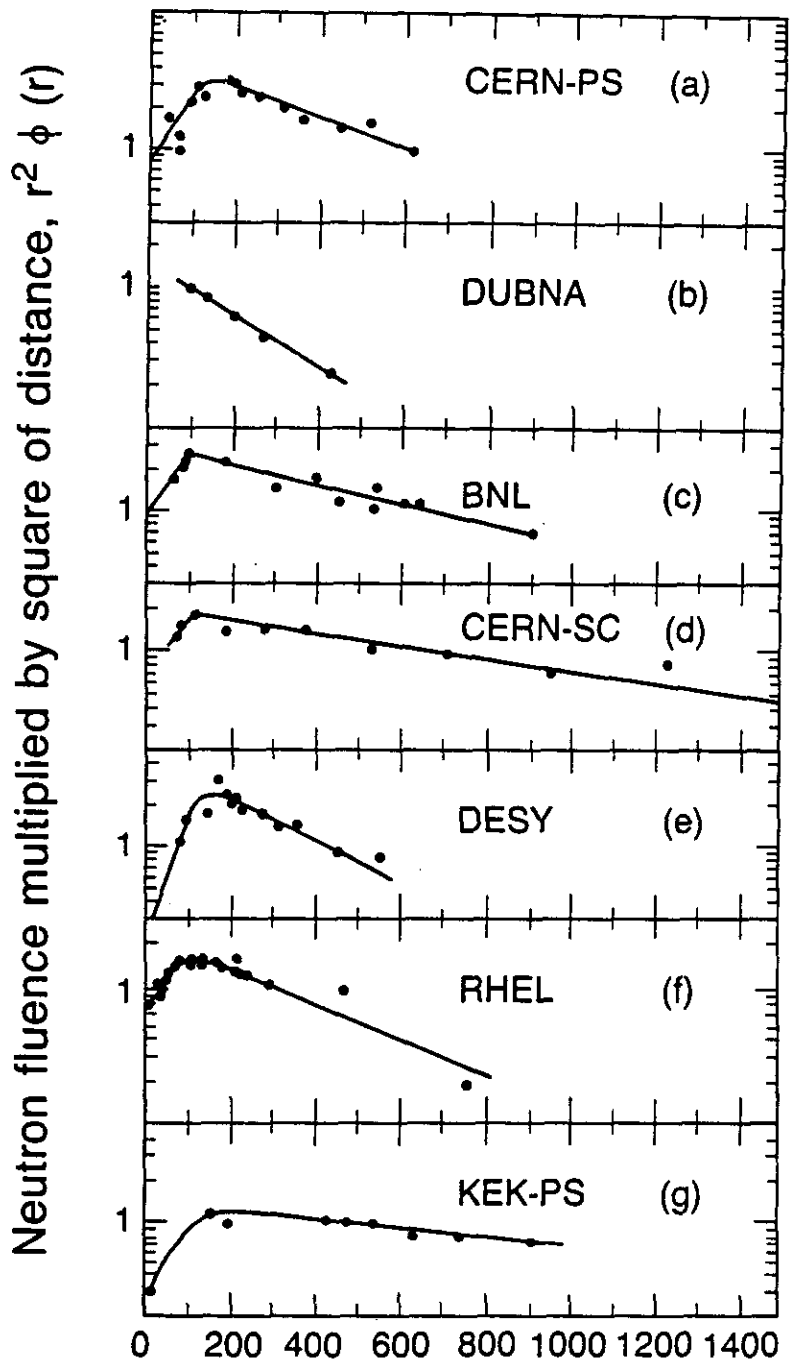

XBL 853-8051

6.1

6.1

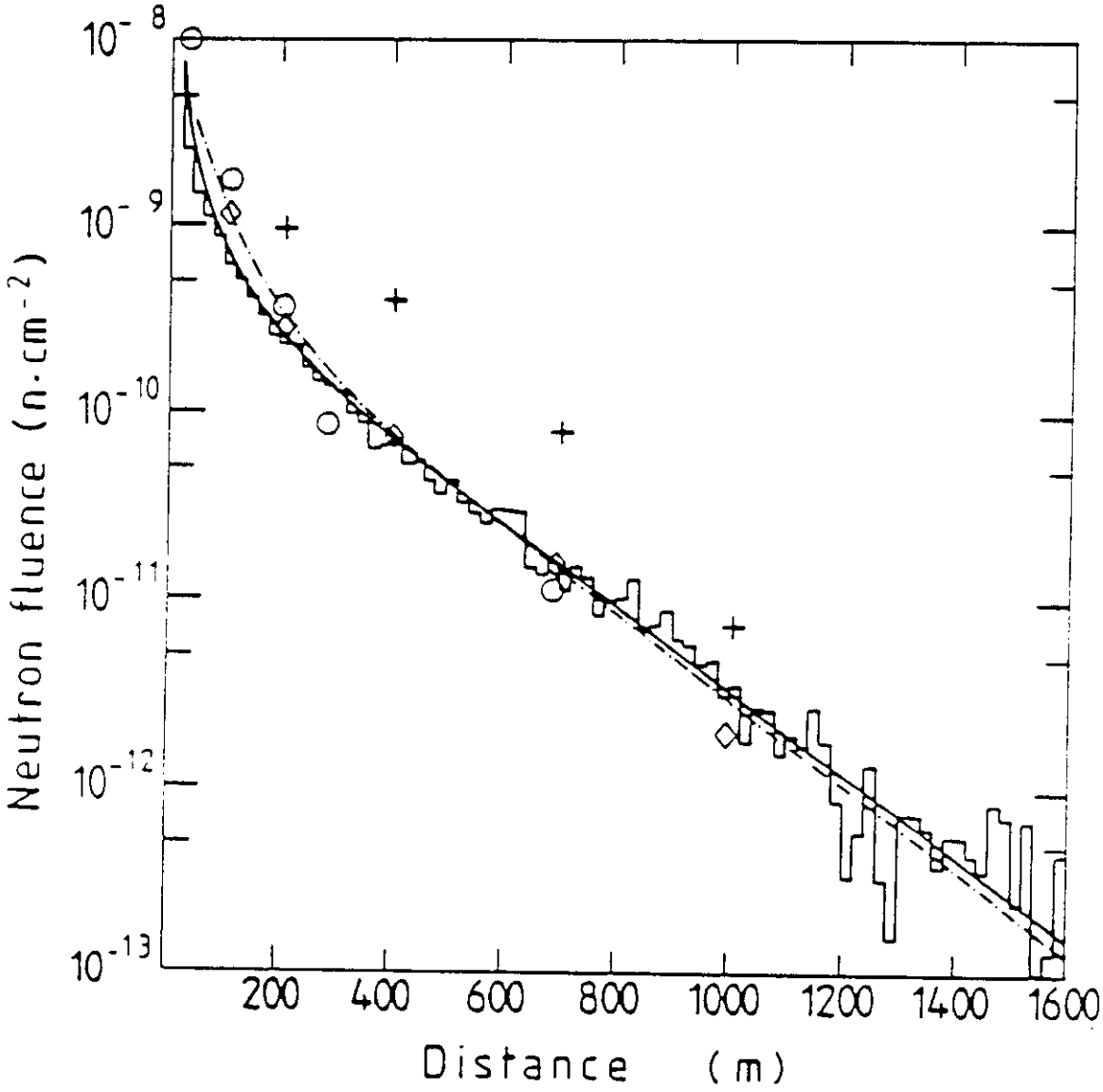
Neutron fluence (n.cm⁻²)
10⁻⁸
10⁻⁹
10⁻¹⁰
10⁻¹¹
10⁻¹²
10⁻¹³
200
400
600
800
1000
1200
1400
1600
Distance (m)

6.2

6.2

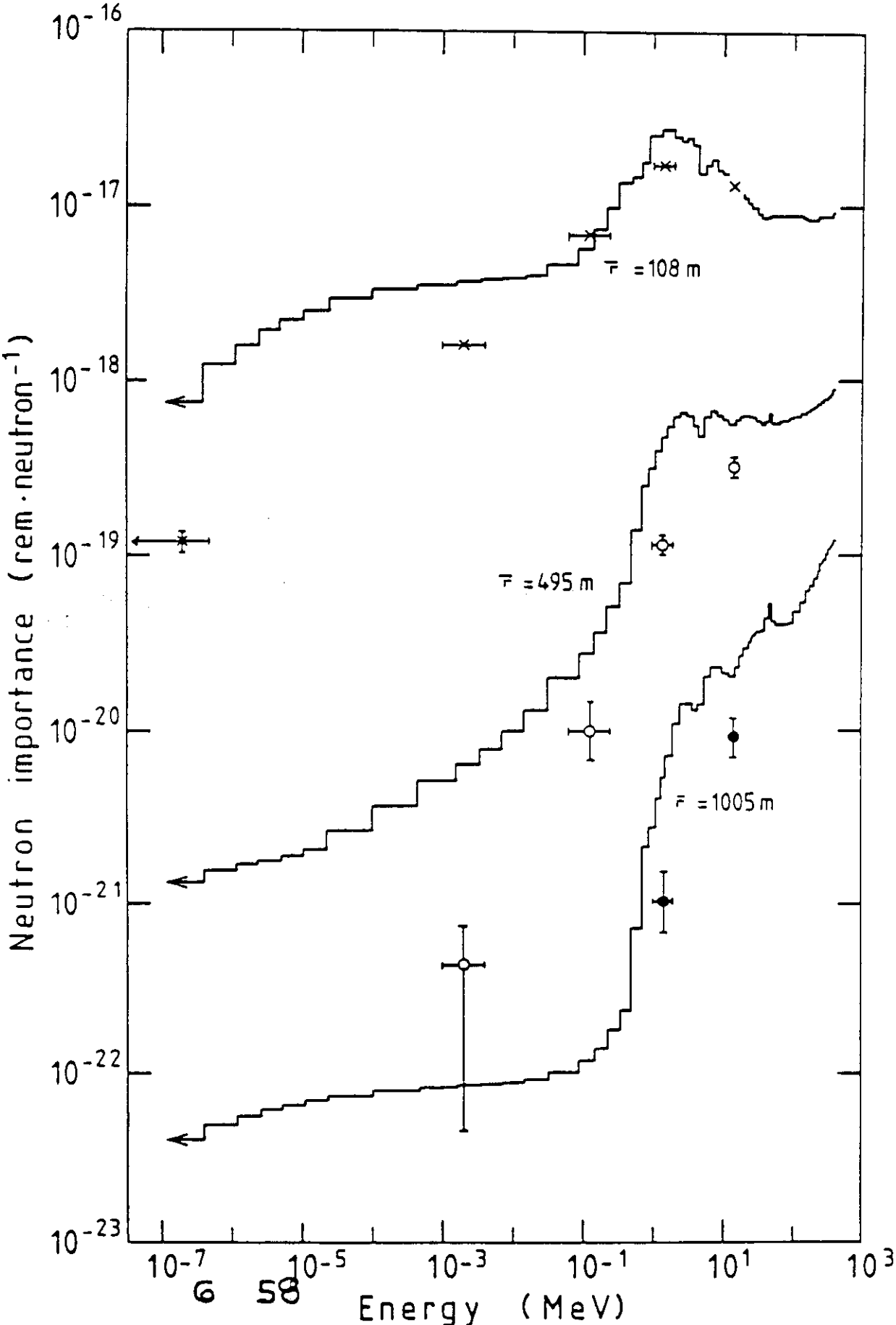
Neutron importance (rem·neutron⁻¹)
10⁻¹⁶
10⁻¹⁷
10⁻¹⁸
10⁻¹⁹
10⁻²⁰
10⁻²¹
10⁻²²
10⁻²³
r̄ = 108 m
r̄ = 495 m
r̄ = 1005 m
10⁻⁷
10⁻⁵
10⁻³
10⁻¹
10¹
10³
Energy (MeV)

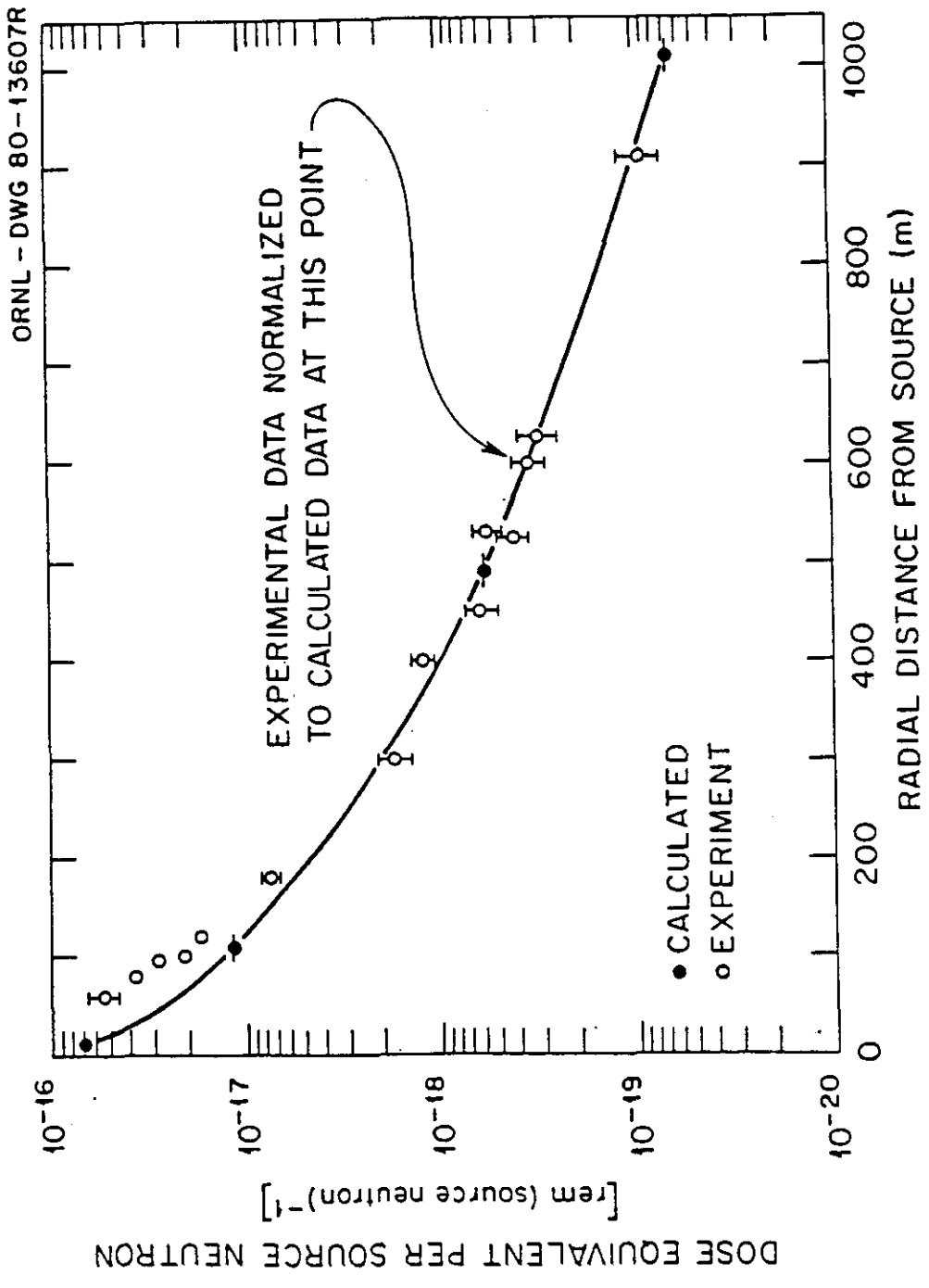
ORNL - DWG 80-13607R
EXPERIMENTAL DATA NORMALIZED
TO CALCULATED DATA AT THIS POINT
• CALCULATED
o EXPERIMENT
DOSE EQUIVALENT PER SOURCE NEUTRON
[rem (source neutron)⁻¹]
RADIAL DISTANCE FROM SOURCE (m)
10⁻¹⁶
10⁻¹⁷
10⁻¹⁸
10⁻¹⁹
10⁻²⁰
0
200
400
600
800
1000

6.4

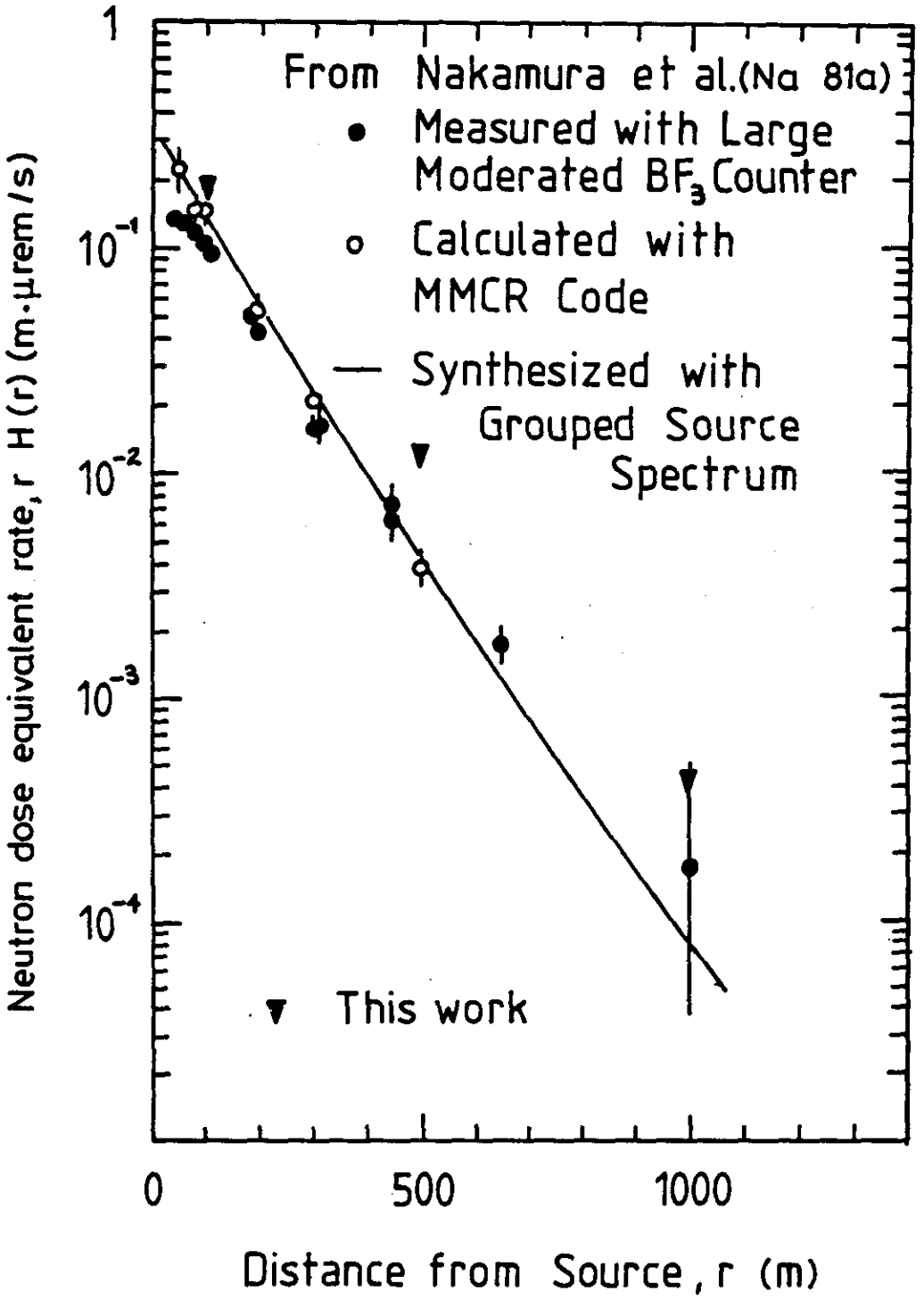
From Nakamura et al.(Na 81a)
Measured with Large Moderated BF_3 Counter
Calculated with MMCR Code
Synthesized with Grouped Source Spectrum
This work
Neutron dose equivalent rate, r H(r) (m·μrem/s)
1
10^{-1}
10^{-2}
10^{-3}
10^{-4}
0
500
1000
Distance from Source, r (m)

6.5

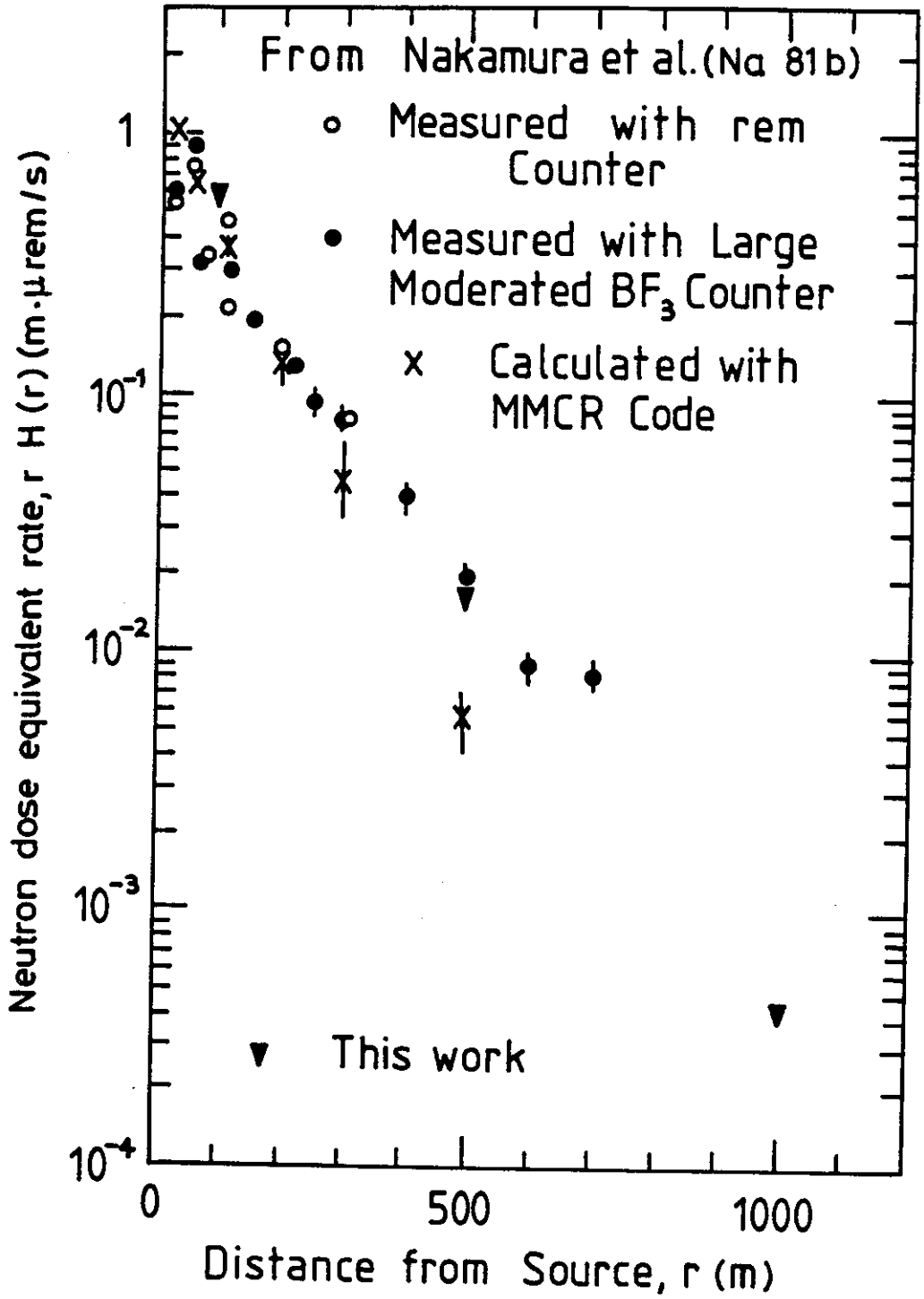
From Nakamura et al. (Na 81b)
Measured with rem Counter
Measured with Large Moderated BF_3 Counter
Calculated with MMCR Code
This work
Neutron dose equivalent rate, r H(r) (m.μrem/s)
1
10^{-1}
10^{-2}
10^{-3}
10^{-4}
0
500
1000
Distance from Source, r (m)

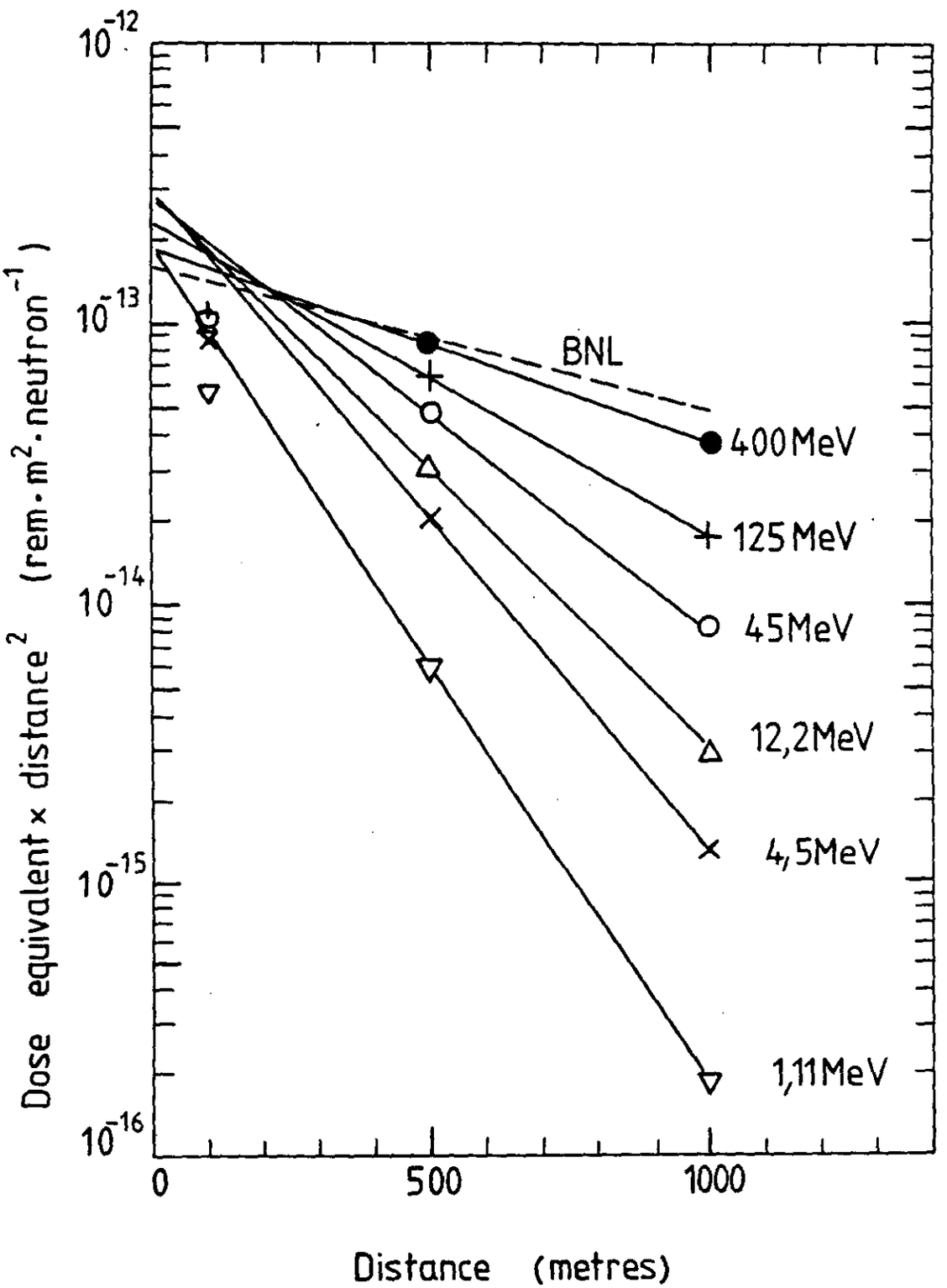
10^{-12}
10^{-13}
10^{-14}
10^{-15}
10^{-16}
Dose equivalent × distance^2 (rem · m^2 · neutron^{-1})
0
500
1000
Distance (metres)
BNL
400 MeV
125 MeV
45 MeV
12,2 MeV
4,5 MeV
1,11 MeV

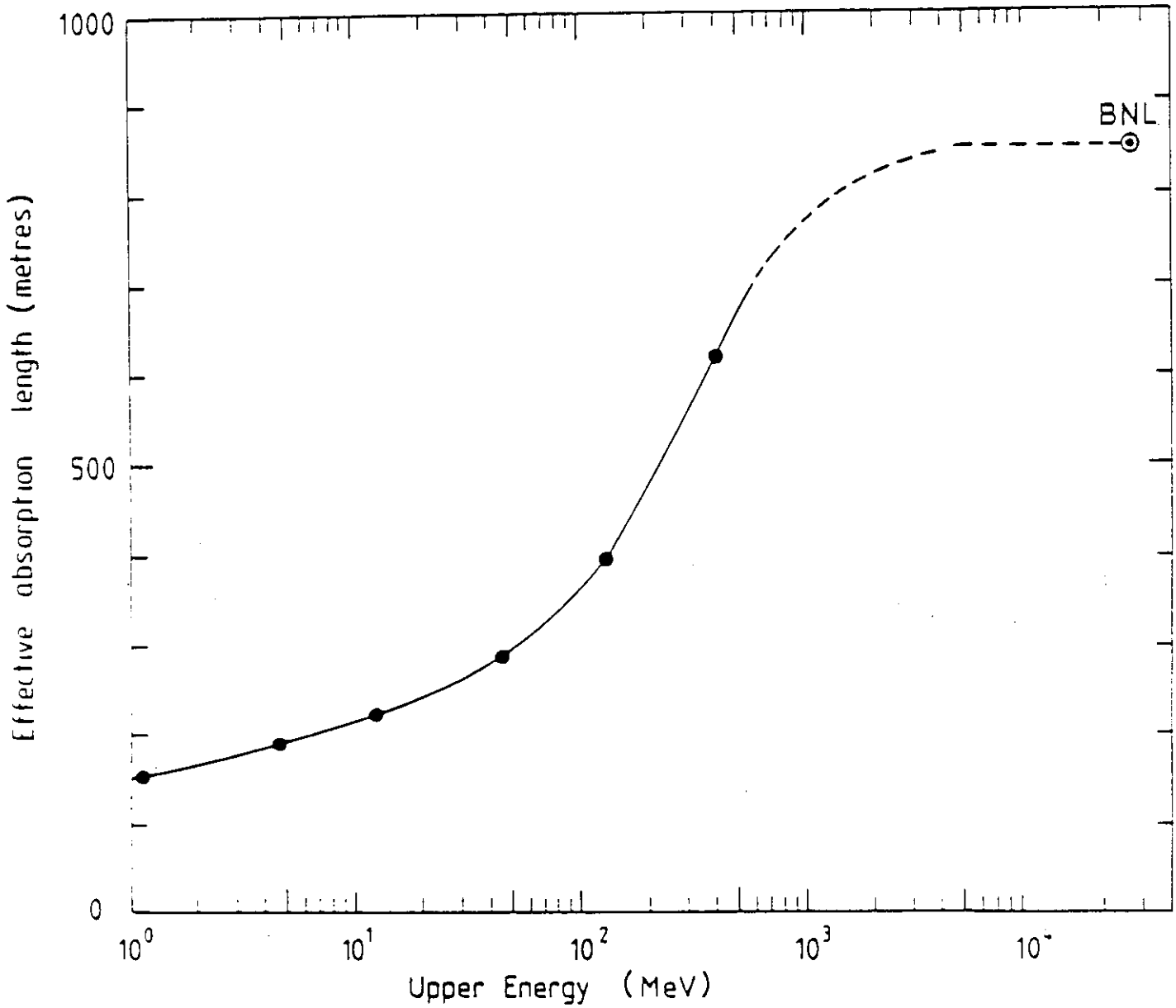
1000
500
0
BNL
Effective absorption length (metres)
10^0
10^1
10^2
10^3
Upper Energy (MeV)

6.8

6.8

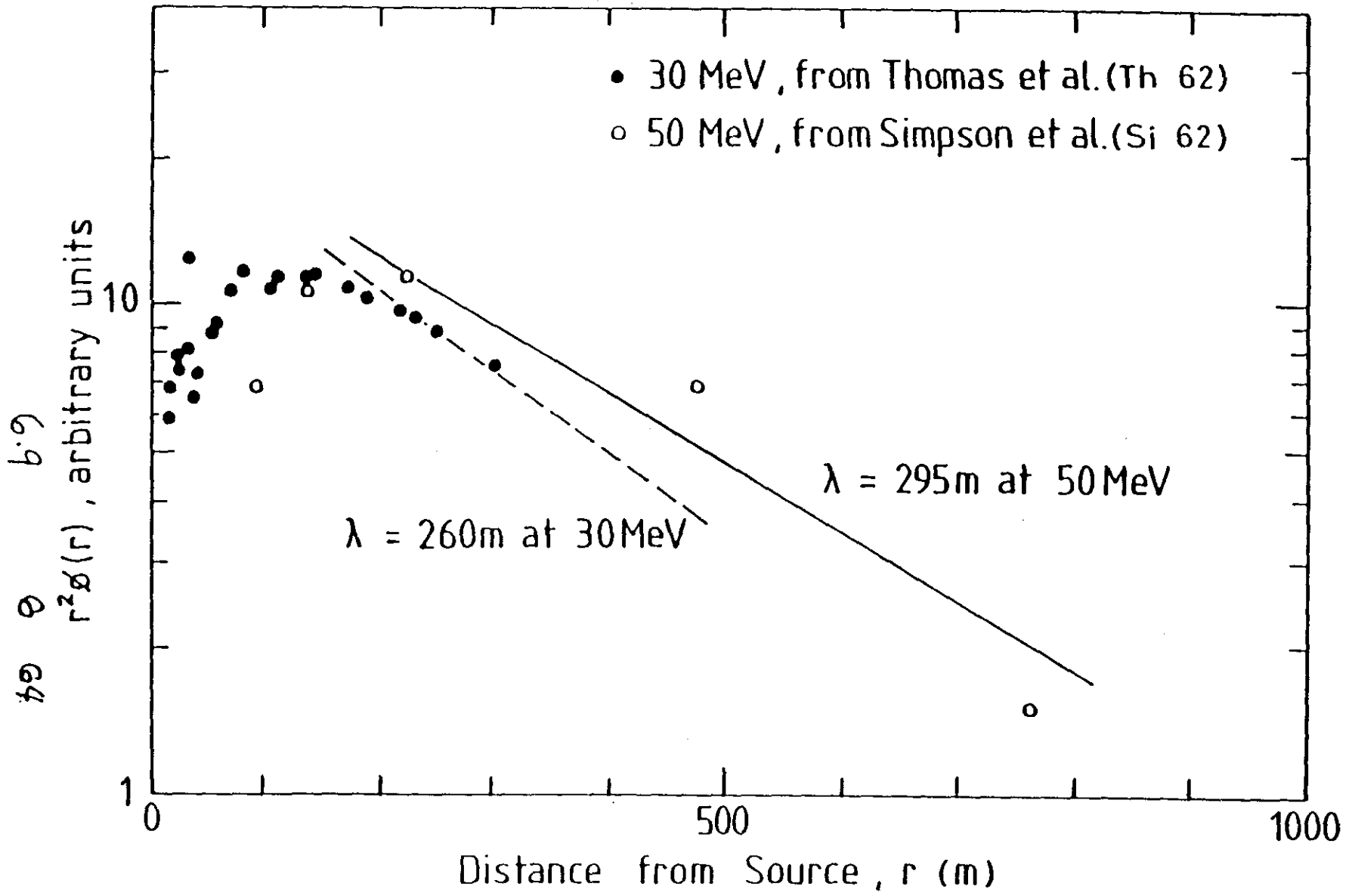
• 30 MeV, from Thomas et al. (Th 62)
○ 50 MeV, from Simpson et al. (Si 62)
λ = 295m at 50 MeV
λ = 260m at 30 MeV
r²ϕ(r), arbitrary units
10
1
0
500
1000
Distance from Source, r (m)

6.9

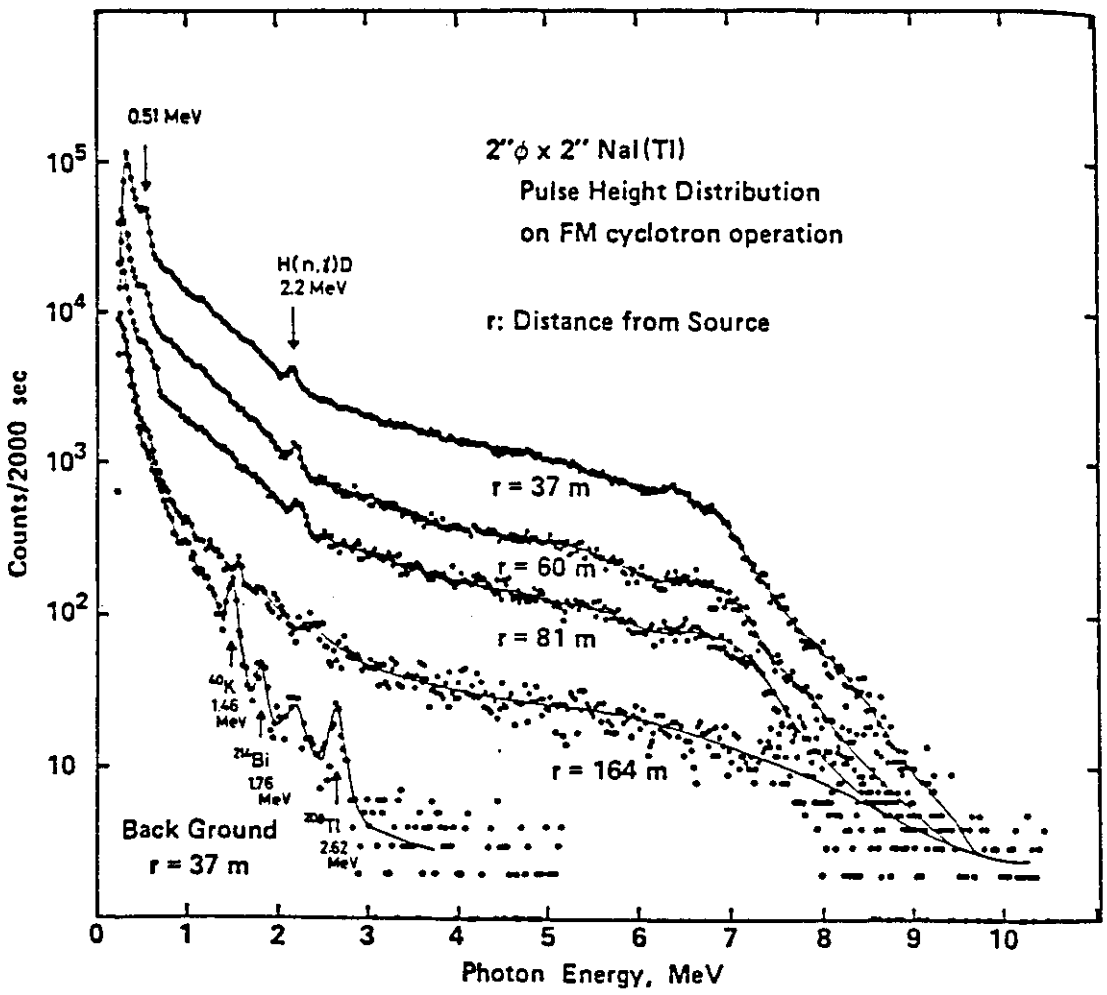
0.51 MeV
2"ϕ x 2" NaI(Tl)
Pulse Height Distribution
on FM cyclotron operation
H(n,γ)D
2.2 MeV
r: Distance from Source
r = 37 m
r = 60 m
r = 81 m
r = 164 m
40K
1.46
MeV
214Bi
1.76
MeV
208Tl
2.62
MeV
Back Ground
r = 37 m
Counts/2000 sec
Photon Energy, MeV

6.10

6.10

XBL 853-8046

6.11

6.11

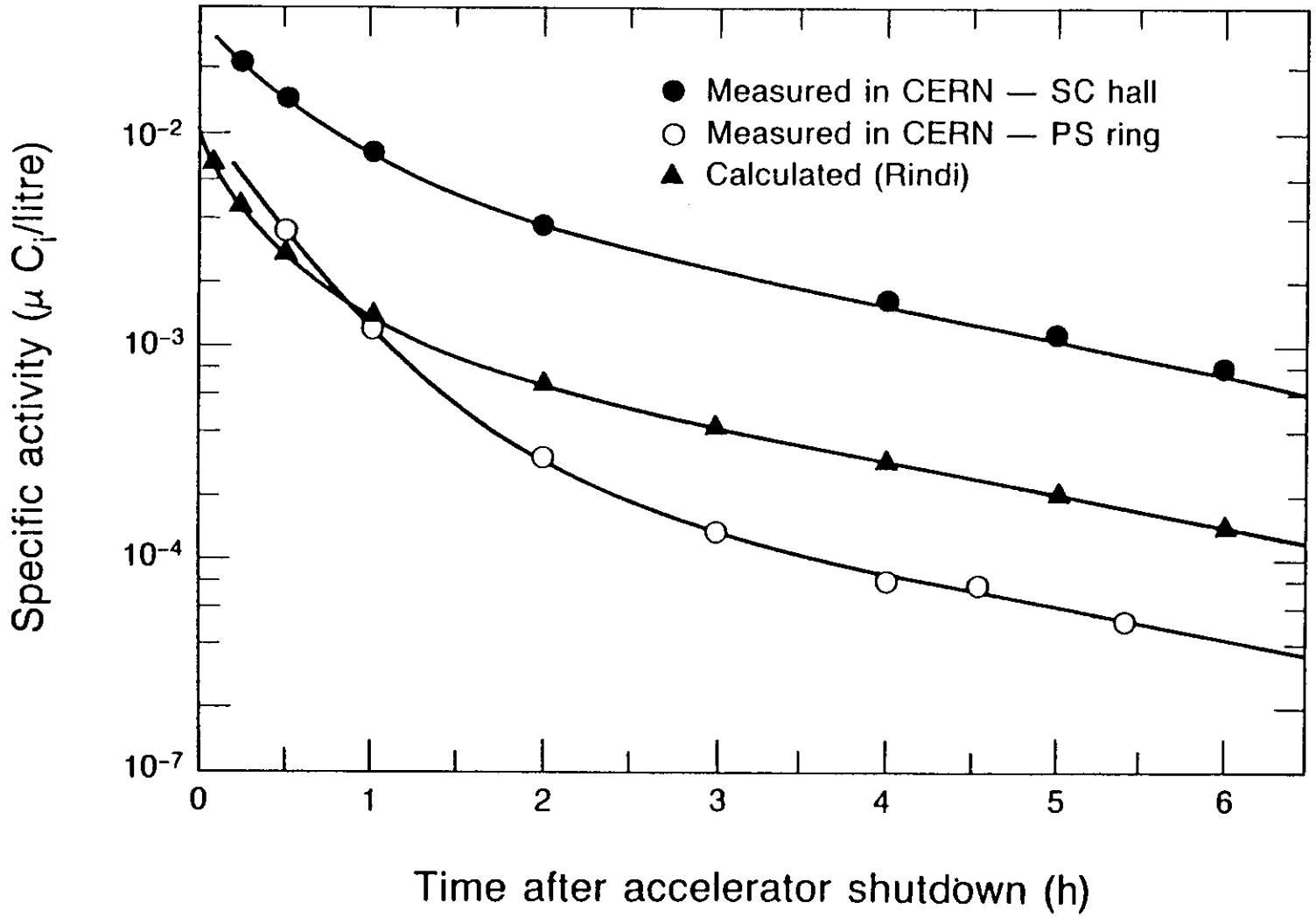
Measured in CERN — SC hall
Measured in CERN — PS ring
Calculated (Rindi)
Specific activity (μ Ci/litre)
10⁻²
10⁻³
10⁻⁴
10⁻⁷
0
1
2
3
4
5
6
Time after accelerator shutdown (h)

XBL 853-8041

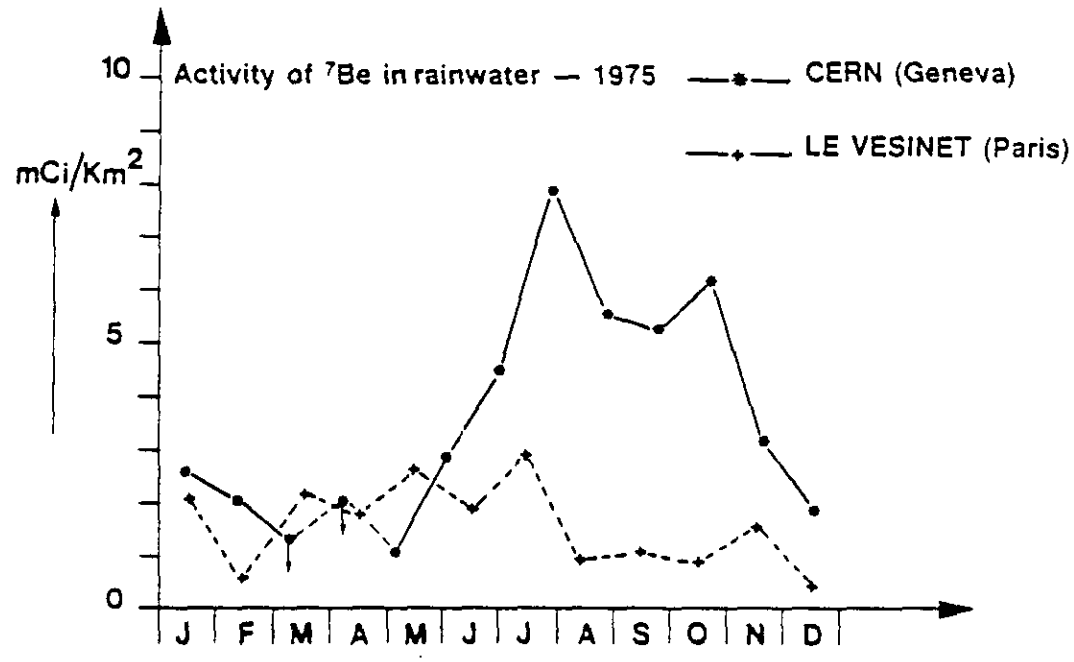

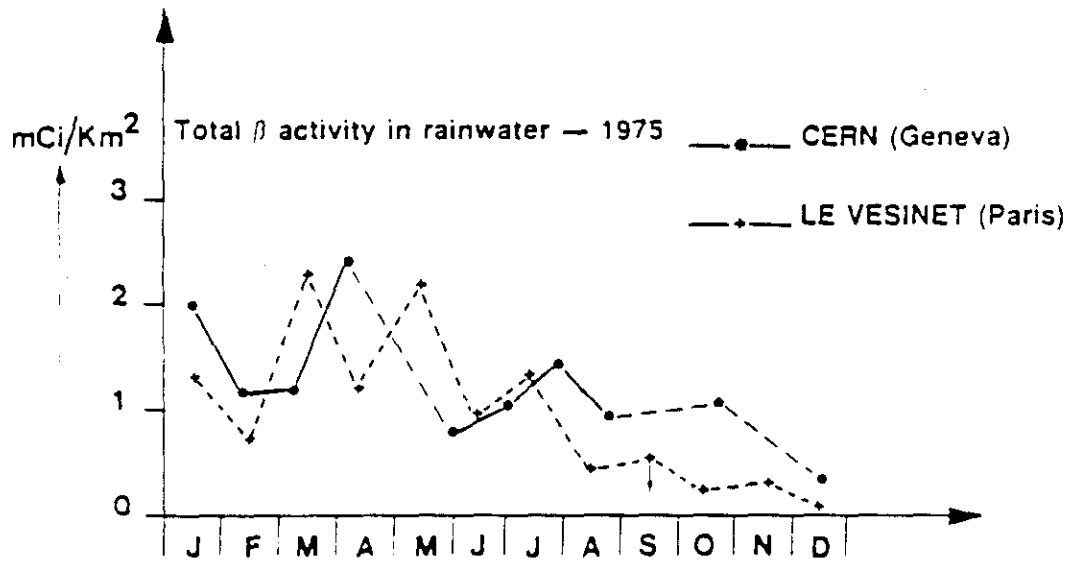

XBL 853-8044

6.13

6.13

6.13

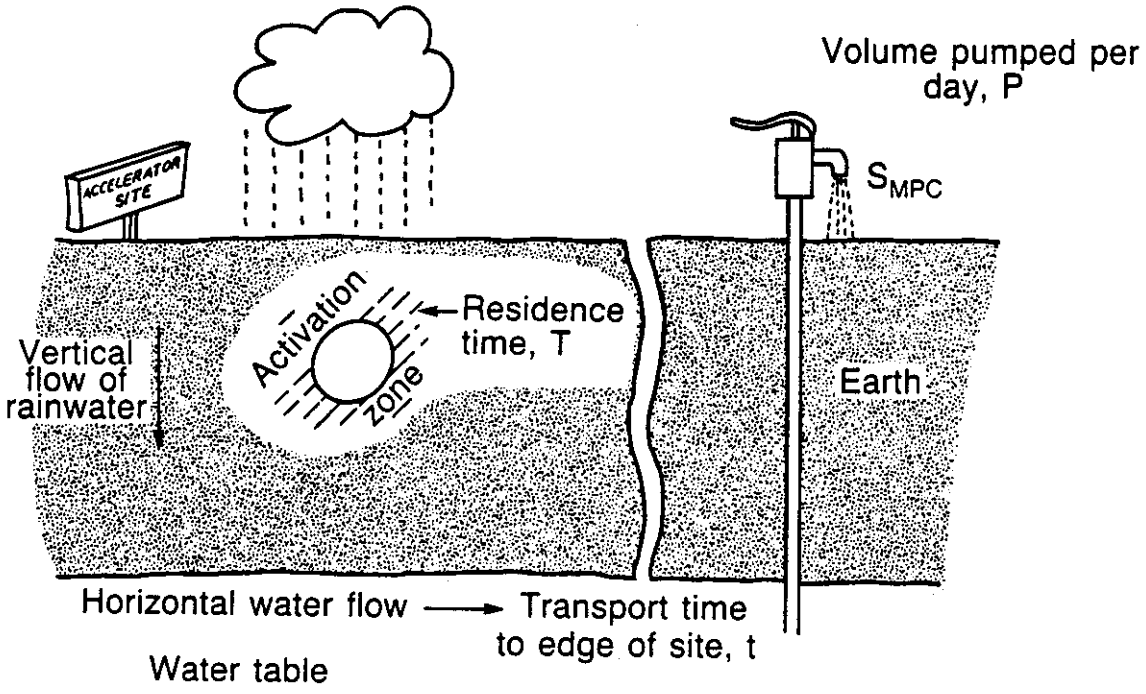

XBL 853-8040

6.14

Appendix 6.1

Neutron Importance Functions

In Tables A.1 to A.3 that follow the neutron importance is given as a function of energy for the specified cosine intervals and for r = 108, 495, and 1005 m respectively.

Appendix 6.1

TABLE A.1

Neutron Importance as a function of Energy
Mean r = 108 m.

		Neutron Importance in sievert				
		cosθ				
E_{high} MeV	E_{low} MeV	0.0-0.2	0.2-0.4	0.4-0.6	0.6-0.8	0.8-1.0
4.00E+02	3.75E+02	3.75E-19	2.36E-19	1.58E-19	1.26E-19	9.34E-20
3.75E+02	3.50E+02	3.59E-19	2.27E-19	1.53E-19	1.21E-19	8.96E-20
3.50E+02	3.25E+02	3.50E-19	2.23E-19	1.50E-19	1.20E-19	8.84E-20
3.25E+02	3.00E+02	3.44E-19	2.21E-19	1.49E-19	1.20E-19	8.83E-20
3.00E+02	2.75E+02	3.39E-19	2.19E-19	1.49E-19	1.20E-19	8.92E-20
2.75E+02	2.50E+02	3.33E-19	2.17E-19	1.48E-19	1.20E-19	8.93E-20
2.50E+02	2.25E+02	3.25E-19	2.12E-19	1.45E-19	1.18E-19	8.76E-20
2.25E+02	2.00E+02	3.16E-19	2.07E-19	1.42E-19	1.15E-19	8.55E-20
2.00E+02	1.75E+02	3.09E-19	2.04E-19	1.40E-19	1.14E-19	8.47E-20
1.75E+02	1.50E+02	3.06E-19	2.02E-19	1.40E-19	1.14E-19	8.52E-20
1.50E+02	1.25E+02	3.06E-19	2.04E-19	1.42E-19	1.17E-19	8.72E-20
1.25E+02	1.00E+02	3.12E-19	2.09E-19	1.45E-19	1.20E-19	9.00E-20
1.00E+02	9.00E+01	3.18E-19	2.11E-19	1.46E-19	1.20E-19	9.10E-20
9.00E+01	8.00E+01	3.24E-19	2.14E-19	1.47E-19	1.20E-19	9.08E-20
8.00E+01	7.00E+01	3.34E-19	2.20E-19	1.50E-19	1.21E-19	9.10E-20
7.00E+01	6.00E+01	3.48E-19	2.29E-19	1.54E-19	1.24E-19	9.21E-20
6.00E+01	5.50E+01	3.55E-19	2.30E-19	1.54E-19	1.22E-19	9.07E-20
5.50E+01	5.00E+01	3.62E-19	2.35E-19	1.56E-19	1.23E-19	9.03E-20
5.00E+01	4.50E+01	4.12E-19	2.66E-19	1.72E-19	1.29E-19	9.08E-20
4.50E+01	4.00E+01	3.82E-19	2.47E-19	1.61E-19	1.21E-19	8.62E-20
4.00E+01	3.50E+01	3.69E-19	2.41E-19	1.58E-19	1.20E-19	8.66E-20
3.50E+01	3.00E+01	3.87E-19	2.55E-19	1.67E-19	1.28E-19	9.19E-20
3.00E+01	2.75E+01	4.09E-19	2.70E-19	1.77E-19	1.35E-19	9.74E-20
2.75E+01	2.50E+01	4.14E-19	2.75E-19	1.81E-19	1.38E-19	1.00E-19
2.50E+01	2.25E+01	4.20E-19	2.82E-19	1.88E-19	1.44E-19	1.05E-19
2.25E+01	2.00E+01	4.24E-19	2.89E-19	1.95E-19	1.51E-19	1.12E-19
2.00E+01	1.75E+01	4.28E-19	2.95E-19	2.02E-19	1.59E-19	1.20E-19
1.75E+01	1.49E+01	4.32E-19	3.05E-19	2.12E-19	1.70E-19	1.30E-19
1.49E+01	1.35E+01	3.77E-19	2.77E-19	2.03E-19	1.73E-19	1.39E-19
1.35E+01	1.22E+01	3.78E-19	2.78E-19	2.05E-19	1.76E-19	1.42E-19
1.22E+01	1.00E+01	3.77E-19	2.82E-19	2.12E-19	1.87E-19	1.55E-19
1.00E+01	8.19E+00	3.77E-19	2.85E-19	2.17E-19	1.96E-19	1.63E-19
8.19E+00	6.70E+00	4.04E-19	3.04E-19	2.36E-19	2.18E-19	1.87E-19
6.70E+00	5.49E+00	4.23E-19	3.19E-19	2.38E-19	2.13E-19	1.76E-19
5.49E+00	4.49E+00	3.89E-19	2.92E-19	2.16E-19	1.89E-19	1.54E-19
4.49E+00	3.68E+00	5.10E-19	4.12E-19	3.09E-19	2.70E-19	2.26E-19
3.68E+00	3.01E+00	5.17E-19	4.22E-19	3.21E-19	2.88E-19	2.47E-19
3.01E+00	2.47E+00	4.68E-19	3.78E-19	2.95E-19	2.72E-19	2.33E-19
2.47E+00	2.02E+00	4.91E-19	3.92E-19	3.10E-19	2.84E-19	2.45E-19
2.02E+00	1.65E+00	5.46E-19	4.44E-19	3.52E-19	3.14E-19	2.75E-19
1.65E+00	1.35E+00	5.40E-19	4.39E-19	3.50E-19	3.06E-19	2.74E-19
1.35E+00	1.11E+00	5.23E-19	4.24E-19	3.34E-19	2.88E-19	2.53E-19
1.11E+00	9.07E-01	4.86E-19	4.09E-19	3.23E-19	2.82E-19	2.53E-19
9.07E-01	7.43E-01	3.60E-19	2.85E-19	2.27E-19	2.02E-19	1.79E-19
7.43E-01	4.98E-01	2.93E-19	2.36E-19	1.89E-19	1.64E-19	1.48E-19
4.98E-01	3.34E-01	2.30E-19	2.00E-19	1.68E-19	1.42E-19	1.38E-19
3.34E-01	2.24E-01	1.59E-19	1.38E-19	1.16E-19	1.01E-19	9.77E-20
2.24E-01	1.50E-01	1.18E-19	1.03E-19	8.78E-20	7.56E-20	7.44E-20
1.50E-01	8.65E-02	8.55E-20	7.66E-20	6.70E-20	5.76E-20	5.81E-20
8.65E-02	3.18E-02	5.82E-20	5.54E-20	5.10E-20	4.39E-20	4.64E-20
3.18E-02	1.50E-02	4.44E-20	4.41E-20	4.23E-20	3.64E-20	3.97E-20
1.50E-02	7.10E-03	4.17E-20	4.21E-20	4.08E-20	3.52E-20	3.86E-20
7.10E-03	3.35E-03	4.06E-20	4.11E-20	4.01E-20	3.45E-20	3.79E-20
3.35E-03	1.58E-03	3.93E-20	3.99E-20	3.91E-20	3.37E-20	3.69E-20
1.58E-03	4.54E-04	3.76E-20	3.85E-20	3.78E-20	3.28E-20	3.58E-20
4.54E-04	1.01E-04	3.51E-20	3.60E-20	3.55E-20	3.08E-20	3.34E-20
1.01E-04	2.26E-05	3.16E-20	3.24E-20	3.17E-20	2.76E-20	2.97E-20
2.26E-05	1.07E-05	2.77E-20	2.81E-20	2.74E-20	2.36E-20	2.52E-20
1.07E-05	5.04E-06	2.53E-20	2.55E-20	2.46E-20	2.12E-20	2.24E-20
5.04E-06	2.38E-06	2.25E-20	2.25E-20	2.15E-20	1.84E-20	1.93E-20
2.38E-06	1.13E-06	1.93E-20	1.91E-20	1.80E-20	1.54E-20	1.59E-20
1.13E-06	4.14E-07	1.58E-20	1.53E-20	1.42E-20	1.21E-20	1.23E-20
4.14E-07	1.00E-10	1.02E-20	9.86E-21	9.04E-21	7.89E-21	7.67E-21

Appendix 6.1

TABLE A.2

Neutron Importance as a function of Energy
Mean r = 495 m.

		Neutron Importance in sievert				
E_{high} MeV	E_{low} MeV	cosθ 0.0-0.2	0.2-0.4	0.4-0.6	0.6-0.8	0.8-1.0
4.00E+02	3.75E+02	6.04E-20	3.72E-20	2.39E-20	1.71E-20	9.01E-21
3.75E+02	3.50E+02	5.80E-20	3.57E-20	2.29E-20	1.63E-20	8.53E-21
3.50E+02	3.25E+02	5.62E-20	3.46E-20	2.23E-20	1.59E-20	8.28E-21
3.25E+02	3.00E+02	5.47E-20	3.37E-20	2.17E-20	1.55E-20	8.14E-21
3.00E+02	2.75E+02	5.32E-20	3.28E-20	2.12E-20	1.51E-20	7.97E-21
2.75E+02	2.50E+02	5.17E-20	3.18E-20	2.05E-20	1.46E-20	7.74E-21
2.50E+02	2.25E+02	5.00E-20	3.07E-20	1.98E-20	1.41E-20	7.46E-21
2.25E+02	2.00E+02	4.83E-20	2.95E-20	1.90E-20	1.35E-20	7.15E-21
2.00E+02	1.75E+02	4.67E-20	2.85E-20	1.83E-20	1.30E-20	6.90E-21
1.75E+02	1.50E+02	4.52E-20	2.76E-20	1.77E-20	1.25E-20	6.71E-21
1.50E+02	1.25E+02	4.39E-20	2.67E-20	1.72E-20	1.21E-20	6.53E-21
1.25E+02	1.00E+02	4.24E-20	2.58E-20	1.66E-20	1.17E-20	6.33E-21
1.00E+02	9.00E+01	4.12E-20	2.51E-20	1.61E-20	1.13E-20	6.20E-21
9.00E+01	8.00E+01	4.04E-20	2.47E-20	1.59E-20	1.12E-20	6.07E-21
8.00E+01	7.00E+01	3.94E-20	2.43E-20	1.57E-20	1.11E-20	5.96E-21
7.00E+01	6.00E+01	3.83E-20	2.39E-20	1.56E-20	1.11E-20	5.89E-21
6.00E+01	5.50E+01	3.70E-20	2.34E-20	1.52E-20	1.09E-20	5.77E-21
5.50E+01	5.00E+01	3.57E-20	2.29E-20	1.51E-20	1.09E-20	5.79E-21
5.00E+01	4.50E+01	3.37E-20	2.31E-20	1.59E-20	1.19E-20	6.54E-21
4.50E+01	4.00E+01	3.16E-20	2.13E-20	1.45E-20	1.08E-20	5.86E-21
4.00E+01	3.50E+01	2.99E-20	2.00E-20	1.36E-20	1.02E-20	5.62E-21
3.50E+01	3.00E+01	2.79E-20	1.92E-20	1.34E-20	1.03E-20	5.89E-21
3.00E+01	2.75E+01	2.57E-20	1.83E-20	1.31E-20	1.03E-20	6.12E-21
2.75E+01	2.50E+01	2.41E-20	1.75E-20	1.27E-20	1.01E-20	6.19E-21
2.50E+01	2.25E+01	2.26E-20	1.66E-20	1.22E-20	9.97E-21	6.25E-21
2.25E+01	2.00E+01	2.12E-20	1.58E-20	1.18E-20	9.77E-21	6.29E-21
2.00E+01	1.75E+01	1.97E-20	1.49E-20	1.12E-20	9.48E-21	6.28E-21
1.75E+01	1.49E+01	1.77E-20	1.35E-20	1.03E-20	8.86E-21	6.00E-21
1.49E+01	1.35E+01	1.28E-20	1.02E-20	8.24E-21	7.63E-21	5.65E-21
1.35E+01	1.22E+01	1.27E-20	1.01E-20	8.21E-21	7.64E-21	5.71E-21
1.22E+01	1.00E+01	1.29E-20	1.03E-20	8.37E-21	7.89E-21	6.00E-21
1.00E+01	8.19E+00	1.46E-20	1.13E-20	9.10E-21	8.45E-21	6.36E-21
8.19E+00	6.70E+00	1.38E-20	1.10E-20	8.98E-21	8.57E-21	6.72E-21
6.70E+00	5.49E+00	1.42E-20	1.09E-20	8.75E-21	8.10E-21	6.09E-21
5.49E+00	4.49E+00	1.28E-20	9.56E-21	7.42E-21	6.59E-21	4.78E-21
4.49E+00	3.68E+00	9.02E-21	8.00E-21	6.95E-21	6.80E-21	5.55E-21
3.68E+00	3.01E+00	9.63E-21	8.64E-21	7.61E-21	7.62E-21	6.32E-21
3.01E+00	2.47E+00	1.25E-20	1.04E-20	8.76E-21	8.41E-21	6.65E-21
2.47E+00	2.02E+00	1.27E-20	1.05E-20	8.63E-21	8.05E-21	6.27E-21
2.02E+00	1.65E+00	9.05E-21	8.09E-21	6.98E-21	6.69E-21	5.47E-21
1.65E+00	1.35E+00	6.93E-21	6.51E-21	5.79E-21	5.66E-21	4.80E-21
1.35E+00	1.11E+00	6.20E-21	5.72E-21	5.01E-21	4.80E-21	4.00E-21
1.11E+00	9.07E-01	4.14E-21	3.99E-21	3.62E-21	3.61E-21	3.16E-21
9.07E-01	7.43E-01	4.63E-21	3.98E-21	3.34E-21	3.14E-21	2.50E-21
7.43E-01	4.98E-01	2.31E-21	2.06E-21	1.76E-21	1.67E-21	1.37E-21
4.98E-01	3.34E-01	7.41E-22	7.71E-22	7.36E-22	7.11E-22	6.89E-22
3.34E-01	2.24E-01	5.95E-22	6.01E-22	5.61E-22	5.47E-22	5.07E-22
2.24E-01	1.50E-01	3.96E-22	4.11E-22	3.92E-22	3.82E-22	3.65E-22
1.50E-01	8.65E-02	2.72E-22	2.91E-22	2.84E-22	2.77E-22	2.74E-22
8.65E-02	3.18E-02	1.79E-22	1.97E-22	1.98E-22	1.89E-22	1.99E-22
3.18E-02	1.50E-02	1.13E-22	1.25E-22	1.28E-22	1.20E-22	1.31E-22
1.50E-02	7.10E-03	8.68E-23	9.62E-23	9.91E-23	9.16E-23	1.01E-22
7.10E-03	3.35E-03	6.85E-23	7.59E-23	7.83E-23	7.20E-23	8.01E-23
3.35E-03	1.58E-03	5.45E-23	6.03E-23	6.23E-23	5.71E-23	6.38E-23
1.58E-03	4.54E-04	4.37E-23	4.84E-23	5.02E-23	4.59E-23	5.15E-23
4.54E-04	1.01E-04	3.15E-23	3.48E-23	3.61E-23	3.30E-23	3.70E-23
1.01E-04	2.26E-05	2.28E-23	2.50E-23	2.60E-23	2.38E-23	2.66E-23
2.26E-05	1.07E-05	1.77E-23	1.94E-23	2.02E-23	1.86E-23	2.09E-23
1.07E-05	5.04E-06	1.62E-23	1.78E-23	1.85E-23	1.72E-23	1.93E-23
5.04E-06	2.38E-06	1.50E-23	1.65E-23	1.72E-23	1.61E-23	1.82E-23
2.38E-06	1.13E-06	1.39E-23	1.53E-23	1.61E-23	1.52E-23	1.72E-23
1.13E-06	4.14E-07	1.25E-23	1.38E-23	1.47E-23	1.41E-23	1.61E-23
4.14E-07	1.00E-10	9.83E-24	1.09E-23	1.17E-23	1.18E-23	1.36E-23

Appendix 6.1

TABLE A.3

Neutron Importance as a function of Energy
Mean r = 1005 m.

		Neutron Importance in sievert				
		cosθ				
E_{high} MeV	E_{low} MeV	0.0-0.2	0.2-0.4	0.4-0.6	0.6-0.8	0.8-1.0
4.00E+02	3.75E+02	1.64E-20	1.01E-20	5.70E-21	3.11E-21	1.21E-21
3.75E+02	3.50E+02	1.58E-20	9.68E-21	5.42E-21	2.94E-21	1.14E-21
3.50E+02	3.25E+02	1.52E-20	9.27E-21	5.17E-21	2.79E-21	1.08E-21
3.25E+02	3.00E+02	1.47E-20	8.87E-21	4.92E-21	2.65E-21	1.03E-21
3.00E+02	2.75E+02	1.41E-20	8.43E-21	4.65E-21	2.49E-21	9.60E-22
2.75E+02	2.50E+02	1.35E-20	7.98E-21	4.36E-21	2.31E-21	8.87E-22
2.50E+02	2.25E+02	1.29E-20	7.55E-21	4.08E-21	2.15E-21	8.15E-22
2.25E+02	2.00E+02	1.23E-20	7.08E-21	3.79E-21	1.97E-21	7.42E-22
2.00E+02	1.75E+02	1.17E-20	6.63E-21	3.51E-21	1.81E-21	6.77E-22
1.75E+02	1.50E+02	1.10E-20	6.14E-21	3.22E-21	1.65E-21	6.13E-22
1.50E+02	1.25E+02	1.02E-20	5.60E-21	2.90E-21	1.47E-21	5.45E-22
1.25E+02	1.00E+02	9.09E-21	4.98E-21	2.58E-21	1.31E-21	4.79E-22
1.00E+02	9.00E+01	8.16E-21	4.51E-21	2.33E-21	1.17E-21	4.18E-22
9.00E+01	8.00E+01	7.51E-21	4.22E-21	2.22E-21	1.14E-21	4.06E-22
8.00E+01	7.00E+01	6.76E-21	3.91E-21	2.11E-21	1.11E-21	4.05E-22
7.00E+01	6.00E+01	5.92E-21	3.55E-21	1.98E-21	1.08E-21	4.07E-22
6.00E+01	5.50E+01	5.22E-21	3.25E-21	1.86E-21	1.04E-21	4.00E-22
5.50E+01	5.00E+01	4.64E-21	2.97E-21	1.76E-21	1.02E-21	4.19E-22
5.00E+01	4.50E+01	3.44E-21	2.56E-21	1.70E-21	1.12E-21	5.42E-22
4.50E+01	4.00E+01	3.23E-21	2.29E-21	1.47E-21	9.38E-22	4.35E-22
4.00E+01	3.50E+01	2.91E-21	2.02E-21	1.28E-21	8.08E-22	3.77E-22
3.50E+01	3.00E+01	2.31E-21	1.68E-21	1.11E-21	7.32E-22	3.69E-22
3.00E+01	2.75E+01	1.77E-21	1.36E-21	9.42E-22	6.55E-22	3.53E-22
2.75E+01	2.50E+01	1.51E-21	1.19E-21	8.39E-22	5.99E-22	3.37E-22
2.50E+01	2.25E+01	1.28E-21	1.03E-21	7.39E-22	5.42E-22	3.18E-22
2.25E+01	2.00E+01	1.09E-21	8.87E-22	6.48E-22	4.82E-22	2.94E-22
2.00E+01	1.75E+01	9.14E-22	7.51E-22	5.56E-22	4.24E-22	2.67E-22
1.75E+01	1.49E+01	7.29E-22	6.03E-22	4.52E-22	3.52E-22	2.28E-22
1.49E+01	1.35E+01	4.61E-22	3.98E-22	3.19E-22	2.73E-22	2.03E-22
1.35E+01	1.22E+01	4.48E-22	3.90E-22	3.15E-22	2.71E-22	2.03E-22
1.22E+01	1.00E+01	4.80E-22	4.08E-22	3.27E-22	2.82E-22	2.15E-22
1.00E+01	8.19E+00	6.22E-22	4.95E-22	3.79E-22	3.12E-22	2.30E-22
8.19E+00	6.70E+00	5.21E-22	4.31E-22	3.42E-22	2.96E-22	2.30E-22
6.70E+00	5.49E+00	5.31E-22	4.32E-22	3.34E-22	2.78E-22	2.05E-22
5.49E+00	4.49E+00	4.44E-22	3.48E-22	2.60E-22	2.07E-22	1.43E-22
4.49E+00	3.68E+00	1.85E-22	1.84E-22	1.66E-22	1.59E-22	1.31E-22
3.68E+00	3.01E+00	2.01E-22	1.98E-22	1.78E-22	1.71E-22	1.43E-22
3.01E+00	2.47E+00	3.22E-22	2.76E-22	2.21E-22	1.90E-22	1.45E-22
2.47E+00	2.02E+00	2.78E-22	2.34E-22	1.82E-22	1.52E-22	1.10E-22
2.02E+00	1.65E+00	1.18E-22	1.15E-22	9.94E-23	9.13E-23	7.26E-23
1.65E+00	1.35E+00	7.10E-23	7.30E-23	6.68E-23	6.45E-23	5.43E-23
1.35E+00	1.11E+00	5.71E-23	5.79E-23	5.22E-23	4.95E-23	4.08E-23
1.11E+00	9.07E-01	3.22E-23	3.35E-23	3.14E-23	3.10E-23	2.74E-23
9.07E-01	7.43E-01	4.20E-23	3.85E-23	3.20E-23	2.83E-23	2.18E-23
7.43E-01	4.98E-01	1.12E-23	1.09E-23	9.51E-24	8.77E-24	7.15E-24
4.98E-01	3.34E-01	2.27E-24	2.45E-24	2.42E-24	2.39E-24	2.37E-24
3.34E-01	2.24E-01	1.84E-24	1.97E-24	1.91E-24	1.91E-24	1.83E-24
2.24E-01	1.50E-01	1.32E-24	1.43E-24	1.41E-24	1.41E-24	1.41E-24
1.50E-01	8.63E-02	1.04E-24	1.13E-24	1.14E-24	1.14E-24	1.19E-24
8.63E-02	3.18E-02	8.64E-25	9.44E-25	9.67E-25	9.37E-25	1.03E-24
3.18E-02	1.50E-02	7.58E-25	8.30E-25	8.62E-25	8.15E-25	9.25E-25
1.50E-02	7.10E-03	7.25E-25	7.95E-25	8.30E-25	7.79E-25	8.92E-25
7.10E-03	3.35E-03	7.01E-25	7.70E-25	8.07E-25	7.55E-25	8.68E-25
3.35E-03	1.58E-03	6.80E-25	7.48E-25	7.86E-25	7.35E-25	8.47E-25
1.58E-03	4.54E-04	6.58E-25	7.25E-25	7.65E-25	7.15E-25	8.24E-25
4.54E-04	1.01E-04	6.27E-25	6.93E-25	7.32E-25	6.86E-25	7.90E-25
1.01E-04	2.26E-05	5.91E-25	6.53E-25	6.91E-25	6.51E-25	7.49E-25
2.26E-05	1.07E-05	5.50E-25	6.07E-25	6.43E-25	6.08E-25	6.99E-25
1.07E-05	5.04E-06	5.21E-25	5.75E-25	6.07E-25	5.76E-25	6.63E-25
5.04E-06	2.38E-06	4.89E-25	5.37E-25	5.66E-25	5.39E-25	6.19E-25
2.38E-06	1.13E-06	4.52E-25	4.94E-25	5.19E-25	4.96E-25	5.67E-25
1.13E-06	4.14E-07	4.11E-25	4.46E-25	4.65E-25	4.47E-25	5.06E-25
4.14E-07	1.00E-10	3.50E-25	3.76E-25	3.86E-25	3.75E-25	4.11E-25

Appendix 6.2

Photon Importance Functions

In Tables B.1 to B.3 that follow similar results to those of Appendix 6.1 are given for the photon importance.

Appendix 6.2

TABLE B.1

Photon Importance as a function of Energy
Mean r = 108 m.

		Photon Importance in sievert				
E_{high} MeV	E_{low} MeV	cosθ 0.0-0.2	0.2-0.4	0.4-0.6	0.6-0.8	0.8-1.0
1.40E+01	1.20E+01	3.46E-21	1.42E-21	8.42E-22	6.86E-22	6.61E-22
1.20E+01	1.00E+01	3.40E-21	1.42E-21	8.32E-22	6.62E-22	6.31E-22
1.00E+01	8.00E+00	3.31E-21	1.42E-21	8.19E-22	6.32E-22	5.64E-22
8.00E+00	7.50E+00	3.49E-21	1.42E-21	7.95E-22	6.08E-22	5.75E-22
7.50E+00	7.00E+00	3.48E-21	1.42E-21	7.95E-22	6.02E-22	5.63E-22
7.00E+00	6.50E+00	3.47E-21	1.43E-21	7.97E-22	5.98E-22	5.51E-22
6.50E+00	6.00E+00	3.46E-21	1.44E-21	8.02E-22	5.95E-22	5.39E-22
6.00E+00	5.50E+00	3.44E-21	1.46E-21	8.11E-22	5.95E-22	5.21E-22
5.50E+00	5.00E+00	3.43E-21	1.48E-21	8.23E-22	5.97E-22	5.20E-22
5.00E+00	4.50E+00	3.40E-21	1.50E-21	8.36E-22	6.00E-22	5.39E-22
4.50E+00	4.00E+00	3.37E-21	1.52E-21	8.52E-22	6.04E-22	5.25E-22
4.00E+00	3.50E+00	3.32E-21	1.55E-21	8.72E-22	6.12E-22	5.12E-22
3.50E+00	3.00E+00	3.26E-21	1.58E-21	9.01E-22	6.27E-22	5.14E-22
3.00E+00	2.50E+00	3.18E-21	1.62E-21	9.40E-22	6.50E-22	5.06E-22
2.50E+00	2.00E+00	3.07E-21	1.67E-21	9.94E-22	6.88E-22	5.07E-22
2.00E+00	1.50E+00	2.92E-21	1.73E-21	1.07E-21	7.44E-22	5.18E-22
1.50E+00	1.00E+00	2.69E-21	1.79E-21	1.16E-21	8.20E-22	5.46E-22
1.00E+00	4.00E-01	2.60E-21	1.75E-21	1.16E-21	8.43E-22	6.06E-22
4.00E-01	2.00E-01	1.69E-21	1.21E-21	8.52E-21	6.43E-22	5.13E-22
2.00E-01	1.00E-01	8.83E-22	6.58E-22	4.89E-22	3.81E-22	3.28E-22
1.00E-01	1.00E-02	4.34E-23	3.28E-23	2.33E-23	1.93E-23	1.47E-23

Appendix 6.2

TABLE B.2

Photon Importance as a function of Energy
Mean r = 495 m.

		Photon Importance in sievert				
E_{high} MeV	E_{low} MeV	cosθ 0.0-0.2	0.2-0.4	0.4-0.6	0.6-0.8	0.8-1.0
1.40E+01	1.20E+01	3.45E-22	1.32E-22	4.68E-23	1.62E-23	1.77E-23
1.20E+01	1.00E+01	3.27E-22	1.27E-22	4.58E-23	1.56E-23	1.60E-23
1.00E+01	8.00E+00	3.04E-22	1.20E-22	4.49E-23	1.54E-23	1.36E-23
8.00E+00	7.50E+00	3.11E-22	1.24E-22	4.50E-23	1.42E-23	1.36E-23
7.50E+00	7.00E+00	3.02E-22	1.21E-22	4.42E-23	1.37E-23	1.29E-23
7.00E+00	6.50E+00	2.93E-22	1.18E-22	4.45E-23	1.43E-23	1.22E-23
6.50E+00	6.00E+00	2.83E-22	1.15E-22	4.55E-23	1.41E-23	1.14E-23
6.00E+00	5.50E+00	2.71E-22	1.12E-22	4.47E-23	1.51E-23	1.08E-23
5.50E+00	5.00E+00	2.58E-22	1.08E-22	4.40E-23	1.61E-23	1.03E-23
5.00E+00	4.50E+00	2.43E-22	1.03E-22	4.33E-23	1.60E-23	9.66E-24
4.50E+00	4.00E+00	2.26E-22	9.82E-23	4.23E-23	1.55E-23	9.56E-24
4.00E+00	3.50E+00	2.07E-22	9.21E-23	4.11E-23	1.78E-23	8.87E-24
3.50E+00	3.00E+00	1.85E-22	8.48E-23	3.95E-23	1.90E-23	8.21E-24
3.00E+00	2.50E+00	1.60E-22	7.61E-23	3.73E-23	1.94E-23	7.60E-24
2.50E+00	2.00E+00	1.32E-22	6.56E-23	3.43E-23	1.98E-23	8.60E-24
2.00E+00	1.50E+00	1.00E-22	5.30E-23	3.00E-23	1.93E-23	8.73E-24
1.50E+00	1.00E+00	6.64E-23	3.85E-23	2.42E-23	1.75E-23	8.67E-24
1.00E+00	4.00E-01	3.48E-23	2.33E-23	1.57E-23	1.20E-23	6.54E-24
4.00E-01	2.00E-01	7.50E-24	5.88E-24	4.45E-24	3.71E-24	2.55E-24
2.00E-01	1.00E-01	1.67E-24	1.45E-24	1.20E-24	1.08E-24	8.65E-25
1.00E-01	1.00E-02	1.32E-29	1.03E-29	6.95E-30	4.91E-30	3.79E-30

Appendix 6.2

TABLE B.3

Photon Importance as a function of Energy
Mean r = 1005 m.

		Photon Importance in sievert				
E_{high} MeV	E_{low} MeV	cosθ 0.0-0.2	0.2-0.4	0.4-0.6	0.6-0.8	0.8-1.0
1.40E+01	1.20E+01	5.00E-23	1.70E-23	3.62E-24	3.90E-25	5.10E-26
1.20E+01	1.00E+01	4.50E-23	1.53E-23	3.58E-24	3.94E-25	4.90E-26
1.00E+01	8.00E+00	3.88E-23	1.34E-23	3.32E-24	4.70E-25	4.43E-26
8.00E+00	7.50E+00	3.68E-23	1.34E-23	3.35E-24	4.79E-25	4.40E-26
7.50E+00	7.00E+00	3.46E-23	1.26E-23	3.21E-24	4.93E-25	4.44E-26
7.00E+00	6.50E+00	3.23E-23	1.19E-23	3.09E-24	4.79E-25	4.21E-26
6.50E+00	6.00E+00	2.97E-23	1.10E-23	2.92E-24	4.63E-25	4.15E-26
6.00E+00	5.50E+00	2.70E-23	1.01E-23	2.89E-24	4.43E-25	3.78E-26
5.50E+00	5.00E+00	2.41E-23	9.13E-24	2.69E-24	4.18E-25	3.72E-26
5.00E+00	4.50E+00	2.11E-23	8.12E-24	2.50E-24	4.04E-25	3.66E-26
4.50E+00	4.00E+00	1.81E-23	7.08E-24	2.29E-24	3.92E-25	3.34E-26
4.00E+00	3.50E+00	1.50E-23	5.97E-24	2.01E-24	4.18E-25	3.10E-26
3.50E+00	3.00E+00	1.18E-23	4.83E-24	1.72E-24	4.33E-25	4.28E-26
3.00E+00	2.50E+00	8.70E-24	3.68E-24	1.40E-24	4.35E-25	5.40E-26
2.50E+00	2.00E+00	5.82E-24	2.55E-24	1.06E-24	4.04E-25	7.67E-26
2.00E+00	1.50E+00	3.33E-24	1.54E-24	7.11E-25	3.34E-25	1.12E-25
1.50E+00	1.00E+00	1.48E-24	7.41E-25	3.96E-25	2.31E-25	1.09E-25
1.00E+00	4.00E-01	3.56E-25	2.51E-25	1.65E-25	1.12E-25	5.97E-26
4.00E-01	2.00E-01	1.76E-26	1.54E-26	1.19E-26	9.54E-27	6.48E-27
2.00E-01	1.00E-01	1.68E-27	1.66E-27	1.45E-27	1.32E-27	1.08E-27
1.00E-01	1.00E-02	2.28E-38	1.57E-38	1.05E-38	6.94E-39	5.84E-39

CHAPTER 7

SOURCES OF INFORMATION AND BIBLIOGRAPHY ON ACCELERATOR RADIATION PROTECTION

'In Nature's infinite book of secrecy a little
can I read.'

from 'Antony and Cleopatra'
William Shakespeare (1564-1616)

CHAPTER 7

SOURCES OF INFORMATION AND BIBLIGRAPHY ON ACCELERATOR RADIATION PROTECTION

It is not possible within the constraints of space of this manual to discuss adequately the many complex topics that comprise accelerator radiation protection. It is possible only to indicate the highlights of the subject and to provide guidance to other sources of information.

In general, most information on accelerator radiation phenomena has been obtained at the larger national laboratories engaging in accelerator design and construction for nuclear and high-energy physics research. These institutions can provide resources commensurate with the magnitude of the problems to be solved and have a continuing interest in their study. By contrast, small university departments, radiotherapy departments in medical centers and industrial facilities must often depend on the advice of extramural consultants and usually are not able to conduct research in accelerator health physics. Furthermore, much of the information that has been collected is unpublished and not widely available.

The principle sources of information on accelerator radiation phenomena are:

1. Monographs
2. Proceedings of symposia and conferences
3. Accelerator design studies
4. Reports of national and international organizations
5. Review articles

These most important sources are described, followed by listings in the General Bibliography.

7.1 MONOGRAPHS

The past decade has seen the appearance of a handful of monographs discussing accelerator health physics and associated topics in high-energy radiation phenomena. These monographs have served to delineate accelerator health physics as an independent discipline in its own right.

In the summer of 1970, Kase and Nelson gave a series of seminars at the Stanford Medical Center on radiation dosimetry. These seminars attempted to clarify the basic concepts of radiation dosimetry and to incorporate experience with high-energy electrons, obtained at the Stanford Linear Accelerator Center and elsewhere, during the preceding five years. Although publication was delayed until 1978, the lecture notes were available as an internal report and provide a good starting point for the study of electron and photon dosimetry.

Freytag (1972) published the first systematic treatment of radiation phenomena at high-energy electron accelerators. The original

edition was published in German, but a translation into English has now been made available by the U.S. National Aeronautics and Space Administration. A year later, Patterson and Thomas published a more comprehensive monograph discussing electron, proton and heavy-ion accelerators, with a substantial emphasis on the higher energy accelerators. More recently, Pellicioni and Rindi have published a somewhat shorter treatment (in Italian, no English translation available).

Several monographs exist on particular aspects of accelerator health physics, for example, induced radioactivity has been discussed by Barbier; accelerator shielding by Zaitsev, Komochkov and Sychev.

In addition to these monographs, several books are also of great value in dealing with accelerator radiation problems, although their scope is more general. Radiation shielding is discussed in three volumes published under the auspices of the International Atomic Energy Agency and in this compendium the specific problems of particle accelerator shielding are discussed.

7.2 PROCEEDINGS OF CONFERENCES

Perhaps the single, most useful source of information on particle accelerator radiation matters is contained in the proceedings of International Conferences devoted to the topic. The first of these was held in Paris in 1962 and broadly discussed in shielding of high-energy accelerators. It had been preceeded in 1957 by a meeting held in New York which discussed the radiation problems associated with the new weak-focussing synchrotrons at Berkeley and Brookhaven and how this experience could be applied to the second generation of synchrotrons then being designed. With the operation of these second generation accelerators there was a flury of activity and interest and the Atomic Energy Commission of the United States organised three symposia whose proceedings are extremely useful. These symposia were organized in the period 1965-1969. Two years later an international symposium was held in CERN. In 1975 a course on high energy radiation protection and dosimetry was held at the Ettore Majorana Centre for Scientific Culture in Erice under the auspices of the School of Radiation Damage and Protection. The proceedings of this course, 'High Energy Radiation Protection and Dosimetry' were published by the IEEE. The School, under the direction of A. Rindi, has since held several additional courses. The most recent, of interest to accelerator users, were those on 'The Application of Computers to Health Physics' and 'Advances in Radiation Protection and Dosimetry in Medicine', the proceedings of which are published.

The proceedings of some national conferences also provide a useful source of information on accelerator radiation problems and their solution. Since 1965, the IEEE has sponsored a series of biennial national particle accelerator conferences in the United States. The first was held in Washington, D.C. in 1965, followed by others in 1967 and 1969. The 4th conference was held in Chicago in 1971, and since that time the location of the meetings has rotated from Washington, D.C., to Chicago to San Francisco. Proceedings of the conferences are published by the IEEE in special volumes of the Transactions in Nuclear Science. They are valuable source of information on particle accelerator design, as

well as containing a few papers discussing radiation problems.

In the United Kingdom, a conference, 'Radiation Protection in Accelerator Radiation Environments', was held at the Rutherford Laboratory in 1969, the proceedings being published as an internal report. In 1977, the National Laboratory for High Energy Physics (KEK) at Tsukuba, Japan held a conference to discuss radiation shielding which largely addressed particle accelerators. The proceedings are available, although mostly in Japanese.

7.3 ACCELERATOR DESIGN STUDIES

During the design phase of large particle accelerators, a considerable effort is devoted to the study of their radiation problems and to their resolution. These design studies often lead to significant advances in our understanding of accelerator radiation phenomena, design study reports of large accelerators are often, therefore, a rich source of information.

Examples are the design reports for the Stanford 20-GeV linear accelerator, the Los Alamos 800-MeV proton linear accelerator, the Fermilab 500-GeV proton synchrotron, the CERN 300-GeV proton synchrotron, the electron storage ring, PEP, at Stanford and the proton storage ring, ISABELLE, at Brookhaven.

7.4 REPORTS OF NATIONAL AND INTERNATIONAL ORGANIZATIONS

The International Commission on Radiological Protection (ICRP) has published two reports of particular interest to accelerator health physicists: Reports 15 and 21, which provide data of value in assessing dose equivalent resulting from external exposure to ionising radiation. At the time of writing (mid-1985) both reports were being revised.

The International Commission of Radiation Units and Measurements (ICRU) has issued several reports discussing the dosimetry of radiation fields typical of particle accelerators. Because such radiation fields are complex, it is important to have a firm grasp of the basic concepts of radiation dosimetry. Radiation quantities and units are discussed in ICRU Report 33, and ICRU Report 25 discusses the conceptual basis for the determination of dose equivalent. Basic aspects of high energy particle interactions and radiation dosimetry for energies greater than 100 MeV are discussed in ICRU Report 28. Other reports of interest are those on Neutron Fluence, Neutron Spectra and Kerma (Report 13), Linear Energy Transfer and Radiation Protection Instrumentation and its Applications (Report 20).

The International Atomic Energy Agency (IAEA) has issued an extremely useful volume entitled 'Radiological Safety Aspects of the Operations of Electron Linear Accelerators' (IAEA 79). (This volume covers the same ground for high-energy positive ion accelerators.)

7.5. REVIEW ARTICLES

In addition to the sources mentioned, several review articles on various aspects of accelerator radiation problems are of both historical and current interest. They are listed in the General Bibliography.

GENERAL BIBLIOGRAPHY

BASIC TEXTS ON OCCUPATIONAL HEALTH AND SAFETY

General Safety

Calabrese, E.J., Methodological Approach to Deriving Environmental and Occupational Health Standards, John Wiley and Sons, New York (1978).

Chissick, S.S. and Derricott, R. (Eds.), Occupational Health and Safety Managements, John Wiley and Sons, Chichester (1981).

Cooper, M.G. (Ed.), Risk of Man-Made Hazards to Man, Clarenden Press, Oxford (1985).

Crandall, R.W. and Lave, L.B. (Eds.), The Scientific Basis of Health and Safety Regulation, Brookings Institutions, Washington, DC (1981).

De Reamer, R., Modern Safety and Health Technology, John Wiley and Sons, New York (1981).

Griffiths , R.F. (Ed.), Dealing with Risk, John Wiley, New York (1981).

Lave, L.B. (Eds.), Quantitative Risk Assessment in Regulation, The Brookings Institutions, Washington, DC

Lawrence, W.W., Off Acceptable Risk, William Kauffmann, Los Altos, California (1976).

National Council on Radiation Protection and Measurements, 'Perceptions of Risk', Proceedings of the Fifteenth Annual Meeting of the NCRP, March 14-15, 1979, Washington, DC (1980).

National Council on Radiation Protection and Measurements, 'Qualitative Risk in Standards Setting', Proceedings of the Sixteenth Annual Meeting of the NCRP, April 2-3, 1980, Washington, DC (1981).

National Safety Council, Accident Prevention Manual for Industrial Operations, 7th Edition, Chicago, IL (1978).

Petersen, D., Safety Management, Aloray, Fairview, NJ (1975).

Petersen, D., Techniques of Safety Management, McGraw Hill, New York (1978).

Steere, N.V. (Ed.), Handbook of Laboratory Safety, CRC Press, Cleveland, OH (1976).

Occupational Medicine

Barth, P.S. and Allan-Hunt, H., Workers' Compensation and Work-Related Illnesses and Diseases, The M.I.T. Press, Cambridge, Mass. (1980).

Dagett Norwood, W., Health Protection of Radiation Workers, Charles C. Thomas, Springfield, Ill. (1975).

Essex-Cater, A.J., A Manual of Public Health and Community Medicine, John Wright and Sons, Ltd., Bristol (1979).

Hobson, W. (Ed.), The Theory and Practice of Public Health, Oxford (1979).

Holland, W.W., Detels, R. and Knox, G. (Eds.), Oxford Text Book of Public Health, Oxford University Press, Oxford.

Vol. 1. History, Determinants, Scope and Strategies (1984).

Vol. 2. Processes for Public Health Protection (1985).

Vol. 3. Investigative Methods in Public Health (1985).

Vol. 4. Specific Applications (1985).

Hunter, D., The Diseases of Occupations, Hodder and Stoughton, London (1980).

LaDou, J., Occupational Health Law-A Guide for Industry, Marcel Dekker, New York (1981).

Last, J.M. (Ed.), Maxey-Rosenau: Public Health and Preventive Medicine, Appleton-Century-Crofts, New York (1980).

Mechanic, D. (Ed.), Handbook of Health, Health Care, and the Health Professions, The Free Press (McMillan), New York (1983).

Preger, L. (Ed.), Induced Disease-Drug, Irradiation, Occupation, Grune and Stratton, New York (1980).

Schilling, R.S.F. (Ed.), Occupational Health Practice, Butterworths, London (1982).

Singleton, W.T. and Debney, L.M., Occupational Disability, MTP Press Limited, Lancaster (1982).

Zenz, C. (Ed.), Developments in Occupational Medicine, Year Book Medical Publishers, Inc., Chicago (1980).

Zenz, C. (Ed.), Occupational Medicine, Year Book Medical Publishers, Inc., Chicago (1975).

Industrial (or Occupational) Hygiene

Ballantyne, B. and Schwabe, P.H., Respiratory Protection, Chapman Hall, London (1981).

Clay's Handbook of Environmental Health, (Revised by W.H. Bassett and F.G. Davies) H.K. Lewis and Co. Ltd., London (1981).

National Safety Council, Fundamentals of Industrial Hygiene, NSC, Chicago, Illinois (1979).

National Institute for Occupational Safety and Health, The Industrial Environment-Its Evaluation and Control, U.S. Department of Health Education and Welfare, National Institute for Occupational Safety and Health, U.S. Government Printing Office, Washington, DC (1973).

Occupational Safety and Health Administration, U.S. Department of Labor, OSHA Safety and Health Standards (29 CFR 1910)-General Industry, OSHA-2201, Revised March 11, 1983.

Occupational Safety and Health Administration, Employment Safety and Health Guide No. 680. OSHA Industrial Hygiene Technical Manual, Commerce Clearing House Chicago, Illinois (1984).

Patty's Industrial Hygiene and Toxicology (Third Revised Edition), Vol. I, General Principles, C.D. Clayton and F.E. Clayton (Eds.), John Wiley and Sons, New York (1978).

Patty's Industrial Hygiene and Toxicology (Third Revised Edition), Vol. IIa, Toxicology, C.D. Clayton and F.E. Clayton (Eds.), John Wiley and Sons, New York (1981).

Patty's Industrial Hygiene and Toxicology (Third Revised Edition), Vol. IIb, Toxicology, C.D. Clayton and F.E. Clayton (Eds.), John Wiley and Sons, New York (1981).

Patty's Industrial Hygiene and Toxicology (Third Revised Edition), Vol. IIc, Toxicology, C.D. Clayton and F.E. Clayton (Eds.), John Wiley and Sons, New York (1981).

Patty's Industrial Hygiene and Toxicology (Third Revised Edition), Vol. III. Theory and Rationale of Industrial Hygiene Practice, L.J. Cralley and L.V. Cralley (Eds.), John Wiley and Sons, New York (1979).

Peterson, J.E., Industrial Health, Prentice Hall, Englewood Cliffs, N.J. (1977).

Waldron, H.A. and Harrington, J.M., Occupational Hygiene, Blackwell, Oxford (1980).

Toxicology

Anderson, K. and Scott, K., Fundamentals of Industrial Toxicology, Ann Arbor Science Publishers, Ann Arbor (1981).

Doull, J., Klaassen, C.D. and Amdur, M.O., Casarett and Doull's Toxicology, Macmillan (1980).

Letavet, A.A. and Kurylandskaya, E.B., The Toxicology of Radioactive Substances, Pergamon Press, Oxford.

Vol. 1. Strontium, Caesium, Ruthenium, Radon, translated by E. Lloyd (1962).

Vol. 2. Radioactive Cobalt, Sodium, Phosphorus and Gold, translated by R.E. Travers, translation edited by E. Lloyd (1963).

Vol. 3. Iron-59, translated by R.E. Travers (1967).

Vol. 4. Thorium-232 and Uranium-238, translated by A. Crozy, translation edited by G.W. Dolphin (1970).

Vol. 5. Zinc-65, translated by A. Cruzy, translation edited by G.W. Dolphin (1970).

Moutschen, J., Introduction to Genetic Toxicology, John Wiley and Sons, Chichester (1985).

National Academy of Sciences, Prudent Practices for Handling Hazardous Chemicals in Laboratories, National Academy Press, Washington (1981).

National Academy of Sciences, Prudent Practice for Disposal of Chemicals from Laboratories, National Academy Press, Washington (1983).

Nenot, J.C. and Stather, J. W., The Toxicity of Plutonium, Americium, and Curium, published for the Commission of the European Communities by

Pergamon Press, Oxford (1979).

Plunkett, E.R., Handbook of Industrial Toxicology, Chemical Publishing Co., New York (1976).

Proctor, N.H. and Hughes, J.P., Chemical Hazards in the Workplace, J.P. Lippincott, Philadelphia (1978).

Sax, N.I., Dangerous Properties of Industrial Materials, Van Nostrand Reinhold (1975).

REFERENCES ON NUCLEAR AND PARTICLE PHYSICS

Evans, R.D., The Atomic Nucleus, McGraw Hill, New York (1955).

Halliday, D., Introductory Nuclear Physics, 2nd Edition., John Wiley, New York (1955).

Heitler, W., The Quantum Theory of Radiation, Oxford University Press, Oxford (1954).

Rossi, B., High-Energy Particles, Prentice-Hall, Englewood Cliffs, NJ (1956).

Segrè, E., 'Nuclei and Particles', W.A. Benjamin, Inc., New York (1965).

BASIC TEXTS ON RADIOBIOLOGY AND RADIATION EFFECTS

Bacq, Z.M. and Alexander, P., Fundamentals of Radiobiology, 2nd Edition Pergamon Press, Oxford (1961).

Boice, J.D. and Fraumeni, J.F., Radiation Carcinogenesis-Epidemiology and Biological Significance, Raven Press, New York (1984).

Fabrikant, J.I., Radiobiology, Medical Publishers, Inc., Chicago (1972).

Fullerton, G.D., Keep, D.T., Waggener, R.G. and Webster, W. (Editors), Biological Risks of Medical Irradiations. Medical Monographs No. 5, American Association of Physicists in Medicine, American Institute of Physics, New York (1980).

Grosch, D.S. and Hopwood, L.E., Biological Effects of Radiations, Academic Press, New York (1979).

Lea, D.E., Actions of Radiations on Living Cells, Cambridge University Press (1962).

National Academy of Sciences, 'The Effects on Populations of Exposure to Low Levels of Ionizing Radiation: 1980', National Academy Press, Washington, DC (1980).

Pizzarello, D.J. and Witcofski, R.L., Basic Radiation Biology, Lea and Febiger, Philadelphia, PA (1975).

UNSCEAR, 'Ionizing Radiation: Sources and Biological Ion Effects', United Nations Committee on the Effects of Atomic Radiation, 1982, Report to the General Assembly with Annexes, United Nations, New York (1982).

BASIC TEXTS ON RADIOLOGICAL PROTECTION

Cember, H., Introduction to Health Physics, 2nd Edition, Pergamon Press, Oxford, (1983).

Hughes, D., 'Notes on Ionizing Radiation: Quantities Units, Biological Units and Permissible Doses', Occupational Monograph No. 5, Science Reviews, Leeds (1982).

Lapp, R.E., Andrews, H.P., Nuclear Radiation Physics, 4th Edition, Prentice-Hall, Englewood Cliffs, NJ (1972).

Morgan, K.Z., Turner, J.E. (Eds.), Principles of Radiation Protection, John Wiley, New York (1967).

Oliver, R., Radiation Physics in Radiology, Blackwell, Oxford (1966).

Rees, D.J., Health Physics, The MIT Press, Cambridge, MA (1967).

Shapiro, J., Radiation protection-A Guide for Scientists and Physicians, Harvard University Press, Cambridge, MA (1972).

Stewart, D.C., Handling Radioactivity, John Wiley, New York (1981).

CONCEPTS AND STANDARDS IN RADIOLOGICAL PROTECTION

Council of the European Community, 'Council Directive Laying Down the Revised Basic Safety Standards for the Health Protection of the General Public and Workers against the Dangers of Ionizing Radiation', Official Journal of the European Communities, Vol. 19, No. L187, Luxembourg (1976).

International Atomic Energy Agency, Basic Safety Standards for Radiation Protection, Safety Series No. 9, 1967 Edition, IAEA, Vienna (1967).

International Commission on Radiological Protection, 'Recommendations of the International Commission on Radiological Protection', ICRP Publication No. 26, Pergamon Press, Oxford (1977).

International Commission on Radiological Protection, 'Problems Involved in Developing an Index of Harm', Publication 27, Pergamon Press, Oxford (1977).

International Commission on Radiological Protection, 'Statement from the 1978 Stockholm Meeting of the ICRP', Annals of the ICRP 2, (1) (1978).

International Commission on Radiological Protection, 'Statement and Recommendations of the 1980 Brighton Meeting of the ICRP', Annals of the ICRP 4, (3/4) (1980).

International Commission on Radiological Protection, 'Limits of the Intakes of Radionuclides by Workers', ICRP Publication 30,
Part 1. Annals of the ICRP 2, (3/4) (1979).
Supplement to Part 1. Annals of the ICRP 3, (1-4) (1979).
Part 2. Annals of the ICRP 4 (3/4), (1980).
Supplement to Part 2. Annals of the ICRP 5, (1-6) (1981).
Part 3. Addendum to Parts 1 and 2. Annals of the ICRP 6, (2/3) (1981).
Supplement A to Part 3. Annals of the ICRP 7, (2/3) (1982).
Supplement B to Part 3. Addendum to the Supplements to Parts 1 and 2. Annals of the ICRP 8, (1-3) (1982).

Index. Annals of the ICRP 8, (4) (1982).

International Commission on Radiological Protection, 'Cost Benefit Analysis in the Optimization of Radiation Protection', Publication 37 [Annals of the ICRP 10, (2/3), 1983], Pergamon Press, Oxford (1983).

International Commission on Radiological Protection, 'Nonstochastic Effects of Ionizing Radiation', Publication 41 [Annals of the ICRP 14, (3), 1984], Pergamon Press, Oxford (1984).

International Commission on Radiological Protection, 'A Compilation of the Major Concepts and Quantities in Use by the ICRP', Publication 42 [Annals of the ICRP 14, (4), 1982], Pergamon Press, Oxford (1984).

International Commission on Radiation Units and Measurements, 'Conceptual Basis for the Determination of Dose Equivalent', ICRU Report No. 25, Washington, DC (1976).

International Commission on Radiation Units and Measurements, 'Radiation Quantities and Units', ICRU Report No. 33, Washington, DC (1985).

International Commission on Radiation Units and Measurements, 'Determination of Dose Equivalents Resulting from External Radiations', ICRU Report 39, Washington, DC (1985).

National Council on Radiation Protection and Measurements, 'Basic Radiation Protection Criteria', NCRP Report No. 39, Washington, DC (1971).

National Council of Radiation Protection and Measurements, 'Review of the Current Status of Radiation Protection Philosophy', NCRP Report No. 43, Washington, DC (1975).

National Council on Radiation Protection and Measurements, 'Critical Issues in Setting Radiation Dose Limits', Proc. Seventeenth Annual Meeting of the NCRP, April 8-9, 1981, Washington, DC (1982).

National Council on Radiation Protection and Measurements, 'Some Issues Important in developing Basic Radiation Protection Recommendations', Proc. Twentieth Annual Meeting of the NCRP, April 4-5, 1984, Washington, DC (1984).

Taylor, L.S., 'Organization for Radiation Protection', U.S. Department of Energy Report DOE/TIC-10124 (1979).

BASIC REFERENCES ON DOSIMETRY AND INSTRUMENTATION

Attix, F.H. (Ed.), Topics in Radiation Dosimetry, Radiation Dosimetry, Supplement 1, Academic Press, New York (1972).

Attix, F.H., Roesch, W.C. and Tochilin, E., (Eds.), Radiation Dosimetry, 2nd ed. (in three volumes: Vol. I: Fundamentals; Vol. II: Instrumentation; Vol. III: Sources, Fields, Measurements and Applications), Academic Press, New York (1968, 1966, 1969).

Becker, K., Solid State Dosimetry, CRC Press, Cleveland, OH (1973).

Booz, J. and Dietze, G., 'Radiation Protection Quantities for External Exposure', Proceedings of a Seminar held at Braunschweig, 19-21 March 1985, Rad. Protection Dosim. 12(2) (1985).

Greening, J.R., Fundamentals of Radiation Dosimetry, Adam Hilger (1981).

Handloser, J.S., Health Physics Instrumentation, Pergamon Press, London (1959).

Hine, G.J. and Brownell, G.L. (Eds.), Radiation Dosimetry, Academic Press, New York (1956).

Holm, N.W. and Berry, R.J., Manual on Radiation Dosimetry, Marcel Dekker, New York (1970).

International Commission on Radiation Units and Measurements-Report 20. Radiation Protection Instrumentation and its Application, ICRU, Washington, DC (1971).

Kase, K.R. and Nelson, W.R., Concepts of Radiation Dosimetry, Pergamon Press, Oxford (1978).

Kiefer, H. and Maushart, R. (translated by R. Friese), Radiation Protection Measurement, Pergamon Press (1972).

Lawrence Berkeley Laboratory, Instrumentation for Environmental Monitoring, Eds. Budnitz, R.J., Nero, A.V., Murphy, D.J., and Graven, R., Environmental Instrumentation Survey, Vol. 1, Radiation, John Wiley, New York (1983).

Mann, W.B., Ayres, R.L. and Garfinkel, S.B., Radioactivity and its Measurement (Second Edition), Pergamon Press, Oxford (1980).

McKinley, A.F., Thermoluminescence Dosimetry, Adam Hilger, Bristol (1981).

National Council in Radiation Protection and Measurements, 'Instrumentation and Monitoring Methods for Radiation Protection', Report 57, Washington, DC (1978).

National Council in Radiation Protection and Measurements, 'A Handbook of Radioactivity Measurement Procedures', Report 58, Washington, DC (1978).

Price, W.J., Nuclear Radiation Detection, McGraw-Hill, New York (1958).

Rossi, B.B. and Staub, H.H., Ionization Chambers and Counters: Experimental Techniques, McGraw-Hill, New York (1949).

Thomas, R.H. and Perez-Mendez, V. (Eds.), Advances in Radiation Protection and Dosimetry in Medicine, Proceedings of the third Course of the International School of Radiation Protection and Damage 'Ettore Majorana', Plenum Press, New York (1980).

Swanson, W.P., 'Radiological Safety Aspects of the Operation of Electron Linear Accelerators', Technical Report Series No. 188, IAEA, Vienna (1979).

TEXTBOOKS AND REVIEW ARTICLES ON ACCELERATOR HEALTH PHYSICS

Brynjolfsson, A. and Martin, T.G., III, 'Bremsstrahlung Production and Shielding of Static and Linear Electron Accelerators below 50 MeV. Toxic Gas Production, Required Exhaust Rates, and Radiation Instrumentation', Int. J. Appl. Radiat. Isot. 22, 29 (1971).

Freytag, E., 'Strahlenschutz an Hochenergiebeschleunigern', G. Braun Karlsruhe (1972), (in German), English translation available: 'Radiation Protection of High-Energy Accelerators', Technical Translation NASATT-F-16,910, National Aeronautics and Space Administration, Washington, DC 20546 (April 1976).

Goebel, K., 'Radiation Problems Encountered in the Design of Multi-GeV Research Facilities', CERN Report CERN 71-21 (1971).

Patterson, H.W. and Thomas, R.H., 'Experimental Shielding Studies-A Review', Particle Accelerators 2, 77 (1971).

Patterson, H.W. and Thomas, R.H., 'Accelerator Health Physics', Academic Press, New York (1973).

Rindi, A. and Thomas, R.H., 'The Radiological Environmental Impact of High-Energy Accelerators', Critical Reviews of Environmental Control, Vol. 9, No. 1, p. 51 (1979).

Rindi, A. and Thomas R.H., 'Skyshine-A Paper Tiger'? Particle Accelerators 7, 23 (1975).

Stevenson, G.R., 'The Radiation Environment of Proton Accelerators and Storage Rings', CERN Report CERN 76-04 (1976).

Thomas, R.H. and Stevenson, G.R., 'Radiation Protection Around High-Energy Accelerators', Radiat. Prot. Dosim. 10 (1-4), 283 (1985).

Tobias, C.A. and Todd, P., Space Radiation Biology and Related Topics, Academic Press, New York (1974).

ACCELERATOR-PRODUCED RADIATIONS (GENERAL)

American National Standards Institute and National Bureau of Standards, 'Radiological Safety in the Design and Operation of Particle Accelerators', NBS Handbook No. 107, Washington, DC (1970).

Gundaker, W.E. and Boggs, R.F., 'Recommendations for the Safe Operation of Particle Accelerators', United States Department of Health, Education and Welfare, National Center for Radiological Health, Report No. MORP 68-2, Rockville, MD (1968).

International Commission on Radiation Units and Measurements, 'Basic Aspects of High-Energy Particle Interactions and Radiation Dosimetry', ICRU Report No. 28, Washington, DC (1978).

International Commission on Radiological Protection, 'Data for Protection Against Ionizing Radiation from External Sources: Supplement to ICRP Publication 15, Report of Committee 3', ICRP Publication No. 21, Pergamon Press, Oxford (1973).

National Council on Radiation Protection and Measurements, 'Protection Against Betatron-Synchrotron Radiation up to 100 Million Electron Volts', NCRP Report No. 14, published as National Bureau of Standards Handbook No. 55, US National Bureau of Standards, Washington, DC (1954).

National Council on Radiation Protection and Measurements, 'Radiation Protection Design Guidelines for 0.1-100 MeV Particle Accelerator Facilities', NCRP Report No. 51, Washington, DC (1977).

United States National Bureal of Standards, National Council on Radiation Protection and Measurements, 'Shielding for High-Energy Electron Accelerator Installations', NBS Handbook No. 97 and NCRP Report No. 31, Washington, DC (1964).

ACCELERATOR-PRODUCED NEUTRONS

Boggs, R.F., 'Radiobiological Safety Aspects of the Operation of Neutron Generators', Safety Series No. 42, IAEA, Vienna (1976).

International Commission on Radiation Units and Measurements, 'Neutron Fluence, Neutron Spectra and Kerma', ICRU Report No. 13, Washington, DC (1969).

National Bureau of Standards, 'Protection Against Neutron Radiation up to 30 Million Electron Volts', NBS Handbook No. 63, Washington, DC (1957).

National Council on Radiation Protection and Measurements, 'Protection Against Neutron Radiation', Report 38, Washington, DC (1971).

National Council on Radiation Protection and Measurements, 'Radiation Protection and Measurement for Low-Voltage Accelerators', Report 72, Washington, DC (1983).

National Council on Radiation Protection and Measurements, 'Neutron Contamination for Medical Electron Accelerators', Report 79, Washington, DC (1984).

CONFERENCE PROCEEDINGS ON ACCELERATOR-PRODUCED RADIATIONS

Proceedings of the 1970 Proton Linac Accelerator Conference, National Accelerator Laboratory, Batavia, IL, Sept. 28 - Oct. 2, 1970, 2 Vols., NAL Report (19).

Proceedings of the 1972 Proton Linear Accelerator Conference, Oct. 10-13, 1972, Los Alamos Scientific Laboratory, NM, Report LA-5115 (Nov. 1972).

Proceedings of the 1976 Proton Linear Accelerator Conference, Sept. 14-17, 1976, AECL-5677 (1976).

Bonet-Maury, M., and Duhamel, M. (Eds.), Premier Colloque International sur La Protection Auprès des Grands Accelerateurs, Presses Universitaires De France, Paris (1962).

'Ettore Majorana' Center for Scientific Culture, International School of Radiation Damage and Protection, 'First Course on High Energy Radiation Dosimetry and Protection, held at Erice, 1-11 Oct. 1975', IEEE Trans. Nucl. Sci. NS-23 (4), 1318 (1976).

European Organization for Nuclear Research, Proceedings of International Congress on Protection Against Accelerator and Space Radiation, Held at Geneva, 26-30 Apr. 1971, CERN Report No. 71-16, Geneva (1971).

Katoh, K. and Hirayama, H. (Eds.), Proceedings of the Symposium on Shielding Design of Accelerators, Tsukuba, Japan, 7-8 November (1977),

National Laboratory for High Energy Physics (KEK), Internal Report KEK-77-31, March 1978.

Nelson, W.R. and Jenkins, T.M., (Eds.), 'The Applications of Computers to Health Physics', Proceedings of the Second Course of the International School of Radiation Protection and Damage, Erice, Italy , Plenum Press, New York, 1979.

'Proceedings of the First National Accelerator Conference, Washington, DC, 10-12 March 1965', IEEE Trans. Nuclear Science NS-12, 3 (June 1965).

'Proceedings of the Second National Accelerator Conference, Washington, DC 1-3 March 1967', IEEE Trans. Nucl. Science NS-14, 3 (June 1967).

'Proceedings of the Third National Accelerator Conference, Washington, DC, 5-7 March 1969', IEEE Trans. Nucl. Science NS-16, 3 (June 1969).

'Proceedings of the Fourth National Accelerator Conference, Chicago, 1-3 March 1971', IEEE Trans. Nucl. Science NS-18, 3 (June 1971).

'Proceedings of the 1973 Particle Accelerator Conference, Accelerator Engineering and Technology, San Francisco 5-7 March 1973', IEEE Trans. Nucl. Sci. NS-20, 3 (June 1973).

'Proceedings of 1975 Particle Accelerator Conference, Accelerator Engineering and Technology, Washington, DC, 12-14 March 1975', IEEE Trans. Nucl. Sci. NS-22, 3 (June 1975).

'Proceedings of 1977 Particle Accelerator Conference, Accelerator Engineering and Technology, San Francisco, 12-14 March 1979', IEEE Trans. Nucl. Sci. NS-26, 3 (June 1979).

Solon, L.E. (Ed.), Proceedings of the Conference on Shielding High Energy Accelerators, New York, April 11-13, 1957, USAEC Report TID-7543 (1957).

Stevenson, G.R. (Ed.), Proceedings of the Conference on Radiation Protection in Accelerator Environments, Held at the Rutherford Laboratory, March 1969, Chilton, Didcot, Oxon, (1969).

Thomas, R.H. and Perez-Mendez, V. (Eds.), 'Advances in Radiation Protection and Dosimetry in Medicine', Proceedings of the Third Course of the International School of Radiation Protection and Damage, Erice, Italy, Plenum Press, New York (1980).

United States Atomic Energy Commission, Proceedings of USAEC First Symposium on Accelerator Radiation Dosimetry and Experience, Held at Brookhaven National Laboratory, Upton, NY, 3-5 Nov. 1965, USAEC, Div. Technical Information, Report CONF-651109, Washington, DC (1965).

United States Atomic Energy Commission, Proceedings of Second International Conference on Accelerator Dosimetry and Experience, Held at the Stanford Linear Accelerator Center, Stanford, CA, 5-7 Nov. 1969, USAEC, Div. Technical Information, Rep. CONF-691101, Washington, DC (1969).

United States Atomic Energy Commission, Conference. Particle Accelerators in Radiation Therapy, Held at Los Alamos Scientific Laboratory, 2-5 Oct. 1972, USAEC and Los Alamos Scientific Laboratory Rep. LA-5180-C, available from Technical Information Center, Oak Ridge, TN (1972).

Wallace, R.W. (Ed.), Proceedings of the First International Symposium on the Biological Interpretation of Dose From Accelerator-Produced Radiation, Berkeley, California, March 13–16, 1967, USAEC Report Conf-670305 (1967).

GENERAL REFERENCES ON RADIATION SHIELDING

Chilton, A.B., Shultis, J.K. and Faw, R.E., Principles of Radiation Shielding, Prentice Hall, Inc., Englewood Cliffs, NJ (1980).

Davison, B., Neutron Transport Theory, Clarendon Press, Oxford (1957).

Hafner, J.W., Radiation and Shielding in Space, Academic Press, New York (1967).

Jaeger, R.G., Blizard, E.P., Chilton, A.B., Grotenhuis, M., Honig, A., Jaeger, T.A. and Eisenlohr, H.H. (Eds.), Engineering Compendium on Radiation Shielding, Vol. I: Shielding Fundamentals and Methods; Vol. II: Shielding Materials, Vol. III: Shield Design and Engineering, IAEA Vienna, Springer-Verlag, Berlin (1968, 1975, 1970).

Nelson, W.R. and Jenkins, T.M. (Eds.), 'Computer Techniques in Radiation Transport and Dosimetry', Proceedings of the Second Course of the International School of Radiation Damage and Protection, 'Ettore Majorana', Plenum Press, New York (1978).

Price, B.T., Horton, C.C. and Spinney, K.T., Radiation Shielding, Pergamon Press, Oxford (1957).

Rockwell, T., III (Ed.), Reactor Shielding Design Manual, Van Nostrand, Princeton, NJ (1956).

Schaeffer, N.M. (Ed.), Reactor Shielding for Nuclear Engineers, United States Atomic Energy Commission, Office of Technical Services, Report TID-25951, Oak Ridge, TN (1973).

Zaitsev, L.N., Komochkov, M.M, and Sychev., B.S., Fundamentals of Shielding For Accelerators, Atomizdat, Moscow [in Russian] (1971).

ADVISORY MATERIAL ON RADIOLOGICAL PROTECTION, USEFUL AT ACCELERATOR INSTALLATIONS, BUT BROADER IN SCOPE

International Atomic Energy Agency, 'The Provision of Radiological Protection Services', Safety Series No. 13, IAEA, Vienna (1965).

International Atomic Energy Agency, 'Radiation Protection Procedures', Safety Series No. 38, IAEA, Vienna (1973).

National Bureau of Standards, 'A Manual of Radioactivity Procedures', NBS Handbook No. 80 and NCRP Report No. 28, Washington, DC (1961).

National Bureau of Standards, 'Physical Aspects of Irradiation', NBS Handbook No. 85 and ICRU Report No. 10b, Washington, DC (1964).

National Council on Radiation Protection and Measurements, 'Safe Handling of Radioactive Materials', Report 29, (NBS Handbook No. 92), Washington, DC (1964).

National Council on Radiation Protection and Measurements, 'Medical Exposure of Pregnant and Potentially Pregnant Women', Report 54, Washington, DC (1979).

National Council on Radiation Protection and Measurements, 'Operational Safety Program', Report 59, Washington, DC (1978).

National Council on Radiation Protection and Measurements, 'Management of Persons Accidently Contaminated with Radionuclides', Report 65, Washington, DC (1980).

National Council on Radiation Protection and Measurements, 'Radio-Frequency Electromagnetic Fields', Report 67, Washington, DC (1981).

ADVISORY MATERIAL RELATED TO RADIATION MONITORING

International Atomic Energy Agency, 'The Use of Film Badges for Personnel Monitoring', Safety Series No. 8, IAEA, Vienna (1962).

International Atomic Energy Agency, 'The Basic Requirement for Personnel Monitoring', Safety Series No. 14, IAEA, Vienna (1965).

International Atomic Energy Agency, 'Personnel Dosimetry Systems for External Radiation Exposures', Technical Reports Series No. 109, IAEA, Vienna (1970).

International Atomic Energy Agency, 'Handbook on Calibration of Radiation Protection Monitoring Instruments', Technical Reports Series No. 133, IAEA, Vienna (1971).

International Commission on Radiation Units and Measurements, 'Radiation Protection Instrumentation and its Applications', ICRU Report No. 20, Washington, DC (1971).

International Commission on Radiological Protection, 'General Principles of Monitoring for Radiation Protection of Workers', ICRP Publication No. 35, [Annals of the ICRP 9, 4 (1982)], Pergamon Press, London (1969).

International Commission on Radiation Units and Measurements, 'Radiological Monitoring Methods and Instruments', NCRP Report No. 10 and NBS Handbook No. 51, Washington, DC (1952).

International Commission on Radiation Units and Measurements, 'Instrumentation and Monitoring Methods for Radiation Protection', Report 57, Washington DC (1978).

International Commission on Radiological Protection, 'Principles of Monitoring for the Radiation Protection of the Population', Publication 43 [Annals of the ICRP 15, 1 (1985)], Pergamon Press, Oxford (1985).

HANDBOOKS AND DATA TABULATIONS

Berger, M.J. and Seltzer, S.M., 'Tables of Energy Losses and Ranges of Electrons and Positrons', National Aeronautics and Space Administration, Rep. NASA-SP-3012, Washington, DC (1974); 'Additional Stopping Power and Range Tables for Protons, Mesons, and Electrons', National Aeronautics and Space Administration, Rep. NASA SP-3036, Washington, DC (1966).

(These reports are available at the Office of Technical Services, Washington, DC 20230).

Bureau of Radiological Health, Radiological Health Handbook, Bureau of Radiological Health, Public Health Service, United States Department of Health, Education and Welfare, Rockville, MD (1970).

Goldman, D.T. and Roesser, J.R., Chart of the Nuclides, 9th ed., Knolls Atomic Power Laboratory, General Electric Co., Schenectady, NY (1966).

Hubbell, J.H., 'Photon Cross Sections, Attenuation Coefficients, and Energy Absorption Coefficients from 10 keV to 100 GeV', United States National Bureau of Standards, Publication No. NSRDS-NBS 29, Washington, DC (1969).

Lederer, C.M., Hollander, J.M. and Perlman, I., Table of Isotopes, 7th Edition, John Wiley, New York (1978).

Nachtigall, D., Table of Specific Gamma Ray Constants, Karl Thiemig, Munich (1969).

Pages, L., Bertel, E., Joffre, H. and Sklavenitis, L., 'Energy Loss, Range, and Bremsstrahlung Yield for 10-keV to 100-MeV Electrons in Various Elements and Chemical Compounds', At. Data Nucl. Data Tables 4, 1, pp. 1–27 (1972).

Particle Data Group, Review of Particle Properties, Lawrence Berkeley Laboratory Report LBL-100, revised, Phys. Letters 111B, April (1982).

Plechaty, E.F., Cullen, D.E., Howerton, R.J., 'Tables and Graphs of Photon Interaction Cross Sections from 1.0 keV to 100 MeV Derived from the LLL Evaluated Nuclear Data Library', Lawrence Livermore Laboratory Report UCRL-50400, Vol. 26, Rev. 1 (1975).

Seelmann-Eggebert, W., Pfenning G. and Munzel, H., 'Nuklidkarte', 3rd ed., Institut fur Radiochemie, Kernforschungszentrum Karlsruhe, Bundesminister fur Wissenschaftliche Forschug, Bonn (1968).

Storm, E. and Israel, H.I., 'Photon Cross Sections from 0.001 to 100 MeV for Elements 1 through 100', Los Alamos Scientific Laboratory Report LA-3753 (1967); 'Photon Cross Sections from 1 keV to 100 MeV for Elememts Z = 1 to Z = 100', Nuclear Data Tables A7, Academic Press, New York, pp. 565–681 (1970).

Veigele, W.J., 'Photon Cross Sections from 0.1 keV to 1 MeV for Elements Z = 1 to Z = 94', At. Data Tables 5 1 (1973) 51–111.

Wang, Y., Ed., Handbook of Radioactive Nuclides, Chemical Rubber Co., Cleveland, Ohio (1969).

ENVIRONMENTAL RADIATION

Eisenbud, M., Environmental Radioactivity, Academic Press, New York (1973).

Goebel, K., 'Radio-Ecological Considerations for Operating Particle Accelerators', CERN Internal Report CERN 79-09 (1979).

Goebel, K. (Ed.), 'The Radiological Impact of the LEP Project on the Environment', CERN Internal Report CERN 81-08 (20 July 1981).

National Council on Radiation Protection and Measurements, 'Environmental Radiation Measurements', Report 50, Washington, DC (1977).

National Council on Radiation Protection and Measurements, 'Natural Background Radiation in the United States', Report 45, Washington, DC (1975).

Rindi, A. and Thomas, R.H., 'Radiological Environmental Impact of High-Energy Accelerators', CRC Critical Reviews in Environmental Control 9, 51 (1979).

Slade, D.H. (Ed.), 'Methodology and Atomic Energy 1968', United States Atomic Energy Commission Div. of Tech. Information, Washington, DC, Rep. No. TID-24190 (1968); available from Clearinghouse for Federal Scientific and Technical Information, Springfield, VA.

Thomas, R.H., 'The Radiological Impact of High-Energy Accelerators on the Environment', National Laboratory of High-Energy Physics, Japan, Internal Report KEK-78-20 (1978).

ACCELERATOR DESIGN STUDIES

CERN, 'The 300 GeV Program', CERN Report CERN/1050 (1972).

Fermi National Accelerator Laboratory, 'A Report on the Design of the Fermi National Accelerator Laboratory Superconducting Accelerator', Batavia, IL (May 1979).

Hobbis, L.C.W., Rees., G.H. and Stirling, G.C., 'A Pulsed Neutron Facility for Condensed Matter Research', Rutherford Laboratory Report RL-77-064-C (June 1977).

'National Accelerator Laboratory-Design Report', Universities Research Association Internal Report (July 1968).

Lawrence Berkeley Laboratory, 'The 200-BeV Accelerator Design Study', 2 vols., internal report, UCRL-16000 (June 1965).

Lawrence Berkeley Laboratory, 'High Intensity Uranium Beams from the SuperHILAC and the Bevalac', Proposal 32 (May 1975).

Lawrence Berkeley Laboratory, 'The Heavy Ion Medical Accelerator', internal report, Pub-5122 (June 1984).

Neale, R.D. (Ed.), 'The Stanford Two-Mile Accelerator', Benjamin, New York (1968).

'PEP Conceptual Design Report', Lawrence Berkeley Laboratory and Stanford Linear Accelerator Center, internal report, LBL-4288/SLAC-185 (February 1976).

Sanford, J.R. (Ed.), 'Isabelle-A Proton-Proton Colliding Beam Facility', Brookhaven National Laboratory Internal Report BNL-5078 (January 1978).

U.S. Department of Energy, 'Superconducting Super Collider Reference Design Study', Reference Designs Study Group, Lawrence Berkeley Laboratory, May 8, 1984.

PROBLEMS OF INDUCED RADIOACTIVITY

Barbier, M., Induced Radioactivity, North Holland, Amsterdam, 1969.

Blasewitz, A.G., Davis, J.M. and Smith, M.R., The Treatment and Handling of Radioactive Waste, Battelle Press, Columbus, OH (1983).

Opelka, J.H., Mundis. R.L., Marmer, G.J., Peterson, J.M., Siskind, B., and Kitka, M.J., 'Particle-Accelerator Decommissioning', Argonne National Laboratory Report ANL/ES-82 (December 1979).

Stewart, D.C., Handling Radioactivity, John Wiley, New York (1981).

ACCELERATOR RADIATION SAFETY MANUALS

CERN, 'Radiation Safety Manual', European Organization for Nuclear Research, Geneva (1975).

Lawrence Berkeley Laboratory, 'Health and Safety Manual', Pub-3000 (1980 and subsequent revisions).

Martin, T.G. (Ed.), 'Accelerator Radiation Protection', U.S. Army Natick Laboratories Technical Report TR-73-7, Natick, MA (1972).

Particle Accelerator Manual (Prepared by W.M. Brobeck and Associates), U.S. Department of Health, Education and Welfare, Report MORP 68-12, National Center for Radiological Health, Rockville, MD (1968).